LOCAL ASPECTS OF SLEEP AND WAKEFULNESS

EDITED BY: Giulio Bernardi, Francesca Siclari and Michele Bellesi
PUBLISHED IN: Frontiers in Neuroscience

frontiers Research Topics

frontiers

Frontiers eBook Copyright Statement

The copyright in the text of individual articles in this eBook is the property of their respective authors or their respective institutions or funders. The copyright in graphics and images within each article may be subject to copyright of other parties. In both cases this is subject to a license granted to Frontiers.

The compilation of articles constituting this eBook is the property of Frontiers.

Each article within this eBook, and the eBook itself, are published under the most recent version of the Creative Commons CC-BY licence. The version current at the date of publication of this eBook is CC-BY 4.0. If the CC-BY licence is updated, the licence granted by Frontiers is automatically updated to the new version.

When exercising any right under the CC-BY licence, Frontiers must be attributed as the original publisher of the article or eBook, as applicable.

Authors have the responsibility of ensuring that any graphics or other materials which are the property of others may be included in the CC-BY licence, but this should be checked before relying on the CC-BY licence to reproduce those materials. Any copyright notices relating to those materials must be complied with.

Copyright and source acknowledgement notices may not be removed and must be displayed in any copy, derivative work or partial copy which includes the elements in question.

All copyright, and all rights therein, are protected by national and international copyright laws. The above represents a summary only. For further information please read Frontiers' Conditions for Website Use and Copyright Statement, and the applicable CC-BY licence.

ISSN 1664-8714
ISBN 978-2-88963-565-8
DOI 10.3389/978-2-88963-565-8

About Frontiers

Frontiers is more than just an open-access publisher of scholarly articles: it is a pioneering approach to the world of academia, radically improving the way scholarly research is managed. The grand vision of Frontiers is a world where all people have an equal opportunity to seek, share and generate knowledge. Frontiers provides immediate and permanent online open access to all its publications, but this alone is not enough to realize our grand goals.

Frontiers Journal Series

The Frontiers Journal Series is a multi-tier and interdisciplinary set of open-access, online journals, promising a paradigm shift from the current review, selection and dissemination processes in academic publishing. All Frontiers journals are driven by researchers for researchers; therefore, they constitute a service to the scholarly community. At the same time, the Frontiers Journal Series operates on a revolutionary invention, the tiered publishing system, initially addressing specific communities of scholars, and gradually climbing up to broader public understanding, thus serving the interests of the lay society, too.

Dedication to Quality

Each Frontiers article is a landmark of the highest quality, thanks to genuinely collaborative interactions between authors and review editors, who include some of the world's best academicians. Research must be certified by peers before entering a stream of knowledge that may eventually reach the public - and shape society; therefore, Frontiers only applies the most rigorous and unbiased reviews.
Frontiers revolutionizes research publishing by freely delivering the most outstanding research, evaluated with no bias from both the academic and social point of view. By applying the most advanced information technologies, Frontiers is catapulting scholarly publishing into a new generation.

What are Frontiers Research Topics?

Frontiers Research Topics are very popular trademarks of the Frontiers Journals Series: they are collections of at least ten articles, all centered on a particular subject. With their unique mix of varied contributions from Original Research to Review Articles, Frontiers Research Topics unify the most influential researchers, the latest key findings and historical advances in a hot research area! Find out more on how to host your own Frontiers Research Topic or contribute to one as an author by contacting the Frontiers Editorial Office: researchtopics@frontiersin.org

LOCAL ASPECTS OF SLEEP AND WAKEFULNESS

Topic Editors:
Giulio Bernardi, IMT School for Advanced Studies Lucca, Italy
Francesca Siclari, Lausanne University Hospital (CHUV), Switzerland
Michele Bellesi, University of Bristol, United Kingdom

Citation: Bernardi, G., Siclari, F., Bellesi, M., eds. (2020). Local Aspects of Sleep and Wakefulness. Lausanne: Frontiers Media SA. doi: 10.3389/978-2-88963-565-8

Table of Contents

frontiers in Neuroscience

EDITORIAL
published: 07 February 2020
doi: 10.3389/fnins.2020.00058

Editorial: Local Aspects of Sleep and Wakefulness

Giulio Bernardi[1]*, *Francesca Siclari*[2]* and *Michele Bellesi*[3]*

[1] IMT School for Advanced Studies Lucca, Lucca, Italy, [2] Lausanne University Hospital (CHUV), Lausanne, Switzerland, [3] School of Physiology, Pharmacology & Neuroscience, University of Bristol, Bristol, United Kingdom

Keywords: sleep, hd-EEG, MEG, fMRI-EEG, K-complex, slow wave, spindle, connectivity

Editorial on the Research Topic

Local Aspects of Sleep and Wakefulness

In the last two decades, the traditional view of sleep and wakefulness as global, whole-brain states has been challenged by a growing body of evidence indicating that both sleep and wake are regulated locally and that sleep- and wake-like activity can often co-occur across distinct brain areas. This change in perspective has led to a better understanding of sleep physiology and pathophysiology. The present Research Topic highlights current research and views on the local regulation of sleep and wakefulness in multiple species, models and systems. The articles, which include both original research and reviews, describe results obtained using a variety of experimental techniques and analytical methods.

Several articles explore the local aspects of sleep hallmarks, including slow waves, K-complexes (KCs) and spindles, and evaluate how they could relate to typical features and known functions of sleep, including sensory disconnection and memory consolidation. Using magnetoencephalographic (MEG) recordings in N2-sleep, Ioannides et al. demonstrate that KCs, commonly considered as "global" events, are characterized by important inter-regional differences. The authors show that spontaneous KCs are associated with changes in brain activity that mostly involve medial frontal and cingulate areas, whereas more lateral and posterior regions are usually spared. In addition, their results indicate that KCs are preceded by specific activity changes that are circumscribed to the dorsal caudal anterior cingulate cortex. Laurino et al. complement these observations through the study of sensory evoked KCs. Using source modeling of high-density electroencephalographic (hd-EEG) recordings, they show that the first component of KCs is a positive signal deflection with a specific cortical distribution that depends on the nature of the administered sensory stimulus. This positive wave, which is associated with an increase in high-frequency activity, appears to travel toward frontal brain regions where the main negative component of the KC is eventually ignited.

Other two studies focused on the local correlates of sleep spindles. Specifically, Alfonsi et al. used source modeling of scalp EEG data to identify the cortical sources of sleep spindles and their variations across a night of sleep. They confirm that faster spindles predominate over parietal cortical areas, while slower spindles involve more frontal regions. Moreover, the authors show that activity of frontal slow spindles tends to decrease from the beginning to the end of the night, while, within each cycle, activity of both frontal and parietal spindles follows a U-shaped curve. Fang et al.

OPEN ACCESS

Edited and reviewed by:
Luis de Lecea,
Stanford University, United States

***Correspondence:**
Giulio Bernardi
giulio.bernardi@imtlucca.it
Francesca Siclari
francesca.siclari@chuv.ch
Michele Bellesi
michele.bellesi@bristol.ac.uk

Specialty section:
This article was submitted to Sleep and Circadian Rhythms, a section of the journal Frontiers in Neuroscience

Received: *10 January 2020*
Accepted: *15 January 2020*
Published: *07 February 2020*

Citation:
Bernardi G, Siclari F and Bellesi M (2020) Editorial: Local Aspects of Sleep and Wakefulness. Front. Neurosci. 14:58. doi: 10.3389/fnins.2020.00058

used simultaneous fMRI-EEG to study cortical and subcortical areas involved in sleep spindles and to evaluate their potential relationship with cognitive skills. They report activations in the thalamus, bilateral striatum, middle cingulate cortex, and cerebellum. Further, spindle activation in a subset of these structures correlated with reasoning abilities, but not short-term memory or verbal abilities.

In their opinion piece, Geva-Sagiv and Nir outline available evidence linking local changes in slow waves and spindles to experience-dependent brain plasticity and learning. They show how cortical and thalamic sleep oscillations are coupled with hippocampal activity and may thus support memory consolidation. The authors also describe how recent discoveries of novel tools allowing to artificially modulate sleep oscillations could potentially be used to modulate sleep-dependent memory processing. Finally, they underscore the need to achieve a better understanding of how the local regulation and co-regulation of slow waves and spindles relates to changes in hippocampal activity.

The local regulation of sleep may have important implications not only for experience-dependent brain plasticity, but also for the maintenance of an efficient sensory disconnection during sleep. Tamaki and Sasaki used source localization of hd-EEG recordings to confirm and extend their recent observation of an inter-hemispheric asymmetry in NREM slow wave activity during the first night of sleep in an unfamiliar environment. Interestingly, they show that while a similar asymmetry in brain activity is not present during REM sleep, in phasic REM periods the amplitude of evoked brain responses to deviant tones is greater during the first relative to the second night. These findings suggest the presence of distinct brain mechanisms to monitor an unfamiliar environment during NREM and REM sleep.

Two review articles highlight the importance of employing distinct animal models to achieve a deeper understanding of the local regulation of sleep and wakefulness. Rattenborg et al. describe similarity and differences in local sleep regulation across different species of birds and mammals. While evidence clearly indicates that wakefulness, NREM and REM sleep often manifest as non-discrete states in many different species, inter-species differences and peculiarities may hold the key to understand the functions and mechanisms of sleep-related brain activity. Moreover, Vantomme et al. outline evidence from animal studies supporting a possible role of the thalamic reticular nucleus (TRN) in the local regulation of sleep oscillations. In fact, while recent research especially focused on the cortical mechanisms of local sleep regulation, the involvement of subcortical structures is still poorly investigated and understood. Here, Vantomme and colleagues show that subcortical circuits may contribute to the tuning of regional sleep patterns and suggest that alterations of such circuits could potentially explain aberrant local changes in cortical brain activity observed in distinct pathological conditions.

The falling asleep and the awakening processes represent transitional states associated with changes in activity that do not occur simultaneously across all brain regions. The study of these states may thus provide essential information regarding the local cortical and subcortical regulation of sleep. For the first time, two studies explore here how brain activity and connectivity change at sleep onset following a period of acute sleep deprivation. Gorgoni et al. show that recovery sleep is characterized by a stronger and more diffuse frontal increase in low-frequency activity relative to sleep onset in baseline conditions. In contrast, changes in sigma and beta activity, respectively characterized by an increase over centro-parietal areas and a widespread decrease, are scarcely affected by sleep loss. In addition, Fernandez Guerrero and Achermann show that sleep onset is characterized by an anterior-to-posterior decoupling within the so-called default mode network (DMN), while increased connectivity from posterior cingulate cortex to other nodes of the DMN is observed for most frequencies. Increased sleep drive caused by sleep deprivation leads to similar changes, but with decreased connectivity among several pairs of areas, especially in the high-frequency range.

The fact that sleep is locally regulated implies that islands of sleep-like activity could also appear during behavioral and electrophysiological wakefulness. Two review papers describe the physiological meaning and possible behavioral and cognitive impact of these "local sleep" episodes during periods of waking. D'Ambrosio et al. summarize the neurophysiological bases of local sleep and compare it to other forms of intrusions of sleep into wakefulness, such as microsleep episodes. Importantly, local sleep episodes increase in number and extension with time spent awake and have a proven negative impact on behavioral performance. Thus, the authors suggest that local sleep may represent a signature of brain fatigue, potentially accounting for many of the cognitive and behavioral manifestations of sleepiness. Andrillon et al. further suggest that local sleep intrusions could affect subjective experience associated with attentional lapses, leading to either mind wandering or mind blanking. Their proposed framework may have important implications for our understanding of inter-individual differences in attentional lapses in physiological and pathological conditions, such as attention deficit hyperactivity disorder (ADHD). In fact, alterations in the local regulation of sleep and wakefulness could contribute to explain still poorly understood symptoms of many pathological conditions. In line with this, Christensen et al. demonstrate that insomnia patients are characterized by a stronger expression of sleep patterns characteristic of light sleep or wakefulness, even during the deepest stages of sleep, indicating a deep sleep fragility.

Finally, in their work Héricé and Sakata show that even a simple network model of the sleep–wake cycle can be associated with complex behaviors. Their results indicate the importance of carefully taking into account the complexity of sleep-wake regulation circuits when designing *in vivo* experiments and interpreting their results, but also show the fundamental complementary role of computational models in studying the physiological mechanisms regulating sleep-related brain activity.

Overall, this Research Topic underscores the importance of combining multiple experimental models and approaches to broaden our understanding of sleep regulation. The editors hope that the papers published herein will stimulate further

investigations aimed at elucidating the complex mechanisms underpinning the local regulation of sleep and wakefulness, and their implications for behavior and cognition in both physiological and pathological conditions.

AUTHOR CONTRIBUTIONS

GB wrote the first draft. All authors revised and edited the manuscript.

Conflict of Interest: The authors declare that the research was conducted in the absence of any commercial or financial relationships that could be construed as a potential conflict of interest.

Copyright © 2020 Bernardi, Siclari and Bellesi. This is an open-access article distributed under the terms of the Creative Commons Attribution License (CC BY). The use, distribution or reproduction in other forums is permitted, provided the original author(s) and the copyright owner(s) are credited and that the original publication in this journal is cited, in accordance with accepted academic practice. No use, distribution or reproduction is permitted which does not comply with these terms.

frontiers in Neuroscience

ORIGINAL RESEARCH
published: 04 December 2018
doi: 10.3389/fnins.2018.00912

Intracortical Causal Information Flow of Oscillatory Activity (Effective Connectivity) at the Sleep Onset Transition

Antonio Fernandez Guerrero[1,2] *and Peter Achermann*[1,2,3,4]*

[1] *Institute of Pharmacology and Toxicology, University of Zurich, Zurich, Switzerland,* [2] *Neuroscience Center Zurich, University of Zurich and ETH Zurich, Zurich, Switzerland,* [3] *The KEY Institute for Brain-Mind Research, Department of Psychiatry, Psychotherapy and Sychosomatics, University Hospital of Psychiatry, Zurich, Switzerland,* [4] *Zurich Center for Interdisciplinary Sleep Research, University of Zurich, Zurich, Switzerland*

We investigated the sleep onset transition in humans from an effective connectivity perspective in a baseline condition (approx. 16 h of wakefulness) and after sleep deprivation (40 h of sustained wakefulness). Using EEG recordings (27 derivations), source localization (LORETA) allowed us to reconstruct the underlying patterns of neuronal activity in various brain regions, e.g., the default mode network (DMN), dorsolateral prefrontal cortex and hippocampus, which were defined as regions of interest (ROI). We applied isolated effective coherence (iCOH) to assess effective connectivity patterns at the sleep onset transition [2 min prior to and 10 min after sleep onset (first occurrence of stage 2)]. ICOH reveals directionality aspects and resolves the spectral characteristics of information flow in a given network of ROIs. We observed an anterior-posterior decoupling of the DMN, and moreover, a prominent role of the posterior cingulate cortex guiding the process of the sleep onset transition, particularly, by transmitting information in the low frequency range (delta and theta bands) to other nodes of DMN (including the hippocampus). In addition, the midcingulate cortex appeared as a major cortical relay station for spindle synchronization (originating from the thalamus; sigma activity). The inclusion of hippocampus indicated that this region might be functionally involved in sigma synchronization observed in the cortex after sleep onset. Furthermore, under conditions of increased homeostatic pressure, we hypothesize that an anterior-posterior decoupling of the DMN occurred at a faster rate compared to baseline overall indicating weakened connectivity strength within the DMN. Finally, we also demonstrated that cortico-cortical spindle synchronization was less effective after sleep deprivation than in baseline, thus, reflecting the reduction of spindles under increased sleep pressure.

Keywords: effective connectivity, default mode network, central executive network, delta activity, sigma activity, sleep deprivation

OPEN ACCESS

Edited by:
Francesca Siclari,
Lausanne University Hospital (CHUV), Switzerland

Reviewed by:
George K. Kostopoulos,
University of Patras, Greece
Maurizio Gorgoni,
Sapienza University of Rome, Italy

***Correspondence:**
Peter Achermann
acherman@pharma.uzh.ch

Specialty section:
This article was submitted to Sleep and Circadian Rhythms, a section of the journal Frontiers in Neuroscience

Received: *11 September 2018*
Accepted: *20 November 2018*
Published: *04 December 2018*

Citation:
Fernandez Guerrero A and Achermann P (2018) Intracortical Causal Information Flow of Oscillatory Activity (Effective Connectivity) at the Sleep Onset Transition. Front. Neurosci. 12:912. doi: 10.3389/fnins.2018.00912

INTRODUCTION

Falling asleep is a process characterized by the relative disengagement from the external environment and a loss of consciousness, yet, little is known about its neurophysiological basis (Ogilvie, 2001; Marzano et al., 2013). Given that conscious awareness is attributed to the capability to integrate activity originating from diverse brain regions (particularly cortico-cortical and cortico-thalamic interactions), a suitable approach to examine how this process unfolds is by applying connectivity methods which are able to describe how distinct brain oscillations transmit information between brain regions (Massimini et al., 2005; Esser et al., 2009; Chow et al., 2013; Tononi et al., 2016). With a seed-based approach or by independent component analyses (ICA), several brain networks were identified during rest (resting state networks, RSNs), with nodes clustered together according to a shared pattern of temporal correlations (Park and Friston, 2013; Amico et al., 2014). Two prominent networks stand out, the default mode network (DMN, thought to be involved in mind-wandering, creativity and emotional processing) and the central executive network (CEN, involved in cognition, planning and working memory), generally being anti-correlated to the DMN (Buckner et al., 2008; Douw et al., 2014; Salone et al., 2016). This study aims to investigate connectivity changes paralleling the sleep onset (SOn) transition, on a selection of nodes that combines these two principal networks, which have been previously related with consciousness and sleep (Sämann et al., 2011; Heine et al., 2012; Uehara et al., 2014).

Identifying potential interactions arising in a network of connected brain regions is one of the most important and relevant problems in neuroscience (He and Evans, 2010; Park and Friston, 2013). In this context, connectivity can be addressed in three major ways by investigating structural, functional, and effective connectivity (Sporns and Betzel, 2016; Stam et al., 2016). Briefly summarized, structural connectivity deals with the topology of white matter tracts physically linking different brain areas, functional connectivity reflects temporal correlations between regions, and effective connectivity completes and corrects the deficiencies of functional connectivity, by pruning potential indirect connections and by adding causal and directionality aspects (Friston, 2011; Valdes-Sosa et al., 2011; Stam et al., 2016). The use of the EEG, as in this study, and in contrast to fMRI research (typically limited to the mere predominant directionality of slow components due to the low temporal resolution of fMRI), allows for an additional spectral representation of effective connectivity coupling due to its much higher characteristic sampling rate (Pascual-Marqui et al., 2011). In this paper, we will focus on effective connectivity to study the SOn transition from a connectivity perspective including directionality.

Effective connectivity methods are mathematical tools created to best characterize the influence that one neuronal group is impinging on another one in the context of neuronal networks (in principle, composed of an arbitrary number of nodes) (Friston, 2011; Liu and Aviyente, 2012). Pioneers in the study of causal relationships among a set of signals were Akaike (with a method called Noise Contribution Ratio) and Granger (with a causality method named after him), laying the analytical foundation for this field, which has advanced substantially since then, yet, continuing to be under development (Akaike, 1968; Granger, 1969). In general, effective connectivity methods can be formulated either in the time or frequency domain and can have either linear or non-linear characteristics in the underlying equations (Geweke, 1982; Bakhshayesh et al., 2014; Khadem and Hossein-Zadeh, 2014). Some well-known effective connectivity methods are: Granger Causality (GC), Partial Directed Coherence (PDC), Transfer Entropy (TE), Phase Slope Index (PSI) or Dynamic Causal Modeling (DCM) (Barnett et al., 2009; Silfverhuth et al., 2012; Ewald et al., 2013; Friston et al., 2014).

In order to assess effective connectivity changes characterizing the SOn transition, we applied isolated effective coherence (iCOH) (Pascual-Marqui et al., 2014a). Intuitively, this method provides a normalized measure (between 0 and 1) of the coupling strength between a pair of nodes in the frequency domain, which is sensitive to the directionality of the interaction by index permutation (i.e., *A* directs *B*, versus the opposite, which can vary remarkably, a distinction neglected by functional connectivity methods) (Kralemann et al., 2014). By mathematical construction, iCOH prunes away any indirect path linking two particular brain areas, which could distort the results in a major way (especially for complex networks). For example, if node *A* directs *B*, and *B* directs *C*, but there is no direct connection between *A* and *C* (existing only indirectly), then, iCOH results preserve the actual causal order, whereas other techniques (e.g., GC or Directed Transfer Function) would tend to incorrectly indicate a direct connection between *A* and *C*, biasing the causal structure of a network (Baccala and Sameshima, 2001; Faes et al., 2010). In addition, the frequency representation of iCOH allows to study the relevant information contained in its spectral characteristics and can be used to deduce which frequency bands (indicated by either absolute or local maxima) are preferentially involved in the information transfer between a set of brain regions (Pascual-Marqui et al., 2014a).

MATERIALS AND METHODS

Data Description and Preprocessing

The EEG data analyzed in this study are from recordings in eight healthy young right-handed men of a previous study (Finelli et al., 2000, 2001a,b). The EEG signals were sampled at 128 Hz [band-pass filter: 0.16–30 Hz; for additional details see (Finelli et al., 2001b)]. The sleep stages were scored for 20-s epochs (C3A2 derivation) according to Rechtschaffen and Kales (1968). Artifacts were identified as described in Finelli et al. (2001b). Additionally, 4-s epochs containing artifacts were replaced by the preceding epoch free of artifacts (12-s epochs, i.e., three consecutive 4-s epochs were analyzed). The total number of recording channels was 27, placed evenly on the scalp according to the international 10/20 system. Although a technical reference (placed 5% rostral to Cz) was originally used in the recordings, in the subsequent processing, all EEG data were re-referenced to the average reference. EEG recordings were performed during

a baseline night (bedtime 23:00–7:00 hours), and recovery sleep (23:00–11:00 hours) following 40 h of sustained wakefulness (within-subject design). The local ethics committee approved the study protocol and written informed consent was obtained from the participants prior to the study. For further details on participants (inclusion, exclusion criteria; protocol) and recordings see (Finelli et al., 2000, 2001b). Effective connectivity data were computed by means of iCOH (implemented in eLORETA) in the following frequency bands: delta (0.5–5 Hz), theta (5–8 Hz), alpha (8–12 Hz), sigma (12–16 Hz) and beta (16–24 Hz).

Even when the SOn process is a gradual phenomenon that unfolds continuously as a function of time (Ogilvie, 2001; Prerau et al., 2014; Siclari et al., 2014), data have to be aligned in order to statistically compare and analyze the process of SOn. Thus, SOn was operationally defined as the first occurrence of an epoch of stage 2 non-rapid eye movement (NREM) sleep. Multivariate autoregressive (MVAR) models, on which the iCOH method relies, were fitted to consecutive 12-s EEG epochs. Outputs were averaged to obtain a single effective connectivity response, representing a 2-min interval per subject, and subsequently averaged across subjects to yield the final group result. Sleep latency (first occurrence of stage 2) was shorter in recovery sleep (4.1 ± 1.2 versus 12.1 ± 1.6 min; SEM; $p < 0.01$; Wilcoxon signed-rank test). Before SOn there was only a single 2-min interval with the contribution of all participants in both conditions. After SOn, 10 min were selected, resulting in five consecutive 2-min intervals, which were averaged to have a unified picture of the connectivity behavior both before and after SOn. The eLORETA version used for the analyses was version 20160611 (most updated at the time of running this study; available as free academic software[1]).

Isolated Effective Coherence (iCOH)

The algorithm to compute iCOH starts with the estimation of a MVAR model. For details on the mathematical deduction of the iCOH method based on a MVAR model, explained step by step, we refer to (Pascual-Marqui et al., 2014a). Since this effective connectivity analysis is performed at the source level (resulting in spurious results at the scalp level), it is necessary to use a source localization method for the computation of iCOH (Grech et al., 2008; Jatoi et al., 2014). The equation representing iCOH (derived in the frequency domain) takes the following expression:

$$k_{i \leftarrow j}(\omega) = \frac{S_{\varepsilon_{ii}}^{-1} \left| \breve{A}(\omega)_{ij} \right|^2}{S_{\varepsilon_{ii}}^{-1} \left| \breve{A}(\omega)_{ij} \right|^2 + S_{\varepsilon_{jj}}^{-1} \left| \breve{A}(\omega)_{jj} \right|^2}$$

satisfying the normalization condition: $0 \leq k_{i \leftarrow j}(\omega) \leq 1$ (Pascual-Marqui et al., 2014a). Here, $k_{i \leftarrow j}(\omega)$ represents the iCOH value at a given frequency ω between regions of interest (ROIs) j and i, where the arrow indicates that j influences i (both indexes range from 1 to N, the number of ROIs). The matrix $\breve{A}(\omega) = I - A(\omega)$, with I being the unit matrix of order N, relates to the matrix $A(\omega)$ derived by least square fitting of the MVAR model of order p (estimated by the Akaike information criterion). The matrix S_ε represents the covariance of the residual errors of the MVAR model in the frequency domain and improves the result by adding a weight proportional to the accuracy of the accompanying parameters. The software LORETA is able to compute automatically all necessary parameters in this equation (including the optimal order p of the MVAR model; $p = 23$ in our case), rendering an iCOH spectrum as output, when providing a given set of EEG data as input.

The particular expression of the iCOH formula (specifically, as seen in the denominator), aims to convey that all connections besides the one of interest (j to i) are mathematically "severed". For details about mathematical properties satisfied by iCOH, as well as a comparison with another effective connectivity techniques [the generalized partial directed coherence (gPDC)], we refer to (Pascual-Marqui et al., 2014a,b).

iCOH is normalized and is thus basically independent of the strength of the underlying sources [current source density (CSD); see also (Pascual-Marqui et al., 2014b) for examples of simulated data] similar as it is for coherence and power (Achermann and Borbély, 1998).

Selection of ROIs

In order to study statistical changes in effective connectivity accompanying the SOn transition, a suitable selection of ROIs needs to be made, aiming to capture the most relevant aspects from a neurobiological perspective, thus, constituting a crucial step in the process of the analysis (Sämann et al., 2011). The inverse solution provided by eLORETA allows for a ROI definition either by providing the Montreal Neurological Institute coordinates of seed regions or by direct selection of Brodmann areas by the user. A total of nine ROIs were selected: the medial prefrontal cortex (MPFC), mid-cingulate gyrus (MCC), posterior cingulate cortex (PCC), bilateral inferior parietal lobule (IPL), bilateral dorsolateral prefrontal cortex (DLPFC) and bilateral hippocampus (H). The rational for these particular ROIs comes from their close relationship with two principal brain networks: the DMN and the CEN (Sporns et al., 2007; Sämann et al., 2011). The first five ROIs define major hubs of the DMN (first two in the anterior, and last three in the posterior part), whereas the DLPFC is the most important hub of the CEN (Andrews-Hanna et al., 2010; Larson-Prior et al., 2011). On the other hand, the hippocampus is sometimes included in the definition of DMN regions, whereas other authors prefer to consider the hippocampus separately as a limbic structure (therefore, excluded from DMN analysis), which nevertheless is acknowledged to interact with cortical hubs of the DMN (e.g., during autobiographical recall) (Buckner et al., 2008; Horovitz et al., 2009; Sämann et al., 2010). Either way, the main reason for adding the hippocampus to our ROI selection is due to its relationship with sleep spindles occurring at the SOn transition, as revealed by intracranial recordings (Nir et al., 2011; Sarasso et al., 2014). Sleep spindles are generated in the thalamus, specifically in the reticular nucleus (Fuentealba and Steriade, 2005; Magnin et al., 2010). Thus, inclusion of the thalamus as a ROI would have made sense. However, we cannot locate thalamic activity with LORETA, as the thalamus is a too deep lying subcortical region for source localization.

[1] http://uzh.ch/keyinst/loreta

The computation of iCOH involves a matrix inversion which limits the number of ROIs that could be included. Eight to nine ROIs (in conjunction with the 127 frequency bins) are the limit avoiding numerical instability in calculating the matrix inversion.

In practice, ROIs were defined by a sphere surrounding the centroid of each ROI. Nevertheless, an unavoidable tradeoff is present, as a small radius would not give the best precision (given that noise effects in the LORETA calculation of spectral current generators do not cancel out when the number of averaged vectors is small), whereas a large radius would tend to produce wrong results for sensitive interactions. In addition, if the radius is too big, the averaged current vector can be even close to 0 in all directions. Thus, as a compromise, the radius for each ROI was defined as 15 mm (Siclari et al., 2014). The cartesian coordinates (Montreal Neurological Institute system, MNI) representing the centroids of our selected ROIs are listed in **Table 1**.

Statistical Analyses and Presentation of Results

We carried out statistical tests based on the method of non-parametric randomization of the maximum statistic, which has the advantage of correcting for multiple testing, and of not relying on the assumption of any specific or exact statistical distribution (e.g., Gaussian, Student, Fisher; statistical non-parametric mapping, SnPM) (Nichols and Holmes, 2002; Faes et al., 2012). With SnPM, surrogate permutations (5,000 in our case) are created rendering a histogram which provides the statistical threshold (Pascual-Marqui et al., 2014a).

Results are presented in two ways in this paper. Firstly, as iCOH values computed by eLORETA, representing connectivity strength (effect size) as a function of frequency for any pair of ROIs (plots are arranged as a square matrix of order 9; **Figures 1**–**3**). Columns represent "senders", while rows are "receivers" of information flow. The correspondence between ROI and position in the square matrix, which is the same for rows and columns, follows the same order as they appear in **Table 1**. The frequency axis ranges from 0.5 Hz up to the Nyquist frequency (64 Hz), in 0.5 Hz steps. The *y*-axis represents the iCOH values. Dots below the curves indicate differences between conditions A and B (e.g., recovery versus baseline; gray dots A > B; black dots A < B). Secondly, significant differences between conditions A and B are plotted in matrix fashion for specific frequency bands (**Figures 4**, **5**). Red squares indicate A > B, blue ones A < B. All comparisons were corrected for multiple comparisons (see above). Additionally, light and dark red or blue reflect different significance thresholds (light color $p < 0.05$ corrected; dark color approximately $p < 0.025$ corrected) to give an indication on the hierarchy of the changes. We increased the threshold to twice (or if not possible because of being out of range, approximately twice) the 0.05 level.

TABLE 1 | Regions of interests (ROIs) selected for the effective connectivity analysis (iCOH) at the sleep onset transition.

Name of region of interest (ROI)	Abbreviation	X (mm)	Y (mm)	Z (mm)
Medial prefrontal cortex	MPFC	0.0	45.0	13.3
Mid-cingulate cortex	MCC	0.0	−17.5	37.5
Posterior cingulate cortex	PCC	0.0	−52.5	27.5
Left inferior parietal lobule	LIPL	−45.0	−45.0	52.5
Right inferior parietal lobule	RIPL	45.0	−45.0	52.5
Left dorsolateral prefrontal cortex	LDLPFC	−37.5	40.0	25.0
Right dorsolateral prefrontal cortex	RDLPFC	37.5	40.0	25.0
Left hippocampus	LH	−21.6	−28.3	−10.0
Right hippocampus	RH	21.6	−28.3	−10.0

Indicated are the centroid positions of the ROIs in MNI coordinates.

RESULTS

iCOH Spectra

Baseline Condition

Figure 1 illustrates the iCOH spectra before and after SOn in the baseline condition [performed on a 2-min window prior to SOn (red curve) and averaged five 2-min windows after SOn (blue curve); group averaged across subjects]. Information flow was clearly asymmetrical with the MCC and PCC as major sources, i.e., drivers and the other regions as receivers, i.e., targets.

Before SOn (**Figure 1**, red curves), the MCC had the largest impact bilaterally on the IPL and hippocampus with the absolute maximum of iCOH located at 3.5 Hz (delta range) and to a smaller degree to the PCC and bilaterally to the DLPFC. Information flow from the MCC to the MPFC occurred in the theta range (maximum at 5 Hz) and in the beta range (maxima at 20 Hz) bilaterally to the IPL and hippocampus. A further important source was the PCC, with predominantly theta (5.5 Hz) and to a smaller degree sigma (14.5 Hz) flow bilaterally to the IPL and hippocampus. These connections were less strong than those from the MCC.

After SOn (**Figure 1**, blue curves), one recognizes major changes that occurred after the transition into sleep compared to pre-SOn. Now, the PCC achieved the greatest prominence as a driving source of information flow in the theta range, projecting bilaterally to the IPL [at 5.5 Hz (LIPL) and 6.5 Hz (RIPL)] and hippocampus [at 5.5 Hz (LH) and at 7.5 Hz (RH)]. Further, the PCC projected to all other ROIs in the sigma range (related to spindles) with varying strength. The PCC is anatomically close to the thalamus, the actual generator of sleep spindles (De Gennaro and Ferrara, 2003; Fuentealba and Steriade, 2005), thus, the PCC could be acting as one of its main cortical "relay stations" of spindle propagation (Amico et al., 2014). Secondly, after SOn, the MCC was still exerting influence at various strength levels on all other ROIs mainly in the high delta (4 Hz), low theta (5 Hz) and in the sigma (14.5 Hz) range.

Dots in **Figure 1** represent the statistical comparison between the conditions, i.e., the changes that occurred after SOn. Gray dots indicate frequency bins at which effective connectivity was enhanced after SOn, black dots those at which it was decreased.

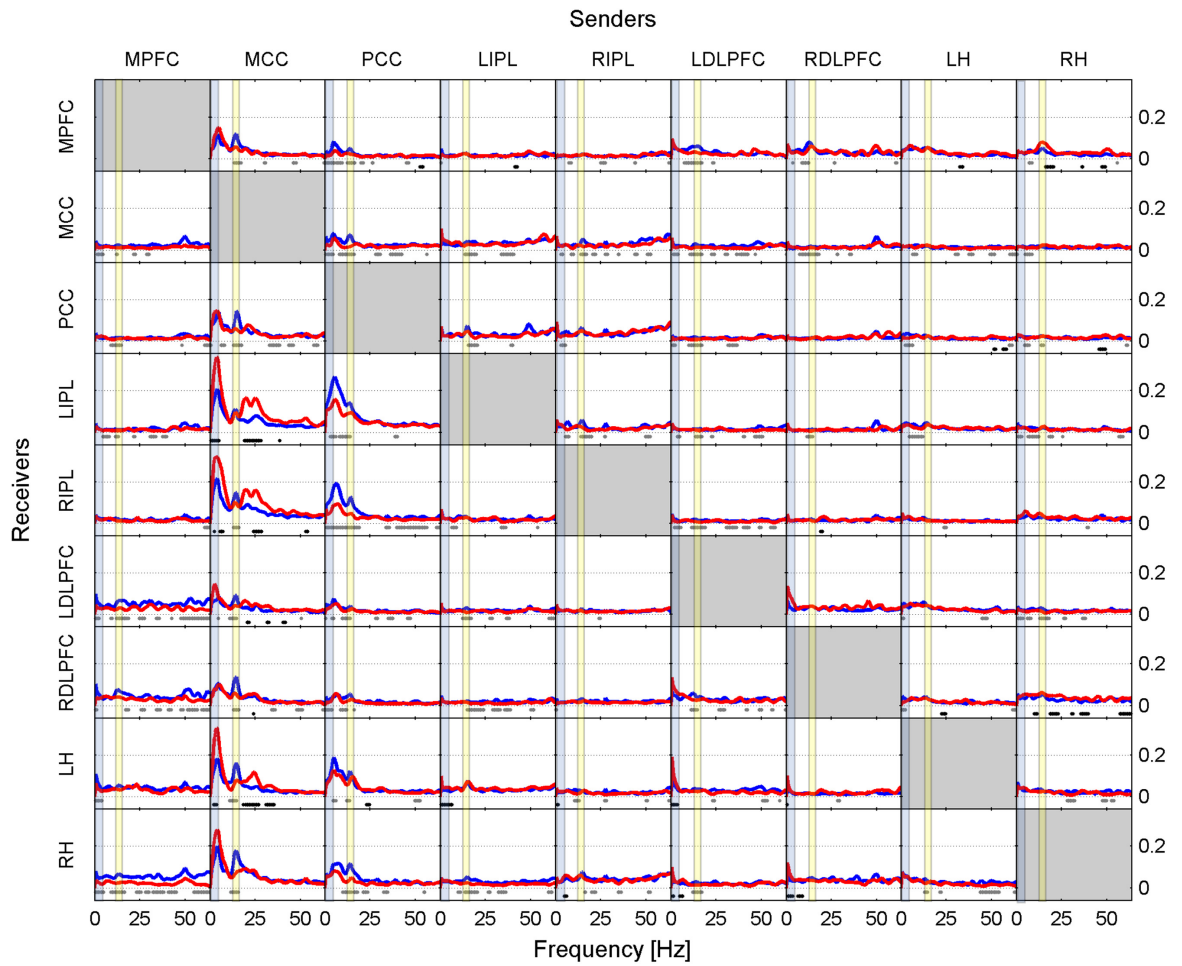

FIGURE 1 | Effective connectivity assessed by iCOH at the SOn transition in baseline. iCOH values representing connectivity strength (effect size) as a function of frequency for any pair of ROIs. Plots arranged as a square matrix of order 9; columns represent "senders", rows are "receivers" of information flow. For the abbreviations of the ROIs see **Table 1**. iCOH spectra before SOn (red curves) and after SOn (blue curves) are depicted and the frequency range is from 0.5 to 64 Hz (0.5-Hz resolution). Dots below the curves indicate significant differences between iCOH after SOn vs. iCOH before SOn: gray dots iCOH after SOn > iCOH before SOn; black dots iCOH after SOn < iCOH before SOn. To facilitate orientation, the delta (0.5–5 Hz) and sigma (12–16 Hz) band have been highlighted by light blue and light yellow, respectively.

The general picture reveals that prevalent connections present before SOn originating from the MCC were weakened after SOn in the low frequency range (delta and theta bands) and strengthened when originating from the PCC. In addition, causal flow in the beta range (located at 20 Hz and beyond) originating from the MCC was reduced. Finally, synchronization in the sigma band (related to sleep spindles) evolved mainly originating from the PCC and MCC.

Figure 1 also reveals connections from LDLPFC to LH and from RDLPFC to RH very close to 0 Hz. We consider this as a non-biological effect (artifact), i.e., caused by leakage (smearing) of the DC component (0 Hz) also known as Gibbs phenomenon in signal-processing theory.

Recovery Condition

Figure 2, similarly to **Figure 1**, shows iCOH spectra before (red) and after (blue) SOn in recovery after 40 h of sustained wakefulness. As in baseline, information flow was asymmetric with the MCC and PCC as major drivers. The connectivity patterns were like the ones observed in the baseline condition although with a different effect size (see below). Also, the comparison between post- and pre-SOn revealed a similar picture of change as in baseline.

Like in **Figures 1**, **2** revealed spurious connectivity very close to 0 Hz, e.g., between the left and right DLPFC (Gibbs phenomenon).

Statistical Contrast Between Baseline and Recovery

Comparing iCOH spectra prior to SOn between baseline and recovery revealed essentially no significant difference. **Figure 3** represents statistical comparison between recovery and baseline sleep for the period after SOn, comparing the blue iCOH spectra of **Figures 1**, **2**.

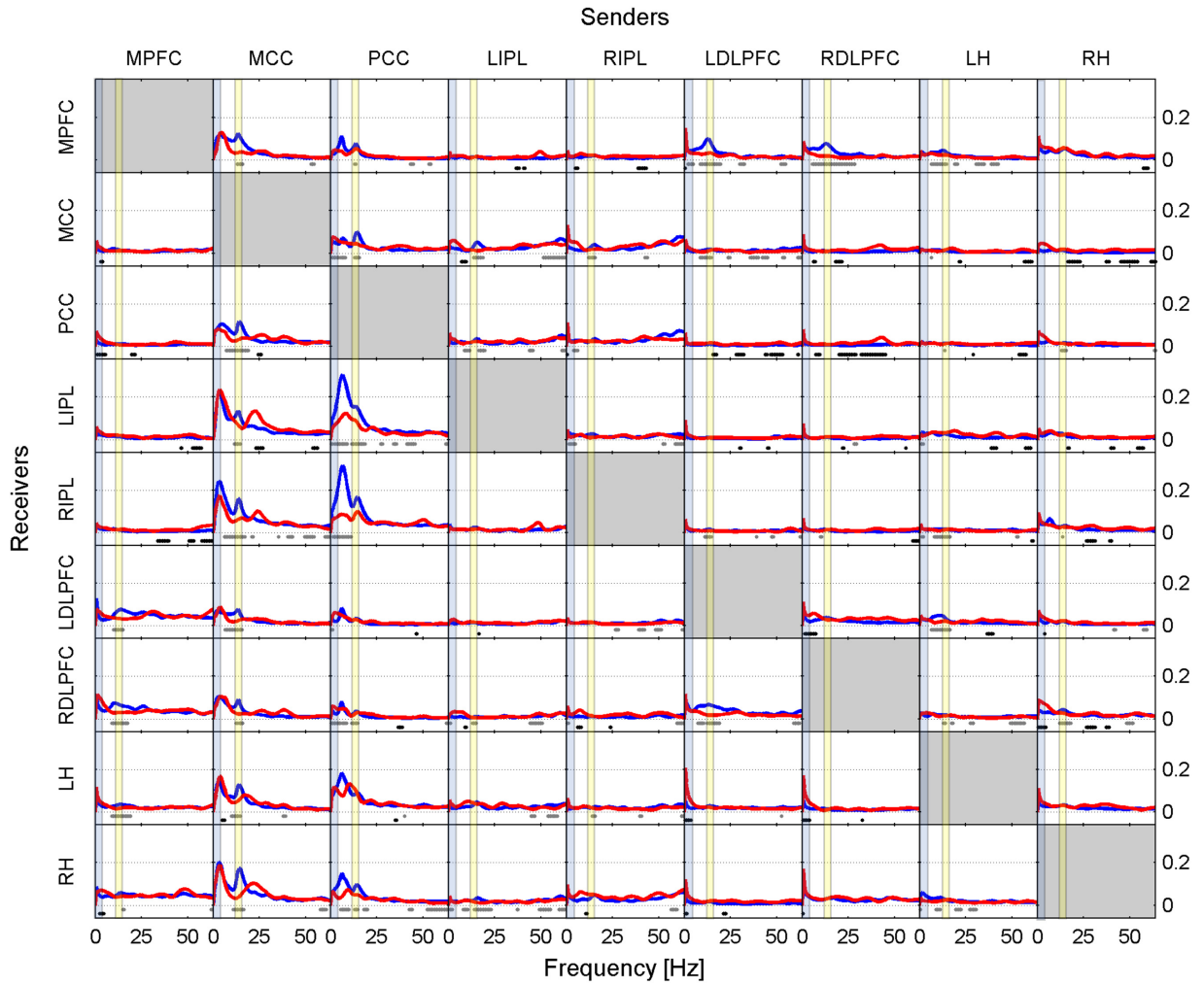

FIGURE 2 | Effective connectivity assessed by iCOH at the SOn transition in recovery after 40 h of sustained wakefulness. For details of the representation see **Figure 1**.

The overall picture revealed a reduction of iCOH values (effect size) in recovery compared to the baseline following the SOn transition (**Figure 3**, black dots) across many pairs of ROIs. It affected broad frequency ranges (many of them with low effect sizes), often the beta and gamma range. Increased connectivity due to increased sleep pressure were observed for the following projections: mainly PCC to LIPL and RIPL (theta, alpha and sigma range), and MCC to MPFC, LIPL and RIPL (theta, upper alpha and sigma range). A few pairs of ROIs (out of a total of 72 connections) hardly showed any change: MPFC to RH, PCC to LH, RH to LH, and RIPL to MCC.

iCOH of Specific Frequency Bands

We also investigated causal information flow in classical frequency bands. **Figure 4** illustrates significant effective connectivity changes following SOn in the delta (0.5–5 Hz) and sigma (12–16 Hz) band (left and right columns, respectively) for baseline and recovery (upper and middle rows) and the contrast recovery to baseline (bottom row). Changes in effective connectivity of the theta (5–8 Hz), alpha (8–12 Hz) and beta (16–24 Hz) band are illustrated accordingly in **Figure 5**. Two levels of the significance ($p < 0.05$ and $p < 0.025$) were applied to provide some information on the hierarchy of the changes, i.e., not all connectivity changes are equally salient in terms of significant increases or decreases as SOn unfolds. This also reduced the type I error. Further, also the strength of the connections and their change revealed by the iCOH spectra (**Figures 1**–**3**) helps to get an idea about the hierarchy.

Delta Band

In baseline, delta activity (0.5–5 Hz) showed significant changes in information flow between 22 ($p < 0.05$; 11 $p < 0.025$, respectively) pairs of ROIs after SOn, 17 (7) increased and 5 (4) decreased (**Figure 4**, upper left panel). The PCC acted as a major low frequency synchronizer, connectivity to all ROIs except to the RH was increased (only increases to the MPFC and MCC remained at $p < 0.025$). On the other hand, the MCC,

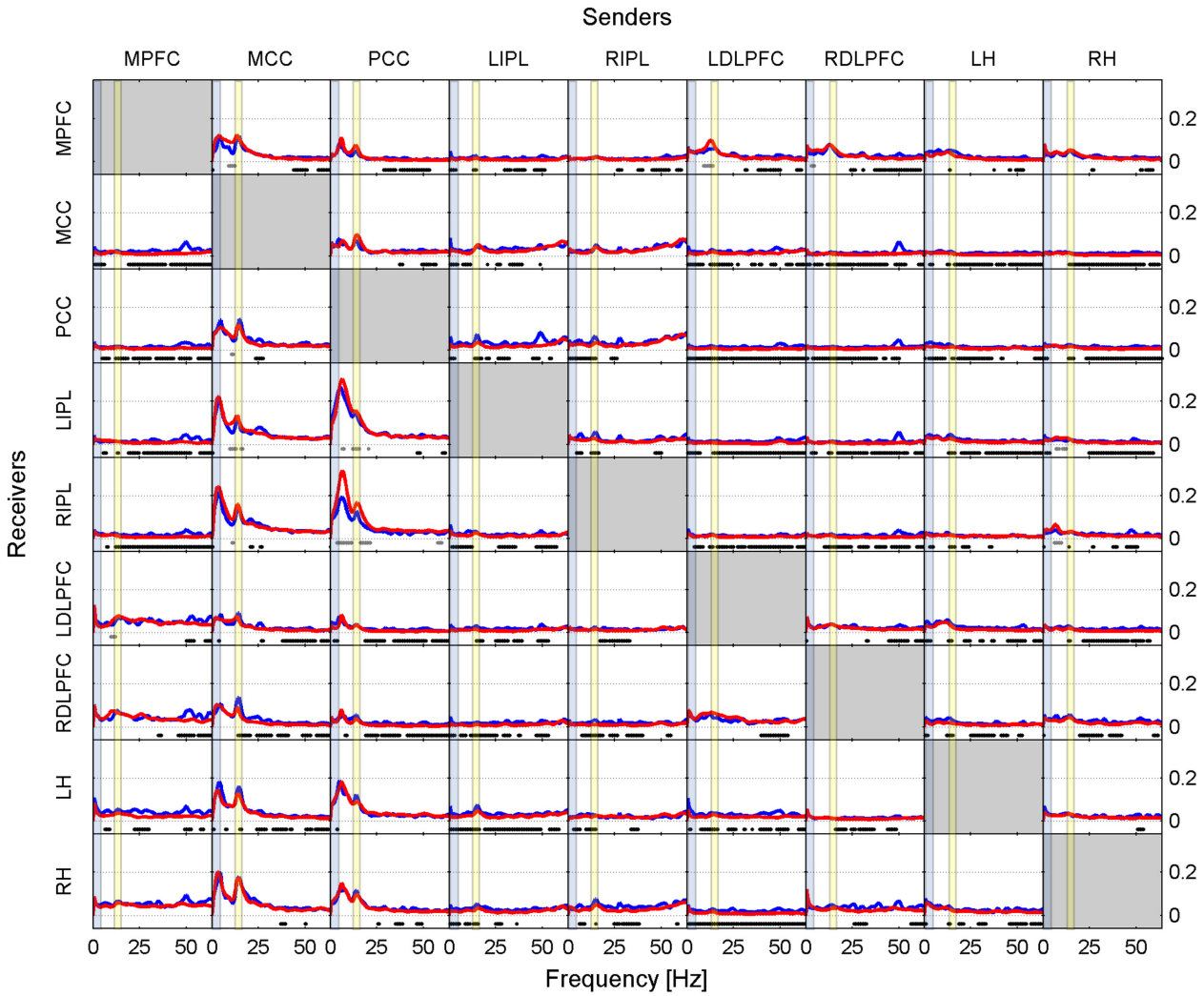

FIGURE 3 | Effective connectivity assessed by iCOH after the SOn transition in baseline (blue curves) and recovery (red curves). For details of the representation see **Figure 1**. Dots below the curves indicate significant differences between iCOH after SOn in baseline vs. iCOH after SOn in recovery: gray dots iCOH recovery > iCOH baseline; black dots iCOH recovery < iCOH baseline. To facilitate orientation, the delta (0.5–5 Hz)) and sigma (12–16 Hz) band have been highlighted by light blue and light yellow, respectively.

the other major source, showed weakened connections to the LIPL ($p < 0.025$) and the LH ($p < 0.05$). All other changes concerned low effect sizes. Connectivity between the MPFC and the MCC ($p < 0.05$), the LDLPFC ($p < 0.025$), the LH and the RH ($p < 0.025$), between the LIPL and the MPFC ($p < 0.025$), between the LDLPFC and the MCC and the RIPL (both $p < 0.05$), between the LH and the PCC ($p < 0.025$), and the RH and the LIPL ($p < 0.05$) and the LDLPFC ($p < 0.025$) was strengthened. Decreases (weakened connections) occurred from the LDLPFC to the LH ($p < 0.025$), and from the RDLPFC to the RH ($p < 0.025$).

In recovery, information flow between only 16 (8) pairs of ROIs changed [6 (3) pairs less than in baseline], 7 (3) increased and 9 (5) decreased (**Figure 4**, left middle panel) after SOn in the delta band. The PCC continued to be a main driver of delta flow (however, displaying less significant connections), with increased connectivity strength to the MCC ($p < 0.025$), bilaterally to the IPL, to the RDLPFC ($p < 0.025$) and to the RH ($p < 0.05$). Connections from the MCC to all other ROIs did not change. Weak connections changed as follows: the RIPL showed increased connectivity with the LIPL ($p < 0.05$), and the LH with the MPFC ($p < 0.05$). Decreased connectivity was observed between the MPFC and the MCC ($p < 0.05$), the PCC ($p < 0.025$) and the RH ($p < 0.05$), between the RIPL and the MCC ($p < 0.05$), between the LDLPFC and the LH ($p < 0.025$) and RH ($p < 0.05$), between the RDLPFC and the LDLPFC ($p < 0.025$) and the LH ($p < 0.025$), and between the RH and the RDLPFC ($p < 0.025$).

Comparing baseline and recovery, significant changes in connectivity basically only occurred after SOn. The general picture revealed decreased effective connectivity in the delta band with increased sleep pressure (**Figure 4**, lower left panel). Twenty-three (16) pairs of ROIs showed decreased iCOH values during recovery compared to baseline. Thus, connectivity

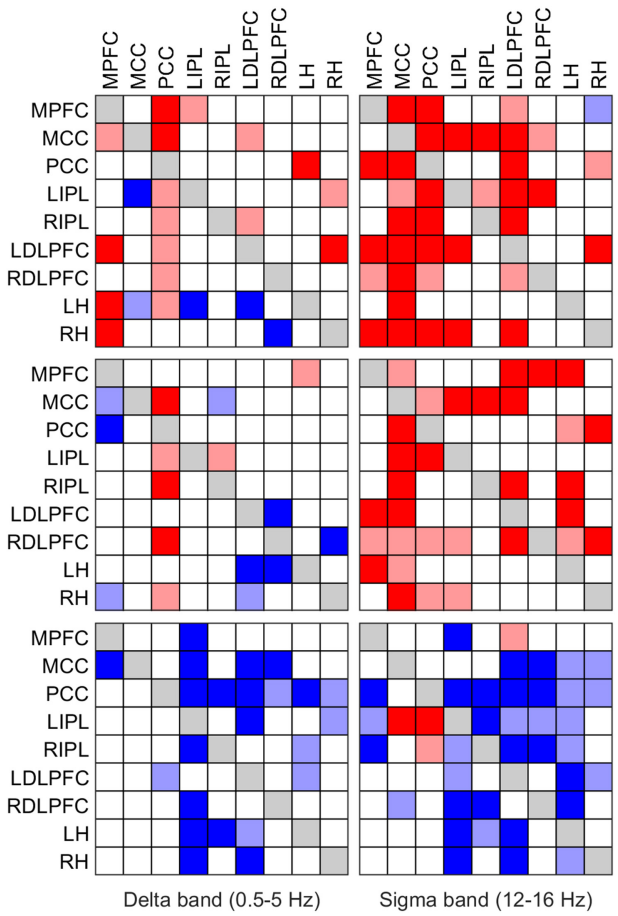

FIGURE 4 | Significant change of iCOH (connectivity) in the delta (left column) and sigma band (right column) at the SOn transition in baseline (top) and recovery (middle) and after SOn between baseline and recovery (bottom). Significant differences between conditions are plotted in matrix fashion; columns represent "senders", rows are "receivers" of information flow. For the abbreviations of the ROIs see **Table 1**. Red squares (light and dark) indicate connectivity before SOn < connectivity after SOn (top two rows) and connectivity at baseline < connectivity at recovery (bottom row); blue squares (light and dark) indicate the opposite change. Two significance thresholds were applied to reveal the hierarchy of changes: the lighter colors correspond to $p < 0.05$ (SnPM), the darker ones to $p < 0.025$ (SnPM).

strength was higher in baseline. The MCC and PCC as major drivers did not show any change in connection strength with increased sleep pressure except for a reduction in information flow from the PCC to the LDLPFC ($p < 0.05$). All other reductions concerned iCOH values of low effect size.

Sigma Band

Sigma activity (power in the sigma band) is closely related to sleep spindles (Dijk et al., 1993). Our results relate to changes in the sigma band. However, for some interpretations (due to the aforementioned relationship) we refer to sleep spindles although we did not identify spindles in the present context.

In baseline, 36 (27) significant changes in connectivity occurred, 35 (27) of them representing an increase in the information flow with SOn in the sigma band (12–16 Hz; **Figure 4**, upper right panel). The MCC occurred to be the main cortical driver of sigma flow in our selection of ROIs, with significantly increased projections to all other ROIs and overall displaying the highest significant increases with the SOn transition ($p < 0.025$). Similarly, the PCC also appeared as an important sigma driver (although less than the MCC), directing connections to all ROIs [$p < 0.025$, except to LIPL ($p < 0.05$)], except to the LH. All other connections showed weak (low effect size) to very weak changes. The MPFC increased transmission to the PCC ($p < 0.025$), bilaterally to the DLPFC and to the RH ($p < 0.025$); the LIPL to the MCC ($p < 0.025$), the LDLPFC ($p < 0.025$) and the RH ($p < 0.025$); the RIPL to the MCC ($p < 0.025$) and the LIPL ($p < 0.05$); the LDLPFC to its right counterpart ($p < 0.05$) and the MPFC ($p < 0.05$), and weakly to the MCC and PCC ($p < 0.025$), bilaterally to the IPL and the RH ($p < 0.025$); the RDLPFC to the MCC ($p < 0.05$) and LIPL ($p < 0.025$). Finally, the RH decreased sigma transmission to the MPFC ($p < 0.05$), but increased it to the PCC ($p < 0.05$) and LDLPFC ($p < 0.025$).

In recovery, 31 (20) connections showed increased information flow between pairs of ROIs [5 (7) less than in baseline] after SOn (**Figure 4**, middle right panel). Most of them overlapped with those of baseline; some disappeared, and a few weak ones occurred with higher sleep pressure. Again, with the MCC and PCC being the main cortical drivers of sigma flow.

Connectivity in baseline and recovery basically differed only after SOn. Generally, decreased effective connectivity with increased sleep pressure was observed between 35 (20) pairs of ROIs and increased connectivity between 4 (2) pairs (**Figure 4**, lower right panel). The MCC exerted a stronger impact on the LIPL ($p < 0.025$), and a reduced one on the RDLPFC ($p < 0.05$). The PCC showed heightened information flow to the LIPL ($p < 0.025$) and RIPL ($p < 0.05$). Most other changes concerned weak connectivity.

Further Frequency Bands

Changes in effective connectivity of the theta (5–8 Hz), alpha (8–12 Hz) and beta (16–24 Hz) band are illustrated in **Figure 5**. In the theta and alpha bands at baseline (top row), mostly increased effective connectivity was observed. In the alpha band, the PCC was a major driver of causal flow at the transition. Changes were less obvious in the beta band (fewer connectivity changes with SOn). In recovery (middle row), qualitatively similar changes as in baseline occurred in all bands, although with fewer changes than in baseline. Nonetheless, the PCC could still be identified as the most important ROI causally affecting other ROIs. Comparing baseline and recovery (bottom row), an overall reduction of iCOH occurred after SOn in all frequency bands (in the alpha band, there were several exceptions to this general tendency). If the stricter threshold ($p < 0.025$) was applied, about half of the connections were removed in baseline and recovery (**Figure 5**, upper and middle row). In the statistical contrast between baseline and recovery (bottom row), most changes remained with stricter threshold ($p < 0.025$), in particular in the theta and beta band.

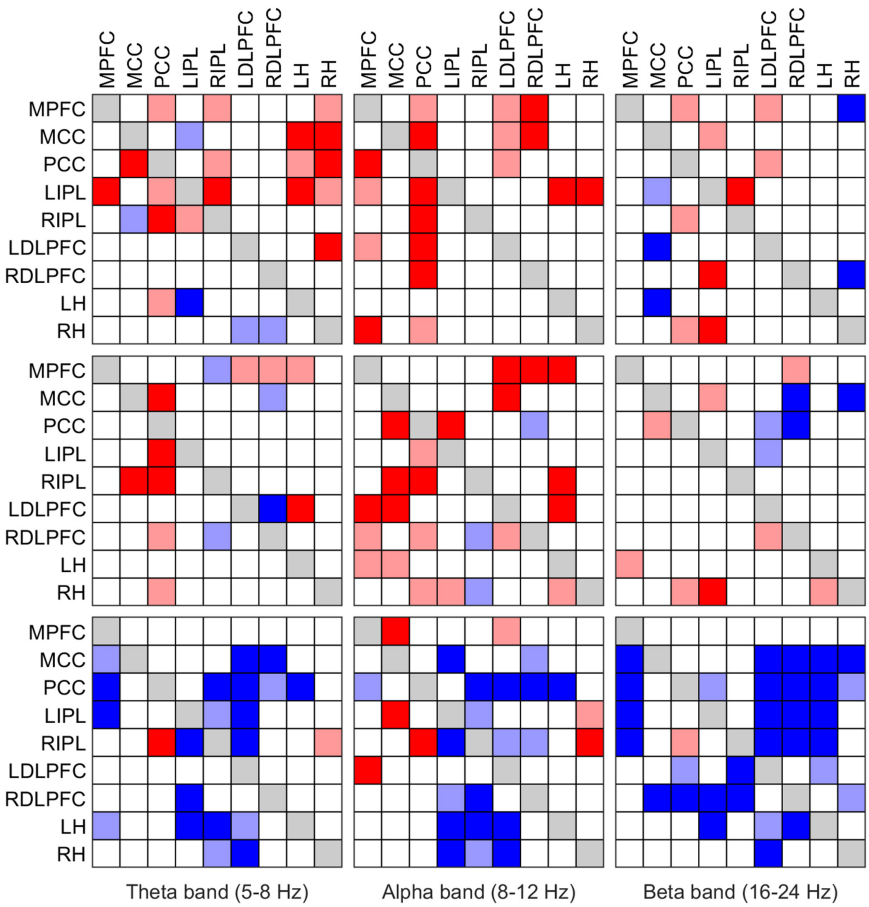

FIGURE 5 | Significant change of iCOH (connectivity) in the theta (left column), alpha (middle column) and beta band (right column) at the SOn transition in baseline (top) and recovery (middle) and after SOn between baseline and recovery (bottom). For details see **Figure 4**.

DISCUSSION

Overall, we found significant effective connectivity changes, as assessed by iCOH, during the SOn transition, which are congruent with the role of the PCC (a major hub of the DMN) in regulating consciousness (Amico et al., 2014; Herbet et al., 2014). In addition, we showed that, in the cortex, the MCC (and to a lower extent, the PCC) acted as a main relay stations of the thalamus for fast sigma (spindle) synchronization after SOn (Andrillon et al., 2011).

Relevant Spectral Features of iCOH

Baseline

Low frequency transmission arising from the MCC, and to a smaller extent from the PCC to the hippocampus and posterior parts of the DMN appear to be the major causal drivers characterizing the period prior to SOn in the baseline condition (**Figure 1**, red curves). After the SOn transition the PCC emerged as the most salient structure and principal driver of synchronization, sending theta flow to basically all investigated ROIs (**Figure 1**, blue curves and **Figure 4**, top row). The MCC still exerted a prominent role, transmitting causal flow at slightly higher frequencies (high delta/low theta) than before SOn. After SOn, spindle synchronization (sigma band; fast spindle range) occurred throughout all defined ROIs, driven by both the MCC and the PCC. However, this does not necessarily imply that spindles must be considered as a global cortical phenomenon, as local contributions from fronto-parietal areas might be the most important (Andrillon et al., 2011; Del Felice et al., 2014) and additionally may relate to underlying thalamocortical projections (Andrillon et al., 2011).

Recovery

Prior to SOn, a delta and theta flow from the MCC (acting as principal source of synchronization), directed to the remaining ROIs was observed (**Figure 2**, red curves). There was an additional beta flow component from the MCC and PCC, mainly projecting bilaterally to the IPL and hippocampus.

After SOn, firstly theta flow originating from the PCC as main driver, and a secondary delta flow arising from the MCC was present (**Figure 2**, blue curves). Secondly, sigma synchronization spread across all ROIs (sinks), originating from the MCC and PCC, hence, localizing cortical sources of fast spindles compatible with previous studies (Del Felice et al., 2014; Park et al., 2015).

Furthermore, sigma synchronization displayed higher clustering in the frontal lobe during recovery than in baseline, as shown by the enhanced dorsolateral prefrontal contribution (compare **Figure 2** with **Figure 1**; see also **Figure 4**). The DLPFC, a cortical structure well-known to produce enhanced delta activity during recovery sleep, also received low frequency input, thereby, possibly facilitating the generation of slow waves (De Gennaro et al., 2000; Marzano et al., 2013).

In general, the changes at SOn in recovery were qualitatively similar to the ones in baseline (main differences pertain to the iCOH levels, i.e., effect size), confirming the relevance of the MCC as predominant source of sigma synchronization, with a secondary contribution of the PCC.

Recovery Versus Baseline

Most evident was a reduction in connectivity after SOn in recovery compared to baseline (**Figure 3**, black dots). This effect was most noticeable in the beta range conveying the notion of significantly less beta flow in the sleep deprived brain (associated with cortical and body arousal), although not exclusively restricted to the high frequency range (Kuo et al., 2016; Sena et al., 2016). We can reasonably attribute the significant reduction of strength in cortical communication to the breakdown of effective connectivity accompanying SOn (Massimini et al., 2005; Esser et al., 2009). Nevertheless, there were also connections undergoing a local increase in recovery at certain frequencies. In general, the frequency bands with increased connectivity pertained either the upper alpha or low sigma range, potentially reflecting spindle synchronization.

Topographical Properties and Neurobiological Interpretation

In a previous analysis, we estimated the cortical sources underlying brain oscillatory activity at SOn using LORETA (Fernandez Guerrero and Achermann, 2018). The temporal evolution of CSD in different frequency bands was investigated. The most salient findings were observed in the low frequency (delta and theta bands) and in the spindle frequency range (sigma band). Delta activity followed an exponential increase with highest values observed in antero-central areas encompassing also bilaterally the DLPFC, the MPFC and the MCC. Therefore, these regions seem to play a pivotal role at the SO transition, both from an activity and connectivity perspective. Sleep deprivation accelerated the exponential increase and accentuated activity in the afore-mentioned ROIs and eventually in the entire cortex, while effective connectivity decreased after sleep deprivation. Sigma activity followed an inverted U-shape affecting mostly posterior areas, in particular the parietal cortex (the bilateral IPL was also among our ROIs). Sleep deprivation diminished sigma activity levels (including the parietal lobe) and the activity peak shifted to an earlier time (reflecting a fastening of the temporal dynamics) similar to the proposed accelerated temporal dynamics in the DMN connectivity disintegration. Theta and alpha activity increased with time and higher levels were observed with increased sleep pressure while again connectivity was diminished. This diverging response to sleep deprivation of source strength and connectivity in various frequency bands points to the independence of the two measures.

Changes in effective connectivity in the delta band paralleling the SOn transition indicated a greater cortical breakdown affecting fronto-parietal DMN nodes during the recovery condition (**Figure 4**, left column) (Massimini et al., 2005; Bonhomme et al., 2016). Indeed, integrity of the DMN, particularly the coupling between anterior and posterior parts, has been associated to the degree of conscious arousal or alertness (Horovitz et al., 2009; Chow et al., 2013; Franzen et al., 2013; Britton et al., 2014). For instance, functional connectivity in fMRI studies (based on linear temporal correlations analyses, using DMN nodes as seed regions) applied to the SOn transition have also indicated decoupling of anterior and posterior parts of the DMN with increased sleep depth (Sämann et al., 2011). Consequently, the gradual disruption of anterior to posterior parts of the DMN shown by iCOH might correlate at a subjective level with the progressive fading of consciousness during SOn (Heine et al., 2012; Speth and Speth, 2016).

Our effective connectivity analyses also indicated that this disruptive process occurs at an accelerated rate when the brain is exposed to increased sleep pressure, a behavior also observed with functional connectivity in fMRI (based on cross-correlations, a technique far less rigorous than ours) (Sämann et al., 2010). Thus, **Figure 4** would indicate that the reversible "impairment" of consciousness defining the sleep state is more profound during the recovery condition, as a result of reaching a higher network disconnection than in baseline (Boly et al., 2008; Barrett et al., 2012). Hence, the fronto-parietal disconnection (**Figure 4**, left middle panel) may be seen as a temporally accelerated connectivity change reaching a deeper loss of conscious awareness.

Effective connectivity analyses pointed to the PCC as the major hub affecting effective connectivity breakdown during SOn. The predominance of the PCC holds in terms of both the largest effect size and in the frequency of statistically significant differences observed as critical sending hub in the delta, alpha and sigma frequency bands (also for theta when the more lenient threshold is considered). Indeed, this structure has been shown in many studies to play a crucial, necessary, albeit possibly not sufficient, role in maintenance of a normal state of consciousness, or alternation between different states of consciousness (Vogt and Laureys, 2005; Amico et al., 2014; Herbet et al., 2014; Leech and Sharp, 2014). Moreover, the PCC plays a crucial role in the normal DMN functioning, and its relevance is highlighted by the fact that it has the highest metabolic rate of the brain and the highest degree of functional connectivity to other brain areas in resting-state analyses performed with fMRI studies (Vogt and Laureys, 2005; Sämann et al., 2011).

Finally, as another prominent feature the hippocampus received less delta flow from the prefrontal cortex in the recovery condition, and in turn, sent less flow itself (**Figure 4**). The hippocampus is a structure known to be involved in both short-term and long-term memory, and has also been implicated in working memory in conjunction with the prefrontal cortex (Lavenex and Amaral, 2000; Leszczynski, 2011). Furthermore, the hippocampus is documented to play a pivotal role in

transferring of declarative memories gathered during the day to the cortex for long-term storage, a process that happens principally during stage 2 and deep sleep (Born et al., 2006; Rasch and Born, 2013). We hypothesize that this prefrontal-hippocampal effective connectivity breakdown may constitute a neurobiological explanation for impaired declarative memory consolidation under conditions of sleep deprivation (Lavenex and Amaral, 2000; Gais and Born, 2004).

In general, the topology of the network indicating major statistical changes unfolding with the SOn transition in the sigma range (**Figure 4**, right column) exhibited a great similarity between the two conditions, although the number of statistically significant connections was a bit higher at baseline (36 significant connections, compared to 30 in the recovery condition). The lower number of significant connections in the recovery condition could indicate a reduced capacity to generate and propagate spindles throughout the cortical mantle when subjects are under higher sleep pressure (Olbrich et al., 2014). This may also relate to the inverse relationship between delta and sigma activity (delta activity increasing with sleep pressure), and as such leading to lower sigma activity (less spindles) in recovery sleep (Carrier et al., 2001; Finelli et al., 2001b). The topology was mainly governed by fronto-parietal connections, generally indicating a statistical increase in iCOH values, hence, in agreement with sigma synchronization at SOn (De Gennaro et al., 2000; Anderer et al., 2001).

As we defined the sigma band as 12–16 Hz, effective connectivity results relate to fast (rather than slow) spindles (Aeschbach and Borbély, 1993; Aeschbach et al., 1997; De Gennaro and Ferrara, 2003). Although spindles have a thalamic origin (LORETA cannot localize deep subcortical structures), as a relay, the major cortical hub acting as a driver for spindle synchronization (in this case, fast spindles) was the MCC, both in baseline and recovery conditions (Amico et al., 2014). Given that fast spindles show maximum power spectral density along the parietal lobe, the spatial location of MCC is optimal for being the driver of fast spindles (Anderer et al., 2001; Marzano et al., 2013). This structure is compatible with other studies of source localization using LORETA (Anderer et al., 2001; Andrillon et al., 2011; Del Felice et al., 2014).

For both delta and sigma activity, the general trend, with few exceptions, was a reduction of connectivity strength in the recovery condition. The spatial organization of the network indicating significant changes remains remarkably similar in the two conditions, suggesting that the recovery condition is not characterized by a new spatial configuration, different from baseline, but rather by a loss of connectivity strength within the same main fronto-parietal networks. On the other hand, the increases of connectivity with the transition may reflect an endogenous mechanism to reinforce the gradual disengagement from the external environment (e.g., by enhancing slow wave activity spreading, with a prominent role of the IPL) or, quite the opposite, counter-balancing mechanisms that are impeding the consolidation of the SOn process (as, e.g., in insomnia patients). If the reinforcement hypothesis is correct, healthy sleepers should exhibit increased connectivity to a greater extent (either in effect size, frequency of significance or both) than insomniacs. On the other hand, if increased connectivity is due to a counter-balancing mechanism hindering SOn, it should be more noticeable in insomniac than healthy subjects.

The anterior-posterior decoupling following the SOn transition has also been observed using yet another effective connectivity technique different from the iCOH, the Direct Transfer Function (DTF) (De Gennaro et al., 2004). In this regard, the DTF showed, for the period preceding SOn (emergence of first spindle or K complex), a prevalence of occipital to frontal information flow in the delta, theta and alpha bands. However, after SOn, the directionality pattern inverted, and the predominant direction of transmission was fronto-parietal to occipital at all frequency bands. Although this analysis was based on the scalp EEG and did not define brain networks, the observed behavior was compatible with a breakdown of the DMN. In addition, a later study confirmed and extended the previous finding based on the DTF (De Gennaro et al., 2005). In this study, the effects on connectivity resulting from total sleep deprivation were also assessed by means of the DTF. With increased sleep pressure, the anterior-to-posterior directionality of coupling could be already detected before the SOn transition, therefore, constituting a time advance shift compared to the baseline condition. This speed-up of the dynamics has also been observed investigating the temporal evolution of the cortical sources of oscillatory activity at the SOn transition (Fernandez Guerrero and Achermann, 2018). Regarding the above-mentioned mentioned DTF connectivity patterns preceding SOn, our results do not necessarily contradict these findings given that we used different time intervals and pursued a different approach to investigate connectivity (iCOH instead of the DTF). De Gennaro et al. (2005) defined the "pre-sleep onset period" as the interval of 5 min before the first occurrence of a spindle or K complex (first epoch of stage 2), compared to the "post-sleep onset period", of 5 min duration. Therefore, our analyses intervals differ considerably as we analyzed 2 min prior to and 10 min after SOn. We did not observe significant differences between baseline and recovery in the 2-min interval preceding SOn. Nonetheless, we cannot exclude that effects would have been detected with longer intervals. However, our participants fell asleep very fast prohibiting the analysis of a longer pre-sleep interval. Furthermore, variability in the 2-min intervals prior to SOn might have been too large, i.e., power of our study might have been insufficient given the relatively small number of participants (see section "Limitations").

Our connectivity analyses revealed to some degree interhemispheric asymmetries, e.g., between the LDLPFC and the RDLPFC or the LH and the RH in the delta and sigma range. Interhemispheric asymmetries during SOn have also been reported at the level of power spectral density (Ioannides et al., 2017). With our small sample size, we are not confident to make strong claims, but the asymmetries might be related to functional laterality (participants were right-handed).

Finally, a fRMI study and an EEG based one of functional connectivity and graph theory also concluded that the SOn transition is accompanied by a breakdown of cortico-cortical connectivity as sleep progresses into slow wave sleep (Spoormaker et al., 2010; Vecchio et al., 2017). The delta and theta

band revealed lower levels of small-world properties, indicative of reduced connectivity after SOn, while the opposite was observed for sigma activity reflecting emerging spindle synchronization (Vecchio et al., 2017). The breakdown in cortico-cortical connectivity between anterior and posterior nodes of the DMN serves as a neurophysiological explanation for disengagement from the external world, as it hinders the capacity of cortical areas to integrate information received from other brain areas. However, before entering into slow wave sleep, cortico-cortical connectivity was observed to be higher than in wakefulness, which fits with our data (in particular, synchronization of spindles). Additionally, sleep studies also using graph theory in order to measure small-world properties are consistent with the network reorganization we observed after SOn (Ferri et al., 2007, 2008).

Limitations

Some limitations of the current analysis are important to note. Twenty-seven EEG electrodes were used which is at the lower limit for source localization and a general head model was employed. We cannot neglect the blurring of the solutions that increases for deeper sources (Grech et al., 2008; Pascual-Marqui et al., 2014a). The blurring introduced by the LORETA method may affect not only the current density maps, but also connectivity results (Jatoi et al., 2014).

A new method has been proposed recently called "innovations orthogonalization" in order to tackle some arising pitfalls in the application of iCOH, due to leakage or mixing of signals produced by both volume conduction and the low spatial resolution of techniques such as LORETA (Pascual-Marqui et al., 2017). Through this type of correction, spectral responses are more accurate; however, we reckon that the subtle correction performed by the innovations orthogonalization method does not conflict with our results, as it mostly pertains a subtle spectral resolution of effective connectivity.

Also, our selection of ROIs has an impact on the results and their interpretation. As we, e.g., did not differentiate between hemispheres for MPFC, MCC and PCC or between dorsal or ventral MPFC and dorsal or ventral hippocampus, interpretations may be limited. However, we were cautious with the selection of ROIs (see section "Materials and Methods") and think that the global picture was captured with our selection.

Spindles in the hippocampus were observed in intracranial recordings of epileptic patients (Sarasso et al., 2014). Given that the precision of LORETA is expected to decrease with increasing depth, we do not know whether spindles occurred in the hippocampus. Nonetheless, spectral changes in the sigma range of iCOH passed the statistical tests, so we may assume that they relate to hippocampal activity.

Further, a homogenous sample of eight healthy good sleepers was included in the analyses which is a relatively small sample. However, changes congruent to published findings were observed but we cannot rule out that statistical power was insufficient.

Finally, we cannot exclude that some of the connectivity patterns observed after SOn resemble NREM sleep in general. However, the comparison pre-sleep to post-sleep is specific for the SOn process.

CONCLUSION

iCOH proved to be a valuable tool to reveal the effective connectivity patterns at the transition into sleep revealing the spectral characteristics of the information transmission. A posterior to anterior decoupling of the DMN in the low frequency range was observed, reflecting the progressive disengagement from the external environment at the transition to sleep. The PCC played a major role in the unfolding of the SOn transition, guiding the other nodes, particularly, in the delta-theta range. Furthermore, the MCC appeared as a principal cortical relay station of the thalamus in sigma synchronization (related to spindles) throughout the cortex. Lower overall cortical connectivity was present after sustained wakefulness, thus, the SOn transition exhibited a smaller connectivity reduction than in baseline but still leading to a disconnection of the major nodes of the DMN.

ETHICS STATEMENT

The local ethical committee for research on human subjects approved the study protocol.

AUTHOR CONTRIBUTIONS

AFG and PA designed the analyses and wrote the paper. AFG conducted the analyses.

FUNDING

The study was supported by the Swiss National Science Foundation (Grant 32003B_146643).

ACKNOWLEDGMENTS

We thank Dr. Thomas Rusterholz for the help in creating the figures.

REFERENCES

Achermann, P., and Borbély, A. A. (1998). Temporal evolution of coherence and power in the human sleep electroencephalogram. *J. Sleep Res.* 7(Suppl. 1), 36–41. doi: 10.1046/j.1365-2869.7.s1.6.x

Aeschbach, D., and Borbély, A. A. (1993). All-night dynamics of the human sleep EEG. *J. Sleep Res.* 2, 70–81. doi: 10.1111/j.1365-2869.1993.tb00065.x

Aeschbach, D., Dijk, D. J., and Borbély, A. A. (1997). Dynamics of EEG spindle frequency activity during extended sleep in humans: relationship to slow-wave

activity and time of day. *Brain Res.* 748, 131–136. doi: 10.1016/S0006-8993(96)01275-9

Akaike, H. (1968). On use of a linear model for identification of feedback systems. *Ann. Inst. Stat. Math.* 20, 425–439. doi: 10.1007/BF02911655

Amico, E., Gomez, F., Di Perri, C., Vanhaudenhuyse, A., Lesenfants, D., Boveroux, P., et al. (2014). Posterior cingulate cortex-related co-activation patterns: a resting state fMRI study in propofol-induced loss of consciousness. *PLoS One* 9:e100012. doi: 10.1371/journal.pone.0100012

Anderer, P., Klosch, G., Gruber, G., Trenker, E., Pascual-Marqui, R. D., Zeitlhofer, J., et al. (2001). Low-resolution brain electromagnetic tomography revealed simultaneously active frontal and parietal sleep spindle sources in the human cortex. *Neuroscience* 103, 581–592. doi: 10.1016/S0306-4522(01)00028-8

Andrews-Hanna, J. R., Reidler, J. S., Sepulcre, J., Poulin, R., and Buckner, R. L. (2010). Functional-anatomic fractionation of the brain's default network. *Neuron* 65, 550–562. doi: 10.1016/j.neuron.2010.02.005

Andrillon, T., Nir, Y., Staba, R. J., Ferrarelli, F., Cirelli, C., Tononi, G., et al. (2011). Sleep spindles in humans: insights from intracranial EEG and unit recordings. *J. Neurosci.* 31, 17821–17834. doi: 10.1523/JNEUROSCI.2604-11.2011

Baccala, L., and Sameshima, K. (2001). Partial directed coherence: a new concept in neural structure determination. *Biol. Cybern.* 84, 463–474. doi: 10.1007/PL00007990

Bakhshayesh, H., Fitzgibbon, S. P., and Pope, K. J. (2014). "Detection of coupling with linear and nonlinear synchronization measures for EEG," in *Proceedings of the 2nd Middle East Conference on Biomedical Engineering (MECBME)*, Doha, 240–243. doi: 10.1109/MECBME.2014.6783249

Barnett, L., Barrett, A. B., and Seth, A. K. (2009). Granger causality and transfer entropy are equivalent for Gaussian variables. *Phys. Rev. Lett.* 103:238701. doi: 10.1103/PhysRevLett.103.238701

Barrett, A., Murphy, M., Bruno, M., Noirhomme, Q., Boly, M., Laureys, S., et al. (2012). Granger causality analysis of steady-state electroencephalographic signals during propofol-induced anaesthesia. *PLoS One* 7:e29072. doi: 10.1371/journal.pone.0029072

Boly, M., Phillips, C., Tshibanda, L., Vanhaudenhuyse, A., Schabus, M., Dang-Vu, T. T., et al. (2008). Intrinsic brain activity in altered states of consciousness - How conscious is the default mode of brain function? *Ann. N. Y. Acad. Sci.* 1129, 119–129. doi: 10.1196/annals.1417.015

Bonhomme, V., Vanhaudenhuyse, A., Demertzi, A., Bruno, M. A., Jaquet, O., Bahri, M. A., et al. (2016). Resting-state network-specific breakdown of functional connectivity during ketamine alteration of consciousness in volunteers. *Anesthesiology* 125, 873–888. doi: 10.1097/ALN.0000000000001275

Born, J., Rasch, B., and Gais, S. (2006). Sleep to remember. *Neuroscientist* 12, 410–424. doi: 10.1177/1073858406292647

Britton, W. B., Lindahl, J. R., Cahn, B. R., Davis, J. H., and Goldman, R. E. (2014). Awakening is not a metaphor: the effects of Buddhist meditation practices on basic wakefulness. *Ann. N. Y. Acad. Sci.* 1307, 64–81. doi: 10.1111/nyas.12279

Buckner, R. L., Andrews-Hanna, J. R., and Schacter, D. L. (2008). The brain's default network - anatomy, function, and relevance to disease. *Ann. N. Y. Acad. Sci.* 2008, 1–38. doi: 10.1196/annals.1440.011

Carrier, J., Land, S., Buysse, D., Kupfer, D., and Monk, T. (2001). The effects of age and gender on sleep EEG power spectral density in the middle years of life (ages 20-60 years old). *Psychophysiology* 38, 232–242. doi: 10.1111/1469-8986.3820232

Chow, H. M., Horovitz, S. G., Carr, W. S., Picchioni, D., Coddington, N., Fukunaga, M., et al. (2013). Rhythmic alternating patterns of brain activity distinguish rapid eye movement sleep from other states of consciousness. *Proc. Natl. Acad. Sci. U.S.A.* 110, 10300–10305. doi: 10.1073/pnas.1217691110

De Gennaro, L., and Ferrara, M. (2003). Sleep spindles: an overview. *Sleep Med. Rev.* 7, 423–440. doi: 10.1053/smrv.2002.0252

De Gennaro, L., Ferrara, M., and Bertini, M. (2000). Effect of slow-wave sleep deprivation on topographical distribution of spindles. *Behav. Brain Res.* 116, 55–59. doi: 10.1016/S0166-4328(00)00247-3

De Gennaro, L., Vecchio, F., Ferrara, M., Curcio, G., Rossini, P. M., and Babiloni, C. (2004). Changes in fronto-posterior functional coupling at sleep onset in humans. *J. Sleep Res.* 13, 209–217. doi: 10.1111/j.1365-2869.2004.00406.x

De Gennaro, L., Vecchio, F., Ferrara, M., Curcio, G., Rossini, P. M., and Babiloni, C. (2005). Antero-posterior functional coupling at sleep onset: changes as a function of increased sleep pressure. *Brain Res. Bull.* 65, 133–140. doi: 10.1016/j.brainresbull.2004.12.004

Del Felice, A., Arcaro, C., Storti, S. F., Fiaschi, A., and Manganotti, P. (2014). Electrical source imaging of sleep spindles. *Clin. EEG Neurosci.* 45, 184–192. doi: 10.1177/1550059413497716

Dijk, D. J., Hayes, B., and Czeisler, C. A. (1993). Dynamics of electroencephalographic sleep spindles and slow wave activity in men: effect of sleep deprivation. *Brain Res.* 626, 190–199. doi: 10.1016/0006-8993(93)90579-C

Douw, L., Nieboer, D., van Dijk, B. W., Stam, C. J., and Twisk, J. W. R. (2014). A healthy brain in a healthy body: brain network correlates of physical and mental fitness. *PLoS One* 9:e88202. doi: 10.1371/journal.pone.0088202

Esser, S. K., Hill, S., and Tononi, G. (2009). Breakdown of effective connectivity during slow wave sleep: investigating the mechanism underlying a cortical gate using large-scale modeling. *J. Neurophysiol.* 102, 2096–2111. doi: 10.1152/jn.00059.2009

Ewald, A., Avarvand, F. S., and Nolte, G. (2013). Identifying causal networks of neuronal sources from EEG/MEG data with the phase slope index: a simulation study. *Biomed. Eng. Biomed. Tech.* 58, 165–178. doi: 10.1515/bmt-2012-0028

Faes, L., Erla, S., and Nollo, G. (2012). Measuring connectivity in linear multivariate processes: definitions, interpretation, and practical analysis. *Comput. Math. Methods Med.* 2012:140513. doi: 10.1155/2012/140513

Faes, L., Erla, S., Tranquillini, E., Orrico, D., and Nollo, G. (2010). An identifiable model to assess frequency-domain Granger causality in the presence of significant instantaneous interactions. *Conf. Proc. IEEE Eng. Med. Biol. Soc.* 2010, 1699–1702. doi: 10.1109/IEMBS.2010.5626839

Fernandez Guerrero, A., and Achermann, P. (2018). Brain dynamics during the sleep onset transition: an EEG source localization study. *Neurobiol. Sleep Circadian Rhythms* (in press).

Ferri, R., Rundo, F., Bruni, O., Terzano, M. G., and Stam, C. J. (2007). Small-world network organization of functional connectivity of EEG slow-wave activity during sleep. *Clin. Neurophysiol.* 118, 449–456. doi: 10.1016/j.clinph.2006.10.021

Ferri, R., Rundo, F., Bruni, O., Terzano, M. G., and Stam, C. J. (2008). The functional connectivity of different EEG bands moves towards small-world network organization during sleep. *Clin. Neurophysiol.* 119, 2026–2036. doi: 10.1016/j.clinph.2008.04.294

Finelli, L. A., Achermann, P., and Borbély, A. A. (2001a). Individual "fingerprints" in human sleep EEG topography. *Neuropsychopharmacology* 25, S57–S62.

Finelli, L. A., Borbély, A. A., and Achermann, P. (2001b). Functional topography of the human nonREM sleep electroencephalogram. *Eur. J. Neurosci.* 13, 2282–2290. doi: 10.1046/j.0953-816x.2001.01597.x

Finelli, L. A., Baumann, H., Borbély, A. A., and Achermann, P. (2000). Dual electroencephalogram markers of human sleep homeostasis: correlation between theta activity in waking and slow-wave activity in sleep. *Neuroscience* 101, 523–529. doi: 10.1016/S0306-4522(00)00409-7

Franzen, J. D., Heinrichs-Graham, E., White, M. L., Wetzel, M. W., Knott, N. L., and Wilson, T. W. (2013). Atypical coupling between posterior regions of the default mode network in attention-deficit/hyperactivity disorder: a pharmaco-magnetoencephalography study. *J. Psychiatry Neurosci.* 38, 333–340. doi: 10.1503/jpn.120054

Friston, K. J. (2011). Functional and effective connectivity: a review. *Brain Connect.* 1, 13–36. doi: 10.1089/brain.2011.0008

Friston, K. J., Bastos, A. M., Oswal, A., van Wijk, B., Richter, C., and Litvak, V. (2014). Granger causality revisited. *Neuroimage* 101, 796–808. doi: 10.1016/j.neuroimage.2014.06.062

Fuentealba, P., and Steriade, M. (2005). The reticular nucleus revisited: intrinsic and network properties of a thalamic pacemaker. *Prog. Neurobiol.* 75, 125–141. doi: 10.1016/j.pneurobio.2005.01.002

Gais, S., and Born, J. (2004). Declarative memory consolidation: mechanisms acting during human sleep. *Learn. Memory* 11, 679–685. doi: 10.1101/lm.80504

Geweke, J. (1982). Measurement of linear-dependence and feedback between multiple time-series. *J. Am. Stat. Assoc.* 77, 304–313. doi: 10.1080/01621459.1982.10477803

Granger, C. (1969). Investigating causal relations by econometric models and cross-spectral methods. *Econometrica* 37, 424–438. doi: 10.2307/1912791

Grech, R., Cassar, T., Muscat, J., Camilleri, K. P., Fabri, S. G., Zervakis, M., et al. (2008). Review on solving the inverse problem in EEG source analysis. *J. Neuroeng. Rehabil.* 5:25. doi: 10.1186/1743-0003-5-25

He, Y., and Evans, A. (2010). Graph theoretical modeling of brain connectivity. *Curr. Opin. Neurol.* 23, 341–350. doi: 10.1097/WCO.0b013e32833aa567

Heine, L., Soddu, A., Gomez, F., Vanhaudenhuyse, A., Tshibanda, L., Thonnard, M., et al. (2012). Resting state networks and consciousness alterations of multiple resting state network connectivity in physiological, pharmacological, and pathological consciousness states. *Front. Psychol.* 3:295. doi: 10.3389/fpsyg.2012.00295

Herbet, G., Lafargue, G., de Champfleur, N. M., Moritz-Gasser, S., le Bars, E., Bonnetblanc, F., et al. (2014). Disrupting posterior cingulate connectivity disconnects consciousness from the external environment. *Neuropsychologia* 56, 239–244. doi: 10.1016/j.neuropsychologia.2014.01.020

Horovitz, S. G., Braun, A. R., Carr, W. S., Picchioni, D., Balkin, T. J., Fukunaga, M., et al. (2009). Decoupling of the brain's default mode network during deep sleep. *Proc. Natl. Acad. Sci. U.S.A.* 106, 11376–11381. doi: 10.1073/pnas.0901435106

Ioannides, A. A., Liu, L. C., Poghosyan, V., and Kostopoulos, G. K. (2017). Using MEG to understand the progression of light sleep and the emergence and functional roles of spindles and K-complexes. *Front. Hum. Neurosci.* 11:313. doi: 10.3389/fnhum.2017.00313

Jatoi, M. A., Kamel, N., Malik, A. S., and Faye, I. (2014). EEG based brain source localization comparison of sLORETA and eLORETA. *Australas. Phys. Eng. Sci. Med.* 37, 713–721. doi: 10.1007/s13246-014-0308-3

Khadem, A., and Hossein-Zadeh, G. A. (2014). Estimation of direct nonlinear effective connectivity using information theory and multilayer perceptron. *J. Neurosci. Methods* 229, 53–67. doi: 10.1016/j.jneumeth.2014.04.008

Kralemann, B., Pikovsky, A., and Rosenblum, M. (2014). Reconstructing effective phase connectivity of oscillator networks from observations. *New J. Phys.* 16:085013. doi: 10.1088/1367-2630/16/8/085013

Kuo, T. B. J., Chen, C. Y., Hsu, Y. C., and Yang, C. C. H. (2016). EEG beta power and heart rate variability describe the association between cortical and autonomic arousals across sleep. *Auton. Neurosci.* 194, 32–37. doi: 10.1016/j.autneu.2015.12.001

Larson-Prior, L. J., Power, J. D., Vincent, J. L., Nolan, T. S., Coalson, R. S., Zempel, J., et al. (2011). Modulation of the brain's functional network architecture in the transition from wake to sleep. *Prog. Brain Res.* 193, 277–294. doi: 10.1016/B978-0-444-53839-0.00018-1

Lavenex, P., and Amaral, D. G. (2000). Hippocampal-neocortical interaction: a hierarchy of associativity. *Hippocampus* 10, 420–430. doi: 10.1002/1098-1063(2000)10:4<420::AID-HIPO8>3.0.CO;2-5

Leech, R., and Sharp, D. J. (2014). The role of the posterior cingulate cortex in cognition and disease. *Brain* 137, 12–32. doi: 10.1093/brain/awt162

Leszczynski, M. (2011). How does hippocampus contribute to working memory processing? *Front. Hum. Neurosci.* 5:168. doi: 10.3389/fnhum.2011.00168

Liu, Y., and Aviyente, S. (2012). Quantification of effective connectivity in the brain using a measure of directed information. *Comput. Math. Methods Med.* 2012:635103. doi: 10.1155/2012/635103

Magnin, M., Rey, M., Bastuji, H., Guillemant, P., Mauguiere, F., and Garcia-Larrea, L. (2010). Thalamic deactivation at sleep onset precedes that of the cerebral cortex in humans. *Proc. Natl. Acad. Sci. U.S.A.* 107, 3829–3833. doi: 10.1073/pnas.0909710107

Marzano, C., Moroni, F., Gorgoni, M., Nobili, L., Ferrara, M., and De Gennaro, L. (2013). How we fall asleep: regional and temporal differences in electroencephalographic synchronization at sleep onset. *Sleep Med.* 14, 1112–1122. doi: 10.1016/j.sleep.2013.05.021

Massimini, M., Ferrarelli, F., Huber, R., Esser, S. K., Singh, H., and Tononi, G. (2005). Breakdown of cortical effective connectivity during sleep. *Science* 309, 2228–2232. doi: 10.1126/science.1117256

Nichols, T. E., and Holmes, A. P. (2002). Nonparametric permutation tests for functional neuroimaging: a primer with examples. *Hum. Brain Mapp.* 15, 1–25. doi: 10.1002/hbm.1058

Nir, Y., Staba, R. J., Andrillon, T., Vyazovskiy, V. V., Cirelli, C., Fried, I., et al. (2011). Regional slow waves and spindles in human sleep. *Neuron* 70, 153–169. doi: 10.1016/j.neuron.2011.02.043

Ogilvie, R. D. (2001). The process of falling asleep. *Sleep Med. Rev.* 5, 247–270. doi: 10.1053/smrv.2001.0145

Olbrich, E., Landolt, H. P., and Achermann, P. (2014). Effect of prolonged wakefulness on electroencephalographic oscillatory activity during sleep. *J. Sleep Res.* 23, 253–260. doi: 10.1111/jsr.12123

Park, D. H., Ha, J. H., Ryu, S. H., Yu, J., and Shin, C. J. (2015). Three-dimensional electroencephalographic changes on low-resolution brain electromagnetic tomography (LORETA) during the sleep onset period. *Clin. EEG Neurosci.* 46, 340–346. doi: 10.1177/1550059414536713

Park, H. J., and Friston, K. J. (2013). Structural and functional brain networks: from connections to cognition. *Science* 342:1238411. doi: 10.1126/science.1238411

Pascual-Marqui, R. D., Biscay, R. J., Bosch-Bayard, J., Lehmann, D., Kochi, K., Kinoshita, T., et al. (2014a). Assessing direct paths of intracortical causal information flow of oscillatory activity with the isolated effective coherence (iCoh). *Front. Hum. Neurosci.* 8:448. doi: 10.3389/fnhum.2014.00448

Pascual-Marqui, R. D., Rolando, J. B., Bosch-Bayard, J., Lehmann, D., Kochi, K., Yoshimura, M., et al. (2014b). Advances in EEG methods applied to intra-cortical connectivity inference and to functional imaging: examples in psychiatry research. *Int. J. Psychophysiol.* 94, 121–121. doi: 10.1016/j.ijpsycho.2014.08.589

Pascual-Marqui, R. D., Biscay, R. J. L., Bosch, J., Faber, P. L., Kinoshita, T., Kochi, K., et al. (2017). *Innovations Orthogonalization: A Solution to the Major Pitfalls of EEG/MEG "Leakage Correction"*. Ithaca, NY: Cornell University Library.

Pascual-Marqui, R. D., Lehmann, D., Koukkou, M., Kochi, K., Anderer, P., Saletu, B., et al. (2011). Assessing interactions in the brain with exact low-resolution electromagnetic tomography. *Philos. Trans. R. Soc. A* 369, 3768–3784. doi: 10.1098/rsta.2011.0081

Prerau, M. J., Hartnack, K. E., Obregon-Henao, G., Sampson, A., Merlino, M., Gannon, K., et al. (2014). Tracking the sleep onset process: an empirical model of behavioral and physiological dynamics. *PLoS Comput. Biol.* 10:e1003866. doi: 10.1371/journal.pcbi.1003866

Rasch, B., and Born, J. (2013). About sleep's role in memory. *Physiol. Rev.* 93, 681–766. doi: 10.1152/physrev.00032.2012

Rechtschaffen, A., and Kales, A. (1968). *A Manual of Standardized Terminology, Techniques and Scoring System of Sleep Stages in Human Subjects*. Los Angeles, CA: Brain Information Service/Brain Research Institute.

Salone, A., Di Giacinto, A., Lai, C., De Berardis, D., Iasevoli, F., Fornaro, M., et al. (2016). The interface between neuroscience and neuro-psychoanalysis: focus on brain connectivity. *Front. Hum. Neurosci.* 10:20. doi: 10.3389/fnhum.2016.00020

Sämann, P. G., Tully, C., Spoormaker, V. I., Wetter, T. C., Holsboer, F., Wehrle, R., et al. (2010). Increased sleep pressure reduces resting state functional connectivity. *Magn. Reson. Mater. Phys. Biol. Med.* 23, 375–389. doi: 10.1007/s10334-010-0213-z

Sämann, P. G., Wehrle, R., Hoehn, D., Spoormaker, V. I., Peters, H., Tully, C., et al. (2011). Development of the brain's default mode network from wakefulness to slow wave sleep. *Cereb. Cortex* 21, 2082–2093. doi: 10.1093/cercor/bhq295

Sarasso, S., Proserpio, P., Pigorini, A., Moroni, F., Ferrara, M., De Gennaro, L., et al. (2014). Hippocampal sleep spindles preceding neocortical sleep onset in humans. *Neuroimage* 86, 425–432. doi: 10.1016/j.neuroimage.2013.10.031

Sena, P., d'Amore, M., Brandimonte, M. A., Squitieri, R., and Fiorentino, A. (2016). "Experimental framework for simulators to study driver cognitive distraction: brake reaction time in different levels of arousal," in *Proceedings of 6th Transport Research Arena Tra*, Warsaw.

Siclari, F., Bernardi, G., Riedner, B. A., LaRocque, J. J., Benca, R. M., and Tononi, G. (2014). Two distinct synchronization processes in the transition to sleep: a high-density electroencephalographic study. *Sleep* 37, 1621–1637. doi: 10.5665/sleep.4070

Silfverhuth, M., Hintsala, H., Kortelainen, J., and Seppanen, T. (2012). Experimental comparison of connectivity measures with simulated EEG signals. *Med. Biol. Eng. Comput.* 50, 683–688. doi: 10.1007/s11517-012-0911-y

Speth, C., and Speth, J. (2016). The borderlands of waking: quantifying the transition from reflective thought to hallucination in sleep onset. *Conscious. Cogn.* 41, 57–63. doi: 10.1016/j.concog.2016.01.009

Spoormaker, V. I., Schroter, M. S., Gleiser, P. M., Andrade, K. C., Dresler, M., Wehrle, R., et al. (2010). Development of a large-scale functional brain network during human non-rapid eye movement sleep. *J. Neurosci.* 30, 11379–11387. doi: 10.1523/JNEUROSCI.2015-10.2010

Sporns, O., and Betzel, R. F. (2016). Modular brain networks. *Ann. Rev. Psychol.* 67, 613–640. doi: 10.1146/annurev-psych-122414-033634

Sporns, O., Honey, C. J., and Kotter, R. (2007). Identification and classification of hubs in brain networks. *PLoS One* 2:e1049. doi: 10.1371/journal.pone.0001049

Stam, C. J., van Straaten, E. C. W., Van Dellen, E., Tewarie, P., Gong, G., Hillebrand, A., et al. (2016). The relation between structural and functional connectivity patterns in complex brain networks. *Int. J. Psychophysiol.* 103, 149–160. doi: 10.1016/j.ijpsycho.2015.02.011

Tononi, G., Boly, M., Massimini, M., and Koch, C. (2016). Integrated information theory: from consciousness to its physical substrate. *Nat. Rev. Neurosci.* 17, 450–461. doi: 10.1038/nrn.2016.44

Uehara, T., Yamasaki, T., Okamoto, T., Koike, T., Kan, S., Miyauchi, S., et al. (2014). Efficiency of a "small-world" brain network depends on consciousness level: a resting-state fMRI study. *Cereb. Cortex* 24, 1529–1539. doi: 10.1093/cercor/bht004

Valdes-Sosa, P. A., Roebroeck, A., Daunizeau, J., and Friston, K. J. (2011). Effective connectivity: influence, causality and biophysical modeling. *Neuroimage* 58, 339–361. doi: 10.1016/j.neuroimage.2011.03.058

Vecchio, F., Miraglia, F., Gorgoni, M., Ferrara, M., Iberite, F., Bramanti, P., et al. (2017). Cortical connectivity modulation during sleep onset: a study via graph theory on EEG data. *Hum. Brain Mapp.* 38, 5456–5464. doi: 10.1002/hbm.23736

Vogt, B. A., and Laureys, S. (2005). Posterior cingulate, precuneal and retrosplenial cortices: cytology and components of the neural network correlates of consciousness. *Prog. Brain Res.* 150, 205–217. doi: 10.1016/S0079-6123(05)50015-3

Conflict of Interest Statement: The authors declare that the research was conducted in the absence of any commercial or financial relationships that could be construed as a potential conflict of interest.

Copyright © 2018 Fernandez Guerrero and Achermann. This is an open-access article distributed under the terms of the Creative Commons Attribution License (CC BY). The use, distribution or reproduction in other forums is permitted, provided the original author(s) and the copyright owner(s) are credited and that the original publication in this journal is cited, in accordance with accepted academic practice. No use, distribution or reproduction is permitted which does not comply with these terms.

frontiers in Neuroscience

ORIGINAL RESEARCH
published: 06 February 2019
doi: 10.3389/fnins.2019.00046

Brain Activation Time-Locked to Sleep Spindles Associated With Human Cognitive Abilities

*Zhuo Fang[1,2], Laura B. Ray[1,3], Adrian M. Owen[1,4] and Stuart M. Fogel[1,2,3,4,5]**

[1] Brain and Mind Institute, Western University, London, ON, Canada, [2] School of Psychology, University of Ottawa, Ottawa, ON, Canada, [3] Sleep Unit, The Royal's Institute of Mental Health Research, University of Ottawa, Ottawa, ON, Canada, [4] Department of Psychology, Western University, London, ON, Canada, [5] University of Ottawa Brain and Mind Research Institute, Ottawa, ON, Canada

Simultaneous electroencephalography and functional magnetic resonance imaging (EEG–fMRI) studies have revealed brain activations time-locked to spindles. Yet, the functional significance of these spindle-related brain activations is not understood. EEG studies have shown that inter-individual differences in the electrophysiological characteristics of spindles (e.g., density, amplitude, duration) are highly correlated with "Reasoning" abilities (i.e., "fluid intelligence"; problem solving skills, the ability to employ logic, identify complex patterns), but not short-term memory (STM) or verbal abilities. Spindle-dependent reactivation of brain areas recruited during new learning suggests night-to-night variations reflect offline memory processing. However, the functional significance of stable, trait-like inter-individual differences in brain activations recruited during spindle events is unknown. Using EEG–fMRI sleep recordings, we found that a subset of brain activations time-locked to spindles were specifically related to Reasoning abilities but were unrelated to STM or verbal abilities. Thus, suggesting that individuals with higher fluid intelligence have greater activation of brain regions recruited during spontaneous spindle events. This may serve as a first step to further understand the function of sleep spindles and the brain activity which supports the capacity for Reasoning.

Keywords: sleep, spindles, cognitive abilities, simultaneous EEG–fMRI, NREM

OPEN ACCESS

Edited by:
Michele Bellesi,
University of Bristol, United Kingdom

Reviewed by:
Fabio Ferrarelli,
University of Pittsburgh School of Medicine, United States
Sofia Isabel Ribeiro Pereira,
Cardiff University, United Kingdom

***Correspondence:**
Stuart M. Fogel
sfogel@uottawa.ca

Specialty section:
This article was submitted to Sleep and Circadian Rhythms, a section of the journal Frontiers in Neuroscience

Received: *22 October 2018*
Accepted: *17 January 2019*
Published: *06 February 2019*

Citation:
Fang Z, Ray LB, Owen AM and Fogel SM (2019) Brain Activation Time-Locked to Sleep Spindles Associated With Human Cognitive Abilities. Front. Neurosci. 13:46. doi: 10.3389/fnins.2019.00046

INTRODUCTION

Sleep spindles are one of the defining features of non-rapid eye movement (NREM) sleep. Spindles are traditionally defined as bursts of waxing and waning neural oscillations between 11 and 16 Hz (Iber et al., 2007), which stand out from the ongoing, background electroencephalographic (EEG) activity (Rechtschaffen and Kales, 1968). The brain regions activated during spontaneous spindle events have been identified (Laufs et al., 2007; Schabus et al., 2007; Tyvaert et al., 2008; Andrade et al., 2011; Caporro et al., 2012). However, the functional significance of these brain activations has yet to be elucidated, thereby limiting our understanding of the function of sleep spindles. Spindles are remarkably stable from night-to-night, but vary considerably from one individual to another, and because of the trait-like nature of spindles (Silverstein and Levy, 1976), they have even been suggested to be an "electrophysiological fingerprint" (De Gennaro et al., 2005).

Recent work by our group and others (Nader and Smith, 2001, 2003; Bódizs et al., 2005, 2008; Schabus et al., 2006; Fogel et al., 2007; Ujma et al., 2014, 2015; Fang et al., 2017) suggests that spindles are electrophysiological markers of specific cognitive abilities, and in particular, Reasoning abilities (i.e., "fluid intelligence"; problem solving skills, the ability to employ logic, identify complex patterns). However, the neural basis of this relationship is not known; there is no direct evidence investigating the relationship between trait-like cognitive abilities and interindividual differences in spindle-dependent brain activations. Thus, as a first step, we sought to explore what brain activations time-locked to spontaneous spindle events are correlated with various domains of human intellectual abilities. This might shed light on the functional significance of brain activations time-locked to sleep spindles, and the neural functional correlates which explain individual differences in trait-like cognitive strengths and weaknesses.

In an effort to identify the functional brain areas recruited during spontaneous spindle events, a handful of studies have employed simultaneous electroencephalography and functional magnetic resonance imaging (EEG–fMRI) to explore brain activations time-locked to spindles (Laufs et al., 2007; Schabus et al., 2007; Tyvaert et al., 2008; Andrade et al., 2011; Caporro et al., 2012). Spindle-related activations have been consistently found in the thalamus and the temporal lobe, for both fast spindles and slow spindles (Laufs et al., 2007; Schabus et al., 2007; Tyvaert et al., 2008; Andrade et al., 2011; Caporro et al., 2012), as well as activation of the cingulate cortex and motor areas (Andrade et al., 2011; Caporro et al., 2012). Interestingly, activation of the putamen has also been found to be associated with spindle events (Tyvaert et al., 2008; Caporro et al., 2012) and Andrade et al. (2011) found a strong interaction between spindle occurrence and hippocampal formation functional connectivity, suggesting that spindles may be related to memory and cognitive functioning. However, they did not report any relationship between these activations and cognitive abilities. In addition, by directly comparing fast spindles vs. slow spindles, Schabus et al. (2007) observed increased activations associated with slow spindles in the superior temporal gyrus while fast spindles recruited activation in sensorimotor areas, mesial frontal cortex, hippocampus, and cerebellum; important memory centers of the brain. However, in the absence of any direct relationship between spindle-dependent activation and cognitive performance, the functional significance of these spindle-related activations could only be speculated based alone on the brain regions recruited. Taken together, the extant literature, not-surprisingly, suggests that brain activations associated with the action of sleep spindles involve well-known spindle-generating regions (e.g., thalamic and cortical regions), as well as, more intriguingly, regions which subserve executive functioning [prefrontal cortex (PFC)], declarative memory (hippocampus), motor skills (motor cortex and cerebellum), and procedural memory (the striatum). However, these studies are limited in that they can only tell us what brain regions are recruited during spindle events. The functional significance of these activations with respect to the trait-like nature of spindles remains to be elucidated.

Notably, the sleep spindle is the only known spontaneous neural oscillation that has been identified as an electrophysiological marker of cognitive abilities and aptitudes, that are typically assessed by intelligence quotient (IQ) tests (for review, see Fogel and Smith, 2011). The association between sleep spindles and individual differences in cognitive abilities has been well documented. More specifically, previous studies have revealed that interindividual differences in spindle characteristics are related to the capacity for Reasoning (i.e., the ability to identify complex patterns and relationships, the use of logic, existing knowledge, skills, and experience to solve novel problems (Nader and Smith, 2001, 2003; Bódizs et al., 2005, 2008; Schabus et al., 2006; Fogel et al., 2007; Ujma et al., 2014, 2015; Fang et al., 2017). For example, Nader and Smith (2001, 2003) found that both the number of sleep spindles and sigma power (12–14 Hz) was correlated with Performance IQ scores. Further studies revealed this relationship to be specific to these Reasoning-related abilities, over-and-above (i.e., controlling for) Verbal IQ (Fogel et al., 2007; Fang et al., 2017). Consistently, several studies (Bódizs et al., 2005; Schabus et al., 2006) found that fast spindles were positively correlated with similar metrics of Reasoning abilities (i.e., "fluid intelligence"), measured by the Raven's Progressive Matrices (Raven et al., 1976). Similar studies identified a positive correlation between right-parietal fast spindles and visuospatial abilities assessed by the Rey–Osterrieth complex figure test (Bódizs et al., 2008). They identified a positive correlation between spindles and intellectual abilities measured by the Cattell Culture Fair Intelligence test, specifically in woman but not in men (Ujma et al., 2014). Although a relationship in men was subsequently identified by the same group in daytime sleep (Ujma et al., 2015). Taken together, these studies support the notion that sleep spindles are an electrophysiological marker of cognitive abilities, and specifically, the ability to solve problems using logic and Reasoning. These studies have provided insight into the electrophysiological correlates of Reasoning abilities, insofar as to indirectly suggest that efficient functioning of the neural substrates that support spindle generation and those that are recruited during spontaneous spindle events may be related to the capacity for these cognitive skills. Two recent studies employing simultaneous EEG–fMRI have investigated the association between sleep spindle-related brain activation and memory consolidation, including declarative (Bergmann et al., 2012) and procedural memory (Fogel et al., 2017a). However, both of these studies were interested in investigating memory trace reactivation following new learning (i.e., acute effects of learning on subsequent sleep), and did not investigate the stable, trait-like interindividual differences in cognitive abilities and how they relate to inter-individual differences in spindle-dependent brain activation. Thus, the functional significance of spontaneous spindle-related brain activations, and whether these activations related to specific domains of cognitive abilities [e.g., Reasoning, Verbal, Short-Term Memory (STM)] in healthy individuals remains to be investigated, which is the principle aim of the current study.

Therefore, here, using simultaneous EEG–fMRI recordings during sleep, we sought to identify, for the first time, the neuroanatomical function correlates of the well-established

relationship between sleep spindles and specific cognitive abilities. We hypothesized that the neural activation patterns, time-locked to spindles would be related to distinct cognitive abilities whereby, consistent with previous cognitive and EEG studies, spindle-related brain activations would be correlated to a greater extent with Reasoning, but not STM or Verbal abilities, and include brain regions known to be involved in spindle generation, and also known to support Reasoning abilities (e.g., thalamus, PFC, striatum, cerebellum). This will provide insight into the functional significance of sleep spindles.

MATERIALS AND METHODS

Participants

To be included in the study, all participants were non-shift workers and medication-free; had no history of head injury or seizures; had a normal body mass index (<25); and did not consume excessive caffeine, nicotine, or alcohol. Interested participants had to score <10 on the Beck Depression (Beck et al., 1974) (BDI) and the Beck Anxiety (Beck et al., 1988) (BAI) inventories and have no history or signs of sleep disorders, indicated by the Sleep Disorders Questionnaire (Douglass et al., 1994). Extreme morning and evening types were excluded based on the Morningness–Eveningness Questionnaire (Horne and Ostberg, 1976). A total of 35 healthy right-handed adults (20 female) between 20 and 35 years old (M = 23.69, SD = 3.57) who met these initial screening criteria were recruited to participate in this study. In addition, participants were given a letter of information, provided informed written consent before participation, and were financially compensated for their participation. All study procedures and methods adhered to the Declaration of Helsinki and were approved by the Western University Health Science research ethics board.

To ensure the absolute minimum amount of data required for EEG and fMRI analyses, and to ensure a minimum sleep duration, quality, and continuity of sleep, participants were required to sleep for a period of at least 5 min of uninterrupted NREM sleep during the sleep session in the MRI scanner to be included in the analyses. Among the 35 participants recruited in the study, only 5 participants did not meet the 5-min consolidated NREM sleep criteria for the sleep session, and one participant did not complete the Cambridge Brain Sciences (CBS) online test. Therefore, 29 participants (M = 23.97, SD = 3.83, 17 female) were included in the final data analyses, that slept on average for 44 min. The detailed sleep architecture and sleep spindle parameters are reported in the section "Results" and **Table 1**.

The necessary sample size was determined *a priori* based on previous studies, and power calculated, where possible using G*Power for Mac version 3.1 (Faul et al., 2007, 2009). Based on the most comparable simultaneous EEG–fMRI studies (Laufs et al., 2007; Schabus et al., 2007; Tyvaert et al., 2008; Andrade et al., 2011; Caporro et al., 2012), previous studies have employed sample sizes $N < 15$. A recent study by our group using the same cognitive tests as the current study (Fang et al., 2017) found robust associations between spindles and cognitive abilities in a sample size of N = 24, replicating previous findings in smaller samples (e.g., $N < 12$; Fogel and Smith, 2006; Fogel et al., 2007). Based on power calculation for correlation with p (two-tailed) = 0.05 (b = 0.20, effect size = 0.56) (Fang et al., 2017), an N = 22 was required. Thus, N = 29 subjects included in this study was considered to provide adequate statistical power for the main effects of interest.

TABLE 1 | Sleep architecture and sleep spindle parameters for spindles during NREM sleep from EEG–fMRI recording sessions.

	M	*SD*
	Sleep architecture	
Wake (min) (N = 26)	26.87	20.25
NREM1 (min) (N = 26)	5.84	4.38
NREM2 (min) (N = 29)	23.87	14.50
SWS (min) (N = 20)	14.77	17.17
NREM (min)	39.29	19.33
REM (N = 8)	17.80	10.76
Total sleep	44.20	23.84
Sleep latency	8.16	10.11
	Total bandwidth (11–16 Hz) spindles at Cz	
Number	334.74	212.29
Duration (s)	0.49	0.05
Amplitude (μV)	27.21	6.43
Density	8.22	2.34

NREM, non-rapid eye movement sleep; NREM1, stage 1 sleep; NREM2, stage 2 sleep; SWS, slow wave sleep; REM, rapid eye movement sleep.

Cognitive Ability Test

The CBS platform is a web-based test battery[1], which has previously been used in large-scale (Hampshire et al., 2012; Wild et al., 2018) and smaller-scale studies (Brewer-Deluce et al., 2017; Fang et al., 2017; Fogel et al., 2018; Phan et al., 2018). The CBS trials include 12 cognitive tests that measure a broad range of cognitive abilities including reasoning, problem solving, planning, attention, and memory. The CBS trials are advantageous as the 12 tasks are adapted from well-known, well-established paradigms from the cognitive neuroscience literature, that assess a wide range of aspects of cognition. As opposed to conventional tests which are based solely on the face-validity of the constructs of interest, CBS subscales are derived quantitatively from a data-driven approach using factor analysis, conducted on a large population from a previous study (Hampshire et al., 2012). In addition, the CBS test is non-verbal in nature and computerized. Therefore, it has the advantage of ease of administration, and is also not dependent on verbal comprehension. In addition, automated scoring and consistent test administration minimizes error. More importantly, and particularly for the aims of the current study, sleep spindles have been found to be correlated with Reasoning ability scores derived from the CBS test battery, using the same testing approach used here (Fang et al., 2017). In addition, the neural correlates of each factor have been investigated previously using neuroimaging (Hampshire et al., 2012). Therefore, we chose the CBS platform to investigate the neural correlates between sleep spindles and cognitive abilities.

[1]https://www.cambridgebrainsciences.com/science/tasks

All 12 subtests are based on classic paradigms from cognitive psychology. For example, the Reasoning factor is best described in terms of performance on five tests adapted from the cognitive literature, including deductive reasoning (Cattell, 1940), spatial rotation (Silverman et al., 2000), feature match (Treisman and Gelade, 1980), spatial planning (Shallice, 1982), and polygons (Folstein et al., 1975). STM is best described in terms of four tests, including visuospatial working memory (Inoue and Matsuzawa, 2007), spatial span (Corsi, 1972), paired associates (Gould et al., 2006), and self-ordered search (Collins et al., 1998). Finally, verbal ability is best captured by performance on three tests, including verbal reasoning (Baddeley, 1968), color-word remapping (Stroop, 1935), and digit span (Wechsler, 1981). More detailed information of the 12 subtests can be found in the **Supplementary Material**.

During the orientation session, participants were informed about the study requirements and procedures, and given detailed instructions of the online CBS tests. All participants were required to register and complete the CBS tests online at home after the orientation session. Participants were required to use a computer mouse to perform the task. Completion of the 12 tests takes between 30 and 60 min in total. The order of the tasks was randomized across participants. Prior to each test, specific instructions on how to perform the respective test were displayed onscreen.

CBS Scores Calculation

Consistent with the previous literature (Hampshire et al., 2012), the raw scores from each of the 12 subtests were normalized using the mean and standard deviation obtained from a large, young population (N = 44,600; age 20–35 years) of subjects who completed the CBS Trials (Hampshire et al., 2012) (Equation 1). Each subtest was then weighted according to the factor loadings from Hampshire et al. (2012) (Equation 2). Finally, the respective sub-tests were averaged to create the Reasoning, STM, and Verbal sub-scales and transformed to standard scores (Equation 3), so that test scores were readily comparable to results from similar studies that employed test batteries tapping into Reasoning and Verbal abilities, such as the Multidimensional Aptitude Battery – II (Fogel and Smith, 2006; Fogel et al., 2007) and other commonly used batteries of cognitive abilities (e.g., Wechsler Adult Intelligence Scale (Wechsler, 1981). The descriptive statistics of each subtest are shown in **Table 2**.

$$Z\text{-score} = (X_{\text{raw}} - M_{\text{norm}})/SD_{\text{norm}} \quad (1)$$

$$\text{Weighted Score} = Z\text{-score} * \text{factor loadings} \quad (2)$$

$$\text{Standard score} = 100 + \text{Weighted Score} * 15 \quad (3)$$

where X_{raw}, raw score of each test item in the current study; M_{norm}, mean score of each test item from the literature; SD_{norm}, standard deviation of each test item from the literature; factor loading, weight of each test item from the literature.

Experimental Procedure

An overview of the study procedure is shown in **Figure 1**. Participants underwent an initial screening prior to the study by completing the Sleep Disorder Questionnaires (Douglass et al., 1994), BDI (Beck et al., 1974), BAI (Beck et al., 1988) scales, Horne–Ostberg Morningness–Eveningness Questionnaire (Horne and Ostberg, 1976), and the MRI safety screening questionnaire to screen for signs of sleep disorders, unusual sleep habits, depression, or anxiety and MRI compatibility. Participants who met all these criteria were included in the study and visited the sleep lab for an orientation session at least 1 week prior to the EEG–fMRI sleep recording night. During the orientation session, participants were informed about the study requirements and procedures, and given detailed instructions of the online CBS tests. All participants were required to complete the CBS tests online at home after the orientation session, during which participants were not allowed to consume caffeinated, alcoholic, or nicotine products. Participants were required to keep a regular sleep-wake cycle (bed-time between 2200 and 2400 h, wake-time between 0700 and 0900 h), to abstain from taking daytime naps at least 7 days prior to and throughout participation in the study. Compliance with this schedule was assessed using both sleep diaries and wrist actigraphy (Actiwatch 2, Philips Respironics, Andover, MA, United States) worn on the non-dominant wrist for 1 week prior to the EEG–fMRI sleep recording night. Participants who met these requirements were scheduled for the EEG–fMRI sleep recording session. The experimental sleep session started between 21h00 and 24h00, during which time simultaneous EEG–fMRI was recorded while participants slept in the scanner. Specifically, the scan procedure normally started at 21h00, at which point, the EEG equipment was installed and tested. This was followed by localizer scans, a T1 MPRAGE structural scan, and an awake resting scan. These procedures took more than 30 min to complete. The sleep recording ("lights out") normally started after 22h00, within the range of the subject's habitual bedtime. The average sleep latency was 8.16 ± 10.11 min (**Table 1**) and the average sleep onset time, when participants fell asleep in the scanner was 22h22 (±25 min). Following the EEG–fMRI sleep session, participants were allowed to sleep in the nearby sleep laboratory for the remainder of the night.

TABLE 2 | Descriptive statistics of the three CBS subscales (Reasoning, STM, and Verbal abilities).

IQ measures	Range	Mean ± SD	Median
Reasoning	78.84–108.17	95.65 ± 7.20	96.46
STM	84.38–115.33	101.60 ± 6.77	102.30
Verbal	88.51–110.92	99.62 ± 5.12	99.52

Polysomnographic Recording and Analysis

Recording Parameters

Simultaneous polysomnography was comprised of 64-channel MR-compatible EEG cap which included one electrocardiogram (ECG) lead (Braincap MR, Easycap, Herrsching, Germany) and two MR-compatible 32-channel amplifiers (Brainamp MR plus, Brain Products GmbH, Gilching, Germany). EEG recordings were taken referenced to FCz. Skin resistance was reduced below 5 KOhm using high-chloride abrasive electrode paste

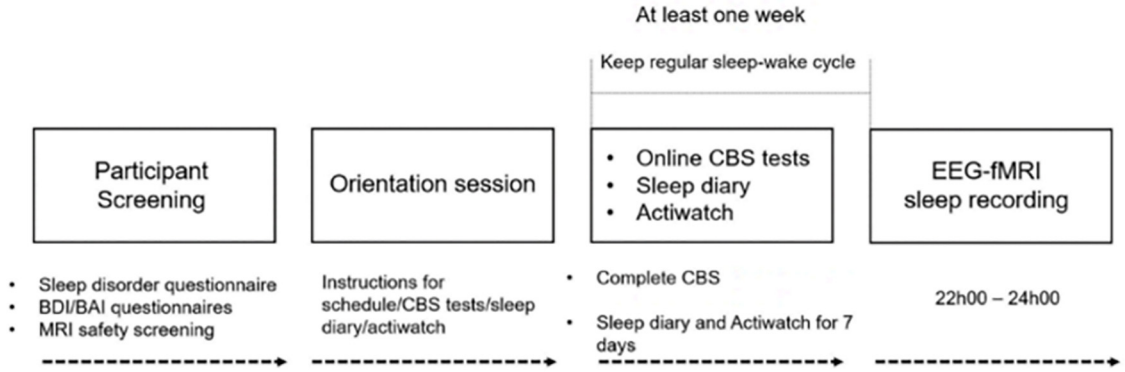

FIGURE 1 | Experimental procedure of the study. Participants underwent initial screening to exclude any signs of sleep disorders, unusual sleep habits, or other health-related ineligibility and MRI compatibility. Eligible participants visited the sleep lab for the orientation session at least a week prior to the EEG–fMRI sleep recording night, in which participants were given detailed instructions about the study procedure, CBS tests, sleep diary, and actiwatch. All participants completed the CBS tests online and kept a regular sleep-wake cycle for at least 1 week prior to the sleep recording. Compliance with this schedule was assessed using both sleep diaries and wrist actigraphy. Participants who met these requirements were scheduled for the EEG–fMRI sleep recording session. MRI scanning started at 21h00, and lights out was from 22h00 to as late as 24h00.

(Abralyt 2000 HiCL; Easycap, Herrsching, Germany). The single drop-down ECG electrode from the EEG cap can have less than optimal visualization of the R-peak of the QRS complex. For this reason, we used additional bipolar electrodes for three ECG derivations to obtain high-quality recordings in order to accurately identify *R*-peaks, using an MR-compatible 16-channel bipolar amplifier (Brainamp ExG MR, Brain Products GmbH, Gilching, Germany). This was done in order to increase the chances of acquiring at least one ECG channel with high quality *R*-peaks, necessary for effective ballistocardiographic (BCG) correction. In addition, as recommended by Mullinger et al. (2011), we repositioned subjects in the MRI scanner so that the subjects were shifted away from iso-center of the magnetic field by 40 mm. At this position, the MRI images are not impacted, but the BCG artifact has been reported to be reduced by up to 40%, thereby improving EEG quality after BCG correction. EEG data were transferred via fiber optic cables to a personal laptop where Brain Products Recorder Software, Version 1.x (Brain Products, Gilching, Germany) was synchronized to the scanner clock. Data were digitized with a resolution of 500-nv/bit at 5 kHZ and were analog filtered by a band-limiter low pass filter at 500 Hz and a high pass filter with a 10-s time constant corresponding to a high pass frequency of 0.0159 Hz.

EEG Data Processing

Electroencephalographic data were first corrected for gradient-induced and cardioballistic artifacts in two separate steps: In the first step, MRI gradient artifacts were removed using an adaptive average template subtraction method (Allen et al., 2000) implemented in Brain Products Analyzer, and down-sampled to 250 Hz. Sleep-fMRI parameters were chosen to ensure that the lowest residual gradient artifacts (18.52 Hz) would not compromise the sleep spindle frequency (11–16 Hz). Due to safety and data quality concerns, the Helium pump was not allowed to be switched off during the EEG–fMRI acquisition. However, through the pilot tests, we confirmed that the frequency of the pump noise is >80 Hz, which is outside EEG frequencies of interest in our study (e.g., 11–16 Hz for spindles), and would not impact slower frequencies needed for accurate visual sleep scoring. In the second step, the *R*-peaks in the ECG were semi-automatically detected, visually verified, manually adjusted when necessary, to correct both false positives and false negative *R*-peak detections. Then, adaptive template subtraction (Allen et al., 1998) was used to remove BCG artifacts time-locked to the *R*-peak of the QRS complex of the cardiac rhythm. After these two steps, we visually verified the quality of the data and inspected the amplitude of the residual artifacts time-locked to the *R*-peaks (**Supplementary Figure S1**). An independent component analyses (ICAs)-based approach (Srivastava et al., 2005; Mantini et al., 2007) was applied to remove any remaining BCG residual artifact if the peak of the maximum amplitude of the residual artifact exceeded 3 μV during the QRS complex (e.g., 0–600 ms). Finally, a low-pass filter (60 Hz) was applied to the EEG data, which were then re-referenced to averaged mastoids. A sample of the EEG traces after correction is shown in **Supplementary Figure S2**.

Following the artifact correction, sleep stages were scored in accordance with standard criteria (Iber et al., 2007) using the "VisEd Marks" toolbox[2] for eeglab (Delorme and Makeig, 2004). Automatic spindle detection was carried out using a previously published and validated (Ray et al., 2015) method (*n.b.*, against both multiple expert scorers and using crowd-sourcing from a large sample of non-experts) employing EEGlab-compatible (Delorme and Makeig, 2004) software[3] written for MATLAB R2014a (The MathWorks Inc., Natick, MA, United States). The detailed processing steps and procedures and validation are reported elsewhere (Ray et al., 2015) and are thus presented only briefly here. The spindle data were extracted from movement artifact-free, NREM sleep epochs. The detection method

[2]https://github.com/jadesjardins/vised_marks

[3]github.com/stuartfogel/detect_spindles

(Ray et al., 2015) used a complex demodulation transformation of the EEG signal with a bandwidth of 5 Hz centered about a carrier frequency of 13.5 Hz (i.e., 11–16 Hz) (Iber et al., 2007). Spindle detection was visually verified by an expert following automated detection. The variables of interest extracted from this method include spindle amplitude, duration, and density (number of spindles per minute of NREM sleep) for each participant and at each derivation (Fz, Cz, and Pz). However, given the limited amount of sleep in the current study, there was an insufficient number of spindle events to further subdivide spindles into slow (e.g., 11–13.5 Hz at Fz) and fast (e.g., 13.6–16 Hz at Pz) spindle types without excluding subjects due to missing data or insufficient number of spindle onsets. Thus, only results from full bandwidth spindles at Cz in NREM sleep were reported and included in the final analyses.

Relationship Between Sleep Spindle EEG Characteristics and Cognitive Abilities

Linear regression analyses were used to examine the effects of sleep spindles on cognitive abilities (Reasoning, STM, and Verbal) assessed by the CBS test battery. Sleep spindle duration, amplitude, and density were entered into each model as dependent variables separately; Reasoning, STM, and Verbal subscale factors were entered into the models as independent variables. Inspection of the resulting partial correlation coefficients was conducted to identify which subscale (e.g., Reasoning, Verbal, or STM) accounted for the greatest proportion of unique interindividual variability for each spindle characteristic. The regression models included gender and whole brain volume as covariates of non-interest. These were included given that the relationship between spindles and Reasoning ability was reportedly different in men and women (Ujma et al., 2014), and brain volume might influence NREM slow wave oscillations (Saletin et al., 2013), sleep quality (Branger et al., 2016), or be related to cognitive abilities (Casey et al., 2005).

MRI Imaging Acquisition and Analysis

Recording Parameters

Functional magnetic resonance imaging was performed at a 3.0T Magnetom Prisma MR imaging system (Siemens, Erlangen, Germany) using a 64-channel head coil. High-resolution anatomic images were acquired using a standard 3D Multislice MPRAGE sequence (TR = 2300 ms, TE = 2.98 ms, TI = 900 ms, FA = 9°, 176 slices, FoV = 256 × 256 mm^2, matrix size = 256 × 256 × 176, voxel size = 1 × 1 × 1 mm^3). During the sleep session, T2*-weighted fMRI images were acquired with a gradient echo-planar imaging (EPI) sequence using axial slice orientation (TR = 2160 ms, TE = 30 ms, FA = 90°, 40 transverse slices, 3 mm slice thickness, 10% inter-slice gap, FoV = 220 × 220 mm^2, matrix size = 64 × 64 × 40, voxel size = 3.44 × 3.44 × 3 mm^3). Sleep-fMRI parameters were chosen to ensure that the lowest residual gradient artifacts (18.52 Hz) would not compromise the sleep spindle frequency (11–16 Hz). This was achieved by setting the MR scan repetition time to 2160 ms, such that it matched a common multiple of the EEG sample time (0.2 ms), the product of the scanner clock precision (0.1 μs), and the number of slices (40 slices) used (Mulert and Lemieux, 2009). Among all participants, up to 2 h of sleep EEG–fMRI data was acquired. An expert, registered polysomnographic technologist scored the EEG data acquired during the simultaneous EEG–fMRI sleep recordings according to standard criteria (Iber et al., 2007).

Image Preprocessing

Functional images were preprocessed and analyzed using SPM8[4] (Welcome Department of Imaging Neuroscience, London, United Kingdom) implemented in MATLAB (ver. 8.5 R2015a) for Windows (Microsoft, Inc. Redmond, WA, United States). For each subject, functional images were corrected for slice acquisition time differences and realigned to correct head motion using rigid body transformation. A mean realigned image was then created from the resulting images. The structural T1-image was coregistered to this mean volume of functional images. Using DARTEL in SPM8, the coregistered structural images were segmented into gray matter, white matter, and cerebrospinal fluid, and an average subject-based template was created. All functional and anatomical images were then spatially normalized using the resulting template, which was generated from the structural scans. Finally, spatial smoothing was applied on all functional images (Gaussian kernel, 8 mm full-width at half-maximum (FWHM).

First-Level Individual GLM

The onset time and duration of each spindle were identified from the EEG data. Given that the EEG and fMRI recordings were recorded simultaneously and precisely synchronized, the brain activations time-locked to each spindle could be estimated using the onset of each spindle (converted to TR) and duration of each spindle in a fixed effects GLM using an even-related fMRI design. The BOLD time series data were modeled using a canonical hemodynamic response function (HRF). In total, 27 nuisance variables were entered in the model to be removed, including the Friston-24 movement parameters (Friston et al., 1996), the mean white matter intensity, and the mean cerebral spinal fluid intensity for each participant. In addition, the spectral power (μV^2) in the delta band (0.5–4 Hz) for each TR window (2160 ms) was also entered as a nuisance variable, given that slow wave activity is a defining characteristic of NREM sleep (Iber et al., 2007), and is related to spindle generation (Siapas and Wilson, 1998; Mölle et al., 2011). High-pass filtering was implemented in the design using a cut-off at 128 s to remove low frequency drifts from the time series. These analyses generated spindle-related contrast maps of the *t*-statistic [SPM(*t*)] for all spindle events.

Second-Level Group GLM

The SPM(*t*) maps generated from the first-level GLM were entered into second-level GLMs for group-level analyses. One

[4]http://www.fil.ion.ucl.ac.uk/spm/software/spm8/

sample *t*-tests were conducted for the brain activations time-locked to spindles. In addition, to investigate the relationship between the magnitude of the spindle-dependent activations and the cognitive abilities assessed by the CBS subscales, whole-brain spatial multiple regression analyses were conducted at the group level using the SPM8 toolbox. Spindle-related contrast maps of the *t*-statistic [SPM(*t*)] from first-level GLM were selected, and cognitive test scores for each subtest (e.g., Reasoning, Verbal, and STM) were entered as covariates of interest in the described GLMs, separately. Gender and whole brain volume were included in the models as variables of non-interest. Multiple regression analyses were conducted at the whole-brain level voxel by voxel [i.e., no region of interest (ROI) mask was applied] to explore which brain regions recruited during spindle events were correlated to each CBS subtest. Statistical inferences were performed at a threshold of $p < 0.001$ (uncorrected) at the whole-brail level and $p < 0.05$, family wise error (FWE) corrected at the cluster level.

Statistical Comparisons of Brain–Behavior Correlations Among Three Cambridge Brain Sciences (CBS) Subtests

Reasoning ability was highly inter-correlated with Verbal ability ($r = 0.596$; $p = 0.001$), and marginally correlated with STM ability ($r = 0.357$; $p = 0.058$). To further test whether the relationship between Reasoning ability and the spindle-related activations could be accounted for by Verbal or STM abilities, we directly compared the correlations between spindle-related activations and three CBS subtests (Reasoning, Verbal, and STM). Due to high multicollinearity, we could not include all subtests scores into one design matrix model in SPM. Therefore, we employed a ROI approach for this comparison. We selected three main regions for further analyses, including the thalamus, the anterior cingulate cortex/middle cingulate cortex (ACC/MCC), and the bilateral putamen, because in the current study, we found the brain activation in these three regions were time-locked to spindle events and also correlated with Reasoning abilities. In addition, these three regions have been consistently reported to be recruited during spindle events in the extant literature (Schabus et al., 2007; Tyvaert et al., 2008). In order to employ an independent ROI analysis to avoid circularity (Kriegeskorte et al., 2009), the three ROIs were defined based on the coordinates reported in the previous literature which also used EEG–fMRI approach to investigate the spindle-related brain activation, using the MarsBaR toolbox[5]. The thalamus ROI was derived from Tyvaert et al. (2008) (L: −14, −10, 6; R: 19, −10, 5, radiums: 6 mm); the ACC/MCC was derived from Schabus et al. (2007) (ACC, L: −6, 34, 14; R: 6, 38, 12; MCC, −2, 26, 24, radiums: 6 mm); the bilateral putamen was derived from Tyvaert et al. (2008) (L: −29, −3, 7; R: 28, −7, 13, radiums: 6 mm). Using the MarsBaR toolbox, we calculated parametric estimate activation values in response to spindle events in the three independent ROIs and conducted standard multiple linear regressions. Brain activation parametric estimate values in the thalamus, the ACC/MCC, and the bilateral putamen were included in the models as dependent variables and Reasoning, Verbal, and STM scores were entered as independent variables. Gender and whole brain volume were included as covariates of non-interest.

[5]http://marsbar.sourceforge.net/

Overlap Between Spindle-Related Maps and Reasoning-Spindle Correlation Maps

To illustrate the overlap of activations between the spindle-related activation maps and Reasoning-spindle correlation maps, the conjunction was taken as the minimum *t*-statistic using the conjunction null hypothesis (Friston et al., 2005; Nichols et al., 2005) over:

(1) a *t*-map testing for the main effect of the spindle events during the sleep session and
(2) a *t*-map testing for the main effect of the correlation between the Reasoning ability and spindle events.

These two statistical maps were thresholded at $p < 0.001$ (uncorrected) at the whole-brain level and $p < 0.05$, FWE corrected at the cluster level.

RESULTS

Sleep Architecture

An overview of the study procedure is shown in **Figure 1**. Of the $N = 35$ participants recruited in the study, only 5 participants did not meet the 5-min consolidated NREM sleep criteria for the sleep session, and one participant did not complete the CBS online test. Therefore, $N = 29$ participants were included in the final analyses. As shown in **Table 1**, among these 29 participants, $N = 26$ participants experienced NREM1 sleep, all $N = 29$ participants experienced NREM2 sleep, $N = 20$ had SWS sleep, and $N = 8$ had rapid eye movement (REM) sleep. The ($N = 29$) participants had at least 14.67 min of sleep, and on average, a total of 44.20 ($SD = 23.84$) min of sleep (including REM) during the sleep recording session in the MRI scanner. The average sleep latency of these 29 participants was 8.16 ± 10.11 min and the average sleep onset time when participants fell asleep in the scanner was 22h22 (±25 min). Given the focus of the current investigation on NREM spindles, we analyzed only the NREM data of the 29 subjects. The average duration of NREM sleep was 39.29 ($SD = 19.33$) min and participants had on average 334.74 ($SD = 212.29$, min = 63, max = 1035) sleep spindles during NREM sleep.

Relationship Between Sleep Spindle Characteristics and Cognitive Abilities

Standard multiple linear regression analyses revealed that, taken together, Reasoning, STM, and Verbal abilities assessed by the CBS trials (**Table 2**) significantly accounted for variability in spindle amplitude [$F(5,23) = 3.424$, $R^2 = 0.427$, $p = 0.019$], but not duration [$F(5,23) = 0.366$, $R^2 = 0.074$, $p = 0.867$), or density [$F(5,23) = 1.489$, $R^2 = 0.245$, $p = 0.232$] during NREM sleep (**Table 3**). Similar to previous studies (Fogel et al., 2007; Fang et al., 2017), follow-up inspection of the

TABLE 3 | Multiple regression analyses of the relationship between CBS trials and spindles (**Figure 2**).

	Overall regression effect		
Sleep spindle parameter	**Unadjusted R^2**	**$F(5,23)$**	***p***
Amplitude	0.427	3.424	**0.019***
Duration	0.074	0.366	0.867
Density	0.245	1.489	0.232
	Follow-up analyses for amplitude		
CBS measures	**Semipartial *r***	***t*(23)**	***p***
Reasoning	0.435	2.314	**0.030***
Verbal	0.133	0.642	0.527
STM	0.082	0.394	0.697

Statistically significant results indicated by an asterisk (*) at $p < 0.05$; STM, short-term memory.

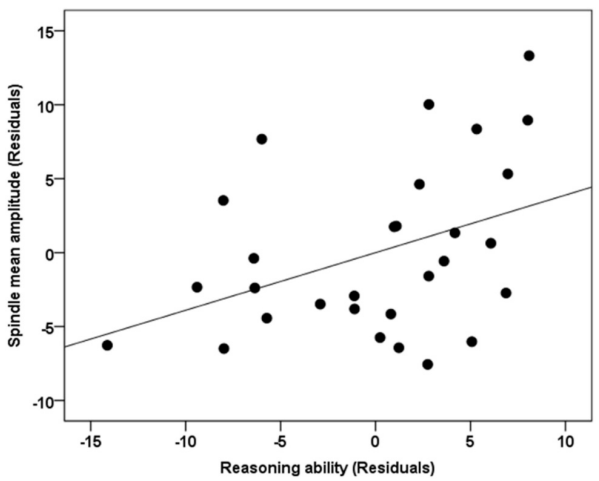

FIGURE 2 | Correlation between spindle amplitude and Reasoning ability. The unique relationship (i.e., partial correlation, $r = 0.435$, $p = 0.030$) between Reasoning ability, controlling for STM and Verbal abilities with spindle amplitude during NREM sleep. Gender and the whole brain volume were included in the model as covariates of no interest. Values reported in the scatterplot are residuals (showing the partial correlation) and shown in standardized arbitrary units.

partial coefficients revealed that Reasoning ability, controlling for STM and Verbal abilities [$t(23) = 2.314$, $r = 0.435$, $p = 0.030$] accounted for variability in spindle amplitude (**Figure 2**). By contrast, neither STM, controlling for Reasoning and Verbal abilities [$t(23) = 0.394$, $r = 0.082$, $p = 0.697$), nor Verbal abilities, controlling for STM and Reasoning abilities [$t(23) = 0.642$, $r = 0.133$, $p = 0.527$) accounted for variability in sleep spindle amplitude. Thus, Reasoning abilities (but not STM or Verbal abilities) were uniquely related to spindle characteristics. To further explore which subtest score (i.e., deductive reasoning, spatial rotation, feature match, spatial planning, and polygons) from the Reasoning subscale was correlated with spindle amplitude, partial correlation analysis revealed that deductive reasoning, spatial planning, and polygons were all significantly correlated with spindle amplitude ($p < 0.05$), while spatial rotation and spatial planning were marginally correlated ($p < 0.10$) with spindle amplitude (**Supplementary Table S1**).

Activation of Brain Regions Time-Locked to Spindles During NREM Sleep

As expected, and consistent with previous studies (Laufs et al., 2007; Schabus et al., 2007; Tyvaert et al., 2008; Andrade et al., 2011; Caporro et al., 2012), as shown in **Figure 3A**, activations time-locked to spindles were observed in the thalamus/midbrain, the bilateral striatum (putamen/globus pallidus and caudate), the medial frontal cortex, the cerebellum, and the brain stem (statistical inferences were performed at a threshold of $p < 0.001$ uncorrected at the whole-brain level and $p < 0.05$, FWE corrected at the cluster level, **Table 4**).

Correlation Between Brain Activations Time-Locked to Spindles and Cognitive Abilities

To examine the correlation between the level of activation of neural substrates recruited during spindles events and cognitive abilities, we conducted whole-brain spatial correlation analyses between brain activation maps time-locked to spindles and the scores on the three distinct cognitive subscales (Reasoning, STM, and Verbal abilities) assessed by the

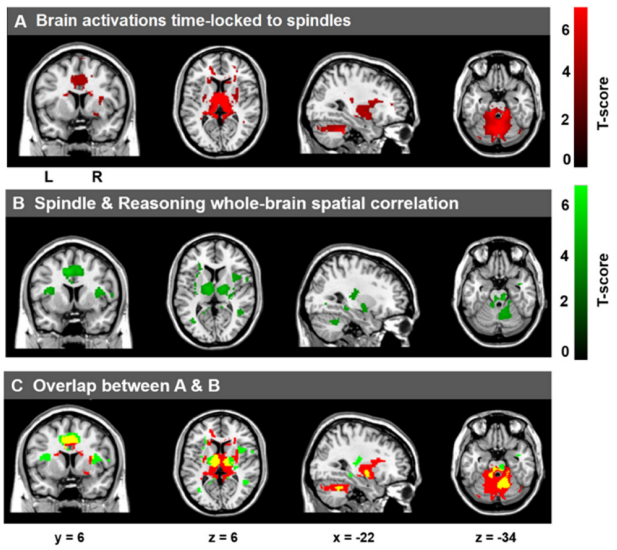

FIGURE 3 | Cerebral activations time-locked to sleep spindles and correlation between spindle-related activation and Reasoning abilities. **(A)** Activations time-locked to sleep spindles during NREM sleep. **(B)** Spatial correlation maps between activations time-locked to sleep spindles and Reasoning abilities. **(C)** Overlap between **A** (red) and **B** (green), with the conjunction of **A** and **B** shown in yellow. Statistical inferences were performed at a threshold of $p < 0.001$ (uncorrected) at the whole-brail level and $p < 0.05$, FWE corrected at the cluster level.

TABLE 4 | Statistically significant activations time-locked to sleep spindles (**Figure 3A**).

Hemisphere	Region	MNI coordinate			Peak *z*-score	FWE-corrected *p*-value
		X	*Y*	*Z*		
Right	Thalamus	10	−22	10	6.14	< 0.001
Left	Thalamus	−12	−24	18	6.03	< 0.001
Left	Caudate	−14	12	12	6.07	< 0.001
Left	Putamen/pallidum	−18	−2	−4	4.22	0.001
Right	Putamen/pallidum	18	−4	−4	5.32	< 0.05
Bilateral	Cerebellum	2	−62	−10	5.88	< 0.001
Left	Anterior cingulate	−16	32	18	5.16	0.001
Right	Anterior cingulate	12	22	28	3.94	0.001
Middle	Middle cingulate	0	24	32	4.53	0.001

Significant brain responses after FWE correction $p < 0.05$ at the cluster level.

TABLE 5 | Whole brain correlations between Reasoning ability and spindle-related activations (**Figure 3B**).

Hemisphere	Region	MNI coordinate			Peak *z*-score	Cluster-level FWE corrected *p*-value
		X	*Y*	*Z*		
Left	Paracentral lobule	−12	−32	58	4.83	< 0.001
Middle	Anterior cingulate	−6	12	26	4.19	< 0.001
Middle	Middle cingulate	−6	10	42	4.30	< 0.001
Left	Precuneus	−14	−58	32	4.83	< 0.001
Left	Putamen/pallidum	−16	−6	−2	4.34	< 0.001
Left	Thalamus	−12	−10	6	3.99	< 0.001
Right	Thalamus	16	−10	8	3.88	< 0.001
Right	Brain stem	14	−32	−32	4.58	< 0.001
Left	Brain stem	−8	−30	−26	4.09	< 0.001
Right	Cerebellum	14	−64	−34	3.94	< 0.001
Left	Temporal lobe	−42	−58	−2	4.01	< 0.05
Right	Temporal lobe	48	−52	−4	4.14	< 0.005

Significant brain responses after FWE correction $p < 0.05$ at the cluster level.

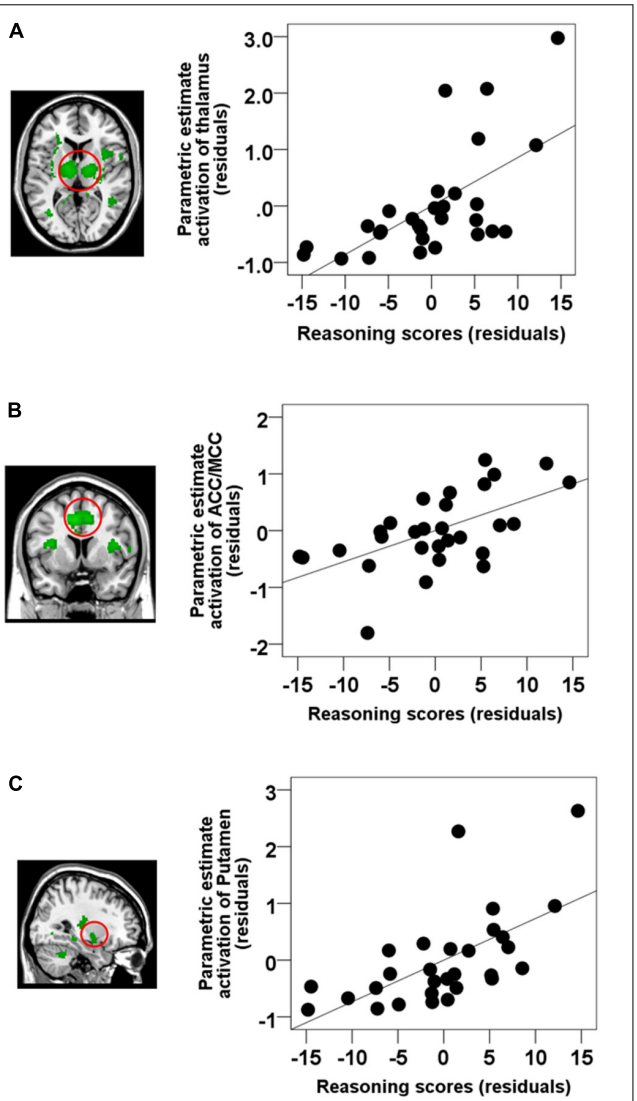

FIGURE 4 | Semi-partial correlations between brain activations time-locked to spindles and Reasoning scores. ROI analyses revealed that Reasoning abilities were correlated with activations in the **(A)** the thalamus (partial correlation, $r = 0.628$, $p < 0.001$), **(B)** ACC/MCC (partial correlation, $r = 0.585$, $p = 0.001$), and **(C)** the bilateral putamen (partial correlation, $r = 0.616$, $p = 0.001$). Gender and the whole brain volume were included in the model as covariates of no interests. Values are standardized residuals (showing the partial correlation) and shown in standardized arbitrary units.

CBS trials. As shown in **Figure 3B**, Reasoning ability was significantly correlated with activations time-locked to spindle events in the thalamus, bilateral putamen, brainstem/pons, ACC, the MCC, the paracentral lobe, the posterior cingulate cortex, the precuneus, and bilateral temporal lobe (statistical inferences were performed at a threshold of $p < 0.001$ uncorrected at the whole-brail level and $p < 0.05$, FWE corrected at the cluster level (**Table 5**). To illustrate these relationships more clearly, the semi-partial correlations are shown in **Figure 4**. The ROIs of ACC/MCC, thalamus, and bilateral putamen were defined independently based on the previous literature, as described in the "Materials and Methods" section.

Remarkably, no activations time-locked to spindle events were significantly related to STM or Verbal ability when considered as the covariate of interest (cluster-level *FWE* correction, $p < 0.05$). Moreover, very few results were significant even at a much less conservative, $p < 0.001$, without correction for multiple comparisons for Verbal abilities, and no results for STM at that threshold.

Comparisons of Brain–Behavior Correlations Between Reasoning, STM, and Verbal Abilities

Reasoning ability was highly inter-correlated with Verbal ability ($r = 0.596$, $p = 0.001$), and marginally correlated

with STM ability (r = 0.357, p = 0.058), thus preventing all three scales to be included in a whole brain regression analysis due to high multicollinearity. Thus, in order to further examine whether the significant relationship between activations time-locked to spindle events and Reasoning ability could be accounted for by STM or Verbal abilities, we selected three ROI based on the spindle activations consistently observed in the extant literature (see the section "Materials and Methods" for details). ROIs included: the thalamus, the ACC/MCC, and the bilateral putamen. We extracted the beta weights from these three independent ROIs from coordinates determined from the literature. We then conducted standard multiple linear regressions whereby parametric brain activation estimate values in the thalamus, the ACC/MCC, and the bilateral putamen were included in the models as dependent variables, and Reasoning, Verbal, and STM scores were included in the models as independent variables. Similar to the whole-brain analysis (**Table 6**), altogether, Reasoning, STM, and Verbal abilities significantly accounted for brain activation time-locked to spindles in the thalamus (R^2 = 0.425, p = 0.019), the cingulate cortex (R^2 = 0.627, p = 0.033), and the putamen (R^2 = 0.456, p = 0.011). Importantly, follow-up inspection of the partial coefficients revealed that Reasoning ability uniquely accounted for spindle-related activation in the thalamus (r = 0.460, p = 0.021), the cingulate cortex (r = 0.434, p = 0.030), and the putamen (r = 0.458, p = 0.021) over and above Verbal and STM (i.e., controlling for STM and Verbal abilities). The same partial correlation analyses were conducted between the five subtests scores and the spindle-related brain activation in the three main regions of interest (i.e., thalamus, ACC/MCC, putamen). As shown in **Supplementary Table S2**, all subtests were correlated with brain activations time-locked to spindles in thalamus and putamen ($p < 0.05$) except for feature match. In addition, the ACC/MCC activation was significantly correlated with deductive reasoning, spatial rotation, and polygons ($p < 0.05$), and marginally correlated with spatial planning (p = 0.06).

TABLE 6 | Multiple regression analyses of the relationship between CBS trials and brain activation time-locked to spindles.

	Overall regression effect		
Correlated region	**Unadjusted R^2**	**F(5,23)**	**p**
Thalamus	0.425	3.394	**0.019***
ACC/MCC	0.627	2.974	**0.033***
Putamen	0.456	3.855	**0.011***
	Follow-up analyses for the thalamus		
CBS measures	**Partial r**	**t(23)**	**p**
Reasoning	0.460	2.486	**0.021***
Verbal	0.210	1.029	0.314
STM	−0.091	−0.436	0.667
	Follow-up analyses for the ACC/MCC		
CBS measures	**Partial r**	**t(23)**	**p**
Reasoning	0.434	2.307	**0.030***
Verbal	0.229	1.128	0.271
STM	−0.198	−0.971	0.342
	Follow-up analyses for the putamen		
CBS measures	**Partial r**	**t(23)**	**p**
Reasoning	0.458	2.473	**0.021***
Verbal	0.293	1.470	0.155
STM	−0.241	−1.193	0.245

Statistically significant results indicated by an asterisk (*) at $p < 0.05$; STM, short-term memory.

Overlap Between Activations Time-Locked to Spindles and Reasoning-Related Spindle Activations

From **Figure 3**, we can see that there were several overlapping regions between the spindle activation maps (**Figure 3A**) and the maps that show activations time-locked to spindles that were correlated with Reasoning abilities (**Figure 3B**). To follow-up this observation, the overlap ($p < 0.05$, FWE at the cluster level) between the spindle activation maps and the Reasoning-related spindle correlation maps (**Figure 3C**, yellow regions) show several regions were consistently high and jointly activated in both the spindle maps (**Figure 3A**) and Reasoning-spindle correlation maps (**Figure 3B**), including the thalamus, medial frontal cortex, bilateral putamen, and the cerebellum. Thus, suggesting that a subset of the spontaneous spindle-related activations was uniquely correlated with Reasoning abilities.

DISCUSSION

Advancements in simultaneous EEG–fMRI technology and techniques has enabled the investigation of the functional brain activation recruited during well-known electrophysiological events such as sleep spindles. This can provide a window into understanding what brain areas are involved in sleep processes and their function. Given the challenging nature of applying these techniques to study sleep, only a handful of studies have explored the brain activations correlated with sleep spindles (Laufs et al., 2007; Schabus et al., 2007; Tyvaert et al., 2008; Andrade et al., 2011; Caporro et al., 2012). While important in terms of advancing the understanding of the neurophysiology and functional anatomy of the spindle, unfortunately, we can only infer the functional significance of these brain activations from these studies. Thus, limiting our understanding of the related functions of sleep spindles and their neural correlates. Previous EEG and behavioral studies have identified sleep spindles as a biological marker of cognitive abilities, and in particular, Reasoning abilities (Bódizs et al., 2005; Schabus et al., 2006; Fogel et al., 2007; Fogel and Smith, 2011; Ujma et al., 2014, 2015; Fang et al., 2017). While providing important information about the functional significance of the sleep spindle, the neuroanatomical substrates and neural mechanisms which support the relationship between spindles and Reasoning abilities can only be inferred indirectly from these studies. Here, we

identified the neural activation patterns time-locked to spindles that are correlated to cognitive abilities. Using simultaneous EEG–fMRI sleep recordings, the results of the present study support three main findings:

(1) similar to previous studies (Fogel et al., 2007; Fang et al., 2017), the electrophysiological spindle characteristics (e.g., amplitude) during NREM sleep were related to Reasoning but not STM or Verbal abilities,
(2) similar to previous studies (Laufs et al., 2007; Schabus et al., 2007; Tyvaert et al., 2008; Andrade et al., 2011; Bergmann et al., 2012; Caporro et al., 2012; Fogel et al., 2017a), activations time-locked to spindles were observed in the thalamus, bilateral striatum, MCC, and cerebellum, and importantly,
(3) Reasoning abilities, but not STM or Verbal abilities, were correlated with spindle-related activations in a subset of these regions including the thalamus, bilateral putamen, medial frontal gyrus, MCC, and precuneus.

These results provide evidence that individuals with greater neural activation time-locked to spindle events have greater Reasoning abilities (i.e., "fluid intelligence"; problem solving skills, the ability to employ logic, identify complex patterns). Altogether, our results identified for the first time, that a subset of spontaneous spindle-related activations are correlated specifically with Reasoning abilities but are unrelated to other abilities such as STM and Verbal abilities. Thus, suggesting that the extent of spindle-related activations reflect an individual's capacity for reasoning.

Association Between Spindle Amplitude and Reasoning Abilities

The three subtests (i.e., Reasoning, STM, and Verbal) that assess sub-domains of general cognitive abilities are highly inter-correlated with one another. However, among these three inter-correlated subtests, only Reasoning abilities were found to be correlated with spindles, when the overlapping variability was controlled using multiple regression. This finding has been reported previously whereby the electrophysiological characteristics of spindles were correlated with Reasoning abilities (Fang et al., 2017) and Performance intelligence (Fogel et al., 2007), but not Verbal abilities. Also, it is consistent with the extant literature and the well-established finding that spindles are related to a subset of cognitive abilities that tap into reasoning and the ability to solve problems, i.e., fluid intelligence (Nader and Smith, 2001, 2003; Schabus et al., 2006; Ujma et al., 2014, 2015). Using CBS tests, Hampshire et al. (2012) identified that the network of brain regions which support these three subtests of cognitive abilities were distinct from each other. Therefore, indicating that although these three subtest are inter-correlated with each other, they are associated with distinct neural substrates. Our findings further suggest that BOLD brain activations during spindle events are uniquely related to Reasoning abilities, over and above STM and Verbal abilities. It is also worth noting that according to previous studies (Bódizs et al., 2005; Schabus et al., 2006; Fogel et al., 2007; Fogel and Smith, 2011; Hoedlmoser et al., 2014; Róbert Bódizs et al., 2014; Ujma et al., 2014, 2015, 2016; Tessier et al., 2015; Fang et al., 2017), there is no single or unique spindle electrophysiological characteristic that is correlated with cognitive abilities (i.e., fluid intelligence, reasoning, problem solving, etc.). Several spindle parameters have been found to be correlated with cognitive abilities. For example, spindle amplitude (Bódizs et al., 2014; Ujma et al., 2014, 2016; Fang et al., 2017), spindle activity (duration × amplitude) (Schabus et al., 2006; Hoedlmoser et al., 2014; Tessier et al., 2015), and spindle density (Bódizs et al., 2005; Fogel et al., 2007) have all been reported to be correlated with cognitive abilities. In the current study, we observed the strongest association between spindle amplitude and reasoning ability. This is consistent with the finding of a recent meta-analysis study (Ujma, 2018), which reported that only spindle amplitude is unambiguously associated with cognitive ability.

Spontaneous Brain Responses Time-Locked to Sleep Spindles

As expected, and consistent with previous EEG–fMRI studies of spontaneous spindle-related activations (Laufs et al., 2007; Schabus et al., 2007; Tyvaert et al., 2008; Andrade et al., 2011; Bergmann et al., 2012; Caporro et al., 2012; Fogel et al., 2017a), our results identified and confirmed the brain regions associated with spindle events during NREM sleep in both cortical (including the media prefrontal, ACC, and MCC), subcortical areas (including the thalamus and bilateral caudate, putamen, and pallidum), and the cerebellum. Thus, confirming the recruitment of cortico-thalamic-striatal circuitry in spindle generation. These human neuroimaging findings are supported by a large body of animal studies, which at the cellular level, suggest that spindles reflect oscillatory activity in widespread thalamocortical circuits, and involve complex interactions between reticular, thalamocortical, and pyramidal cells (Steriade, 2005). Unfortunately, due to the limited duration, and high inter-subject variability of sleep in the scanner, we did not have sufficient sleep to investigate slow and fast spindles separately, or enough SWS to test whether a different pattern of results was observed during SWS. This limitation is not unexpected given the difficulty in obtaining long, consolidated bouts of sleep in an MRI environment. As scanner technology becomes more comfortable and less noisy, future studies may succeed at obtaining longer duration sleep in the MRI simultaneously with EEG. Taken together, animal and recent human neuroimaging studies, including the current study, support the involvement of thalamocortical, striatal, and cerebellar circuitry in spindle generation. However, these findings do not directly investigate the functional correlates of spontaneous spindle-related brain activation, discussed in the following section.

Association Between Spindle-Related Activation and Reasoning Ability

The results of the current study identified, for the first time, that brain activations recruited during spontaneous spindle events

were specifically associated with Reasoning abilities, but not STM or Verbal abilities, including the thalamus, the PFC (i.e., the ACC/MCC), the bilateral putamen, the cerebellum, and the precuneus. Thus, suggesting that interindividual differences in the extent of activations in cortico–thalamic–striatal circuitry time-locked spindles are related to individual cognitive strengths, and in particular, Reasoning abilities. The extent of these activations does not relate to other cognitive abilities, e.g., STM or Verbal abilities. Given the widespread nature and heterogeneity of the brain regions activated, further investigation to explore the network dynamics (e.g., using functional connectivity analyses) is warranted. This may reveal network hubs of communication, for which the strength of connectivity with other areas might provide further insight into the relationship between spindles and intellectual abilities. It is important to note that the results of this study are entirely correlational, and the possibility remains that the observed correlation can be explained by other confounding or unrelated factors. Moreover, the directionality of this relationship cannot be determined from the results of this study. Future studies employing similar techniques in cases where spindle activity is abnormal and where specific cognitive deficits occur such as Autism (Limoges et al., 2013), learning disabilities (Shibagaki et al., 1982), and in schizophrenia (Wamsley et al., 2012) may provide additional insight into the neural basis of the relationship between spindles and Reasoning abilities. However, this study is an important first step in investigating the functional significance of spindle-related activations in young, healthy populations.

The network of brain regions identified here, activated during spindles, correlated with Reasoning abilities are convergent with the extant literature. For example, thalamo–cortical circuitry (e.g., thalamus and the PFC region) is implicated in modulation of cognitive performance, such as memory, executive functioning, and attention (Van Der Werf et al., 2000; Van der Werf et al., 2003; Blair, 2006; Mitchell and Chakraborty, 2013; Ferguson and Gao, 2015). Similar to the current study, thalamic activations have been observed while solving fluid intelligence tasks, including problem solving (Fangmeier et al., 2006), reasoning tasks (Melrose et al., 2007), and particularly, inductive reasoning (Jia et al., 2011; Liang et al., 2014). Other neuroanatomical studies (Bohlken et al., 2014) found that thalamic volume was significantly correlated with general intellectual functioning. In addition, at least one study identified structural and functional abnormalities in the thalamus in adults with reduced intellectual functioning who experienced prenatal exposure to alcohol (Clark et al., 2000). Similarly, a large body of literature has identified the role of the PFC in fluid intelligence and Reasoning (Baker et al., 1996; Waltz et al., 1999; Duncan, 2000; Gray et al., 2003; Coricelli and Nagel, 2009). For example, patients with damage to the PFC exhibited a selective and catastrophic deficit for both deductive and inductive reasoning tasks (Waltz et al., 1999). In addition, Gray et al. (2003) found that individuals with higher fluid intelligence have greater activations in the PFC. Coricelli and Nagel (2009) have shown that Reasoning abilities correlate with neural activity in the medial PFC. Additionally, at least one neuroanatomical MRI study employing voxel-based morphometry has revealed a positive correlation between gray matter intensity in the medial PFC and Reasoning abilities assessed by Cattell's Culture Fair Intelligence Test, and also the WAIS-R (Gong et al., 2005). In addition, several studies have observed robust activations in the basal ganglia for Reasoning-related tasks compared to other cognitive tasks, including the caudate nucleus, putamen, and globus pallidus (Melrose et al., 2007; Rodriguez-Moreno and Hirsch, 2009). Specifically, Sandman et al. (2014) has reported that the morphometry of the putamen was associated with performance on Reasoning-related subtests of the WAIS including block design, matrix Reasoning, and perceptual index in preadolescent children. Although overlooked in some studies, the cerebellum is activated during the deductive reasoning processing (Goel et al., 2000; Goel and Dolan, 2004). Thus, taken together, suggesting that integrity and functioning of these regions (e.g., thalamus, PFC, striatum, cerebellum) are required for intact Reasoning abilities, however, this possibility remains to be explicitly investigated. Our results suggest that individuals with greater spindle-related activation of this circuitry is associated with greater Reasoning abilities. Thus, spindles may be an important marker of Reasoning abilities, and a window into understanding the interindividual differences in the activation patterns of neural substrates related to specific cognitive abilities.

The clinical significance and applications of the relationship between spindles and cognitive abilities is yet to be realized. Interestingly, spindle production is reduced with age (Carrier et al., 2001, 2011; Lafortune et al., 2012; Martin et al., 2013; Fogel et al., 2014; Fogel et al., 2017b), and abnormal in developmental disorders, such as Autism (Limoges et al., 2005), learning disabilities (Shibagaki et al., 1982), and in schizophrenia (Wamsley et al., 2012). Deficient or dysfunctional spindle generation has been found to be associated with compromised intellectual functioning. More specifically, it has been suggested that deficient gating mechanisms of thalamocortical circuitry (Bixler and Rhodes, 1968) may explain abnormal spindle production in children with mental disability (Gibbs and Gibbs, 1962; Shibagaki and Kiyono, 1983). Moreover, the present study is an important first step which may lead to the development of novel interventions utilizing spindle-enhancing neuromodulatory techniques (e.g., neurofeedback, transcranial direct current stimulation, pharmacological techniques) to improve daytime cognitive performance and explore the physiological mechanisms which support the function of sleep for memory and cognitive performance. Thus, such an approach could target cognitive deficits, in cases where spindle production is abnormal such as in learning disabilities (Gibbs and Gibbs, 1962; Shibagaki and Kiyono, 1983), below normal cognitive functioning (Fogel and Smith, 2011), normal, healthy aging (Carrier et al., 2011; Fogel et al., 2014, 2017b), developmental disorders (Limoges et al., 2005), and in schizophrenia (Wamsley et al., 2012). A better understanding of the neural basis of the relationship between spindles and cognitive abilities may ultimately help to better understand biological basis of normal and abnormal cognitive functioning in healthy individuals and neurological conditions. This may eventually lead to novel interventions to precisely target cases where spindle production is abnormal or non-optimal.

However, there are limitations of the current study worth mentioning. First, sleep was recorded only for a short time at the beginning of the night, in an MRI environment. Thus, we would expect that the architecture of sleep and spindle parameters are not perfectly comparable to a whole night of natural, nocturnal sleep in a normal sleeping environment. It should be mentioned that the density of sleep spindles in the current study was higher than some previous EEG studies. There are several possible reasons for this discrepancy. First, studies have shown that spindle density is highest near the start of the first NREM cycle in a night (Zeitlhofer et al., 1997; Purcell et al., 2017) and the density of sleep spindles is decreased with the deepening of sleep (Steriade and Amzica, 1998; De Gennaro et al., 2000; Himanen et al., 2002). In the current study, we recorded sleep only at the beginning of the night, and under conditions where deep sleep is less likely. Thus, spindle density would be expected to be higher than whole-night studies under normal conditions. Moreover, the continuous noise from the MRI scanner throughout the sleep session may have had an unavoidable impact on spindle production. A number of previous studies have shown that sleep spindles can protect sleep from external stimuli (Peters and Jones, 1991; Elton et al., 1997; Cote et al., 2000; Vyazovskiy et al., 2004; Dang-Vu et al., 2010; Schabus et al., 2012). For example, Dang-Vu et al. (2010) have demonstrated that individuals who generate a greater number of sleep spindles maintain sleep better in the face of disruptive stimuli. Therefore, it is possible that participants who slept better generated a greater number of spindles. Finally, sleep in an MR environment is likely more comparable to daytime napping recordings (i.e., light, fragmented sleep). Accordingly, the density of sleep spindles reported in the current study is comparable to a previous daytime napping study using the same spindle detection method (Albouy et al., 2013). Second, while the majority of subjects (N = 20) achieved SWS, there is however, enormous inter-subject variability in terms of the actual duration (spindle number range: 1–752, mean = 133.35, Std = 177.93). Furthermore, only 12 subjects had more than 30 spindle events (spindle number range: 42–752, mean = 218, Std = 189.18) during slow wave sleep, which is the minimum reasonable number necessary to carry out the analyses. As a result of these issues, we were not confident of the results for SWS only. In addition, we do not have any specific *a priori* hypotheses about SWS spindles in particular. Therefore, we did not separate the stage 2 sleep and slow wave sleep in the current study. Finally, the goal of the current study was to investigate the event-related functional brain activations in the BOLD signal time course that occur during spindle events. Therefore, similar to previous EEG–fMRI sleep studies investigating spindle-related brain activations (Schabus et al., 2007; Andrade et al., 2011; Fogel et al., 2017a), spindles at the midline derivation (re; Fz, Cz, Pz) were detected to identify the onsets of spindle events given that the topographical distribution of visually scored and automatically detected sleep spindles is prevalent on central leads, especially the centroparietal midline derivation (McCormick et al., 1997; Zeitlhofer et al., 1997). Also, it has been reported that most spindles are detected simultaneously from multiple channels, whereby spindles tend to co-occur at midline channels more than half the time (Hagler et al., 2018). However, it is important to note that in spite of the prevalence and concurrence patterns of spindles maximal at central derivation spindles, there is evidence that sleep spindles also occur locally (Andrillon et al., 2011; Nir et al., 2011; Piantoni et al., 2016; Hagler et al., 2018). Local spindles occurring in isolation may be associated with specific aspects of cognitive functions, such as working memory (Buchmann et al., 2014), memory consolidation (Johnson et al., 2010), and global cognitive integration (Manoach et al., 2016). While beyond the scope of the objectives of the current study, deep-source EEG localization techniques could provide corroborative or converging evidence in regards to whether EEG sources correspond to BOLD brain activations time-locked to sleep spindles from a single scalp location (e.g., Boutin et al., 2018). This may shed light on the functional significance of local vs. global spindle events.

In summary, we investigated the spindle-related neural substrates that support cognitive strengths and weaknesses. There are considerable interindividual differences in sleep spindles, which are very trait-like (Silverstein and Levy, 1976; Gaillard and Blois, 1981). While the neural circuitry and generating mechanisms of spindles are well-understood, the neurophysiological basis of the relationship between spindles and cognitive abilities remains to be fully elucidated. Our results show for the first time the neuroanatomical functional correlates of the relationship between sleep spindles and specific intellectual abilities. In particularly, our study found that the extent of the brain activations time-locked to sleep spindles were correlated with interindividual differences in Reasoning, but not Verbal or STM abilities. These findings provide new insights to understand the function of sleep spindles.

AUTHOR CONTRIBUTIONS

SF and AO designed the study and supervised the research. SF, ZF, and LR carried out the research and collected the data. ZF, SF, and LR contributed to data analyses. ZF, SF, and LR prepared the figures and wrote the manuscript. All authors discussed the results and commented on the manuscript.

FUNDING

This research was funded by a Canada Excellence Research Chair (CERC) grant number (#215063) to AO. This study was previously released as a pre-print at BioRxiv (Fang et al., 2017). We want to confirm here that this study or any part of this study has not been published in any other peer-reviewed journal. It is also worth noting that the manuscript submitted to Frontiers in Neuroscience has been heavily revised with significant improvements to the analyses after it was released in pre-print.

SUPPLEMENTARY MATERIAL

The Supplementary Material for this article can be found online at: https://www.frontiersin.org/articles/10.3389/fnins.2019.00046/full#supplementary-material

REFERENCES

Albouy, G., Fogel, S., Pottiez, H., Nguyen, V. A., Ray, L., Lungu, O., et al. (2013). Daytime sleep enhances consolidation of the spatial but not motoric representation of motor sequence memory. *PLoS One* 8:e52805. doi: 10.1371/journal.pone.0052805

Allen, P. J., Josephs, O., and Turner, R. (2000). A method for removing imaging artifact from continuous EEG recorded during functional MRI. *Neuroimage* 12, 230–239. doi: 10.1006/nimg.2000.0599

Allen, P. J., Polizzi, G., Krakow, K., Fish, D. R., and Lemieux, L. (1998). Identification of EEG events in the MR scanner: the problem of pulse artifact and a method for its subtraction. *Neuroimage* 8, 229–239. doi: 10.1006/nimg.1998.0361

Andrade, K. C., Spoormaker, V. I., Dresler, M., Wehrle, R., Holsboer, F., Samann, P. G., et al. (2011). Sleep spindles and hippocampal functional connectivity in human NREM Sleep. *J. Neurosci.* 31, 10331–10339. doi: 10.1523/JNEUROSCI.5660-10.2011

Andrillon, T., Nir, Y., Staba, R. J., Ferrarelli, F., Cirelli, C., Tononi, G., et al. (2011). Sleep spindles in humans: insights from intracranial EEG and unit recordings. *J. Neurosci.* 31, 17821–17834. doi: 10.1523/JNEUROSCI.2604-11.2011

Baddeley, A. D. (1968). A 3 min reasoning test based on grammatical transformation. *Psychon. Sci.* 10, 341–342. doi: 10.3758/BF03331551

Baker, S. C., Rogers, R. D., Owen, A. M., Frith, C. D., Dolan, R. J., Frackowiak, R. S. J., et al. (1996). Neural systems engaged by planning: a PET study of the tower of London task. *Neuropsychologia* 34, 515–526. doi: 10.1016/0028-3932(95)00133-6

Beck, A. T., Epstein, N., Brown, G., and Steer, R. A. (1988). An inventory for measuring clinical anxiety: psychometric properties. *J. Consul. Clin. Psychol.* 56, 893–897. doi: 10.1037/0022-006X.56.6.893

Beck, A. T., Rial, W. Y., and Rickels, K. (1974). Short form of depression inventory: cross-validation. *Psychol. Rep.* 34, 1184–1186.

Bergmann, T. O., Mölle, M., Diedrichs, J., Born, J., and Siebner, H. R. (2012). Sleep spindle-related reactivation of category-specific cortical regions after learning face-scene associations. *Neuroimage* 59, 2733–2742. doi: 10.1016/j.neuroimage.2011.10.036

Bixler, E. O., and Rhodes, J. M. (1968). Spindle activity during sleep in cultural-familial mild retardates. *Psychophysiology* 5:212.

Blair, C. (2006). How similar are fluid cognition and general intelligence? A developmental neuroscience perspective on fluid cognition as an aspect of human cognitive ability. *Behav. Brain Sci.* 29, 109–160. doi: 10.1017/S0140525X06009034

Bódizs, R., Gombos, F., Ujma, P. P., and Kovács, I. (2014). Sleep spindling and fluid intelligence across adolescent development: sex matters. *Front. Hum. Neurosci.* 8:952. doi: 10.3389/fnhum.2014.00952

Bódizs, R., Kis, T., Lázár, A. S., Havrán, L., Rigó, P., Clemens, Z., et al. (2005). Prediction of general mental ability based on neural oscillation measures of sleep. *J. Sleep Res.* 14, 285–292. doi: 10.1111/j.1365-2869.2005.00472.x

Bódizs, R., Lázár, A. S., and Rigó, P. (2008). Correlation of visuospatial memory ability with right parietal EEG spindling during sleep. *Acta Physiol. Hung.* 95, 297–306. doi: 10.1556/APhysiol.95.2008.3.5

Bohlken, M. M., Brouwer, R. M., Mandl, R. C. W., van Haren, N. E. M., Brans, R. G. H., van Baal, G. C. M., et al. (2014). Genes contributing to subcortical volumes and intellectual ability implicate the thalamus. *Hum. Brain Mapp.* 35, 2632–2642. doi: 10.1002/hbm.22356

Boutin, A., Pinsard, B., Boré, A., Carrier, J., Fogel, S. M., and Doyon, J. (2018). Transient synchronization of hippocampo-striato-thalamo-cortical networks during sleep spindle oscillations induces motor memory consolidation. *Neuroimage* 169, 419–430. doi: 10.1016/j.neuroimage.2017.12.066

Branger, P., Arenaza-Urquijo, E. M., Tomadesso, C., Mézenge, F., André, C., de Flores, R., et al. (2016). Relationships between sleep quality and brain volume, metabolism, and amyloid deposition in late adulthood. *Neurobiol. Aging* 41, 107–114. doi: 10.1016/j.neurobiolaging.2016.02.009

Brewer-Deluce, D., Wilson, T. D., and Owen, A. M. (2017). Cognitive function in varsity football athletes is maintained in the absence of concussion. *FASEB J.* 31, 745–747.

Buchmann, A., Dentico, D., Peterson, M. J., Riedner, B. A., Sarasso, S., Massimini, M., et al. (2014). Reduced mediodorsal thalamic volume and prefrontal cortical spindle activity in schizophrenia. *Neuroimage* 102, 540–547. doi: 10.1016/j.neuroimage.2014.08.017

Caporro, M., Haneef, Z., Yeh, H. J., Lenartowicz, A., Buttinelli, C., Parvizi, J., et al. (2012). Functional MRI of sleep spindles and K-complexes. *Clin. Neurophysiol.* 123, 303–309. doi: 10.1016/j.clinph.2011.06.018

Carrier, J., Land, S., Buysse, D. J., Kupfer, D. J., and Monk, T. H. (2001). The effects of age and gender on sleep EEG power spectral density in the middle years of life (ages 20-60 years old). *Psychophysiology* 38, 232–242. doi: 10.1111/1469-8986.3820232

Carrier, J., Viens, I., Poirier, G., Robillard, R., Lafortune, M., Vandewalle, G., et al. (2011). Sleep slow wave changes during the middle years of life. *Eur. J. Neurosci.* 33, 758–766. doi: 10.1111/j.1460-9568.2010.07543.x

Casey, B. J., Tottenham, N., Liston, C., and Durston, S. (2005). Imaging the developing brain: what have we learned about cognitive development? *Trends Cogn. Sci.* 9, 104–110.

Cattell, R. B. (1940). A culture-free intelligence test. I. *J. Educ. Psychol.* 31, 161–179. doi: 10.1037/h0059043

Clark, C. M., Li, D., Conry, J., Conry, R., and Loock, C. (2000). Structural and functional brain integrity of fetal alcohol syndrome in nonretarded cases. *Pediatrics* 105, 1096–1099. doi: 10.1542/peds.105.5.1096

Collins, P., Roberts, A. C., Dias, R., Everitt, B. J., and Robbins, T. W. (1998). Perseveration and strategy in a novel spatial self-ordered sequencing task for nonhuman primates: effects of excitotoxic lesions and dopamine depletions of the prefrontal cortex. *J. Cogn. Neurosci.* 10, 332–354. doi: 10.1162/089892998562771

Coricelli, G., and Nagel, R. (2009). Neural correlates of depth of strategic reasoning in medial prefrontal cortex. *Proc. Nat. Acad. Sci. U.S.A.* 106, 9163–9168. doi: 10.1073/pnas.0807721106

Corsi, P. (1972). *Human Memory and the Medial Temporal Region of the Brain*. Ph.D. thesis, McGill University, Montreal.

Cote, K. A., Epps, T. M., and Campbell, K. B. (2000). The role of the spindle in human information processing of high-intensity stimuli during sleep. *J. Sleep Res.* 9, 19–26. doi: 10.1046/j.1365-2869.2000.00188.x

Dang-Vu, T. T., McKinney, S. M., Buxton, O. M., Solet, J. M., and Ellenbogen, J. M. (2010). Spontaneous brain rhythms predict sleep stability in the face of noise. *Curr. Biol.* 20, 626–627. doi: 10.1016/j.cub.2010.06.032

De Gennaro, L., Ferrara, M., and Bertini, M. (2000). Topographical distribution of spindles: variations between and within nrem sleep cycles. *Sleep Res. Online* 3, 155–160.

De Gennaro, L., Ferrara, M., Vecchio, F., Curcio, G., and Bertini, M. (2005). An electroencephalographic fingerprint of human sleep. *Neuroimage* 26, 114–122. doi: 10.1016/j.neuroimage.2005.01.020

Delorme, A., and Makeig, S. (2004). EEGLAB: an open source toolbox for analysis of single-trial EEG dynamics including independent component analysis. *J. Neurosci. Methods* 134, 9–21. doi: 10.1016/j.jneumeth.2003.10.009

Douglass, A. B., Bornstein, R., Nino-Murcia, G., Keenan, S., Miles, L., Zarcone, V. P. Jr., et al. (1994). The sleep disorders questionnaire. I: creation and multivariate structure of SDQ. *Sleep* 17, 160–167. doi: 10.1093/sleep/17.2.160

Duncan, J. (2000). A neural basis for general intelligence. *Science* 289, 457–460. doi: 10.1126/science.289.5478.457

Elton, M., Winter, O., Heslenfeld, D., Loewy, D., Campbell, K., and Kok, A. (1997). Event-related potentials to tones in the absence and presence of sleep spindles. *J. Sleep Res.* 6, 78–83. doi: 10.1046/j.1365-2869.1997.00033.x

Fang, Z., Sergeeva, V., Ray, L. B., Viczko, J., Owen, A. M., and Fogel, S. M. (2017). Sleep spindles and intellectual ability: epiphenomenon or directly related? *J. Cogn. Neurosci.* 29, 167–182. doi: 10.1162/jocn_a_01034

Fangmeier, T., Knauff, M., Ruff, C. C., and Sloutsky, V. (2006). fMRI evidence for a three-stage model of deductive reasoning. *J. Cogn. Neurosci.* 18, 320–334. doi: 10.1162/jocn.2006.18.3.320

Faul, F., Erdfelder, E., Buchner, A., and Lang, A.-G. (2009). Statistical power analyses using G*Power 3.1: tests for correlation and regression analyses. *Behav. Res. Methods* 41, 1149–1160. doi: 10.3758/BRM.41.4.1149

Faul, F., Erdfelder, E., Lang, A.-G., and Buchner, A. (2007). GPOWER: a general power analysis program. *Behav. Res. Methods* 39, 175–191. doi: 10.3758/BF03193146

Ferguson, B. R., and Gao, W.-J. (2015). Development of thalamocortical connections between the mediodorsal thalamus and the prefrontal cortex and

its implication in cognition. *Front. Hum. Neurosci.* 8:1027. doi: 10.3389/fnhum.2014.01027

Fogel, S., Albouy, G., King, B. R., Lungu, O., Vien, C., Bore, A., et al. (2017a). Reactivation or transformation? Motor memory consolidation associated with cerebral activation time-locked to sleep spindles. *PLoS One* 12:e0174755. doi: 10.1371/journal.pone.0174755

Fogel, S., Vien, C., Karni, A., Benali, H., Carrier, J., and Doyon, J. (2017b). Sleep spindles: a physiological marker of age-related changes in gray matter in brain regions supporting motor skill memory consolidation. *Neurobiol. Aging* 49, 154–164. doi: 10.1016/j.neurobiolaging.2016.10.009

Fogel, S., Albouy, G., Vien, C., Popovicci, R., King, B. R., Hoge, R. D., et al. (2014). fMRI and sleep correlates of the age-related impairment in motor memory consolidation. *Hum. Brain Mapp.* 35, 3625–3645. doi: 10.1002/hbm.22426

Fogel, S., Ray, L., Sergeeva, V., De Koninck, J., and Owen, A. M. (2018). A novel approach to dream content analysis reveals links between learning-related dream incorporation and cognitive abilities. *Front. Psychol.* 9:1398. doi: 10.3389/fpsyg.2018.01398

Fogel, S., and Smith, C. T. (2006). Learning-dependent changes in sleep spindles and Stage 2 sleep. *J. Sleep Res.* 15, 250–255. doi: 10.1111/j.1365-2869.2006.00522.x

Fogel, S. M., Nader, R., Cote, K. A., and Smith, C. T. (2007). Sleep spindles and learning potential. *Behav. Neurosci.* 121, 1–10. doi: 10.1037/0735-7044.121.1.1

Fogel, S. M., and Smith, C. T. (2011). The function of the sleep spindle: a physiological index of intelligence and a mechanism for sleep-dependent memory consolidation. *Neurosci. Biobehav. Rev.* 35, 1154–1165. doi: 10.1016/j.neubiorev.2010.12.003

Folstein, M. F., Folstein, S. E., and McHugh, P. R. (1975). Mini-mental state. *J. Psychiatr. Res.* 12, 189–198. doi: 10.1016/0022-3956(75)90026-6

Friston, K., Penny, W., and Glaser, D. E. (2005). Conjunction revisited. *Neuroimage* 25, 661–667. doi: 10.1016/j.neuroimage.2005.01.013

Friston, K. J., Williams, S., Howard, R., Frackowiak, R. S. J., and Turner, R. (1996). Movement-related effects in fMRI time-series. *Magn. Reson. Med.* 35, 346–355. doi: 10.1002/mrm.1910350312

Gaillard, J. M., and Blois, R. (1981). Spindle density in sleep of normal subjects. *Sleep* 4, 385–391. doi: 10.1093/sleep/4.4.385

Gibbs, E. L., and Gibbs, F. A. (1962). Extreme spindles: correlation of electroencephalographic sleep pattern with mental retardation. *Science* 138, 1106–1107. doi: 10.1126/science.138.3545.1106

Goel, V., Buchel, C., Frith, C., and Dolan, R. J. (2000). Dissociation of mechanisms underlying syllogistic reasoning. *Neuroimage* 12, 504–514. doi: 10.1006/nimg.2000.0636

Goel, V., and Dolan, R. J. (2004). Differential involvement of left prefrontal cortex in inductive and deductive reasoning. *Cognition* 93, B109–B121. doi: 10.1016/j.cognition.2004.03.001

Gong, Q. Y., Sluming, V., Mayes, A., Keller, S., Barrick, T., Cezayirli, E., et al. (2005). Voxel-based morphometry and stereology provide convergent evidence of the importance of medial prefrontal cortex for fluid intelligence in healthy adults. *Neuroimage* 25, 1175–1186. doi: 10.1016/j.neuroimage.2004.12.044

Gould, R. L., Brown, R. G., Owen, A. M., Bullmore, E. T., and Howard, R. J. (2006). Task-induced deactivations during successful paired associates learning: an effect of age but not Alzheimer's disease. *Neuroimage* 31, 818–831. doi: 10.1016/j.neuroimage.2005.12.045

Gray, J. R., Chabris, C. F., and Braver, T. S. (2003). Neural mechanisms of general fluid. *Nat. Neurosci.* 6, 316–322. doi: 10.1038/nn1014

Hagler, D. J., Ulbert, I., Wittner, L., Erőss, L., Madsen, J. R., Devinsky, O., et al. (2018). Heterogeneous origins of human sleep spindles in different cortical layers. *J. Neurosci.* 38, 3013–3025. doi: 10.1523/JNEUROSCI.2241-17.2018

Hampshire, A., Highfield, R. R., Parkin, B. L., and Owen, A. M. (2012). Fractionating human intelligence. *Neuron* 76, 1225–1237. doi: 10.1016/j.neuron.2012.06.022

Himanen, S. L., Virkkala, J., Huhtala, H., and Hasan, J. (2002). Spindle frequencies in sleep EEG show U-shape within first four NREM sleep episodes. *J. Sleep Res.* 11, 35–42. doi: 10.1046/j.1365-2869.2002.00273.x

Hoedlmoser, K., Heib, D. P. J., Roell, J., Peigneux, P., Sadeh, A., Gruber, G., et al. (2014). Slow sleep spindle activity, declarative memory, and general cognitive abilities in children. *Sleep* 37, 1501–1512. doi: 10.5665/sleep.4000

Horne, J. A., and Ostberg, O. (1976). A self-assessment questionnaire to determine morningness-eveningness in human circadian rhythms. *Int. J. Chronobiol.* 4, 97–110.

Iber, C., Ancoli-Israel, S., Chesson, A. L., and Quan, S. F. (2007). *The AASM Manual for the Scoring of Sleep and Associated Events: Rules, Terminology and Technical Specifications*. Westchester, IL: American Academy of Sleep Medicine.

Inoue, S., and Matsuzawa, T. (2007). Working memory of numerals in chimpanzees. *Curr. Biol.* 17, R1004–R1005. doi: 10.1016/j.cub.2007.10.027

Jia, X., Liang, P., Lu, J., Yang, Y., Zhong, N., and Li, K. (2011). Common and dissociable neural correlates associated with component processes of inductive reasoning. *Neuroimage* 56, 2292–2299. doi: 10.1016/j.neuroimage.2011.03.020

Johnson, L. A., Euston, D. R., Tatsuno, M., and McNaughton, B. L. (2010). Stored-trace reactivation in rat prefrontal cortex is correlated with down-to-up state fluctuation density. *J. Neurosci.* 30, 2650–2661. doi: 10.1523/JNEUROSCI.1617-09.2010

Kriegeskorte, N., Simmons, W. K., Bellgowan, P. S., and Baker, C. I. (2009). Circular analysis in systems neuroscience: the dangers of double dipping. *Nat. Neurosci.* 12, 535–540. doi: 10.1038/nn.2303

Lafortune, M., Gagnon, J. F., Latreille, V., Vandewalle, G., Martin, N., Filipini, D., et al. (2012). Reduced slow-wave rebound during daytime recovery sleep in middle-aged subjects. *PLoS One* 7:e43224. doi: 10.1371/journal.pone.0043224

Laufs, H., Walker, M. C., and Lund, T. E. (2007). 'Brain activation and hypothalamic functional connectivity during human non-rapid eye movement sleep: an EEG/fMRI study'–its limitations and an alternative approach. *Brain* 130(Pt 7), e75; authorrely e76. doi: 10.1093/brain/awm084

Liang, P., Jia, X., Taatgen, N. A., Zhong, N., and Li, K. (2014). Different strategies in solving series completion inductive reasoning problems: an fMRI and computational study. *Int. J. Psychophysiol.* 93, 253–260. doi: 10.1016/j.ijpsycho.2014.05.006

Limoges, E., Bolduc, C., Berthiaume, C., Mottron, L., and Godbout, R. (2013). Relationship between poor sleep and daytime cognitive performance in young adults with autism. *Res. Dev. Disabil.* 34, 1322–1335. doi: 10.1016/j.ridd.2013.01.013

Limoges, E., Mottron, L., Bolduc, C., Berthiaume, C., and Godbout, R. (2005). Atypical sleep architecture and the autism phenotype. *Brain* 128, 1049–1061. doi: 10.1093/brain/awh425

Manoach, D. S., Pan, J. Q., Purcell, S. M., and Stickgold, R. (2016). Reduced sleep spindles in schizophrenia: a treatable endophenotype that links risk genes to impaired cognition? *Biol. Psychiatry* 80, 599–608. doi: 10.1016/j.biopsych.2015.10.003

Mantini, D., Perrucci, M. G., Cugini, S., Ferretti, A., Romani, G. L., and Del Gratta, C. (2007). Complete artifact removal for EEG recorded during continuous fMRI using independent component analysis. *Neuroimage* 34, 598–607. doi: 10.1016/j.neuroimage.2006.09.037

Martin, N., Lafortune, M., Godbout, J., Barakat, M., Robillard, R., Poirier, G., et al. (2013). Topography of age-related changes in sleep spindles. *Neurobiol. Aging* 34, 468–476. doi: 10.1016/j.neurobiolaging.2012.05.020

McCormick, L., Nielsen, T., Nicolas, A., Ptito, M., and Montplaisir, J. (1997). Topographical distribution of spindles and K-complexes in normal subjects. *Sleep* 20, 939–941. doi: 10.1093/sleep/20.11.939

Melrose, R. J., Poulin, R. M., and Stern, C. E. (2007). An fMRI investigation of the role of the basal ganglia in reasoning. *Brain Res.* 2, 146–158. doi: 10.1016/j.brainres.2007.01.060

Mitchell, A. S., and Chakraborty, S. (2013). What does the mediodorsal thalamus do? *Front. Syst. Neurosci.* 7:37. doi: 10.3389/fnsys.2013.00037

Mölle, M., Bergmann, T. O., Marshall, L., and Born, J. (2011). Fast and slow spindles during the sleep slow oscillation: disparate coalescence and engagement in memory processing. *Sleep* 34, 1411–1421. doi: 10.5665/SLEEP.1290

Mulert, C., and Lemieux, L. (eds). (2009). *EEG(-)fMRI: Physiological Basis, Technique, and Applications*. Berlin: Springer.

Mullinger, K. J., Yan, W. X., and Bowtell, R. (2011). Reducing the gradient artefact in simultaneous EEG-fMRI by adjusting the subject's axial position. *Neuroimage* 54, 1942–1950. doi: 10.1016/j.neuroimage.2010.09.079

Nader, R. S., and Smith, C. (2001). The relationship between stage 2 sleep spindles and intelligence. *Sleep* 24:A160.

Nader, R. S., and Smith, C. (2003). A role for Stage 2 sleep in memory processing. *Sleep Brain Plast.* 1, 87–99. doi: 10.1093/acprof:oso/9780198574002.003.0005

Nichols, T., Brett, M., Andersson, J., Wager, T., and Poline, J.-B. (2005). Valid conjunction inference with the minimum statistic. *Neuroimage* 25, 653–660. doi: 10.1016/j.neuroimage.2004.12.005

Nir, Y., Staba, R. J., Andrillon, T., Vyazovskiy, V. V., Cirelli, C., Fried, I., et al. (2011). Regional slow waves and spindles in human sleep. *Neuron* 70, 153–169. doi: 10.1016/j.neuron.2011.02.043

Peters, A., and Jones, E. G. (eds). (1991). *Normal and Altered States of Function*, Vol. 9. Boston, MA: Springer. doi: 10.1007/978-1-4615-6622-9

Phan, D.-V., Chan, C.-L., Pan, R.-H., Yang, N.-P., Hsu, H.-C., Ting, H.-W., et al. (2018). A study of the effects of daily physical activity on memory and attention capacities in college students. *J. Healthc. Eng.* 2018:2942930. doi: 10.1155/2018/2942930

Piantoni, G., Halgren, E., and Cash, S. S. (2016). Spatiotemporal characteristics of sleep spindles depend on cortical location. *Neuroimage* 146, 236–245. doi: 10.1016/j.neuroimage.2016.11.010

Purcell, S. M., Manoach, D. S., Demanuele, C., Cade, B. E., Mariani, S., Cox, R., et al. (2017). Characterizing sleep spindles in 11,630 individuals from the national sleep research resource. *Nat. Commun.* 8:15930. doi: 10.1038/ncomms15930

Raven, J. C., Court, J. H., and Raven, J. (1976). *Manual for Raven's Progressive Matrices*. San Antonio, TX: Harcourt Assessment.

Ray, L. B., Sockeel, S., Soon, M., Bore, A., Myhr, A., Stojanoski, B., et al. (2015). Expert and crowd-sourced validation of an individualized sleep spindle detection method employing complex demodulation and individualized normalization. *Front. Hum. Neurosci.* 9:507. doi: 10.3389/fnhum.2015.00507

Rechtschaffen, A., and Kales, A. (1968). *Manual of Standardized Terminology, Techniques and Scoring System for Sleep Stages of Human Subjects*. Los Angeles, CA: UCLA Brain Information Service.

Rodriguez-Moreno, D., and Hirsch, J. (2009). The dynamics of deductive reasoning: an fMRI investigation. *Neuropsychologia* 47, 949–961. doi: 10.1016/j.neuropsychologia.2008.08.030

Saletin, J. M., van der Helm, E., and Walker, M. P. (2013). Structural brain correlates of human sleep oscillations. *Neuroimage* 83, 658–668. doi: 10.1016/j.neuroimage.2013.06.021

Sandman, C. A., Head, K., Muftuler, L. T., Su, L., Buss, C., and Poggi, E. (2014). Neuroimage Shape of the basal ganglia in preadolescent children is associated with cognitive performance. *Neuroimage* 99, 93–102. doi: 10.1016/j.neuroimage.2014.05.020

Schabus, M., Dang-Vu, T. T., Albouy, G., Balteau, E., Boly, M., Carrier, J., et al. (2007). Hemodynamic cerebral correlates of sleep spindles during human non-rapid eye movement sleep. *Proc. Natl. Acad. Sci. U.S.A.* 104, 13164–13169. doi: 10.1073/pnas.0703084104

Schabus, M., Dang-Vu, T. T., Heib, D. P. J., Boly, M., Desseilles, M., Vandewalle, G., et al. (2012). The fate of incoming stimuli during NREM sleep is determined by spindles and the phase of the slow oscillation. *Front. Neurol.* 3:40. doi: 10.3389/fneur.2012.00040

Schabus, M., Hödlmoser, K., Gruber, G., Sauter, C., Anderer, P., Klösch, G., et al. (2006). Sleep spindle-related activity in the human EEG and its relation to general cognitive and learning abilities. *Eur. J. Neurosci.* 23, 1738–1746. doi: 10.1111/j.1460-9568.2006.04694.x

Shallice, T. (1982). Specific impairments of planning. *Philos. Trans. R. Soc. B Biol. Sci.* 298, 199–209. doi: 10.1098/rstb.1982.0082

Shibagaki, M., and Kiyono, S. (1983). Duration of spindle bursts during nocturnal sleep in mentally retarded children. *Electroencephalogr. Clin. Neurophysiol.* 55, 645–651. doi: 10.1016/0013-4694(83)90274-2

Shibagaki, M., Kiyono, S., and Watanabe, K. (1982). Spindle evolution in normal and mentally retarded children: a review. *Sleep* 5, 47–57. doi: 10.1093/sleep/5.1.47

Siapas, A. G., and Wilson, M. A. (1998). Coordinated interactions between hippocampal ripples and cortical spindles during slow-wave sleep. *Neuron* 21, 1123–1128.

Silverman, I., Choi, J., Mackewn, A., Fisher, M., Moro, J., and Olshansky, E. (2000). Evolved mechanisms underlying wayfinding. *Evol. Hum. Behav.* 21, 201–213. doi: 10.1016/S1090-5138(00)00036-2

Silverstein, L. D., and Levy, C. M. (1976). The stability of the sigma sleep spindle. *Electroencephalogr. Clin. Neurophysiol.* 40, 666–670. doi: 10.1016/0013-4694(76)90142-5

Srivastava, G., Crottaz-Herbette, S., Lau, K. M., Glover, G. H., and Menon, V. (2005). ICA-based procedures for removing ballistocardiogram artifacts from EEG data acquired in the MRI scanner. *Neuroimage* 24, 50–60. doi: 10.1016/j.neuroimage.2004.09.041

Steriade, M. (2005). Sleep, epilepsy and thalamic reticular inhibitory neurons. *Trends Neurosci.* 28, 317–324. doi: 10.1016/j.tins.2005.03.007

Steriade, M., and Amzica, F. (1998). Coalescence of sleep rhythms and their chronology in corticothalamic networks. *Sleep Res. Online* 1, 1–10.

Stroop, J. R. (1935). Studies of interference in serial verbal reactions. *J. Exp. Psychol.* 18, 643–662. doi: 10.1037/h0054651

Tessier, S., Lambert, A., Chicoine, M., Scherzer, P., Soulières, I., and Godbout, R. (2015). Intelligence measures and stage 2 sleep in typically-developing and autistic children. *Int. J. Psychophysiol.* 97, 58–65. doi: 10.1016/j.ijpsycho.2015.05.003

Treisman, A. M., and Gelade, G. (1980). A feature-integration theory of attention. *Cogn. Psychol.* 12, 97–136. doi: 10.1016/0010-0285(80)90005-5

Tyvaert, L., Levan, P., Grova, C., Dubeau, F., and Gotman, J. (2008). Clinical neurophysiology effects of fluctuating physiological rhythms during prolonged EEG-fMRI studies. *Clin. Neurophysiol.* 119, 2762–2774. doi: 10.1016/j.clinph.2008.07.284

Ujma, P. P. (2018). Sleep spindles and general cognitive ability – a meta-analysis. *Sleep Spindles Cortical Up States* 1–17. doi: 10.1556/2053.2.2018.01 [Epub ahead of print].

Ujma, P. P., Bódizs, R., Gombos, F., Stintzing, J., Konrad, B. N., Genzel, L., et al. (2015). Nap sleep spindle correlates of intelligence. *Sci. Rep.* 5:17159. doi: 10.1038/srep17159

Ujma, P. P., Konrad, B. N., Genzel, L., Bleifuss, A., Simor, P., Pótári, A., et al. (2014). Sleep spindles and intelligence: evidence for a sexual dimorphism. *J. Neurosci.* 34, 16358–16368. doi: 10.1523/JNEUROSCI.1857-14.2014

Ujma, P. P., Sándor, P., Szakadát, S., Gombos, F., and Bódizs, R. (2016). Sleep spindles and intelligence in early childhood–developmental and trait-dependent aspects. *Dev. Psychol.* 52, 2118–2129. doi: 10.1037/dev0000233

Van der Werf, Y. D., Jolles, J., Witter, M. P., and Uylings, H. B. M. (2003). Contributions of thalamic nuclei to declarative memory functioning. *Cortex* 39, 1047–1062. doi: 10.1016/S0010-9452(08)70877-3

Van Der Werf, Y. D., Witter, M. P., Uylings, H. B. M., and Jolles, J. (2000). Neuropsychology of infarctions in the thalamus: a review. *Neuropsychologia* 38, 613–627. doi: 10.1016/S0028-3932(99)00104-9

Vyazovskiy, V. V., Achermann, P., Borbely, A. A., and Tobler, I. (2004). The dynamics of spindles and EEG slow-wave activity in NREM sleep in mice. *Arch. Ital. Biol.* 142, 511–523.

Waltz, J. A., Knowlton, B. J., Holyoak, K. J., Boone, K. B., Mishkin, F. S., de Menezes Santos, M., et al. (1999). A system for relational reasoning in human prefrontal cortex. *Psychol. Sci.* 10, 119–125. doi: 10.1111/1467-9280.00118

Wamsley, E. J., Tucker, M. A., Shinn, A. K., Ono, K. E., McKinley, S. K., Ely, A. V., et al. (2012). Reduced sleep spindles and spindle coherence in schizophrenia: mechanisms of impaired memory consolidation? *Biol. Psychiatry* 71, 154–161. doi: 10.1016/j.biopsych.2011.08.008

Wechsler, D. A. (1981). *Wechsler Adult Intelligence Scale–Revised*. New York, NY: Psychological Corporation.

Wild, C. J., Nichols, E. S., Battista, M. E., Stojanoski, B., and Owen, A. M. (2018). Dissociable effect of self-reported daily sleep duration on high-level cognitive abilities. *Sleep* 41:zsy182. doi: 10.1093/sleep/zsy182

Zeitlhofer, J., Gruber, G., Anderer, P., Asenbaum, S., Schimicek, P., and Saletu, B. (1997). Topographic distribution of sleep spindles in young healthy subjects. *J. Sleep Res.* 6, 149–155. doi: 10.1046/j.1365-2869.1997.00046.x

Conflict of Interest Statement: The authors declare that the research was conducted in the absence of any commercial or financial relationships that could be construed as a potential conflict of interest.

Copyright © 2019 Fang, Ray, Owen and Fogel. This is an open-access article distributed under the terms of the Creative Commons Attribution License (CC BY). The use, distribution or reproduction in other forums is permitted, provided the original author(s) and the copyright owner(s) are credited and that the original publication in this journal is cited, in accordance with accepted academic practice. No use, distribution or reproduction is permitted which does not comply with these terms.

frontiers in Neuroscience

ORIGINAL RESEARCH
published: 03 April 2019
doi: 10.3389/fnins.2019.00312

The Spatiotemporal Pattern of the Human Electroencephalogram at Sleep Onset After a Period of Prolonged Wakefulness

*Maurizio Gorgoni[1], Chiara Bartolacci[1], Aurora D'Atri[1], Serena Scarpelli[1], Cristina Marzano[1], Fabio Moroni[1], Michele Ferrara[2] and Luigi De Gennaro[1,3]**

[1] Department of Psychology, Sapienza University of Rome, Rome, Italy, [2] Department of Biotechnological and Applied Clinical Sciences, University of L'Aquila, L'Aquila, Italy, [3] IRCCS Santa Lucia Foundation, Rome, Italy

During the sleep onset (SO) process, the human electroencephalogram (EEG) is characterized by an orchestrated pattern of spatiotemporal changes. Sleep deprivation (SD) strongly affects both wake and sleep EEG, but a description of the topographical EEG power spectra and oscillatory activity during the wake-sleep transition after a period of prolonged wakefulness is still missing. The increased homeostatic sleep pressure should induce an earlier onset of sleep-related EEG oscillations. The aim of the present study was to assess the spatiotemporal EEG pattern at SO following SD. A dataset of a previous study was analyzed. We assessed the spatiotemporal EEG changes (19 cortical derivations) during the SO (5 min before vs. 5 min after the first epoch of Stage 2) of a recovery night after 40 h of SD in 39 healthy subjects, analyzing the EEG power spectra (fast Fourier transform) and the oscillatory activity [better oscillation (BOSC) detection method]. The spatiotemporal pattern of the EEG power spectra mostly confirmed the changes previously observed during the wake-sleep transition at baseline. The comparison between baseline and recovery showed a wide increase of the post- vs. pre-SO ratio during the recovery night in the frequency bins $\leq$10 Hz. We found a predominant alpha oscillatory rhythm in the pre-SO period, while after SO the theta oscillatory activity was prevalent. The oscillatory peaks showed a generalized increase in all frequency bands from delta to sigma with different predominance, while beta activity increased only in the fronto-central midline derivations. Overall, the analysis of the EEG power replicated the topographical pattern observed during a baseline night of sleep but with a stronger intensity of the SO-induced changes in the frequencies $\leq$10 Hz, and the detection of the rhythmic activity showed the rise of several oscillations at SO after SD that was not observed during the wake-sleep transition at baseline (e.g., alpha and frontal theta in correspondence of their frequency peaks). Beyond confirming the local nature of the EEG pattern at SO, our results show that SD has an impact on the spatiotemporal modulation of cortical activity during the falling-asleep process, inducing the earlier emergence of sleep-related EEG oscillations.

Keywords: sleep onset, sleep deprivation, EEG topography, oscillatory activity, BOSC

OPEN ACCESS

Edited by:
Giulio Bernardi,
IMT School for Advanced Studies Lucca, Italy

Reviewed by:
Stuart Fogel,
University of Ottawa, Canada
Marco Laurino,
Institute of Clinical Physiology (IFC), Italy

***Correspondence:**
Luigi De Gennaro
luigi.degennaro@uniroma1.it

Specialty section:
This article was submitted to Sleep and Circadian Rhythms, a section of the journal Frontiers in Neuroscience

Received: *23 January 2019*
Accepted: *19 March 2019*
Published: *03 April 2019*

Citation:
Gorgoni M, Bartolacci C, D'Atri A, Scarpelli S, Marzano C, Moroni F, Ferrara M and De Gennaro L (2019) The Spatiotemporal Pattern of the Human Electroencephalogram at Sleep Onset After a Period of Prolonged Wakefulness. Front. Neurosci. 13:312. doi: 10.3389/fnins.2019.00312

INTRODUCTION

Sleep is widely considered as a local and use-dependent process, since regional patterns of activation and deactivation coexist in the brain during sleep, and recent evidence suggests that large regional heterogeneities also occur during specific transitional states (for review see Ferrara and De Gennaro, 2011; Siclari and Tononi, 2017). Indeed, the sleep onset (SO) period represents a complex phenomenon of transition between two different functional states (i.e., wakefulness and sleep) of the brain in which the fluctuation of consciousness seems to result from topographically heterogeneous cortical activities (Gorgoni et al., 2019). In particular, the falling-asleep process is characterized by: (a) wide regional and temporal frequency-specific changes in the scalp electroencephalogram (EEG) (De Gennaro et al., 2001a,b; Marzano et al., 2013; Siclari et al., 2014); (b) asynchronies between cortical and deep structures in the appearance of sleep rhythms (Magnin et al., 2010; Sarasso et al., 2014); (c) modifications of the dynamic interactions between functionally specialized regions (De Gennaro et al., 2004; Larson-Prior et al., 2009; Vecchio et al., 2017; Fernandez Guerrero and Achermann, 2018); (d) changes in cerebral metabolic activity (Kjaer et al., 2002; Kotajima et al., 2005; Horovitz et al., 2008).

At the scalp level, the human EEG power spectra at SO show the cohabitation of wake-like and sleep-like activities, with an earlier synchronization of the fronto-central areas expressed by the anterior increase of the slow-wave activity (SWA), a temporo-occipital diffusion in the theta frequency range, a shift from a posterior to an anterior prevalence of the alpha activity, an increase in the sigma frequency range mostly at a centro-parietal level and a generalized decrease in the beta frequency (Marzano et al., 2013). The direct assessment of the genuine oscillatory nature of the EEG at SO by means of the application of the Better OSCillation detection method (BOSC analysis; Caplan et al., 2001; Whitten et al., 2011) suggested that the pattern of synchronization during SO apparently does not include alpha and frontal theta oscillations (Marzano et al., 2013). However, we cannot exclude that these unexpected findings were due to the short window considered for the SO period (i.e., the two 5-min intervals before and after the first epoch of stage 2), which could make not viable the observation of specific EEG oscillatory activities with a more delayed build-up.

What is still missing is the description of the spatial and temporal modification of the EEG power spectra and rhythmic oscillations at SO after a period of prolonged wakefulness. It is well-known that sleep deprivation (SD) strongly affects the human EEG during wake (Finelli et al., 2000; Tinguely et al., 2006; De Gennaro et al., 2007; Gorgoni et al., 2014) and recovery sleep (Cajochen et al., 1999; Finelli et al., 2001; Tinguely et al., 2006; Marzano et al., 2010), mainly with a generalized increase of the slowest frequencies. Moreover, SD also has an influence on the EEG activity during the transition from recovery sleep to wake (i.e., the process of awakening) (Tassi et al., 2006; Gorgoni et al., 2015). Surprisingly, albeit several findings underlined that a period of prolonged wakefulness induced marked changes in functional coupling (De Gennaro et al., 2005), effective connectivity (Fernandez Guerrero and Achermann, 2018) and in the brain dynamics assessed with EEG source localization (Fernandez Guerrero and Achermann, 2019) during the wake-sleep transition, the effect of SD on the SO-related scalp topographical changes in the EEG power and oscillatory activity has been not systematically studied. Since SD induces (a) an acceleration of the baseline electrophysiological dynamics at SO (De Gennaro et al., 2005; Fernandez Guerrero and Achermann, 2019) and (b) an increase of the delta, theta and alpha activity during REC sleep (Marzano et al., 2010), we hypothesize that the higher homeostatic sleep pressure should determine an earlier onset of oscillatory EEG changes during the falling-asleep process that usually occurs later during a night of sleep under normal conditions. If this is true, we should observe a greater concordance between spectral and oscillatory data: while in the BSL night the spectral power and the oscillatory activity differed because no post-SO changes were observed in the alpha and frontal theta oscillatory peaks (Marzano et al., 2013), SD should provoke an earlier build-up of the alpha and theta oscillations, mirroring the increase in the spectral power in these frequency bands.

The aim of the present study was to assess the wake-sleep transition after 40 h of SD in the same 40 healthy subjects previously investigated at BSL (Marzano et al., 2013). We assessed the single-Hz changes in spatial EEG at SO and the temporal dynamics of the frequency bands before and after SO. Subsequently, we used the BOSC method which measures oscillatory activity within an EEG signal containing a non-rhythmic portion, in order to detect sleep EEG oscillations before and after SO, and then their spatial and temporal variations have been investigated.

MATERIALS AND METHODS

Participants

Data for the present analyses were obtained by the sample of previous studies (Marzano et al., 2010, 2013). Forty right-handed healthy subjects (20 males and 20 females; age range = 18–29, mean age = 23.8 $\pm$ 2.88 years) were selected from a university student population. The inclusion criteria were: normal sleep duration and schedule (habitual sleep time: midnight-8:00 am $\pm$ 1 h), no daytime nap habits, no excessive daytime sleepiness, no other sleep, medical, neurological or psychiatric disorder, as assessed by a 1-week sleep log and by a clinical interview. Participants were required to avoid napping throughout the experiment; compliance was controlled by actigraphic recordings (AMI Mini motion logger). One subject was excluded from the analyses because he did not show artifact-free epoch before the SO. Therefore, analyses were conducted on 39 subjects.

All subjects gave their written informed consent. The study was approved by the Institutional Ethics Committee of the Department of Psychology of "Sapienza" University of Rome and was conducted in accordance with the Declaration of Helsinki.

Procedure

After 2 weeks of regular sleep/wake habits monitored with sleep log and (in the last 2 days before the beginning of the study) actigraphic recordings, subjects participated in a sleep/wake protocol across four consecutive days and nights. Sleep was recorded during the first night (adaptation), the second night [baseline (BSL)], and the fourth night [recovery (REC)]. After awakening from BSL sleep, a protocol of 40-h SD started at 10.00 am. For the purposes of the present study, the main analyses have been performed on the REC night, while the BSL condition has been considered only for the comparison of polysomnographic (PSG) measures and post- vs. pre-SO changes in the EEG power topography.

Sleep recordings have been carried out in a sound-proof, temperature-controlled room. The subjects' sleep was undisturbed, started at midnight, and ended after 7.5 h of accumulated sleep (as visually checked online by expert sleep researchers).

Polysomnographic Recordings

An Esaote Biomedica VEGA 24 polygraph was used for PSG recordings. EEG signals were analogically filtered (high-pass filter at 0.50 Hz and antialiasing low-pass filter at 30 Hz [−30 dB/octave]). The 19 unipolar EEG derivations of the international 10–20 system (Fp1, Fp2, F7, F8, F3, F4, Fz, C3, C4, Cz, P3, P4, Pz, T3, T4, T5, T6, O1, O2) were recorded from scalp electrodes with averaged mastoid reference. The submental electromyogram (EMG) was recorded with a time constant of 0.03 s. Bipolar horizontal electrooculogram (EOG) was recorded from electrodes placed approximately 1 cm from the medial and lateral canthi of the dominant eye with a time constant of 1 s. The impedance of these electrodes was kept below 5 kOhm.

Data Analysis

PSG and Quantitative Analyses of EEG Signals

The midline central EEG derivation (Cz), EMG, and EOG were used to visually score sleep stages in 12-s epochs, according to the standard criteria (Rechtschaffen and Kales, 1968). PSG measures were submitted to paired *t*-tests comparing BSL and REC nights (alpha level = 0.05).

The polygraphic signals (19 EEG channels, EOG, and EMG) were analog-to-digital converted online with a sampling rate of 128 Hz and stored on the disk of a personal computer. We considered the 0.50- to 25.00-Hz frequency range, computing power spectra by a fast Fourier transform (FFT) routine for 4-s periodograms. Spectra from three consecutive 4-s epochs were averaged to allow alignment with the visual scoring of sleep stages, based on 12-s epochs. EEG topography was evaluated by comparing the 5-min pre-SO vs. post-SO intervals. Ocular and muscle artifacts were carefully excluded offline by visual inspection. Epochs in which eyes were open were also excluded. After the exclusion of the artifacts, the mean duration of the REC falling-asleep period (pre- and post-SO) included in the spectral analysis was 5.95 ± 0.98 min (range: 3.4–8.8 min). Individual time series of EEG power values were aligned as a function of the first epoch of sleep defined on the basis of the appearance of the first K-complex or sleep spindle. Data analysis was mostly performed with the software package MATLAB (The Mathworks, Inc., Natick, MA, United States) and its signal analysis and statistics toolbox.

Single-Hz EEG Topography

Data were reduced to a 1-Hz bin width by collapsing four adjacent 0.25-Hz bins before statistical analyses. The only exception was the 0.50- to 1.00-Hz bin, for which two adjacent 0.25-Hz bins were collapsed. The bins were referred to and plotted by the center frequency included in our study (e.g., the 2-Hz bin referred to the averaged values of the following bins: 2.00, 2.25, 2.50, and 2.75 Hz). The log-transformed EEG power values for each 1-Hz frequency bin of the REC night were considered as dependent measures and compared in the 5-min pre- and post-SO intervals by paired *t*-tests. As a standard procedure for EEG power, this log-transformation reduces violations of normality.

With the aim to assess the influence of SD on the magnitude of the SO-related topographical changes, we also compared the post- vs. pre-SO ratio of the raw EEG power between the REC and the BSL night for each frequency bin. Such comparison was computed using the Wilcoxon signed-rank tests, since only 52% of our data had a normal distribution (Lilliefors test). The difference between REC and BSL post- vs. pre-SO ratio has been calculated with the aim to depict the direction of the findings.

For every statistical comparison performed on topographical data, the Bonferroni correction for multiple comparisons was applied.

Time Course of the EEG Frequency Bands

Due to the variable length of the pre-SO and post-SO intervals and of the first sleep cycle, we adopted for the REC night the procedure previously used for the analysis of the time course during SO at BSL (Marzano et al., 2013) to make the individual time courses comparable: (1) the individual time courses were aligned as a function of the first spindle or K-complex; (2) the time series of 12-s epochs during the pre-SO interval were divided into five segments, while the post-SO time series were divided into 20 segments (percentiles); and (3) we removed epochs with muscle, movement, or ocular artifacts and averaged individual time courses across subjects. In this way, each pre- and post-SO interval represented a fifth and a 20th percentile of the total pre- and post-sleep intervals, respectively. Neither skipped first REM sleep episodes nor SO REM sleep episodes were present in our recordings.

For the five time intervals preceding and following SO, EEG power maps were computed for the following frequency EEG bands: delta (0.50–4.75 Hz), theta (5.00–7.75 Hz), alpha (8.00–11.75 Hz), sigma (12.00–15.75 Hz), and beta (16.00–24.75 Hz). Power maps at the 10th, 15th, and 20th time intervals were also calculated, with the aim to provide a synoptic description of the kinetics of EEG topography across the first sleep cycle.

Detection of Oscillatory Activity

As previously observed (Marzano et al., 2013), the FFT algorithm of the EEG signal does not necessarily imply an underlying oscillatory activity at that specific frequency. The FFT is mainly

designed for stationary and regular signals and is characterized by a limited time-frequency resolution. However, the EEG pattern during the SO period is more likely characterized by changes in oscillatory (non-stationary) activity. For this reason, we also applied to the EEG signals of the REC night the BOSC detection method introduced by Caplan et al. (2001). BOSC is considered a powerful method to detect oscillatory neural activity minimizing bias across frequencies, electrodes, tasks, electrophysiological states and species (Whitten et al., 2011). This method is aimed to detect oscillatory activity within an EEG signal containing a non-rhythmic portion, considering the functional form of the background non-rhythmic portion of the signal and revealing segments of the recording that significantly deviate from the spectral characteristics of the background. We recently applied the BOSC method to detect oscillatory activity during wake (D'Atri et al., 2015), NREM and REM sleep (Marzano et al., 2011; Moroni et al., 2012; Scarpelli et al., 2015) and in the wake-sleep transition at BSL (Marzano et al., 2013).

The analysis was separately performed for each frequency of interest (in the 0.50–24.25-Hz range), cortical derivation and 5-min time segment before and after SO, and then averaged across subjects. For each frequency, an oscillatory episode was defined as an epoch longer than a duration threshold (DT, set to three cycles in our analysis) during which wavelet power at frequency exceeded a power threshold (PT). BOSC identifies a power increase, above PT, of a minimum duration (DT), rejecting transient events that are not oscillatory but can induce increases in the spectral power that may be erroneously considered as rhythmic activity. This PT threshold was chosen as follows in the selected segments before and after SO: (1) the EEG was wavelet transformed (Morlet wavelet, window = 6 cycles) at 47 logarithmically spaced frequencies in the 0.50- to the 24.25-Hz range. The average of the log-transform of these wavelet values yielded the wavelet power spectrum; (2) the background noise spectrum assumed the form Power(f) = A$f^{-\alpha}$. We used two different fits of background window for pre- and post-SO periods. The estimate of this background has been obtained by fitting the observed spectrum at each electrode with a linear regression in the log to log units. The background at f^* has been estimated on the mean of its corresponding $\chi^2(2)$ probability distribution function. The power threshold (P_T) was set to the 95th percentile of the theoretical probability distribution. The proportion of time in which significant oscillations were detected before and after SO is termed $P_{episode}$ (Caplan and Glaholt, 2007).

As previously done for the BSL night (Marzano et al., 2013), to provide a statistical assessment of the SO-related topographical changes in the oscillatory activity during the REC night, for the frequency peak of each band we compared the proportion of time in which significant oscillations were detected in the pre-SO and post-SO periods, separately for each cortical derivation. Since the majority of the derivations (74%) showed a normal distribution (Lilliefors test) and given the robustness of parametric t-tests to violation of normality (Siclari et al., 2017), we used paired t-tests.

Finally, the time course of the values of $P_{episode}$ resulting from five pre-SO and post-SO time intervals was reported for each frequency and scalp location.

RESULTS

PSG Measures

Table 1 reports the results of the comparisons (paired t-tests) between PSG measures of BSL and REC nights. The macrostructural variables of sleep point to a pattern of significant differences between BSL and REC nights, representing the typical consequences of a night of SD: REC night was characterized by a shortening in the latency of NREM sleep stages, by an increase of the percentage of SWS and a decrease of stage 1, by a decreased percentage of WASO, number of awakenings and arousals; sleep efficiency was increased, while TBT was significantly decreased; with respect to REM sleep, its latency did not change, while its amount during REC sleep decreased.

Single-Hz EEG Topography

Figure 1 shows the topographic distribution of the EEG power before and after SO during the REC night and their comparison (ratio and t-values). We found a significant ($p \leq 0.0005$ corresponding to $t \geq 3.79$ after the Bonferroni correction) differences between pre- and post-SO in all cortical derivations in the $\leq$8 Hz frequency range, in the direction of a power increase after SO. The EEG power under 2 Hz exhibited a clear prevalence in the anterior regions both before and after SO, and the widespread significant increase of EEG power after SO in this frequency range reached its maximum in the left fronto-temporal area (2 Hz bin) and the centro-parietal derivations (0.5 and 1 Hz bins). The EEG topography in the 3–4 Hz bins showed a central prevalence before and after SO, but the statistical comparisons pointed to frontal maxima. The theta frequency range (5–7 Hz) also exhibited a maximal EEG power in the central area both

TABLE 1 | Polysomnographic measures.

Variables	*BSL*		*REC*		*t*(1,38)	*p*
	Mean	***SD***	**Mean**	***SD***		
Stage 1 latency (min)	6.73	5.81	1.93	2.09	5.8	**0.0001**
Stage 2 latency (min)	11.40	11.46	3.27	2.37	4.8	**0.0001**
Stage 1 (%)	6.36	2.94	2.85	1.71	8.84	**0.0001**
Stage 2 (%)	59.25	6.76	58.65	8.48	0.6	0.55
Stage 3 (%)	7.75	3.77	11.87	3.89	7.73	**0.0001**
Stage 4 (%)	2.21	3.27	5.89	6.01	6.32	**0.0001**
SWS (%)	9.96	6.06	17.76	7.71	11.94	**0.0001**
REM (%)	24.42	4.42	20.74	5.73	4.15	**0.0002**
WASO (min)	26.44	19.30	11.69	7.66	4.96	**0.0001**
Awakenings (#)	28.67	10.74	20.51	7.61	5.61	**0.0001**
Arousals (#)	35.54	17.79	26.18	18.74	3.16	**0.003**
TST (min)	440.90	39.03	449.30	20.27	1.49	0.14
TBT (min)	476.98	40.69	463.61	21.98	2.21	**0.03**
SEI % (TST/TBT)	92.51	4.21	96.92	1.72	6.51	**0.0001**

Means and standard deviations (SD) of the PSG variables, during baseline (BSL) and recovery (REC) nights in 39 subjects. The results of paired t-tests are also reported. SWS, slow-wave sleep; REM, rapid eye movement; WASO, wake after sleep onset; TST, total sleep time; TBT, total bed time; SEI, sleep efficiency index. Significant results ($p < 0.05$) were reported in bold.

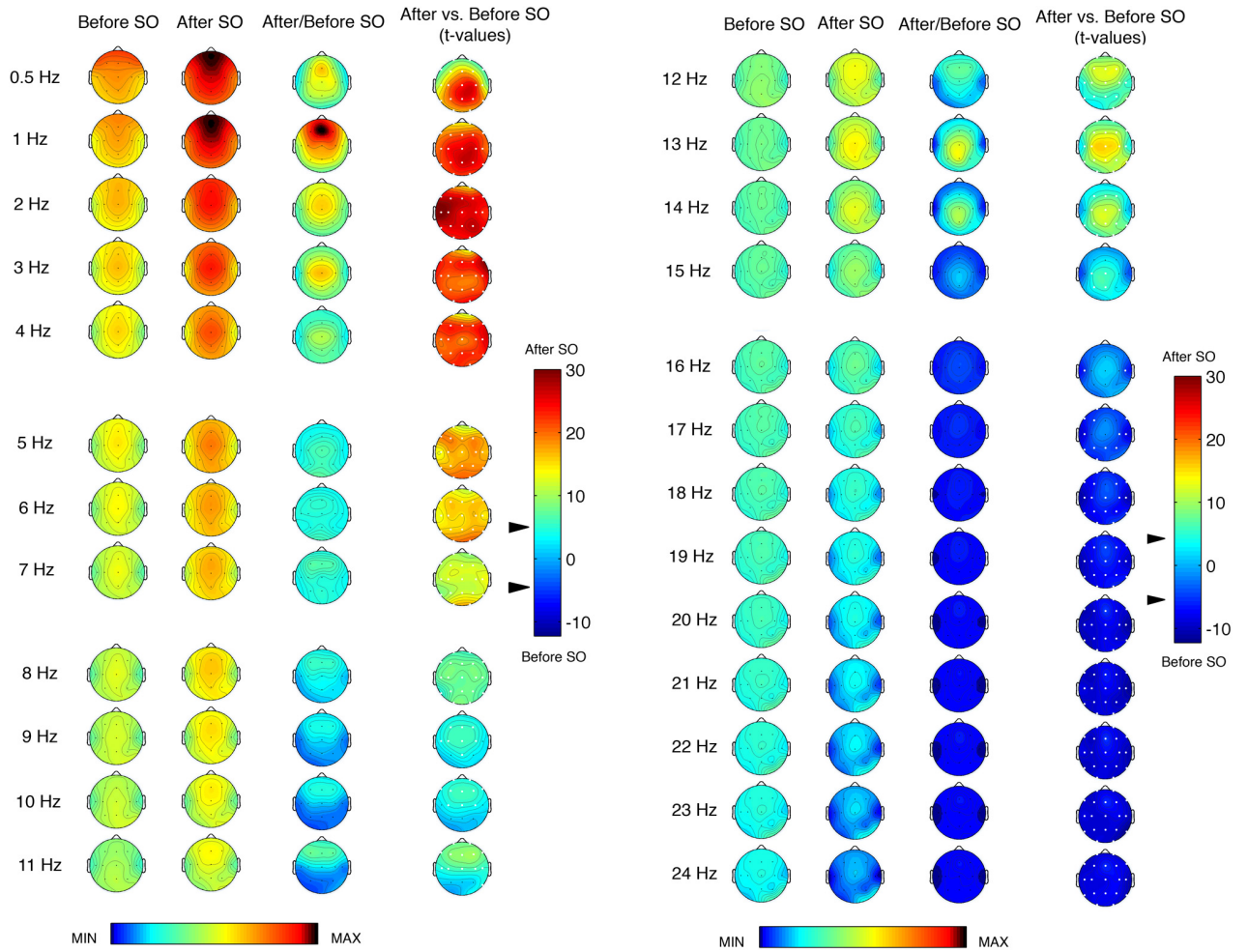

FIGURE 1 | Single-Hz electroencephalographic (EEG) topography (left side, frequency range = 0.50–11 Hz; right side, frequency range = 12–24 Hz) at sleep onset (SO) after a period of prolonged wakefulness. In both halves of the figure, the first two columns show the topographic distribution of absolute EEG power in the 5-min intervals before SO and after SO, respectively. The maps were scaled between minimal (min) and maximal (max) values calculated for all frequencies and derivations in before SO and after SO periods. The third column shows the relative EEG changes expressed as the ratio between after SO and before SO periods. The maps were scaled between min and max values in before SO and after SO periods. The fourth column depicts the topographical statistical EEG power differences (assessed by paired *t*-tests) between these 5-min periods. Values are expressed in *t*-values: positive *t*-values indicate a prevalence of the after SO period and vice versa. The two-tailed level of significance is indicated by the arrow in correspondence of the *t*-values color bar ($p \leq 0.0005$ corresponding to $t \geq 3.79$ after the Bonferroni correction). White dots indicate significant differences after the Bonferroni corrections. Values are color-coded and plotted at the corresponding position on the planar projection of the scalp surface and are interpolated (biharmonic spline) between electrodes. The maps are based on the 19 unipolar EEG derivations of the international 10–20 system with averaged mastoid reference, and they are plotted for each frequency Hz bin in the 0.50- to the 24.75-Hz range.

before and after SO, and the *t*-values maps pointed to a larger post-SO increase in the occipital region.

The EEG power topography in the 8–12 Hz frequency range was characterized by a transition from a posterior prevalence before SO to a frontal prevalence after SO. The statistical comparisons showed a post-SO significant increase in all cortical areas at 8 and 12 Hz, and in the fronto-central areas in the frequency bins between 9 and 11 Hz, extended to the temporal (9 Hz: T3; 11 Hz: T3, T4, T6) and parietal (9 Hz: Pz) derivations. All these frequency bins showed a maximum post-SO increase in the frontal region.

The sigma frequency range (13–15 Hz) was characterized by marked differences between pre- and post-SO, due to the scoring of SO as the first epoch of stage 2. Such differences, all in the direction of a post-SO increase, reached the statistical significance in all cortical derivations at 13 Hz, in a wide number of derivations at 14 Hz (C3, C4, Cz, F3, F4, Fz, O1, O2, P3, P4, Pz, T5, T6) and in some centro-parietal locations at 15 Hz (C3, Cz, P3, Pz). Prevalence in the midsagittal centro-parietal areas was detectable in all these frequency bins.

While the significant difference between pre- and post-SO in the $\leq$15 Hz frequencies pointed to a power increase after SO, in the $\geq$16 Hz frequency range we observed a change in the direction of these differences, that is a post-SO power decrease. In the 16 Hz bin, such power decrease reached the statistical significance only in two temporal derivations (T3, T4). The 17

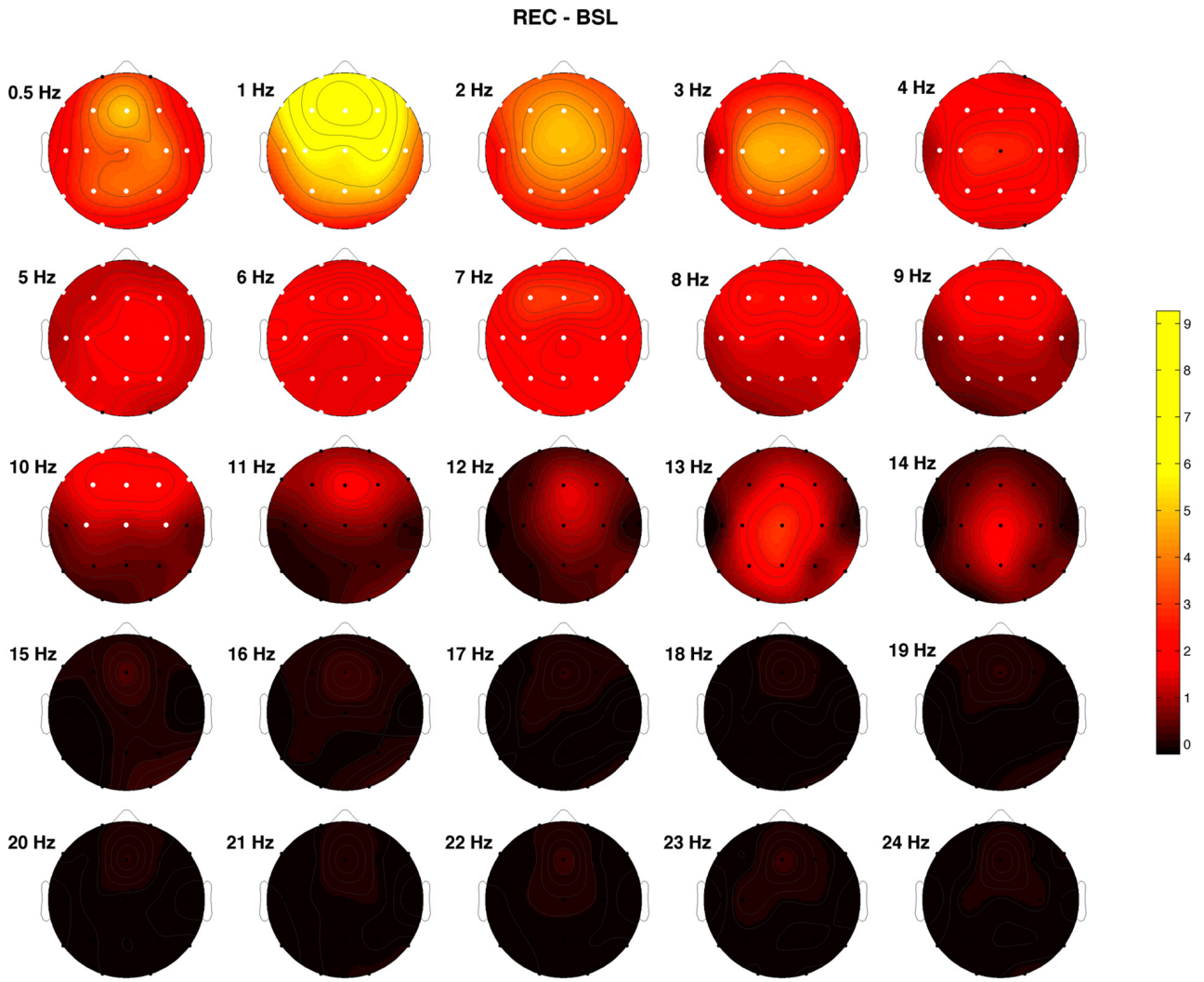

FIGURE 2 | Topographical EEG power differences between recovery (REC) and baseline (BSL) conditions performed on the relative EEG changes expressed as the ratio between after SO and before SO periods (post-SO/pre-SO). Positive values indicate a higher post-SO/pre-SO ratio in the REC condition and vice versa. White dots indicate significant differences at the Wilcoxon signed-rank tests after the Bonferroni corrections ($p \leq 0.0003$). Values are color-coded and plotted at the corresponding position on the planar projection of the scalp surface and are interpolated (biharmonic spline) between electrodes. The maps are based on the 19 unipolar EEG derivations of the international 10–20 system with averaged mastoid reference, and they are plotted for each frequency Hz bin in the 0.50- to 24.75-Hz range.

and 18 Hz frequencies showed a widespread significant power decrease after SO, and in the ≥19 Hz frequencies these significant changes concerned to all cortical derivations, without a specific topographical prevalence.

Figure 2 shows the difference between REC and BSL night concerning the post-SO/pre-SO ratio of the raw EEG power. White dots indicate the significant differences at the Wilcoxon signed-rank tests after Bonferroni correction ($p \leq 0.0003$). A significantly higher ratio in the REC condition was observed in the frequency bins ≤9 Hz in all (1–3, 6 and 7 Hz) or almost all (0.5, 4 and 5, 8 and 9 Hz) cortical derivations, and in the 10 Hz bin at a fronto-central level (F1, F2, F3, F4, F7, F8, Fz, C3, C4, Cz), representing an index of higher synchronized activity (i.e., higher sleep pressure) during the REC night.

Time Course of EEG Frequency Bands

Figure 3 depicts the time course of the EEG power across the SO point and during the first NREM sleep episode of the REC night. The delta activity showed a gradually increasing fronto-central prevalence in the pre-SO intervals. After SO, a phenomenon of anteriorization of this frequency range was clearly visible, with maximal power values over the midsagittal frontal derivation, that decreased only in close proximity to the end of the first NREM episode (i.e., the time interval just before the 20th percentile).

The theta frequency range was characterized by a growing fronto-central prevalence before and after SO. An increase in the occipital area was visible in close proximity to SO and persisted across the first NREM sleep episode.

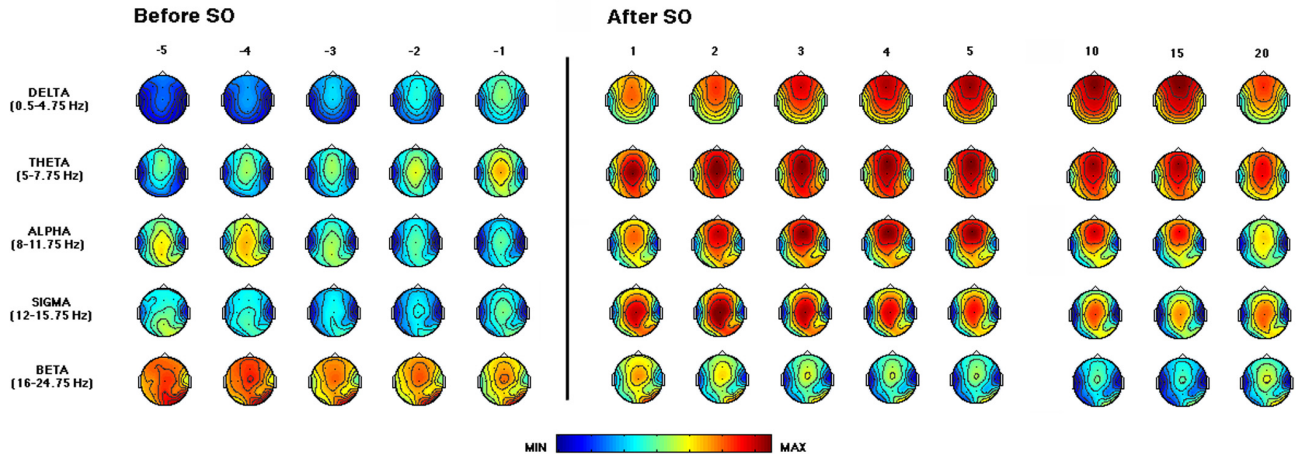

FIGURE 3 | Time course of EEG frequency bands during the recovery (REC) night. From the left, topographic EEG shows changes across the interval preceding SO (i.e., from the lights-off to the first epoch of sleep). The power maps obtained by subdividing the pre-SO interval into five equal parts (from the -fifth to -first). Data were calculated for each subject and then averaged across subjects. After the vertical line, indicating the first epoch of stage 2 sleep, the first five intervals after SO (from the first-fifth) are plotted. The last three columns on the right side show power maps at the 10th, 15th, and 20th time intervals calculated across the first sleep cycle. Values are color-coded and plotted at the corresponding position on the planar projection of the scalp surface and are interpolated (biharmonic spline) between electrodes. The maps are based on the 19 unipolar EEG derivations of the international 10–20 system with averaged mastoid reference. Maps are plotted for the following EEG bands: delta (0.50–4.75 Hz), theta (5.00–7.75 Hz), alpha (8.00–11.75 Hz), sigma (12.00–15.75 Hz), and beta (16.00–24.75 Hz).

The alpha activity showed a centro-posterior prevalence in the pre-sleep intervals that progressively decreases, while after SO we observed a gradual increase in this frequency range, particularly in fronto-central areas, that showed a reduction only at the end of the first NREM episode.

The sigma frequency range exhibited a marked increase after SO, with a clear centro-parietal localization, as expected since the operational definition of SO.

The beta activity showed fronto-central and occipital prevalence, and its power progressively decreased across the SO point.

Detection and Topography of Oscillatory Activity

The EEG oscillatory activity averaged across all the derivations during the SO of the REC night is illustrated in **Figure 4**, while **Figure 5** depicts its topographical modulation. Pre-sleep EEG was characterized by a prevalent alpha oscillatory activity, with a peak at 9.85 Hz, followed by the theta and beta activity, peaking at 6.06 and 18.38 Hz, respectively. The oscillation of the delta activity was already present. In the post-SO period, the prevalence of the theta range was visible, with a peak at 7.46 Hz, followed by sigma (peak at 12.12 Hz) and delta (peak at 3.73 Hz) activity. At a topographical level (**Figure 5**), pre-SO alpha showed a prevalence in posterior areas, and post-SO theta activity had a clear occipital predominance. Delta oscillatory activity $\leq$ 2 Hz had a frontal predominance after SO, while at 3–4 Hz it was more evident at central areas in both pre- and post-SO conditions.

Figure 6 shows the topographical maps of the comparison (*t*-test) between pre-SO and post-SO intervals in the frequency peak of each band, concerning the proportion of time in which significant oscillations were detected. Results showed a significant ($p \leq 0.001$ corresponding to $t \geq 3.55$ after Bonferroni correction) increase of all frequency peaks after SO in the whole scalp topography, except the beta band that significantly increased only in the midline centro-parietal derivations (Cz; Pz). The delta and theta activity showed a prevalence in posterior areas, reaching their maximum in the left occipital derivation, while alpha and sigma activity showed a more evident increase in the frontal locations.

Time Course of the Oscillatory Activity

Figure 7 depicts the time course of the oscillatory activity across the SO point of the REC night. The pre-sleep period was characterized by a generalized slight prevalence of the alpha oscillations, that gradually shift in the direction of a theta predominance just before SO, particularly evident in the cortical derivations along the midline. After SO, a wide increase of the oscillatory activity in the frequency bands between delta and sigma was observed, albeit with different topography and intensity. The occipital regions were characterized by an increasing post-SO prevalence of the theta oscillations, progressively extended to the delta range. In the parietal area, the sleep period was steadily dominated by delta and theta oscillations, with a progressive increase in alpha and sigma activities and in the slowest frequency bins. According to an anteroposterior gradient, delta oscillations dominated the post-SO period in frontal and central areas and became stronger with time. Alpha and sigma activities showed a wide and progressive increase during the sleep period, while beta oscillations mostly disappeared, albeit the slowest bins in the beta rage exhibited a stable level after SO.

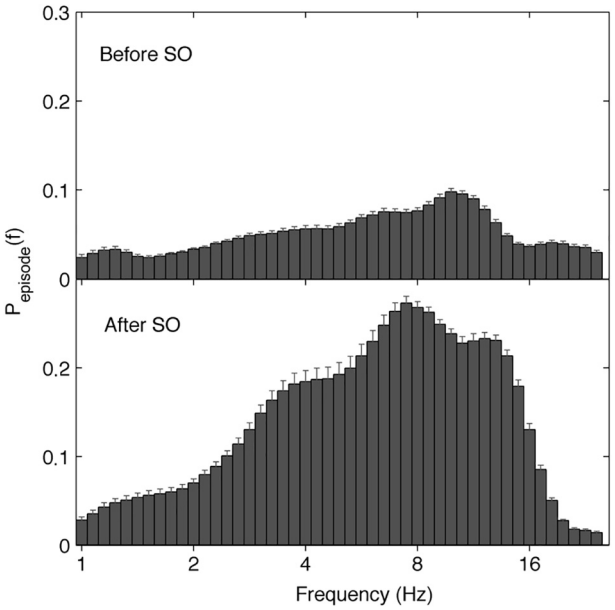

FIGURE 4 | Electroencephalographic oscillations averaged across the whole derivations at SO during the recovery (REC) night. The figure plots the mean proportion of time ($P_{episode}$ [*f*]) of the EEG before (upper panel) and after (lower panel) SO in which oscillations were detected at each frequency. The detection of oscillations has been made by the better oscillation detection method (see section Materials and Methods) on the 19 EEG electrodes. Error bars denote interlocation variability. Units of frequency are expressed in Hz and are plotted in 47 logarithmically spaced frequency values in the 0.50- to 24.25 Hz frequency range.

DISCUSSION

To the best of our knowledge, this is the first study to describe the complete topography of the EEG power spectra and oscillatory activity across the wake-sleep transition after SD.

The spatio-temporal dynamic of the EEG power at SO after prolonged wakefulness substantially replicated findings in the wake-sleep transition during the BSL night in the same sample (Marzano et al., 2013), suggesting that SD does not alter the topographical pattern of the EEG power at SO. Interestingly, also the assessment of effective connectivity during the wake-sleep transition shows changes after SO qualitatively similar in the BSL and REC conditions (Fernandez Guerrero and Achermann, 2018). On the other hand, the direct comparison between REC and BSL revealed a generalized increase after SD of the post- vs. pre-SO ratio of the EEG power in the bins $\leq$9 Hz, that became fronto-centrally localized at 10 Hz. This finding suggests that a period of prolonged wakefulness increases the intensity of the SO-induced topographical EEG changes with an exacerbation of the EEG synchronization process, representing a sign of the higher homeostatic sleep need, in the absence of strong differences in the higher frequencies.

Concerning the analysis of the rhythmic oscillations, we found that SD had an influence on the modulation of the oscillatory activity during the falling-asleep process. Considering the average oscillatory activity across derivations, we found in the REC night that the theta rhythm was prevalent after SO, followed by sigma and delta rhythms, while the post-SO period at BSL (Marzano et al., 2013) was characterized by a dominant sigma oscillatory activity. These phenomena were topographically and temporally modulated, substantially confirming the EEG power findings. The topographic distribution of the frequency peaks of oscillatory activity showed a generalized increase after SO in all frequency bands from delta to sigma, albeit with different predominance (centro-posterior for delta activity, occipital for theta activity, anterior for alpha and sigma rhythms), while beta rhythm significantly increased only in the midline centro-parietal derivations. As expected, the procedure of SD induced an increase of alpha and frontal theta oscillatory activity in their frequency peaks after SO, not observed in normal conditions (Marzano et al., 2013), showing more consistent results between FFT and BOSC analysis compared to BSL. Our results support the hypothesis that the short window considered for the SO period (i.e., the two 5-min intervals before and after the first epoch of stage 2) may make difficult to detect several EEG oscillatory activities with a more delayed build-up (alpha and frontal theta) during a normal night of sleep, while the increased homeostatic sleep pressure after prolonged wakefulness leads to an earlier onset of such sleep-related rhythmic oscillations.

Delta Activity

Delta power exhibited its classical fronto-central prevalence and a strong and generalized increase after SO, with the time course of this effect pointing to a progressive anteriorization that begins before the SO point. Changes in this frequency band represent the most prominent and fastest SO-related EEG power modifications, confirming and extending to a REC condition the previous findings in a normal night of sleep (De Gennaro et al., 2001a,b; Marzano et al., 2013).

The comparison between BSL and REC conditions showed a global increase of the post- vs. pre-SO ratio in the delta frequency bins, consistent with the consolidated role of sleep SWA as the marker of homeostatic sleep need after prolonged wakefulness (for a review see Achermann and Borbély, 2017).

The assessment of the oscillatory activity substantially confirmed the results obtained with the FFT, revealing a generalized enhancement of delta rhythm in its frequency peak during sleep, albeit with a peculiar maximum increase in the occipital area. However, the detailed topographical distribution of the EEG oscillations (**Figure 5**) showed that frontal, central and parietal areas exhibited a genuine peak of the delta oscillations after SO, while in the occipital region the great oscillatory activity around 3.73 Hz appeared as a by-product of the prevalent theta peak.

It is worth noting that, according to several findings, the SO process seems characterized by the consecutive emergence of different types of slow waves (Siclari et al., 2014; Spiess et al., 2018), and the EEG power maps and sources of several sub-bands in the delta range were differentially affected by SD during the first NREM sleep episode (Bersagliere et al., 2018). Such findings suggest the need for a more detailed characterization of

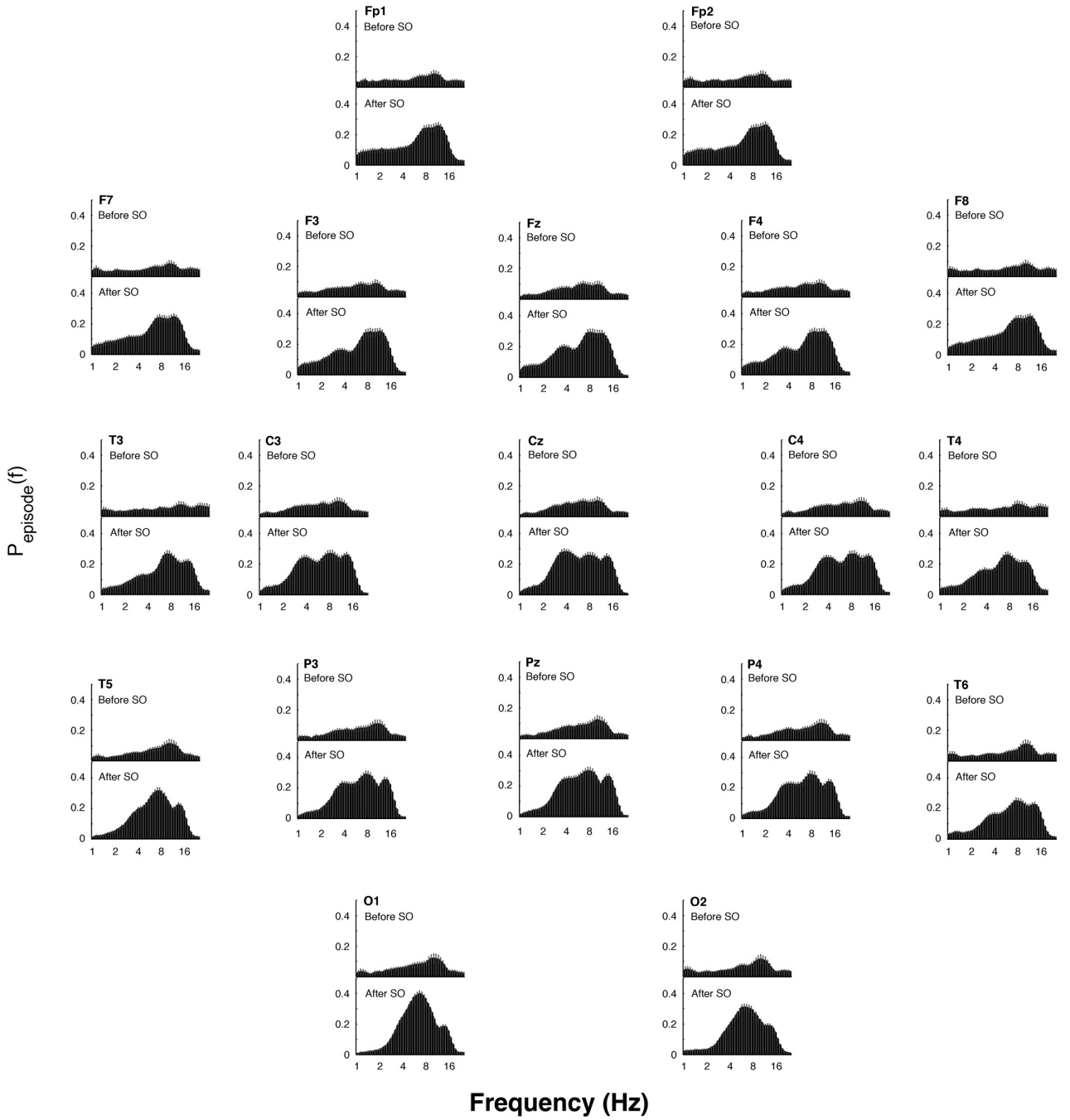

FIGURE 5 | Topographic distribution of the EEG oscillations detailed by the better oscillation method during the 5-min segments before and after SO (upper and lower panels, respectively) in the recovery (REC) night. The mean proportion of time ($P_{episode}$ [*f*]) of the EEG before and after SO in which oscillations were detected for each scalp location is plotted. Error bars denote intersubject variability. Units of frequency are expressed in Hz and are plotted in 47 logarithmically spaced frequency values in the 0.50- to 24.25 Hz frequency range.

the spatio-temporal dynamics of the different kinds of slow waves at SO after sustained wakefulness in future studies.

Theta Activity

The spatio-temporal pattern of the theta power was mostly similar to that observed in the delta range, with a global power increase after SO and a progressive fronto-central consolidation, consistently with BSL findings (Marzano et al., 2013).

Electroencephalogram activity in the theta frequency range was one of the most affected by SD. Similar to the delta range, theta power exhibited a widespread increase of the post-SO changes in the REC compared to the BSL condition. Theta

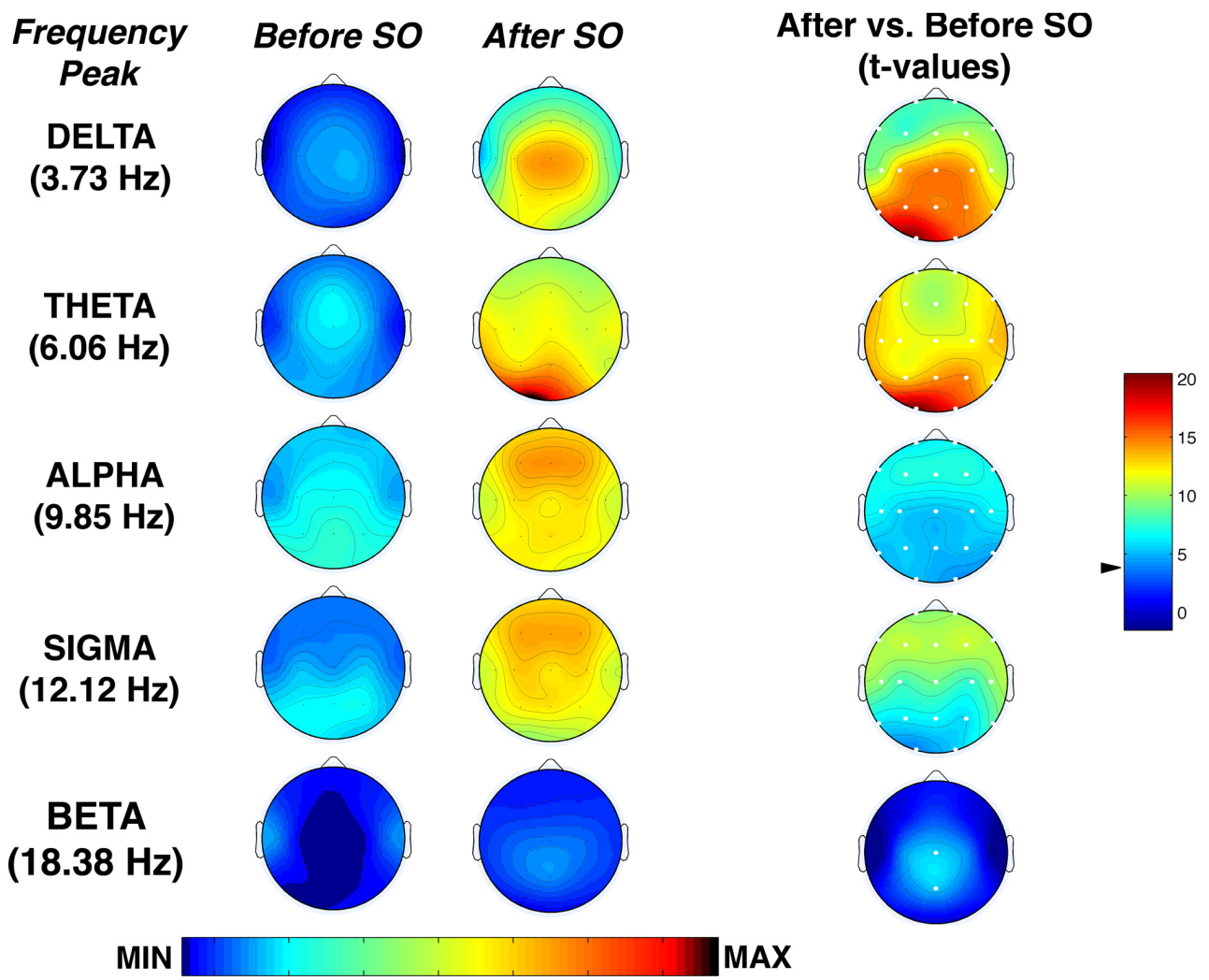

FIGURE 6 | Topographic distribution of the frequency peak of oscillatory activity within each EEG frequency bands at SO during the recovery (REC) night. From the left, the first two columns show the topographic distribution of the mean proportion of time in which oscillations were detected ($P_{episode}$ [*f*]) in correspondence of five selected frequencies of interest (3.73, 6.06, 9.85, 12.02, 18.38 Hz) among the five frequency bands (delta, theta, alpha, sigma, beta) in the 5-min intervals before SO and after SO, respectively. The maps were scaled between minimal (min) and maximal (max) values in the before SO and after SO periods. The first column on the right side shows topographical statistical $P_{episode}$ differences (assessed by paired *t*-tests) between after SO and before SO periods. Values are expressed in *t*-values: positive *t*-values indicate a prevalence of the after SO over the before SO period, and vice versa. The two-tailed level of significance is indicated by the arrow in correspondence of the *t*-values color bar ($p \leq 0.001$ corresponding to $t \geq 3.55$ after Bonferroni correction). White dots indicate significant differences after the Bonferroni corrections. Values are color-coded and plotted at the corresponding position on the planar projection of the scalp surface and are interpolated (biharmonic spline) between electrodes. The maps are based on the 19 unipolar EEG derivations of the international 10–20 system with averaged mastoid reference.

rhythm was prevalent in the oscillatory activity averaged across derivations after SO, differently from the BSL condition that was characterized by a maximum peak in the sigma range (Marzano et al., 2013). Moreover, we found a post-SO frontal enhancement in the theta oscillatory peak not observable at BSL (Marzano et al., 2013). An anterior involvement of the theta activity during the SO process in a REC night has been recently observed also with EEG source localization (Fernandez Guerrero and Achermann, 2019). The theta activity is considered a sensitive marker of homeostatic sleep pressure during wake (Finelli et al., 2000; Tinguely et al., 2006; De Gennaro et al., 2007; Vyazovskiy et al., 2011; Hung et al., 2013; Gorgoni et al., 2014), associated with impaired behavioral performance (Gorgoni et al., 2014; Bernardi et al., 2015; Fattinger et al., 2017; Nir et al., 2017) and characterized by a fronto-central maximum increase after SD interpreted as a higher recovery need in these areas (Horne, 1993; Finelli et al., 2001; Mander et al., 2010). The theta activity also exhibited a wide increase during REC sleep after sustained wakefulness, sharing with the delta activity a fronto-central predominance (Finelli et al., 2001; Marzano et al., 2010). During the SO process at BSL, the delta and theta activity showed similar "small world" features, interpreted as signs of functional disconnection (Vecchio et al., 2017). Together with these findings, our present results strongly

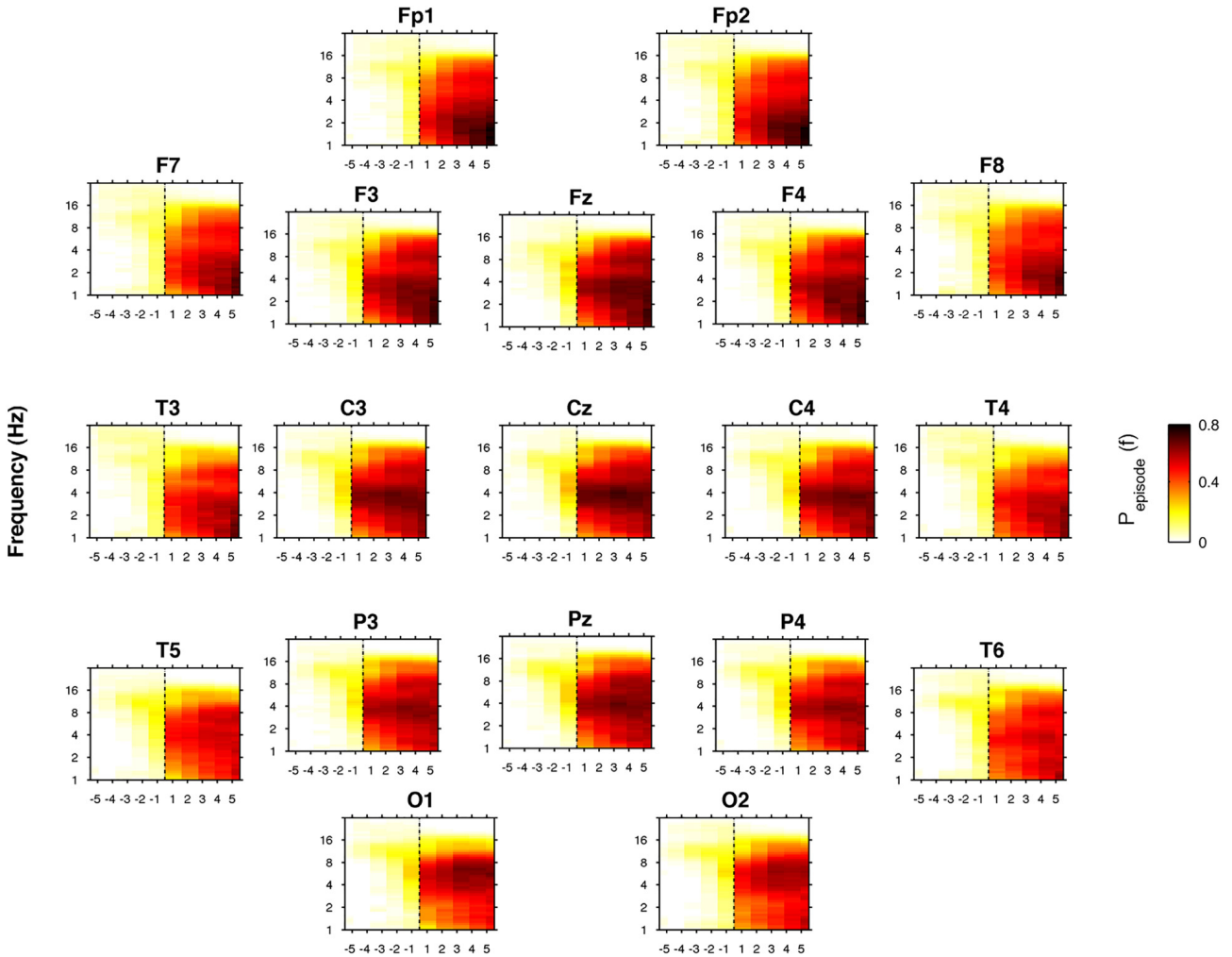

FIGURE 7 | Time course of oscillatory activity at SO during the recovery (REC) night. Topographic time-frequency plots of the five intervals before (from the fifth-first) and after (from the first-fifth) SO, averaged across subjects at the 19 scalp derivations. The pre- and post-SO intervals were divided into five equal parts as in **Figure 2**. Data were calculated for each subject and then were averaged across subjects. Darker colors (red brown) are indicative of increase oscillatory ($P_{episode}$) activity for a specific frequency of oscillation in the 0.50- to 24.25 Hz frequency range. SO is indicated by black dotted line.

support the notion of a crucial role of the theta activity during sleep (and not only during wake) as a biological marker of homeostatic sleep need.

Differently from the delta activity, however, an occipital maximum peak in both EEG power and oscillatory activity has been observed in our study, consistently with previous observations at SO in BSL (Wright et al., 1995; Marzano et al., 2013; Park et al., 2015). Moreover, occipital theta activity after SD showed a strong increase (secondary to the anterior one) during wake (De Gennaro et al., 2007; Gorgoni et al., 2014) and REC sleep (Finelli et al., 2001). Supported by findings in a single epileptic patient at SO (Marzano et al., 2013), we previously interpreted the scalp occipital theta oscillations after SO as a reflection of a peculiar local activity of the calcarine cortex, suggesting a possible involvement of this regional EEG feature in dreamlike mental activity and hypnagogic hallucinations, often observed during the falling-asleep process. Albeit no direct evidence for this hypothesis has been provided so far, recent findings with EEG source localization at SO seem to go in this direction (Fernandez Guerrero and Achermann, 2019).

Alpha Activity

As observed in the BSL night (Hasan and Broughton, 1994; Tanaka et al., 1997; De Gennaro et al., 2001b; Marzano et al., 2013), also in the REC condition the alpha activity gradually declined before SO, and then increased during sleep, showing an inversion from a pre-SO posterior to a post-SO anterior prevalence. It has been proposed that such posterior-to-anterior shift may represent a modification of the functional meaning of the alpha activity during the falling-asleep process (Pivik and Harman, 1995; De Gennaro et al., 2004): the occipital prevalence in the pre-SO period should represent the typical "idle rhythm" of the relaxed eyes-closed wakefulness (Adrian and Matthews, 1934; Niedermeyer, 1997), while the post-SO

fronto-central rise in alpha activity should be considered as part of the synchronization process, associated with sleep-maintaining mechanisms. Our findings indirectly corroborate this hypothesis: (a) the increase in the post- vs. pre-SO ratio in the REC condition compared to BSL in almost all the alpha frequency bins (with a specific fronto-central localization at 10 Hz) supports the existence of a relation between greater homeostatic sleep pressure and higher alpha activity during sleep, particularly in fronto-central areas; (b) the global post-SO increase in correspondence of the alpha oscillatory peak, not observed in normal condition (Marzano et al., 2013), suggests that the alpha activity at SO after prolonged wakefulness can be considered as a genuine rhythmic activity. Similarly, assessing EEG source localization, it has been observed a faster and higher increase of alpha activity after SO during a REC night, that progressively involve the frontal areas with increasing time (Fernandez Guerrero and Achermann, 2019). The authors proposed that this finding may be indicative of a genuine alpha increase instead of an enhancement of slow spindles (which mainly falls in the alpha frequency range) since spindle activity is usually reduced after sleep loss (De Gennaro and Ferrara, 2003). The greater SO-induced increase in the alpha frequency in REC compared to BSL observed in the present research supports this hypothesis.

Sigma Activity

The sigma frequency range progressively increased after SO, exhibiting the centro-parietal predominance that characterizes sleep spindles (De Gennaro and Ferrara, 2003). This result partially represents a by-product of the methodological choice to set the beginning of sleep in correspondence of the first epoch of stage 2 (i.e., the emergence of sleep spindles and/or K-complexes). However, similar findings have been observed in a BSL night by using a different method to define the timing of the SO period (Siclari et al., 2014).

Notably, no differences between BSL and REC have been found in the sigma power post- vs. pre-SO ratio. A reduction of spindle/sigma activity has been previously observed in a REC night after different protocols of SD (Borbély et al., 1981; De Gennaro et al., 2000; Curcio et al., 2003; De Gennaro and Ferrara, 2003; Marzano et al., 2010). Moreover, tracking the temporal dynamics of brain activity at SO with EEG source localization, Fernandez Guerrero and Achermann (2019) recently found a reduced ability to generate sigma activity after SD. However, they considered a different timing to define SO (2 min pre- vs. 10 min post-SO). It is plausible that the post-SD spindle reduction may not be observed comparing the shorter post-sleep intervals considered in our study (5 min pre- and post-SO).

The detection of the oscillatory activity showed a global increase of the sigma rhythm after SO, mostly confirming BSL findings (Marzano et al., 2013) albeit with a lower oscillatory peak (BSL: 13.00 Hz; REC: 12.12 Hz) that seems consistent with the previously observed reduction of the spindle frequency during REC sleep (Knoblauch et al., 2003; Olbrich et al., 2014).

Beta Activity

The frequency bins $\geq$ 18 Hz were characterized by a progressive and generalized decrease during the falling-asleep process, that begins before the SO without a specific topographical predominance, extending previous observation at BSL and representing an arousal reduction (Merica et al., 1991; Merica and Gaillard, 1992; De Gennaro et al., 2001a; Marzano et al., 2013).

No significant changes in the REC condition compared to BSL were observed for the post- vs. pre-SO ratio. The influence of SD on the EEG power during the falling-asleep process, then, seems to be expressed more in term of higher deactivation (i.e., stronger synchronization) than reduced activation. Consistently, analyzing the cortical sources of the beta activity at SO, Fernandez Guerrero and Achermann (2019) found that less that 10% of the voxels differed between BSL and REC conditions, although the reduction of the beta activity was faster in REC.

Albeit the spatio-temporal modulation of the oscillatory activity in the beta frequency pointed to a progressive reduction in this frequency range, the comparison between pre- and post-SO periods in the beta frequency peak showed an increase in the midline centro-parietal derivation, not observed during the BSL night (Marzano et al., 2013). This result is surprising (a) considering the parallel decrease in the EEG beta power, (b) starting from the evidence of a beta activity reduction at SO (Merica et al., 1991; De Gennaro et al., 2001a; Marzano et al., 2013) (c) bearing in mind that beta activity is usually considered an electrophysiological marker of arousal and motor/cognitive functioning (Basar-Eroglu et al., 1996; Neuper and Pfurtscheller, 2001; Kilavik et al., 2013; Merker, 2013).

On the other hand, an increase in beta power during REC sleep has been observed after SWS deprivation (Ferrara et al., 2002) and (albeit not significantly) after total SD (Marzano et al., 2010). It should be considered that fast frequencies are also generated during the depolarizing phase of the slow sleep oscillations, and not only during activation processes (Steriade, 2001). Moreover, analyzing the EEG dynamics during active and quite wake in rats, Grønli et al. (2016) found that during active wakefulness the beta (and gamma) activity was increased, while in quite wakefulness the beta activity paralleled the delta and theta activity in tracking the sleep need, with consistent modifications of the cortical lactate concentration (a measure of cerebral glucose utilization). Albeit these findings do not give an elucidation about the increase of the beta rhythm observed in our study, they point to the need for further characterization of state-dependent beta oscillations.

CONCLUSION

The interest for the characterization of the local brain activity during the SO process is growing, and our findings appear complementary to recent observations on the effect of SD on the wake-sleep transition assessed with EEG source localization and effective connectivity (Fernandez Guerrero and Achermann, 2018, 2019). Beyond confirming the local nature of the falling-asleep process, our results provide for the first time a window on the spatio-temporal dynamics of the EEG power spectra

and oscillatory activity at SO after a period of prolonged wakefulness. We found that SD (a) affected the EEG power at SO, increasing the magnitude of SO-related changes in the frequencies ≤10 Hz, (b) induced a predominant theta oscillatory rhythm, and (c) promoted an earlier appearance of sleep-related rhythmic oscillations like alpha and frontal theta, not observed at BSL, enhancing the concordance between FFT and BOSC.

From a methodological standpoint, our results confirm the BOSC method as a useful tool to characterize the EEG spatiotemporal dynamics during different states of consciousness (and the transition between them), providing information on the genuine rhythmic nature of the electrophysiological activities observed.

Finally, we must remember that SD is extremely diffuse, and its price in terms of working and car accidents is dramatically high. The characterization of the electrophysiological processes during the SO period after sustained wakefulness could represent an essential contribute to help the prevention of the damages provoked by sleep loss, e.g., detecting the possible frequency-specific spatio-temporal targets for brain stimulation protocols aimed at the promotion of vigilance and the reduction of sleepiness (Annarumma et al., 2018).

DATA AVAILABILITY

The datasets generated for this study are available on request to the corresponding author.

AUTHOR CONTRIBUTIONS

MG, LDG, and MF: substantial contributions to the conception and design of the work, interpretation of data, and drafting the work and revising it critically for important intellectual content. MG, CB, ADA, SS, CM, and FM: acquisition and analysis of data. MG, CB, ADA, SS, CM, FM, MF, and LDG: final approval of the paper and agreement to be accountable for all aspects of the work in ensuring that questions related to the accuracy or integrity of any part of the work are appropriately investigated and resolved.

FUNDING

This work was supported by a grant from Sapienza University of Rome, Avvio alla Ricerca 2016 (AR216154C970DF9F) to MG.

REFERENCES

Achermann, P., and Borbély, A. A. (2017). "Sleep homeostasis and models of sleep regulation," in *Principles and Practice of Sleep Medicine*, 6th Edn, eds M. H. Kryger, T. Roth, and W. C. Dement (Amsterdam: Elsevier), 377–387. doi: 10.1016/B978-0-323-24288-2.00036-2

Adrian, E. D., and Matthews, B. H. (1934). The Berger rhythm: potential changes from the occipital lobes in man. *Brain* 57, 355–385. doi: 10.1093/brain/57.4.355

Annarumma, L., D'Atri, A., Alfonsi, V., and De Gennaro, L. (2018). The efficacy of transcranial current stimulation techniques to modulate resting-state EEG, to affect vigilance and to promote sleepiness. *Brain Sci.* 8:E137. doi: 10.3390/brainsci8070137

Basar-Eroglu, C., Struber, D., Schurmann, M., Stadler, M., and Basar, E. (1996). Gamma-band responses in the brain: a short review of psychophysiological correlates and functional significance. *Int. J. Psychophysiol.* 24, 101–112. doi: 10.1016/S0167-8760(96)00051-7

Bernardi, G., Siclari, F., Yu, X., Zennig, C., Bellesi, M., Ricciardi, E., et al. (2015). Neural and behavioral correlates of extended training during sleep deprivation in humans: evidence for local, task-specific effects. *J. Neurosci.* 35, 4487–4500. doi: 10.1523/JNEUROSCI.4567-14.2015

Bersagliere, A., Pascual-Marqui, R. D., Tarokh, L., and Achermann, P. (2018). Mapping slow waves by EEG topography and source localization: effects of sleep deprivation. *Brain Topogr.* 31, 257–269. doi: 10.1007/s10548-017-0595-6

Borbély, A. A., Baumann, F., Brandeis, D., Strauch, I., and Lehmann, D. (1981). Sleep-deprivation- effect on sleep stages and EEG power density in man. *Electroencephalogr. Clin. Neurophysiol.* 51, 483–493. doi: 10.1016/0013-4694(81)90225-X

Cajochen, C., Foy, R., and Dijk, D. J. (1999). Frontal predominance of a relative increase in sleep delta and theta EEG activity after sleep loss in humans. *Sleep Res. Online* 2, 65–69.

Caplan, J. B., and Glaholt, M. G. (2007). The roles of EEG oscillations in learning relational information. *Neuroimage* 38, 604–616. doi: 10.1016/j.neuroimage.2007.07.054

Caplan, J. B., Madsen, J. R., Raghavachari, S., and Kahana, M. J. (2001). Distinct patterns of brain oscillations underlie two basic parameters of human maze learning. *J. Neurophysiol.* 86, 368–380. doi: 10.1152/jn.2001.86.1.368

Curcio, G., Ferrara, M., Pellicciari, M. C., Cristiani, R., and De Gennaro, L. (2003). Effect of total sleep deprivation on the landmarks of stage 2 sleep. *Clin. Neurophysiol.* 114, 2279–2285. doi: 10.1016/S1388-2457(03)00276-1

D'Atri, A., De Simoni, E., Gorgoni, M., Ferrara, M., Ferlazzo, F., Rossini, P. M., et al. (2015). Frequency-dependent effects of oscillatory-tDCS on EEG oscillations: a study with Better OSCillation detection method (BOSC). *Arch. Ital. Biol.* 153, 134–144. doi: 10.12871/000398292015237

De Gennaro, L., and Ferrara, M. (2003). Sleep spindles: an overview. *Sleep. Med. Rev.* 7, 423–440. doi: 10.1053/smrv.2002.0252

De Gennaro, L., Ferrara, M., and Bertini, M. (2000). Effect of slow-wave sleep deprivation on topographical distribution of spindles. *Behav. Brain Res.* 116, 55–59. doi: 10.1016/S0166-4328(00)00247-3

De Gennaro, L., Ferrara, M., and Bertini, M. (2001a). The boundary between wakefulness and sleep: quantitative electroencephalographic changes during the sleep onset period. *Neuroscience* 107, 1–11.

De Gennaro, L., Ferrara, M., Curcio, G., and Cristiani, R. (2001b). Antero-posterior EEG changes during the wakefulness-sleep transition. *Clin. Neurophysiol.* 112, 1901–1911.

De Gennaro, L., Marzano, C., Veniero, D., Moroni, F., Fratello, F., Curcio, G., et al. (2007). Neurophysiological correlates of sleepiness: a combined TMS and EEG study. *Neuroimage* 36, 1277–1287. doi: 10.1016/j.neuroimage.2007.04.013

De Gennaro, L., Vecchio, F., Ferrara, M., Curcio, G., Rossini, P. M., and Babiloni, C. (2004). Changes in fronto-posterior functional coupling at sleep onset in humans. *J. Sleep Res.* 13, 209–217. doi: 10.1111/j.1365-2869.2004.00406.x

De Gennaro, L., Vecchio, F., Ferrara, M., Curcio, G., Rossini, P. M., and Babiloni, C. (2005). Antero-posterior functional coupling at sleep onset: changes as a function of increased sleep pressure. *Brain Res. Bull.* 65, 133–140. doi: 10.1016/j.brainresbull.2004.12.004

Fattinger, S., Kurth, S., Ringli, M., Jenni, O. G., and Huber, R. (2017). Theta waves in children's waking electroencephalogramresemble local aspects of sleep during wakefulness. *Sci. Rep.* 7:11187. doi: 10.1038/s41598-017-11577-3

Fernandez Guerrero, A., and Achermann, P. (2018). Intracortical causal information flow of oscillatory activity (effective connectivity) at the sleep onset transition. *Front. Neurosci.* 12:912. doi: 10.3389/fnins.2018.00912

Fernandez Guerrero, A., and Achermann, P. (2019). Brain dynamics during the sleep onset transition: an EEG source localization study. *Neurobiol. Sleep Circadian Rhythms* 6, 24–34. doi: 10.1016/j.nbscr.2018.11.001

Ferrara, M., and De Gennaro, L. (2011). Going local: Insights from EEG and stereo-EEG studies of the human sleep-wake cycle. *Curr. Top. Med. Chem.* 11, 2423–2427. doi: 10.2174/156802611797470268

Ferrara, M., De Gennaro, L., Curcio, G., Cristiani, R., Corvasce, C., and Bertini, M. (2002). Regional differences of the human sleep electroencephalogram in

response to selective slow-wave sleep deprivation. *Cereb. Cortex* 12, 737–748. doi: 10.1093/cercor/12.7.737

Finelli, L. A., Baumann, H., Borbély, A. A., and Achermann, P. (2000). Dual electroencephalogram markers of human sleep homeostasis: correlation between theta activity in waking and slow-wave activity in sleep. *Neuroscience* 101, 523–529. doi: 10.1016/S0306-4522(00)00409-7

Finelli, L. A., Borbély, A. A., and Achermann, P. (2001). Functional topography of the human nonREM sleep electroencephalogram. *Eur. J. Neurosci.* 13, 2282–2290. doi: 10.1046/j.0953-816x.2001.01597.x

Gorgoni, M., D'Atri, A., Scarpelli, S., Ferrara, M., and De Gennaro, L. (2019). "Timing and topography of sleep onset: asynchronies and regional changes of brain activity," in *Handbook of Sleep Research*, ed. H. Dringenberg (Amsterdam: Elsevier).

Gorgoni, M., Ferlazzo, F., Ferrara, M., Moroni, F., D'Atri, A., Fanelli, S., et al. (2014). Topographic electroencephalogram changes associated with psychomotor vigilance task performance after sleep deprivation. *Sleep Med.* 15, 1132–1139. doi: 10.1016/j.sleep.2014.04.022

Gorgoni, M., Ferrara, M., D'Atri, A., Lauri, G., Scarpelli, S., Truglia, I., et al. (2015). EEG topography during sleep inertia upon awakening after a period of increased homeostatic sleep pressure. *Sleep Med.* 16, 883–890. doi: 10.1016/j.sleep.2015.03.009

Grønli, J., Rempe, M., Clegern, W., Schmidt, M., and Wisor, J. P. (2016). Beta EEG reflects sensory processing in active wakefulness and homeostatic sleep drive in quiet wakefulness. *J. Sleep Res.* 25, 257–268. doi: 10.1111/jsr.12380

Hasan, J., and Broughton, R. (1994). "Quantitative topographic EEG mapping during drowsiness and sleep onset," in *Sleep Onset: Normal and Abnormal Processes*, eds R. D. Ogilvie and J. R. Harsh (Washington, DC: American Psychological Association), 219–235. doi: 10.1037/10166-013

Horne, J. A. (1993). Human sleep, sleep loss and behaviour. Implications for the prefrontal cortex and psychiatric disorder. *Br. J. Psychiatry* 162, 413–419. doi: 10.1192/bjp.162.3.413

Horovitz, S. G., Fukunaga, M., de Zwart, J. A., van Gelderen, P., Fulton, S. C., Balkin, T. J., et al. (2008). Low frequency BOLD fluctuations during resting wakefulness and light sleep: a simultaneous EEG-fMRI study. *Hum. Brain Mapp.* 29, 671–682. doi: 10.1002/hbm.20428

Hung, C. S., Sarasso, S., Ferrarelli, F., Riedner, B., Ghilardi, M. F., Cirelli, C., et al. (2013). Local experience-dependent changes in the wake EEG after prolonged wakefulness. *Sleep* 36, 59–72. doi: 10.5665/sleep.2302

Kilavik, B. E., Zaepffel, M., Brovelli, A., MacKay, W. A., and Riehle, A. (2013). The ups and downs of β oscillations in sensorimotor cortex. *Exp. Neurol.* 245, 15–26. doi: 10.1016/j.expneurol.2012.09.014

Kjaer, T. W., Law, I., Wiltschiotz, G., Paulson, O. B., and Madsen, P. L. (2002). Regional cerebral blood flow during light sleep–a H(2)(15)OPET study. *J. Sleep Res.* 11, 201–207. doi: 10.1046/j.1365-2869.2002.00303.x

Knoblauch, V., Martens, W. L. J., Wirz-Justice, A., and Cajochen, C. (2003). Human sleep spindle characteristics after sleep deprivation. *Clin. Neurophysiol.* 114, 2258–2267. doi: 10.1016/S1388-2457(03)00238-4

Kotajima, F., Meadows, G. E., Morrell, M. J., and Corfield, D. R. (2005). Cerebral blood flow changes associated with fluctuations in alpha and theta rhythm during sleep onset in humans. *J. Physiol.* 568, 305–313. doi: 10.1113/jphysiol.2005.092577

Larson-Prior, L. J., Zempel, J. M., Nolan, T. S., Prior, F. W., Snyder, A. Z., and Raichle, M. E. (2009). Cortical network functional connectivity in the descent to sleep. *Proc. Natl. Acad. Sci. U.S.A.* 106, 4489–4494. doi: 10.1073/pnas.0900924106

Magnin, M., Rey, M., Bastuji, H., Guillemant, P., Mauguiere, F., and Garcia-Larrea, L. (2010). Thalamic deactivation at sleep onset precedes that of the cerebral cortex in humans. *Proc. Natl. Acad. Sci. U.S.A.* 107, 3829–3833. doi: 10.1073/pnas.0909710107

Mander, B. A., Reid, K. J., Baron, K. G., Tjoa, T., Parrish, T. B., Paller, K. A., et al. (2010). EEG measures index neural and cognitive recovery from sleep deprivation. *J. Neurosci.* 30, 2686–2693. doi: 10.1523/JNEUROSCI.4010-09.2010

Marzano, C., Ferrara, M., Curcio, G., and De Gennaro, L. (2010). The effects of sleep deprivation in humans: Topographical electroencephalographic changes in NREM versus REM sleep. *J. Sleep Res.* 19, 260–268. doi: 10.1111/j.1365-2869.2009.00776.x

Marzano, C., Ferrara, M., Mauro, F., Moroni, F., Gorgoni, M., Tempesta, D., et al. (2011). Recalling and forgetting dreams: theta and alpha oscillations during sleep predict subsequent dream recall. *J. Neurosci.* 31, 6674–6683. doi: 10.1523/JNEUROSCI.0412-11.2011

Marzano, C., Moroni, F., Gorgoni, M., Nobili, L., Ferrara, M., and De Gennaro, L. (2013). How we fall asleep: regional and temporal differences in electroencephalographic synchronization at sleep onset. *Sleep Med.* 14, 1112–1122. doi: 10.1016/j.sleep.2013.05.021

Merica, H., Fortune, R. D., Gaillard, J. M., et al. (1991). "Hemispheric temporal organization during the onset of sleep in normal subjects," in *Phasic Events and Dynamic Organization of Sleep*, eds M. G. Terzano, P. L. Halász, and A. C. Declerck (New York, NY: Raven Press), 73–83.

Merica, H., and Gaillard, J. M. (1992). The EEG of the sleep onset period in insomnia: a discriminant analysis. *Physiol. Behav.* 52, 199–204. doi: 10.1016/0031-9384(92)90258-4

Merker, B. (2013). Cortical gamma oscillations: the functional key is activation, not cognition. *Neurosci. Biobehav. Rev.* 37, 401–417. doi: 10.1016/j.neubiorev.2013.01.013

Moroni, F., Nobili, L., De Carli, F., Massimini, M., Francione, S., Marzano, C., et al. (2012). Slow EEG rhythms and inter-hemispheric synchronization across sleep and wakefulness in the human hippocampus. *Neuroimage* 60, 497–504. doi: 10.1016/j.neuroimage.2011.11.093

Neuper, C., and Pfurtscheller, G. (2001). Event-related dynamics of cortical rhythms: frequencyspecific features and functional correlates. *Int. J. Psychophysiol.* 43, 41–58. doi: 10.1016/S0167-8760(01)00178-7

Niedermeyer, E. (1997). Alpha rhythms as physiological and abnormal phenomena. *Int. J. Psychophysiol.* 26, 31–49. doi: 10.1016/S0167-8760(97)00754-X

Nir, Y., Andrillon, T., Marmelshtein, A., Suthana, N., Cirelli, C., Tononi, G., et al. (2017). Selective neuronal lapses precede human cognitive lapses following sleep deprivation. *Nat. Med.* 23, 1474–1480. doi: 10.1038/nm.4433

Olbrich, E., Landolt, H. P., and Achermann, P. (2014). Effect of prolonged wakefulness on electroencephalographic oscillatory activity during sleep. *J. Sleep Res.* 23, 255–262. doi: 10.1111/jsr.12123

Park, D. H., Ha, J. H., Ryu, S. H., Yu, J., and Shin, C. J. (2015). Three-dimensional electroencephalographic changes on Low-resolution brain electromagnetic tomography (LORETA) during the sleep onset period. *Clin. EEG Neurosci.* 46, 340–346. doi: 10.1177/1550059414536713

Pivik, R. T., and Harman, K. (1995). A reconceptualization of EEG alpha activity as an index of arousal during sleep: all alpha activity is not equal. *J. Sleep Res.* 4, 131–137. doi: 10.1111/j.1365-2869.1995.tb00161.x

Rechtschaffen, A., and Kales, A. (1968). *A Manual of Standardized Terminology, Techniques and Scoring System for Sleep Stages of Human Subjects*. Los Angeles: UCLA Brain Information Service.

Sarasso, S., Proserpio, P., Pigorini, A., Moroni, F., Ferrara, M., De Gennaro, L., et al. (2014). Hippocampal sleep spindles preceding neocortical sleep onset in humans. *Neuroimage* 86, 425–432. doi: 10.1016/j.neuroimage.2013.10.031

Scarpelli, S., Marzano, C., D'Atri, A., Gorgoni, M., Ferrara, M., and De Gennaro, L. (2015). State-or trait-like individual differences in dream recall: preliminary findings from a within-subjects study of multiple nap REM sleep awakenings. *Front. Psychol.* 6:928. doi: 10.3389/fpsyg.2015.00928

Siclari, F., Baird, B., Perogamvros, L., Bernardi, G., LaRocque, J., Riedner, B., et al. (2017). The neural correlates of dreaming. *Nat. Neurosci.* 20, 872–878. doi: 10.1038/nn.4545

Siclari, F., Bernardi, G., Riedner, B., LaRocque, J., Benca, M. R., and Tononi, G. (2014). Two distinct synchronization processes in the transition to sleep: a high-density electroencephalographic study. *Sleep* 37, 1621–1637. doi: 10.5665/sleep.4070

Siclari, F., and Tononi, G. (2017). Local aspects of sleep and wakefulness. *Curr. Opin. Neurobiol.* 44, 222–227. doi: 10.1016/j.conb.2017.05.008

Spiess, M., Bernardi, G., Kurth, S., Ringli, M., Wehrle, F. M., Jenni, O. G., et al. (2018). How do children fall asleep? A high-density EEG study of slow waves in the transition from wake to sleep. *Neuroimage* 178, 23–35. doi: 10.1016/j.neuroimage.2018.05.024

Steriade, M. (2001). Impact of network activities on neuronal properties in corticothalamic systems. *J. Neurophysiol.* 86, 1–39. doi: 10.1152/jn.2001.86.1.1

Tanaka, H., Hayashi, M., and Hori, T. (1997). Topographical characteristics and principal component structure of the hypnagogic EEG. *Sleep* 20, 523–534. doi: 10.1093/sleep/20.7.523

Tassi, P., Bonnefond, A., Engasser, O., Hoeft, A., Eschenlauer, R., and Muzet, A. (2006). EEG spectral power and cognitive performance during sleep inertia: the effect of normal sleep duration and partial sleep deprivation. *Physiol. Behav.* 87, 177–184. doi: 10.1016/j.physbeh.2005.09.017

Tinguely, G., Finelli, L. A., Landolt, H. P., Borbély, A. A., and Achermann, P. (2006). Functional EEG topography in sleep and waking: state-dependent and state-independent features. *Neuroimage* 32, 283–292. doi: 10.1016/j.neuroimage.2006.03.017

Vecchio, F., Miraglia, F., Gorgoni, M., Ferrara, M., Iberite, F., Bramanti, P., et al. (2017). Cortical connectivity modulation during sleep onset: a study via graph theory on EEG data. *Hum. Brain Map.* 38, 5456–5464. doi: 10.1002/hbm.23736

Vyazovskiy, V. V., Olcese, U., Hanlon, E. C., Nir, Y., Cirelli, C., and Tononi, G. (2011). Local sleep in awake rats. *Nature* 472, 443–447. doi: 10.1038/nature10009

Whitten, T. A., Hughes, A. M., Dickson, C. T., and Caplan, J. B. (2011). A better oscillation detection method robustly extracts EEG rhythms across brain state changes: the human alpha rhythm as a test case. *Neuroimage* 54, 860–874. doi: 10.1016/j.neuroimage.2010.08.064

Wright, K. P., Badia, P., and Wauquier, A. (1995). Topographical and temporal patterns of brain activity during the transition from wakefulness to sleep. *Sleep* 18, 880–889. doi: 10.1093/sleep/18.10.880

Conflict of Interest Statement: The authors declare that the research was conducted in the absence of any commercial or financial relationships that could be construed as a potential conflict of interest.

Copyright © 2019 Gorgoni, Bartolacci, D'Atri, Scarpelli, Marzano, Moroni, Ferrara and De Gennaro. This is an open-access article distributed under the terms of the Creative Commons Attribution License (CC BY). The use, distribution or reproduction in other forums is permitted, provided the original author(s) and the copyright owner(s) are credited and that the original publication in this journal is cited, in accordance with accepted academic practice. No use, distribution or reproduction is permitted which does not comply with these terms.

frontiers in Neuroscience

REVIEW
published: 05 June 2019
doi: 10.3389/fnins.2019.00567

Local Aspects of Avian Non-REM and REM Sleep

Niels C. Rattenborg[1], Jacqueline van der Meij[1], Gabriël J. L. Beckers[2] and John A. Lesku[3]*

[1] Avian Sleep Group, Max Planck Institute for Ornithology, Seewiesen, Germany, [2] Cognitive Neurobiology and Helmholtz Institute, Utrecht University, Utrecht, Netherlands, [3] School of Life Sciences, La Trobe University, Melbourne, VIC, Australia

Birds exhibit two types of sleep that are in many respects similar to mammalian rapid eye movement (REM) and non-REM (NREM) sleep. As in mammals, several aspects of avian sleep can occur in a local manner within the brain. Electrophysiological evidence of NREM sleep occurring more deeply in one hemisphere, or only in one hemisphere – the latter being a phenomenon most pronounced in dolphins – was actually first described in birds. Such asymmetric or unihemispheric NREM sleep occurs with one eye open, enabling birds to visually monitor their environment for predators. Frigatebirds primarily engage in this form of sleep in flight, perhaps to avoid collisions with other birds. In addition to interhemispheric differences in NREM sleep intensity, the intensity of NREM sleep is homeostatically regulated in a local, use-depended manner within each hemisphere. Furthermore, the intensity and temporo-spatial distribution of NREM sleep-related slow waves varies across layers of the avian hyperpallium – a primary visual area – with the slow waves occurring first in, and propagating through and outward from, thalamic input layers. Slow waves also have the greatest amplitude in these layers. Although most research has focused on NREM sleep, there are also local aspects to avian REM sleep. REM sleep-related reductions in skeletal muscle tone appear largely restricted to muscles involved in maintaining head posture. Other local aspects of sleep manifest as a mixture of features of NREM and REM sleep occurring simultaneously in different parts of the neuroaxis. Like monotreme mammals, ostriches often exhibit brainstem-mediated features of REM sleep (muscle atonia and REMs) while the hyperpallium shows EEG slow waves typical of NREM sleep. Finally, although mice show slow waves in thalamic input layers of primary sensory cortices during REM sleep, this is not the case in the hyperpallium of pigeons, suggesting that this phenomenon is not a universal feature of REM sleep. Collectively, the local aspects of sleep described in birds and mammals reveal that wakefulness, NREM sleep, and REM sleep are not always discrete states.

Keywords: sleep, bird, mammal, unihemispheric, atonia, evolution, slow wave, propagation

OPEN ACCESS

Edited by:
Michele Bellesi,
University of Bristol, United Kingdom

Reviewed by:
Vladyslav Vyazovskiy,
University of Oxford, United Kingdom
Giorgio F. Gilestro,
Imperial College London, United Kingdom

****Correspondence:***
Niels C. Rattenborg
rattenborg@orn.mpg.de

Specialty section:
This article was submitted to Sleep and Circadian Rhythms, a section of the journal Frontiers in Neuroscience

Received: *15 March 2019*
Accepted: *17 May 2019*
Published: *05 June 2019*

Citation:
Rattenborg NC, van der Meij J, Beckers GJL and Lesku JA (2019) Local Aspects of Avian Non-REM and REM Sleep. Front. Neurosci. 13:567. doi: 10.3389/fnins.2019.00567

INTRODUCTION

Wakefulness and sleep, as well as the two types of sleep found in mammals and birds – rapid eye movement (REM) and non-REM (NREM) sleep – are often treated as mutually exclusive states distinguished by a suite of behavioral, electroencephalographic, and electromyographic traits. In mammals and birds, NREM sleep is distinguished from wakefulness by the presence of

high-amplitude slow waves in electroencephalogram (EEG) or local field potential (LFP) recordings. These slow waves result from the slow oscillation, or alternation, of neuronal membrane potentials between a hyperpolarized state with neuronal quiescence and a depolarized state with action potentials (Steriade et al., 1993; Reiner et al., 2001; Steriade, 2006). Slow waves – typically quantified as slow wave activity (SWA) (approximately 0.5–4.5 Hz power density) – increase and decrease as a function of time spent awake and asleep, respectively, in both mammals and birds, suggesting that they reflect homeostatically regulated processes (Jones et al., 2008; Martinez-Gonzalez et al., 2008; Rattenborg et al., 2009; Lesku et al., 2011b). However, although thalamocortical spindles are present during NREM sleep in mammals (Astori et al., 2013), they are apparently absent in birds (van der Meij et al., 2019a). EEG activity during wakefulness and REM sleep are similar in both mammals and birds; although the hippocampal theta rhythm present in mammals has not been detected in birds (Rattenborg et al., 2011). REM sleep is distinguished from wakefulness by increased arousal thresholds and reduced muscle tone (only partial in birds; Dewasmes et al., 1985), intermittently interrupted by twitching of skeletal muscle groups, including those controlling eye movements. As in mammals, thermoregulatory responses are suppressed during avian REM sleep (Heller et al., 1983; Graf et al., 1987; Scriba et al., 2013), and in both altricial mammals and birds, the amount of REM sleep is highest in young, decreasing across early ontogeny (Roffwarg et al., 1966; Jouvet-Mounier et al., 1970; Scriba et al., 2013). Finally, REM sleep is homeostatically regulated in both groups (Tobler and Borbély, 1988; Martinez-Gonzalez et al., 2008; Newman et al., 2008; Lesku et al., 2011b).

To explore the mechanisms and functions of NREM and REM sleep, researchers examine changes in the time spent in each state following experimental manipulations. Interspecific differences in the time spent in these states is also used to identify biological or ecological traits that predict their variation, and thereby, possibly, the functions of each state (Lesku et al., 2009). Quantifying the time spent in each state necessarily requires treating wakefulness, NREM sleep, and REM sleep as mutually exclusive states. However, in practice, the transitions from one state to another can be gradual (e.g., wakefulness to NREM sleep), rendering the boundary between states arbitrary. In some species, sleep and wakefulness can also occur unihemispherically, a specialized adaptation that enables animals to partially sleep under ecological circumstances when being fully asleep would be disadvantageous (Rattenborg et al., 2000, 2016; Lyamin et al., 2008b, 2018). However, such *local sleep* is not restricted to these animals. As new technology allows more brain regions to be examined simultaneously, it is becoming evident that even in conventional mammalian models for studying sleep, such as rodents and humans, traits used to define different states can occur at the same time in different brain regions (Nir et al., 2011, 2017; Vyazovskiy et al., 2011b; Emrick et al., 2016; Funk et al., 2016; Tamaki et al., 2016; Durán et al., 2018). Herein, we review the various types of local sleep found in birds, including those not known to occur in mammals.

LOCAL ASPECTS OF NREM SLEEP

Asymmetric and Unihemispheric Sleep

The discovery that some animals can engage in NREM sleep with one cerebral hemisphere at a time (unihemispheric sleep), or more deeply with one hemisphere than the other (asymmetric sleep) undoubtedly contributed to current views regarding the local nature of NREM sleep (Krueger and Obál, 1993; Lima and Rattenborg, 2007; Rattenborg et al., 2012; Siclari and Tononi, 2017; Castelnovo et al., 2018; Krueger et al., 2019). These asymmetric forms of NREM sleep (also known as unihemispheric or asymmetric slow wave sleep) have been described in Odontocete cetaceans (e.g., dolphins, porpoises, and the beluga whale) (Mukhametov et al., 1977; Lyamin et al., 2008b), pinnipeds in the superfamily Otarioidea (fur seals, sea lions, and walruses) (Lyamin et al., 2012, 2018), one manatee (order Sirenia) (Mukhametov et al., 1992), and several species of birds (Spooner, 1964; Peters et al., 1965; Ookawa and Takagi, 1968; Ball et al., 1988; Szymczak et al., 1996; Rattenborg et al., 1999a,b, 2000, 2001, 2016; Ayala-Guerrero et al., 2003; Ookawa, 2004; Low et al., 2008; Fuchs et al., 2009). In the mammalian and avian species in which eye state was examined in conjunction with EEG recordings, usually the eye contralateral to the sleeping (or more deeply sleeping) hemisphere is closed while the eye contralateral to the awake (or more lightly sleeping) hemisphere is open (Peters et al., 1965; Ookawa and Takagi, 1968; Ball et al., 1988; Rattenborg et al., 1999a,b, 2001; Lyamin et al., 2002, 2004; Low et al., 2008; Fuchs et al., 2009).

A Note on Nomenclature

Although asymmetric forms of NREM sleep occur in marine mammals and birds, comparing the extent of this phenomenon across taxonomic groups has been hindered by the use of different approaches to characterize these forms of sleep. The criteria for classifying NREM sleep as unihemispheric, asymmetric, or symmetric (bihemispheric) varies across studies depending, in part, on the relative emphasis given to EEG or behavioral indicators of sleep. In studies that emphasize EEG activity, the boundaries between these states are defined by the degree of interhemispheric asymmetry in NREM sleep-related EEG SWA. In marine mammals, an asymmetry index (AI) in the level of SWA has been calculated as: AI = (left hemisphere SWA – right SWA)/(left SWA + right SWA) (Lyamin et al., 2008a,b). The commonly used thresholds, AI ≤ -0.3 or ≥ 0.3 and ≤ -0.6 or ≥ 0.6, reflect increasing degrees of interhemispheric asymmetry, with the former usually considered asymmetric and the later unihemispheric; however, the exact term (i.e., asymmetric or unihemispheric) ascribed to episodes of mammalian NREM sleep exceeding these thresholds varies across studies (Lyamin et al., 2008a,b, 2016, 2018). Historically, in birds, the relationship between unilateral eye closure and interhemispheric asymmetries in EEG slow waves was simply mentioned anecdotally (Spooner, 1964; Peters et al., 1965; Ookawa and Takagi, 1968). Later, Ball et al. (1988) showed that visually identified periods of pronounced interhemispheric asymmetry in EEG slow waves were usually associated with unilateral eye closure in glaucous-winged gulls

(*Larus glaucescens*). Later, Rattenborg et al. (1999a,b) showed that unilateral eye closure was associated with a statistically significant average interhemispheric asymmetry in SWA in mallard ducks (*Anas platyrhynchos*), with SWA levels in the hemisphere contralateral to the open eye higher than (bihemispheric) wakefulness, but lower than that occurring during bihemispheric NREM sleep (Rattenborg et al., 1999a,b; see also Fuchs et al., 2009). Given that the mallards had one eye open and seemed to use this eye to monitor their environment (see below), such asymmetries were classified as unihemispheric NREM sleep. Based on the relationships between unilateral eye closure and interhemispheric asymmetries in SWA described in EEG studies, eye state alone has been used as an indicator of unihemispheric sleep in several behavioral studies (Ball et al., 1988; Mascetti and Vallortigara, 2001; Boerema et al., 2003; Nelini et al., 2010, 2012; Mascetti, 2016). Finally, the AI thresholds used in dolphins and seals were recently employed to classify NREM sleep as unihemispheric, asymmetric, or symmetric in great frigatebirds (*Fregata minor*) in the wild where eye state could not be monitored (Rattenborg et al., 2016).

None of the terms used to describe the asymmetric forms of sleep and wakefulness fully capture all EEG and behavioral aspects of these states. Unihemispheric sleep inherently implies unihemispheric wakefulness. This seemingly makes sense when applied to fur seals, but not dolphins. When sleeping in the water, fur seals float on one side with their nostrils held above the surface to breath. This posture is maintained by unilateral movements of the front flipper in the water which is presumably controlled by the contralateral awake hemisphere. Interestingly, the eye facing down in the water is open while the other is closed (Lyamin et al., 2004), possibly enabling seals to detect predatory sharks and orcas; this might explain why fur seals in the wild float on their side during the day, when they could visually detect predators, but not at night (Trites et al., 2009). Consequently, in fur seals, the EEG asymmetry is clearly associated with a motor asymmetry, as well as an apparent sensory asymmetry associated with having one eye open. Hence, the term unihemispheric sleep (or unihemispheric wakefulness) accurately describes the neurophysiology and the behavior. Dolphins also have one eye open during unihemispheric sleep. However, unlike fur seals, dolphins can swim in a coordinated and directed manner while sleeping unihemispherically, indicating that at least some subcortical motor systems are bilaterally "awake" (Siegel, 2008). Consequently, the term unihemispheric sleep fails to adequately describe all waking aspects of this state in dolphins. Similarly, the converse, emphasizing the bilateral wake-like behavior and categorizing a dolphin's state as fully awake when they are swimming with one eye closed and exhibiting unilateral cortical slow waves, obviously deemphasizes the behavioral (eye closure) and unilateral EEG signs of sleep (Siegel, 2008). Overall, given the mosaic of behavioral and EEG signs of wakefulness and sleep occurring in marine mammals and birds, it is perhaps not surprising that researchers have struggled to find simple terms that adequately describe these complex states.

Adaptive Use of the Open Eye

Determining whether sleeping with one eye open serves an adaptive function would likely enhance our understanding of asymmetric/unihemispheric sleep and the relative importance that should be given to eye state. One possibility is that having one eye open is simply a functionless byproduct of having one hemisphere awake (or sleeping less deeply) for some other reason. For example, when sleeping in the water, do fur seals keep one eye open to watch for threats, or is this simply an epiphenomenon of keeping one hemisphere awake to control unilateral flipper movements? Although it is unknown whether the open eye can detect threats in fur seals, research on birds and dolphins provide insight into the answer. Captive ducks sleeping on the ground at the edge of a group spend a greater proportion of NREM sleep with one eye open (rather than both eyes closed) when compared to ducks sleeping flanked on both sides by other ducks (Rattenborg et al., 1999a,b). Moreover, only ducks at the group edge show a preference for looking away from the other birds when sleeping with one eye open. Given that they were not exhibiting any asymmetrical motor activity, this directional preference in and of itself strongly suggests that ducks are able to visually detect threats when sleeping with one eye open. Indeed, ducks respond rapidly to a threatening visual stimulus presented to the open eye, indicating that at least some components of wakefulness are online even though the corresponding hemisphere shows SWA levels intermediate between unequivocal NREM sleep and unequivocal wakefulness. In the wild, this may be sufficient for detecting approaching predators. Nonetheless, further research is needed to identify the brain regions that mediate this anti-predator response and to determine whether other aspects of wakefulness are compromised by the presence of intermediate levels of SWA in the hemisphere connected to the open eye.

Dolphins also actively use the open eye to monitor their environment during unihemispheric sleep. However, in contrast to ducks, captive dolphins direct the open eye toward conspecifics. Pacific white-sided dolphins (*Lagenorhynchus obliquidens*) swimming side-by-side in a group of four directed their open eye toward the other dolphins (Goley, 1999). In addition, during the first few weeks following birth, bottlenose dolphin mothers and their calves keep the eye facing each other open and the other closed when sleeping while continuously swimming (Gnone et al., 2006; Sekiguchi et al., 2006; Lyamin et al., 2007). Importantly, in both species, the dolphins were swimming side-by-side in a circle around their pool. Consequently, despite exhibiting the same asymmetry in motor activity needed to swim in a given circular direction, the dolphins on the inside and outside of the circle kept a different eye open and different hemisphere awake. Although the responsiveness of the open eye has not been examined, the lack of a relationship with motor activity and the preference for directing the open eye toward conspecifics suggest that maintaining visual awareness is one function of unihemispheric sleep in dolphins. Finally, in addition to maintaining unilateral visual awareness, if the ear connected to the awake hemisphere remains responsive to sounds, unihemispheric sleep may explain how dolphins are able

to sustain periods of acoustic responsiveness for several days (Ridgway et al., 2006, 2009; Branstetter et al., 2012).

Unihemispheric and Asymmetric Sleep in Flight

The research outlined above suggests that asymmetric forms of sleep instill animals with some of the adaptive benefits of wakefulness. However, research on sleep in flying birds suggests that these partial waking states are insufficient to meet all ecological demands for wakefulness, at least under certain circumstances. Several avian species engage in long, non-stop flights: bar-tailed godwits (*Limosa lapponica baueri*) fly from Alaska to New Zealand in 8.1 days spanning 11,690 km of sustained flight (Gill et al., 2009); great frigatebirds fly around the Indian Ocean for up to 2 months without landing on the water (Weimerskirch et al., 2016); and Alpine swifts (*Tachymarptis melba*) and Common swifts (*Apus apus*) can fly for 200 and 300 days, respectively (Liechti et al., 2013; Hedenström et al., 2016). Many other birds also make multiday, non-stop flights (reviewed in Rattenborg, 2017). The discovery that dolphins can swim in a coordinated manner during unihemispheric sleep and ducks can switch to asymmetric sleep when needed on the ground, led to the assumption that flying birds maintain aerodynamic control and navigation by sleeping with one eye open (Rattenborg, 2017).

Sleep in flight was recently demonstrated for the first time in great frigatebirds (Rattenborg et al., 2016). Using a head-mounted EEG and acceleration data logger (**Figure 1A**), Rattenborg et al. (2016) found that sleep mainly occurred at night while the birds were soaring on rising air currents, and never when they flapped their wings. As expected, NREM sleep was more often asymmetric in flight when compared to sleep on land. In flight, nearly half of the asymmetric sleep exceeded the threshold for unihemispheric sleep (i.e., AI ≤ -0.6 or ≥ 0.6), as typically defined in marine mammals. Episodes of asymmetric sleep were usually short, but could last up to several minutes (**Figure 1B**). Unexpectedly, the frigatebirds also engaged in episodes of bihemispheric sleep, which could also last for several minutes. However, this form of sleep did not affect their aerodynamic control of flight, raising the question, why did they usually sacrifice sleep in one hemisphere by primarily sleeping asymmetrically. The accelerometry recordings revealed when the birds were circling to the left or right, and this suggested that they relied on asymmetric sleep to watch where they were going. When circling, the hemisphere opposite to the direction of the turn showed the lowest SWA and the highest gamma (30–80 Hz) activity (**Figure 1C**), suggesting that the eye facing into the turn was open (**Figure 1D**). Given that frigatebirds have no predators when over the ocean, they might sleep this way to avoid head-on collisions with other birds circling in the opposite direction in the same air mass.

Nonetheless, other lines of evidence suggest that sleeping asymmetrically is not sufficient to meet all of their demands for wakefulness while on the wing at night. Despite spending most of the nighttime hours soaring, when sleep could occur, the frigatebirds slept <1 h per night. This suggests that even at night while soaring, when frigatebirds are not known to feed, their need for attention usually exceeds that afforded by sleeping

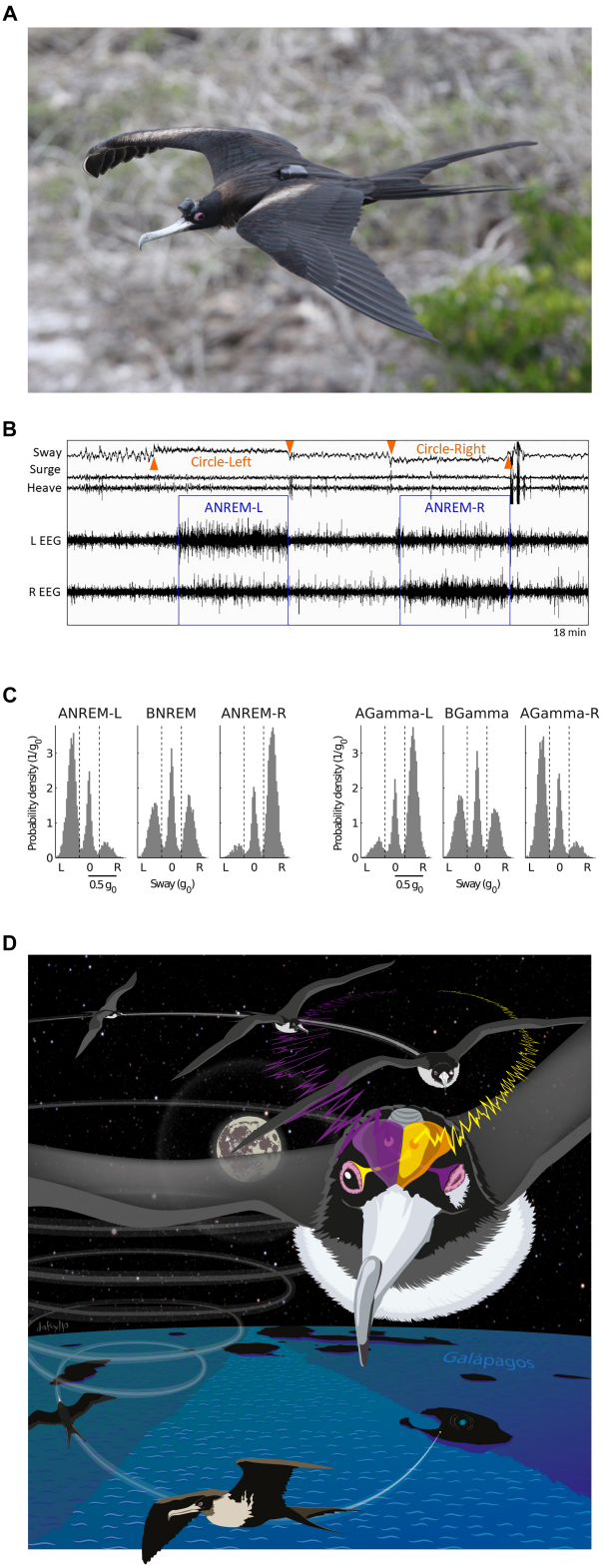

FIGURE 1 | Sleep in flight. **(A)** Female great frigatebird with a head mounted data logger for recording the EEG from both cerebral hemispheres and triaxial acceleration. A GPS logger mounted on the back recorded position and

(Continued)

FIGURE 1 | Continued
altitude. **(B)** Electroencephalogram (EEG) and accelerometry (sway, surge, and heave) recording from a frigatebird sleeping while circling in rising air currents. When the bird circled to the left (as indicated by centripetal acceleration detected in the sway axis) the bird showed asymmetric NREM sleep (ANREM) with the left hemisphere sleeping deeper (larger slow waves) than the right (ANREM-L), and when the bird circled to the right the right hemisphere slept deeper than the left (ANREM-R); during the other recording segments the bird was awake. **(C)** The relationship between interhemispheric asymmetries in slow wave activity (SWA, 0.75–4.5 Hz) and gamma activity (30–80 Hz) during NREM sleep for all birds combined ($N = 14$). During ANREM, the birds usually circled toward the side with greater SWA and lower gamma activity. By contrast, during bihemispheric NREM (BNREM) without asymmetries in SWA or gamma (BGamma), the birds showed no preference for circling in one particular direction. AGamma-L and AGamma-R indicate NREM with greater gamma in the left and right hemispheres, respectively. **(D)** Illustration showing a bird circling to the right while sleeping with the right hemisphere. Although the birds' eye state is not known, based on studies from other birds, the EEG asymmetries suggest that the frigatebirds kept the eye connected to the more awake (lower SWA and higher gamma) hemisphere open and facing the direction of the turn. Panels **(A–C)** reproduced with permission from Rattenborg et al. (2016). Photo by Bryson Voirin. Illustration by Damond Kyllo.

with one hemisphere awake. Otherwise, one would have expected them to maximize the time spent sleeping asymmetrically or unihemispherically. Although the exact cognitive challenges that require bihemispheric wakefulness remain unclear, great frigatebirds follow eddies – productive parts of the ocean with increased foraging opportunities – at night, even though they only feed during the day (Tew Kai et al., 2009). By following eddies, frigatebirds may ensure that they are over a productive area at daybreak. How frigatebirds track eddies at night is unknown (Tew Kai et al., 2009), but the unexpectedly low amount of sleep in flight suggests that this and, perhaps, other cognitive demands require attention exceeding that occurring during asymmetric or unihemispheric sleep. Thus, although keeping an eye open may allow ducks, dolphins, fur seals, and, apparently, frigatebirds to visually monitor their environment during asymmetric or unihemispheric sleep, this unilateral awareness is probably not sufficient to meet all demands for wakefulness. Consequently, even in animals capable of asymmetric forms of sleep, the time spent sleeping may be greatly reduced under challenging ecological circumstances (Rattenborg et al., 2004, 2016; Lesku et al., 2012).

Unihemispheric or Asymmetric Sleep in Other Animals?

Collectively, these studies indicate that having one eye open to monitor the environment is an important adaptive component of asymmetric or unihemispheric sleep, even if processing in the contralateral hemisphere is limited. Interestingly, the ability to sleep with one eye open is common among birds (Ball et al., 1988), and might even predate their evolution (Rattenborg et al., 2000). Given that birds are reptiles in the taxonomic clade Dinosauria (Brusatte et al., 2015), non-avian reptiles might be expected to also sleep with one eye open. Indeed, non-avian reptiles, including crocodilians – the closest living relatives to birds – have been observed resting with one eye open (Rattenborg et al., 2000; Mathews et al., 2006; Kelly et al., 2015). Moreover, similar to ducks sleeping at the edge of a group, Western fence lizards (*Sceloporus occidentalis*) and juvenile saltwater crocodiles (*Crocodylus porosus*) direct the open eye toward potential threats (Mathews et al., 2006; Kelly et al., 2015). Despite these behavioral similarities, due to the lack of systematic electrophysiological studies, it is unclear whether closure of one eye is associated with asymmetric or unihemispheric sleep in non-avian reptiles (Rattenborg et al., 2000; Kelly et al., 2015).

The prevalence of sleep with one eye open in birds, and a potentially similar state in reptiles, questions why this type of sleep is not more widespread among mammals. Certainly, there are many terrestrial species that might benefit from being able to sleep asymmetrically or unihemispherically when needed. Interestingly, a recent study suggests that humans might be able to modulate the intensity of sleep unilaterally in response to ecologically relevant challenges (Tamaki et al., 2016). On the first night spent sleeping in a new (potentially dangerous) environment, people slept less deeply with parts of the left hemisphere (based on EEG SWA), whereas on the second night, both hemispheres slept deeply. Importantly, on the first, but not the second night, people were also more responsive to sounds presented to the right ear than the left, suggesting that the EEG asymmetry enhanced auditory awareness unilaterally. Given that this phenomenon was only recently discovered in humans, the capacity to modulate interhemispheric sleep intensity in response to changing ecological demands may be more widespread among terrestrial mammals than currently recognized. If so, it may have served as a precursor for the evolution of more asymmetric forms of sleep which evolved independently three times when the terrestrial ancestors to dolphins and porpoises, seals in the superfamily Otarioidea, and manatees transitioned to living and sleeping in a marine environment (Rattenborg et al., 2000).

Local NREM Sleep Homeostasis

The discovery that NREM sleep can occur independently in the two hemispheres of some animals raised the question as to whether NREM sleep is homeostatically regulated independently in each hemisphere. Homeostasis can manifest as an increase in time spent in, or intensity of, NREM sleep, the latter measured as EEG SWA (Tobler, 2011). Early studies of dolphins did indeed suggest that NREM sleep is regulated intrahemispherically. Following unihemispheric sleep deprivation in dolphins, the hemisphere that had been kept awake usually (seven of nine experiments performed on five dolphins) showed an increase above preceding baseline levels in the time spent in NREM sleep (Oleksenko et al., 1992). Although the amount of recovery sleep did not correlate with the duration of sleep deprivation (see Lyamin et al., 2008b), it is possible that some of the recovery manifested as an increase in NREM sleep intensity. Unfortunately, SWA during NREM sleep was not quantified. In fur seals, the amount of bihemispheric NREM sleep on land increased following extended periods in the water, wherein sleep primarily occurred asymmetrically or unihemispherically (Lyamin et al., 2018). However, it is unclear whether the increase in bihemispheric sleep reflects two independent, intrahemispheric homeostatic responses occurring at the same time, a propensity for NREM sleep to primarily

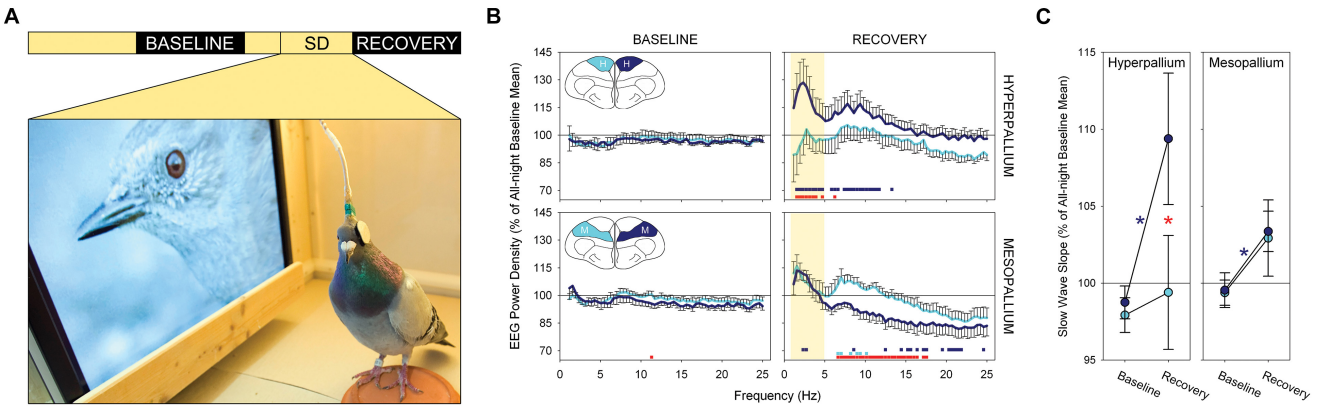

FIGURE 2 | Local sleep homeostasis in the avian brain. **(A)** Experimental design: a 12 h baseline night, 8 h period of bihemispheric sleep deprivation with unilateral visual stimulation (SD) and a 12 h recovery night. Photograph shows the experimental environment during the treatment. **(B)** Spectral power density (0.78–25.00 Hz) during NREM sleep for the first quarter of the baseline and recovery nights for the stimulated (dark blue) and visually deprived (light blue) hyperpallia and mesopallia. Data are presented as mean ± SE. Colored squares at the bottom of each recovery night plot reflect a significant pairwise comparison between the baseline and recovery night of the stimulated (dark blue) and visually deprived (light blue) hyperpallia; red squares denote a significant asymmetry between the left and right brain region during recovery sleep. Although the experimental treatment induced interhemispheric asymmetries across a wide range of frequencies, slow wave activity (yellow shading) in the hyperpallium showed the largest asymmetry. Insets: frontal view of a transverse section through the cerebrum of a pigeon highlighting the hyperpallium (H) and mesopallium (M). **(C)** Up slope of NREM sleep slow waves in the hyperpallium and mesopallium contralateral to the stimulated eye (dark blue) and deprived eye (light blue) during the first quarter of the baseline and recovery night. Data are presented as mean ± SE. Significant changes in slope between the baseline and recovery nights are marked with an asterisk (contralateral to the stimulated eye in dark blue; contralateral to the deprived eye, non-significant); significant asymmetries between the left and right hemisphere for a given brain region are denoted by a red asterisk. Note the asymmetry between the stimulated and visually deprived hyperpallia during recovery sleep, with the stimulated hyperpallium showing steeper slopes, and the symmetric mean increase in the mesopallium. Reproduced with permission from Lesku et al. (2011b).

occur bihemispherically on land (Lyamin et al., 2008c), or both. As in the dolphin studies, SWA during NREM sleep was not reported. In future studies, it would be interesting to determine whether NREM sleep time or intensity increase unilaterally following sleep deprivation of only one hemisphere while fur seals sleep unihemispherically in the water. Finally, although unihemispheric sleep deprivation has not been performed in birds, several behavioral studies in chicken chicks have shown small, but significant, changes in the time spent with only the left or right eye closed in response to treatments thought to selectively activate one hemisphere or the other (e.g., Mascetti et al., 2007; Nelini et al., 2010, 2012; Quercia et al., 2018; reviewed in Mascetti, 2016), suggesting that sleep may be homeostatically regulated independently in each hemisphere. It will be important for future studies to determine the extent to which these changes in eye state correlate with changes in hemispheric sleep measured electrophysiologically (see Lesku et al., 2011b).

Even though the hemispheric regulation of NREM sleep needs further study in mammals and birds, several lines of evidence suggest the NREM sleep intensity is homeostatically regulated in a local, use-dependent manner *within* a hemisphere in both taxonomic groups (reviewed in Rattenborg et al., 2012). The local, use-dependent homeostatic regulation of NREM sleep-related SWA in the neocortex was established in a series of studies on humans (Kattler et al., 1994; Huber et al., 2004; Landsness et al., 2009) and rats (Vyazovskiy et al., 2000; Yasuda et al., 2005; Vyazovskiy and Tobler, 2008; Hanlon et al., 2009). In these studies, selectively activating certain cortical regions during wakefulness induced a local increase in EEG SWA in those regions during subsequent NREM sleep. Interestingly, reducing activation of a cortical region during wakefulness later diminished SWA in that region during sleep (Huber et al., 2006). Collectively, these studies demonstrate that the local level of NREM sleep intensity is determined by the prior local level of brain use, or disuse, during wakefulness in mammals.

One study has provided electrophysiological evidence for local sleep homeostasis in birds (Lesku et al., 2011b). Lesku et al. (2011b) implanted electrodes over the left and right hyperpallia (a primary visual area) and left and right mesopallia (a non-visual processing area). The left eye of each bird was capped, while the right eye was directed toward a monitor showing videos of wild birds (**Figure 2A**), during which they were prevented from having their normal daytime naps in either hemisphere. In this way, the left hyperpallia, which receives projections primarily from the right eye, was stimulated more than the right hyperpallia, which received reduced visual input, but both hemispheres were kept similarly awake. At the end of the day, the cap was removed and the birds were allowed to sleep undisturbed. During recovery sleep, the left and right mesopallium showed an increase in SWA relative to the baseline night (**Figure 2B**); the increase was symmetric because the level of SWA was determined only by the amount of wakefulness during the previous day. Conversely, there was an asymmetry in SWA in the hyperpallium with only the stimulated hyperpallium showing an increase. The absence of an increase in SWA in the unstimulated hyperpallium likely reflects the net effect of competing processes that increase (time awake) and decrease (sensory deprivation) (e.g., Huber et al., 2006) SWA relative to

baseline. The slope of NREM sleep slow waves – a proposed correlate of synaptic potentiation induced during wakefulness (Vyazovskiy et al., 2011a) – also showed the greatest increase in the stimulated hyperpallium (**Figure 2C**). Thus, the intensity of NREM sleep is shaped locally within a hemisphere as a function of the duration and intensity of prior wakefulness.

Finally, it conceivable that sleep is homeostatically regulated at an even more local level in the avian brain. During sleep deprivation in mammals, localized neocortical sleep-related oscillations can intrude into global wakefulness, resulting in deficits in waking performance (Vyazovskiy et al., 2011b; Nir et al., 2017). The same phenomenon might occur in the avian hyperpallium, the most dorsal part of the telencephalon from which the EEG is usually recorded. However, the high-density multiunit or cellular recordings of the hyperpallium needed to differentiate between sleep-like potentials resulting from local sleep-related processes and those arising from other sources during active wakefulness (see Boiko and Bureś, 1985; Yang et al., 2008) have not been performed in birds. In addition, birds provide little opportunity to examine the intrusion of sleep-related oscillations into quiet wakefulness, as they usually transition to NREM sleep within seconds of becoming inactive. Nonetheless, if future studies detect localized sleep-related oscillations intruding into wakefulness, it will be interesting to determine whether they adversely impact neurobehavioral performance, as shown in mammals and predicted by modeling (Lima and Rattenborg, 2007). It will also be important to determine the extent to which such brief, localized sleep can compensate for the loss of global sleep during periods of prolonged wakefulness.

Slow Wave Origin and Propagation

At any point in time during NREM sleep, different parts of the neocortex may be engaged in the hyperpolarized or depolarized phase of the slow oscillation of neuronal membrane potentials. This local aspect of slow oscillations, and resulting EEG slow waves, arises from the fact that slow oscillations originate from multiple neocortical regions and propagate horizontally across the neocortex as a traveling wave (Massimini et al., 2004; Murphy et al., 2009; Nir et al., 2011). Although the neocortex is capable of generating slow oscillations following recovery from thalamotomy, input from the thalamus plays an important role in the generation of slow waves under normal conditions (Crunelli and Hughes, 2010; Timofeev and Chauvette, 2011; Lemieux et al., 2014). Slow waves typically occur first within layer 5 (a thalamorecipient layer) (Constantinople and Bruno, 2013) and propagate vertically within cortical columns (Chauvette et al., 2010; Capone et al., 2019). Although the mechanisms underlying the layer-specific, horizontal propagation of slow waves have been investigated under anesthesia (Sanchez-Vives and McCormick, 2000; Luczak et al., 2007; Sakata and Harris, 2009; Chauvette et al., 2011; Wester and Contreras, 2012; Reyes-Puerta et al., 2015; Capone et al., 2019), little is known about how slow waves propagate horizontally during natural NREM sleep. The functions (if any) of the traveling aspect of slow waves are poorly understood (Muller et al., 2018).

Recently, the spatiotemporal properties of slow waves were characterized in the avian hyperpallium (van der Meij et al., 2019a). Most of the hyperpallium is involved in processing visual information and is, in many respects, homologous to the mammalian primary visual cortex (Medina and Reiner, 2000). Like the primary visual cortex, the hyperpallium is composed of layers, some of which receive extensive input from the thalamic lateral geniculate nucleus (Karten et al., 1973; Watanabe et al., 1983). Although the hyperpallium lacks pyramidal neurons with apical dendrites spanning multiple layers, the layers are interconnected via axonal projections (Medina and Reiner, 2000). Van der Meij and colleagues used high-density silicone electrode arrays to record LFP across the various layers of the pigeon's hyperpallium (**Figure 3A**). Interestingly, the thalamic input layers – interstitial part of hyperpallium apicale (IHA) and the hyperpallium intercalatum (HI) – play a prominent role in slow waves; slow waves have the highest amplitude within these layers (**Figures 3B,C**), and they tend to appear first in and propagate through, and outward from, these layers (**Figures 3D,E**; van der Meij et al., 2019a). Collectively, this suggests that thalamic input might be involved in the genesis of avian slow waves. Alternatively, properties intrinsic to neurons in these layers or the associated cytoarchitecture may favor the initiation and propagation of slow waves. Regardless, this study demonstrates that, as in the mammalian neocortex, slow waves propagate through the avian brain during NREM sleep (see also Beckers et al., 2014).

The mechanisms that mediate avian slow wave propagation remain unclear. Nonetheless, from multi-electrode recordings of anesthesia-induced slow waves, which in many aspects, including propagation pattern, resemble NREM slow waves (van der Meij et al., 2019b), it is clear that the extracellular depolarization of LFP waves is spatio-temporally closely matched by local action potential activity (Beckers et al., 2014), as is the case during NREM sleep in the human neocortex (Nir et al., 2011). Consequently, propagating slow waves appear to reflect the sequential local activation of neurons in the avian brain.

LOCAL ASPECTS OF REM SLEEP

Research on the local aspects of sleep has primarily focused on the cortical manifestation of NREM sleep in mammals and birds. However, in birds, muscle tone during REM sleep also appears to be regulated at a local level. In addition to sleeping with their head turned over the shoulder, birds can also sleep with their head facing forward. Interestingly, when geese sleep with their head facing forward, it slowly drops during REM sleep, presumably reflecting the loss of some tone in the neck muscles (Dewasmes et al., 1985). However, nuchal EMG recordings rarely show a reduction in tone during this behavior; the same behavior and EMG findings have also been reported in several other avian species (e.g., van Twyver and Allison, 1972; Šušić and Kovaèević, 1973; Tobler and Borbély, 1988; Szymczak et al., 1993). Nonetheless, when geese sleep with their head resting fully supported on their back, the same EMG recordings often show hypotonia or atonia (Dewasmes et al., 1985). Importantly, this

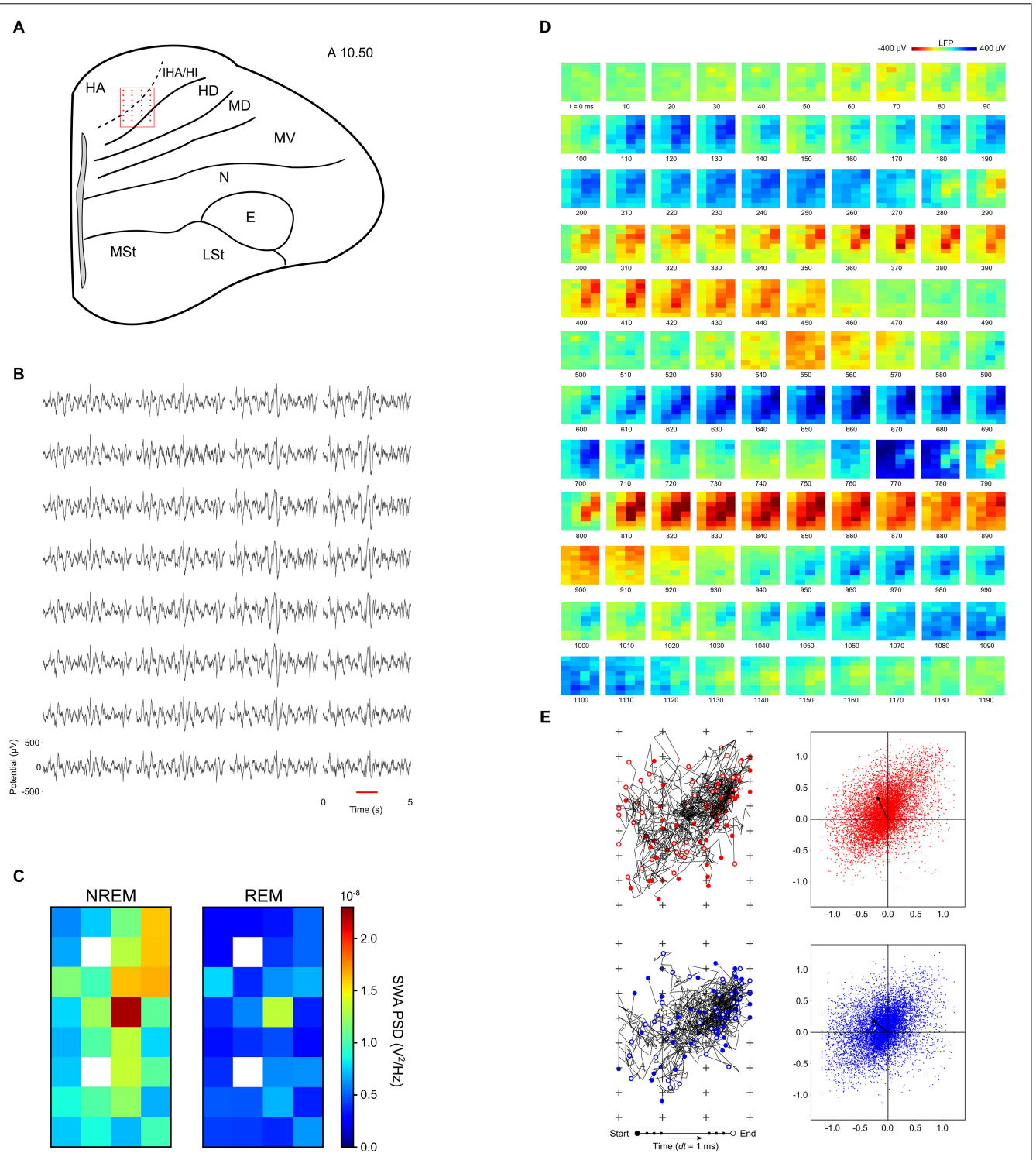

FIGURE 3 | Neurophysiology of the avian hyperpallium during natural sleep. **(A)** Position of a 32-channel silicon electrode probe in the hyperpallium of a pigeon. The orientation of the electrode grid (red) is always depicted with the medial side to the left and the surface of the brain on top. Input from the avian lateral geniculate nucleus (LGN) projects primarily to the interstitial part of hyperpallium apicale (IHA) and the hyperpallium intercalatum (HI). The underlying hyperpallium densocellulare (HD) receives relatively little input from the LGN. The hyperpallium overlies and is interconnected with the dorsal and ventral mesopallium (MD and MV) and nidopallium (N). **(B)** Five-second example of local field potentials showing the spatial distribution of slow waves in the hyperpallium during NREM sleep. **(C)** Mean slow wave activity (SWA; 1.5–4.5 Hz; *N* = 4 birds) over all episodes of NREM and REM sleep reveals greater SWA recorded from the electrodes positioned along the diagonal corresponding to the primary thalamic input layers, IHA and HI. SWA during REM sleep decreases from NREM sleep levels across all layers of the

(Continued)

FIGURE 3 | Continued
hyperpallium. White squares indicate missing data for some birds. **(D)** Propagating slow waves during NREM sleep. Red underlined episode from panel **(B)** is visualized in a sequence of image plots where pixels represent electrode sites and electrical potential is coded in color. **(E)** Trajectories and net propagation of the negative (red) and positive (blue) components of slow waves from a pigeon during NREM sleep. Left: trajectories for 50 randomly selected negative and positive waves (plus signs depict electrode sites). Right: net wave propagation calculated for every negative and positive wave in a 2 h recording; the black dot shows the mean propagation for negative and positive waves. Panels **(D,E)** demonstrate that both negative and positive potentials propagate most prominently along the thalamic input layers, and slightly into the overlying hyperpallium apicale (HA). E, entopallium; LSt, striatum lateral; MSt, striatum medial. Reproduced with permission from van der Meij et al. (2019a).

difference was not due to a lengthening of REM sleep bouts and a resulting progressive reduction in muscle tone when the head was supported, as bouts of REM sleep were similarly short regardless of head position. Consequently, the presence or absence of EMG atonia was specifically related to whether the head was supported or unsupported during REM sleep. Thus, even though the head drops when facing forward, the higher level of neck EMG activity indicates that some tone is maintained, possibly to partially counteract or control the drop. Consistent with the presence of some tone, the drops are usually slow (i.e., not a free-fall) and, in some cases, interrupted by brief halts or jerks (Walker and Berger, 1972; Ayala-Guerrero and Vasconcelos-Dueñas, 1988; Ayala-Guerrero, 1989; Ayala-Guerrero et al., 2003). Collectively, these findings indicate that neck muscle tone is regulated during avian REM sleep to accommodate differing postural demands.

In addition to the neck muscles, birds appear to sustain some tone in the muscles involved in standing during REM sleep. Most mammals lie down to sleep, due, in part, to the loss of skeletal muscle tone during REM sleep. Even horses, giraffes, and elephants, which can stand during NREM sleep, usually engage in REM sleep while lying (Ruckebusch, 1972; Tobler, 1992; Tobler and Schwierin, 1996; see also Gravett et al., 2017). Although horses have a leg locking mechanism (stay apparatus) that reduces the muscular tone needed to stand (Schuurman et al., 2003), apparently this level of tone can only be maintained during NREM sleep. Indeed, when horses are reluctant to lie down, due to pain or perceived vulnerability, they stumble and, in some cases, injure themselves when they enter REM sleep (Aleman et al., 2008; see also Schiffmann et al., 2018). In contrast to horses, birds often engage in REM sleep while standing, even on one foot, without falling (Dewasmes et al., 1985; Szymczak et al., 1993). Several lines of evidence suggest that this is not due to a more effective passive standing mechanism, but rather to the maintenance of some muscle tone during REM sleep. The ability to sleep while standing is often attributed to an "automatic digital flexor mechanism" that causes tendons to pull the foot closed around a perch when the bird relaxes and allows its weight to flex the ankle (Galton and Shepherd, 2012) and a "digital tendon locking mechanism" consisting of interlocking ridges in the digit tendons and overlying tendon sheaths that help to keep the digits closed (Quinn and Baumel, 1990). Some species of bats use a similar digital tendon locking mechanism (Quinn and Baumel, 1993) that allows them to engage in NREM and REM sleep while hanging upside down (Zhao et al., 2010), apparently without any muscular effort, as dead bats are found still hanging (Neuweiler, 2000). However, birds that die in their sleep do not remain perched up-right in trees, and freshly dead or anesthetized starlings are unable to passively grasp a perch (Galton and Shepherd, 2012). Similarly, although some birds may require less muscle tone to balance while standing on the ground on one foot due to the arrangement of the bones in the hip (Stolpe, 1932; Chang and Ting, 2017), it seems likely that some tone is still required to balance (Necker, 2006), let alone to hold one foot up (Necker, 2010). The ability to engage in REM sleep while standing on one foot likely relies on the same mechanisms that enable geese and other birds to maintain neck muscle tone when sleeping with their head unsupported. Finally, similar mechanisms may explain how frigatebirds can engage in brief bouts of REM sleep while soaring (Rattenborg et al., 2016).

The mechanisms mediating the local regulation of muscle tone during avian REM sleep are unknown. In mammals, glutamatergic neurons in the pontine sublaterodorsal nucleus (SLD) project to GABA/glycine inhibitory neurons in the ventromedial medulla (vmM) which in turn hyperpolarize somatic motor neurons resulting in atonia of the postural muscles (Valencia Garcia et al., 2018). The local regulation of muscle tone in birds is difficult to reconcile with this centralized, top-down model of muscle tone regulation in mammals. Assuming that the same central brainstem pathways also mediate reductions in muscle tone in birds, local competitive processes might modulate the impact that this central signal has on motor neurons and muscle tone depending on the postural demands for sustained tone.

The local regulation of muscle tone during avian REM sleep may have implications for understanding the functions of atonia. Traditionally, atonia is thought to prevent dream-related motor cortex output from causing animals to act out their dreams during REM sleep (Jouvet and Delorme, 1965; Morrison, 1983; Mahowald and Schenck, 2005). According to this hypothesis, the phasic twitches that occur during REM sleep are thought to reflect momentary failures of the atonia mechanism that prevents dream-related motor cortex output from reaching the muscles. Neurodegeneration of this brainstem mechanism is thought to give rise to REM sleep behavior disorder, a condition wherein people in REM sleep exhibit elevated muscle tone and complex behaviors that have been attributed to the enactment of dreams (Mahowald and Schenck, 2005). However, several lines of evidence indicate that twitches do not reflect a response to REM sleep-related activity in the motor cortex (Blumberg and Plumeau, 2016). First, dreams also occur during NREM sleep (Siclari et al., 2017), when muscle tone is sustained, but they do not result in dream enactment. Second, twitches persist in cats and week-old rats when the motor cortex is disconnected from the brainstem (Marchiafava and Pompeiano, 1964;

Villablanca, 1966; Kreider and Blumberg, 2000). Finally, in intact young rats, activity in the motor cortex follows, rather than precedes twitches (Tiriac et al., 2014). Clearly, twitches do not simply reflect output from the motor cortex during REM sleep, but instead output from the brainstem.

Rather than being a functionless byproduct of dreaming, twitches appear to play an important role in the development and perhaps maintenance of the motor cortex. During wakefulness, deliberate movements are accompanied by a corollary discharge that effectively informs the sensorimotor cortex that a movement has been initiated and the resulting sensory feedback (reafference) should be ignored. By contrast, during REM sleep, reafference resulting from twitches generated by the brainstem reaches the sensorimotor cortex where it induces large responses that are thought to play an active role in the development of sensorimotor neural circuits (Tiriac et al., 2014). Atonia is thought to contribute to this process by increasing the signal-to-noise ratio of sensory signals resulting from twitches. In adults, twitches may also update and recalibrate these sensorimotor circuits (Tiriac and Blumberg, 2016).

Becoming completely atonic and twitchy does not seem to pose a problem for very young birds which do not need to maintain up-right postures. However, it is unclear how adult birds reconcile this seemingly fundamental need for atonia and twitching with the local regulation of muscle tone during REM sleep. Presumably, the muscle groups controlling the digits, legs, etc., involved in standing also need to twitch. Indeed, the fact that reduced muscle tone persists, in at least some muscle groups, during certain postures emphasizes its importance; if it did not serve an important function natural selection should have done away with it altogether. Given the presence of atonia in the neck muscles of geese during REM sleep only when the head is supported (Dewasmes et al., 1985), it is conceivable that the muscles involved in standing become atonic and twitch when birds engage in REM sleep while sitting down. In effect, just as birds can engage in NREM sleep with one hemisphere at a time, they might be able to determine when REM sleep functions attributed to atonia and twitching take place in different parts of the body. Determining how birds reconcile the seemingly competing demands for postural control on the one hand, with atonia and twitching, on the other, might provide novel perspectives on the mechanisms and functions of REM sleep-related atonia and twitching, in general.

MIXED NREM/REM SLEEP STATES

The heterogeneity of states is not limited to the combination of wakefulness and NREM sleep, in the case of unihemispheric sleep, or in topographic variations in SWA during NREM sleep or REM sleep-related muscle tone. Comparative research reveals that mixed states can arise through the combination of aspects of NREM sleep occurring simultaneously with features of REM sleep. The first evidence for such mixture was gleaned from several studies on monotreme mammals. Owing to the retention of ancestral traits, such as egg-laying (Warren et al., 2008), monotremes might also retain ancestral sleep traits that would have been present in the most recent common ancestor to all mammals. Several studies of sleeping monotremes revealed only cortical slow waves typical of NREM sleep (Allison et al., 1972; Siegel et al., 1996, 1999; but see Nicol et al., 2000). However, concurrent with EEG signs of NREM sleep, were REM sleep-like brainstem unit activity in the short-beaked echidna (*Tachyglossus aculeatus*; Siegel et al., 1996) and REM sleep-related, brainstem-generated phenomena, including REMs and reduced muscle tone in the platypus (*Ornithorhynchus anatinus*; Siegel et al., 1999). The temporal integration and spatial segregation of NREM and REM sleep in the brains of monotremes, suggested that this was the ancestral condition, wherein REM sleep first appeared in the brainstem of early mammals, and later extended to the cortex in the common ancestor to metatherian (marsupial) and eutherian (placental) mammals (Siegel et al., 1998). This hypothesis was strengthened by the absence of similar activity in the brainstem of sleeping turtles (Eiland et al., 2001).

Motivated by the research on monotremes, Lesku et al. (2011a) investigated sleep in a Palaeognath bird. First, phylogenetically, there are two main groups of living birds: the clade Palaeognathae includes the large flightless ratites (e.g., ostriches, emus, rheas, and cassowaries), small flightless kiwi, and small volant tinamous. The sister clade, Neognathae, includes all other birds. Like monotremes, the Palaeognaths retain ancestral traits, including their reptilian palate anatomy, not found in Neognaths (Mitchell et al., 2014). Interestingly, in addition to a REM sleep state with cortical activation typical of other birds, ostriches (*Struthio camelus*) also have a monotreme-like sleep state characterized by EEG slow waves occurring in conjunction with REMs under closed eyelids, and behavioral and physiological signs of reduced neck muscle tone (**Figure 4**; Lesku et al., 2011a). This monotreme-like mixed sleep state led Lesku et al. (2011a) to tentatively suggest that the evolution of REM sleep followed a similar trajectory in mammals and birds, occurring first in the brainstem and later becoming exclusively associated with cortical activation. However, unlike other birds, ostriches maintain an unusual sleep posture with the head held periscopically above the ground during unequivocal NREM sleep and entry into this mixed sleep state. Moreover, although the head drops during the mixed state, as a result of reduced muscle tone, the neck remains held off the ground. Consequently, just as geese modulate muscle tone during REM sleep depending on their head position (Dewasmes et al., 1985), it is conceivable that ostriches incorporate features of NREM sleep into REM sleep to maintain some control over their falling head. If true, then such a mixed state might not have any relevance for understanding the evolution of avian sleep states, and we would predict that other Palaeognath birds that sleep with their head better supported (by body or ground) to exhibit distinct sleep states like those observed in Neognath birds (Roth et al., 2006). Moreover, although ostriches exhibit some ancestral traits, they bear little resemblance to early birds, which were small and flighted. For all these reasons, the study of tinamous, which retain the ancestral small size and ability to fly (Mitchell et al., 2014), might be more relevant to understanding how NREM and REM sleep evolved in birds. Unlike their Palaeognath kin, the elegant crested tinamou (*Eudromia elegans*) has sleep states like those

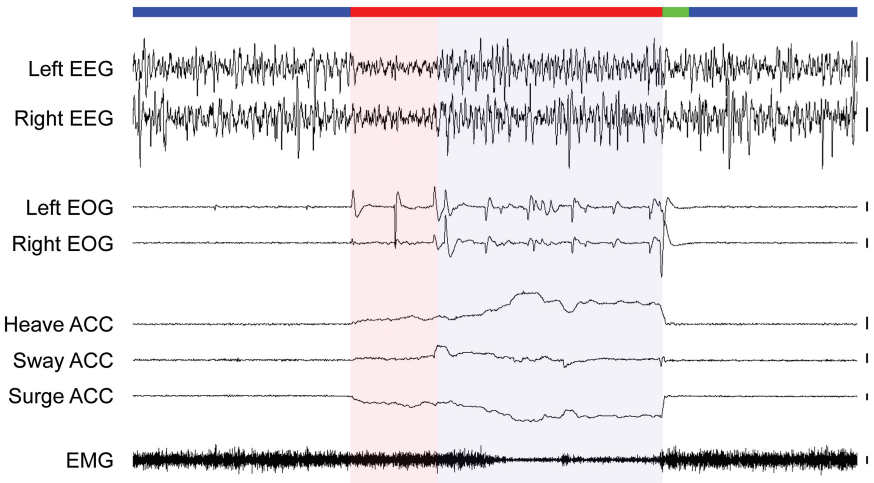

FIGURE 4 | Sleep states in an ostrich. The recording begins and ends with periods of NREM sleep (blue bar) characterized by high amplitude, slow waves in the electroencephalogram (EEG), the absence of rapid eye movements (measured via electrooculogram, EOG), and head movements (accelerometer, ACC), and moderate neck muscle tone (electromyogram, EMG). NREM sleep is interrupted by a period of REM sleep (red bar) with either EEG activation (red shading) or slow waves (blue shading). Irrespective of the type of EEG activity, rapid eye movements, a forward falling and swaying head with moderate-to-low muscle tone occurred invariably during REM sleep in the ostrich. Heave ACC: movement along the dorso-ventral axis with an upward slope denoting downward movement, Sway ACC: lateral axis with up denoting movement to the right, Surge ACC: anterior-posterior axis with down denoting movement forward. Vertical bars to the right of each EEG, EOG, and EMG trace denote 100 μV, and 100 mg-forces to the right of each ACC trace. Trace duration: 60 s. Reproduced with permission from Lesku et al. (2011a).

of all other birds studied, as characterized by the EEG, EOG, EMG and head movements captured by video recordings and accelerometry (Tisdale et al., 2017). Consequently, it seems that the mixed sleep state described in ostriches does not reflect the ancestral state for birds, but rather a peculiarity of ostriches, perhaps somehow related to their unusual sleep posture.

Indirectly, these findings from two Palaeognath species, also question whether the mixed sleep state found in monotremes reflects the ancestral state for mammals, especially given recent reports of a REM sleep-like state, with wake-like cortical activation, in the bearded dragon lizard (*Pogona vitticeps*) (Shein-Idelson et al., 2016; Libourel et al., 2018). Perhaps even more relevant is the discovery that the cortical correlates of REM sleep-like states vary dramatically, even among different species of lizards recorded using the same methods in the same lab. Unlike bearded dragons, the Argentine tegu (*Salvator merianae*) does not exhibit wake-like cortical activation during putative REM sleep, but rather a novel beta rhythm, rarely observed during wakefulness (Libourel et al., 2018). Collectively, these studies suggest that the cortical correlates of (ostensibly) REM sleep in non-avian reptiles are more diverse than previously recognized, an exciting finding that complicates attempts to draw simple stories for the evolution of sleep states in vertebrates.

Recent studies suggest that slow waves occurring during REM sleep might be more common than previously thought, even in more traditional mammalian models for investigating sleep, such as rodents and humans. Intracortical records from mice revealed that slow waves persist in the thalamic input layers of primary sensory cortices during REM sleep (Funk et al., 2016). By contrast, secondary/association cortices show LFP activation across all layers. Recently, in a high-density EEG study of humans, slow waves were also recorded from at least some primary cortices (Bernardi et al., 2019). Funk et al. (2016) suggest that slow waves occurring in the input layers of primary sensory cortices might gate sensory input, and thereby explain why arousal thresholds are elevated during REM sleep. These studies demonstrate that cortical slow waves can occur during mammalian REM sleep, and thereby question whether this phenomenon explains the presence of slow waves in monotremes exhibiting signs of REM sleep. However, as the EEG electrodes were placed over the parietal and sensorimotor cortex in echidnas (Siegel et al., 1996) and motor cortex in platypuses (Siegel et al., 1999), it is unclear whether slow waves in monotremes and mice reflect the same phenomena. High density EEG and intracortical recordings are needed in monotremes and more placental species, to clarify the generality and potential functions of slow waves during REM sleep.

Recent intra-"cortical" recordings from pigeons demonstrate that slow waves occurring in the thalamic input layers of primary sensory areas is not a universal feature of animals with REM sleep. As described above, during NREM sleep, slow waves in the visual hyperpallium – the avian homolog of the mammalian primary visual cortex – are most evident in thalamic input layers. However, during REM sleep, these layers show a large reduction in slow wave power from prior NREM sleep levels (**Figure 3C**). Furthermore, in some recordings, these input layers also exhibit bursts of 70–90 Hz gamma activity during REM sleep (van der Meij et al., 2019a). These finding indicate that thalamic input layers of primary sensory cortices do not always exhibit slow waves during REM sleep. In addition, the intra-"cortical" recordings from pigeons indicate that the presence of EEG slow waves occurring in conjunction with signs of REM sleep in ostriches (Lesku et al., 2011a) cannot be attributed

to the phenomenon described in mice (Funk et al., 2016). As in most studies of birds, the EEG was recorded from the visual hyperpallium in ostriches, but only ostriches show slow waves occurring in conjunction with other signs of REM sleep. Consequently, slow waves during REM sleep reflect a unique feature of the ostrich hyperpallium, rather than a general feature of the avian hyperpallium during REM sleep.

CONCLUSION

In several respects, the local aspects of sleep are similar in mammals and birds. Nonetheless, there are also some potentially informative differences. In both groups, at least some species mitigate the simultaneous ecological need to be awake and the physiological need to sleep by engaging in NREM sleep unihemispherically. Although the evidence for sleep homeostasis at the hemispheric level remains somewhat equivocal, the presence of local use-dependent homeostasis within a hemisphere suggests that homeostasis at the hemispheric level is likely. In both mammals and birds, thalamic input layers play a prominent role in the initiation of propagating slow waves. Despite the similar local aspects of NREM sleep, birds exhibit local aspects of REM sleep not found in mammals. Although birds show visible signs of reduced tone in the muscles supporting the head during REM sleep, the muscles involved in maintaining a standing posture (even on one foot) rarely show reductions in tone during REM sleep. In addition, birds are able to modulate tone in the neck muscles to accommodate different head positions during REM sleep. Like monotreme mammals, ostriches exhibit a mixed sleep state characterized by cortical slow waves occurring with brainstem-mediated features of REM sleep. However, comparisons with other birds and reptiles, challenge the hypothesis that this mixed sleep state reflects an ancestral form of sleep in mammals or birds. Instead, an emerging pattern from recent comparative work is that the EEG correlates of REM sleep may be far more diverse than previously recognized: ostriches have slow waves, but their close tinamou relatives have activation typical of other birds; pogona lizards have wake-like cortical activation, but tegu lizards exhibit a beta rhythm rarely found during wakefulness; and mice exhibit slow waves in the thalamic input layers of the primary visual cortex, but pigeons show activation in these layers. We suspect that as the diversity of species and the number of brain regions examined increases, our ability to package sleep into two, simple, mutually exclusive states will become even more difficult. Although this may tax our ability to define sleep, this diversity also serves as a rich resource for exploring the mechanisms and functions of sleep-related brain activity.

AUTHOR CONTRIBUTIONS

NR and JL wrote the initial draft of the manuscript. All authors provided the input on the manuscript. JL and JvdM contributed to the figures.

FUNDING

NR and JvdM were supported by the Max Planck Society. JvdM is a member of the International Max Planck Research School for Organismal Biology. GB is part of the Consortium on Individual Development (CID), which is funded through the Gravitation Program of the Dutch Ministry of Education, Culture, and Science and the Netherlands Organization for Scientific Research (NWO; Grant Number 024.001.003). JL was supported by the Australian Research Council (DP170101003).

ACKNOWLEDGMENTS

We thank Gianina Ungurean and Dolores Martinez-Gonzalez for their valuable comments on the manuscript.

REFERENCES

Aleman, M., Williams, D. C., and Holliday, T. (2008). Sleep and sleep disorders in horses. *AAEP Proc.* 54, 180–185.

Allison, T., van Twyver, H., and Goff, W. R. (1972). Electrophysiological studies of the echidna, Tachyglossus aculeatus. I. Waking and sleep. *Arch. Ital. Biol.* 110, 145–184. doi: 10.4449/aib.v110i2.2469

Astori, S., Wimmer, R. D., and Lüthi, A. (2013). Manipulating sleep spindles–expanding views on sleep, memory, and disease. *Trends Neurosci.* 36, 738–748. doi: 10.1016/j.tins.2013.10.001

Ayala-Guerrero, F. (1989). Sleep patterns in the parakeet Melopsittacus undulatus. *Physiol. Behav.* 46, 787–791. doi: 10.1016/0031-9384(89)90038-3

Ayala-Guerrero, F., Mexicano, G., and Ramos, J. I. (2003). Sleep characteristics in the turkey *Meleagris gallopavo*. *Physiol. Behav.* 78, 435–440. doi: 10.1016/S0031-9384(03)00032-5

Ayala-Guerrero, F., and Vasconcelos-Dueñas, I. (1988). Sleep in the dove *Zenaida asiatica*. *Behav. Neural. Biol.* 49, 133–138. doi: 10.1016/S0163-1047(88)90451-7

Ball, N. J., Amlaner, C. J., Shaffery, J. P., and Opp, M. R. (1988). "Asynchronous eye closure and unihemispheric quiet sleep of birds," in *Sleep 86*, eds W. P. Koella, F. Obál, H. Schulz, and P. Visser (New York, NY: Gustav Fischer), 151–153.

Beckers, G. J. L., van der Meij, J., Lesku, J. A., and Rattenborg, N. C. (2014). Plumes of neuronal activity propagate in three dimensions through the nuclear avian brain. *BMC Biol.* 12:16. doi: 10.1186/1741-7007-12-16

Bernardi, G., Betta, M., Ricciardi, E., Pietrini, P., Tononi, G., and Siclari, F. (2019). Regional delta waves in human rapid-eye movement sleep. *J. Neurosci.* 39, 2686–2697. doi: 10.1523/JNEUROSCI.2298-18.2019

Blumberg, M. S., and Plumeau, A. M. (2016). A new view of "dream enactment" in REM sleep behavior disorder. *Sleep Med. Rev.* 30, 34–42. doi: 10.1016/j.smrv.2015.12.002

Boerema, A. S., Riedstra, B., and Strijkstra, A. M. (2003). Decrease in monocular sleep after sleep deprivation in the domestic chicken. *Behaviour* 140, 1415–1420. doi: 10.1163/156853903771980657

Boiko, V. P., and Bureś, J. (1985). Electrical phenomena in the telencephalon of the pigeon during pecking. *Neurosci. Behav. Physiol.* 15, 265–270.

Branstetter, B. K., Finneran, J. J., Fletcher, E. A., Weisman, B. C., and Ridgway, S. H. (2012). Dolphins can maintain vigilant behavior through echolocation for 15 days without interruption or cognitive impairment. *PLoS One* 7:e47478. doi: 10.1371/journal.pone.0047478

Brusatte, S. L., O'Connor, J. K., and Jarvis, E. D. (2015). The origin and diversification of birds. *Curr. Biol.* 25, R888–R898. doi: 10.1016/j.cub.2015.08.003

Capone, C., Rebollo, B., Muñoz, A., Illa, X., Del Giudice, P., Sanchez-Vives, M. V., et al. (2019). Slow waves in cortical slices: how spontaneous activity is shaped by laminar structure. *Cereb. Cortex* 9, 319–335. doi: 10.1093/cercor/bhx326

Castelnovo, A., Lopez, R., Proserpio, P., Nobili, L., and Dauvilliers, Y. (2018). NREM sleep parasomnias as disorders of sleep-state dissociation. *Nat. Rev. Neurol.* 14, 470–481. doi: 10.1038/s41582-018-0030-y

Chang, Y. H., and Ting, L. H. (2017). Mechanical evidence that flamingos can support their body on one leg with little active muscular force. *Biol. Lett.* 13, 20160948. doi: 10.1098/rsbl.2016.0948

Chauvette, S., Crochet, S., Volgushev, M., and Timofeev, I. (2011). Properties of slow oscillation during slow-wave sleep and anesthesia in cats. *J. Neurosci.* 31, 14998–15008. doi: 10.1523/JNEUROSCI.2339-11.2011

Chauvette, S., Volgushev, M., and Timofeev, I. (2010). Origin of active states in local neocortical networks during slow sleep oscillation. *Cereb. Cortex* 20, 2660–2674. doi: 10.1093/cercor/bhq009

Constantinople, C. M., and Bruno, R. M. (2013). Deep cortical layers are activated directly by thalamus. *Science* 340, 1591–1594. doi: 10.1126/science.1236425

Crunelli, V., and Hughes, S. W. (2010). The slow (< 1 Hz) rhythm of non-REM sleep: a dialogue between three cardinal oscillators. *Nat. Neurosci.* 13, 10–18. doi: 10.1038/nn.2445

Dewasmes, G., Cohen-Adad, F., Koubi, H., and Le Maho, Y. (1985). Polygraphic and behavioral study of sleep in geese: existence of nuchal atonia during paradoxical sleep. *Physiol. Behav.* 35, 67–73. doi: 10.1016/0031-9384(85)90173-8

Durán, E., Oyanedel, C. N., Niethard, N., Inostroza, M., and Born, J. (2018). Sleep stage dynamics in neocortex and hippocampus. *Sleep* 41:zsy060. doi: 10.1093/sleep/zsy060

Eiland, M. M., Lyamin, O. I., and Siegel, J. M. (2001). State-related discharge of neurons in the brainstem of freely moving box turtles, *Terrapene carolina* major. *Arch. Ital. Biol.* 139, 23–36. doi: 10.4449/aib.v139i1.202

Emrick, J. J., Gross, B. A., Riley, B. T., and Poe, G. R. (2016). Different simultaneous sleep states in the hippocampus and neocortex. *Sleep* 39, 2201–2209. doi: 10.5665/sleep.6326

Fuchs, T., Maury, D., Moore, F. R., and Bingman, V. P. (2009). Daytime micro-naps in a nocturnal migrant: an EEG analysis. *Biol. Lett.* 5, 77–80. doi: 10.1098/rsbl.2008.0405

Funk, C. M., Honjoh, S., Rodriguez, A. V., Cirelli, C., and Tononi, G. (2016). Local slow waves in superficial layers of primary cortical areas during REM sleep. *Curr. Biol.* 26, 396–403. doi: 10.1016/j.cub.2015.11.062

Galton, P. M., and Shepherd, J. D. (2012). Experimental analysis of perching in the European starling (*Sturnus vulgaris*: Passeriformes; Passeres), and the automatic perching mechanism of birds. *J. Exp. Zool. A Ecol. Genet. Physiol.* 317, 205–215. doi: 10.1002/jez.1714

Gill, R. E., Tibbitts, T. L., Douglas, D. C., Handel, C. M., Mulcahy, D. M., Gottschalck, J. C., et al. (2009). Extreme endurance flights by landbirds crossing the Pacific Ocean: ecological corridor rather than barrier? *Proc. R. Soc. B* 276, 447–458. doi: 10.1098/rspb.2008.1142

Gnone, G., Moriconi, T., and Gambini, G. (2006). Sleep behaviour: activity and sleep in dolphins. *Nature* 441, E10–E11. doi: 10.1038/nature04899

Goley, P. D. (1999). Behavioral aspects of sleep in Pacific white-sided dolphins (*Lagenorhynchus obliquidens*, Gill 1865). *Mar. Mam. Sci.* 15, 1054–1064. doi: 10.1111/j.1748-7692.1999.tb00877.x

Graf, R., Heller, H. C., Sakaguchi, S., and Krishna, S. (1987). Influence of spinal and hypothalamic warming on metabolism and sleep in pigeons. *Am. J. Physiol.* 252, R661–R667. doi: 10.1152/ajpregu.1987.252.4.R661

Gravett, N., Bhagwandin, A., Sutcliffe, R., Landen, K., Chase, M. J., Lyamin, O. I., et al. (2017). Inactivity/sleep in two wild free-roaming African elephant matriarchs - Does large body size make elephants the shortest mammalian sleepers? *PLoS One* 12:e0171903. doi: 10.1371/journal.pone.0171903

Hanlon, E. C., Faraguna, U., Vyazovskiy, V. V., Tononi, G., and Cirelli, C. (2009). Effects of skilled training on sleep slow wave activity and cortical gene expression in the rat. *Sleep* 32, 719–729. doi: 10.1093/sleep/32.6.719

Hedenström, A., Norevik, G., Warfvinge, K., Andersson, A., Bäckman, J., and Åkesson, S. (2016). Annual 10-month aerial life phase in the common swift *Apus apus*. *Curr. Biol.* 26, 1–5. doi: 10.1016/j.cub.2016.09.014

Heller, H. C., Graf, R., and Rautenberg, W. (1983). Circadian and arousal state influences on thermoregulation in the pigeon. *Am. J. Physiol.* 245, R321–R328. doi: 10.1152/ajpregu.1983.245.3.R321

Huber, R., Ghilardi, M. F., Massimini, M., Ferrarelli, F., Riedner, B. A., Peterson, M. J., et al. (2006). Arm immobilization causes cortical plastic changes and locally decreases sleep slow wave activity. *Nat. Neurosci.* 9, 1169–1176. doi: 10.1038/nn1758

Huber, R., Ghilardi, M. F., Massimini, M., and Tononi, G. (2004). Local sleep and learning. *Nature* 430, 78–81. doi: 10.1038/nature02663

Jones, S. G., Vyazovskiy, V. V., Cirelli, C., Tononi, G., and Benca, R. M. (2008). Homeostatic regulation of sleep in the white-crowned sparrow (*Zonotrichia leucophrys gambelii*). *BMC Neurosci.* 9:47. doi: 10.1186/1471-2202-9-47

Jouvet, M., and Delorme, F. (1965). Locus Coeruleus et Sommeil Paradoxal. *C. R. Seances Soc. Biol. Fil.* 159, 895–899.

Jouvet-Mounier, D., Astic, L., and Lacote, D. (1970). Ontogenesis of the states of sleep in rat, cat, and guinea pig during the first postnatal month. *Dev. Psychobiol.* 2, 216–239. doi: 10.1002/dev.420020407

Karten, H. J., Hodos, W., Nauta, W. J., and Revzin, A. M. (1973). Neural connections of the "visual wulst" of the avian telencephalon. Experimental studies in the pigeon (*Columba livia*) and owl (*Speotyto cunicularia*). *J. Comp. Neurol.* 150, 253–277. doi: 10.1002/cne.901500303

Kattler, H., Dijk, D. J., and Borbély, A. A. (1994). Effect of unilateral somatosensory stimulation prior to sleep on the sleep EEG in humans. *J. Sleep Res.* 3, 159–164. doi: 10.1111/j.1365-2869.1994.tb00123.x

Kelly, M. L., Peters, R. A., Tisdale, R. K., and Lesku, J. A. (2015). Unihemispheric sleep in crocodilians? *J. Exp. Biol.* 218, 3175–3178. doi: 10.1242/jeb.127605

Kreider, J. C., and Blumberg, M. S. (2000). Mesopontine contribution to the expression of active 'twitch' sleep in decerebrate week-old rats. *Brain Res.* 872, 149–159. doi: 10.1016/S0006-8993(00)02518-X

Krueger, J. M., Nguyen, J. T., Dykstra-Aiello, C. J., and Taishi, P. (2019). Local sleep. *Sleep Med. Rev.* 43, 14–21. doi: 10.1016/j.smrv.2018.10.001

Krueger, J. M., and Obál, F. (1993). A neuronal group theory of sleep function. *J. Sleep Res.* 2, 63–69. doi: 10.1111/j.1365-2869.1993.tb00064.x

Landsness, E. C., Crupi, D., Hulse, B. K., Peterson, M. J., Huber, R., Ansari, H., et al. (2009). Sleep-dependent improvement in visuomotor learning: a causal role for slow waves. *Sleep* 32, 1273–1284. doi: 10.1093/sleep/32.10.1273

Lemieux, M., Chen, J. Y., Lonjers, P., Bazhenov, M., and Timofeev, I. (2014). The impact of cortical deafferentation on the neocortical slow oscillation. *J. Neurosci.* 34, 5689–5703. doi: 10.1523/JNEUROSCI.1156-13.2014

Lesku, J. A., Meyer, L. C. R., Fuller, A., Maloney, S. K., Dell'Omo, G., Vyssotski, A. L., et al. (2011a). Ostriches sleep like platypuses. *PLoS One* 6:e23203. doi: 10.1371/journal.pone.0023203

Lesku, J. A., Vyssotski, A. L., Martinez-Gonzalez, D., Wilzeck, C., and Rattenborg, N. C. (2011b). Local sleep homeostasis in the avian brain: convergence of sleep function in mammals and birds? *Proc. R. Soc. B* 278, 2419–2428. doi: 10.1098/rspb.2010.2316

Lesku, J. A., Rattenborg, N. C., Valcu, M., Vyssotski, A. L., Kuhn, S., Kuemmeth, F., et al. (2012). Adaptive sleep loss in polygynous pectoral sandpipers. *Science* 337, 1654–1658. doi: 10.1126/science.1220939

Lesku, J. A., Roth, T. C., Rattenborg, N. C., Amlaner, C. J., and Lima, S. L. (2009). History and future of comparative analyses in sleep research. *Neurosci. Biobehav. Rev.* 33, 1024–1036. doi: 10.1016/j.neubiorev.2009.04.002

Libourel, P. A., Barrillot, B., Arthaud, S., Massot, B., Morel, A. L., Beuf, O., et al. (2018). Partial homologies between sleep states in lizards, mammals, and birds suggest a complex evolution of sleep states in amniotes. *PLoS Biol.* 16:e2005982. doi: 10.1371/journal.pbio.2005982

Liechti, F., Witvliet, W., Weber, R., and Bächler, E. (2013). First evidence of a 200-day non-stop flight in a bird. *Nat. Commun.* 4:2554. doi: 10.1038/ncomms3554

Lima, S. L., and Rattenborg, N. C. (2007). A behavioural shutdown can make sleeping safer: a strategic perspective on the function of sleep. *Anim. Behav.* 74, 189–197. doi: 10.1016/j.anbehav.2006.12.007

Low, P. S., Shank, S. S., Sejnowski, T. J., and Margoliash, D. (2008). Mammalian-like features of sleep structure in zebra finches. *Proc. Natl. Acad. Sci. U.S.A.* 105, 9081–9086. doi: 10.1073/pnas.0703452105

Luczak, A., Barthó, P., Marguet, S. L., Buzsáki, G., and Harris, K. D. (2007). Sequential structure of neocortical spontaneous activity in vivo. *Proc. Natl. Acad. Sci. U.S.A.* 104, 347–352. doi: 10.1073/pnas.0605643104

Lyamin, O., Pryaslova, J., Kosenko, P., and Siegel, J. (2007). Behavioral aspects of sleep in bottlenose dolphin mothers and their calves. *Physiol. Behav.* 92, 725–733. doi: 10.1016/j.physbeh.2007.05.064

Lyamin, O. I., Kosenko, P. O., Korneva, S. M., Vyssotski, A. L., Mukhametov, L. M., and Siegel, J. M. (2018). Fur seals suppress REM sleep for very long periods without subsequent rebound. *Curr. Biol.* 28, 2000–2005. doi: 10.1016/j.cub.2018.05.022

Lyamin, O. I., Kosenko, P. O., Lapierre, J. L., Mukhametov, L. M., and Siegel, J. M. (2008c). Fur seals display a strong drive for bilateral slow-wave sleep while on land. *J. Neurosci.* 28, 12614–12621. doi: 10.1523/JNEUROSCI.2306-08.2008

Lyamin, O. I., Kosenko, P. O., Vyssotski, A. L., Lapierre, J. L., Siegel, J. M., and Mukhametov, L. M. (2012). Study of sleep in a walrus. *Dokl. Biol. Sci.* 444, 188–191. doi: 10.1134/S0012496612030143

Lyamin, O. I., Lapierre, J. L., Kosenko, P. O., Kodama, T., Bhagwandin, A., Korneva, S. M., et al. (2016). Monoamine release during unihemispheric sleep and unihemispheric waking in the fur seal. *Sleep* 39, 625–636. doi: 10.5665/sleep.5540

Lyamin, O. I., Lapierre, J. L., Kosenko, P. O., Mukhametov, L. M., and Siegel, J. M. (2008a). Electroencephalogram asymmetry and spectral power during sleep in the northern fur seal. *J. Sleep Res.* 17, 154–165. doi: 10.1111/j.1365-2869.2008.00639.x

Lyamin, O. I., Manger, P. R., Ridgway, S. H., Mukhametov, L. M., and Siegel, J. M. (2008b). Cetacean sleep: an unusual form of mammalian sleep. *Neurosci. Biobehav. Rev.* 32, 1451–1484. doi: 10.1016/j.neubiorev.2008.05.023

Lyamin, O. I., Mukhametov, L. M., and Siegel, J. M. (2004). Relationship between sleep and eye state in Cetaceans and Pinnipeds. *Arch. Ital. Biol.* 142, 557–568. doi: 10.4449/aib.v142i4.427

Lyamin, O. I., Mukhametov, L. M., Siegel, J. M., Nazarenko, E. A., Polyakova, I. G., and Shpak, O. V. (2002). Unihemispheric slow wave sleep and the state of the eyes in a white whale. *Behav. Brain Res.* 129, 125–129. doi: 10.1016/S0166-4328(01)00346-1

Mahowald, M., and Schenck, C. (2005). Insights from studying human sleep disorders. *Nature* 437, 1279–1285. doi: 10.1038/nature04287

Marchiafava, P. L., and Pompeiano, O. (1964). Pyramidal influences of spinal cord during desynchronized sleep. *Arch. Ital. Biol.* 102, 500–529. doi: 10.1007/BF00364696

Martinez-Gonzalez, D., Lesku, J. A., and Rattenborg, N. C. (2008). Increased EEG spectral power density during sleep following short-term sleep deprivation in pigeons (*Columba livia*): evidence for avian sleep homeostasis. *J. Sleep Res.* 17, 140–153. doi: 10.1111/j.1365-2869.2008.00636.x

Mascetti, G. G. (2016). Unihemispheric sleep and asymmetrical sleep: behavioral, neurophysiological, and functional perspectives. *Nat. Sci. Sleep* 8, 221–238. doi: 10.2147/NSS.S71970

Mascetti, G. G., Rugger, M., Vallortigara, G., and Bobbo, D. (2007). Monocular-unihemispheric sleep and visual discrimination learning in the domestic chick. *Exp. Brain Res.* 176, 70–84. doi: 10.1007/s00221-006-0595-3

Mascetti, G. G., and Vallortigara, G. (2001). Why do birds sleep with one eye open? Light exposure of the chick embryo as a determinant of monocular sleep. *Curr. Biol.* 11, 971–974. doi: 10.1016/S0960-9822(01)00265-2

Massimini, M., Huber, R., Ferrarelli, F., Hill, S., and Tononi, G. (2004). The sleep slow oscillation as a traveling wave. *J. Neurosci.* 24, 6862–6870. doi: 10.1523/JNEUROSCI.1318-04.2004

Mathews, C. G., Lesku, J. A., Lima, S. L., and Amlaner, C. J. (2006). Asynchronous eye closure as an anti-predator behavior in the western fence lizard (*Sceloporus occidentalis*). *Ethology* 112, 286–292. doi: 10.1111/j.1439-0310.2006.01138.x

Medina, L., and Reiner, A. (2000). Do birds possess homologues of mammalian primary visual, somatosensory and motor cortices? *Trends Neurosci.* 23, 1–12. doi: 10.1016/S0166-2236(99)01486-1

Mitchell, K. J., Llamas, B., Soubrier, J., Rawlence, N. J., Worthy, T. H., Wood, J., et al. (2014). Ancient DNA reveals elephant birds and kiwi are sister taxa and clarifies ratite bird evolution. *Science* 344, 898–900. doi: 10.1126/science.1251981

Morrison, A. (1983). A window on the sleeping brain. *Sci. Am.* 248, 94–102. doi: 10.1038/scientificamerican0483-94

Mukhametov, L. M., Lyamin, O. I., Chetyrbok, I. S., Vassilyev, A. A., and Diaz, R. (1992). Sleep in an Amazonian manatee, *Trichechus inunguis*. *Experientia* 48, 417–419.

Mukhametov, L. M., Supin, A. Y., and Polyakova, I. G. (1977). Interhemispheric asymmetry of the electroencephalographic sleep patterns in dolphins. *Brain Res.* 134, 581–584. doi: 10.1016/0006-8993(77)90835-6

Muller, L., Chavane, F., Reynolds, J., and Sejnowski, T. J. (2018). Cortical travelling waves: mechanisms and computational principles. *Nat. Rev. Neurosci.* 19, 255–268. doi: 10.1038/nrn.2018.20

Murphy, M., Riedner, B. A., Huber, R., Massimini, M., Ferrarelli, F., and Tononi, G. (2009). Source modeling sleep slow waves. *Proc. Natl. Acad. Sci. U.S.A.* 106, 1608–1613. doi: 10.1073/pnas.0807933106

Necker, R. (2006). Specializations in the lumbosacral vertebral canal and spinal cord of birds: evidence of a function as a sense organ which is involved in the control of walking. *J. Comp. Physiol. A. Neuroethol. Sens. Neural Behav. Physiol.* 192, 439–448. doi: 10.1007/s00359-006-0105-x

Necker, R. (2010). Stehen der Vögel auf einem Bein: mechanismen und mögliche Funktionen - eine Übersicht (Birds standing on one leg: mechanisms and possible functions - a review). *Vogelwarte* 48, 43–44.

Nelini, C., Bobbo, D., and Mascetti, G. G. (2010). Local sleep: a spatial learning task enhances sleep in the right hemisphere of domestic chicks (*Gallus gallus*). *Exp. Brain Res.* 205, 195–204. doi: 10.1007/s00221-010-2352-x

Nelini, C., Bobbo, D., and Mascetti, G. G. (2012). Monocular learning of a spatial task enhances sleep in the right hemisphere of domestic chicks (*Gallus gallus*). *Exp. Brain Res.* 218, 381–388. doi: 10.1007/s00221-012-3023-x

Neuweiler, G. (2000). *The Biology of Bats*. Oxford: Oxford University Press.

Newman, S. M., Paletz, E. M., Rattenborg, N. C., Obermeyer, W. H., and Benca, R. M. (2008). Sleep deprivation in the pigeon using the disk-over-water method. *Physiol. Behav.* 93, 50–58. doi: 10.1016/j.physbeh.2007.07.012

Nicol, S. C., Andersen, N. A., Phillips, N. H., and Berger, R. J. (2000). The echidna manifests typical characteristics of rapid eye movement sleep. *Neurosci. Lett.* 283, 49–52. doi: 10.1016/S0304-3940(00)00922-8

Nir, Y., Andrillon, T., Marmelshtein, A., Suthana, N., Cirelli, C., Tononi, G., et al. (2017). Selective neuronal lapses precede human cognitive lapses following sleep deprivation. *Nat. Med.* 23, 1474–1480. doi: 10.1038/nm.4433

Nir, Y., Staba, R. J., Andrillon, T., Vyazovskiy, V. V., Cirelli, C., Fried, I., et al. (2011). Regional slow waves and spindles in human sleep. *Neuron* 70, 153–169. doi: 10.1016/j.neuron.2011.02.043

Oleksenko, A. I., Mukhametov, L. M., Polyakova, I. G., Supin, A. Y., and Kovalzon, V. M. (1992). Unihemispheric sleep deprivation in bottlenose dolphins. *J. Sleep Res.* 1, 40–44. doi: 10.1111/j.1365-2869.1992.tb00007.x

Ookawa, T. (2004). The electroencephalogram and sleep in the domestic chicken. *Avian Poult. Biol. Rev.* 15, 1–8. doi: 10.3184/147020604783637453

Ookawa, T., and Takagi, K. (1968). Electroencephalograms of free behavioral chicks at various developmental ages. *Jpn. J. Physiol.* 18, 87–99.

Peters, J., Vonderahe, A., and Schmid, D. (1965). Onset of cerebral electrical activity associated with behavioral sleep and attention in the developing chick. *J. Exp. Zool.* 160, 255–262.

Quercia, A., Bobbo, D., and Mascetti, G. G. (2018). The effect of monocular deprivation on unihemispheric sleep in light and dark incubated/reared domestic chicks. *Laterality* 23, 166–183. doi: 10.1080/1357650X.2017.1347180

Quinn, T. H., and Baumel, J. J. (1990). The digital tendon locking mechanism of the avian foot (Aves). *Zoomorphology* 109, 281–293. doi: 10.1007/BF00312195

Quinn, T. H., and Baumel, J. J. (1993). Chiropteran tendon locking mechanism. *J. Morph.* 216, 197–208. doi: 10.1002/jmor.1052160207

Rattenborg, N. C. (2017). Sleeping on the wing. *Interface Focus* 7:20160082. doi: 10.1098/rsfs.2016.0082

Rattenborg, N. C., Amlaner, C. J., and Lima, S. L. (2000). Behavioral, neurophysiological and evolutionary perspectives on unihemispheric sleep. *Neurosci. Biobehav. Rev.* 24, 817–842. doi: 10.1016/S0149-7634(00)00039-7

Rattenborg, N. C., Amlaner, C. J., and Lima, S. L. (2001). Unilateral eye closure and interhemispheric EEG asymmetry during sleep in the pigeon (*Columba livia*). *Brain Behav. Evol.* 58, 323–332. doi: 10.1159/000057573

Rattenborg, N. C., Lima, S. L., and Amlaner, C. J. (1999a). Facultative control of avian unihemispheric sleep under the risk of predation. *Behav. Brain Res.* 105, 163–172. doi: 10.1016/S0166-4328(99)00070-4

Rattenborg, N. C., Lima, S. L., and Amlaner, C. J. (1999b). Half-awake to the risk of predation. *Nature* 397, 397–398. doi: 10.1038/17037

Rattenborg, N. C., Lima, S. L., and Lesku, J. A. (2012). Sleep locally, act globally. *Neuroscientist* 18, 533–546. doi: 10.1177/1073858412441086

Rattenborg, N. C., Mandt, B. H., Obermeyer, W. H., Winsauer, P. J., Huber, R., Wikelski, M., et al. (2004). Migratory sleeplessness in the white-crowned sparrow (*Zonotrichia leucophrys gambelii*). *PloS Biol.* 2:E212. doi: 10.1371/journal.pbio.0020212

Rattenborg, N. C., Martinez-Gonzalez, D., and Lesku, J. A. (2009). Avian sleep homeostasis: convergent evolution of complex brains, cognition and sleep functions in mammals and birds. *Neurosci. Biobehav. Rev.* 33, 253–270. doi: 10.1016/j.neubiorev.2008.08.010

Rattenborg, N. C., Martinez-Gonzalez, D., Roth, T. C., and Pravosudov, V. V. (2011). Hippocampal memory consolidation during sleep: a comparison of mammals and birds. *Biol. Rev. Camb. Philos. Soc.* 86, 658–691. doi: 10.1111/j.1469-185X.2010.00165.x

Rattenborg, N. C., Voirin, B., Cruz, S. M., Tisdale, R., Dell'Omo, G., Lipp, H.-P., et al. (2016). Evidence that birds sleep in mid-flight. *Nat. Commun.* 7:12468. doi: 10.1038/ncomms12468

Reiner, A., Stern, E. A., and Wilson, C. J. (2001). Physiology and morphology of intratelencephalically projecting corticostriatal-type neurons in pigeons as revealed by intracellular recording and cell filling. *Brain Behav. Evol.* 58, 101–114. doi: 10.1159/000047264

Reyes-Puerta, V., Sun, J. J., Kim, S., Kilb, W., and Luhmann, H. J. (2015). Laminar and columnar structure of sensory-evoked multineuronal spike sequences in adult rat barrel cortex in vivo. *Cereb. Cortex* 25, 2001–2021. doi: 10.1093/cercor/bhu007

Ridgway, S., Carder, D., Finneran, J., Keogh, M., Kamolnick, T., Todd, M., et al. (2006). Dolphin continuous auditory vigilance for five days. *J. Exp. Biol.* 209, 3621–3628. doi: 10.1242/jeb.02405

Ridgway, S., Keogh, M., Carder, D., Finneran, J., Kamolnick, T., Todd, M., et al. (2009). Dolphins maintain cognitive performance during 72 to 120 hours of continuous auditory vigilance. *J. Exp. Biol.* 212, 1519–1527. doi: 10.1242/jeb.027896

Roffwarg, H. P., Muzio, J. N., and Dement, W. C. (1966). Ontogenetic development of the human sleep-dream cycle. *Science* 152, 604–619. doi: 10.1126/science.152.3722.604

Roth, T. C., Lesku, J. A., Amlaner, C. J., and Lima, S. L. (2006). A phylogenetic analysis of the correlates of sleep in birds. *J. Sleep Res.* 15, 395–402. doi: 10.1111/j.1365-2869.2006.00559.x

Ruckebusch, Y. (1972). Relevance of drowsiness in circadian cycle of farm animals. *Anim. Behav.* 20, 637–643. doi: 10.1016/S0003-3472(72)80136-2

Sakata, S., and Harris, K. D. (2009). Laminar structure of spontaneous and sensory-evoked population activity in auditory cortex. *Neuron* 64, 404–418. doi: 10.1016/j.neuron.2009.09.020

Sanchez-Vives, M. V., and McCormick, D. A. (2000). Cellular and network mechanisms of rhythmic recurrent activity in neocortex. *Nat. Neurosci.* 3, 1027–1034. doi: 10.1038/79848

Schiffmann, C., Hoby, S., Wenker, C., Hård, T., Scholz, R., Clauss, M., et al. (2018). When elephants fall asleep: a literature review on elephant rest with case studies on elephant falling bouts, and practical solutions for zoo elephants. *Zoo Biol.* 37, 133–145. doi: 10.1002/zoo.21406

Schuurman, S. O., Kersten, W., and Weijs, W. A. (2003). The equine hind limb is actively stabilized during standing. *J. Anat.* 202, 355–362. doi: 10.1046/j.1469-7580.2003.00166.x

Scriba, M. F., Ducrest, A.-L., Henry, I., Vyssotski, A. L., Rattenborg, N. C., and Roulin, A. (2013). Linking melanism to brain development: expression of a melanism-related gene in barn owl feather follicles covaries with sleep ontogeny. *Front. Zool.* 10:42. doi: 10.1186/1742-9994-10-42

Sekiguchi, Y., Arai, K., and Kohshima, S. (2006). Sleep behaviour: sleep in continuously active dolphins. *Nature* 441, E9–E10. doi: 10.1038/nature04898

Shein-Idelson, M., Ondracek, J. M., Liaw, H. P., Reiter, S., and Laurent, G. (2016). Slow waves, sharp waves, ripples, and REM in sleeping dragons. *Science* 352, 590–595. doi: 10.1126/science.aaf3621

Siclari, F., Baird, B., Perogamvros, L., Bernardi, G., LaRocque, J. J., Riedner, B., et al. (2017). The neural correlates of dreaming. *Nat. Neurosci.* 20, 872–878. doi: 10.1038/nn.4545

Siclari, F., and Tononi, G. (2017). Local aspects of sleep and wakefulness. *Curr. Opin. Neurobiol.* 44, 222–227. doi: 10.1016/j.conb.2017.05.008

Siegel, J. M. (2008). Do all animals sleep? *Trends Neurosci.* 31, 208–213. doi: 10.1016/j.tins.2008.02.001

Siegel, J. M., Manger, P. R., Nienhuis, R., Fahringer, H. M., and Pettigrew, J. D. (1996). The echidna *Tachyglossus aculeatus* combines REM and non-REM aspects in a single sleep state: implications for the evolution of sleep. *J. Neurosci.* 16, 3500–3506. doi: 10.1523/JNEUROSCI.16-10-03500.1996

Siegel, J. M., Manger, P. R., Nienhuis, R., Fahringer, H. M., and Pettigrew, J. D. (1998). Monotremes and the evolution of rapid eye movement sleep. *Philos. Trans. R. Soc. B* 353, 1147–1157. doi: 10.1098/rstb.1998.0272

Siegel, J. M., Manger, P. R., Nienhuis, R., Fahringer, H. M., Shalita, T., and Pettigrew, J. D. (1999). Sleep in the platypus. *Neurosci.* 91, 391–400. doi: 10.1016/S0306-4522(98)00588-0

Spooner, C. E. (1964). *Observations on the Use of the Chick in the Pharmacological Investigation of the Central Nervous System*. Ph. D. dissertation. Los Angeles, CA: University of California.

Steriade, M. (2006). Grouping of brain rhythms in corticothalamic systems. *Neuroscience* 137, 1087–1106. doi: 10.1016/j.neuroscience.2005.10.029

Steriade, M., Nuñez, A., and Amzica, F. (1993). A novel slow (< 1 Hz) oscillation of neocortical neurons in vivo: depolarizing and hyperpolarizing components. *J. Neurosci.* 13, 3252–3265. doi: 10.1523/JNEUROSCI.13-08-03252.1993

Stolpe, M. (1932). Physiologisch-anatomische untersuchungen über die hintere extremität der vögel. *J. Ornithol.* 80, 161–247.

Šušić, V. T., and Kovaèević, R. M. (1973). Sleep patterns in the owl *Strix aluco*. *Physiol. Behav.* 11, 313–317. doi: 10.1016/0031-9384(73)90005-X

Szymczak, J. T., Helb, H. W., and Kaiser, W. (1993). Electrophysiological and behavioral correlates of sleep in the blackbird (*Turdus merula*). *Physiol. Behav.* 53, 1201–1210. doi: 10.1016/0031-9384(93)90380-X

Szymczak, J. T., Kaiser, W., Helb, H. W., and Beszczyńska, B. (1996). A study of sleep in the European blackbird. *Physiol. Behav.* 60, 1115–1120. doi: 10.1016/0031-9384(96)00231-4

Tamaki, M., Bang, J. W., Watanabe, T., and Sasaki, Y. (2016). Night watch in one brain hemisphere during sleep associated with the first-night effect in humans. *Curr. Biol.* 26, 1190–1194. doi: 10.1016/j.cub.2016.02.063

Tew Kai, E., Rossi, V., Sudre, J., Weimerskirch, H., Lopez, C., Hernandez-Garcia, E., et al. (2009). Top marine predators track Lagrangian coherent structures. *Proc. Natl. Acad. Sci. U.S.A.* 106, 8245–8250. doi: 10.1073/pnas.0811034106

Timofeev, I., and Chauvette, S. (2011). Thalamocortical oscillations: local control of EEG slow waves. *Curr. Top. Med. Chem.* 11, 2457–2471. doi: 10.2174/156802611797470376

Tiriac, A., and Blumberg, M. S. (2016). The case of the disappearing spindle burst. *Neural. Plast.* 2016:8037321. doi: 10.1155/2016/8037321

Tiriac, A., Del Rio-Bermudez, C., and Blumberg, M. S. (2014). Self-generated movements with "unexpected" sensory consequences. *Curr. Biol.* 24, 2136–2141. doi: 10.1016/j.cub.2014.07.053

Tisdale, R. K., Vyssotski, A. L., Lesku, J. A., and Rattenborg, N. C. (2017). Sleep-related electrophysiology and behavior of tinamous (*Eudromia elegans*): tinamous don't sleep like ostriches. *Brain Behav. Evol.* 89, 249–261. doi: 10.1159/000475590

Tobler, I. (1992). Behavioral sleep in the Asian elephant in captivity. *Sleep* 15, 1–12. doi: 10.1093/sleep/15.1.1

Tobler, I. (2011). "Phylogeny of sleep regulation," in *Principles and Practice of Sleep Medicine*, 5th Edn, eds M. H. Kryger, T. Roth, and W. C. Dement (Amsterdam: Elsevier Health Sciences), 112–125.

Tobler, I., and Borbély, A. A. (1988). Sleep and EEG spectra in the pigeon (*Columba livia*) under baseline conditions and after sleep deprivation. *J. Comp. Physiol. A* 163, 729–738. doi: 10.1007/BF00604050

Tobler, I., and Schwierin, B. (1996). Behavioural sleep in the giraffe (*Giraffa camelopardalis*) in a zoological garden. *J. Sleep Res.* 5, 21–32. doi: 10.1046/j.1365-2869.1996.00010.x

Trites, A. W., Lestenkof, P., and Battaile, B. (2009). *Identifying Foraging Habitat of Lactating Northern Fur Seals and the Spatial Overlap with Commercial Fisheries in the Eastern Bering Sea. NPRB Project* 636 Final Report. Vancouver: North Pacific Universities Marine Mammal Research Consortium.

Valencia Garcia, S., Brischoux, F., Clément, O., Libourel, P. A., Arthaud, S., Lazarus, M., et al. (2018). Ventromedial medulla inhibitory neuron inactivation induces REM sleep without atonia and REM sleep behavior disorder. *Nat. Commun.* 9:504. doi: 10.1038/s41467-017-02761-0

van der Meij, J., Martinez-Gonzalez, D., Beckers, G. J. L., and Rattenborg, N. C. (2019a). Intra-"cortical" activity during avian non-REM and REM sleep: variant and invariant traits between birds and mammals. *Sleep* 42:zsy230. doi: 10.1093/sleep/zsy230

van der Meij, J., Martinez-Gonzalez, D., Beckers, G. J. L., and Rattenborg, N. C. (2019b). Neurophysiology of avian sleep: comparing natural sleep and isoflurane anesthesia. *Front. Neurosci.* 13:262. doi: 10.3389/fnins.2019.00262

van Twyver, H., and Allison, T. (1972). A polygraphic and behavioral study of sleep in the pigeon (*Columba livia*). *Exp. Neurol.* 35, 138–153. doi: 10.1016/0014-4886(72)90065-9

Villablanca, J. (1966). Behavioral and polygraphic study of "sleep" and "wakefulness" in chronic decerebrate cats. *Electroencephalogr. Clin. Neurophysiol.* 21, 562–577. doi: 10.1016/0013-4694(66)90175-1

Vyazovskiy, V. V., Borbély, A. A., and Tobler, I. (2000). Unilateral vibrissae stimulation during waking induces interhemispheric EEG asymmetry during subsequent sleep in the rat. *J. Sleep Res.* 9, 367–371. doi: 10.1046/j.1365-2869.2000.00230.x

Vyazovskiy, V. V., Cirelli, C., and Tononi, G. (2011a). Electrophysiological correlates of sleep homeostasis in freely behaving rats. *Prog. Brain Res.* 193, 17–38. doi: 10.1016/B978-0-444-53839-0.00002-8

Vyazovskiy, V. V., Olcese, U., Hanlon, E. C., Nir, Y., Cirelli, C., and Tononi, G. (2011b). Local sleep in awake rats. *Nature* 472, 443–447. doi: 10.1038/nature10009

Vyazovskiy, V. V., and Tobler, I. (2008). Handedness leads to interhemispheric EEG asymmetry during sleep in the rat. *J. Neurophysiol.* 99, 969–975. doi: 10.1152/jn.01154.2007

Walker, J. M., and Berger, R. J. (1972). Sleep in the domestic pigeon (*Columba livia*). *Behav. Biol.* 7, 195–203. doi: 10.1016/S0091-6773(72)80199-8

Warren, W. C., Hillier, L. W., Marshall Graves, J. A., Birney, E., Ponting, C. P., Grützner, F., et al. (2008). Genome analysis of the platypus reveals unique signatures of evolution. *Nature* 453, 175–183. doi: 10.1038/nature06936

Watanabe, M., Ito, H., and Masai, H. (1983). Cytoarchitecture and visual receptive neurons in the Wulst of the Japanese quail (*Coturnix coturnix japonica*). *J. Comp. Neurol.* 213, 188–198. doi: 10.1002/cne.902130206

Weimerskirch, H., Bishop, C., Jeanniard du Dot, T., Prudor, A., and Sachs, G. (2016). Frigate birds track atmospheric conditions over months-long transoceanic flights. *Science* 353, 74–78. doi: 10.1126/science.aaf4374

Wester, J. C., and Contreras, D. (2012). Columnar interactions determine horizontal propagation of recurrent network activity in neocortex. *J. Neurosci.* 32, 5454–5471. doi: 10.1523/JNEUROSCI.5006-11.2012

Yang, Y., Cao, P., Yang, Y., and Wang, S. R. (2008). Corollary discharge circuits for saccadic modulation of the pigeon visual system. *Nat. Neurosci.* 11, 595–602. doi: 10.1038/nn.2107

Yasuda, T., Yasuda, K., Brown, R. A., and Krueger, J. M. (2005). State-dependent effects of light-dark cycle on somatosensory and visual cortex EEG in rats. *Am. J. Physiol. Regul. Integr. Comp. Physiol.* 289, R1083–R1089. doi: 10.1152/ajpregu.00112.2005

Zhao, X., Sun, H., Tang, Z., Flanders, J., Zhang, S., and Ma, Y. (2010). Characterization of the sleep architecture in two species of fruit bat. *Behav. Brain Res.* 208, 497–501. doi: 10.1016/j.bbr.2009.12.027

Conflict of Interest Statement: The authors declare that the research was conducted in the absence of any commercial or financial relationships that could be construed as a potential conflict of interest.

Copyright © 2019 Rattenborg, van der Meij, Beckers and Lesku. This is an open-access article distributed under the terms of the Creative Commons Attribution License (CC BY). The use, distribution or reproduction in other forums is permitted, provided the original author(s) and the copyright owner(s) are credited and that the original publication in this journal is cited, in accordance with accepted academic practice. No use, distribution or reproduction is permitted which does not comply with these terms.

frontiers in Neuroscience

MINI REVIEW
published: 05 June 2019
doi: 10.3389/fnins.2019.00576

Regulation of Local Sleep by the Thalamic Reticular Nucleus

*Gil Vantomme, Alejandro Osorio-Forero, Anita Lüthi and Laura M. J. Fernandez**

Department of Fundamental Neurosciences, University of Lausanne, Lausanne, Switzerland

In spite of the uniform appearance of sleep as a behavior, the sleeping brain does not produce electrical activities in unison. Different types of brain rhythms arise during sleep and vary between layers, areas, or from one functional system to another. Local heterogeneity of such activities, here referred to as local sleep, overturns fundamental tenets of sleep as a globally regulated state. However, little is still known about the neuronal circuits involved and how they can generate their own specifically-tuned sleep patterns. NREM sleep patterns emerge in the brain from interplay of activity between thalamic and cortical networks. Within this fundamental circuitry, it now turns out that the thalamic reticular nucleus (TRN) acts as a key player in local sleep control. This is based on a marked heterogeneity of the TRN in terms of its cellular and synaptic architecture, which leads to a regional diversity of NREM sleep hallmarks, such as sleep spindles, delta waves and slow oscillations. This provides first evidence for a subcortical circuit as a determinant of cortical local sleep features. Here, we review novel cellular and functional insights supporting TRN heterogeneity and how these elements come together to account for local NREM sleep. We also discuss open questions arising from these studies, focusing on mechanisms of sleep regulation and the role of local sleep in brain plasticity and cognitive functions.

Keywords: sleep spindles, slow wave activity, delta waves, neural circuit, thalamocortical

OPEN ACCESS

Edited by:
Giulio Bernardi,
IMT School for Advanced Studies Lucca, Italy

Reviewed by:
Sakiko Honjoh,
University of Tsukuba, Japan
Anna Castelnovo,
Ospedale Regionale di Lugano, Switzerland

****Correspondence:***
Laura M. J. Fernandez
laura.fernandez@unil.ch

Specialty section:
This article was submitted to Sleep and Circadian Rhythms, a section of the journal Frontiers in Neuroscience

Received: *20 March 2019*
Accepted: *21 May 2019*
Published: *05 June 2019*

Citation:
Vantomme G, Osorio-Forero A, Lüthi A and Fernandez LMJ (2019) Regulation of Local Sleep by the Thalamic Reticular Nucleus. Front. Neurosci. 13:576. doi: 10.3389/fnins.2019.00576

INTRODUCTION

Sleep serves distinct needs for the mammalian brain and the body, ranging from restorative and metabolic functions to offline memory consolidation (Rasch and Born, 2013). Sleep-like states occur also in jellyfish (Nath et al., 2017), the earliest metazoan species containing a nervous system, suggesting a beneficial purpose of sleep for even the simplest neural circuits. Local variations of sleep rhythms, i.e., specific to restrained portions of the mammalian brain, could account for neural circuit-specific sleep needs and sleep functions. In this review we use the term local sleep to refer to these local variations. During Non-Rapid-Eye-Movement (NREM) sleep, local sleep is now shown for major rhythms: slow-oscillation (SO, <∼1.5 Hz), delta (1.5–4 Hz) and sleep spindles (∼10–15 Hz). The SO is well-documented in rodents, cats, ferrets and humans, as a nesting oscillation composed of a silent and an active state, the latter carrying spindles and high frequency gamma rhythms (∼30–80 Hz) (Steriade et al., 1993; Achermann and Borbély, 1997; Rasch and Born, 2013; Halász et al., 2014; Neske, 2015; Crunelli et al., 2018). The cortical origin of the SO has been partly elucidated, in particular regarding the initiation, maintenance and termination of the active state (Sanchez-Vives and McCormick, 2000; Timofeev et al., 2000; Luczak et al., 2007; Sakata and Harris, 2009; Chauvette et al., 2010) (for review see, Neske, 2015). In contrast to the

SO, delta waves are homeostatically regulated (Borbély and Tobler, 2011), and their generation mechanism are less clear—although the thalamus makes a strong contribution (Steriade et al., 1993; Halász et al., 2014; Crunelli et al., 2018; Fernandez et al., 2018). SO and delta, jointly described as a slow-wave activity (SWA, ∼0.5–4 Hz), show a decaying antero-posterior gradient in the human brain (Werth et al., 1997). SWA can also appear as single and seemingly independent events in local brain areas (Nir et al., 2011). Finally, sleep spindles can emerge in spatially confined regions, independently from the corresponding contralateral side (Nir et al., 2011), over regions probably corresponding to the size of functionally defined areas (Kim et al., 2015; Piantoni et al., 2017; Fernandez et al., 2018).

The description of local sleep in mammals is a fortunate development for endeavors attempting to dissect circuit functions of sleep. This is because developing techniques to identify and manipulate sleep locally might reveal directly the distinct assets of different sleep types for neural circuit properties, including in particular the role of one sleep rhythm over the others. An intriguing possibility is that local sleep is crucial for the maintenance and protection of the cellular and synaptic wiring of neural circuits and their plasticity. Prior studies have indeed proposed beneficial effects relevant for neural circuits such as: the regulation of synaptic strength and spine structure (Tononi and Cirelli, 2014; de Vivo et al., 2017), ion homeostasis of intracellular Ca^{2+} levels (Maret et al., 2007), cell-type-specific forms of excitability and plasticity (Kurotani et al., 2008; Astori et al., 2013), sensory receptive field regulation (Durkin et al., 2017), and undeniably more aspects still to be discovered. Local-sleep driven circuit reactivation also contributes to experience-dependent plasticity of local circuits (Huber et al., 2004; Bergmann et al., 2012; Johnson et al., 2012; Tamaki et al., 2013).

An influential hypothesis posits that wake-related area-specific increases in synaptic strength underlie local differences in SWA, suggesting that SWA takes on restorative functions in response to experience-dependent plasticity (Tononi and Cirelli, 2006). However, besides this hypothesis, so far there are no cellular or synaptic mechanisms known that underlie local differences in the spectral mix of sleep. Among the key players generating sleep patterns, there are the thalamus and the surrounding thalamic reticular nucleus (TRN) (Steriade and Llinas, 1988; Magnin et al., 2010; Halassa et al., 2014). The TRN is a peculiar shell-like inhibitory nucleus long known for its anatomical and functional heterogeneity. A large body of literature documents the role of the TRN in sleep rhythm generation, notably in sleep spindles, but also in delta and SO (Steriade and Llinas, 1988; Crunelli et al., 2018). However, despite its high heterogeneity and its crucial implication in sleep rhythms, the TRN contribution to local aspects of sleep has been considered only recently. This is even more surprising given that the TRN is strongly innervated by cortical inputs and is part of reciprocally connected and focalized thalamocortical loops, at least in sensory systems (Crabtree, 1999; Pinault, 2004). The cortical activity could drive the TRN, which would in return influence the cortex in a heterogeneous local manner.

Here, we explore how the TRN regulates sleep heterogeneity. Our review attempts to bring together the different anatomical, morphological and functional aspects of the TRN, disclosing a local circuit framework that shapes sleep spatial variability.

FAR FROM BEING A HOMOGENEOUS INHIBITORY NUCLEUS, THE TRN SHOWS ANATOMICAL, MORPHOLOGICAL AND NEUROCHEMICAL DIVERSITY

Anatomical Diversity

The origin of cortical and subcortical afferents and the thalamic target of TRN neurons define anatomical subregions in the TRN. To describe these subregions, we focus here on the TRN's thalamic targets. The postero-dorsal portion of the TRN is involved in visual (Crabtree and Killackey, 1989), auditory (Shosaku and Sumitomo, 1983) and somatosensory modalities (Crabtree, 1996). A gustatory sector (Hayama et al., 1994) and a visceral sector (Stehberg et al., 2001) overlap in the ventral portion of the TRN and extend from the posterior to the intermediate region along the anteroposterior axis. The anterior sector of the TRN is involved in motor and limbic structures (Gonzalo-Ruiz and Lieberman, 1995a,b; Zikopoulos and Barbas, 2007; **Figure 1A**, left). Primary sensory sectors of TRN (Crabtree, 1999) provide focalized and dense projections to first-order thalamic nuclei (Pinault and Deschênes, 1998), with the large majority of TRN cells targeting exactly one nucleus in a topographical order. The projections to higher-order thalamic sensory areas typically originate from the same sectors of TRN that target the first-order sensory areas, yet TRN cells projecting to higher-order nuclei have a final terminal arborization that extends over greater areas (Pinault et al., 1995). The TRN sector projecting to prefrontal-projecting thalamic nuclei occupies most of the rostral pole of the nucleus and is, at least in rodent, clearly segregated from the posterior sensory sectors. Projections into midline and intralaminar nuclei are made through small and less dense terminal arborizations compared to primary sensory projections (Pinault and Deschênes, 1998), with a less strict topographical organization (Cornwall et al., 1990; Kolmac and Mitrofanis, 1997).

Morphological Diversity

Beyond this anatomical subdivision, early histological studies reveal several cytoarchitectonic and cellular differences in the TRN of ferret (Clemence and Mitrofanis, 1992), cat (Clemence and Mitrofanis, 1992; Lubke, 1993), rabbit (Lubke, 1993) and rat (Requena et al., 1991; Spreafico et al., 1991; Lubke, 1993). Spreafico undertakes a classification of three morphologically different types of neurons based on their soma shape, their dendritic arborization and their localization within the TRN (**Figure 1A**, middle). The R-type cells have a round soma and are preferentially located in anterior-limbic portions of TRN, whereas the small fusiform-shaped f-type cells are located in sensory sectors. Large fusiform F-type cells are found throughout the nucleus and have an axonal arborization within the TRN (Spreafico et al., 1988). Large F-type neurons receive chemical

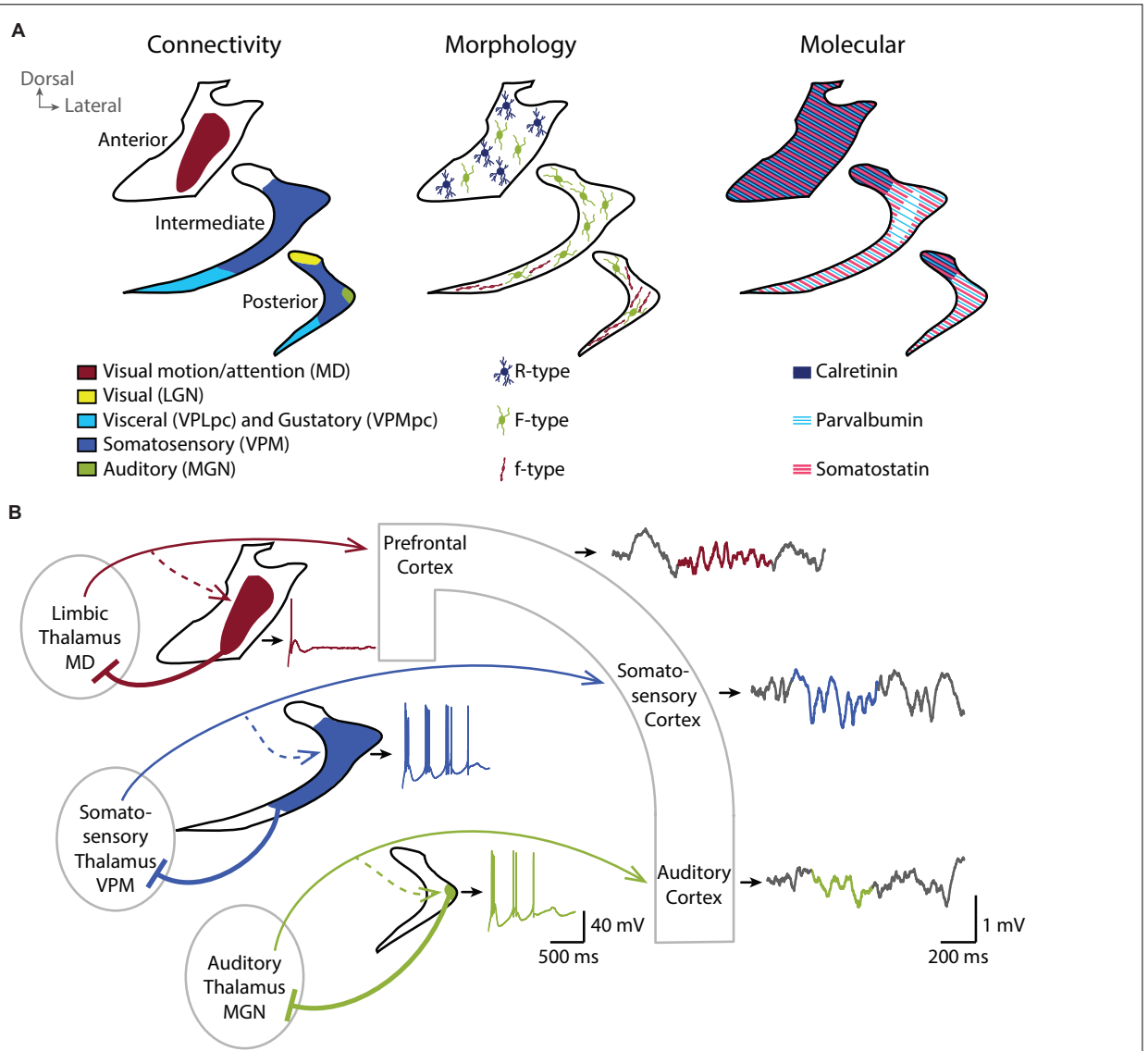

FIGURE 1 | TheTRN is a heterogeneous nucleus and shapes local sleep through parallel thalamocortical loops. **(A)** Coronal schemes of the anterior, intermediate and posterior TRN showing the diversity of the connectivity (left), the repartition of TRN neurons with different morphological properties (middle), and the expression pattern of some of the major molecular markers (right). **(B)** Coronal scheme of three parallel thalamocortical loops showing the impact of distinct firing properties of TRN neurons in the different functional TRN sectors on the local activity of related cortices. Cortical inputs to the TRN are not depicted for clarity. *In vitro* whole-cell current-clamp traces of TRN neurons are shown next to the related TRN drawing (black outline). TRN neurons show rebound burst firing after a hyperpolarization step from –60 to –100 mV. Neurons in sensory sectors (green and blue) show more repetitive burst firing than the neuron in limbic sector (red). *In vivo* local field potentials simultaneously recorded in the different cortices during NREM sleep with detected spindle event (color highlighted) are shown on the right. Sensory cortices, in particular the somatosensory cortex in mice, are enriched in sleep spindles compared to prefrontal cortex. Whole-cell recording traces are adapted from Fernandez et al., 2018 (CC BY 4.0). MD, mediodorsal thalamic nucleus; VPLpc, Ventroposterolateral parvicellular thalamic nucleus; VPMpc, Ventroposteromedial parvicellular thalamic nucleus; LGN, Lateral geniculate thalamic nucleus; VPM, Ventroposteromedial thalamic nucleus; MGN, Medial geniculate thalamic nucleus.

and electrical connections in similar proportion whereas small f-type seems to receive predominantly chemical synapses (Deleuze and Huguenard, 2006). The extent of the axonal arborization is also variable between TRN neurons. Cox et al. (1996) describe three patterns of projection into the ventrobasal thalamus of rat (cluster, intermediate and diffuse) and correlates the axonal arborization with the strength of inhibitory control over the thalamus (Cox et al., 1997). Diffuse axonal arborizations do not respect the boundaries of thalamic somatosensory vibrissae representation (called barreloids) and extend to a large region of the ventrobasal thalamus. On the contrary, neurons with clustered branching pattern form focal projections within barreloids, corresponding to the axonal arborizations described by Pinault and Deschênes (1998) and Desîlets-Roy et al. (2002). The intermediate axonal arborization covers an area fourfold greater than the clustered projection.

Neurochemical Diversity

Additionally, the TRN neurons stain for a variety of neurochemical markers, most of which are not homogeneously distributed and not necessarily conserved across species. TRN cells stain homogeneously, and most prominently within the brain for the neurotransmitter gamma aminobutyric acid (GABA) (Penny et al., 1984), for Glutamic acid decarboxylase (GAD67) (Houser et al., 1980) and for vesicular transporter of GABA, such as VGAT2 (Halassa et al., 2011) from rodents to humans, consistent with the broad inhibitory synaptic transmission they convey to the thalamus. However, Ca^{2+}-binding proteins such as calretinin and calbindin are not homogeneously expressed throughout the TRN. For example, calretinin and the KCl cotransporter KCC2 are preferentially expressed in the anterior and in the dorsal part of the rat TRN (Lizier et al., 1997; Bartho et al., 2004; **Figure 1A**, right). Calbindin-expressing neurons are instead found mostly in the posterior and intermediate regions of the rabbit TRN, corresponding to sensory sectors (Contreras-Rodriguez et al., 2003). The Ca^{2+}-binding protein parvalbumin (PV) as well as the somatostatin (SOM)-expressing TRN neurons seem to form largely separate subpopulations that are intermingled throughout sectors, albeit to varying degrees (**Figure 1A**, right). For example, the inner tier of intermediate mouse TRN seems devoid of SOM-expressing neurons (Clemente-Perez et al., 2017). Other peptides, such as thyrotropin-releasing hormone (Segerson et al., 1987), vaso-active intestinal peptide (Burgunder et al., 1999), prolactin-releasing peptide (Roland et al., 1999) are also described in the rat TRN with disparate expression patterns throughout the nucleus (for review see, Pinault, 2004).

HETEROGENEOUS TRN-THALAMO-CORTICAL FUNCTIONAL LOOPS SHAPE LOCAL SLEEP IN CORTEX

Sectorial Differences in TRN Cell Function

Our recent paper (Fernandez et al., 2018) is a first step towards demonstrating that TRN heterogeneity is essential to determine local sleep. We used optogenetically-assisted circuit mapping of TRN cell sectors in mice to define the functional properties of TRN cells based on their sectorial localization. In doing so, we identified both marked and graded differences in the endogenous discharge characteristics of TRN cells along sectors (**Figure 1B**). Cells in the somatosensory sector of the TRN showed the most vigorous endogenous repetitive bursting. The burst discharge of cells in the auditory sector of the TRN, while also pronounced, was weaker than in the somatosensory sector. In marked contrast, TRN cells innervated by the limbic mediodorsal thalamic nucleus failed to discharge in repetitive bursts. Burst differences are likely one of a number of several cellular and synaptic heterogeneities in TRN sectors that remain to be explored with respect to their impact on thalamic inhibition. In particular, whether these sectorial differences in discharge characteristics correspond to neurochemically distinct neuronal subtypes, such as PV- or SOM-expressing cells as described by Clemente-Perez remains to be determined (Clemente-Perez et al., 2017). Moreover, activity of TRN cells is differentially modulated depending on the sector of the TRN, visual or limbic, and the brain state, wakefulness or NREM sleep (Halassa et al., 2014). TRN-mediated inhibition of thalamic nuclei thus has unequal origins and might be recruited during different brain states and neuromodulatory conditions.

Local Sleep Properties Correlate With Heterogeneity in TRN Burst Discharge

To determine whether sectorial differences in discharge patterns of TRN cells correspond to differences in local NREM sleep, we recorded multi-site local field potentials in the corresponding cortical areas (**Figure 1B**; Fernandez et al., 2018). These parallel recordings revealed marked differences in the local spectral composition of sleep. In particular, cortical somatosensory areas, that form loops with strongly bursting somatosensory TRN sector, produced fast and large spindles. This result is in line with previous findings in mice of prominent sigma power (10–15 Hz) in sensory-motor (Fernandez et al., 2017) and somatosensory regions (Kim et al., 2015). Intriguingly, human NREM sleep shows a clear sigma power peak and highest sleep spindle density in central derivations that include primary sensorimotor areas (Cox et al., 2017; Piantoni et al., 2017). Thus, some aspects of the spatial organization of NREM sleep spindles are similar in mice and humans. We next found that the power profile of local sleep in auditory and limbic prefrontal cortices does not contain such a strong sigma component, which correlates with the moderate repetitive bursting capacity of cells contained within the corresponding TRN sectors. Altogether, our findings offer evidence that heterogeneous cellular characteristics of TRN are linked to local sleep.

Manipulating TRN Activity to Switch the Type of Local Sleep

To establish the causal relation between TRN bursting activity and local sleep properties in this study (Fernandez et al., 2018), we used either chemogenetic hyperpolarization of TRN cells, or genetic removal of the $Ca_V3.3$ calcium channel, an essential element of TRN bursting (Astori et al., 2011; Pellegrini et al., 2016). Chemogenetic inhibition of TRN cells in the sensory sectors suppressed bursting and simultaneously hyperpolarized the cellular resting membrane potential, thus reducing excitability. Genetic removal of the $Ca_V3.3$ channel suppressed bursting while maintaining regular firing. In both cases, local sleep in somatosensory cortex was largely depleted of sleep spindles, which indicates that repetitive bursting of TRN cells is the major determinant of sleep spindle density in these cortical areas. Instead, in prefrontal areas, in which spindles were less prominent, genetic removal of $Ca_V3.3$ did not significantly affect the spectral composition of sleep nor of the properties of individual spindle events. Besides sleep spindles, the manipulation of TRN bursting also reduced power in the SO band, while upregulating delta power. Therefore, the TRN is important to regulate the spectral content of local sleep.

These experiments open the possibility to modify local sleep by manipulating burst discharge of TRN sectors, for example through modulating the membrane potential of these cells.

Recent studies using optogenetic inhibition of TRN activity (Lewis et al., 2015; Herrera et al., 2016) also report alterations in the spectral characteristics of NREM sleep, yet without focusing on local variations in this specific vigilance state. Activating hypothalamic GABAergic input to the TRN switches the brain state from NREM sleep to wake (Herrera et al., 2016); while direct photoinhibition of the TRN in NREM sleep decreases the 1–4 Hz frequency band, but no distinction was made between the SO and delta range (Lewis et al., 2015). Our recent study finds in particular that local sleep in sensory cortex switches between spindle– and delta–enriched forms depending on the membrane potential of these cells. Multiple mechanisms regulate the membrane potential of TRN cells during natural sleep, in particular neuromodulation (Bal and McCormick, 1993; Ni et al., 2016) and activation of extrasynaptic NMDA receptors (Zhang et al., 2009). The exact conditions under which these are activated and whether there are sectorial differences remains to be elaborated.

IMPLICATIONS OF THALAMICALLY–DRIVEN LOCAL SLEEP FOR LOCAL NEURAL CIRCUITS

We explore here how experimental manipulations of TRN advance insights into the functions of local sleep, in particular when it comes to understanding its role in the maintenance and plasticity of neural circuits.

Sleep Need of Local Neural Circuits

The amount of SWA during NREM sleep is homeostatically regulated according to the time spent awake, and primarily involves an increase in the delta component of SWA (Borbély and Tobler, 2011). SWA can also be upregulated locally in a cortical area according to its recent use. Somatosensory stimulation during wakefulness enhances SWA and spindles locally in the somatosensory areas in humans (Kattler et al., 1994), while SWA diminishes following a period of arm immobilization during wakefulness (Huber et al., 2006). Enhanced SWA indicates an enhanced need for sleep; therefore, somatosensory stimulation during the day augments the need of somatosensory thalamocortical loops to enter deep NREM sleep. Therefore, interference with local SWA increase after a period of sensory stimulation could help to explore local circuit alterations in a brain that otherwise sleeps normally. For example, intense sensory stimulation (e.g., whisker stimulation) during waking is known for enhancing SWA locally during NREM sleep in related sensory cortex (Vyazovskiy et al., 2000, 2004). Acute depolarization of TRN cells (Lewis et al., 2015; Fernandez et al., 2018) could be applied to see whether the use-dependent increase in the delta component of SWA can be prevented. Consequences on the functional and structural organization of the barrel cortex could then be traced to local sleep modification. This experimental approach could represent a step forward as it circumvents the non-specific effects of total sleep deprivation previously used to monitor circuit alterations in response to global homeostatic upregulation of NREM sleep. Moreover, it will unravel the distinct implication of the low-frequency (SO) and the high-frequency (delta) components of the SWA in local neural circuits.

Developmental Regulation of Neural Circuits

A poorly explored aspect of local sleep is whether it is beneficial for the maturation and maintenance of neural connectivity. As considerably documented in the literature, local rhythmic activity occurs at early developmental stages in rodents (Tiriac and Blumberg, 2016) and in humans (Whitehead et al., 2017). Of particular interest is an immature form of spindle-related activity, the "neonatal spindle burst," which results from self-generated muscle activity in the periphery, such as twitches of muscles or whiskers. The neonatal spindle burst is a predominant form of synchronized brain activity early in development (from late prenatal stages to the first postnatal weeks) and appears locally in cortical areas. These local rhythmic events are probably crucial for the establishment of sensorimotor maps (Del Rio-Bermudez and Blumberg, 2018). Although the relationship to mature sleep spindles is not clear, mechanistic similarities suggest that they could be forerunners (or at least immature signs) of the circuitries generating mature sleep spindles (Del Rio-Bermudez and Blumberg, 2018). Once the brain is adult, could local spindles continue to play a role in thalamocortical connectivity? This is supported by evidence that synchronized Ca^{2+} entry in thalamocortical cells—which also occurs during spindles—controls axonal outgrowth and synaptic refinement (Mire et al., 2012; Moreno-Juan et al., 2017). Furthermore, repetitive low-threshold bursting in TC cells induces waves of Ca^{2+} entry and increases in intracellular cAMP levels (Lüthi and McCormick, 1999) at frequencies that are known to serve as codes for growth cone responsiveness (Nicol et al., 2011). Barrel formation depends on the activity of adenylyl cyclase type I (AC I), a calcium-dependent version of the enzymes catalyzing synthesis of the intracellular messenger cAMP (Welker et al., 1996; Abdel-Majid et al., 1998; Lu et al., 2003). Disruption of the AC I-encoding gene results in the "barrelless" mouse model that lacks cortical barrels (Welker et al., 1996; Abdel-Majid et al., 1998). Loss of AC I in the sensory thalamus reproduces this developmental defect, disrupting cortical barrel patterns (Suzuki et al., 2015). To summarize, local sleep, by reactivating specific thalamocortical loops and triggering cAMP-dependent signaling cascades could maintain and reorganize connectivity of thalamocortical systems. Such possibilities can now be explored through manipulating local sleep via interfering with activity in TRN sectors.

CONCLUSION AND PERSPECTIVES

Local sleep, as spatial variations of sleep rhythms within the brain, is shaped by differences in thalamocortical connectivity rooted in the anatomy and functional activity of the TRN.

In support of this, we summarize evidence that the TRN is segregated into different sectors with different cellular properties that tune the type of regional sleep patterns. We also argue that the TRN, due to the strong dependence of its discharge patterns on membrane potential, could be a versatile area to modify local sleep in response to use, experience and learning (Huber et al., 2004; Johnson et al., 2012; Tamaki et al., 2013). It remains to be seen whether compromised local neural circuits involving the TRN may produce aberrant local changes in the cortex. For example, a local wake state in motor areas is isolated in the sleeping brain in sleepwalking parasomniac patients (Terzaghi et al., 2009). Alternatively, in neuropsychotic diseases such as schizophrenia, strong deficits in sleep spindles possibly arise due to impaired TRN activity (Castelnovo et al., 2017; Thankachan et al., 2019), pointing to the hypothesis that sleep rhythm abnormalities in these diseases could be related to aberrant activity in the local sectors of the TRN. Dysregulation and abnormal compartmentalization of sleep could impact other diseases for which the link has not yet been established, compromising brain connectivity and learning processes. Further understanding of the mechanisms regulating the TRN will be essential in delineating the importance of the spatial heterogeneity of NREM sleep for local neural circuits in restorative and cognitive functions.

AUTHOR CONTRIBUTIONS

All authors wrote, read, and corrected the manuscript. GV and LF elaborated the figure.

FUNDING

This work was supported by the Swiss National Science Foundation (grant 31003A_166318) and Etat de Vaud.

REFERENCES

Abdel-Majid, R. M., Leong, W. L., Schalkwyk, L. C., Smallman, D. S., Wong, S. T., Storm, D. R., et al. (1998). Loss of adenylyl cyclase I activity disrupts patterning of mouse somatosensory cortex. *Nat. Genet.* 19, 289–291. doi: 10.1038/980

Achermann, P., and Borbély, A. A. (1997). Low-frequency (< 1 Hz) oscillations in the human sleep electroencephalogram. *Neuroscience* 81, 213–222. doi: 10.1016/s0306-4522(97)00186-3

Astori, S., Wimmer, R. D., and Luthi, A. (2013). Manipulating sleep spindles—expanding views on sleep, memory, and disease. *Trends Neurosci.* 36, 738–748. doi: 10.1016/j.tins.2013.10.001

Astori, S., Wimmer, R. D., Prosser, H. M., Corti, C., Corsi, M., Liaudet, N., et al. (2011). The CaV3.3 calcium channel is the major sleep spindle pacemaker in thalamus. *Proc. Natl. Acad. Sci. U.S.A.* 108, 13823–13828. doi: 10.1073/pnas.1105115108

Bal, T., and McCormick, D. A. (1993). Mechanisms of oscillatory activity in guinea-pig nucleus reticularis thalami in vitro: a mammalian pacemaker. *J. Physiol.* 468, 669–691. doi: 10.1113/jphysiol.1993.sp019794

Bartho, P., Payne, J. A., Freund, T. F., and Acsady, L. (2004). Differential distribution of the KCl cotransporter KCC2 in thalamic relay and reticular nuclei. *Eur. J. Neurosci.* 20, 965–975. doi: 10.1111/j.1460-9568.2004.03562.x

Bergmann, T. O., Mölle, M., Diedrichs, J., Born, J., and Siebner, H. R. (2012). Sleep spindle-related reactivation of category-specific cortical regions after learning face-scene associations. *Neuroimage* 59, 2733–2742. doi: 10.1016/j.neuroimage.2011.10.036

Borbély, A. A., and Tobler, I. (2011). Manifestations and functional implications of sleep homeostasis. *Handb. Clin. Neurol.* 98, 205–213. doi: 10.1016/b978-0-444-52006-7.00013-7

Burgunder, J. M., Heyberger, B., and Lauterburg, T. (1999). Thalamic reticular nucleus parcellation delineated by VIP and TRH gene expression in the rat. *J. Chem. Neuroanat.* 17, 147–152. doi: 10.1016/s0891-0618(99)00033-2

Castelnovo, A., Graziano, B., Ferrarelli, F., and D'Agostino, A. (2017). Sleep spindles and slow waves in schizophrenia and related disorders: main findings, challenges and future perspectives. *Eur. J. Neurosci.* 48, 2738–2758. doi: 10.1111/ejn.13815

Chauvette, S., Volgushev, M., and Timofeev, I. (2010). Origin of active states in local neocortical networks during slow sleep oscillation. *Cereb. Cortex* 20, 2660–2674. doi: 10.1093/cercor/bhq009

Clemence, A. E., and Mitrofanis, J. (1992). Cytoarchitectonic heterogeneities in the thalamic reticular nucleus of cats and ferrets. *J. Comp. Neurol.* 322, 167–180. doi: 10.1002/cne.903220203

Clemente-Perez, A., Makinson, S. R., Higashikubo, B., Brovarney, S., Cho, F. S., Urry, A., et al. (2017). Distinct thalamic reticular cell types differentially modulate normal and pathological cortical rhythms. *Cell Rep.* 19, 2130–2142. doi: 10.1016/j.celrep.2017.05.044

Contreras-Rodriguez, J., Gonzalez-Soriano, J., Martinez-Sainz, P., Marin-Garcia, P., and Rodriguez-Veiga, E. (2003). Neurochemical heterogeneity of the thalamic reticular and perireticular nuclei in developing rabbits: patterns of calbindin expression. *Brain Res. Dev. Brain Res.* 144, 211–221. doi: 10.1016/s0165-3806(03)00194-9

Cornwall, J., Cooper, J. D., and Phillipson, O. T. (1990). Projections to the rostral reticular thalamic nucleus in the rat. *Exp. Brain Res.* 80, 157–171.

Cox, C. L., Huguenard, J. R., and Prince, D. A. (1996). Heterogeneous axonal arborizations of rat thalamic reticular neurons in the ventrobasal nucleus. *J. Comp. Neurol.* 366, 416–430. doi: 10.1002/(sici)1096-9861(19960311)366:3<416::aid-cne4>3.0.co;2-7

Cox, C. L., Huguenard, J. R., and Prince, D. A. (1997). Nucleus reticularis neurons mediate diverse inhibitory effects in thalamus. *Proc. Natl. Acad. Sci. U.S.A.* 94, 8854–8859. doi: 10.1073/pnas.94.16.8854

Cox, R., Schapiro, A. C., Manoach, D. S., and Stickgold, R. (2017). Individual differences in frequency and topography of slow and fast sleep spindles. *Front. Hum Neurosci.* 11:433. doi: 10.3389/fnhum.2017.00433

Crabtree, J. W. (1996). Organization in the somatosensory sector of the cat's thalamic reticular nucleus. *J. Comp. Neurol.* 366, 207–222. doi: 10.1002/(sici)1096-9861(19960304)366:2<207::aid-cne2>3.3.co;2-m

Crabtree, J. W. (1999). Intrathalamic sensory connections mediated by the thalamic reticular nucleus. *Cell Mol. Life. Sci.* 56, 683–700. doi: 10.1007/s000180050462

Crabtree, J. W., and Killackey, H. P. (1989). The topographic organization and axis of projection within the visual sector of the rabbit's thalamic reticular nucleus. *Eur. J. Neurosci.* 1, 94–109. doi: 10.1111/j.1460-9568.1989.tb00777.x

Crunelli, V., Lörincz, M. L., Connelly, W. M., David, F., Hughes, S. W., Lambert, R. C., et al. (2018). Dual function of thalamic low-vigilance state oscillations: rhythm-regulation and plasticity. *Nat. Rev. Neurosci.* 19, 107–118. doi: 10.1038/nrn.2017.151

de Vivo, L., Bellesi, M., Marshall, W., Bushong, E. A., Ellisman, M. H., Tononi, G., et al. (2017). Ultrastructural evidence for synaptic scaling across the wake/sleep cycle. *Science* 355, 507–510. doi: 10.1126/science.aah5982

Del Rio-Bermudez, C., and Blumberg, M. S. (2018). Active sleep promotes functional connectivity in developing sensorimotor networks. *Bioessays* 40:e1700234. doi: 10.1002/bies.201700234

Deleuze, C., and Huguenard, J. R. (2006). Distinct electrical and chemical connectivity maps in the thalamic reticular nucleus: potential roles in synchronization and sensation. *J. Neurosci.* 26, 8633–8645. doi: 10.1523/jneurosci.2333-06.2006

Desîlets-Roy, B., Varga, C., Lavallée, P., and Deschênes, M. (2002). Substrate for cross-talk inhibition between thalamic barreloids. *J. Neurosci.* 22:RC218.

Durkin, J., Suresh, A. K., Colbath, J., Broussard, C., Wu, J., Zochowski, M., et al. (2017). Cortically coordinated NREM thalamocortical oscillations play an essential, instructive role in visual system plasticity. *Proc. Natl. Acad. Sci. U.S.A.* 114, 10485–10490. doi: 10.1073/pnas.1710613114

Fernandez, L. M., Vantomme, G., Osorio-Forero, A., Cardis, R., Béard, E., and Lüthi, A. (2018). Thalamic reticular control of local sleep in mouse sensory cortex. *Elife* 7:e39111. doi: 10.7554/eLife.39111

Fernandez, L. M. J., Comte, J. C., Le Merre, P., Lin, J. S., Salin, P. A., and Crochet, S. (2017). Highly dynamic spatiotemporal organization of low-frequency activities during behavioral states in the mouse cerebral cortex. *Cereb. Cortex* 27, 5444–5462. doi: 10.1093/cercor/bhw311

Gonzalo-Ruiz, A., and Lieberman, A. R. (1995a). GABAergic projections from the thalamic reticular nucleus to the anteroventral and anterodorsal thalamic nuclei of the rat. *J. Chem. Neuroanat.* 9, 165–174. doi: 10.1016/0891-0618(95)00078-x

Gonzalo-Ruiz, A., and Lieberman, A. R. (1995b). Topographic organization of projections from the thalamic reticular nucleus to the anterior thalamic nuclei in the rat. *Brain Res. Bull.* 37, 17–35. doi: 10.1016/0361-9230(94)00252-5

Halassa, M. M., Chen, Z., Wimmer, R. D., Brunetti, P. M., Zhao, S., Zikopoulos, B., et al. (2014). State-dependent architecture of thalamic reticular subnetworks. *Cell* 158, 808–821. doi: 10.1016/j.cell.2014.06.025

Halassa, M. M., Siegle, J. H., Ritt, J. T., Ting, J. T., Feng, G., and Moore, C. I. (2011). Selective optical drive of thalamic reticular nucleus generates thalamic bursts and cortical spindles. *Nat. Neurosci.* 14, 1118–1120. doi: 10.1038/nn.2880

Halász, P., Bódizs, R., Parrino, L., and Terzano, M. (2014). Two features of sleep slow waves: homeostatic and reactive aspects–from long term to instant sleep homeostasis. *Sleep Med.* 15, 1184–1195. doi: 10.1016/j.sleep.2014.06.006

Hayama, T., Hashimoto, K., and Ogawa, H. (1994). Anatomical location of a taste-related region in the thalamic reticular nucleus in rats. *Neurosci. Res.* 18, 291–299. doi: 10.1016/0168-0102(94)90165-1

Herrera, C. G., Cadavieco, M. C., Jego, S., Ponomarenko, A., Korotkova, T., and Adamantidis, A. (2016). Hypothalamic feedforward inhibition of thalamocortical network controls arousal and consciousness. *Nat. Neurosci.* 19, 290–298. doi: 10.1038/nn.4209

Houser, C. R., Vaughn, J. E., Barber, R. P., and Roberts, E. (1980). GABA neurons are the major cell type of the nucleus reticularis thalami. *Brain Res.* 200, 341–354. doi: 10.1016/0006-8993(80)90925-7

Huber, R., Ghilardi, M. F., Massimini, M., Ferrarelli, F., Riedner, B. A., Peterson, M. J., et al. (2006). Arm immobilization causes cortical plastic changes and locally decreases sleep slow wave activity. *Nat. Neurosci.* 9, 1169–1176. doi: 10.1038/nn1758

Huber, R., Ghilardi, M. F., Massimini, M., and Tononi, G. (2004). Local sleep and learning. *Nature* 430, 78–81. doi: 10.1038/nature02663

Johnson, L. A., Blakely, T., Hermes, D., Hakimian, S., Ramsey, N. F., and Ojemann, J. G. (2012). Sleep spindles are locally modulated by training on a brain-computer interface. *Proc. Natl. Acad. Sci. U.S.A.* 109, 18583–18588. doi: 10.1073/pnas.1207532109

Kattler, H., Dijk, D. J., and Borbély, A. A. (1994). Effect of unilateral somatosensory stimulation prior to sleep on the sleep EEG in humans. *J. Sleep Res.* 3, 159–164. doi: 10.1111/j.1365-2869.1994.tb00123.x

Kim, D., Hwang, E., Lee, M., Sung, H., and Choi, J. H. (2015). Characterization of topographically specific sleep spindles in mice. *Sleep* 38, 85–96. doi: 10.5665/sleep.4330

Kolmac, C. I., and Mitrofanis, J. (1997). Organisation of the reticular thalamic projection to the intralaminar and midline nuclei in rats. *J. Comp. Neurol.* 377, 165–178. doi: 10.1002/(sici)1096-9861(19970113)377:2<165::aid-cne2>3.0.co;2-1

Kurotani, T., Yamada, K., Yoshimura, Y., Crair, M. C., and Komatsu, Y. (2008). State-dependent bidirectional modification of somatic inhibition in neocortical pyramidal cells. *Neuron* 57, 905–916. doi: 10.1016/j.neuron.2008.01.030

Lewis, L. D., Voigts, J., Flores, F. J., Schmitt, L. I., Wilson, M. A., Halassa, M. M., et al. (2015). Thalamic reticular nucleus induces fast and local modulation of arousal state. *Elife* 4:e08760. doi: 10.7554/eLife.08760

Lizier, C., Spreafico, R., and Battaglia, G. (1997). Calretinin in the thalamic reticular nucleus of the rat: distribution and relationship with ipsilateral and contralateral efferents. *J. Comp. Neurol.* 377, 217–233. doi: 10.1002/(sici)1096-9861(19970113)377:2<217::aid-cne5>3.0.co;2-6

Lu, H. C., She, W. C., Plas, D. T., Neumann, P. E., Janz, R., and Crair, M. C. (2003). Adenylyl cyclase I regulates AMPA receptor trafficking during mouse cortical 'barrel' map development. *Nat. Neurosci.* 6, 939–947. doi: 10.1038/nn1106

Lubke, J. (1993). Morphology of neurons in the thalamic reticular nucleus (TRN) of mammals as revealed by intracellular injections into fixed brain slices. *J. Comp. Neurol.* 329, 458–471. doi: 10.1002/cne.903290404

Luczak, A., Bartho, P., Marguet, S. L., Buzsaki, G., and Harris, K. D. (2007). Sequential structure of neocortical spontaneous activity in vivo. *Proc. Natl. Acad. Sci. U.S.A.* 104, 347–352. doi: 10.1073/pnas.0605643104

Lüthi, A., and McCormick, D. A. (1999). Modulation of a pacemaker current through Ca2+-induced stimulation of cAMP production. *Nat. Neurosci.* 2, 634–641. doi: 10.1038/10189

Magnin, M., Rey, M., Bastuji, H., Guillemant, P., Mauguiere, F., and Garcia-Larrea, L. (2010). Thalamic deactivation at sleep onset precedes that of the cerebral cortex in humans. *Proc. Natl. Acad. Sci. U.S.A.* 107, 3829–3833. doi: 10.1073/pnas.0909710107

Maret, S., Dorsaz, S., Gurcel, L., Pradervand, S., Petit, B., Pfister, C., et al. (2007). Homer1a is a core brain molecular correlate of sleep loss. *Proc. Natl. Acad. Sci. U.S.A.* 104, 20090–20095. doi: 10.1073/pnas.0710131104

Mire, E., Mezzera, C., Leyva-Díaz, E., Paternain, A. V., Squarzoni, P., Bluy, L., et al. (2012). Spontaneous activity regulates robo1 transcription to mediate a switch in thalamocortical axon growth. *Nat. Neurosci.* 15, 1134–1143. doi: 10.1038/nn.3160

Moreno-Juan, V., Filipchuk, A., Antón-Bolaños, N., Mezzera, C., Gezelius, H., Andrés, B., et al. (2017). Prenatal thalamic waves regulate cortical area size prior to sensory processing. *Nat. Commun.* 8:14172. doi: 10.1038/ncomms14172

Nath, R. D., Bedbrook, C. N., Abrams, M. J., Basinger, T., Bois, J. S., Prober, D. A., et al. (2017). The jellyfish Cassiopea exhibits a sleep-like state. *Curr. Biol.* 27:e2983. doi: 10.1016/j.cub.2017.08.014

Neske, G. T. (2015). The slow oscillation in cortical and thalamic networks: mechanisms and functions. *Front. Neural Circ.* 9:88. doi: 10.3389/fncir.2015.00088

Ni, K. M., Hou, X. J., Yang, C. H., Dong, P., Li, Y., Zhang, Y., et al. (2016). Selectively driving cholinergic fibers optically in the thalamic reticular nucleus promotes sleep. *Elife* 5:e10382. doi: 10.7554/eLife.10382

Nicol, X., Hong, K. P., and Spitzer, N. C. (2011). Spatial and temporal second messenger codes for growth cone turning. *Proc. Natl. Acad. Sci. U.S.A.* 108, 13776–13781. doi: 10.1073/pnas.1100247108

Nir, Y., Staba, R. J., Andrillon, T., Vyazovskiy, V. V., Cirelli, C., Fried, I., et al. (2011). Regional slow waves and spindles in human sleep. *Neuron* 70, 153–169. doi: 10.1016/j.neuron.2011.02.043

Pellegrini, C., Lecci, S., Lüthi, A., and Astori, S. (2016). Suppression of sleep spindle rhythmogenesis in mice with deletion of CaV3.2 and CaV3.3 T-type Ca2+ channels. *Sleep* 39, 875–885. doi: 10.5665/sleep.5646

Penny, G. R., Conley, M., Schmechel, D. E., and Diamond, I. T. (1984). The distribution of glutamic acid decarboxylase immunoreactivity in the diencephalon of the opossum and rabbit. *J. Comp. Neurol.* 228, 38–56. doi: 10.1002/cne.902280106

Piantoni, G., Halgren, E., and Cash, S. S. (2017). Spatiotemporal characteristics of sleep spindles depend on cortical location. *Neuroimage* 146, 236–245. doi: 10.1016/j.neuroimage.2016.11.010

Pinault, D. (2004). The thalamic reticular nucleus: structure, function and concept. *Brain Res. Brain Res. Rev.* 46, 1–31. doi: 10.1016/j.brainresrev.2004.04.008

Pinault, D., Bourassa, J., and Deschênes, M. (1995). The axonal arborization of single thalamic reticular neurons in the somatosensory thalamus of the rat. *Eur. J. Neurosci.* 7, 31–40. doi: 10.1111/j.1460-9568.1995.tb01017.x

Pinault, D., and Deschênes, M. (1998). Projection and innervation patterns of individual thalamic reticular axons in the thalamus of the adult rat: a three-dimensional, graphic, and morphometric analysis. *J. Comp. Neurol.* 391, 180–203. doi: 10.1002/(sici)1096-9861(19980209)391:2<180::aid-cne3>3.0.co;2-z

Rasch, B., and Born, J. (2013). About sleep's role in memory. *Physiol. Rev.* 93, 681–766. doi: 10.1152/physrev.00032.2012

Requena, V., Diaz, F., Villena, A., Vidal, L., and Perez de Vargas, I. (1991). Histoenzymatic study of the neurons in the visual sector of the thalamic reticular nucleus in the adult rat. *J. Hirnforsch.* 32, 459–467.

Roland, B. L., Sutton, S. W., Wilson, S. J., Luo, L., Pyati, J., Huvar, R., et al. (1999). Anatomical distribution of prolactin-releasing peptide and its receptor suggests

additional functions in the central nervous system and periphery. *Endocrinology* 140, 5736–5745. doi: 10.1210/en.140.12.5736

Sakata, S., and Harris, K. D. (2009). Laminar structure of spontaneous and sensory-evoked population activity in auditory cortex. *Neuron* 64, 404–418. doi: 10.1016/j.neuron.2009.09.020

Sanchez-Vives, M. V., and McCormick, D. A. (2000). Cellular and network mechanisms of rhythmic recurrent activity in neocortex. *Nat. Neurosci.* 3, 1027–1034. doi: 10.1038/79848

Segerson, T. P., Hoefler, H., Childers, H., Wolfe, H. J., Wu, P., Jackson, I. M., et al. (1987). Localization of thyrotropin-releasing hormone prohormone messenger ribonucleic acid in rat brain in situ hybridization. *Endocrinology* 121, 98–107. doi: 10.1210/endo-121-1-98

Shosaku, A., and Sumitomo, I. (1983). Auditory neurons in the rat thalamic reticular nucleus. *Exp. Brain Res.* 49, 432–442.

Spreafico, R., Battaglia, G., and Frassoni, C. (1991). The reticular thalamic nucleus (RTN) of the rat: cytoarchitectural, Golgi, immunocytochemical, and horseradish peroxidase study. *J. Comp. Neurol.* 304, 478–490. doi: 10.1002/cne.903040311

Spreafico, R., de Curtis, M., Frassoni, C., and Avanzini, G. (1988). Electrophysiological characteristics of morphologically identified reticular thalamic neurons from rat slices. *Neuroscience* 27, 629–638. doi: 10.1016/0306-4522(88)90294-1

Stehberg, J., Acuna-Goycolea, C., Ceric, F., and Torrealba, F. (2001). The visceral sector of the thalamic reticular nucleus in the rat. *Neuroscience* 106, 745–755. doi: 10.1016/s0306-4522(01)00316-5

Steriade, M., and Llinas, R. R. (1988). The functional states of the thalamus and the associated neuronal interplay. *Physiol. Rev.* 68, 649–742. doi: 10.1152/physrev.1988.68.3.649

Steriade, M., McCormick, D. A., and Sejnowski, T. J. (1993). Thalamocortical oscillations in the sleeping and aroused brain. *Science* 262, 679–685. doi: 10.1126/science.8235588

Suzuki, A., Lee, L. J., Hayashi, Y., Muglia, L., Itohara, S., Erzurumlu, R. S., et al. (2015). Thalamic adenylyl cyclase 1 is required for barrel formation in the somatosensory cortex. *Neuroscience* 290, 518–529. doi: 10.1016/j.neuroscience.2015.01.043

Tamaki, M., Huang, T. R., Yotsumoto, Y., Hämäläinen, M., Lin, F. H., Náñez, J. E. Sr., et al. (2013). Enhanced spontaneous oscillations in the supplementary motor area are associated with sleep-dependent offline learning of finger-tapping motor-sequence task. *J. Neurosci.* 33, 13894–13902. doi: 10.1523/JNEUROSCI.1198-13.2013

Terzaghi, M., Sartori, I., Tassi, L., Didato, G., Rustioni, V., LoRusso, G., et al. (2009). Evidence of dissociated arousal states during NREM parasomnia from an intracerebral neurophysiological study. *Sleep* 32, 409–412. doi: 10.1093/sleep/32.3.409

Thankachan, S., Katsuki, F., McKenna, J. T., Yang, C., Shukla, C., Deisseroth, K., et al. (2019). Thalamic reticular nucleus parvalbumin neurons regulate sleep spindles and electrophysiological aspects of schizophrenia in mice. *Sci. Rep.* 9:3607. doi: 10.1038/s41598-019-40398-9

Timofeev, I., Grenier, F., Bazhenov, M., Sejnowski, T. J., and Steriade, M. (2000). Origin of slow cortical oscillations in deafferented cortical slabs. *Cereb. Cortex* 10, 1185–1199. doi: 10.1093/cercor/10.12.1185

Tiriac, A., and Blumberg, M. S. (2016). The case of the disappearing spindle burst. *Neural Plast.* 2016:8037321. doi: 10.1155/2016/8037321

Tononi, G., and Cirelli, C. (2006). Sleep function and synaptic homeostasis. *Sleep Med. Rev.* 10, 49–62. doi: 10.1016/j.smrv.2005.05.002

Tononi, G., and Cirelli, C. (2014). Sleep and the price of plasticity: from synaptic and cellular homeostasis to memory consolidation and integration. *Neuron* 81, 12–34. doi: 10.1016/j.neuron.2013.12.025

Vyazovskiy, V., Borbély, A. A., and Tobler, I. (2000). Unilateral vibrissae stimulation during waking induces interhemispheric EEG asymmetry during subsequent sleep in the rat. *J. Sleep Res.* 9, 367–371. doi: 10.1046/j.1365-2869.2000.00230.x

Vyazovskiy, V. V., Welker, E., Fritschy, J. M., and Tobler, I. (2004). Regional pattern of metabolic activation is reflected in the sleep EEG after sleep deprivation combined with unilateral whisker stimulation in mice. *Eur. J. Neurosci.* 20, 1363–1370. doi: 10.1111/j.1460-9568.2004.03583.x

Welker, E., Armstrong-James, M., Bronchti, G., Ourednik, W., Gheorghita-Baechler, F., Dubois, R., et al. (1996). Altered sensory processing in the somatosensory cortex of the mouse mutant barrelless. *Science* 271, 1864–1867. doi: 10.1126/science.271.5257.1864

Werth, E., Achermann, P., and Borbély, A. A. (1997). Fronto-occipital EEG power gradients in human sleep. *J. Sleep Res.* 6, 102–112. doi: 10.1046/j.1365-2869.1997.d01-36.x

Whitehead, K., Pressler, R., and Fabrizi, L. (2017). Characteristics and clinical significance of delta brushes in the EEG of premature infants. *Clin. Neurophysiol. Pract.* 2, 12–18. doi: 10.1016/j.cnp.2016.11.002

Zhang, Y., Llinas, R. R., and Lisman, J. E. (2009). Inhibition of NMDARs in the nucleus reticularis of the thalamus produces delta frequency bursting. *Front. Neural Circ.* 3:20. doi: 10.3389/neuro.04.020.2009

Zikopoulos, B., and Barbas, H. (2007). Circuits formultisensory integration and attentional modulation through the prefrontal cortex and the thalamic reticular nucleus in primates. *Rev. Neurosci.* 18, 417–438.

Conflict of Interest Statement: The authors declare that the research was conducted in the absence of any commercial or financial relationships that could be construed as a potential conflict of interest.

Copyright © 2019 Vantomme, Osorio-Forero, Lüthi and Fernandez. This is an open-access article distributed under the terms of the Creative Commons Attribution License (CC BY). The use, distribution or reproduction in other forums is permitted, provided the original author(s) and the copyright owner(s) are credited and that the original publication in this journal is cited, in accordance with accepted academic practice. No use, distribution or reproduction is permitted which does not comply with these terms.

frontiers in Neuroscience

ORIGINAL RESEARCH
published: 09 July 2019
doi: 10.3389/fnins.2019.00598

Data-Driven Analysis of EEG Reveals Concomitant Superficial Sleep During Deep Sleep in Insomnia Disorder

Julie Anja Engelhard Christensen[1,2†], Rick Wassing[3†], Yishul Wei[3], Jennifer R. Ramautar[3], Oti Lakbila-Kamal[3], Poul Jørgen Jennum[1] and Eus J. W. Van Someren[3,4,5]*

[1] Danish Center for Sleep Medicine, Department of Clinical Neurophysiology, Rigshospitalet Glostrup, Glostrup, Denmark, [2] Department of Health Technology, Technical University of Denmark, Kongens Lyngby, Denmark, [3] Department of Sleep and Cognition, Netherlands Institute for Neuroscience, an Institute of the Royal Netherlands Academy of Arts and Sciences, Amsterdam, Netherlands, [4] Department of Integrative Neurophysiology, Center for Neurogenomics and Cognitive Research (CNCR), Amsterdam Neuroscience, VU University Amsterdam, Amsterdam, Netherlands, [5] Amsterdam UMC, Vrije Universiteit, Psychiatry, Amsterdam Neuroscience, Amsterdam, Netherlands

Study Objectives: The subjective suffering of people with Insomnia Disorder (ID) is insufficiently accounted for by traditional sleep classification, which presumes a strict sequential occurrence of global brain states. Recent studies challenged this presumption by showing concurrent sleep- and wake-type neuronal activity. We hypothesized enhanced co-occurrence of diverging EEG vigilance signatures during sleep in ID.

Methods: Electroencephalography (EEG) in 55 cases with ID and 64 controls without sleep complaints was subjected to a Latent Dirichlet Allocation topic model describing each 30 s epoch as a mixture of six vigilance states called Topics (T), ranked from N3-related T1 and T2 to wakefulness-related T6. For each stable epoch we determined topic dominance (the probability of the most likely topic), topic co-occurrence (the probability of the remaining topics), and epoch-to-epoch transition probabilities.

Results: In stable epochs where the N1-related T4 was dominant, T4 was more dominant in ID than in controls, and patients showed an almost doubled co-occurrence of T4 *during* epochs where the N3-related T1 was dominant. Furthermore, patients had a higher probability of switching from T1- to T4-dominated epochs, at the cost of switching to N3-related T2-dominated epochs, and a higher probability of switching from N2-related T3- to wakefulness-related T6-dominated epochs.

Conclusion: Even during their deepest sleep, the EEG of people with ID express more N1-related vigilance signatures than good sleepers do. People with ID are moreover more likely to switch from deep to light sleep and from N2 sleep to wakefulness. The findings suggest that hyperarousal never rests in ID.

Keywords: insomnia, indiscrete labeling of sleep, vigilance states, topic modeling, data-driven analysis, polysomnography, latent Dirichlet allocation

Abbreviations: AASM, American Academy of Sleep Medicine; CAP, cyclic alternating pattern; EEG, electroencephalography; EOG, electrooculography; ERP, event-related potential; ID, insomnia disorder; ISI, insomnia severity index; LDA, latent Dirichlet allocation; NREM, non-rapid eye movement; PSG, polysomnography; REM, rapid eye movement; TST, total sleep time.

OPEN ACCESS

Edited by:
Francesca Siclari, Lausanne University Hospital (CHUV), Switzerland

Reviewed by:
Alessandro Silvani, University of Bologna, Italy
Simone Sarasso, University of Milan, Italy

***Correspondence:**
Eus J. W. Van Someren
e.j.w.someren@vu.nl

†*Co-first authors*

Specialty section:
This article was submitted to Sleep and Circadian Rhythms, a section of the journal Frontiers in Neuroscience

Received: *27 December 2018*
Accepted: *27 May 2019*
Published: *09 July 2019*

Citation:
Christensen JAE, Wassing R, Wei Y, Ramautar JR, Lakbila-Kamal O, Jennum PJ and Van Someren EJW (2019) Data-Driven Analysis of EEG Reveals Concomitant Superficial Sleep During Deep Sleep in Insomnia Disorder. Front. Neurosci. 13:598. doi: 10.3389/fnins.2019.00598

STATEMENT OF SIGNIFICANCE

Insomnia Disorder (ID) is the most prevalent sleep disorder. It is poorly understood why people with ID experience part of their sleep as being awake. Quantitative EEG analyses may aid to solve the impasse. We used symbolic representations of spectral changes within 3 s windows to describe standard 30 s sleep epochs as a mixture of states. The method revealed that, as compared to controls, people with ID experience twice as much concurrent light sleep during the deepest sleep, suggesting that hyperarousal continues during deep sleep. Future studies could address the value of concurrent light sleep as a biomarker to pursue brain mechanisms involved in ID and understand treatment response variability.

INTRODUCTION

Insomnia disorder (ID) is characterized by persistent difficulty initiating or maintaining sleep associated with daytime dysfunction which cannot be attributed to insufficient opportunity for sleep (American Academy of Sleep Medicine, 2014). More than 6% of the adult population in high-income countries suffer from chronic insomnia, and this number increases to almost 50% when including the acute form of insomnia (Ohayon, 2002). Moreover, ID has been identified as the second most common mental disorder in Europe (Wittchen et al., 2011). Only recently, genome-wide association studies have commenced to reveal biological pathways involved in insomnia (Hammerschlag et al., 2017; Jansen et al., 2019). Phenotypically, ID can be characterized as a persistent state of physiological and psychological hyperarousal, resembling the state normally seen only transiently during stress (Bonnet and Arand, 2010; Riemann et al., 2010). Polysomnography (PSG) findings in subjects with ID include reductions in sleep continuity and in the time spent in slow-wave sleep and rapid-eye-movement (REM) sleep (Baglioni et al., 2014). These reductions, however, hardly correlate with the subjective severity of sleep complaints (Manconi et al., 2010) in ID and typically underestimate it. The question may be raised whether the common PSG variables capture the key neurophysiological impairments in ID.

More recent methods go beyond the standard manual PSG scoring and give a more detailed description of sleep in ID. An important aim of these methods is to close the present gap between the objectively recorded sleep and the subjective experience of ID (Feige et al., 2013). A recent review revealed promising use of auditory stimulation and event-related potential (ERP) recordings for understanding the mismatch between subjective and objective sleep quality and quantity (Bastien et al., 2014). This technique may not readily be available in routine clinical PSG assessment. To quantify intrinsic rather than responsive processes, most methods focus on the analysis of ongoing sleep EEG. A first class of methods utilizes measures of the spectral composition of the EEG signal. The most robust finding may be that the EEG-spectrum of people with ID contains more high frequency power during pre-sleep wakefulness (Freedman, 1986; Colombo et al., 2016a), and during non-REM (NREM) sleep (Israel et al., 2012; Spiegelhalder et al., 2012; Maes et al., 2014), which may be involved in the degree of perceiving sleep as wakefulness (Krystal et al., 2002). A second class of methods focuses on characterization of transient event occurrence. For example, the REM sleep instability model of ID (Riemann et al., 2012) states that micro- and macro-arousals occur more frequently during and around REM sleep; these arousals have been proposed to be involved in more thought-like cognitions (Wassing et al., 2016). Findings on spindles and K-complexes are equivocal. Studies reported either a decreased spindle density in ID (Besset et al., 1998) or no change (Bastien et al., 2009a). K-complex density was reported to be increased (Forget et al., 2011) or normal (Bastien et al., 2009b).

A third class of methods focusses on the temporal dynamics in the EEG signal. Most analyses of the cyclic alternating pattern (CAP) agree that people with ID express an increased CAP rate (Terzano et al., 2003; Chouvarda et al., 2011, 2012), suggested to indicate "destabilization" of sleep in people with ID (Parrino et al., 2004), which may be improved by certain hypnotics (Parrino et al., 2004, 2008; Ozone et al., 2008). One study further concludes that there is a link between CAP phase A2 subtype and sleep state misperception in ID (Parrino et al., 2009). In a recent study, 30 s epochs of staged sleep were regarded as a Markov chain dynamical process with individual-specific probabilities to switch from one state to another (Wei et al., 2017). It was shown that the probability of transitioning from N2 sleep to N1 sleep or wakefulness is most consistently increased in ID. In another approach, stronger long-range temporal correlations in EEG power fluctuations during pre-sleep wakefulness were associated with worse subjective sleep quality within ID and within normal sleepers (Colombo et al., 2016b). In conclusion, it seems that the association between the subjective complaints and objective sleep parameters may be better revealed when the brain activity assessed with EEG is considered as a complex dynamical process.

A consideration when searching for objective measures that better capture subjective complaints is that traditional sleep classifications all presume a strict sequential occurrence of global brain states. Recent studies challenged this presumption by showing evidence for concurrent sleep- and wake-type neuronal activity (Nir et al., 2011; Vyazovskiy et al., 2011; Funk et al., 2016). Thus, ideally, novel objective measures to pursue neural correlates of subjective sleep complaints in insomnia should not be limited to quantifying vigilance states sequentially, but also quantify their concurrency.

Based on these considerations, we here analyzed the sleep EEG of people with ID and controls without sleep complaints, using a data-driven topic model previously developed and validated in our lab (Koch et al., 2014; Christensen et al., 2016). Originally, topic modeling is a probabilistic approach used to reveal underlying themes or topics in text documents, based on the presence and combination of words (Blei et al., 2003). The same method has been employed to describe the proportions of different underlying latent vigilance states that are simultaneously present in each 30 s sleep epoch. Latent vigilance states are determined in a data-driven way based on symbolically represented patterns observed in the EEG power spectrum. Every epoch can be described as a mixture of six topics T (T1-T6),

each related but not equal to a classical sleep stage. The topics T can be ranked from N3-related T1 and T2 to wakefulness-related T6. The topic modeling approach for analyzing sleep EEG has several advantages: (1) It includes high-dimensional information that is lost with manual scoring, (2) it outputs a mixture of states rather than a discrete scoring, and (3) epochs are not biased by subjective interpretation or classification of neighboring epochs. Lastly, although the symbolic representation is based on scaled EEG and EOG spectral measures, this method goes beyond standard spectral analysis methods and analysis of specific micro-sleep phenomena. The method captures latent patterns in each epoch and visualizes this into a graphical two-dimensional representation. It captures latent patterns in each epoch that indicate the sequential occurrence of different vigilance states, but also captures latent patterns that are indicative of several concomitant vigilance states. An important note here is that EEG leads integrate neurophysiological activity across tens- to hundreds of thousands of neurons. Therefore, the seemingly temporal simultaneous vigilance states observed at the level of the scalp, may well be due to spatial differences in vigilance states of small groups of neurons. We use the term "concomitant" to indicate both simultaneous and sequential occurrences of different vigilance states.

By comparing the sleep EEG of people with ID and controls in this data-driven way, we aimed to reveal group differences that might not be detectable by current methods. For instance, local wakefulness intrusions in sleep would imply simultaneous wake- and sleep EEG signatures. We therefore hypothesized a stronger dominance and co-occurrence of wakefulness-related topics in people suffering from ID than in controls without sleep complaints. We moreover expected that the sleep EEG of people with ID would have higher probability to transition from epochs dominated by deeper sleep-related topics to epochs dominated by light sleep-related topics.

MATERIALS AND METHODS

Participants

Participants were recruited through advertisement and the Netherlands Sleep Registry website (NSR[1]) (Benjamins et al., 2017). A total of 55 participants with ID (41 females, 47.8 ± 12.9 years) and 64 controls (42 females, 45.3 ± 14.6 years) were included. The study was approved by the ethics committee of the Amsterdam University Medical Center, Amsterdam, Netherlands. All participants provided written informed consent. Inclusion criteria for ID were in accordance with the Diagnostic and Statistical Manual of Mental Disorders, fifth edition (American Psychiatric Association, 2013). Exclusion criteria for controls were any sleep difficulties. Exclusion criteria for all participants were neurological, psychiatric, somatic conditions, or other diagnosed sleep disorders including sleep apnea, restless legs syndrome, narcolepsy, or circadian rhythm disorder. In addition, no sleep medication in the previous two months was allowed. Demographic and PSG variables are summarized in **Table 1**.

Procedure and EEG Recording

Participants were instructed to maintain a regular sleep/wake schedule during 1 week prior to laboratory assessment. On the days of laboratory assessments, they were furthermore instructed to refrain from alcohol and drugs and to limit their caffeinated beverages to a maximum of two cups before 12:00 noon. EEG was recorded for two consecutive nights between 11:00 PM and 7:00 AM using a 256-electrode HydroCel net connected to a Net Amps 300 amplifier (Electrical Geodesic Inc. (EGI), Eugene, OR, United States; input impedance: 200 MΩ, A/D converter: 24 bits). Electrode impedance was kept below 100 kΩ. Signals were acquired with a sampling frequency of 1,000 Hz and referenced to the Cz electrode. Sleep-stage scoring was performed in accordance to the American Academy of Sleep Medicine (AASM) standard (Iber et al., 2007). Data from the second night of sleep were analyzed.

EEG Preprocessing

Pre-processing steps were performed using the MEEGPIPE toolbox[2] and EEGLAB (Delorme and Makeig, 2004) in Matlab R2014a (The Mathworks Inc., Natick, MA, United States). First, signals were downsampled to 250 Hz with an antialiasing low-pass filter at 80 Hz. Because the original analysis procedure (Koch et al., 2014) was developed and validated on the derivations C3-A2, O1-A2, EOGL-A2, and EOGR-A1, we analyzed the rereferenced signal between those electrode pairs. Visual inspection of data quality employed "EEG viewer," a Matlab based software developed by Miki Nikolic at Danish Center for Sleep Medicine at Rigshospitalet, Glostrup, Denmark (DCSM). In case the signal was of poor quality, a neighboring electrode was selected.

Signals were filtered forward and reverse in time using 4th order Butterworth filters with cutoffs (−3 dB) at 0.3 and 35 Hz for the EEG signals, and 0.3 and 10 Hz for the EOG signals. All epochs between lights off and lights on were analyzed except for epochs in the beginning or end of the night that were visually clearly contaminated by artifacts. The signal quality of each remaining epoch was evaluated using the standard deviation and range of the signal, and the range of the first derivative of the signal. An epoch was rejected in case the epoch-wise mean of any of the three statistics surpasses four median absolute derivations, as previously described in the supplementary materials of Colombo et al. (2016a). Epochs with artifacts were omitted from analysis.

Sleep Analysis Procedure

Artifact-free epochs were analyzed using a validated automated topic modeling procedure (Koch et al., 2014). As described above, based on the occurrence and combination of symbolic representations of spectral patterns in the raw EEG data, the topic model describes each epoch as a mixture of vigilance states rather than as a single sleep stage. Latent Dirichlet Allocation (LDA)

[1]https://www.sleepregistry.org

[2]https://github.com/meegpipe/meegpipe

TABLE 1 | Demographics and sleep characteristics (subjective, AASM-based, and LDA model-based) in ID and controls.

	Controls	ID	P
Demographics			
N	64	55	–
Age [years, $\mu \pm \sigma$]	45.3 ± 14.6	47.8 ± 12.9	0.41
Sex [male/female]	22/42	14/41	0.29
Subjective insomnia			
ISI [$\mu \pm \sigma$]	**3.8 ± 3.7**	**16.5 ± 4.3**	**<0.0001**
AASM-based measures			
TiB [min, $\mu \pm \sigma$]	483.3 ± 52.7	471.6 ± 44.5	0.10
TST [min, $\mu \pm \sigma$]	**421.7 ± 60.7**	**400.6 ± 59.3**	**0.03**
SE [%, $\mu \pm \sigma$]	87.3 ± 8.6	85.1 ± 10.7	0.32
Wake [%, $\mu \pm \sigma$]	11.7 ± 8.7	14.3 ± 10.9	0.23
REM [%, $\mu \pm \sigma$]	20.2 ± 6.7	19.4 ± 8.5	0.45
N1 [%, $\mu \pm \sigma$]	3.6 ± 2.4	5.0 ± 4.1	0.13
N2 [%, $\mu \pm \sigma$]	39.9 ± 9.4	37.8 ± 11.1	0.12
N3 [%, $\mu \pm \sigma$]	23.6 ± 9.0	22.9 ± 10.2	0.62
LDA model-based overall average topic probability			
T1 [%, $\mu \pm \sigma$]	5.69 ± 1.67	5.23 ± 1.50	0.23
T2 [%, $\mu \pm \sigma$]	25.06 ± 2.64	24.86 ± 2.65	0.52
T3 [%, $\mu \pm \sigma$]	31.08 ± 3.14	31.70 ± 2.77	0.44
T4 [%, $\mu \pm \sigma$]	12.81 ± 1.43	13.08 ± 1.38	0.26
T5 [%, $\mu \pm \sigma$]	18.97 ± 2.88	18.76 ± 2.63	0.94
T6 [%, $\mu \pm \sigma$]	5.62 ± 1.66	5.59 ± 1.42	0.56
LDA model-based percentage of time of stable epochs for each stable epoch type and in total (for the subset of participants with a non-zero number of stable epochs)			
Stable T1 epochs [%, $\mu \pm \sigma$] (number of subjects expressing non-zero values)	1.51 ± 2.09 (N_C = 30)	1.11 ± 1.24 (N_{ID} = 22)	0.57
Stable T2 epochs [%, $\mu \pm \sigma$] (number of subjects expressing non-zero values)	19.98 ± 4.71 (N_C = 64)	20.01 ± 4.51 (N_{ID} = 55)	0.94
Stable T3 epochs [%, $\mu \pm \sigma$] (number of subjects expressing non-zero values)	24.33 ± 6.04 (N_C = 64)	24.72 ± 5.38 (N_{ID} = 55)	0.98
Stable T4 epochs [%, $\mu \pm \sigma$] (number of subjects expressing non-zero values)	2.73 ± 2.44 (N_C = 62)	3.42 ± 2.83 (N_{ID} = 55)	0.24
Stable T5 epochs [%, $\mu \pm \sigma$] (number of subjects expressing non-zero values)	7.33 ± 4.43 (N_C = 64)	7.67 ± 4.54 (N_{ID} = 55)	0.46
Stable T6 epochs [%, $\mu \pm \sigma$] (number of subjects expressing non-zero values)	1.59 ± 1.94 (N_C = 44)	1.06 ± 1.26 (N_{ID} = 37)	0.34
Stable epochs in total [%, $\mu \pm \sigma$] (number of subjects expressing non-zero values)	56.08 ± 5.42 (N_C = 64)	57.29 ± 6.59 (N_{ID} = 55)	0.23

The P-value for the statistics on sex is obtained from a Chi-square test. All other P-values were obtained from Wilcoxon rank sum tests. Bold font-style indicates significant group differences. ID, insomnia disorder; ISI, insomnia severity index; TiB, time in bed from lights out time to get up time; TST, total sleep time; SE, sleep efficiency; T1-T6, topic 1 to 6; LDA, latent Dirichlet allocation.

topic modeling is a machine learning method, traditionally used on text documents to reveal the topics based on the presence and combination of words in the document (Blei et al., 2003). In a similar way, we here used the LDA model procedure to reveal underlying vigilance states (*topics*) based on the occurrence of spectral patterns (*words*). **Figure 1** illustrates the procedure of symbolizing the raw EEG and building distributions of spectral patterns denoted as "word" distributions. **Figure 2** illustrates how the LDA model used the "word" distribution within an epoch to estimate the probabilities of latent vigilance states (*topics*) for that epoch.

Symbolization of the Raw EEG

First, we performed fast-fourier spectral analysis on each 1 s bin of the recording to obtain a participant-specific distribution of spectral power within each classical frequency band. Five equally sized categories were defined by the quintiles of these distributions (*Extreme*, *High*, *Median*, *Low*, or *Very low* power; **Figures 1A–C**). Secondly, each 1 s segment was categorized according to these quintile cutoffs (**Figure 1D**), effectively generating a long vector of letters (*E*, *H*, *M*, *L*, or *V*) for each of the classical frequency bands. Then, for each frequency band, 28 3-letter *words* were generated for each 30 s epoch by concatenating the letters from moving 3 s windows with steps of 1 s. Each 3-letter word descibes a specific pattern of change in spectral power (e.g., HLM: high-low-median; **Figure 1E**). Lastly, we counted how often each possible word occurred in the 30 s epoch, creating a word distribution (**Figure 1F**). Note that for two EEG channels (C3-A2 and O1-A2) the word distributions were created for each classical frequency band (δ, θ, α, and β), and for each EOG channel (EOGL-A2 and EOGR-A1) one word distribution was created for the spectral power below 5 Hz, and one for the cross-correlation values between the two EOG channels instead of power (Koch et al., 2014).

LDA Probabilistic Topic Modeling

Figure 2 illustrates how the LDA model combines word distributions across the EEG and EOG channels to estimate the probabilty of occurence of six vigilance states (*topics*) within each epoch. The LDA model has previously been trained and validated

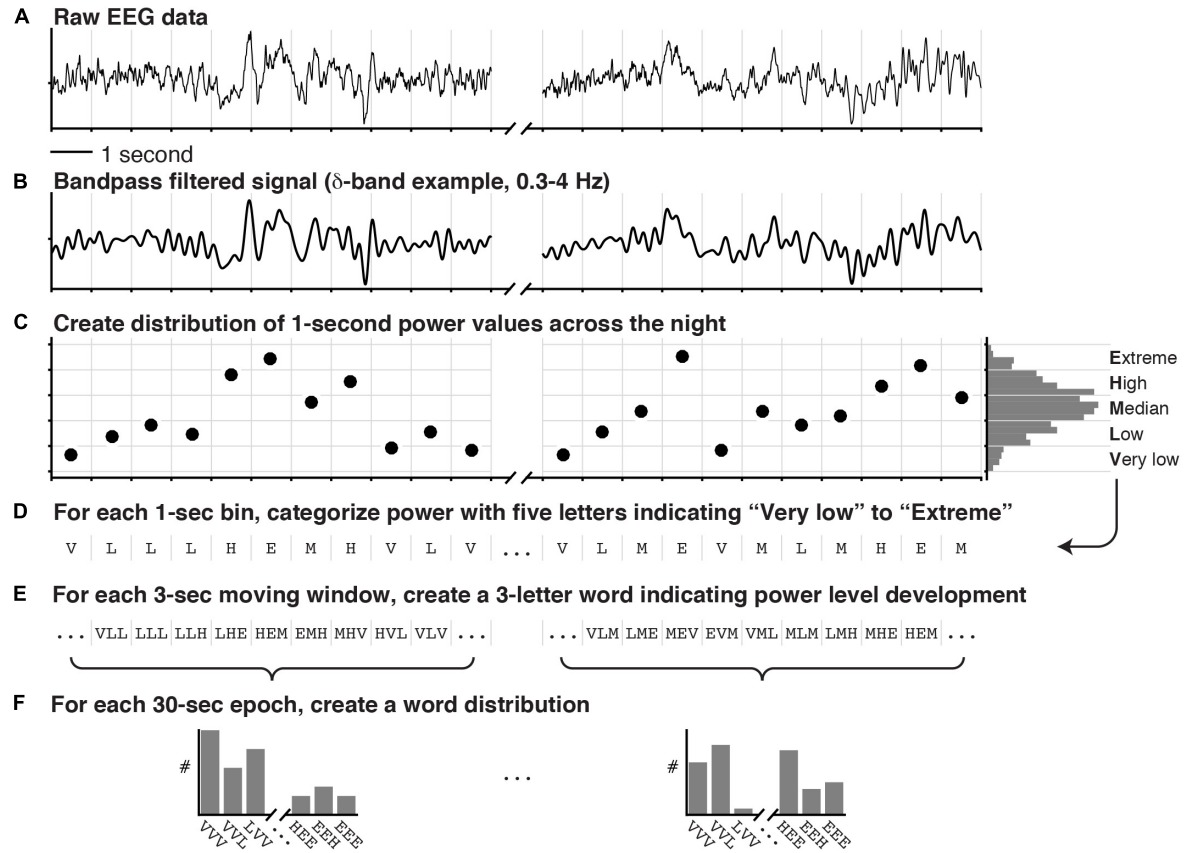

FIGURE 1 | Symbolization of raw EEG for the purpose of Latent Dirichlet Allocation (LDA) topic modeling. The raw data of two EEG signals of which one is depicted in **(A)**, were bandpass filtered into the classical frequency bands (δ, θ, α, and β). **(B)** One bandpass filtered signal is shown. **(C)** The power in each 1 s window was calculated and summarized in a distribution across the entire recording. **(D)** According to quintiles of this distribution, the power in each 1 s window was categorized as either "**V**ery low," "**L**ow," "**M**edian," "**H**igh," or "**E**xtreme," effectively creating a vector of letters. **(E)** For each 3 s sliding window, three consecutive letters were concatenated to create words indicating the spectral power-level development. **(F)** Finally, a word distribution was created for each 30 s epoch by counting how often each of the possible words occurred (5 categories and 3 letters: $5^3 = 125$ words per frequency-band per EEG channel). In addition to the EEG words, an additional 192 words were created in a similar fashion [4 categories and 3 letters: $4^3 = 64$ words per EOG signal (left and right) plus 64 words for the cross-correlation between the EOG signals].

on an independent dataset (Koch et al., 2014). In short, we applied a machine learning approach for non-linear classification of more that two classes (multiclass support vector machine using a radial basis-function kernel) to find that classification in six different topics (rather than 3, 4, 5, or 7) resulted in the highest accuracy for the LDA model output to replicate traditional PSG-scoring. Then we trained the LDA model, where it iteratively learns (1) which words occur together (word distribution patterns), and (2) six distinct latent types of word distribution patterns called topics. The trained model is subsequently validated against a test dataset (Koch et al., 2014), and can thereafter be used on other datasets. Put simply, the *observed* word distributions in an epoch (**Figures 2A,B**, gray bars) are compared to each of the six *expected* word distributions for each topic (**Figure 2B**; colored bars) that were generated by the model. If the observed and expected distribution compare well, the probability of that topic is high, while if the distributions hardly overlap, the probability of that topic is low. The probabilities are normalized to a sum of 1 (**Figure 2C**). In this way, each 30 s epoch is represented as a mixture of six topic probabilities. Repeating this for every 30 s epoch in a recording results in a topic diagram (**Figure 2D**) where each vertical bin is a mixture of six topics, and the height of each stacked bar in that bin represents the probability of each topic. The most likely topic in each bin can be related–but does not equal–to one of the traditional sleep stages.

It should be noted that **Figure 2** only shows the word distributions of δ, θ, α, and β power in one EEG channel, to promote clarity of the visualization. The actual LDA model uses all word distributions, i.e., of δ, θ, α, and β power of two EEG channels (C3-A2 and O1-A2); of the spectral power below 5 Hz of two EOG channels (EOGL-A2 and EOGR-A1); and of the cross-correlation values between the two EOG channels.

Characteristics of Topics

Figure 3 shows four examples of topic diagrams and corresponding manually scored hypnograms. The topic diagram shows the mixture of vigilance states for each epoch. To facilitate understanding of the characteristics represented in each topic,

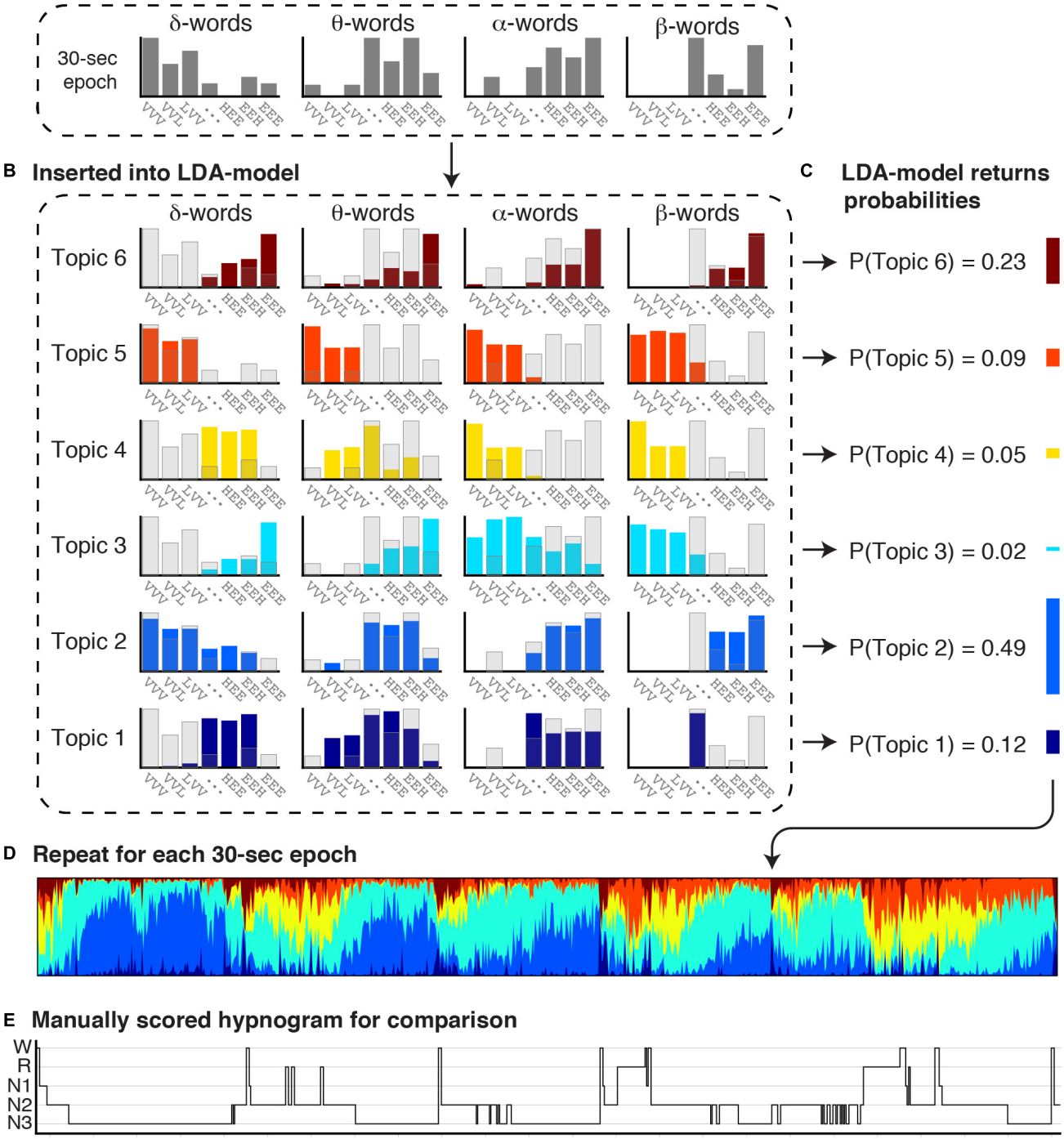

FIGURE 2 | Estimation of concurrent vigilance states in each 30 s epoch. The combined word distributions for each 30 s epoch were inserted into a Latent Dirichlet Allocation (LDA) model, which returns a mixture of topic probabilities for each epoch. The LDA topic model was previously trained to learn the particular distribution of words for six topics (Koch et al., 2014). **(A)** The observed word distributions of one 30 s epoch is inserted into the LDA topic model. **(B)** The *observed* word distributions of the 30 s epoch are depicted in transparent gray bars, and the *expected* word distributions for each topic in colored bars. **(C)** By comparing the observed and expected word distributions, the LDA topic model returns the probability that the observed word distributions comes from the word distribution of each topic. Each 30 s epoch is thereby represented as a mixture of six topics. **(D)** A topic diagram obtained by repeating this procedure for each 30 s epoch in the recording. Each vertical bin in the topic diagram is a mixture of six colors, where the hight of each stacked color represents the probability of a topic. Colors codes range from dark blue (T1) to red (T6). **(E)** For comparison, the manual scored hypnogram is presented below the topic-diagram.

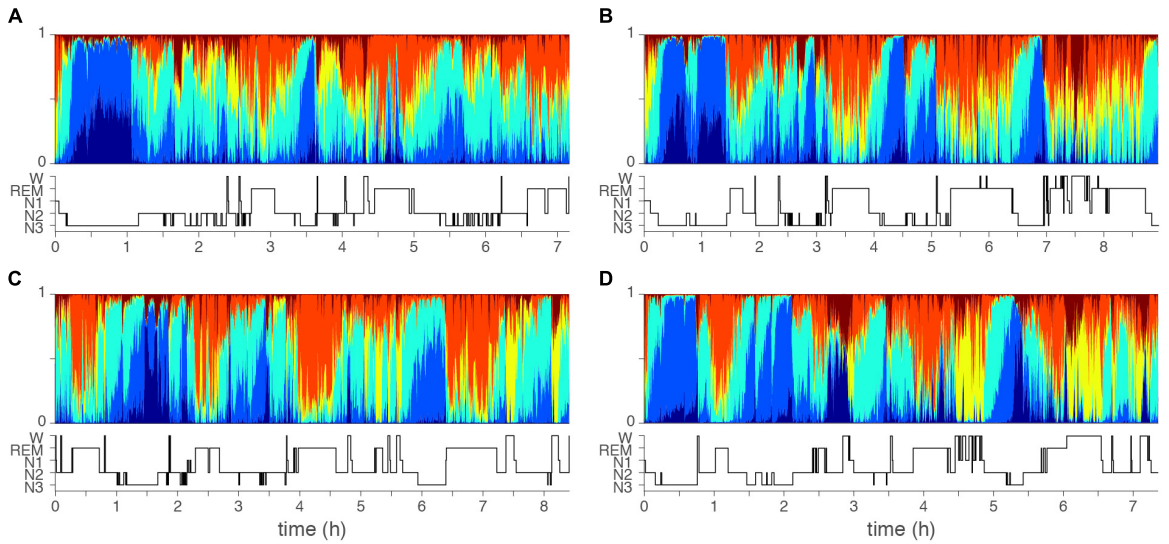

FIGURE 3 | Examples of topic diagrams. Topic diagrams of two normal sleepers **(A,B)** and two insomniac patients **(C,D)**. Each 30 s sleep epoch is represented as a multi-colored vertical bin where the heigth of each stacked color presents the probability that the topic is present. For comparison, the manual scored hypnograms are presented below each diagram. Color codes range from dark blue (T1, mostly seen in deep N3 sleep) to red (T6, mostly seen in wakefulness). Orange (T5) is mostly seen during REM sleep. Note, however, that there is no one-to-one matching of topics and conventional top-down defined qualitative sleep stages. Subtle differences might be seen comparing the two controls **(A,B)** and two cases with insomnia **(C,D)**: In the epochs dominated by the light sleep related topic (yellow), the light sleep related topic is generally stronger (taller yellow bars) for the cases with insomnia as compared to controls.

we here describe the EEG signal in epochs with a particularly high probability of one of the six topics:

1. An epoch with a high probability of Topic 1 (T1, dark blue) has high and consistent delta and theta power. No eye movements are present, but EEG delta activity will be recorded from the EOGL-A2 and EOGR-A2 leads. An epoch rich in T1 will likely be labeled as stage N3 in conventional sleep scoring.
2. An epoch with a high probability of Topic 2 (T2, light blue) has high and consistent delta and theta power, intermediate alpha power and low beta power. No eye movements are present, but some EEG delta activity can be recorded from the EOGL-A2 and EOGR-A2 leads. An epoch rich in T2 will most likely be labeled as stage N3 in conventional sleep scoring.
3. An epoch with a high probability of Topic 3 (T3, turquoise) has intermediate delta, sigma, alpha and beta power in the EEG. No eye movements are present. An epoch rich in T3 will most likely be labeled as stage N2 in conventional sleep scoring.
4. An epoch with a high probability of Topic 4 (T4, yellow) has low delta and theta power, intermediate alpha power and intermediate to high beta power. Eye movements are likely. An epoch rich in T4 will most likely be labeled as stage N1 in conventional sleep scoring.
5. An epoch with a high probability of Topic 5 (T5, orange) has low delta power and low to intermediate theta, alpha and beta power. Eye movements are present. An epoch rich in T5 will most likely be labeled as REM sleep in conventional sleep scoring.
6. An epoch with a high probability of Topic 6 (T6, red) has low delta power, intermediate theta power, and high alpha and beta power. Eye movements are likely. An epoch rich in T6 will most likely be labeled as wakefulness in conventional sleep scoring.

Topic Presence, Dominance, and Dynamics

For the topic diagram of each participant, we extracted several derived measures including topic dominance, and co-occurrence, as well as between-epoch transition probabilities as a measure of vigilance dynamics. First, the topic with the highest probability in an epoch was labeled as the dominant topic. Using this dominance label, we defined epochs as *stable* if they were part of at least three consecutive epochs with the same dominant topic. These stable epochs were selected to extract (1) the probabilities of the dominant topic (*dominance*) and (2) the probabilities of *co-occurence* of the remaining topics (normalized to 1 within each epoch). Finally, we computed *transition probability* as the number of transitions from a stable epoch dominated by one topic to an epoch dominated by any other topic normalized to the total number of possible transitions.

Case-control differences were evaluated for the following outcome measures:

1. The overall average probability of each of the six topics across the night.
2. The percentage of time spent in each of the six stable epoch types across the night.

3. The probability of the dominant topic in each of the six stable epoch types (*dominance)*.
4. The co-occurrance probabilities of each non-dominant topic in each of the six stable epoch types (*co-occurence*).
5. The probabilities to transition from a stable epoch dominated by one topic to an epoch dominated by each of the other topics.

Spectral Analysis

In order to evaluate whether LDA modeling differs from traditional spectral analysis, we performed a fast-fourier spectral analysis of the same EEG channels that were used to compute the word distribution. Absolute spectral power was integrated across the standard clinical frequency bands for each 30-s epoch and averaged within each of the manually identified sleep stages.

Statistical Analyses

Wilcoxon rank-sum tests evaluated group-differences in age and sleep characteristics including the total Insomnia Severity Index (ISI) score, the PSG-based measures, the standard spectral analysis measures, and three of the above LDA model-based measures: the overall average probability of each topic, the percentage of time spent in each of the stable epoch types, and the probability to transition from a stable epoch dominated by one topic to an epoch dominated by each of the other topics.

Because the number of stable epochs for each topic is different across participants, we did not calculate average values for the measures of *dominance* and *co-occurrence* across the night, but rather used mixed-effect general linear models to account for this variability. Accordingly, we evaluated group differences in the *dominance* and *co-occurrence* of each of the topics with group, age, and sex as fixed-effect factors, and a random intercept for each participant.

In addition to describing markers that distinguish ID patients from controls, we evaluated whether the significant markers were associated with the severity of insomnia complaints in the ID group. We used mixed-effects linear models to evaluate the association of the total score of the ISI as a measure of subjective insomnia complaints with topic presence, dominance, and co-occurrence. Age and sex were included in the models as covariates. We calculated partial correlation coefficients between the transition-probabilities and total score of the ISI, controlling for age and sex. In case the effect of the total ISI score was significant, we performed one additional mixed-effects linear regression analysis to elucidate which insomnia symptom could best explain the dependent variable by replacing the total ISI sum score with seven regressors indicating each individual ISI item.

The significance level was set to $\alpha = 0.05$ in all cases. All analyses were performed using MATLAB, R2014a, The MathWorks, Inc., Natick, MA, United States.

RESULTS

Table 1 shows group averages and significance of differences between ID and controls for demographic characteristics, subjective insomnia severity, PSG measures, and LDA model-based measures. Participants with ID subjectively experienced significantly higher insomnia severity. PSG measures were comparable, except for significantly shorter total sleep duration in ID (controls: 421.7 ± 60.7 min, ID: 400.6 ± 59.3 min, Wilcoxon $W = 4249$, $z = 2.18$, $p = 0.03$).

Overall Average Probability of Each of the Six Topics Across the Night

Table 1 reports the overall average probability of each of the six topics for controls and ID. The overall probabilities did not significantly differ between ID and controls for any topic.

Percentage of Time Spent in Each of the Six Stable Epoch Types

Table 1 reports the percentage of time spent in each of the stable epoch types. No significant between-group differences were observed. Furthermore, there was no significant difference in the percentage of stable epochs irrespective of topic dominance between controls [mean (SD) = 56.08% (5.42%)] and ID [57.29% (6.59%); $W = 3526$, $z = 1.20$, $p = 0.23$].

Dominance

Table 2 reports the mean dominance of each stable epoch type for controls and ID. In stable epochs where the N1-related T4 was dominant, T4 was more dominant in ID than in controls (**Figure 4A**). The topic diagrams in **Figures 2D**, **3** shows T4 in yellow. These findings indicate that stable epochs of light sleep in

TABLE 2 | Increased light sleep dominance in ID.

Topic	control	ID	Δ	P
T1[%]	52.40 (49.69–55.11)	51.43 (48.81–54.05)	−1.28 (−5.28–2.72)	0.46
T2 [%]	67.81 (66.15–69.47)	67.46 (65.78–69.13)	−0.35 (−2.72–2.01)	0.48
T3 [%]	57.36 (56.43–58.29)	57.71 (56.67–58.75)	0.35 (−1.04–1.74)	0.68
T4 [%]	**52.59 (51.13–54.05)**	**55.28 (53.68–56.88)**	**2.74 (0.58–4.90)**	**0.03**
T5 [%]	61.11 (59.62–62.60)	61.44 (59.80–63.07)	0.31 (−1.90–2.52)	0.63
T6 [%]	51.75 (48.93–54.58)	50.09 (47.74–52.43)	−2.20 (−5.98–1.58)	0.33

Estimated mean topic dominances defined as the mean probability of each topic when that topic is stable and 95%-confidence intervals for controls and subjects with Insomnia disorder (ID). Bold font-style indicates significant group differences.

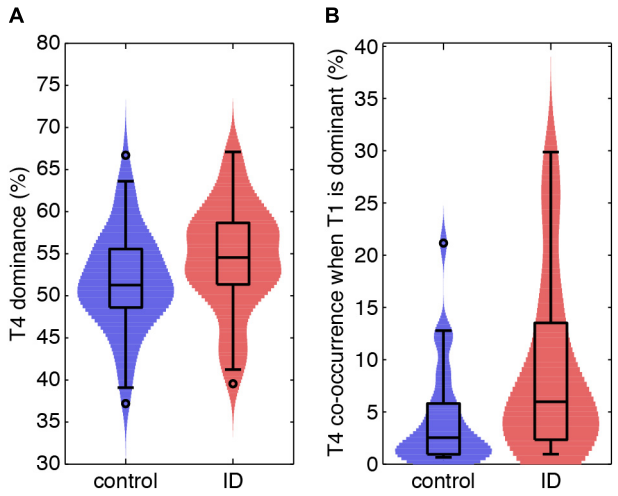

FIGURE 4 | Light sleep-related EEG signatures are more abundant during light and deep sleep in ID than in controls. **(A)** Violin plots for each group (horizontal axis) of the probability of light sleep-related topic T4 when this is stable and dominant (vertical axis). **(B)** Normalized co-occurrence of topic T4 when deep sleep-related topic T1 is stable and dominant (vertical axis).

ID contain more light sleep characteristics than stable epochs of light sleep in controls do.

Co-occurrence

Table 3 reports on the normalized co-occurrence of T2 to T6 in stable epochs dominated by T1 (N3-related topic). As T1 is related to (very) deep sleep, only 30/64 controls and 22/55 participants with ID expressed this stable epoch type (no between group differences in proportion of expression; Chi-square test, $p = 0.45$). For these stable epochs, we found a significantly higher co-occurrence of the N1-related T4 in ID (8.44%) as compared to controls [4.49%, $t(551) = 2.32$, $p = 0.02$; **Figure 4B**]. The co-occurrences of other topics in stable epochs dominated by T1 were not significantly different between ID and controls. These findings indicate that deep sleep in ID contains twice as much of the light sleep characteristics as compared to controls.

Similar tables for the other stable epoch types (stable epochs dominated by T2 to T6) are presented in **Supplementary Table S1**. None of the co-occurrences reported in the **Supplementary Table S1** were found to differ between groups.

Probabilities to Transit From Stable Epochs Dominated by One Topic to an Epoch Dominated by Each of the Other Topics

The probabilities to switch from stable epochs of one topic to an epoch of any other topic are summarized in a Markovian state diagram (**Figure 5**). The transition probability from stable epochs dominated by the N3-related T1 to an epoch dominated by the N1-related T4 was about 8 times higher in participants with ID [$p(T1 \rightarrow T4|ID) = 13.5\%$] compared to controls [$p(T1 \rightarrow T4|C) = 1.7\%$; Wilcoxon $W = 579$, $z = 2.36$, $p = 0.018$]. In addition, the transition probability from the same stable epochs dominated by the N3-related T1 to an epoch dominated by another N3-related topic (T2) was about 6 times lower in participants with ID compared to controls [$p(T1 \rightarrow T2|ID) = 2.6\%$ compared to $p(T1 \rightarrow T2|C) = 15.4\%$;

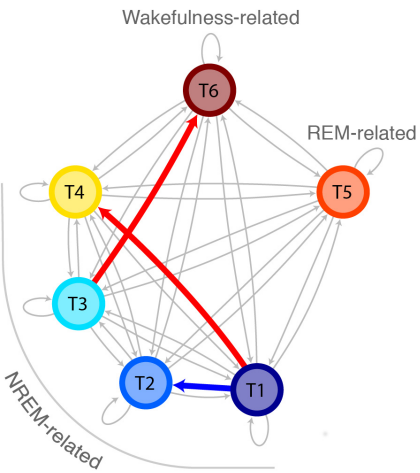

FIGURE 5 | Increased probability for transitions from deep sleep to light sleep in ID as compared to controls. Markovian state diagram for topic transitions. The red arrow indicates a higher probability for participants with ID compared to controls, whereas the blue arrow indicates a lower probability for participants with ID compared to controls. The topics are indicated with colors and arranged in a way so the vertical axis denotes deepness of sleep.

TABLE 3 | Increased N1 sleep-related EEG signatures during deep sleep related periods in ID.

	Controls	ID	Δ	P
Co-occurrence of T2 [%]	33.48 (23.47–43.50)	21.15 (11.80–30.50)	−12.58 (−26.75–1.58)	0.10
Co-occurrence of T3 [%]	9.06 (5.60–12.52)	8.17 (5.62–10.72)	−0.81 (−5.33–3.70)	0.71
Co-occurrence of T4 [%]	**4.49 (2.70–6.29)**	**8.44 (5.43–11.46)**	**4.12 (0.79–7.44)**	**0.02**
Co-occurrence of T5 [%]	7.83 (4.63–11.03)	8.13 (5.39–10.86)	0.56 (−3.84–4.95)	0.84
Co-occurrence of T6 [%]	45.08 (36.71–53.46)	53.59 (43.57–63.62)	8.69 (−4.32–21.70)	0.20

The normalized co-occurrence of topics T2-T6 in periods where the deep sleep-related topic T1 is dominant and stable. The values are reported as estimates, their 95th confidence intervals, and P-values obtained from linear mixed effect models with group, age and sex as fixed-effect factors, and a random intercept for each subject. Bold font-style indicates significant group differences.

Wilcoxon $W = 394.5$, $z = -2.22$, $p = 0.026$]. Finally, the transition probability from stable epochs dominated by the N2-related T3 to an epoch dominated by the wakefulness-related T6 was increased in participants with ID [$p(T3 \rightarrow T6|ID) = 0.7\%$] compared to controls [$p(T3 \rightarrow T6|C) = 0.5\%$; Wilcoxon $W = 3406.5$, $z = 1.97$, $p = 0.048$]. No other transitions were found to differ between groups. These findings indicate that compared to ID, controls have a higher tendency to switch from stable epochs dominated by one deep sleep related topic to epochs dominated by another deep sleep related topic, effectively remaining in deep sleep, whereas participants with ID have a higher tendency to switch to an epoch dominated by a light sleep related topic or from a stable epoch dominated by a N2-related topic to wakefulness.

Spectral Analysis

We found that beta power in the occipital region during N1 sleep was significantly increased in participants with ID [mean(SD) = 93.3 μV (32.1 μV)] compared to controls [mean (SD) = 91.9 μV (90.2 μV); $W = 3340$, $z = -2.20$, $p = 0.03$).

Associations With Subjective Severity of Insomnia Symptoms in People With Insomnia

Firstly, interindividual differences in the transition probabilities "T1→T4," "T1→T2," and "T3→T6," and beta power in the occipital region during N1 sleep, were not significantly associated with total ISI scores ($0.37 \leq p \leq 0.88$). Secondly, whereas interindividual differences in total ISI scores could not explain T4 dominance (β [se] = −0.11 [0.17], $t(1334) = -0.64$, $p = 0.52$), we found that greater T4 co-occurrence in stable epochs dominated by T1 was significantly associated with higher total ISI scores (β [se] = 1.13 [0.23], $t(192) = 4.85$, $p = 2.5 \times 10^{-6}$). The follow-up analysis indicated that greater T4 co-occurrence in stable epochs dominated by T1 was associated with more difficulties staying asleep (β [se] = 4.17 [1.18], $t(186) = 3.54$, $p = 5.0 \times 10^{-4}$), with more worries/distress about sleep problems (β [se] = 5.06 [1.82], $t(186) = 2.78$, $p = 0.006$), and with less problems waking up too early (β [se] = −1.98 [0.94], $t(186) = -2.11$, $p = 0.04$). The other ISI items were not statistically significant ($0.54 \leq p \leq 0.80$).

DISCUSSION

We analyzed the sleep EEG of people with ID and controls with an automatic sleep analysis procedure that expresses every 30-s epoch as a mixture of vigilance states, here called topics, instead of a single sleep stage. Compared to controls, participants with ID had (1) a higher probability of a light sleep-related topic (T4) in stable epochs where light sleep is dominant, (2) a higher co-occurrence of the same light sleep related T4 in stable epochs where a deep sleep related topic (T1) is dominant. Additionally, (3) we found that people with ID had a higher probability to transition from a stable T1-dominant epoch to an epoch where a light sleep-related topic is dominant, while controls were more likely to transition to an epoch where another deep sleep related topic is dominant. Also, (4) we found that people with ID had a higher probability to transition from stable epochs of an N2-sleep related topic (T3) to an epoch dominated by the wakefulness-related topic (T6) as compared to controls. Finally, using a standard spectral analysis (5) we found that people with ID show increased beta power in the occipital region during N1 sleep as compared to controls.

Our findings indicate that people with ID have more EEG signatures typical of light sleep than controls do, both during epochs where light sleep prevails and during epochs where deep sleep prevails. Local sleep and wakefulness would imply simultaneous wake- and sleep EEG signatures, which is what these findings suggest. Together with our findings of increased transitions from deep sleep to light sleep in ID, the present study suggests that people with ID are hyperaroused even in their deepest sleep. Another notable finding is the lack of major differences in standard PSG measures, as a recent review has also concluded (Feige et al., 2013). In a similar vein, we did not find any group-differences in the average probability or time spent in any of the stable epochs dominated by one topic. Only total sleep time (TST) was statistically different. However, with a mere 20 min less TST in ID as compared to controls, this difference cannot explain the severe subjective insomnia complaints. Our novel approach detected that subtle markers of light sleep-related EEG features during deep sleep were associated with the severity of insomnia complaints. Greater co-occurence of light sleep signatures during deep sleep in insomnia were associated with more difficulties staying asleep, more worries/distress about sleep problems, and with less problems waking up too early. These findings indicate that although the differences in light sleep signatures during deep sleep between insomnia patients and controls are small, these subtle changes in sleep do correspond to subjective insomnia complaints. Another important finding is the opposite direction of associations with difficulties staying asleep and waking up too early. The occurrence of light sleep during deep sleep is positively associated with the subjective difficulty staying asleep but negatively with the subjective problem of waking up too early. The suggested differential association appeared in *post hoc* analyses and therefore requires replication.

Although this study utilized the patterns of power-spectral dynamics, our methodology goes beyond standard spectral analysis methods and analysis of specific micro-sleep phenomena. Our method is flexible and fully automated and is applicable for scoring and analyzing PSG data of ID patients. Nonetheless, our findings are in line with previous research that identified increased beta-power during NREM sleep in insomnia disorder (Freedman, 1986; Merica et al., 1998). Furthermore, we have previously implicated (Wei et al., 2017) an increased probability to transition from stage N2 to stage N1 or wakefulness in ID (based on manual scorings following the AASM scoring criteria); similarly, here we found increased transition probabilities from a N2-related T3 to a wakefulness-related T6, and from a deep sleep-related T1 to a light sleep-related T4 in ID.

A future aim could be to examine the temporal dynamics of the topics across the night, as the topic probabilities clearly show cyclic dynamics. Interestingly, for the REM-related topic (T5) we visually observed low probabilities for T5 at the start of the nights which increased with time. In the current study we did not compute an objective measure capturing these temporal dynamics because the current definition of sleep cycles depends

on discrete classification of epochs. New measures of such dynamics need careful examination and validation against this golden standard.

Importance for the Field and Limitations

The automatic sleep analysis procedure used in the current study has provided a more detailed representation of sleep as compared to the AASM standard. Expressing sleep epochs as a mixture of vigilance states allowed us to investigate sleep dynamics in a more refined way, and we identified alterations in sleep patterns of participants with ID that were otherwise not detectable by manual scoring methods. A future aim could be to develop a LDA model that utilizes all EEG leads from high-density EEG recordings. Such a development would extend the spatial dimension of the analysis. Another important consideration for PSG research in general is that the current analysis procedure is bounded by the 30 s epochs. For now, the LDA model is trained to compute topic probabilities for fixed sleep epochs with a constant length of 30 s. A future focus for automated sleep-stage classification could be to both allow indiscrete labeling (more stages at a time), and variable epoch lengths. It should, however, be noted that by allowing data-driven methods to define epoch boundaries and vigilance states, the method might yield sleep stages that are not defined by the AASM today. In addition, the time-scale at which the number of vigilance states is defined is itself a factor that defines the number of vigilance states that can be captured. Nonetheless, overcoming these challenges will increase our conceptual understanding of sleep, and allows for data-driven identification of sleep alterations in health and disease.

A limitation of the present study is that we did not correct for type-1 error-rate inflation. The significance of the results would not have survived a false discovery rate correction. The findings should be considered preliminary until replicated in an independent sample.

The current study has produced important findings that can benefit the understanding of the symptomology of ID in terms of sleep characteristics. In ID, light sleep-related sleep EEG power changes are more prominent not only in light sleep but also even in their deepest sleep.

ETHICS STATEMENT

This study was carried out in accordance with the recommendations of the Central Committee on Research Involving Human Subjects with written informed consent from all subjects. All subjects gave written informed consent in accordance with the Declaration of Helsinki. The protocol was approved by the ethics committee of the Amsterdam University Medical Center, Amsterdam, Netherlands.

AUTHOR CONTRIBUTIONS

JC: study concept and design, development of topic model, and analysis and interpretation of data. RW: study concept and design, analysis and interpretation of data, and acquisition of data. YW: analysis and interpretation of data. JR and OL-K: acquisition and analysis of data. PJ: study concept and design, interpretation of data, and study supervision. EVS: study concept and design, interpretation of data, study supervision, and principal investigator. All the authors critically reviewed the manuscript.

FUNDING

The ESRS Short-Term Research Fellowship 2017 awarded to JC supported this project. Data were collected under the support of the Bial Foundation grants 190/16, 252/12, and 253/12, the Netherlands Organization of Scientific Research (NWO) grant VICI-453.07.001, ZonMw Neuropsychoanalysis Fund Grant 16.561.0001 and the European Research Council Advanced Grant ERC-2014-AdG-671084 INSOMNIA.

SUPPLEMENTARY MATERIAL

The Supplementary Material for this article can be found online at: https://www.frontiersin.org/articles/10.3389/fnins.2019.00598/full#supplementary-material

REFERENCES

American Academy of Sleep Medicine (2014). *International Classification of Sleep Disorders*, 3rd Edn. Darien, IL: American Academy of Sleep Medicine.

American Psychiatric Association (2013). *Diagnostic and Statistical Manual of Mental Disorders*, 5th Edn. Arlington, VA: American Psychiatric Publishing.

Baglioni, C., Regen, W., Teghen, A., Spiegelhalder, K., Feige, B., Nissen, C., et al. (2014). Sleep changes in the disorder of insomnia: a meta-analysis of polysomnographic studies. *Sleep Med. Rev.* 18, 195–213. doi: 10.1016/j.smrv.2013.04.001

Bastien, C. H., Ceklic, T., St-Hilaire, P., Desmarais, F., Pérusse, A. D., Lefrancois, J., et al. (2014). Insomnia and sleep misperception. *Pathol. Biol.* 62, 241–251. doi: 10.1016/j.patbio.2014.07.003

Bastien, C. H., St-Jean, G., Turcotte, I., Morin, C. M., Lavallée, M., and Carrier, J. (2009a). Sleep spindles in chronic psychophysiological insomnia. *J. Psychosom. Res.* 66, 59–65. doi: 10.1016/j.jpsychores.2008.05.013

Bastien, C. H., St-Jean, G., Turcotte, I., Morin, C. M., Lavallée, M., Carrier, J., et al. (2009b). Spontaneous K-complexes in chronic psychophysiological insomnia. *J. Psychosom. Res.* 67, 117–125. doi: 10.1016/j.jpsychores.2009.01.014

Benjamins, J. S., Migliorati, F., Dekker, K., Wassing, R., Moens, S., Blanken, T. F., et al. (2017). Insomnia heterogeneity: characteristics to consider for data-driven multivariate subtyping. *Sleep Med. Rev.* 36, 71–81. doi: 10.1016/j.smrv.2016.10.005

Besset, A., Villemin, E., Tafti, M., and Billiard, M. (1998). Homeostatic process and sleep spindles in patients with sleep-maintenance insomnia (SMI): effect of partial (21 h) sleep deprivation (PSD). *Electroencephalogr. Clin. Neurophysiol.* 107, 122–132. doi: 10.1016/S0013-4694(98)0048-40

Blei, D. M., Ng, A. Y., and Jordan, M. I. (2003). Latent dirichlet allocation. *J. Mach. Learn. Res.* 3, 993–1022.

Bonnet, M. H., and Arand, D. L. (2010). Hyperarousal and insomnia: state of the science. *Sleep Med. Rev.* 14, 9–15. doi: 10.1016/j.smrv.2009.05.002

Chouvarda, I., Mendez, M. O., Rosso, V., Bianchi, A. M., Parrino, L., Grassi, A., et al. (2011). CAP sleep in insomnia: new methodological aspects for sleep microstructure analysis. *Conf. Proc. IEEE Eng. Med. Biol. Soc.* 2011, 1495–1498. doi: 10.1109/IEMBS.2011.6090341

Chouvarda, I., Mendez, M. O., Rosso, V., Bianchi, A. M., Parrino, L., Grassi, A., et al. (2012). Cyclic alternating patterns in normal sleep and insomnia: structure and content differences. *IEEE Trans. Neural Syst. Rehabil. Eng.* 20, 642–652. doi: 10.1109/TNSRE.2012.2208984

Christensen, J. A. E., Jennum, P., Koch, H., Frandsen, R., Zoetmulder, M., Arvastson, L., et al. (2016). Sleep stability and transitions in patients with idiopathic REM sleep behavior disorder and patients with Parkinson's disease. *Clin. Neurophysiol.* 127, 537–543. doi: 10.1016/j.clinph.2015.03.006

Colombo, M. A., Ramautar, J. R., Wei, Y., Gomez-Herrero, G., Stoffers, D., Wassing, R., et al. (2016a). Wake high-density electroencephalographic spatiospectral signatures of insomnia. *Sleep* 39, 1015–1027. doi: 10.5665/sleep.5744

Colombo, M. A., Wei, Y., Ramautar, J. R., Linkenkaer-Hansen, K., Tagliazucchi, E., and Van Someren, E. J. (2016b). More severe insomnia complaints in people with stronger long-range temporal correlations in wake resting-state EEG. *Front. Physiol.* 7:576. doi: 10.3389/fphys.2016.00576

Delorme, A., and Makeig, S. (2004). EEGLAB: an open source toolbox for analysis of single-trial EEG dynamics including independent component analysis. *J. Neurosci. Methods* 134, 9–21. doi: 10.1016/j.neumeth.2003.10.009

Feige, B., Baglioni, C., Spiegelhalder, K., Hirscher, V., Nissen, C., and Riemann, C. (2013). The microstructure of sleep in primary insomnia: an overview and extension. *Int. J. Psychophysiol.* 89, 171–180. doi: 10.1016/j.ijpsycho.2013.04.002

Forget, D., Morin, C. M., and Bastien, C. H. (2011). The role of the spontaneous and evoked K-complex in good-sleeper controls and in individuals with insomnia. *Sleep* 34, 1251–1260. doi: 10.5665/SLEEP.1250

Freedman, R. R. (1986). EEG power spectra in sleep-onset insomnia. *Electroencephalogr. Clin. Neurophysiol.* 63, 408–413. doi: 10.1016/0013-4694(86)90122-7

Funk, C. M., Honjoh, S., Rodriguez, A. V., Cirelli, C., and Tononi, G. (2016). Local slow waves in superficial layers of primary cortical areas during REM sleep. *Curr. Biol.* 26, 396–403. doi: 10.1016/j.cub.2015.11.062

Hammerschlag, A. R., Stringer, S., de Leeuw, C. A., Sniekers, S., Taskesen, E., Watanabe, K., et al. (2017). Genome-wide association analysis of insomnia complaints identifies risk genes and genetic overlap with psychiatric and metabolic traits. *Nat. Genet.* 49, 1584–1592. doi: 10.1038/ng.3888

Iber, C., Ancoli-Israel, S., Chesson, A. L., and Quan, S. F. (2007). *The AASM Manual for the Scoring of Sleep and Associated Events: Rules, Terminology, and Technical Specifications*. Westchester, IL: American Academy of Sleep Medicine.

Israel, B., Buysse, D. J., Krafty, R. T., Begley, A., Miewald, J., and Hall, M. (2012). Short-term stability of sleep and heart rate variability in good sleepers and patients with insomnia: for some measures, one night is enough. *Sleep* 35, 1285–1291. doi: 10.5665/sleep.2088

Jansen, P. R., Watanabe, K., Stringer, S., Skene, N., Bryois, J., Hammerschlag, A. R., et al. (2019). Genome-wide analysis of insomnia in 1,331,010 individuals identifies new risk loci and functional pathways. *Nat. Genet.* 51, 394–403. doi: 10.1038/s41588-018-0333-3

Koch, H., Christensen, J. A., Frandsen, R., Zoetmulder, M., Arvastson, L., Christensen, S. R., et al. (2014). Automatic sleep classification using a data-driven topic model reveals latent sleep states. *J. Neurosci. Methods* 235, 130–137. doi: 10.1016/j.jneumeth.2014.07.002

Krystal, A. D., Edinger, J. D., Wohlgemuth, W. K., and Marsh, G. R. (2002). NREM sleep EEG frequency spectral correlates of sleep complaints in primary insomnia subtypes. *Sleep* 25, 626–636.

Maes, J., Verbraecken, J., Willemen, M., De Volder, I., van Gastel, A., Michiels, N., et al. (2014). Sleep misperception, EEG characteristics and autonomic nervous system activity in primary insomnia: a retrospective study on polysomnographic data. *Int. J. Psychophysiol.* 91, 163–171. doi: 10.1016/j.ijpsycho.2013.10.012

Manconi, M., Ferri, R., Sagrada, C., Punjabi, N. M., Tettamanzi, E., Zucconi, M., et al. (2010). Measuring the error in sleep estimation in normal subjects and in patients with insomnia: insomnia. *J. Sleep Res.* 19, 478–486. doi: 10.1111/j.1365-2869.2009.00801.x

Merica, H., Blois, R., and Gaillard, J. M. (1998). Spectral characteristics of sleep EEG in chronic insomnia. *Eur. J. Neurosci.* 10, 1826–1834. doi: 10.1046/j.1460-9568.1998.00189.x

Nir, Y., Staba, R. J., Andrillon, T., Vyazovskiy, V. V., Cirelli, C., Fried, I., et al. (2011). Regional slow waves and spindles in human sleep. *Neuron* 70, 153–169. doi: 10.1016/j.neuron.2011.02.043

Ohayon, M. M. (2002). Epidemiology of insomnia: what we know and what we still need to learn. *Sleep Med. Rev.* 6, 97–111. doi: 10.1053/smrv.2002.0186

Ozone, M., Yagi, T., Itoh, H., Tamura, Y., Inoue, Y., Uchimura, N., et al. (2008). Effects of zolpidem on cyclic alternating pattern, an objective marker of sleep instability, in Japanese patients with psychophysiological insomnia: a randomized crossover comparative study with placebo. *Pharmacopsychiatry* 41, 106–114. doi: 10.1055/s-2008-1058104

Parrino, L., Ferrillo, F., Smerieri, A., Spaggiari, M. C., Palomba, V., Rossi, M., et al. (2004). Is insomnia a neurophysiological disorder? The role of sleep EEG microstructure. *Brain Res. Bull.* 63, 377–383. doi: 10.1016/j.brainresbull.2003.12.010

Parrino, L., Milioli, G., De Paolis, F., Grassi, A., and Terzano, M. G. (2009). Paradoxical insomnia: the role of CAP and arousals in sleep misperception. *Sleep Med.* 10, 1139–1145. doi: 10.1016/j.sleep.2008.12.014

Parrino, L., Smerieri, A., Giglia, F., Milioli, G., De Paolis, F., and Terzano, M. G. (2008). Polysomnographic study of intermittent zolpidem treatment in primary sleep maintenance insomnia. *Clin. Neuropharmacol.* 31, 40–50. doi: 10.1097/wnf.0b013e3180674e0e

Riemann, D., Spiegelhalder, K., Feige, B., Voderholzer, U., Berger, M., Perlis, M., et al. (2010). The hyperarousal model of insomnia: a review of the concept and its evidence. *Sleep Med. Rev.* 14, 19–31. doi: 10.1016/j.smrv.2009.04.002

Riemann, D., Spiegelhalder, K., Nissen, C., Hirscher, V., Baglioni, C., and Feige, B. (2012). REM sleep instability - a new pathway for insomnia? *Pharmacopsychiatry* 45, 167–176. doi: 10.1055/s-0031-1299721

Spiegelhalder, K., Regen, W., Feige, B., Holz, J., Piosczyk, H., Baglioni, C., et al. (2012). Increased EEG sigma and beta power during NREM sleep in primary insomnia. *Biol. Psychol.* 91, 329–333. doi: 10.1016/j.biopsycho.2012.08.009

Terzano, M. G., Parrino, L., Spaggiari, M. C., Palomba, V., Rossi, M., and Smerieri, A. (2003). CAP variables and arousals as sleep electroencephalogram markers for primary insomnia. *Clin. Neurophysiol.* 114, 1715–1723. doi: 10.1016/s1388-2457(03)00136-6

Vyazovskiy, V. V., Olcese, U., Hanlon, E. C., Nir, Y., Cirelli, C., and Tononi, G. (2011). Local sleep in awake rats. *Nature* 472, 443–447. doi: 10.1038/nature10009

Wassing, R., Benjamins, J. S., Dekker, K., Moens, S., Spiegelhalder, K., Feige, B., et al. (2016). Slow dissolving of emotional distress contributes to hyperarousal. *Proc. Natl. Acad. Sci. U.S.A.* 113, 2538–2543. doi: 10.1073/pnas.1522520113

Wei, Y., Colombo, M. A., Ramautar, J. R., Blanken, T. F., van der Werf, Y. D., Spiegelhalder, K., et al. (2017). Sleep stage transition dynamics reveal specific stage 2 vulnerability in Insomnia. *Sleep* 40:zsx117. doi: 10.1093/sleep/zsx117

Wittchen, H. U., Jacobi, F., Rehm, J., Gustavsson, A., Svensson, M., Jönsson, B., et al. (2011). The size and burden of mental disorders and other disorders of the brain in Europe 2010. *Eur. Neuropsychopharmacol.* 21, 655–679. doi: 10.1016/j.euroneuro.2011.07.018

Conflict of Interest Statement: The authors declare that the research was conducted in the absence of any commercial or financial relationships that could be construed as a potential conflict of interest.

Copyright © 2019 Christensen, Wassing, Wei, Ramautar, Lakbila-Kamal, Jennum and Van Someren. This is an open-access article distributed under the terms of the Creative Commons Attribution License (CC BY). The use, distribution or reproduction in other forums is permitted, provided the original author(s) and the copyright owner(s) are credited and that the original publication in this journal is cited, in accordance with accepted academic practice. No use, distribution or reproduction is permitted which does not comply with these terms.

frontiers in Neuroscience

ORIGINAL RESEARCH
published: 10 July 2019
doi: 10.3389/fnins.2019.00727

Spatiotemporal Dynamics of Sleep Spindle Sources Across NREM Sleep Cycles

*Valentina Alfonsi[1], Aurora D'Atri[1], Maurizio Gorgoni[1], Serena Scarpelli[1], Anastasia Mangiaruga[1], Michele Ferrara[2] and Luigi De Gennaro[1,3]**

[1] Department of Psychology, Sapienza University of Rome, Rome, Italy, [2] Department of Biotechnological and Applied Clinical Sciences, University of L'Aquila, L'Aquila, Italy, [3] IRCCS Santa Lucia Foundation, Rome, Italy

The existence of two different types of sleep spindles (slow and fast) is well-established, according to their topographical distribution at scalp- and cortical-level. Our aim was to provide a systematic investigation focused on the temporal evolution of sleep spindle sources during non-rapid eye movement (NREM) sleep. Spindle activity was recorded and automatically detected in 20 healthy subjects. Low resolution brain electromagnetic tomography (LORETA) was applied for the EEG source localization. Aiming to evaluate the time course of the detected slow and fast spindle sources, we considered the first four NREM sleep cycles and divided each cycle into five intervals of equal duration. We confirmed the preferential localization in the frontal (Brodmann area 10) and parietal (Brodmann area 7) cortical regions, respectively for slow (11.0–12.5) and fast (13.0–14.5) spindles. Across subsequent NREM sleep episodes, the maximal source activation remained systematically located in Brodmann area 10 and Brodmann area 7, showing the topographical stability of the detected generators. However, a different time course was observed as a function of the type of spindles: a linear decrease across subsequent cycles was found for slow spindle but not for fast spindle source. The intra-cycle variations followed a "U" shaped curve for both spindle source, with a trough around third and fourth interval (middle part) and the highest values at the beginning and the end of the considered temporal window. We confirmed the involvement of the frontal and parietal brain regions in spindle generation, showing for the first time their changes within and between consecutive NREM sleep episodes. Our results point to a correspondence between the scalp-recorded electrical activity and the underlying source topography, supporting the notion that spindles are not uniform phenomena: complex region- and time-specific patterns are involved in their generation and manifestation.

Keywords: sleep spindles, slow/fast spindles, EEG source localization, LORETA, time course

OPEN ACCESS

Edited by:
Giulio Bernardi,
IMT School for Advanced Studies Lucca, Italy

Reviewed by:
Péter Przemyslaw Ujma,
Semmelweis University, Hungary
Thomas Andrillon,
Monash University, Australia

***Correspondence:**
Luigi De Gennaro
luigi.degennaro@uniroma1.it

Specialty section:
This article was submitted to Sleep and Circadian Rhythms, a section of the journal Frontiers in Neuroscience

Received: *20 March 2019*
Accepted: *28 June 2019*
Published: *10 July 2019*

Citation:
Alfonsi V, D'Atri A, Gorgoni M, Scarpelli S, Mangiaruga A, Ferrara M and De Gennaro L (2019) Spatiotemporal Dynamics of Sleep Spindle Sources Across NREM Sleep Cycles. Front. Neurosci. 13:727. doi: 10.3389/fnins.2019.00727

INTRODUCTION

Sleep spindles are transient oscillatory activity that appears in electroencephalography (EEG) during NREM sleep. They are typically defined as short (∼0.5–2 s) bursts of waxing and waning pattern within the sigma band (9–16 Hz) (De Gennaro and Ferrara, 2003).

The physiological function of these oscillatory patterns has not yet been completely elucidated. The evidence regarding their role in sleep maintenance appears controversial (Schabus et al., 2012;

Sela et al., 2016), whereas it is well-known their critical role in learning and memory consolidation (Diekelmann and Born, 2010; Cox et al., 2014).

These phenomena are initiated in the reticular nucleus of the thalamus and the reciprocal interactions between specific regions of the cortex shape their duration and amplitude (Steriade and Llinás, 1988; McCormick and Bal, 1997; Ujma et al., 2019).

Spindles are traditionally classified into "slow" and "fast" subtypes, as a function of specific frequency and topography. The former is prevalent in the anterior cortical regions, while the latter spreads mainly in central and posterior areas (Werth et al., 1996; Zeitlhofer et al., 1997).

This regional distribution of scalp-recorded sleep spindles is also displayed at cortical level by studies exploring the activation of underlying cortical generators (Andrillon et al., 2011; Ktonas and Ventouras, 2014). Non-invasive estimation of cortical generators of sleep spindles has been provided by simultaneous EEG and magnetoencephalography recording, through modeling sources as electric current dipoles (Shih et al., 2000; Urakami, 2008). An alternative method is the low-resolution electromagnetic tomography (LORETA) (Pascual-Marqui et al., 2002). LORETA solves the inverse problem and received validation from several fMRI (Vitacco et al., 2002; Mulert et al., 2004) and intracranial recordings studies (Zumsteg et al., 2006). The solution space is restricted to cortical gray matter and modeled as a grid of volume elements (voxels) in the digitized structural template [Montreal Neurological Institute (MNI); Talairach and Tournoux, 1988]. It estimates the intracranial current source density (CSD) underlying global or selected electrical activity relying on a set of scalp-recorded potential differences, consistently with the assumption that contiguous neurons are simultaneously and synchronously active.

A pioneering study investigated the cortical electrical sources of a selected number of fast and slow spindles using LORETA (Anderer et al., 2001). The authors localized simultaneously active spindle generators clustered in frontal and parietal areas. Regions with the highest LORETA activity were mostly identified in the medial prefrontal gyrus and precuneus, respectively for slow and fast spindles. Subsequent studies applying such technique have confirmed the activation of this fronto-parietal network underlying the two types of spindles (Ventouras et al., 2010; Bersagliere et al., 2013; Del Felice et al., 2014) (**Table 1**).

TABLE 1 | Source localization studies of sleep spindle.

	Frequency (Hz)	Brodmann area (BA)	Lobe
Anderer et al., 2001	<13 >13	BA 9,10 BA 7	Frontal Parietal
Ventouras et al., 2010	11–16	BA 17	Occipital
Bersagliere et al., 2013	12–16	BA 5,6,10,11	Frontal, parietal
Del Felice et al., 2013	10–12	BA 10,11,6,45,46	Frontal
	12–14	BA 6,10,11,20,21, 37,40,43,18	Frontal, temporal, parietal, occipital
Del Felice et al., 2014	10–12	BA 9, 10, 6, 21	Frontal, temporal
	12–14	BA 6,10,20,21,7,10	Frontal, temporal, parietal

Together with the regional distribution, also the temporal dynamics across sleep cycles differ between the two types of spindles. Density (number of spindle/minute) of both types of spindles linearly increases across consecutive NREM episodes (Werth et al., 1996), while EEG power values show a gradual decrease of the spectral power for slow spindles and a concomitant increase for fast spindles across consecutive sleep cycles (Tanaka et al., 1997). Consistently with this phenomenon, the frequency (period) of spindles increases over the course of a night's sleep (Dijk et al., 1993; Wei et al., 1999). The spindle density also varies within each sleep cycle. They are more abundant at the beginning and at the end of NREM sleep episodes, typically following a U-shaped curve (Aeschbach et al., 1997; De Gennaro et al., 2000b; Himanen et al., 2002, 2003).

Surprisingly, no study systematically investigated the spatiotemporal dynamics of sleep spindles across the night by assessing the time course of the activation level of their sources. To fill this gap, we applied LORETA to track the temporal evolution of the sleep spindle sources between and within each NREM sleep cycle.

To sum up, the aims of the present study were (a) to confirm the known involvement of frontal and parietal sources in spindle generation and (b) to explore their time-varying activation across different sleep episodes.

MATERIALS AND METHODS

Subjects

Twenty healthy subjects (12 males and 8 females; age range = 20–29, mean age = 23.8 ± 2.45 years) were selected as volunteers from a university student population. The requirements for inclusion were: regular sleep duration and schedule (habitual sleep time: 12:00 am–8:00 am ± 1 h), no daytime nap habits, no excessive daytime sleepiness and no other sleep, medical, neurological or psychiatric disorder, as assessed by a 1-week sleep log and by a clinical interview.

Participants were asked to keep constant their sleep/wake cycle during the week before the experimental night, and their compliance was controlled by daily sleep log and actigraphic recordings.

All subjects provided written informed consent. The study was approved by the Institutional Ethics Committee of the Department of Psychology of "Sapienza" University of Rome and was conducted in accordance with the Declaration of Helsinki.

Procedure

Each subject participated in this study across two consecutive nights. The first night was considered of adaptation, while the following was the experimental night. Polysomnographic (PSG) recordings performed during the experimental night only was considered for the present analyses.

The sleep recordings were carried out in an electrically shielded, sound-proof and temperature-controlled room. Bedtime was scheduled at midnight and ended after 7.5 h of accumulated sleep, as visually checked online by expert sleep researchers.

Polysomnographic Recordings

PSG was recorded using an Esaote Biomedica VEGA 24 polygraph. EEG signals were analogically filtered (high-pass filter at 0.50 Hz and antialiasing low-pass filter at 30 Hz [−30 dB/octave]). The 19 unipolar EEG derivations (Fp1, Fp2, F7, F8, F3, F4, Fz, C3, C4, Cz, P3, P4, Pz, T3, T4, T5, T6, O1, O2) were placed according to the international 10–20 system and recorded from scalp electrodes with linked mastoid electrodes as a reference. Bipolar horizontal electrooculogram (EOG) was recorded from electrodes placed approximately 1 cm from the medial and lateral canthi of the dominant eye. The bipolar submental electromyogram (EMG) was also recorded. The time constants were as follow: 0.03 s for EMGs and 1 s for EOGs. Impedance of these electrodes was maintained below 5 kOhm.

The whole-night sleep recordings (19 EEG channels, EOG, and EMG) were digitalized with a sampling rate of 128 Hz.

Data Analysis

Sleep Stage Scoring

Sleep stages were visually scored (Cz derivation, EMG, and EOG) according to Rechtschaffen and Kales (1968). The sleep stages were scored for every 20 s epoch. Ocular and muscle artifacts were carefully offline excluded by visual inspection. The sleep measures are reported in **Table 2**.

TABLE 2 | Polysomnographic measures.

Variables	Mean (*SD*)
Stage 1 (%)	6.76 (2.21)
Stage 2 (%)	59.34 (6.09)
SWS (%)	9.74 (6.44)
REM (%)	24.14 (4.31)
Awakenings (#)	27.85 (7.42)
Arousals (#)	35.1 (18.49)
TST (min)	451 (29.24)
TBT (min)	473.08 (40.03)
SEI % (TST/TBT)	93.23 (0.02)

Means and standard deviations (SD) of the PSG variables.

Spindle Detection

The automatic spindle detection from the whole night recordings was performed by means of a customized algorithm in MATLAB (The Mathworks, Inc., Natick, MA, United States), adapted from previous studies (Ferrarelli et al., 2007, 2010; Plante et al., 2013, 2015; Gorgoni et al., 2016; D'Atri et al., 2018).

The EEG data for all NREM epochs were band-pass filtered (Chebyshev Type II) between 11 and 15 Hz (−3 dB at 10 and 16 Hz). The detection of a spindle occurred when the mean signal amplitude of each channel exceeded an upper threshold set at six times the mean single channel amplitude. The sleep spindle characteristics are reported in **Table 3**.

Source Localization

In order to estimate the strength and distribution of the intracranial sources (CSD, $\mu A/mm^2$) of EEG activity in the spindle range, we used the freeware eLORETA (exact Low-resolution electromagnetic tomography). We used the most recent version at the time of performing this study (v20170220). eLORETA was applied to estimate the three-dimensional distribution of the current density vector field of sleep spindles. The solution space, restricted to cortical gray matter, is represented by 6239 voxels, with a spatial resolution of 5 mm.

All EEG data containing the detected spindles on each scalp derivation were extracted and segmented for the source localization. The beginning and end of each epoch (total duration: 1 s) were defined as the 0.50 s immediately preceding and following the temporal midpoint of spindles. No repeated epochs were considered in the final analysis.

Before the CSD calculation, all electrodes were adapted to the international 10–20 system and registered to the 3D Montreal Neurological Institute's MNI152 space (Talairach and Tournoux, 1988), producing a spatial transformation matrix for the inverse solution. Then, we determined the LORETA power in the frequency domain via the cross-spectral matrices from the EEG. Finally, CSD maps were extracted through the LORETA pseudoinverse transformation of the information at level of the scalp to the underlying current inside each voxel.

Current source density maps were averaged within- and then between-participants, yielding a grand average for the final group.

A two-step process was performed to identify the active sources underlying slow and fast spindles. The first step consisted of estimating cortical sources for the whole spindle range under investigation (10.0–16.0 Hz) in the frequency domain, with a bin resolution of 0.5 Hz. In a second step, the three bins with the highest CSD were visually identified to define the respective range for slow (11.0–12.5 Hz) and fast (13.0–14.5 Hz) spindles, excluding the central bin due to the activation of both sources (**Figure 1A**). The resulting ROIs [in terms of Brodmann Areas (BA)] with maximal CSD values for slow and fast spindle range were considered as the putative source and used for subsequent analyses.

Time Course Analysis Between Cycles

With the aim of investigating the entity of possible variation across NREM episodes for the two identified spindle sources, we selected the first four consecutive NREM sleep episodes for each subject (i.e., the maximum common number of cycles).

Specifically, the NREM sleep episodes were operationally considered from the first epoch of NREM sleep to the onset of following REM sleep episode. No skipped first REM sleep episodes nor SO REM sleep episodes were present in our recordings.

We considered CSD as dependent variable, and it was computed separately for the slow and fast spindle sources. The CSD values of voxels within the ROIs were averaged.

Data were submitted to a two-way analysis of variance (ANOVA) with Spindle Type (Slow, Fast) and Sleep Cycle (1, 2, 3, 4) as within-subject factors. LSD method was used for planned comparisons ($p \leq 0.05$).

Time Course Analysis Within Cycles

In order to assess the variations of cortical sources within each sleep cycle, we compared consecutive time frames.

TABLE 3 | Global spindle characteristics.

	Slow spindle (11.0–13.0 Hz)			Fast spindle (13.0–15.0 Hz)		
	NREM 2	**NREM 3**	**NREM 4**	**NREM 2**	**NREM 3**	**NREM 4**
Amplitude (μV)	12.13 (1.29)	10.91 (1.50)	10.58 (1.59)	11.79 (1.27)	10.70 (1.63)	10.43 (1.98)
Frequency (Hz)	12.52 (0.08)	12.53 (0.11)	12.56 (0.22)	13.75 (0.17)	13.67 (0.19)	13.74 (0.32)
Duration (s)	1.14 (0.07)	1.06 (0.08)	1.00 (0.24)	0.99 (0.05)	0.84 (0.06)	0.88 (0.23)
Density (number/min)	1.06 (0.34)	0.64 (0.68)	0.31 (0.36)	1.65 (0.39)	0.77 (0.72)	0.38 (0.30)

Means and standard deviations (SD) of detected spindle as a function of sleep cycle (NREM 2,3,4).

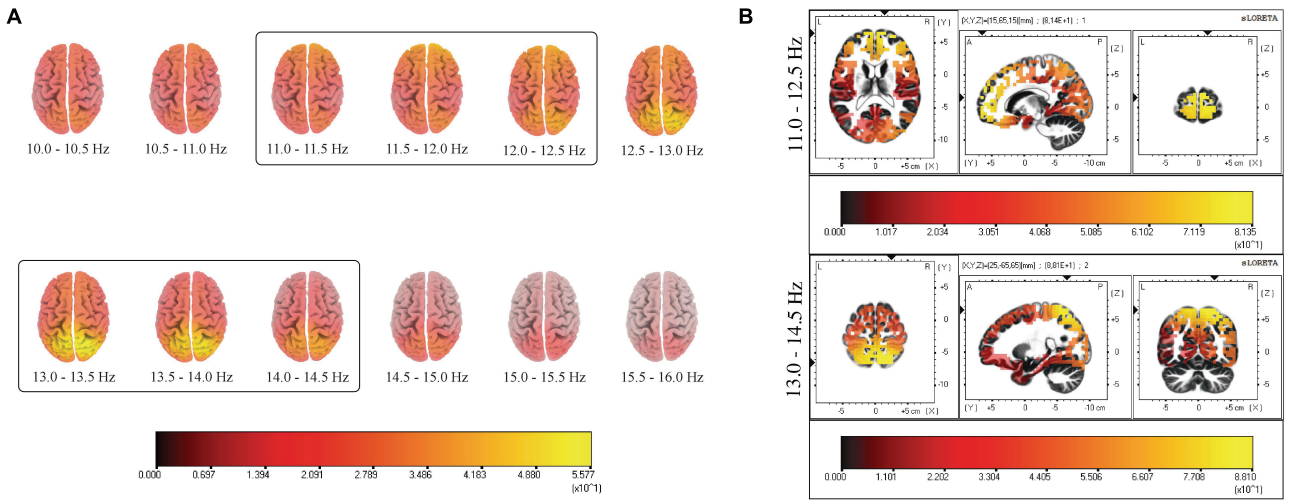

FIGURE 1 | (A) Distribution of mean CSD of the whole spindle frequency range (10.0–16.0 Hz) with a frequency bin resolution of 0.5 Hz. The maximum of the estimated source is indicated in yellow. The prevalent source localization is situated over the anterior regions for low-frequency spindles and posterior regions for high-frequency spindles. **(B)** Distribution of mean CSD of slow (11.0–12.5 Hz) and fast (13.0–14.5 Hz) spindles in NREM sleep cycles. Two local maxima are identified: BA10 and BA7. Each distribution is shown relative to its maximum (in yellow), using axial, sagittal, and coronal slices intersecting at the point of maximal source.

Due to the intra- and inter-individual variability in the duration of NREM sleep cycles, we divided each cycle into five intervals of equal duration, to make their time course comparable (Aeschbach and Borbély, 1993). For each interval of the cycles, CSD of slow and fast spindle sources was computed separately.

Aimed to assess time course within each sleep cycle, two-way ANOVAs considering Spindle Type (Slow, Fast) and Cycle Interval (1, 2, 3, 4, 5) as within-subject factors were carried out. LSD method was used for planned comparisons ($p \leq 0.05$).

RESULTS

Slow and Fast Spindle Sources

The results of source estimation of spindle activity from the 19-channel EEG recordings are depicted in **Figure 1**.

Figure 1B provides a grand average of CSD maps for slow and fast spindles during NREM sleep. LORETA processing revealed two broadly distinct cortical areas for slow and fast spindles, respectively placed in the anterior and posterior cortical brain areas. Multiple cortical sources for slow spindles were identified, scattered throughout the frontal areas. These areas included the superior and medial frontal gyrus (frontal lobe) and anterior cingulate (limbic lobe), with a maximum CSD value in the superior frontal gyrus (BA10). Multiple sources were also identified for fast spindles, mostly restricted and situated in the parietal areas (superior and inferior parietal lobule and post-central gyrus), with the superior parietal lobule (BA7) as the most active region.

The localization and MNI coordinates of local maxima CSD for each detected source of the two types of spindles are reported in **Table 4**.

Variations Between NREM Sleep Cycles

Current source density maps of group average in each NREM sleep episodes are depicted in **Figure 2**. Despite the varying intensity across cycles, we observed that the local maxima of CSD distribution for both slow and fast spindles remained stable.

The repeated measures ANOVA Spindle Type × Sleep Cycle on CSD values (**Figure 3**) showed a significant main effect of the Sleep Cycle ($F_{3,57} = 3.279$, $p = 0.0273$), in the

TABLE 4 | Local maxima of CSD distributions for slow (11.0–12.5 Hz) and fast (13.0–14.5 Hz) spindles.

	Spindle 11.0–12.5 Hz					Spindle 13.0–14.5 Hz				
Local maximum	**Lobe**	**Anatomical region (BA)**	**MNI coordinates**			**Lobe**	**Anatomical region (BA)**	**MNI coordinates**		
1	Frontal lobe	Superior frontal gyrus (10)	15	65	15	Parietal lobe	Superior parietal lobule (7)	25	−65	65
2	Frontal lobe	Superior frontal gyrus (10)	10	65	20	Parietal lobe	Superior parietal lobule (7)	20	−65	65
3	Frontal lobe	Medial frontal gyrus (10)	10	65	15	Parietal lobe	Post-central gyrus (7)	10	−60	70
4	Frontal lobe	Superior frontal gyrus (10)	20	65	10	Parietal lobe	Superior parietal lobule (7)	20	−60	65
5	Frontal lobe	Superior frontal gyrus (10)	5	65	15	Parietal lobe	Post-central gyrus (7)	15	−55	70

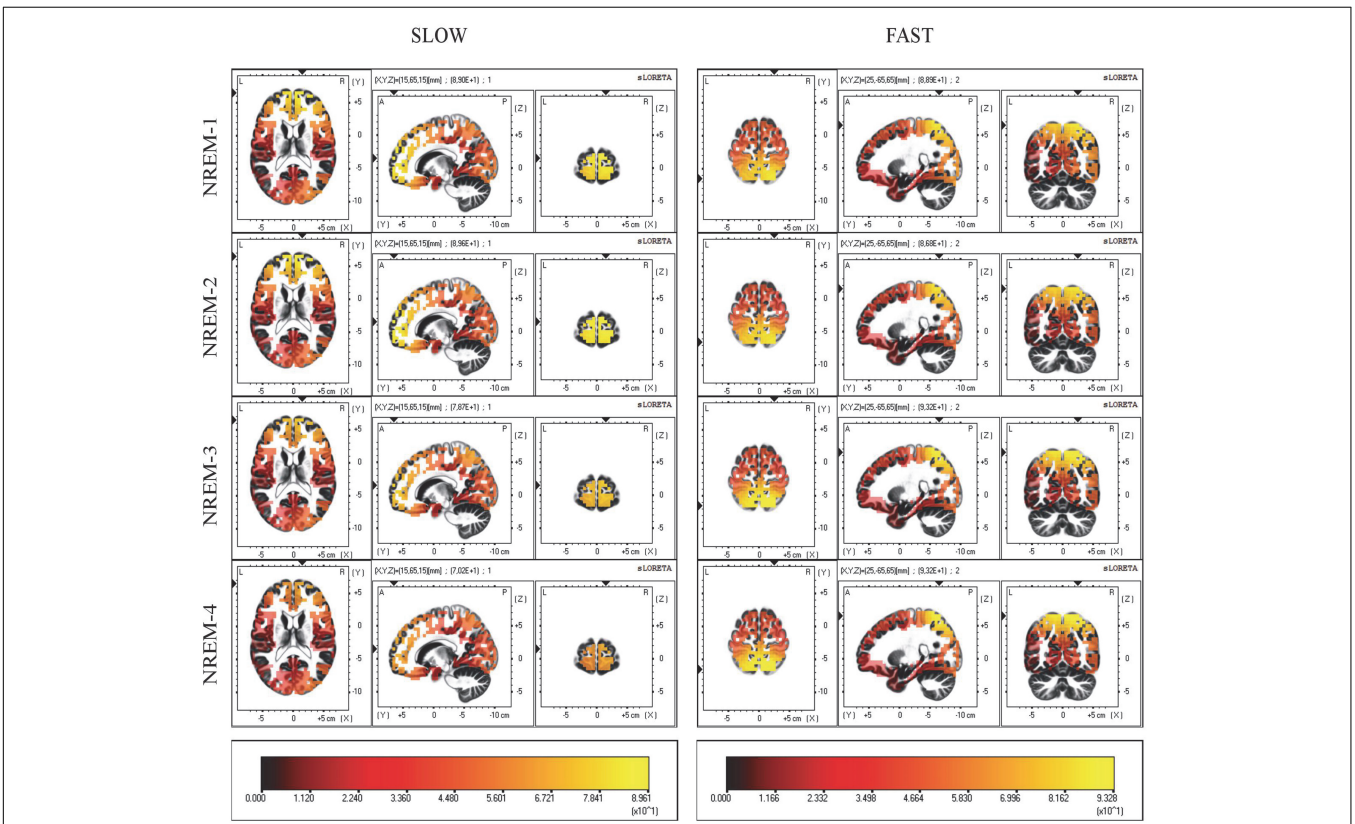

FIGURE 2 | Distribution of mean CSD of slow (11.0–12.5 Hz) and fast (13.0–14.5 Hz) spindles in the first four NREM sleep cycle. Regardless of their current intensity values, local maxima of CSD remain in the same BAs (10,7) across all cycles. Each distribution is shown relative to its maximum (in yellow), using axial, sagittal, and coronal slices intersecting at the point of maximal source.

direction of a clear reduction of CSD values in the fourth cycle compared to the first (p = 0.0223), second (p = 0.0099) and third (p = 0.0113) cycle. No significant main effect of Spindle Type was observed.

A significant interaction effect between the two factors was also observed ($F_{3,57}$ = 4.264, p = 0.0087). LSD *post hoc* comparison showed that while CSD in BA10 (slow spindle source) progressively decreases over time (Cycle 1 vs. Cycle 4: p = 0.0012; Cycle 2 vs. Cycle 4: p = 0.0008; Cycle 2 vs. Cycle 3: p = 0.0504), CSD in BA7 (fast spindle source) showed a different trend. After an initial increase, statistically significant between Cycle 1 and Cycle 3 (p = 0.0266), we found a decrease from Cycle 3 to Cycle 4 (p = 0.0117). CSD of the two types of spindle was different in the first and third cycle, with a prevalence of BA10 within Cycle 1 (p = 0.0399) and of BA7 within Cycle 3 (p = 0.0477).

Variations Within NREM Sleep Cycles

Figure 4 depicts intra-cycle variations of CSD computed from BA10 (slow spindle source) and BA7 (fast spindle source) during the first four sleep cycles.

We carried out four separate ANOVAs, one for each cycle, considering Spindle Type and Cycle Interval as within factors. A statistically significant main effect for the factor Cycle Interval was found for the first ($F_{4,76}$ = 3.334, p = 0.0142) and second ($F_{4,76}$ = 3.866, p = 0.0065) NREM cycle. No effect of Spindle Type or interaction Spindle Type × Cycle Interval was found in any NREM cycle.

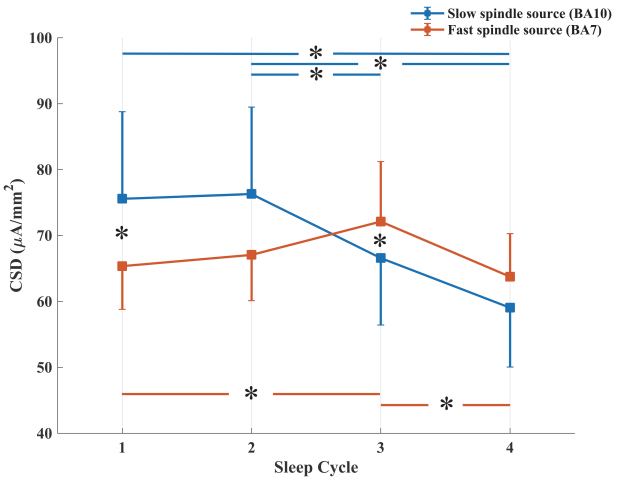

FIGURE 3 | Temporal evolution of mean CSD in BA10 (blue line) and BA7 (orange line) across NREM sleep cycles. *Signficant at $p < 0.05$.

LSD *post hoc* testing for the first NREM cycle showed a significant prevalence of CSD in the first interval as compared to the last three cycle intervals (Interval 1 vs. Interval 3: $p = 0.0015$; Interval 1 vs. Interval 4: $p = 0.0083$; Interval 1 vs. Interval 5: $p = 0.01258$). In the second cycle, we found the same decrease of CSD across different intervals (Interval 1 vs. Interval 3: $p = 0.0031$; Interval 1 vs. Interval 4: $p = 0.0013$; Interval 1 vs. Interval 5: $p = 0.0296$) and a prevalence of CSD in Interval 2 as compared to the Interval 4 ($p = 0.0286$).

DISCUSSION

To our knowledge, this is the first study specifically focused on temporal evolution of cortical spindle generators across the sleep night. Investigating the temporal dynamics of sleep spindle sources could potentially shed light on their involvement in spindle generation as a function of time.

According to the notion that spindling could reveal at least two functionally separated generators, respectively for high- and low- frequency spindles, we applied LORETA source estimation for two complementary purposes: (1) confirming the cortical areas which are involved in the generation of the two types of spindle and (2) tracking their changes between and within each NREM sleep cycle.

Localization of Sleep Spindle Sources

We computed CSD maps in the frequency domain considering a wide frequency range (10.0–16.0 Hz) (**Figure 1A**), with a bin resolution of 0.5 Hz. This frequency-specific analysis identified the ranges 11.0–12.5 and 13.0–14.5 Hz as the frequency intervals with the highest values of CSD, respectively for the "slow" and "fast" spindle type. The frequency resolution allowed us to observe the smoothly changing of detected sources across consecutive bins, with a shift from the anterior activating areas (slower frequencies) to the posterior sources (faster frequencies).

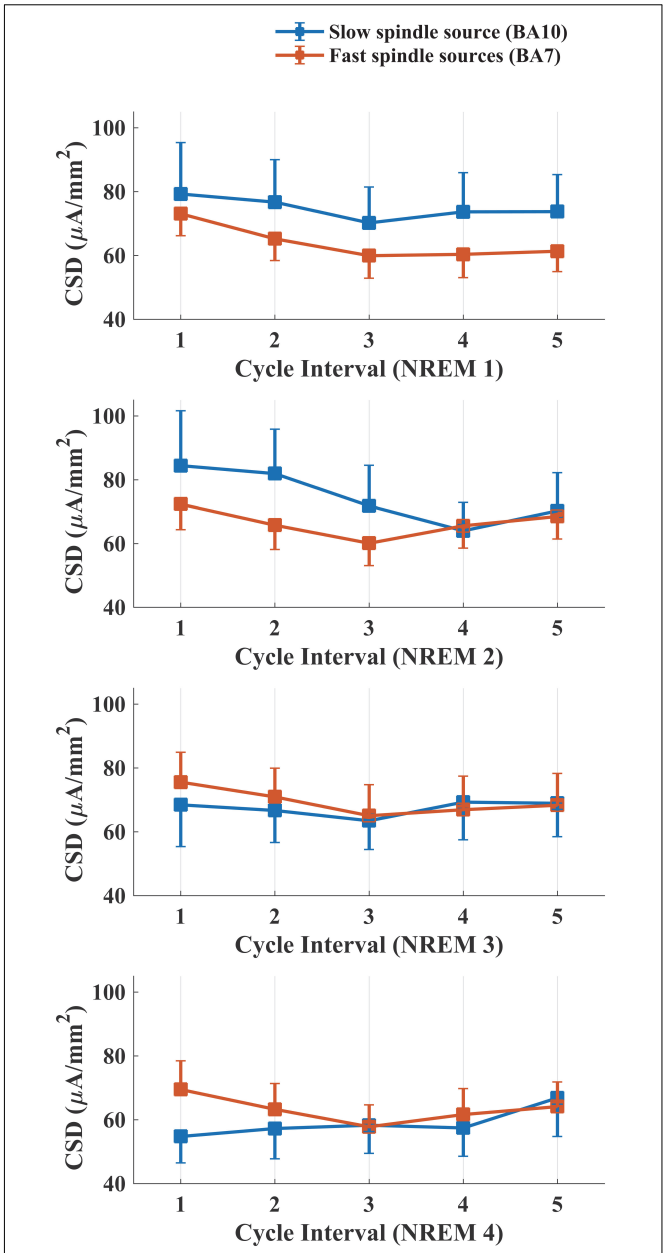

FIGURE 4 | Temporal evolution of mean CSD in BA10 (blue line) and BA7 (orange line) across intervals within each NREM sleep cycle.

The most active source of slow spindles was found in BA10, in the frontal cortex, while fast spindles range reached the absolute maximum in the parietal cortex (BA7) (**Figure 1B**).

The pattern observed at cortical level mirrors the appearance of spindles at the scalp level. This is consistent with the idea that EEG activity reflects the synchronous activation of brain electrical generators. Indeed, the slow spindle oscillations are predominant throughout the anterior derivations, while fast spindles prevail posteriorly (Werth et al., 1996; Zeitlhofer et al., 1997).

Despite the limited number of scalp electrodes (19) may have affected the precision of the inverse solution implemented by

LORETA, the preferential localization of slow and fast spindles sources corresponds to those previously reported in high-density EEG studies (Del Felice et al., 2013, 2014). A strength of the current study is the use of a data-driven approach. Instead of *a priori* division of sleep spindles according to their topographical scalp distribution, the classification was only performed after the source reconstruction through LORETA. The aim was to avoid the pre-selection based on EEG activity.

Time Course of Sleep Spindle Sources

To describe the temporal dynamics of such detected generators across the night, we first computed the average LORETA images for the first four NREM sleep cycles and then for the separate intervals within each cycle.

The maximum value of CSD remained systematically located in BA10 (slow spindle source) and BA7 (fast spindle source) along successive NREM sleep cycles, showing topographical stability of the detected generators (**Figure 2**). However, a gradual decline of CSD in BA10 over consecutive NREM episodes was observed. This decline was paralleled by a concomitant slight increase of CSD in BA7, reaching its peak around the third cycle and then decreasing again (**Figure 3**). The results provided by LORETA showed great inter-individual variability (see SEs in **Figures 3**, **4**). Therefore, the possible absence of consistent pattern across subjects could make it difficult to generalize the observed findings.

Several evidences showed that while EEG power in slow spindle frequency range decreases over the night, an opposite trend is observed for higher frequency power (Tanaka et al., 1997; Cox et al., 2017). Similar results have also been reported for the amount (density) of slow and fast spindles across the night (Werth et al., 1996; Bódizs et al., 2009). Our results on active sources suggest an interesting resemblance with temporal dynamics exhibited by slow and fast spindles on scalp topography (spectral power, density).

The variations within cycles followed a "U" shaped curve for both spindle sources, with a trough around third and fourth interval (middle part) and the highest values at the beginning and the end of the time window investigated (**Figure 4**). As previously reported in EEG studies, such peculiar temporal pattern was also mirrored by EEG topography (Aeschbach et al., 1997; De Gennaro et al., 2000b; Himanen et al., 2002, 2003). The amount of sleep spindles and sigma activity power decreases with the deepening of sleep and increases closer to SO or REM transition (Silverstein and Levy, 1976; Guazzelli et al., 1986; Uchida et al., 1991, 1994; Purcell et al., 2017). In line with this evidence, numerous human and animal studies reported a negative temporal relationship between spindle activity and the low-frequency (0.5–4.0 Hz) and high-amplitude ($\geq$75 μV) slow wave activity (SWA), which are predominant during SWS. Intracellular recordings suggest that spindle and delta waves (1.0–4.0 Hz) are generated by a common thalamocortical mechanism and their differentiation depends on the degree of membrane hyperpolarization of thalamocortical neurons (Steriade et al., 1993; Andrillon et al., 2011).

Moreover, also sleep pressure-related courses of SWA and spindle-frequency activity are negative correlated (Borbély et al., 1981; Dijk et al., 1993; De Gennaro et al., 2000a; Finelli et al., 2001). However, the response to sleep deprivation across the spindle frequency range is not uniform. The reduction of spindle activity only affects high-frequency spindle (>13.0 Hz) (Knoblauch et al., 2002), possibly reflecting a different sensitivity to homeostatic processes for the two types of spindles.

Therefore, the mutual relationship between these two EEG activities could explain both the variations of slow/fast spindle sources between NREM cycles (homeostatic decrease of slow spindle) and in the course of a NREM episode (reduced spindle activity in mid-cycle). However, the lack of comparison analysis between scalp- and source-recorded activities makes this interpretation speculative.

Hashemi et al. (2019) recently examined the interrelationship between sleep-spindles activity and higher frequencies (∼25.0 Hz). In their model, the cortical high frequency activity and its interaction with thalamic oscillation at fast spindle are proposed as key mechanism for the generation of slow spindles. Investigating the relationship between spindle sources and other patterns of brain activity could help understand how the local pattern of spindle activity (e.g., fast vs. slow) emerges. However, an exhaustive description of spindles local features is not possible with LORETA algorithm, due to its limited potential for the identification and localization of multiple and concomitant cortical sources (Nir et al., 2011; Piantoni et al., 2017; Hagler et al., 2018). Moreover, LORETA does not take into account co-localized sources, possibly explaining the key role of modulation of cortical spontaneous activity in the genesis of spindle (Hashemi et al., 2019).

Despite the observed time-related variations, the statistical comparison between slow and fast spindle sources was not significant. The two kinds of spindles, even if distinct, still showed strong overlapping time courses within each NREM episode. This can be interpreted in terms of similar cortical innervation patterns, regardless of different subcortical thalamic generators (Ujma et al., 2019). As highlighted in previous studies (Anderer et al., 2001; Bersagliere et al., 2013; Del Felice et al., 2014), the frontal and parietal spindle sources were directly connected with specific thalamic nuclei, where the spindles are initiated. Subsequent regional variability may stem from local neuronal activity, as suggested by previous researches with intracranial recordings (Andrillon et al., 2011; Nir et al., 2011; Ujma et al., 2019).

The debate about the existence of one or two sleep spindle generators should be considered open. The exploration of the spatiotemporal dynamics of cortical spindle sources could provide new information on this issue. However, given the key role of subcortical sources (thalamus, hippocampus) in spindle generation (McCormick and Bal, 1997; Sarasso et al., 2014), the LORETA solution space restricted to the cortex may represent an important limitation.

CONCLUSION

Low resolution brain electromagnetic tomography combines the high time resolution of the EEG with a spatial accuracy in

source localization, providing a reliable proxy about the complex region- and time-specific patterns of sleep spindles. Thanks to this reliable technique, we confirmed the involvement of the frontal and parietal brain regions in spindle generation. Moreover, we showed for the first time their changes within and between consecutive NREM sleep episodes. Our findings substantially confirm the available observations at the scalp level. Additionally, we can remark the concept that EEG activity reflects the synchronous activation of multiple sources at cortical level. In this regard, an interesting future direction would be the simultaneous exploration of both cortical sources and the corresponding EEG topography, to better characterize the dynamics and nature of the two types of spindles.

DATA AVAILABILITY

The datasets generated for this study are available on request to the corresponding author.

ETHICS STATEMENT

All subjects provided written informed consent. The study was approved by the Institutional Ethics Committee of the Department of Psychology of "Sapienza" University of Rome and was conducted in accordance with the Declaration of Helsinki.

AUTHOR CONTRIBUTIONS

VA, AD'A, and LDG conceived and designed the work. VA, AD'A, MG, SS, and AM acquired and analyzed the data. VA, AD'A, MG, and LDG interpreted the data. VA, AD'A, LDG, and MF drafted the work and revised it critically for important intellectual content. VA, AD'A, MG, SS, AM, MF, and LDG approved the final version of the manuscript and agreed to be accountable for all aspects of the work in ensuring that questions related to accuracy or integrity of any part of the work are appropriately investigated and resolved.

REFERENCES

Aeschbach, D., and Borbély, A. A. (1993). All-night dynamics of the human sleep EEG. *J. Sleep Res.* 2, 70–81. doi: 10.1111/j.1365-2869.1993.tb00065.x

Aeschbach, D., Dijk, D. J., and Borbély, A. A. (1997). Dynamics of EEG spindle frequency activity during extended sleep in humans: relationship to slow-wave activity and time of day. *Brain Res.* 748, 131–136. doi: 10.1016/S0006-8993(96)01275-9

Anderer, P., Klösch, G., Gruber, G., Trenker, E., Pascual-Marqui, R. D., Zeitlhofer, J., et al. (2001). Low-resolution brain electromagnetic tomography revealed simultaneously active frontal and parietal sleep spindle sources in the human cortex. *Neuroscience* 103, 581–592. doi: 10.1016/S0306-4522(01)00028-8

Andrillon, T., Nir, Y., Staba, R. J., Ferrarelli, F., Cirelli, C., Tononi, G., et al. (2011). Sleep spindles in humans: insights from intracranial EEG and unit recordings. *J. Neurosci.* 31, 17821–17834. doi: 10.1523/JNEUROSCI.2604-11.2011

Bersagliere, A., Achermann, P., Lo Russo, G., Proserpio, P., and Nobili, L. (2013). Spindle frequency activity may provide lateralizing information in drug-resistant nocturnal mesial frontal lobe epilepsy: a pilot study on the contribution of sleep recordings. *Seizure* 22, 719–725. doi: 10.1016/j.seizure.2013.05.011

Bódizs, R., Körmendi, J., Rigó, P., and Lázár, A. S. (2009). The individual adjustment method of sleep spindle analysis: methodological improvements and roots in the fingerprint paradigm. *J. Neurosci. Methods* 178, 205–213. doi: 10.1016/j.jneumeth.2008.11.006

Borbély, A. A., Baumann, F., Brandeis, D., Strauch, I., and Lehmann, D. (1981). Sleep deprivation: effect on sleep stages and EEG power density in man. *Electroencephalogr. Clin. Neurophysiol.* 51, 483–493. doi: 10.1016/0013-4694(81)90225-x

Cox, R., Hofman, W. F., de Boer, M., and Talamini, L. M. (2014). Local sleep spindle modulations in relation to specific memory cues. *Neuroimage* 99, 103–110. doi: 10.1016/j.neuroimage.2014.05.028

Cox, R., Schapiro, A. C., Manoach, D. S., and Stickgold, R. (2017). Individual differences in frequency and topography of slow and fast sleep spindles. *Front. Hum. Neurosci.* 11:433. doi: 10.3389/fnhum.2017.00433

D'Atri, A., Novelli, L., Ferrara, M., Bruni, O., and De Gennaro, L. (2018). Different maturational changes of fast and slow sleep spindles in the first four years of life. *Sleep Med.* 42, 73–82. doi: 10.1016/j.sleep.2017.11.1138

De Gennaro, L., and Ferrara, M. (2003). Sleep spindles: an overview. *Sleep Med. Rev.* 7, 423–440. doi: 10.1053/smrv.2002.0252

De Gennaro, L., Ferrara, M., and Bertini, M. (2000a). Effect of slow-wave sleep deprivation on topographical distribution of spindles. *Behav. Brain Res.* 116, 55–59. doi: 10.1016/s0166-4328(00)00247-3

De Gennaro, L., Ferrara, M., and Bertini, M. (2000b). Topographical distribution of spindles: variations between and within nrem sleep cycles. *Sleep Res. Online?* 3, 155–160.

Del Felice, A., Arcaro, C., Storti, S. F., Fiaschi, A., and Manganotti, P. (2013). Slow spindles' cortical generators overlap with the epileptogenic zone in temporal epileptic patients: an electrical source imaging study. *Clin. Neurophysiol.* 124, 2336–2344. doi: 10.1016/j.clinph.2013.06.002

Del Felice, A., Del Arcaro, C., Storti, S. F., Fiaschi, A., and Manganotti, P. (2014). Electrical source imaging of sleep spindles. *Clin. EEG Neurosci.* 45, 184–192. doi: 10.1177/1550059413497716

Diekelmann, S., and Born, J. (2010). The memory function of sleep. *Nat. Rev. Neurosci.* 11:114. doi: 10.1038/nrn2762

Dijk, D.-J., Hayes, B., and Czeisler, C. A. (1993). Dynamics of electroencephalographic sleep spindles and slow wave activity in men: effect of sleep deprivation. *Brain Res.* 626, 190–199. doi: 10.1016/0006-8993(93)90579-c

Ferrarelli, F., Huber, R., Peterson, M. J., Massimini, M., Murphy, M., Riedner, B. A., et al. (2007). Reduced sleep spindle activity in schizophrenia patients. *Am. J. Psychiatry* 164, 483–492. doi: 10.1176/ajp.2007.164.3.483

Ferrarelli, F., Peterson, M. J., Sarasso, S., Riedner, B. A., Murphy, M. J., Benca, R. M., et al. (2010). Thalamic dysfunction in schizophrenia suggested by whole-night deficits in slow and fast spindles. *Am. J. Psychiatry* 167, 1339–1348. doi: 10.1176/appi.ajp.2010.09121731

Finelli, L. A., Borbély, A. A., and Achermann, P. (2001). Functional topography of the human nonREM sleep electroencephalogram. *Eur. J. Neurosci.* 13, 2282–2290. doi: 10.1046/j.0953-816x.2001.01597.x

Gorgoni, M., Lauri, G., Truglia, I., Cordone, S., Sarasso, S., Scarpelli, S., et al. (2016). Parietal fast sleep spindle density decrease in Alzheimer's disease and amnesic mild cognitive impairment. *Neural Plast.* 2016:8376108. doi: 10.1155/2016/8376108

Guazzelli, M., Feinberg, I., Aminoff, M., Fein, G., Floyd, T. C., and Maggini, C. (1986). Sleep spindles in normal elderly: comparison with young adult patterns and relation to nocturnal awakening, cognitive function and brain atrophy. *Electroencephalogr. Clin. Neurophysiol.* 63, 526–539. doi: 10.1016/0013-4694(86)90140-9

Hagler, D. J., Ulbert, I., Wittner, L., Erőss, L., Madsen, J. R., Devinsky, O., et al. (2018). Heterogeneous origins of human sleep spindles in different cortical layers. *J. Neurosci.* 38, 3013–3025. doi: 10.1523/JNEUROSCI.2241-17.2018

Hashemi, N. S., Dehnavi, F., Moghimi, S., and Ghorbani, M. (2019). Slow spindles are associated with cortical high frequency activity. *NeuroImage* 189, 71–84. doi: 10.1016/j.neuroimage.2019.01.012

Himanen, S. L., Virkkala, J., Huhtala, H., and Hasan, J. (2002). Spindle frequencies in sleep EEG show U-shape within first four NREM sleep episodes. *J. Sleep Res.* 11, 35–42. doi: 10.1046/j.1365-2869.2002.00273.x

Himanen, S. L., Virkkala, J., Huupponen, E., Niemi, J., and Hasan, J. (2003). Occurrence of periodic sleep spindles within and across non-REM sleep episodes. *Neuropsychobiology* 48, 209–216. doi: 10.1159/000074639

Knoblauch, V., Kräuchi, K., Renz, C., Wirz-Justice, A., and Cajochen, C. (2002). Homeostatic control of slow-wave and spindle frequency activity during human sleep: effect of differential sleep pressure and brain topography. *Cereb. Cortex* 12, 1092–1100. doi: 10.1093/cercor/12.10.1092

Ktonas, P. Y., and Ventouras, E.-C. (2014). Automated detection of sleep spindles in the scalp EEG and estimation of their intracranial current sources: comments on techniques and on related experimental and clinical studies. *Front. Hum. Neurosci.* 8:998. doi: 10.3389/fnhum.2014.00998

McCormick, D. A., and Bal, T. (1997). Sleep and arousal: thalamocortical mechanisms. *Annu. Rev. Neurosci.* 20, 185–215. doi: 10.1146/annurev.neuro.20.1.185

Mulert, C., Jäger, L., Schmitt, R., Bussfeld, P., Pogarell, O., Möller, H.-J., et al. (2004). Integration of fMRI and simultaneous EEG: towards a comprehensive understanding of localization and time-course of brain activity in target detection. *Neuroimage* 22, 83–94. doi: 10.1016/j.neuroimage.2003.10.051

Nir, Y., Staba, R. J., Andrillon, T., Vyazovskiy, V. V., Cirelli, C., Fried, I., et al. (2011). Regional slow waves and spindles in human sleep. *Neuron* 70, 153–169. doi: 10.1016/j.neuron.2011.02.043

Pascual-Marqui, R. D., Esslen, M., Kochi, K., and Lehmann, D. (2002). Functional imaging with low-resolution brain electromagnetic tomography (LORETA): a review. *Methods Find. Exp. Clin. Pharmacol.* 24(Suppl. C), 91–95.

Piantoni, G., Halgren, E., and Cash, S. S. (2017). Spatiotemporal characteristics of sleep spindles depend on cortical location. *Neuroimage* 146, 236–245. doi: 10.1016/j.neuroimage.2016.11.010

Plante, D. T., Goldstein, M. R., Cook, J. D., Smith, R., Riedner, B. A., Rumble, M. E., et al. (2015). Effects of oral temazepam on sleep spindles during non-rapid eye movement sleep: a high-density EEG investigation. *Eur. Neuropsychopharmacol.* 25, 1600–1610. doi: 10.1016/j.euroneuro.2015.06.005

Plante, D. T., Goldstein, M. R., Landsness, E. C., Peterson, M. J., Riedner, B. A., Ferrarelli, F., et al. (2013). Topographic and sex-related differences in sleep spindles in major depressive disorder: a high-density EEG investigation. *J. Affect. Disord.* 146, 120–125. doi: 10.1016/j.jad.2012.06.016

Purcell, S. M., Manoach, D. S., Demanuele, C., Cade, B. E., Mariani, S., Cox, R., et al. (2017). Characterizing sleep spindles in 11,630 individuals from the national sleep research resource. *Nat. Commun.* 8:15930. doi: 10.1038/ncomms15930

Rechtschaffen, A., and Kales, A. (1968). *A Manual of Standard Terminology: Techniques and Scoring System for Sleep Stages of Human Subjects*. Washington, DC: United States Government Printing Office.

Sarasso, S., Proserpio, P., Pigorini, A., Moroni, F., Ferrara, M., De Gennaro, L., et al. (2014). Hippocampal sleep spindles preceding neocortical sleep onset in humans. *Neuroimage* 86, 425–432. doi: 10.1016/j.neuroimage.2013.10.031

Schabus, M. D., Dang-Vu, T. T., Heib, D. P. J., Boly, M., Desseilles, M., Vandewalle, G., et al. (2012). The fate of incoming stimuli during NREM sleep is determined by spindles and the phase of the slow oscillation. *Front. Neurol.* 3:40. doi: 10.3389/fneur.2012.00040

Sela, Y., Vyazovskiy, V. V., Cirelli, C., Tononi, G., and Nir, Y. (2016). Responses in rat core auditory cortex are preserved during sleep spindle oscillations. *Sleep* 39, 1069–1082. doi: 10.5665/sleep.5758

Shih, J. J., Weisend, M. P., Davis, J. T., and Huang, M. (2000). Magnetoencephalographic characterization of sleep spindles in humans. *J. Clin. Neurophysiol.* 17, 224–231. doi: 10.1097/00004691-200003000-00011

Silverstein, L. D., and Levy, C. M. (1976). The stability of the sigma sleep spindle. *Electroencephalogr. Clin. Neurophysiol.* 40, 666–670. doi: 10.1016/0013-4694(76)90142-5

Steriade, M., and Llinás, R. R. (1988). The functional states of the thalamus and the associated neuronal interplay. *Physiol. Rev.* 68, 649–742. doi: 10.1152/physrev.1988.68.3.649

Steriade, M., McCormick, D. A., and Sejnowski, T. J. (1993). Thalamocortical oscillations in the sleeping and aroused brain. *Science* 262, 679–685. doi: 10.1126/science.8235588

Talairach, J., and Tournoux, P. (1988). *Co-Planar Stereotaxic Atlas of the Human Brain 3-Dimensional Proportional System: An Approach to Cerebral Imaging*. New York, NY: Thieme Medical Publishers, Inc.

Tanaka, H., Hayashi, M., and Hori, T. (1997). Topographical characteristics and principal component structure of the hypnagogic EEG. *Sleep* 20, 523–534. doi: 10.1093/sleep/20.7.523

Uchida, S., Atsumi, Y., and Kojima, T. (1994). Dynamic relationships between sleep spindles and delta waves during a NREM period. *Brain Res. Bull.* 33, 351–355. doi: 10.1016/0361-9230(94)90205-4

Uchida, S., Maloney, T., March, J. D., Azari, R., and Feinberg, I. (1991). Sigma (12–15 Hz) and delta (0.3–3 Hz) EEG oscillate reciprocally within NREM sleep. *Brain Res. Bull.* 27, 93–96. doi: 10.1016/0361-9230(91)90286-s

Ujma, P. P., Hajnal, B., Bodizs, R., Gombos, F., Eross, L., Wittner, L., et al. (2019). The laminar profile of sleep spindles in humans. *bioRxiv*

Urakami, Y. (2008). Relationships between sleep spindles and activities of cerebral cortex as determined by simultaneous EEG and MEG recording. *J. Clin. Neurophysiol.* 25, 13–24. doi: 10.1097/wnp.0b013e318162a8a4

Ventouras, E. M., Ktonas, P. Y., Tsekou, H., Paparrigopoulos, T., Kalatzis, I., and Soldatos, C. R. (2010). Independent component analysis for source localization of EEG sleep spindle components. *Comput. Intell. Neurosci.* 2010:329436. doi: 10.1155/2010/329436

Vitacco, D., Brandeis, D., Pascual-Marqui, R., and Martin, E. (2002). Correspondence of event-related potential tomography and functional magnetic resonance imaging during language processing. *Hum. Brain Mapp.* 17, 4–12. doi: 10.1002/hbm.10038

Wei, H. G., Riel, E., Czeisler, C. A., and Dijk, D.-J. (1999). Attenuated amplitude of circadian and sleep-dependent modulation of electroencephalographic sleep spindle characteristics in elderly human subjects. *Neurosci. Lett.* 260, 29–32. doi: 10.1016/s0304-3940(98)00851-9

Werth, E., Achermann, P., Dijk, D. J., and Borbely, A. A. (1996). Topographic distribution of spindle frequency activity in the sleep EEG. *J. Sleep Res.* 5(Suppl.):252.

Zeitlhofer, J., Gruber, G., Anderer, P., Asenbaum, S., Schimicek, P., and Saletu, B. (1997). Topographic distribution of sleep spindles in young healthy subjects. *J. Sleep Res.* 6, 149–155. doi: 10.1046/j.1365-2869.1997.00046.x

Zumsteg, D., Lozano, A. M., and Wennberg, R. A. (2006). Depth electrode recorded cerebral responses with deep brain stimulation of the anterior thalamus for epilepsy. *Clin. Neurophysiol.* 117, 1602–1609. doi: 10.1016/j.clinph.2006.04.008

Conflict of Interest Statement: The authors declare that the research was conducted in the absence of any commercial or financial relationships that could be construed as a potential conflict of interest.

Copyright © 2019 Alfonsi, D'Atri, Gorgoni, Scarpelli, Mangiaruga, Ferrara and De Gennaro. This is an open-access article distributed under the terms of the Creative Commons Attribution License (CC BY). The use, distribution or reproduction in other forums is permitted, provided the original author(s) and the copyright owner(s) are credited and that the original publication in this journal is cited, in accordance with accepted academic practice. No use, distribution or reproduction is permitted which does not comply with these terms.

frontiers in Neuroscience

ORIGINAL RESEARCH
published: 07 August 2019
doi: 10.3389/fnins.2019.00814

The Emergence of Spindles and K-Complexes and the Role of the Dorsal Caudal Part of the Anterior Cingulate as the Generator of K-Complexes

Andreas A. Ioannides[1], Lichan Liu[1] and George K. Kostopoulos[2]*

[1] Laboratory for Human Brain Dynamics, AAI Scientific Cultural Services Ltd., Nicosia, Cyprus, [2] Neurophysiology Unit, Department of Physiology, School of Medicine, University of Patras, Patras, Greece

The large multicomponent K-complex (KC) and the rhythmic spindle are the hallmarks of non-rapid eye movement (NREM)-2 sleep stage. We studied with magnetoencephalography (MEG) the progress of light sleep (NREM-1 and NREM-2) and emergence of KCs and spindles. Seven periods of interest (POI) were analyzed: wakefulness, the two quiet "core" periods of light sleep (periods free from any prominent phasic or oscillatory events) and four periods before and during spindles and KCs. For each POI, eight 2-s (1250 time slices) segments were used. We employed magnetic field tomography (MFT) to extract an independent tomographic estimate of brain activity from each MEG data sample. The spectral power was then computed for each voxel in the brain for each segment of each POI. The sets of eight maps from two POIs were contrasted using a voxel-by-voxel *t*-test. Only increased spectral power was identified in the four key contrasts between POIs before and during spindles and KCs versus the NREM2 core. Common increases were identified for all four subjects, especially within and close to the anterior cingulate cortex (ACC). These common increases were widespread for low frequencies, while for higher frequencies they were focal, confined to specific brain areas. For the pre-KC POI, only one prominent increase was identified, confined to the theta/alpha bands in a small area in the dorsal caudal part of ACC (dcACC). During KCs, the activity in this area grows in intensity and extent (in space and frequency), filling the space between the areas that expanded their low frequency activity (in the delta band) during NREM2 compared to NREM1. Our main finding is that prominent spectral power increases before NREM2 graphoelements are confined to the dcACC, and only for KCs, sharing common features with changes of activity in dcACC of the well-studied error related negativity (ERN). ERN is seen in awake state, in perceptual conflict and situations where there is a difference between expected and actual environmental or internal events. These results suggest that a KC is the sleep side of the awake state ERN, both serving their putative sentinel roles in the frame of the saliency network.

Keywords: sleep, K-complexes, spindles, magnetoencephalography, magnetic field tomography, error related negativity

OPEN ACCESS

Edited by:
Giulio Bernardi,
IMT School for Advanced Studies Lucca, Italy

Reviewed by:
Raphael Vallat,
University of California, Berkeley, United States
Danilo Menicucci,
University of Pisa, Italy

****Correspondence:***
Andreas A. Ioannides
a.ioannides@aaiscs.com

Specialty section:
This article was submitted to Sleep and Circadian Rhythms, a section of the journal Frontiers in Neuroscience

Received: *30 April 2019*
Accepted: *22 July 2019*
Published: *07 August 2019*

Citation:
Ioannides AA, Liu L and Kostopoulos GK (2019) The Emergence of Spindles and K-Complexes and the Role of the Dorsal Caudal Part of the Anterior Cingulate as the Generator of K-Complexes. Front. Neurosci. 13:814. doi: 10.3389/fnins.2019.00814

INTRODUCTION

Decades of research have established a resilient sleep architecture, fairly reproducible electrophysiological features characterizing the sleep stages and impressive links between sleep macro- and microstructure with very important brain and body functions. Yet, key features of the brain mechanisms dictating these reproducible processes still escape our understanding (Kryger et al., 2017). Here, we focus on two of the most prominent of features of sleep microarchitecture, primarily on the K-complex (KC) and to a lesser degree on spindles. Eight decades after its first description (Loomis et al., 1938), the KC continues to attract the attention of researchers (de Gennaro et al., 2000; Colrain, 2005; Halász, 2005, 2016), because KC appears to be involved in significant sleep functions and several intriguing questions arose in the efforts to understand its underlying mechanisms (Loomis et al., 1938; Roth et al., 1956; Bastien and Campbell, 1992; Amzica and Steriade, 2002; Colrain, 2005; Halász, 2005; Wennberg, 2010; Jahnke et al., 2012).

The KC is a multicomponent event. The main and characterizing component is a large abrupt onset negativity in the electroencephalogram (EEG) (>0.5 s and up to 0.3 mV), often followed by a longer lasting positivity, while a shorter positivity preceding the negative wave may not always be discernible by eye (Cote et al., 2000; Colrain, 2005; Rodenbeck et al., 2006). Interpretation of some of these waves is easier in the case of sensory evoked KCs: Laurino et al. (2014) identify three peaks, or waves distinguished best by their latency (in msec): an early short positive P200, a large negative N550 and a late and longer lasting positive P900. The evoked P200 appears to be a specific sensory response acting as a traveling cortical excitation inducing the bistable cortical response (P550/900) response. A KC is often preceded and is usually followed by spindles (Kokkinos and Kostopoulos, 2011). Furthermore, the KC is a large physiological EEG event with widespread brain topography, its power maximizing frontally, which, along with spindles, characterizes NREM2 stage of sleep (Colrain, 2005). It often emerges at times of brain instability and it is considered both reactive, since it can non-specifically follow sensory responses to various stimuli, but also promote sleep, since it is fairly generalized.

The great practical value of KC is its use to unequivocally mark sleep onset, along with spindles, a demand for all quantitative studies of sleep in health and disease. Beyond that, several important roles for KCs in brain functions have been proposed by both animal experiments (Amzica and Steriade, 2002; Marini et al., 2004; Ji and Wilson, 2007; Cruz-Aguilar et al., 2015) and human brain metabolism (Larson-Prior et al., 2009; Maquet, 2010; Caporro et al., 2012; Jahnke et al., 2012) and EEG/MEG electrophysiological studies (Lu et al., 1992; Numminen et al., 1996; Yoshida et al., 1996; Murphy et al., 2009; Wennberg and Cheyne, 2013; Ioannides et al., 2017). One of these roles of KC is a sentinel role protecting sleep by preventing waking to normal stimuli, which do not present a danger (Jahnke et al., 2012; Halász, 2016). Another suggested function of KCs is to aid the homeostasis of synaptic activation and some stages of memory replay and consolidation (Tononi and Cirelli, 2006; Ji and Wilson, 2007; Johnson et al., 2010; Staresina et al., 2015; Kryger et al., 2017). Through all such "housekeeping" of brain synapses, KCs may pave the way for the uptake of new information after wake-up. Finally, substantial deviations of KC density have been documented in association to aging (Kubicki et al., 1989), epilepsy (Halasz, 1981; Steriade and Amzica, 1998; Geyer et al., 2006; El Helou et al., 2008; Seneviratne et al., 2016), Alzheimer's disease (De Gennaro et al., 2001, 2017) and schizophrenia (Ramakrishnan et al., 2012).

We reported about a decade ago how the progression of sleep stages can be studied in terms of changes in the brain's background activity (quiet "core" periods, free from any prominent phasic or oscillatory EEG or MEG events), especially in the gamma band (Ioannides et al., 2009). More recently we focused on gradual changes upon sleep onset and as sleep progresses through stage non-rapid eye movement (NREM)-1 and NREM-2 as well as before and during spindles and KCs. **Figure 4** of our previous work (Ioannides et al., 2017) shows in one view the large changes in the activity of midline sagittal areas of the brain throughout light sleep. First during "core" periods of light sleep (relative to the activity before sleep), and the smaller changes before and during the large graphoelements of NREM2. With sleep onset fairly widespread increase in low frequency spectral power is identified in NREM1 core periods that extend wider in NREM2 core periods. When the NREM2 core period was contrasted directly with NREM1 core period, modest increases were identified in the alpha and sigma bands in three frontal areas; the area just in front of the genu of the anterior cingulate cortex (ACC), which is often referred to in the literature as rostral ACC (rACC), showed most clearly. The comparison between the periods before spindles with the NREM2 core periods show focal increases in the rACC in the delta band. We have interpreted this sequence of changes, especially in rACC, as a sign of extreme precautions before spindles proceed with their putative memory consolidation task (Ioannides et al., 2017). The apparent precautions before memory consolidation may be important, because memory consolidation during sleep may involve changes in the neural representation of self that is represented by the two midline areas found to consistently increase their gamma band spectral power from awake state to light, deep and finally REM sleep (Ioannides et al., 2009). This midline self-representation core (MSRC) consists of two distinct brain areas; the first, MSRC1, is on the dorsal medial prefrontal cortex and the second, MSRC2, is in the precuneus in the midline posterior parietal cortex (Ioannides, 2018).

The results reported in our earlier work (Ioannides et al., 2017), emphasized spindles because the main motivation was to provide a framework for understanding the role of sleep in learning (Ioannides, 2017) and the neural representation of self (Ioannides, 2018). The sequence of changes from awake state to NREM1 and NREM2 and in particular during the periods before spindles were consistent with preparatory steps designed to ensure accurate and uncorrupted memory consolidation during spindles that related to changes in the neural representation of self. In the earlier work (Ioannides et al., 2017), changes were identified before spindles that seemed to serve a sentinel role, a role better served by the KCs, the question why there is a need

for two sentinel operations, with similar, yet distinct patterns of activations before spindles and KCs was nor addressed. Another key unresolved question of the 2017 paper was how the patterns of activation differentiate before spindles and KCs and in particular whether one or more areas could be seen to play a key role in the generation of KCs. To address these questions, we proceeded in this work using the same methods as the ones used in Ioannides et al. (2017), but analyzed at finer detail the more caudal and dorsal areas to the ones we emphasized in Ioannides et al. (2017). These areas are in the pre-motor cortex and its immediately ventral anterior cingulate cortex (ACC). These areas were not emphasized in the (Ioannides et al., 2017) study because they were swamped by the extensive changes over a wider area during KCs and the KC changes were not central to the discussion. In the current study the results are presented over the frequency ranges from 3.2 to 16 Hz and separately for the periods before and during spindles and KCs for the key areas in the medial frontal cortex identified from the new current analysis and the earlier studies (Ioannides et al., 2009, 2017; Ioannides, 2018). The new analysis anchors the description to the spectral changes before and during spindles and KCs in four nearby areas: the two subdivisions of the premotor cortex and the two areas directly ventral to them on the dorsal caudal ACC (dcACC) that we will refer to as dcACC1 and dcACC2.

Here we will focus on the changes before and to a lesser extend during KCs. Just like in our previous study we find that the controlling role is played by a set of areas in the ACC, and in the overlying ventral premotor areas. We will develop our description around the spectral changes before and during spindles and KCs in two nearby areas on the border of dorsal caudal ACC (dcACC) that we will refer to as dcACC1 and dcACC2 and the ventral premotor areas directly above them. The first area, dcACC1, seems to be involved in the generation of KCs. The second area, dcACC2, is the area of common increase in delta power before spindles and KCs. Our results provide a hint on how the uncertainties in our current understanding of KCs might be resolved and support our earlier results (Ioannides et al., 2017) and the results from other recent studies, claiming that KC-related activity is more prominently identified in frontal cortical areas (Colrain, 2005; Halász, 2005) along the cingulate gyrus. Critically, our results are in full agreement with the first demonstration of focal stimulation, while awake, of a specific cortical area, which seems to correspond to our dcACC1, evoking activity resembling KCs (Voysey et al., 2015). Our results, when seen in the context of numerous other studies of sleep and awake state, suggest that similar mechanisms and networks with key hubs in the ACC deal with pain, saliency detection and environmental monitoring during both sleep and awake states. This supports the suggestion made in our earlier study (Ioannides et al., 2017): the mechanisms that operate in sleep are similar and involve the same networks serving similar roles in awake state. As a consequence, our results are relevant not only for KCs and sleep, but also for fundamental questions about the role of ACC in awake state. We will comment in the Discussion session on how our results may contribute to the current debate about the way emotion, pain and cognitive control are processed in the ACC (Shackman et al., 2011; Jahn et al., 2016).

Our tomographic analysis allows the generators to be throughout the brain. In our description of the results we have focused more on structures close to a midline sagittal section, motivated partly by our own results, earlier studies (Ioannides et al., 2009, 2017) and by the results of the current study that also show distinctive changes on the medial walls of the two hemispheres. It was also motivated by the findings of many past studies reviewed and meta-analyzed in relation to movement and cognition that relate findings about activity patterns close to the medial walls of the two hemispheres both in primates and in human neuroimaging (Picard and Strick, 1996, 2001), related to conflict processing of both cognitive and emotional type (Bush et al., 2000), self-monitoring (Dehaene, 2018), negative affect, pain and cognitive control (Shackman et al., 2011; Jahn et al., 2016). All these studies show distinctive changes on the medial walls of the two hemispheres and this is where we focus the presentation of results. We also show enough of the results along coronal and axial cuts through the identified areas to convey to the reader the full richness of the results, the laterality and which activations are focal and which are extended.

MATERIALS AND METHODS

Background of the MEG Studies

The experiment demanded a number of innovations to make possible, for the first and to the best of our knowledge still the only, set of whole night measurements in the MEG environment. Some details are provided in Ioannides et al. (2004) and its supplementary data and further details in Ioannides et al. (2017). Briefly, to achieve whole night MEG measurements at the time of the experiment (2000), new elements had to be introduced in the hardware of MEG, the data storage capability, the supine arrangement of the recordings and the ease of connecting and disconnecting the subject from the recording system if needed (e.g., to use the toilet in the middle of the night). The last modifications also demanded re-checking/calibrating after the subject returned for the continuation of the recordings. To ensure that all the changes worked well individually and with good synergy the final test was performed "from the inside" by one of us (AAI), who was not a good sleeper so these tests were usually performed after an overseas travel so that AAI was sleep deprived and therefore easier to sleep. On two occasions AAI stopped the recordings early and asked for modifications. On the third occasion (about a year after the start of the preparations for the sleep experiment) AAI slept for the entire night and gave the OK for the experiments to go ahead.

Subjects

The experiment was conducted in RIKEN with RIKEN's ethics committee approval. Before the experiment, all the subjects gave their informed written consent after all procedures were explained to them. Candidate subjects were carefully screened with selection criteria that included regular sleep habits, male, right handed (Annett, 1967) and free of neuropsychiatric illness and all medication. After the set up was ready for recordings and over a period of about a year, the six subjects who passed

TABLE 1 | Subject age at the time of the experiment and number of events (KCm = multiple KC).

Subject #	Age at the time of experiment	Core conditions (control)			EEG graphoelements for NREM2		
		ECW	NREM1	NREM2	Spindles	KC1	KCm
(1)	25	8	8	21	12	8	23
(2)	30	9	11	16	10	10	15
(3)	31	8	10	11	9	11	14
(4)	49	8	9	26	8	9	11

all selection criteria were invited to the lab and performed the planned procedures for the whole night sleep MEG experiments. The first night began with training and placement of auxiliary channels before the subject underwent the sleep acclimatization sleeping on a replica of the MEG bed and with his head inside a replica of the MEG helmet. The next morning the subject was waken up (after 8 h sleep if he had not already waken up) and after debriefing was released and worked as usual with the instruction to stay awake throughout the day. The subject returned to the laboratory after work, had an evening meal and was prepared for the recordings of the main MEG sleep experiment. The data from all seven subjects were scored offline by two sleep experts (six subjects selected and AAI who also satisfied the criteria except for the one for good sleep habits and the fact that he was sleep deprived at the time of the experiment). The two independent scores were compared, a common one agreed and the night hypnogram constructed. For each sleep stage, segments were identified with acceptable signal: free of noise segments, artifacts and good quality signal for MEG, EEG and all auxiliary channels and no indication for head localization coil movement, with head movement below 5 mm between successive head localizations measurements (obtained every 3 min). These conditions were satisfied for three of the six subjects and AAI. The data from these four subjects were prepared for the detailed tomographic analysis. **Table 1** lists for each of the four subjects the age at the time of the experiment and the number of core POIs and good spindles and KCs identified (age 25, 30, 31, and 49).

Data Acquisition and Processing

The MEG was recorded throughout the night using a 151 gradiometer whole-head system (CTF/VSM Omega System, Canada) at a sampling rate of 625 Hz and low pass filter at 208 Hz. The following auxiliary channels were recorded in synchrony with the MEG: scalp EEG from C3 and C4 locations referenced to A2 and A1, respectively, vertical and horizontal EOG and electromyogram (EMG) from the chin. The EEG and EMG channels were pre-processed independently of the MEG using filters appropriate for sleep scoring and/or event identification. Commonly used procedures were employed to score the sleep stages (Rechtschaffen and Kales, 1968). For details on sleep stage scoring and identification of core periods see Ioannides et al. (2004). The data were pre-processed and analyzed in the same way as reported in Ioannides et al. (2017), so only a brief summary of the main points will be given below, with more details provided at the end (see section "Biases in the Presentation and Interpretation of the Results") outlining the logic for the selection of the results to best convey the key findings of the analysis in the context of voluminous related work in a wide range of a fields.

Spindles and single KCs were selected from within segments with clear NREM2 assignment. All periods of interest (POI) were selected by visual inspection of raw MEG data with POIs related to KCs and spindles selected well away from each other, from other graphoelements and noisy or undefined segments like transitions between sleep stages. The 2-s long "before" KC POIs was set for the 2 s segment ending about a 100 ms before the start of KC with no spindle or other large graphoelements within its duration or the 2 s before. The "during" KC POIs were defined as the 2 s beginning a few tens of milliseconds before the KC onset. Typically 8 to 20 KCs and spindles were selected for each subject from the whole night data. Finally, the best 8 (in terms of noise and absence of large amplitude EEGs (other than the KC) were selected for tomographic analysis. The results to be presented here use seven POIs in total: the quiet "core" periods of eyes closed waking (ECW), NREM-1 and NREM-2 and the periods before and during spindles, and the periods before and during KCs. We note that visual inspection alone would not distinguish POIs for NREM2 core periods from NREM2 POIs before spindle and before KCs. The only distinction between them is that the NREM2 core periods are well away, typically (a lot more than) 2 s, from spindles and KCs and any other large graphoelements (e.g., movement artifacts or micro-arousals). The choice of 2 s for the POI "during a KC" and "during spindles" was based on two considerations:

(a) the minimal duration to cover all EEG events. The duration of a KC starting from the initial positive peak and including the late positivity is 0.5−1 or more seconds (Colrain, 2005). Similarly for the POIs for the period "during spindles." A spindle usually lasts for 0.5 to 1.5 s. Therefore 2 s would suffice for either of the events.
(b) the minimal time needed for an accurate power spectral analysis of signals as slow as 1 Hz; while remaining within relevant time limits.

For the rest POIs "before KC," "before spindles," and the core POIs a duration of 2 s was demanded for having the appropriate control for the comparison. The 2 s are also reasonable to capture a generator that precedes the large graphoelements, as recently demonstrated for alpha band activity (Feige et al., 2005): when the alpha component amplitude [extracted from independent component analysis (ICA)] was used as a regressor of the fMRI bold signal time course only signal decreases were found when the standard hemodynamic response function was assumed (with

time delay of about 6 s). The alpha regressor revealed significant positive thalamic and mesencephalic correlations with a mean time delay of 2.5 s. This would be consistent with the true generator of alpha in the thalamus to precede the actual cortical alpha by a few seconds.

In our analysis we treat the core periods, i.e., a quiet periods with no graphoelements, as the foundation of each sleep stage. Conceptually, a core stay plays a role in our analysis, similar to that played by the ground state of a physical system in physics, i.e., a state of a system with the lowest possible energy. Typical examples are the ground state of atoms and nuclei. The core states of different sleep stages are distinct just like the ground states of different atoms are distinct. Specifically, the NREM2 core state is seen as the ground state from which POIs before spindles and before KCs can be "excited." The fact that only increases in spectral power are encountered in the transitions from NREM2 core POI to either the POI before spindles or POIs before KCs adds more credence to the analogy of core states with ground states of atoms. The POIs during KCs are more extreme (energetic) events that are far removed from the core state and hence able to reach a wider range of excited states, something that fits well with the higher amplitude and more widespread increases identified during KCs.

Source Reconstruction

Source analysis of MEG signals for each trial was performed using magnetic field tomography (MFT) (Ioannides et al., 1990; Taylor et al., 1999). For each subject the MFT analysis is performed using a source space fitted to the exact anatomical geometry (extracted from the MRI of the subject). The MFT input is the set of values for the available MEG channels at a single latency (relative to the onset of the stimulus or other time-marked event). These values may be taken from a single trial or from the ensemble average of a set of trials. The MFT output is a three-dimensional distribution of the current density vector field in the source space (i.e., the region of space where active sources can exist) and it is computed completely independently for each time sample of data. For each time sample of each single trial, the continuous estimate of the current density vector is sampled and stored at regular intervals, spaced about 8 mm across and refer to for simplicity hereafter as voxels. The MFT basic algorithm and the mathematical foundation of MFT is described in Ioannides et al. (1990, 2004), Taylor et al. (1999), Poghosyan and Ioannides (2008). Reviews of the MFT analysis and post-MFT statistical and connectivity analysis have been presented in Ioannides (2006, 2007). The majority of MFT studies until about 2010 were devoted in the analysis of MEG data obtained from well controlled stimuli and in particular visual stimuli placed in the quadrants of the visual field so the first entry to the cortical system could be clearly identified and compared to the expected part of the primary visual cortex (Tzelepi et al., 2001). This approach allowed nearly identical experiments to be performed on the same subjects in separate sessions with fMRI and MEG. In this way and using the fMRI localization as a gold standard, it was demonstrated that MFT could localize the activity with millisecond temporal resolution with accuracy of 3 to 5 mm (Moradi et al., 2003), which was as good as the accuracy of the location of the MEG sensors relative to the head, measured by the coregistration of the subject's head in the MEG helmet and the anatomical MRI image of the subject's brain.

The time domain analysis relies on the presence of a time-locking mechanism, usually provided by the onset of a stimulus, to align similar POIs with (sub-)millisecond accuracy. For the analysis of continuous data, e.g., resting state or sleep there is no such time-locking mechanism. For such cases we have first stayed with the time domain analysis and analyzed filtered data within a specific band (ensuring that 2−3 oscillations were present each time) (Ioannides et al., 2009) or carried out the statistical comparisons after the spectral power was computed for each voxel from the time-domain time series. In the second method of analysis frequency bands are used instead of time periods: a sliding window of frequencies (typically frequency band width of 3.2 Hz) is used to compare conditions or search for linked activity. We adopt here this second form of analysis, following exactly the same steps as described in detail in **Figure 1** of Ioannides et al. (2017). The first stage of the analysis maintains the extraction of single trial, sample-by-sample tomographic estimates of activity, as it is done for evoked responses. Then we allow for the uncontrolled blurring in time by transforming each regional time course in the frequency domain using long (duration of 2 s) segments. The outcome of the transformation of the tomographic analysis in the frequency domain shows the spatial distribution of spectral power within a band of frequencies. The statistical comparisons are obtained from the MFT solutions by contrasting spectral power within a 3.2 Hz windows for the two POIs to be compared. The center of this window is initially placed at 3.2 Hz. The center of the window is then shifted by 1.6 Hz and an independent statistical comparison is performed for each new window. The width of 3.2 Hz is about the same as the width of frequency bands below 16 Hz and by stepping every 1.6 Hz we can look separately at the low and high parts of each of these frequency bands. In this way the sliding window center is from 3.2 to 94.4 Hz to cover the frequency range from 1.6 to 96 Hz (**Table 2**).

The EEG frequency band division has been arbitrarily chosen (Buzsaki, 2006), limited by available recording technology, often lacking consensus especially when comparing records at different developmental stage, vigilance state and species recorded. Therefore, in order to have a more complete view of developments in the frequency domain, we adopt a moderate resolution in frequency that can be referred easily to the (not so) standard traditional bands but it has a somewhat finer resolution and an absolute quantitative basis, as described in the previous paragraph. This slightly more detailed and extended range describes well traditional and transitional frequency bands (**Table 2**) and allows us to relate the new results with those of our earlier analysis (Ioannides et al., 2017). The emphasis is on the low frequencies below the beta range, with only one example of changes in higher (gamma) band. This was necessary to keep the size of the manuscript to reasonable length. The activations below the beta band deserve to be grouped together, while separate studies are needed to do justice to the beta and gamma bands. The single

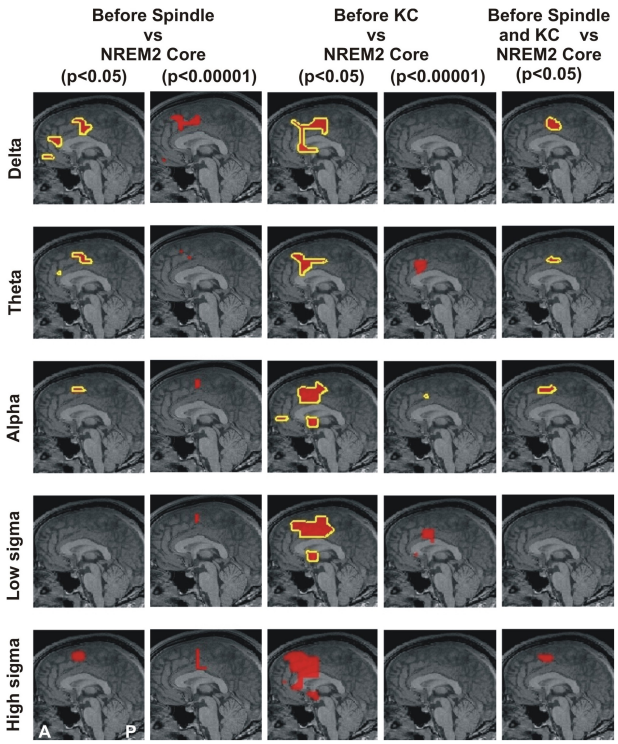

FIGURE 1 | MEG derived tomographic estimates of increases in spectral power before spindles and KC compared to that during the NREM2 core periods. The increases are displayed if they are within 2 mm (on either side) of the displayed midline sagittal cut (Talairach coordinate x = 0). To link the information central to this paper with that presented in Figure 4 of Ioannides et al. (2017), the figure is arranged in the same general way, with each row representing the same frequency band and each column showing the results for a specific combination of POI comparison and statistical significance. The yellow outline denotes common increase in all four subjects. We also display as a the red blob without yellow outline increases in 3 out of 4 subjects in the given comparison and statistical significance, provided there is no other increase with 4/4 subjects anywhere in the brain. The following contrasts are shown: columns 1 and 2 show increases before spindles versus NREM2 control at $p < 0.05$ and $p < 0.00001$; Columns 3 and 4 show increases before KCs versus NREM2 control at $p < 0.05$ and $p < 0.00001$, respectively. Column 5 shows the area with modest increase ($p < 0.05$) identified in separate statistical comparisons from non-overlapping POIs for the periods before spindles and before KCs. The same five frequency bands, as defined in **Table 2**, were used as in Figure 4 of Ioannides et al. (2017): delta (3.2 Hz), theta (6.4 Hz), alpha (9.6 Hz), low sigma (11.2 Hz), and high sigma (14.4 Hz).

result in the gamma band is included to demonstrate the presence of significant changes in activity in the high gamma band and show the distinct pattern of changes (in terms of statistical significance) in the low (below beta) and high (above beta) frequencies.

Common Spectral Statistical Parametric Mapping (sSPM)

We will present results for changes that were identified with the same sign (increases or decreases) and satisfying the *p*-value statistical threshold for each one of the four subjects. All our *p*-values are corrected by the conservative Bonferroni correction

TABLE 2 | Definition of various frequency bands and sub-bands used in this paper.

Frequency band name	Center in Hz	Range in Hz
Delta	3.2	1.6–4.8
Transition delta/theta	4.8	3.2–6.4
Theta	6.4	4.8–8
Transition theta/alpha	8	6.4–9.6
Alpha	9.6	8–11.2
Low sigma	11.2	9.8–12.8
High sigma	14.4	12.8–16
Sub-band of High gamma	57.6	56–59.2

for multiple voxel comparisons. No additional correction was made later because the conservative nature of the Bonferroni correction for the 1,000 or so voxels would have more than compensated for the few frequency bands used in the analysis. The spectral statistical maps of each subject were transformed to MNI template so that they could be combined across subjects and thus identify common changes in brain activity at predefined statistical thresholds. A new *t*-value was assigned in this common space by smoothing the original *t*-values within a sphere of radius 12 mm using a Wood Saxon kernel of radius 7 and decay constant 4 mm. This operation had two effects. First it allowed for possible errors in localization (which through segment selection from periods of very small head movement should be small, within a few millimeters), individual differences in anatomy, and inherent inaccuracy of transformation into a common space. Second it smoothed and further reduced the value of the *t*-test around the peak voxels, thus ensuring that high *t*-values in the common space had also a reasonable extend. The same two threshold levels of significance were used, as the ones used in the 2017 study (Ioannides et al., 2017): the lower significance threshold is set to $p < 0.05$ and corresponding changes will be referred to as "modest." The second threshold is set at a much higher level of significance of $p < 0.00001$ and is correspondingly referred to as "prominent." The grand sSPM results were finally computed, separately for each comparison between two POIs or conditions by counting for each voxel the number of subjects that showed increase or decrease of activity at a pre-defined threshold of *p*-value (always after Bonferroni correction for multiple voxel comparisons).

Automatic identification of contours of similar significance in the sSPMs are naturally blurred by the accuracy of the reconstructions, possible head movement, and particularly the operations for combination across subjects. The smoothing of solutions combines also with the tendency of the plotting routines to smooth over the source space points at which the sSPMs are computed. Nevertheless the shape of the contour is indicative of what the areas might be. When a single area passes the threshold then the contour is a tight spherical shape around the correct brain area. If two areas next to each other pass the threshold then a cylindrical shape will be extracted with the cylinder's symmetry axis along the line joining the two nearby areas. For example if the supplementary motor area (SMA) and pre-SMA are both identified in the sSPMs then the automatic contour computation

will produce a cylindrical solution containing both SMA and pre-SMA, while if SMA and dcACC2 are simultaneously satisfying the threshold set for the sSPMs the contour will have again a cylindrical shape but with the symmetry axis in the ventral-dorsal direction. If all three areas pass the statistical threshold and their (nearby) centers form a right angle then a right angle wedge will result (as we will see in some of our examples in the Results section. By exploring the sSPMs at different frequencies and at different statistical thresholds it then becomes possible to disentangle focal contributions from ROIs because the different areas have a different spectral behavior. Following this analysis we have identified seven key areas, four identified in this study, one in the 2018 study and two others identified in the 2017 study and again showing prominently in the new more detailed analysis.

The resulting grand sSPM results in the MNI space were then back-transformed to the anatomical space of one subject so they could be displayed in the background of that subject's MRI. As a general rule, we will show results when the set statistical threshold ($p < 0.05$ or $p < 0.00001$) is satisfied by each one of the four subjects. In only one case (in **Figure 1**) we have adapted the presentation to show additional cases where the set statistical threshold is satisfied for 3 of the four subjects, provided there was no higher, i.e., 4/4 case anywhere else in the brain. Comparison at different statistical threshold has a specific interpretation in the case of tomographic solutions obtained with our analysis of MEG data. In the time domain increasing the threshold allows us to see events over finer time scales, e.g., to identify the first entry in V1 (Poghosyan and Ioannides, 2008). In the frequency domain identifying a change within a specific frequency band limits the options for neurophysiological interpretation (although details of the mechanisms can only be identified by different experiments).

In summary, we followed the same procedures for analysis and reporting the results so that the new results can be compared and seen in the context of our previous work (Ioannides et al., 2017), with only one exception. In the earlier work, we used the Talairach space as the common template to combine the data across subjects, while in this work we used the MNI space. The data in both works were back-transformed to the MRI of the same subject. This small difference allows a direct comparison whenever results from the same POI contrast and at the same statistical threshold are used. This comparison provides a measure of the distortions that transformation to a common space might introduce, in combination with the other operations (smoothing, interpolations etc.) for the second level (across subjects) statistics.

Biases in the Presentation and Interpretation of the Results

We state from the outset that it is not possible to identify the mechanisms underlying activity in the delta band or fully define any particular EEG event on the basis of spectral power of background (core) activity alone (Amzica and Steriade, 1998). It is also true that the mechanisms underlying delta waves are still a matter of debate, i.e., regarding their emergence from thalamocortical or cortico-cortical circuits (Steriade and Amzica, 1998) and their characterization as type I or type II (Bernardi et al., 2018). The present MEG tomographic study can offer little help in understanding electrophysiological neuronal mechanisms beyond directing attention to particular brain areas with pivotal role in the circuits producing the examined EEG events. However, in an effort to provide a consistent framework to interpret the observed spectral power changes in terms of putative brain functions we considered local power in the delta band (in the sense of slow, 1−4 Hz) as reflecting hyperpolarizing potentials of neurons in the particular area (due to synaptic action, disfacilitation or any other effect (Cash et al., 2009)) and therefore consider the observed increase in delta power as a change toward inhibition. We nevertheless stress that we cannot on the basis of present data alone, commit to any one mechanism conferring bistability, beyond taking into account in our discussion that KC is viewed *as a momentary excursion of the cortex to an unstable state* (Wilson et al., 2006) *or as an evoked neural bistability* (Allegrini et al., 2015).

Upon sleep onset, alpha is blocked. Our finding is the reappearance focal prefrontal brain areas during NREM2 core periods (Ioannides et al., 2017). We consider this as an excitation; the term used at the level of brain functionality rather than at the neuronal neurophysiology level. The correlation of increases in EEG alpha to cognitive processes has long been demonstrated (Wolfgang, 1999), a long with various roles in different aspects of cognition attributed to theta and higher frequency bands activations (Başar et al., 2001). Alpha increases during creative cognition and this may reflect internal processing demands (Fink and Benedek, 2014). Specifically, increased alpha band activity in sleep was shown to correlate to increased sensitivity to environmental noise (McKinney et al., 2011). We therefore consider alpha band activations as indicative of partial return of cognitive processing lost at sleep onset. This leaves theta as a transition zone, possibly acting as a control frequency balancing the putative inhibition from delta and putative excitation from alpha.

The results of this work relate to studies in diverse areas of neuroscience where important definitions regarding locations in the brain and frequency bands are labeled in a fuzzy way, and often inconsistently by experts in different fields, or even within the same field. We compromise the conflicting requirements of relating our work with numerous studies in diverse fields and keeping specificity and accuracy in our presentation of the results by referring as much as possible to precise values of quantities rather than using human labeling and attributions for frequency ranges and brain areas. We computed spectral power and compared the distributions of spectral power for different POIs within frequency bands of fixed width of 3.2 Hz, and we quoted the results for such bands referring to the center frequency (in Hz) of the band. We refer to spatial locations in terms of Talairach coordinates (TC) (Talairach and Tournoux, 1988). When the coordinates that we refer to from other studies are given in the MNI space, we translate them to TC using the Yale BioImage Suite Package[1]. Wherever appropriate, we refer to the popular (but not always consistent) naming of frequency bands and brain locations, also

[1]http://sprout022.sprout.yale.edu/mni2tal/mni2tal.html

providing enough information for the reader to refer to the exact spatial location in TC.

Region of Interest Identification and Interpretation of the sSPMs

In this work we make an indirect region of interest (ROI) analysis using the seven areas defined below.

The first ROI is the frontal area increasing in gamma band from ECW through light and deep sleep, reaching its highest activity during REM (Ioannides et al., 2009); this area was identified as the frontal component of the medial self-representation core (MSRC1) in Ioannides (2018). The second area is the rostral anterior cingulate cortex (rACC). Changes were identified throughout light sleep in rACC consistent with a sentinel role, particularly in the POI before spindles. These changes were interpreted in our previous study as stopping external and internal influences before spindles (Ioannides et al., 2017).

In this work we pay more emphasis on the details of activations in the pre-motor cortex and the immediately ventral part of ACC. We are able to disentangle changes in at least four distinct brain areas by looking in detail in the frequency range from delta to high sigma, before and during spindles and KCs, and for two levels of statistical significance. After transformation to a common space it is clear that these four areas correspond to the distinct cytoarchitectonic areas SMA proper and pre-SMA of the premotor cortex and two other areas directly ventral within the dorsal caudal part of the ACC, which we name dcACC1 and dcACC2. These areas are likely to correspond to two distinct cytoarchitectonic areas in this part of ACC, each with its own somatotopy (Picard and Strick, 1996, 2001).

Finally, the seventh area is in the in the sub genual ACC (sgACC) at the ventral anterior edge of the widespread prominent changes during KCs and hence not easily differentiated from it in the earlier work (Ioannides et al., 2017). It is also identified as a more focal modest increase in the pre-KC POI.

RESULTS

Event Count and Time Domain Analysis

In agreement with the reports for spindles (Frauscher et al., 2015) and KCs (Mak-McCully et al., 2015), for each and every subject we studied, our own tomographic estimates of activity extracted from MEG signals of individual spindles and KCs also show widespread and asynchronous peaks in the time domain and widespread increases in spectral power over the delta, theta and alpha bands. These findings justify our analysis being deliberately insensitive to precise timing. We therefore proceed with detailed analysis of the sSPMs.

Changes Before and During Spindles and KCs Relative to NREM2 Core Periods

Figure 1 displays the common changes across subjects in spectral power (relative to NREM2 core) in the mid-line sagittal cut. For ease of comparison it is set in a similar format as Figure 4 of our previous work (Ioannides et al., 2017) **Figure 1** shows in separate columns the results for POIs before and during spindles (columns 1 and 2) and KCs (column 3 and 4), separating also in different columns results at $p < 0.05$ (columns 1 and 3) and $p < 0.00001$ (column 2 and 4). The fifth column displays the common changes across all subjects that survive the modest threshold of $p < 0.05$ for each subject and for before spindles and before KCs POIs. The Figure shows that only increases (relative to NREM2 core state) were identified. During the 2 s before spindles and KCs, only a single focal prominent activity increase survived with the statistical threshold set to $p < 0.00001$ in each and every one of the four subjects. This prominent increase over NREM2 core periods was only seen before KCs (not seen before spindles) and it was confined to a very small volume in the dcACC. This prominent pre-KC increase was present in all four subjects for only two of the bands, (of 3.2 Hz width): the displayed alpha band (center frequency 9.6 Hz) and the lower band with center frequency at 8 Hz (not displayed). It is the activity within and around this area that grows during the KC, in both intensity and extent and it covers more brain area and a wider range of frequencies. Each figurine displays in red surrounded with a solid yellow contour the regions where all (4/4) subjects satisfy the set criterion. When 3 out of 4 subjects satisfy the set criterion and there is no higher prevalence (i.e., 4/4 subjects) a red blob is displayed with no contour. This representation allows a comprehensive description of the increases in spectra power conveying information about prevalence amongst subjects, frequency bands and spatial location, while maintaining the sharpness of the main result: changes in spectral power before the large NREM2 graphoelements (compared to NREM2 core) are identified with high statistical significance in only one very focal prominent increase in a narrow range of frequencies and only before KCs.

Figure 2 shows the increases in activity relative to NREM2 core periods at 8 Hz in three orthogonal views. Modest increases are shown in parts A (before spindles) and B (before KCs), with part C showing the only prominent focal increase before KCs when the threshold is set at $p < 0.00001$ (no prominent increases are identified before spindles).

The increases in spectral power before spindles and KCs have distinct spatial and spectral properties. In the delta band (center frequency 3.2 Hz, range 1.6 to 4.8 Hz), the increases in spindles and KCs have some overlap but the areas can also be identified where even modest increases are evident in one but not the other condition. This may simply due to the fact that in one contrast increases have not reached the threshold for significance for all subjects. A more careful examination of the data suggest that the changes over NREM2 are very specific in their spatial and spectral details, with spectral power in a specific brain area changing in a characteristic way for spindles and in a different way in a nearby area for KCs. **Figure 3** combines information from the earlier figures to demonstrate the evolution in the frequency domain from a common increase in the delta band in one brain area into distinct increases in nearby areas at the next higher frequency band. **Figure 3C**, shows that for the transition band centered at 4.8 Hz (from 3.2 to 6.4 Hz), there is a clear tendency of the modest increases in spectral power before spindles (yellow contour) and

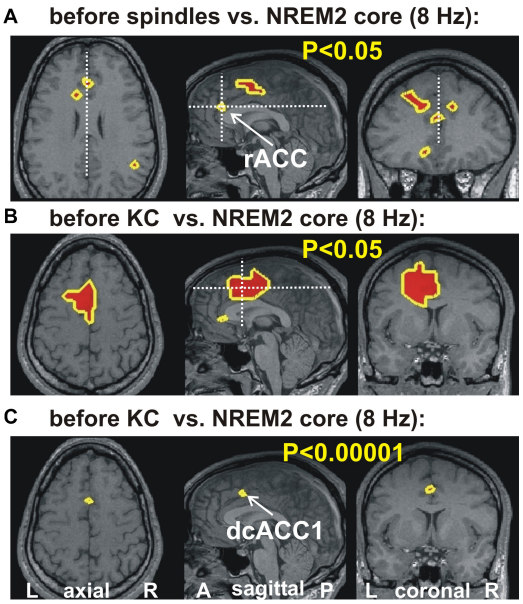

FIGURE 2 | The key areas showing significant change in spectral power, common for all four subjects, at 8 Hz, from the comparison between before spindle, before KC with the NREM2 core POIs. The first two parts show the foci with modest ($p < 0.05$) increase along the midline sagittal cut and through the key area for before spindle **(A)** and before KC **(B)** POIs. **(A)** the axial and coronal cuts are through the rostral ACC area (rACC), which appears to play a key role in controlling the emergence of spindles (Ioannides, 2017). No common increase was identified for the before spindle period at the "prominent" threshold of $p < 0.00001$ in any one frequency band. **(B,C)** show, respectively, the modest ($p < 0.05$) and prominent ($p < 0.00001$) increase for the before KC POIs. In **(B)** a wider but still fairly compact area is seen at more caudal and dorsal along the cingulate; a second very focal increase is identified in the dorsal part of the subgenual ACC (sgACC). In **(C)** only one tiny area survives, and persist into the next frequency band with center at 9.6 Hz (see third row third column in **Figure 1**). The axial and coronal views in both **(B,C)** are through this area which we refer to as dcACC1.

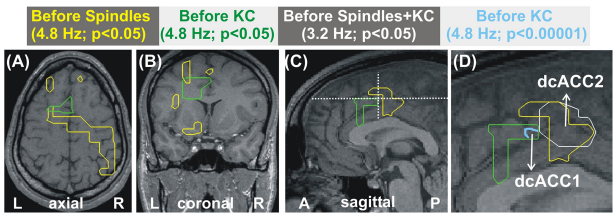

FIGURE 3 | Distinct patterns of increases in spectral power for before spindle and before KC POIs over the NREM2 core periods. The increases are represented as outlines with the color of each outline corresponding to a different contrast as described in the text printed with the same color in each of the panels at the top of the Figure, and described also in this caption below. **(A–C)** show the areas with modest increase ($p < 0.05$) at the center frequency of 4.8 Hz for spindles (yellow) and KCs (green). **(A,B)** are the respective axial and coronal view cut along the lines in the mid-sagittal view in **(C)**. **(D)** shows a zoomed copy of **(C)**, with the focal area in cyan outline showing prominent ($p < 0.00001$) increases before KCs. The white outline marks the areas showing the common overlap for modest increases before spindles and before KCs in the slightly lower band (center at 3.2 Hz). The white outline marks much of the area with before spindle increase because the before KC increase at 3.2 Hz covers almost all of the area of the pre-spindle increase and extends well beyond. The centers of the cyan and white outlines are referred to as dcACC1 and dcACC2.

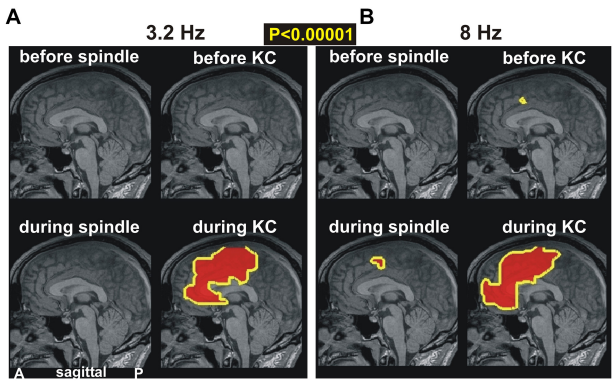

FIGURE 4 | The key prominent changes in spectral power in midline areas for spindles and KCs at frequencies of **(A)** 3.2 Hz and **(B)** 8 Hz, respectively. Top rows show changes before periods while bottom rows for during periods. Left column of each figurine is for spindles while right column for KCs. A prominent broad increase is seen only during KCs in both frequency bands (bottom rows). The top row shows again the only prominent increase in the dcACC1 before KCs. A nearby prominent increase is seen during spindles and a much wider area during KCs.

before KCs (green contour) to be localized in nearby but distinct, not overlapping areas. In **Figure 3D**, the mauve outline shows the very focal prominent increase at 8 and 9.6 Hz for the before KC POI. Finally the overlap region in the delta band where the POIs before both spindles and KCs show a modest increase relative to NREM2 core is shown by the white outline.

In **Figure 4**, we examine prominent ($p < 0.00001$) changes in spectral power in the ACC and surrounding areas. **Figure 4A** shows changes in the lowest computed band (3.2 Hz) and **Figure 4B** at the higher band (8 Hz). The periods before spindles and KCs are displayed in the top row and reiterate the earlier result: the only prominent change in the pre-KC period is the increase in the high delta/low alpha range in the dcACC1. The periods "during" are displayed in the lower rows. During spindles there is a modest increase (not shown), but no prominent increase, in the delta band. A prominent increase is seen during spindles in the theta band that persists in the alpha and low sigma frequency ranges (not shown). What is striking is that this increase in prominent theta, alpha and low sigma bands during spindles maintains the spatial extent (as shown in the left, lower figurine for **Figure 4B**) and surrounds on the caudal and dorsal sides the area of prominent increases before KCs (dcACC1), but has no overlap with it, even when the modest threshold is used. By far the most dominant increase of activity is identified during KCs along the anterior part of the ACC for the entire range of delta, theta (seen in **Figure 4B**) and alpha bands (not shown).

Changes in the Gamma Band Before and During KCs

Increases in spectral power are seen in the gamma band before and during KC POIs relative to the NREM2 core periods. Similar

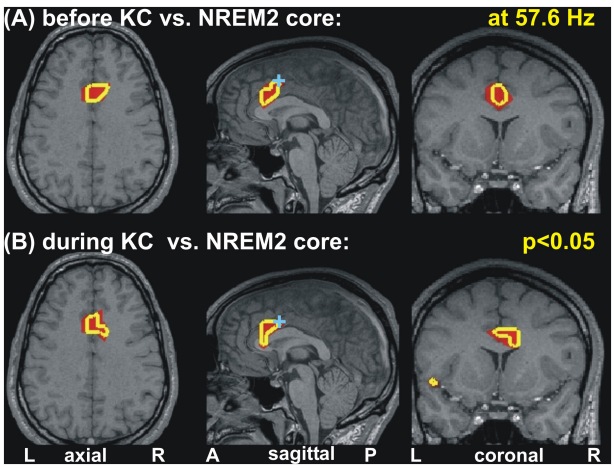

FIGURE 5 | Changes of spectral power at 57.6 Hz before and during KC periods relative to the NREM2 core periods. Modest ($p < 0.05$) increases are seen in similar part of the anterior cingulate for the periods before **(A)** and during **(B)** KCs. A cyan cross in the mid-sagittal cut marks the area (dcACC1) showing prominent increase in upper theta and low alpha band seen before KCs. The axial and coronal cuts are through dcACC1.

gamma band changes are identified for POIs before and during KCs, which, unlike the case in low frequencies remain focal and modest in both POIs. More specifically for gamma band changes, there was no prominent change ($p < 0.00001$) only modest ones ($p < 0.05$), identified within 3−5 successive bands (of width 3.2 Hz). These modest increases in activity before and during the KCs were in different parts of the ACC at different gamma bands. In some of the identified gamma bands, modest increases were identified at very similar locations for before and during KCs POIs. An example of such an increase in gamma band is shown in **Figure 5**, for center frequency at 57.6 Hz with a band width of 3.2 Hz: the area with modest increase is just rostral and ventral to dcACC1.

Gathering Together the Results

The results described above together with the results of our previous two studies (Ioannides et al., 2009, 2017) highlight the critical role played by the ACC and the overlying cortex throughout sleep and specifically in the generation of KCs. The way this role is played out depends critically on changes in spectral power in very specific cortical locations at specific frequency ranges. **Figure 6** displays the cortical geography on the midline cut with the seven key frontal lobe areas, located in either on, or within a few millimeters of the midline sagittal plane. In **Table 3**, we provide for each of the 7 key areas the full details about the increases relative to the NREM2 core periods for all bands up to 17.4 Hz, with center frequency starting at 3.2 Hz stepped by 1.6 Hz till 16 Hz. We emphasize that although there is a sharp transition around 16 Hz, with considerably lower spectral power at higher frequencies, changes are nevertheless seen at higher frequencies, especially in the gamma band as demonstrated by the results in Ioannides et al. (2009) and the example in **Figure 5**.

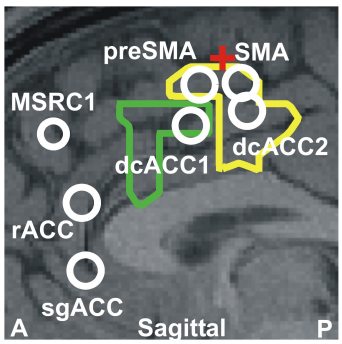

FIGURE 6 | The seven key areas identified in this paper and in our previous studies (Ioannides et al., 2009; Ioannides, 2017); they are the six areas that play a key role in REM2 sleep and the area monotonically increasing its gamma power as sleep progresses from light to deep and finally REM sleep (Ioannides et al., 2009). The areas are displayed onto a mid-sagittal MRI about 2 mm inside the left hemisphere. The area dcACC1 plays a pivotal role in the generation of KCs. Three other areas are identified adjacent to dcACC1. One of these areas lies within dcACC; this area dcACC2 is just caudal to dcACC1 and is related more to spindles but it also plays a role for KCs, especially in the delta band. The area dorsal to dcACC1 is in the pre-SMA and the one rostral to dcACC2 in the SMA. These two areas are activated prominently (with dcACC2) during spindles and seem to make up the generator of the slow spindles. These two premotor areas show modest increases during both KCs and spindles in the theta and alpha bands. The two areas close to rACC seem to play a distinct role. The more dorsal area rACC relates more to spindles. The more ventral area relates to KCs and it is on the subgenual ACC (sgACC), at its more dorsal and ventral part close to the border with rACC. The two outlines showing the modest increase in activity at 4.8 Hz for spindles (yellow) and KCs (green) are also projected on the same MRI slice. The assignment of the two premotor areas to SMA and pre-SMA is made by reference to two earlier works early works for separating Broadman area 6 into SMA and pre-SMA sub-divisions. The first, relates animal studies to early human imaging studies of the areas (Picard and Strick, 2001) and the second is a recent work combining cytoarchitectonic and functional information (Ruan et al., 2018). The red cross marks the location of the rough border of SMA and pre-SMA as defined by the blue cross-hair in Figure 7 of Ruan et al. (2018). The TC of these areas and details of the spectral power changes for each one before and during KCs are given in **Table 3**.

In the final display (**Figure 7**) we show time courses of KC and NREM2 core. The top part, **Figure 7A**, shows the time courses of the EEG signal, showing how the 2 s POIs used in the sSPM analysis are defined in the 4 s long segments extracted for the tomographic analysis. The lower part, **Figure 7B** shows the time courses for regional brain activations before and during the KC on the left and during the (4-s long) NREM2 core period. Part B shows the traces for the two ROIs linked more strongly to KCs, the ROIs for dcACC1 and sgACC. The traces provide a glimpse of the richness in the signal and the tomographic solutions derived from it.

DISCUSSION

Summary of the Results and Their Relevance to Previous Studies

The main contribution of this paper is the delineation of increases in activity in four nearby brain areas before and during spindles

TABLE 3 | A complete representation of the variation in spectral power of the seven midline areas (displayed in **Figure 6**) in the frontal lobes that play a key role before and during spindles and KCs.

ROI TC (x,y,z) mm	Center frequency in Hz								
	3.2	4.8	6.4	8	9.6	11.2	12.8	14.4	16
rACC (0,33,15)									
dcACC1 (0,10,40)									
dcACC2 (0, −1,44)									
Pre-SMA (0,9,48)									
SMA (0,0,50)									
sgACC (0,30,4)									
MSRC1 (−1,40,34)									

*Each column shows the results for a spectral windows starting from 3.2 and ending at 16 Hz (window width of 3.2 Hz and step of 1.6 Hz). Each row represents a different ROI. The first area rACC is discussed in Ioannides et al. (2017). The last area is the center of the edge-surface of MSRC1 (Ioannides et al., 2009; Ioannides, 2018) closest to the midline. The remaining five areas related to the work described in this paper, but some also featuring in the results of Ioannides et al. (2017). Different symbols represent each graphoelement (triangles for KCs and circles for spindles) and POI (open symbols for POIs before and filled symbols for POIs during graphoelements). For ease of reference to POI, the open and filled symbols are placed on the left and right of each cell, respectively. Color is used to represent statistical significance, with black representing modest increases ($p < 0.05$) and red representing prominent increases ($p < 0.00001$). In addition we also mark for emphasis the only prominent increases in the before POIs (only for KCs) with *** and with * the rACC increase in low frequencies before spindles. The contrasts are always between a given POI related to a graphoelement with the NREM2 core period. The rACC is actively inhibited before spindles (shows a modest increase in the delta band) and in the frequency bands centered at 6.4 and 8 Hz. The key area identified in this paper is dcACC1. This area shows the most persistent increase in spectral power before KCs: the only area (i.e., only open red open symbols) with prominent increase in spectral power in a POI before NREM2 graphoelements. This increase is confined to the spectral windows with centers at 8 and 9.6 Hz (the two open red triangles in the dcACC1 row). Before KCs, modest increases are also identified in dcACC1 at lower frequencies (centers from 3.2 to 6.4 Hz) and at one higher band (center at 11.2 Hz). During KCs, dcACC1 shows prominent increases in all bands from 3.2 to 12.8 Hz and modest increases at 14.4 and 16 Hz. Before spindles, dcACC1 shows no increase in spectral power at any frequency band. During spindles dcACC1 show only modest increase for bands with centers from 9.6 to 14.4 Hz. The increase in dcACC2 is almost identical to dcACC1 before and during KCs, without reaching prominent level before KCs. The activity of dcACC2 differs markedly around spindles. Before spindles, dcACC2 shows modest increase in all frequency bands from 3.2 to 8 Hz, and no significant increase at higher frequency bands. During spindles, there is no significant change in activity in the lower bands (with centers at 3.2, 4.8 and 6.4 Hz) and a prominent increase in the next three bands (centers at 8, 9.6, and 11.2 Hz) and modest increases at the higher bands (centers at 12.8, 14.4, and 16 Hz). The changes in spectral power are identical for pre-SMA and SMA for both before and during POIs for spindles and KCs for all bands with centers between 4.8 and 14.4 Hz. The similarity persists in the lowest and highest bands, with only two differences: before KCs at 3.2 Hz (black open triangle) and during KCs at 16 Hz (black filled triangle) resepectively, pre-SMA does not show the modest increase that is evident in SMA. The sgACC shows modest increase in spectral power before KCs, only at the band centered at 8 Hz. Both rACC and sgACC show a focal increases at 8 Hz: rACC before spindles and sgACC before KCs. During KCs both areas show prominent increases in the frequency bands centered from 3.2 to 8 Hz. In the next three higher bands (centered at 9.6Hz) the sgACC continues to show prominent increase but for rACC only modest increases are identified. For sgACC the last two bands, centered at 14.4 and 16 Hz show modest increase. The seventh, most rostral and dorsal area, does not show increase in spectral power before either spindles or KCs. During spindles, it shows modest increase in spectral power at all bands with centers from 3.2 to 11.2 Hz and during KCs modest increase at bands with centers 8, 9.6 and 11.2 Hz.*

and KCs relative to the NREM2 core periods. Two of these areas are in the cingulate cortex, dcACC1 and dcACC2 and the other two are located directly dorsal in the pre-motor cortex, corresponding to its two sub-divisions, the pre-SMA and SMA, respectively. The changes in each of these four areas is specific, complex and principled for the pre- and –during POIs of spindles and KCs. A modest ($p < 0.05$) increase in dcACC1, relative to NREM2, is seen for 3.2 Hz wide bands centered in all frequencies from 3.2 to 11.2 Hz, but this increase reaches prominent level ($p < 0.00001$) only for two bands, centered at 8 and 9.6 Hz. These two prominent increases in dcACC1 in the pre-KC POI, are the only prominent increases identified throughout the brain in the POIs before either spindles or KCs. For spindles no significant change in dcACC1 activity is seen in the pre-spindle POI and modest increases during spindles. The more caudal area dcACC2 shows modest increases relative to NREM2 core POI, for both the pre-spindle and pre-KC POIs for frequency band centers 3.2, 6.4, and 8 Hz, but only for spindles at 6.4 Hz and only for KCs at 9.6, 11.2, and 12.8 Hz. During the POIs before spindles and KCs the changes in SMA and pre-SMA are similar to the pattern of increases dcACC2. **Table 3** provides the more comprehensive description as it puts together the new findings (emphasizing the POIs before spindles and KCs and focusing more on the KCs) and the earlier results describing mainly focal changes for spindles and emphasizing the POIs during spindles and KCs.

In comparing the here presented **Figure 1** with **Figure 4** in Ioannides et al. (2017), the two methodological differences of section 2.5 should be noted (use of MNI rather than TC for intermediate common space and allowing also the display of results satisfied by 75% of subjects). This direct comparison is possible for the first and third columns in **Figure 1** which correspond to the fourth and sixth columns, respectively, of **Figure 4** of the 2017 work (Ioannides et al., 2017), because for these cases exactly the same contrast and threshold are used in

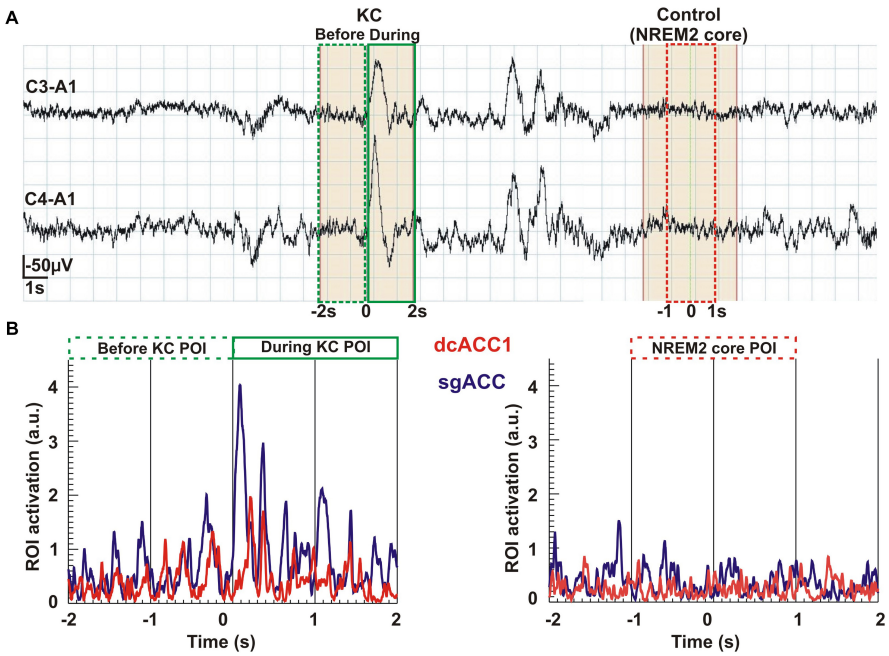

FIGURE 7 | An overview of the analysis from the raw signal and POI selection to regional time courses. The top row Part **(A)** shows the raw EEG signal (high pass at 0.2 Hz) recorded from the two pairs of electrodes (C3-A1 and C4-A1). In the continuous, 37 s long NREM2 record, two KCs are identified. From this segment of data we selected for further analysis the first (single) KC and a period of NREM2 core, at least 2 s after the second (multiple) KC and with no other spindle or KC after its end for the remaining 6 s of the displayed segment. The beginning of the KC as it appeared in the lower of the two EEG channels was used to mark the middle of a 4 s long segment extracted for further analysis. We applied MFT tomography to analyze independently each one of the 2,500 samples of the single KC and each one of the 2,500 samples of the NREM2 core. We used for the Fourier analysis the 1250 samples in each of three POIs: the first 2 s of the KC defined the pre-KC POI and the last 2 s the during-KC POI. The middle 2 s of the NREM2 shaded 4 s were used as a NREM2 core POI for the further analysis. The spectra for each source space point (about 1000 active points in the source space spread in a uniform grid within the brain) was then computed from the time course of each POI. The sSPM were computed independently for each source space point from the statistical comparisons between the distributions for two POIs, each with eight exemplars for each POI. The results were reported after the conservative Bonferoni correction for multiple source space points was applied. Part **(B)** shows the time courses for modulus of activity (time-domain description) for the two ROIs (dcACC1 and sgACC) identified in the sSPM statistics as showing prominent changes before and/or during KCs relative to NREM2 core.

the displays. The second difference allows a more comprehensive description to be given for the highly focal activations before KCs that make up the main result of the current work. The comparison of the third and fourth columns shows the way a compact but not very focal modest increases in spectral power before KCs relative to NREM2 core periods (in the third column) shrink in both the spatial and frequency domain to the prominent and highly focal increases in the alpha band (third figurine of fourth column). Comparing figurines within the third column only, it is evident that the single highly focal prominent increases before KCs in the alpha band (third figurine), persist and remains the only prominent increase in the adjacent theta and low sigma bands (second and fourth figurines) for three of the four subjects. Note that different groups of three subjects could be identified in the different figurines, i.e., a different subject may be the one that has not reached prominent level in the theta from the one that did not reach the prominent level for the low sigma band.

Spectral Patterns of Key Areas in Distinct POIs and First Conclusions

In the Results section we described increases in spectral power from the NREM2 core levels within the rostral and dorsal ACC in the POIs before spindles and KCs. We identified common precursors of spindles and KCs in dcACC2 in the delta band that become distinct in the border band between delta and theta. In the 2 s preceding the start of either spindles or KCs, only one area, the dcACC1, survived at the threshold of $p < 0.00001$: only in the pre-KC but not the pre-spindle period, and only in two adjacent and overlapping frequency bands (high theta and low alpha). The two focal areas dcACC1 and dcACC2 seem to play key roles for KCs and spindles, respectively, but these roles must be seen as the apex of specialization of a unified system (the brain) with areas across the ACC and more dorsal and rostral areas involved in a very specific way around the KC and spindle generation.

Table 3 shows that such a common precursor is the active inhibition (increase in the spectral power in the delta band) in dcACC2 and the immediately dorsal part of SMA (anterior side of SMA). Before spindles but not before KCs a similar active inhibition is evident in rACC and pre-SMA. The opposite (active inhibition before KCs but not before spindles) is seen in dcACC1, the area showing prominent increase in higher frequencies and located where the only area in the brain from where electrical stimulation (in awake state) generates KC-like response (Voysey et al., 2015).

During spindles the changes remain modest and focal, with some prominent and very focal activations in the alpha and low sigma bands in dcACC adjacent dorsal midline cortex and in high sigma band in posterior cortex as described in some detail in Ioannides (2017). During KCs the activity is prominent in the entire ACC and adjacent areas in the delta, theta and alpha bands. These results are consistent with very different operations taking place during spindles and KCs. During spindles the process is finely tuned and precise operations seem to take place as has already been discussed earlier (Ioannides et al., 2017; Ioannides, 2018). A very different picture emerges during KCs: Prominent power increases are seen in the frequencies associated with active inhibition (delta) and with cognitive function (theta and higher bands). Furthermore, modest increases in activity are identified in low and high gamma band (see example in **Figure 5**). These results are consistent with a system running close to a transition, befitting the Janus nature attributed to KCs, a damping effect to promote sleep and an arousing effect for more cognitive tasks that may lead to awakening (Jahnke et al., 2012; Halász, 2016). The findings above, collected from both this work and those previously reported (Ioannides et al., 2009, 2017), converge to the following conclusions:

- The KCs, like spindles, should be considered as the "end product" of a long sequence of processes. This sequence starts with sleep onset in distinct neural networks but becomes most prominent at specific sleep stages, at specific periods before and during KCs and at specific nodes of the brain networks. During this long sequence distinct parts of the ACC play key roles (shown together in **Figure 6**) with changes in spectral power at the very specific frequency bands describe above and listed in **Table 3**.
- The only prominent change in the before POIs is the focal increase of high theta and low alpha spectral power before KCs. This focal increase is in the caudal end of the rostro-caudal part of the anterior cingulate cortex (dcACC1). This area coincides with the area identified recently as the only location where electrical stimulation (while awake) evokes KC-like responses.
- The ACC is involved in environmental and internal monitoring - consistent with a sentinel role. As discussed below, analysis of data from related experiments, for conflict and environment monitoring, identified areas within a few millimeters of the rACC and the two dcACC areas, and the wide ACC areas between them.
- A modest increase is identified in the delta band in the dcACC2 and SMA proper that is common to both spindles and KCs (white outline in rightmost figurine of **Figure 3**. This likely represents a common active inhibition before spindles and KCs. This is probably part of mechanism preventing movement by actively inhibiting the SMA and dcACC2, two areas directly connected with movement initiation (Passingham, 1995; Picard and Strick, 2001). Apart from this common change, the changes in spectral power before KCs were different than those for spindles, either in terms of frequency or in terms of location, but often sharing a common border, see for example how the wider activation in the delta band (center frequency at 3.2 Hz, range from 1.6 to 4.8 Hz) with the common area marked by the white outline, separates in the next band (center frequency at 4.8 Hz, range from 3.2 to 6.4 Hz), into distinct but adjacent increases for spindles and KCs.
- Prominent increases relative to NREM2 core periods are focal in the pre-KC period and extended but well circumscribed (not global) during KCs, as can be seen in **Figures 2–4** of this work and Figures 9–11 in Ioannides (2017).

The Distinct Spectral Signatures Before and During KCs Across Studies

The key areas involved in KC generation are dcACC1, sgACC, and pre-SMA. Before and during KCs, spectral increases are identified in dcACC1 for all bands with centers from 3.2 to 11.2 Hz and for higher frequency bands for the POI during KCs. During the pre-KC period, modest increases are identified for bands with centers from 8 to 11.2 Hz in the pre-SMA. In sgACC, only a modest increase is identified in the pre-KC period and only in one band with center at 8 Hz. During KCs, prominent changes are identified from 3.2 to 12.8 Hz (a modest one in the next band with center at 14.4) in both sgACC and pre-SMA, with a modest increase at 16 Hz only for sgACC. The spectral signature for spindles and KCs are distinct and they provide hints for their possible roles. For KCs the coexistence of delta increases (active inhibition) with increases at higher frequencies (increase cognition) suggest a struggle between external influences and the need to decide whether to wake up or not, and sleep promoting activity, consistent with the proposed sentinel role of KCs (Halász, 2016; Blume et al., 2018). Our analysis adds to the existing literature the identification of this Janus-like behavior of KCs, not only during the main event, but also in the pre-KC period in the frequency range from delta to sigma bands, consistent with recent findings using EEG (Blume et al., 2018).

The results described above and in the previous sub-sections and the first conclusions drawn from them are in excellent agreement with recent literature as the examples of the previous paragraph show. Studies with intracranial electrodes are particularly supporting, including the only study where stimulation of a specific brain area (the dcACC) was causally related to KC-like activation (Voysey et al., 2015). There seemed to be just one apparent exception: in a recent paper (Mak-McCully et al., 2015), it was reported that "*Locally generated KCs were found in all sampled areas, including cingulate, ventral temporal, and occipital cortices. Surprisingly, KCs were smallest and occurred least frequently in anterior prefrontal channels.*" This statement stands in sharp contradiction to the identification of focal initiator of KCs in dcACC in both our study and in the recent intracranial stimulation study (Voysey et al., 2015). A closer examination of the details of Mak-McCully et al. (2015) reveals that the hard facts are actually in full agreement with our findings: the KCs identified by human experts had a local generation in 76% of the cases. The global distribution was identified after more "KC-like" phenomena were included "*using an automatic procedure to look for KC-like activity in the channels*

where KCs were not manually marked, at times when a KC was manually marked in at least one channel. Each channel was band-passed with a zero phase-shift filter from 0.2 to 5 Hz before the detection of KC-like activity. For each channel, a KC template was created by averaging over the manual KC detections from −350 to + 650 ms around the peak. A sliding inner product was then performed between this template and a 1.2 s window when a manual KC occurred in at least one channel. " Filtering with low pass set to 5 Hz eliminates the higher frequencies, e.g., upper theta/low alpha component (Kokkinos et al., 2013) while averaging from the peak negativity further biases the outcome against the other components (positivities before and after the negativity) which have variable time relation with the peak negativity. The combined effect will be a selection of activity near the peak negativity and therefore correspond to the periods "during KCs" of our studies, where we also found widespread activations in the delta band, as seen in Figure 4 of Ioannides (2017) and **Figure 4** of this paper and in **Table 3**. Further, our current study shows that these widespread activations during KCs are seen in similar areas in the theta and alpha bands. The key finding of the present study is that in the 2 s preceding the KC, there is a prominent ($p < 0.00001$) increase in the spectral power in the high theta and low alpha bands over the NREM2 core period confined to dcACC1. As best as one can judge from the published figures (Voysey et al., 2015), this is exactly the area identified as the only area (from the ones where electrodes were placed) that when stimulated causes a KC-like event.

Consistency of the Results and Putative Roles of the KC Generator in ACC

The ACC has been implicated in NREM slow wave generation (Dang-Vu et al., 2008) while it has also been shown to precede sleepwalking episodes (Januszko et al., 2016) and NREM parasomnia arousals (Terzaghi et al., 2012). To advance our understanding of ACC's role however, it is worth integrating relevant evidence from the awake condition as well, beginning by noting that the KC-like event "caused" by stimulation of the dcACC has been seen during awake state (Voysey et al., 2015). Paus (Paus, 2001) emphasized three key roles of ACC in behavior (a) in motor control through dense projections to the motor cortex and spinal cord [see also (Hoffstaedter et al., 2013)], (b) in cognition through reciprocal connections with the lateral prefrontal cortex [see also (Dehaene, 2018)] and (c) in arousal/drive state through extensive afferents from the midline thalamus and brainstem (mainly noradrenergic and dopaminergic nuclei [see also (Vogt and Gabriel, 1993)].

The ACC is generally known to be involved in saliency detection and environmental monitoring, with a rough division into rostral ACC and dorsal ACC sectors corresponding to a rough segregation of emotional (Drevets et al., 2008) and cognitive (Steele and Lawrie, 2004; Taylor et al., 2007) functions, respectively. There are numerous studies demonstrating changes in the ACC with fine experiments attempting to disentangle specific parts of ACC excited differentially by specific tasks, ranging from conflict monitoring in Stroop effect (Pardo et al., 1990), error monitoring (Carter, 1998; Taylor et al., 2007) and its dependence on awareness (O 'connell et al., 2007) and adjustments in control (Kerns et al., 2004). A positron emission tomography study using theory of mind (ToM) tasks showed a reduction of dcACC activity when subjects listened to unlinked sentences compared to actual stories and in two nearby activation in the contrast between ToM and physical stories (Fletcher et al., 1995).

The evidence quoted above and that from our present and earlier (Ioannides et al., 2017) studies converge to the conclusion that similar mechanisms with the same key nodes are involved while awake and sleep to monitor the environment with the ACC playing a central role in both conditions. How this monitoring is used might be different: while awake the results lead to actions biased by intentions; during sleep a simpler choice is selected, to continue sleeping and doing what sleep allows doing or wake up to deal with what just happened. Within such an integrated view the present results help us understand the sentinel function in sleep and the potential key role of KC in it. All sleep functions (i.e., restoration, replenishment and especially memory consolidation through synaptic plasticity and reorganization) demand a brain of low energy consumption and non-biased information processing, i.e., a brain not interfered with and not interrupted by stimuli (environmental or internal). However, complete isolation would render an animal vulnerable to predators or homeostatic emergencies. The compromise between such worthiness of sleep and that of being awake in the face of danger is one of the great challenges in biology. A convenient solution to this challenge could be a sentinel type process, fast evaluating the saliency and/or alarm character of internal and external signals and accordingly lead to awakening or sleep maintenance (Jahnke et al., 2012; Halász, 2016). A sentinel brain system must possess at least three capabilities: sensitivity/responsiveness, cognitive evaluation/decision taking as well as sleep restoration/hypnagogic action; and all of them are potentially met by KC:

(a) There are indications of KC reflecting sensory responsiveness and/or signs of unconscious arousal and being accepted as a reactive wave (Halász, 2016), spontaneously emerging, as an accurate representations of late components (> 400 ms) of sensory evoked potentials by any modality stimuli, (Niiyama et al., 1996; Bastuji and Garcia-Larrea, 1999; Cote et al., 2000; Jahnke et al., 2012) as well as stimuli in anterior cingulate gyrus (Voysey et al., 2015). It is intriguing that the sleeping brain is momentarily more responsive to incoming sensory events just preceding a KC (Sallinen et al., 1997) the time of prominent activation of dcACC (see **Figures 2B,C**), a brain area known to be involved in saliency detection and environmental monitoring (Steele and Lawrie, 2004; Taylor et al., 2007).

(b) There are KC electrophysiological correlates of cognition i.e., fast neural activity of a type – gamma band EEG, but also alpha and theta - known to support cognitive processes (Gross and Gotman, 1999; Başar et al., 2001), required in order to evaluate the saliency of the stimulus. Localized gamma activations have been observed throughout sleep

including NREM2 (Ioannides et al., 2009, 2017). Here we demonstrate that gamma activation in the low and high gamma band is seen just prior and during KCs throughout the ACC with only one example shown in **Figure 4**. In this example, the increase in gamma band power close to 60 Hz in dcACC, just rostral and ventral of the area with prominent high theta and low alpha activations (**Figures 2**, **3**). Interestingly a previous EEG study showed during KCs brief bursts with anterio-posteriorly mobile maximal power and increasing frequency (from high theta to low alpha) (Kokkinos et al., 2013). Consistent with cognitive activity associated with KC are considered its habituation (Bastuji et al., 1995) and its ability to discriminate rare stimuli (Bastuji et al., 1995; Pratt et al., 1999) or stimuli of self-relevance and emotional significance (Perrin et al., 1999; Blume et al., 2017). Importantly, the area where KCs appear to emerge from (ACC) is an area associated with detecting internal or external perturbations (Luu and Pederson, 2004) - further relating KC to a sentinel role.

(c) There is indirect but strong and converging evidence for an hypnagogic (protecting sleep and promoting its maintenance) effect following KC, since the impact of intrusive arousals is lessened and so awareness and awakening is prevented through arousal inhibition, (Wauquier et al., 1995; de Gennaro et al., 2000; Amzica and Steriade, 2002; Colrain, 2005; Halász, 2005; Forget et al., 2011). Also, an increase in KC density has been observed in association with an increase in delta wave leading to slow wave sleep or following a night of fragmented sleep (de Gennaro et al., 2000). A range of different mechanisms have been proposed to describe the KCs sleep promoting role, from the synchronization expected from large and fairly generalized slow negative waves, to the triggering of spindles by KC, to the resetting of brain activity in the transition from Down to Up state (Cash et al., 2009). Any of these mechanisms may theoretically protect sleep.

We conclude that all three demands for a sentinel operation (sensitivity, decision making and restoration of sleeping state) are fulfilled. But, can a tentative synthesis be made? This is a formidable task to tackle, but we think that the appreciation of the fundamental role of dcACC in the emergence of KC (Voysey et al., 2015; Ioannides et al., 2017) points new investigations in specific directions.

Contribution to Old Debates and Speculations

There is considerable debate about the nature of KCs and whether or not they have local or global generation. There is also a seemingly independent controversy about local or distributed nature of awake state processing of distinct physical and cognitive stimuli and situations and specifically pain, cognition, environmental monitoring through error prediction and negative emotion (Shackman et al., 2011; Jahn et al., 2016). In this subsection we will attempt to use the results for the analysis of spectral activity around spindles and KCs to provide bridges between seemingly diverging conclusions and use the resulting synthesis in the final subsection for airing a falsifiable speculation about KCs and ERN.

We begin by noting that distinct brain networks become substantially disconnected during sleep (Massimini et al., 2005), but from time to time particular networks succeed to communicate and lead to a global event (Gemignani et al., 2015). This large amplitude event, however, in NREM sleep cannot enrich consciousness, as in awake, but instead triggers a massive reset of many networks. One of the mechanisms of such resetting could be an evoked neural bistability, which prompted some to describe the nature of KC, as an isolated DOWN state (Cash et al., 2009). Candidate mechanisms for global brain networks resetting include activation of locus coeruleus (Bouret and Sara, 2005). Although consciousness is lost, some unconscious monitoring seems to reappear after sleep onset (Bush et al., 2000; Luu and Pederson, 2004); a strong evidence for this is the focal alpha and low sigma spectral power increases in rACC and other frontal areas in the core periods of NREM2 compared to those of NREM1 (Ioannides et al., 2017). This highly focal change in activity we interpret as a local move away from down states is augmented around KCs. Our results show that both the pre-KC POI and the POI during KC the spectral power relative to that of NREM2 core period is higher in low (delta) and high (theta, alpha, and sigma) frequencies. The increases in the pre-KC POIs are relatively focal, becoming stronger and expanding more widely in the frontal brain in the POIs during KCs. Furthermore, focal increases are encountered in the gamma band which have similar strength and extend in the pre-KC and during KC POIs as can be seen in the example of **Figure 5**.

A related point concerns the question of local or global emergence of KCs. It appears that this debate is won by the former, provided high spatial resolution is afforded (Murphy et al., 2012; Pugin et al., 2015; Ioannides et al., 2017; Siclari and Tononi, 2017). Pre-KC activations in ACC and more dorsal medial frontal cortex appear to be a fundamental component of a sentinel system initiating an unconscious cognitive process which allows a safe and sound, uninterrupted sleep. Both the results presented here and the recent intracranial report of stimulation of dcACC evokes (in awake state) KC-like behavior (Voysey et al., 2015) clearly point to a local generation of KC. This, however, is not the complete story. The study of the intact system in our analysis shows that, at least in the pre-KC POI, focal spectral changes preceding the KCs. During KCs the changes in the spectral power below the beta band are widespread, especially in the frontal cortex where widespread increases survive even at the prominent threshold of $p < 0.00001$.

Our results offer an alternative point about the nature of KCs and the debate whether the emergence of KCs is a local or global phenomenon. Combining our findings with the widespread delta activity around KCs found by Mak-McCully et al. (2015), the evidence suggests that the pre-KC POI is characterized by a local departures from an otherwise widespread down state. Furthermore this pattern of pre-KC increase is a continuation of the changes already taking place in the core periods (well away from spindles and KCs) from NREM1 and NREM2. During the pre-KC POI the potentially disruptive event (the KC) is initiated

at dcACC1 and propagates to a few other areas leading to a set of confined focal events. Under this interpretation, our results suggest that the KC itself (i.e., during KC POI) is not a pure down state, but a bistable disturbance with strong components with spectral power in both the delta band, but also in the higher frequencies. This is very likely a reflection of the Janus face behavior reported by many authors (Jahnke et al., 2012; Kokkinos et al., 2013; Halász, 2016; Blume et al., 2018). This strong statement is made with some reservation because of the low number of subjects in our study. More work with detailed analysis of the coupling between areas, including cross frequency and phase amplitude coupling could provide some additional support and also clarify the precise role of the increases in the transition frequencies (theta band) that now are provisionally seen as the upper bound of the sleep promoting facet of KC (Kokkinos et al., 2013; Gonzalez et al., 2018).

The last key discussion point deals with the functional parcelation of the dorso-caudal part of ACC and the premotor cortex directly dorsal to it; this midline brain area is central to our discussion and it is represented in **Figure 6** by the quartet of four ROIs: dcACC1, dcACC2, SMA and pre-SMA. The reviews by Picard and Strick (Picard and Strick, 1996, 2001) brought together primate microstimulation, human brain imaging (PET and fMRI), physiology and connectivity analysis, attempting to separate distinct of cytoarchitectonic areas on the medial wall related to motor planning and control. Two areas, the SMA-proper (as we also define it), located just rostral to the motor cortex and the cingulate area ventral to it (our dcACC2) were found to have behaviors consistent with direct motor role (e.g., eliciting a time-locked motor output when stimulated), while the pre-SMA appeared concerned more with the selection aspect of motor acts and having no obvious time locked motor output. The same part of the medial wall of the brain figured prominently in a series of other studies using tasks modulated by the level of conflict, error detection, and error prediction. These tasks seemed to elicit a characteristic evoked response potential in the EEG known as error related negativity (ERN) (Bush et al., 2000), apparently generated in the ACC (Herrmann et al., 2004; Dehaene, 2018). More recent intense efforts to understand the functional organization of the SMA, pre-SMA and the rostral and dorsal ACC boils down to the question: is the processing of emotion, pain and cognitive control segregated in distinct subdivisions or are these integrated in a common region? A series of studies, reviewed in Shackman et al. (2011) convincingly demonstrated an overlap of areas identified in tasks involving negative affect, pain and cognitive control. Shackman et al. (2011) reported maxima in separate analysis for each category localized very close to the areas identified in our analysis:

- for negative affect at (TC: −2, 10, 38; within 3 mm of dcACC1) and at (TC: −2, 30, −2; within 3 mm of sgACC).
- for pain at (TC: −2, 0, 44; within 2 mm of dcACC2) and at (TC: −2, 0, 44; between rACC (within 12 mm) and sgACC (within 15 mm).
- for cognitive control at (TC: 0, 12, 42; within 3 mm of dcACC1 and 7 mm of pre-SMA).

A "conjunction map" pooling the pairs of, or all three unitary maps, shows the voxels that were consistently activated across the two or three domains. The resulting conjunction point coincided with the point identified in the unitary map for cognitive control, at (TC: 0, 12, 42) less than 3 mm away from our dcACC1. The cluster maximum for the conjunction between pain and cognitive control (without negative affect) is at (TC: 0, 9, 39) the closest at 1.4 mm away from dcACC1.

In a second study (Jahn et al., 2016), effects of pain, conflict and prediction error (PE) was independently manipulated in a single experiment, allowing a direct comparison of pain and cognitive processing within subjects. The study reported a double dissociation with pain eliciting activations ventral to the cingulate sulcus and cognitive effects localizing more dorsally within the dorsal ACC and spreading into the pre-supplementary motor area, thus supporting the reverse inference meta-analysis of Lieberman and Eisenberger (2015). In general, the cluster maxima, representing foci of significant activations for well segregated properties identified were not as close to the areas identified in our study as the ones identified in Shackman et al. (2011); the closest to our key areas in the (Jahn et al., 2016) study was the cluster maxima for the main effect for Pain at (TC: −2, 28, 13; within 6 mm of rACC), with the other two main effects producing cluster maxima closest to dcACC1 (for PE at TC: −3, 22, 44; within 13 mm) and for Conflict at (TC: 0, 21, 40; within 11 mm).

Spindles and KCs are special processes established by evolution, the greatest experiment of all, to distinguish mechanisms that although starting from a common progenitor (the core state of NREM2) evolve to satisfy different requirements. The identification of distinct foci in the diverse studies discussed above that are very close to the main foci we have identified in our studies provides some supportive evidence. The closeness is particularly impressive in the case of meta-analysis that seek to identify common activations across studies with widely different content (Shackman et al., 2011): nearby foci were identified to each one of the six areas we have identified related to the POIs before and during spindles and KCs. In our view, this consistency is almost inevitable, given the fact that the areas we identify correspond to distinct cytoarchitectonic areas, as already demonstrated for the division of the pre-motor cortex into SMA and pre-SMA (Passingham, 1995; Picard and Strick, 1996, 2001) and the division of the cingulated as already implied by the existence of at least three distinct somatotopic maps (Picard and Strick, 1996, 2001). Significantly, the area identified as the cluster peak of the treble conjunction for negative affect, pain and cognitive control (Shackman et al., 2011) is the same as the one identified in the unitary analysis for cognitive control and only 3 mm away from dcACC1, the highly focal activation that we have identified as the prominent activation in the pre-KC area in the high theta and low alpha range and the only area from where KC-like activity can be elicited in awake state (Voysey et al., 2015). The KC emerges as the general mechanism performing the sentinel duty for whatever disturbance might arise during NREM2 and this can be best described either as a deviation from predicted homeostasis, pain, too strong affect, strong and

unexpected external stimulus. It is therefore to be expected that the areas closely related to the KC will correspond to the areas identified in both the unitary and conjunction maps of the (Shackman et al., 2011) study.

We offer a speculation that emerges from our results that can serve as a guiding hypothesis for future experiments with the same subjects in awake state and sleep. This speculation can be supported, modified or falsified by the future experiments we propose below. We suggest that the KC is the sleep side of the well-studied error related negativity (ERN) that is usually studied in awake state. ERN and KC share a neurophysiological (negative wave) and localization (ACC) characteristics. A recent review of the history of ERN studies (Dehaene, 2018) concludes that ACC is a key area of ERN generation and it is the place where an internal comparison of two signals is made: an unconscious representation of the ongoing action and a conscious representation of the intended one. Although these studies are performed in awake state, ERN may not be unrelated to sleep, since sleep deprivation causes inefficiencies in error-monitoring, as reflected by a reduction in amplitude of the ERN (Fueggle et al., 2018). This speculation opens up a new question. Given that a sentinel role is also encountered for spindles, is there any related spindle activity that might relate to an ERN-like activity during awake state? The way the four areas at the center of this investigation, dcACC1, dcACC2, Pre-SMA and SMA-proper are activated before and during spindles and KCs provide some hints. Although it seems that these four areas are involved in both spindles and KCs, it seems that dcACC1 and pre-SMA are more related to KCs while SMA and dcACC2 are more related to spindles. The earlier studies for the roles and connections of these areas (Picard and Strick, 1996, 2001; Ruan et al., 2018) suggest that there may be a separation between motor specific aspects and learning. The KCs may be more involved in the detection of the need to act and the decision as to whether action should be taken (continue sleeping or wake up) while spindles may be more involved in the enacting of motor acts as part of their role in learning.

Limitations

The small number of subjects (four) is a possible limitation of this study and further studies with more subjects are needed to remove concerns about the generalizability of the results to other subjects. However, the methodology adopted here allows detailed tomographic and statistical analysis of individual subject data, producing very robust results. For the analysis of each subject stringent statistics were applied to reveal commonalities in all four subjects at two statistical thresholds.

A further limitation is that while KCs can also be elicited by sensory stimuli (Laurino et al., 2014), the present study examines only spontaneous KCs. Furthermore, our work indicates the main nodes of the circuits associated with NREM features, the times of their activation and the spectral content, but not the interactions between nodes and the overall properties of the network.

Another limitation of our study is that there was no control of what activities our subject did before sleep. Studies are urgently needed that, like the recent ones reported by the team of Schabus, which relate sleep patterns to different ages (Hoedlmoser et al., 2014) and the subject's activity and learning before sleep (Jegou et al., 2019). In our review of related literature we avoided references to mood disorders that are clearly relevant, since these need to be studied separately in awake state and sleep. Nevertheless the relevance is obvious since in many such clinical conditions have shown abnormalities in the frontal half of the cingulate and surrounding cortex (Dolan et al., 1995; Mayberg, 1997; Etkin, 2010).

Future Outlook

The results outlined in this work add to the growing body of recent sleep research focusing on better understanding of spindles, KCs and slow waves using intracranial recordings (Mak-McCully et al., 2015; Voysey et al., 2015) multichannel EEG (Bernardi et al., 2018; Blume et al., 2018). In this and other of our recent works (Ioannides et al., 2009, 2017; Ioannides, 2018) we relied on the ability of MEG to extract detailed tomographic estimates of activity Focusing almost exclusively on sSPM analysis. However, as can be seen in **Figure 7**, the availability of robust sample by sample estimates of changes in activity in key ROIs opens up new options for detailed time frequency analysis, connectivity analysis and for comparing slow oscillations with single and multiple KCs at unprecedented detail.

Another important way forward is through new experiments that combine at the level of individual subject awake state experiments and whole night sleep studies. Also, from an operational point of view, error in the comparison between ongoing and intended action, is not fundamentally different from saliency detection. We therefore propose that MEG (or EEG) experiments should be performed in awake state and sleep using the same subjects. In the awake state protocols that elicit ERN components should be used, e.g., Go/NOGO experiments with stop signal conditions. The sleep experiments should allow the subjects to reach at least NREM2 so enough spindles and KCs should be collected. Ideally somatosensory and auditory stimulation during NREM2 should also be used. It will also be useful to add stop signals before an expected GO stimulus as well as after. The prediction is that increase activity will be identified in the key areas identified in our study, especially dcACC1, pre-SMA and sgACC for the ERN and before KCs. Activation of dcACC2, SMA and rACC related to ERN could help us clarify not only their role in ERN but their contribution before and especially during spindles. If ERN and KC (and aspects of spindles) are indeed manifestations of the same basic process (e.g., related to impulsivity and response to environmental change) in awake state and sleep, respectively, we would expect the relative contribution from each of these areas to vary from subject to subject but be more similar for KCs and spindles and ERN within each subject. If evoked KCs are available too, then one will be able to map the changes in awake state and sleep from the related sensory areas to the putative ERN

and KC generators and compare their respective evolutions, thus identifying where and how the two evolutions differ.

DATA AVAILABILITY

The raw data supporting the conclusions of this manuscript will be made available by the authors, without undue reservation, to any qualified researcher.

ETHICS STATEMENT

RIKEN's (the institution where the experiment was conducted) ethics committee approved the study, and all the subjects gave their informed written consent after all procedures were explained to them before the experiment.

AUTHOR CONTRIBUTIONS

AI conceived, initiated, and directed the study, for both the experimental phase at the RIKEN BSI and the analysis in Cyprus. All authors contributed to the initial experimental planning, discussed the meaning of the findings, and wrote the manuscript. AI adapted the analysis methods to specific needs of the study and together with LL performed the data analysis in Cyprus.

FUNDING

Some of the work reported here was initially supported by the European Commission under two programs: ARMOR, grant agreement number 287720 under the Seventh Framework Program and SmokeFreeBrain, grant agreement number 681120 under the Horizon 2020 Research and Innovation Program. The work of GK was also supported by University of Patras #51670000-D405. The main part of the work of AI and LL was supported by the European Regional Development Fund and the Cyprus through the Research Promotion Foundation (Project: CONCEPT/0618/0004). The opinions expressed herein belong solely to the authors. The European Commission, the University of Patras and the Research Promotion Foundation had no involvement in the study design, collection, analysis, and interpretation of data, the writing of this manuscript and in the decision to submit this manuscript for publication.

ACKNOWLEDGMENTS

The MEG data were recorded at the Laboratory for Human Brain Dynamics (1998—2009), RIKEN Brain Science Institute, Japan. After the closure of the MEG laboratory, the data were anonymized and transferred under a material transfer agreement to the Laboratory for Human Brain Dynamics at AAI Scientific Cultural Services Ltd. (AAISCS) in Nicosia, Cyprus for follow-up research and data analysis.

REFERENCES

Allegrini, P., Paradisi, P., Menicucci, D., Laurino, M., Piarulli, A., and Gemignani, A. (2015). Self-organized dynamical complexity in human wakefulness and sleep: different critical brain-activity feedback for conscious and unconscious states. *Phys. Rev. E Stat. Nonlin. Soft. Matter Phys.* 92:032808. doi: 10.1103/PhysRevE.92.032808

Amzica, F., and Steriade, M. (1998). Electrophysiological correlates of sleep delta waves. *Electroencephalogr. Clin. Neurophysiol.* 107, 69–83. doi: 10.1016/s0013-4694(98)00051-0

Amzica, F., and Steriade, M. (2002). The functional significance of K-complexes. *Sleep Med. Rev.* 6, 139–149. doi: 10.1053/smrv.2001.0181

Annett, M. (1967). The binomial distribution of right, mixed and left handedness. *Q. J. Exp. Psychol.* 19, 327–333. doi: 10.1080/14640746708400109

Başar, E., Başar-Eroglu, C., Karakaş, S., and Schürmann, M. (2001). Gamma, alpha, delta, and theta oscillations govern cognitive processes. *Int. J. Psychophysiol.* 39, 241–248. doi: 10.1016/s0167-8760(00)00145-8

Bastien, C., and Campbell, K. (1992). The evoked K-complex: all-or-none phenomenon? *Sleep* 15, 236–245. doi: 10.1093/sleep/15.3.236

Bastuji, H., and Garcia-Larrea, L. (1999). Evoked potentials as a tool for the investigation of human sleep. *Sleep Med. Rev.* 3, 23–45. doi: 10.1016/s1087-0792(99)90012-6

Bastuji, H., García-Larrea, L., Franc, C., and Mauguière, F. (1995). Brain processing of stimulus deviance during slow-wave and paradoxical sleep: a study of human auditory evoked responses using the oddball paradigm. *J. Clin. Neurophysiol.* 12, 155–167. doi: 10.1097/00004691-199503000-00006

Bernardi, G., Siclari, F., Handjaras, G., Riedner, B. A., and Tononi, G. (2018). Local and widespread slow waves in stable nrem Sleep: evidence for distinct regulation mechanisms. *Front. Hum. Neurosci.* 12:248. doi: 10.3389/fnhum.2018.00248

Blume, C., del Giudice, R., Lechinger, J., Wislowska, M., Heib, D. P. J., Hoedlmoser, K., et al. (2017). Preferential processing of emotionally and self-relevant stimuli persists in unconscious N2 sleep. *Brain Lang.* 167, 72–82. doi: 10.1016/j.bandl.2016.02.004

Blume, C., del Giudice, R., Wislowska, M., Heib, D. P. J., and Schabus, M. (2018). Standing sentinel during human sleep: continued evaluation of environmental stimuli in the absence of consciousness. *Neuroimage* 178, 638–648. doi: 10.1016/j.neuroimage.2018.05.056

Bouret, S., and Sara, S. J. (2005). Network reset: a simplified overarching theory of locus coeruleus noradrenaline function. *Trends Neurosci.* 28, 574–582. doi: 10.1016/j.tins.2005.09.002

Bush, G., Luu, P., and Posner, M. I. (2000). Cognitive and emotional influences in anterior cingulate cortex. *Trends Cogn. Sci.* 4, 215–222. doi: 10.1016/S1364-6613(00)01483-1482

Buzsaki, G. (2006). *Rhythms of the Brain*. New York, NY: Oxford University Press.

Caporro, M., Haneef, Z., Yeh, H., Lenartowicz, A., Buttinelli, C., Parvizi, J., et al. (2012). Functional MRI of sleep spindles and K-complexes. *Clin. Neurophysiol.* 123, 303–309. doi: 10.1016/j.str.2010.08.012.Structure

Carter, C. S. (1998). Anterior cingulate cortex, error detection, and the online monitoring of performance. *Science* 280, 747–749. doi: 10.1126/science.280.5364.747

Cash, S. S., Halgren, E., Dehghani, N., Rossetti, A. O., Thesen, T., Wang, C., et al. (2009). The human K-complex represents an isolated cortical down-state. *Science* 324, 1084–1087. doi: 10.1126/science.1169626

Colrain, I. M. (2005). The K-complex: a 7-decade history. *Sleep* 28, 255–273. doi: 10.1093/sleep/28.2.255

Cote, K. A., de Lugt, D. R., Langley, S. D., and Campbell, K. B. (2000). Scalp topography of the auditory evoked K-complex in stage 2 and slow wave sleep. *J. Sleep Res.* 8, 263–272. doi: 10.1046/j.1365-2869.1999.00164.x

Cruz-Aguilar, M., Ayala-Guerrero, F., Jimenez-Anguiano, A., Santillan-Doherty, A., and Garcia-Orduna, F. (2015). Sleep in the spider monkey (*Ateles Geoffroyi*): a semi-restrictive, non-invasive, polysomnographic study. *Am. J. Primatol.* 77, 200–210. doi: 10.1002/ajp.22322

Dang-Vu, T. T., Schabus, M., Desseilles, M., Albouy, G., Boly, M., Darsaud, A., et al. (2008). Spontaneous neural activity during human slow wave sleep. *Proc. Natl. Acad. Sci. U.S.A.* 105, 15160–15165. doi: 10.1073/pnas.0801819105

de Gennaro, L., Ferrara, M., and Bertini, M. (2000). The spontaneous K-complex during stage 2 sleep: is it the 'forerunner' of delta waves? *Neurosci. Lett.* 291, 41–43. doi: 10.1016/s0304-3940(00)01366-5

De Gennaro, L., Ferrara, M., Curcio, G., and Cristiani, R. (2001). Antero-posterior EEG changes during the wakefulness–sleep transition. *Clin. Neurophysiol.* 112, 1901–1911. doi: 10.1016/S1388-2457(01)00649-646

De Gennaro, L., Gorgoni, M., Reda, F., Lauri, G., Truglia, I., Cordone, S., et al. (2017). The fall of SLeep K-Complex in Alzheimer Disease. *Sci. Rep.* 7, 1–9. doi: 10.1038/srep39688

Dehaene, S. (2018). The error-related negativity, self-monitoring, and consciousness. *Perspect. Psychol. Sci.* 13, 161–165. doi: 10.1177/1745691618754502

Dolan, R. J., Fletcher, P., Frith, C. D., Friston, K. J., Frackowiak, R. S. J., and Grasby, P. M. (1995). Dopaminergic modulation of impaired cognitive activation in the anterior cingulate cortex in schizophrenia. *Nature* 378, 180–182. doi: 10.1038/378180a0

Drevets, W. C., Savitz, J., and Trimble, M. (2008). The subgenual anterior cingulate cortex in mood disorders. *CNS Spectr.* 13, 663–681. doi: 10.1017/S1092852900013754

El Helou, J., Navarro, V., Depienne, C., Fedirko, E., LeGuern, E., Baulac, M., et al. (2008). K-complex-induced seizures in autosomal dominant nocturnal frontal lobe epilepsy. *Clin. Neurophysiol.* 119, 2201–2204. doi: 10.1016/j.clinph.2008.07.212

Etkin, A. (2010). Functional neuroanatomy of anxiety: a neural circuit perspective. *Curr. Top. Behav. Neurosci.* 2, 251–277. doi: 10.1007/7854_2009_5

Feige, B., Scheffler, K., Esposito, F., Di Salle, F., Hennig, J., and Seifritz, E. (2005). Cortical and subcortical correlates of electroencephalographic alpha rhythm modulation. *J. Neurophysiol.* 93, 2864–2872. doi: 10.1152/jn.00721.2004

Fink, A., and Benedek, M. (2014). EEG alpha power and creative ideation. *Neurosci. Biobehav. Rev.* 44, 111–123. doi: 10.1016/j.neubiorev.2012.12.002

Fletcher, P. C., Happe, F., Frith, U., Baker, S. C., Dolan, R. J., Frackowiak, R. S. J., et al. (1995). Other minds in the brain: a functional imaging study of. *Cognition* 57, 109–128. doi: 10.1016/0010-0277(95)00692-r

Forget, D., Morin, C. M., and Bastien, C. H. (2011). The role of the spontaneous and evoked K-complex in good-sleeper controls and in individuals with insomnia. *Sleep* 34, 1251–1260. doi: 10.5665/sleep.1250

Frauscher, B., von Ellenrieder, N., Dubeau, F., and Gotman, J. (2015). Scalp spindles are associated with widespread intracranial activity with unexpectedly low synchrony. *Neuroimage* 105, 1–12. doi: 10.1016/j.neuroimage.2014.10.048

Fueggle, S. N., Bucks, R. S., and Fox, A. M. (2018). The relationship between naturalistic sleep variation and error monitoring in young adults: an event-related potential (ERP) study. *Int. J. Psychophysiol.* 134, 151–158. doi: 10.1016/J.IJPSYCHO.2018.09.009

Gemignani, A., Menicucci, D., Laurino, M., Piarulli, A., Mastorci, F., Sebastiani, L., et al. (2015). Linking sleep slow oscillations with consciousness theories: new vistas on slow wave sleep unconsciousness. *Arch. Ital. Biol.* 153, 135–143. doi: 10.12871/000398292015238

Geyer, J., Carney, P., and Gilliam, F. (2006). Focal epileptiform spikes in conjuction with K-complexes. *J. Clin. Neurophysiol.* 23, 436–439.

Gonzalez, C., Mak-McCully, R., Rosen, B., Cash, S. S., Chauvel, P., Bastuji, H., et al. (2018). Theta bursts precede, and spindles follow, cortical and thalamic downstates in human NREM sleep. *J. Neurosci.* 38, 9989–10001. doi: 10.1523/JNEUROSCI.0476-18.2018

Gross, D. W., and Gotman, J. (1999). Correlation of high-frequency oscillations with the sleep-wake cycle and cognitive activity in humans. *Neuroscience* 94, 1005–1018. doi: 10.1016/s0306-4522(99)00343-7

Halasz, P. (1981). Generalized epilepsy with spike-wave paroxysms as an epileptic disorder of the function of sleep promotion. *Acta Physiol. Acad. Sci. Hung.* 57, 51–86.

Halász, P. (2005). K-complex, a reactive EEG graphoelement of NREM sleep: an old chap in a new garment. *Sleep Med. Rev.* 9, 391–412. doi: 10.1016/j.smrv.2005.04.003

Halász, P. (2016). The K-complex as a special reactive sleep slow wave - a theoretical update. *Sleep Med. Rev.* 29, 34–40. doi: 10.1016/j.smrv.2015.09.004

Herrmann, M. J., Rommler, J., Ehlis, A., Heidrich, A., and Fallgatter, A. J. (2004). Source localization (LORETA) of the error-related-negativity (ERN/Ne) and positivity (Pe). *Cogn. Brain Res.* 20, 294–299. doi: 10.1016/j.cogbrainres.2004.02.013

Hoedlmoser, K., Heib, D. P. J., Roell, J., Peigneux, P., Sadeh, A., Gruber, G., et al. (2014). Slow sleep spindle activity, declarative memory, and general cognitive abilities in children. *Sleep* 37, 1501–1513. doi: 10.5665/sleep.4000

Hoffstaedter, F., Grefkes, C., Zilles, K., and Eickhoff, S. B. (2013). The "what" and "when" of self-initiated movements. *Cereb. Cortex* 23, 520–530. doi: 10.1093/cercor/bhr391

Ioannides, A., Kostopoulos, G. K. G., Liu, L. L., and Fenwick, P. B. C. (2009). MEG identifies dorsal medial brain activations during sleep. *Neuroimage* 44, 455–468. doi: 10.1016/j.neuroimage.2008.09.030

Ioannides, A. A. (2006). Magnetoencephalography as a research tool in neuroscience: state of the art. *Neuroscientist* 12, 524–544. doi: 10.1177/1073858406293696

Ioannides, A. A. (2007). Dynamic functional connectivity. *Curr. Opin. Neurobiol.* 17, 161–170. doi: 10.1016/j.conb.2007.03.008

Ioannides, A. A. (2017). "Understanding how learning takes place with neuroscience and applying the results to education," in *Brain Function Assessment in Learning*, eds C. Frasson, and G. K. Kostopoulos, (Berlin,: Springer International Publishing AG), 14–35. doi: 10.1007/978-3-319-67615-9

Ioannides, A. A., Bolton, J. P. R., and Clarke, J. J. S. (1990). Continuous probabilistic solutions to the biomagnetic inverse problem. *Physics* 6, 523–542. doi: 10.1088/0266-5611/6/4/005

Ioannides, A. A., Corsi-Cabrera, M., Fenwick, P. B. C., del Rio Portilla, Y., Laskaris, N. A., Khurshudyan, A., et al. (2004). MEG tomography of human cortex and brainstem activity in waking and REM sleep saccades. *Cereb. Cortex* 14, 56–72. doi: 10.1093/cercor/bhg091

Ioannides, A. (2018). Neurofeedback and the neural representation of self: lessons from awake state and sleep. *Front. Hum. Neurosci.* 12:142. doi: 10.3389/fnhum.2018.00142

Ioannides, A.A., liu, L., poghosyan, V., and kostopoulos, G. K. (2017). using meg to understand the progression of light sleep and the emergence and functional roles of spindles and K-complexes. *Front. Hum. Neurosci.* 11:313. doi: 10.3389/fnhum.2017.00313

Jahn, A., Nee, D. E., Alexander, W. H., and Brown, J. W. (2016). distinct regions within medial prefrontal cortex process pain and cognition. *J. Neurosci.* 36, 12385–12392. doi: 10.1523/jneurosci.2180-16.2016

Jahnke, K., von Wegner, F., Morzelewski, A., Borisov, S., Maischein, M., Steinmetz, H., et al. (2012). To wake or not to wake? The two-sided nature of the human K-complex. *Neuroimage* 59, 1631-1638. doi: 10.1016/j.neuroimage.2011.09.013

Januszko, P., Niemcewicz, S., Gajda, T., Wolnyczyk-Gmaj, D., Piotrowska, A. J., Gmaj, B., et al. (2016). Sleepwalking episodes are preceded by arousal-related activation in the cingulate motor area: EEG current density imaging. *Clin. Neurophysiol.* 127, 530–536. doi: 10.1016/j.clinph.2015.01.014

Jegou, A., Schabus, M., Gosseries, O., Dahmen, B., Albouy, G., Desseilles, M., et al. (2019). Cortical reactivations during sleep spindles following declarative learning. *Neuroimage* 195, 104–112. doi: 10.1016/j.neuroimage.2019.03.051

Ji, D., and Wilson, M. A. (2007). Coordinated memory replay in the visual cortex and hippocampus during sleep. *Nat. Neurosci.* 10, 100–107. doi: 10.1038/nn1825

Johnson, L. A., Euston, D. R., Tatsuno, M., and McNaughton, B. L. (2010). Stored-trace reactivation in rat prefrontal cortex is correlated with down-to-up state fluctuation density. *J. Neurosci.* 30, 2650–2661. doi: 10.1523/jneurosci.1617-09.2010

Kerns, J. G., Cohen, J. D., MacDonald, A. W., Cho, R. Y., Stenger, V. A., and Carter, C. S. (2004). Anterior cingulate conflict monitoring and adjustments in control. *Science* 303, 1023–1026. doi: 10.1126/science.1089910

Kokkinos, V., and Kostopoulos, G. K. (2011). Human non-rapid eye movement stage II sleep spindles are blocked upon spontaneous K-complex coincidence and resume as higher frequency spindles afterwards. *J. Sleep Res.* 20, 57–72. doi: 10.1111/j.1365-2869.2010.00830.x

Kokkinos, V., Koupparis, A. M., and Kostopoulos, G. K. (2013). An intra-K-complex oscillation with independent and labile frequency and topography

in NREM sleep. *Front. Hum. Neurosci.* 7:163. doi: 10.3389/fnhum.2013.00163

Kryger, M., Roth, T., and Dement, W. (2017). *Principles and Practice of sleep Medicine*. 6th Edn. Philadelphia: Elsevier.

Kubicki, S., Scheuler, W., Jobert, M., and Pastelak-Price, C. (1989). [The effect of age on sleep spindle and K complex density]. *EEG EMG Z Elektroenzephalogr. Elektromyogr. Verwandte Geb.* 20, 59–63.

Larson-Prior, L. J., Zempel, J. M., Nolan, T. S., Prior, F. W., Snyder, A. Z., and Raichle, M. E. (2009). Cortical network functional connectivity in the descent to sleep. *Proc. Natl. Acad. Sci. U.S.A.* 106, 4489-4494. doi: 10.1073/pnas.0900924106

Laurino, M., Menicucci, D., Piarulli, A., Mastorci, F., Bedini, R., Allegrini, P., et al. (2014). Disentangling different functional roles of evoked K-complex components: mapping the sleeping brain while quenching sensory processing. *Neuroimage* 86, 433-445. doi: 10.1016/j.neuroimage.2013.10.030

Lieberman, M. D., and Eisenberger, N. I. (2015). The dorsal anterior cingulate cortex is selective for pain: results from large-scale reverse inference. *Proc. Nat. Acad. Sci. U.S.A.* 112, 15250–15255. doi: 10.1073/pnas.1515083112

Loomis, A. L., Harvey, E., and Hobart, G. (1938). Disturbance patterns in sleep. *J Neurophysiol.* 2, 413–430.

Lu, S. T., Kajola, M., Joutsiniemi, S. L., Knuutila, J., and Hari, R. (1992). Generator sites of spontaneous MEG activity during sleep. *Electroencephalogr. Clin. Neurophysiol.* 82, 182–196. doi: 10.1016/0013-4694(92)90166-f

Luu, P., and Pederson, S. M. (2004). "The anterior cingulate cortex: regulating Actions in Context," in *Cognitive Neuroscience of Attention*, ed. M. I. Posner, (New York: Guilford Publications Inc.), 232–244.

Mak-McCully, R. A., Rosen, B. Q., Rolland, M., Regis, J., Bartolomei, F., Rey, M., et al. (2015). Distribution, amplitude, incidence, co-occurrence, and propagation of human K-Complexes in focal transcortical recordings. *eNeuro* 2, 1–26. doi: 10.1523/ENEURO.0028-15.2015

Maquet, P. (2010). Understanding non rapid eye movement sleep through neuroimaging. *World J. Biol. Psychiatr.* 11, 9–15. doi: 10.3109/15622971003637736

Marini, G., Ceccarelli, P., and Mancia, M. (2004). Spontanrous K-COMPLEXES in Behaving rats. *Arch. Ital. Biol.* 142, 59–67.

Massimini, M., Ferrarelli, F., Huber, R., Esser, S. K., Singh, H., and Tononi, G. (2005). Breakdown of cortical effective connectivity during sleep. *Science* 309, 2228–2232. doi: 10.1126/science.1117256

Mayberg, S. (1997). Limbic-cortical dysregulation: depression. *J. Neuropsychiatr.* 9, 471–481. doi: 10.1176/jnp.9.3.471

McKinney, S. M., Dang-Vu, T. T., Buxton, O. M., Solet, J. M., and Ellenbogen, J. M. (2011). Covert waking brain activity reveals instantaneous sleep depth. *PLoS One* 6:e17351. doi: 10.1371/journal.pone.0017351

Moradi, F., Liu, L. C., Cheng, K., Waggoner, R. A., Tanaka, K., and Ioannides, A. A. (2003). Consistent and precise localization of brain activity in human primary visual cortex by MEG and fMRI. *Neuroimage* 18, 595–609. doi: 10.1016/s1053-8119(02)00053-8

Murphy, M., Huber, R., Esser, S. A., Riedner, B., Massimini, M., Ferrarelli, F., et al. (2012). The cortical topography of local sleep. *Curr. Top. Med. Chem.* 11, 2438–2446. doi: 10.2174/156802611797470303

Murphy, M., Riedner, B. A., Huber, R., Massimini, M., Ferrarelli, F., and Tononi, G. (2009). Source modeling sleep slow waves. *Proc. Natl. Acad. Sci. U.S.A.* 106, 1608-1613. doi: 10.1073/pnas.0807933106

Niiyama, Y., Satoh, N., Kutsuzawa, O., and Hishikawa, Y. (1996). Electrophysiological evidence suggesting that sensory stimuli of unknown origin induce spontaneous K-complexes. *Electroencephalogr. Clin. Neurophysiol.* 98, 394–400. doi: 10.1016/0013-4694(96)95103-95102

Numminen, J., Mäkelä, J. P., and Hari, R. (1996). Distributions and sources of magnetoencephalographic K-complexes. *Electroencephalogr. Clin. Neurophysiol.* 99, 544–555. doi: 10.1016/s0921-884x(96)95712-4

O 'connell, R. G., Dockree, P. M., Bellgrove, M. A., Kelly, S. P., Hester, R., Garavan, H., et al. (2007). The role of cingulate cortex in the detection of errors with and without awareness: a high-density electrical mapping study. *Eur. J. Neurosci.* 25, 2571–2579. doi: 10.1111/j.1460-9568.2007.05477.x

Pardo, J. V., Pardo, P. J., Janer, K. W., and Raichlet, M. E. (1990). The anterior cingulate cortex mediates processing selection in the Stroop attentional conflict paradigm. *Proc. Nat. Acad. Sci. U.S.A.* 87, 256–259. doi: 10.1073/pnas.87.1.256

Passingham, R. E. (1995). *The Frontal Lobes and Voluntary Action*. Oxford: Oxford University Press.

Paus, T. (2001). Primate anterior cingulate cortex. *Nat. Rev. Neurosci.* 2, 417–424. doi: 10.1038/35077500

Perrin, F., García-Larrea, L., Mauguière, F., and Bastuji, H. (1999). A differential brain esponse to the subject's own name persists during sleep. *Clin. Neurophysiol.* 110, 2153–2164. doi: 10.1016/s1388-2457(99)00177-7

Picard, N., and Strick, P. L. (1996). Motor areas of the medial wall: a review of their location and functional activation. *Cereb. Cortex* 6, 342–353. doi: 10.1093/cercor/6.3.342

Picard, N., and Strick, P. L. (2001). Imaging the premotor areas. *Curr. Opin. Neurobiol.* 11, 663–672. doi: 10.1016/S0959-4388(01)00266-265

Poghosyan, V., and Ioannides, A. A. (2008). Attention modulates earliest responses in the primary auditory and visual cortices. *Neuron* 58, 802–813. doi: 10.1016/j.neuron.2008.04.013

Pratt, H., Berlad, I., and Lavie, P. (1999). 'Oddball' event-related potentials and information processing during REM and non-REM sleep. *Clin. Neurophysiol.* 110, 53–61. doi: 10.1016/S0168-5597(98)00044-46

Pugin, F., Metz, A. J., Wolf, M., Achermann, P., Jenni, O. G., and Huber, R. (2015). Local increase of sleep slow wave activity after three weeks of working memory training in children and adolescents. *Sleep* 38, 607–614. doi: 10.5665/sleep.4580

Ramakrishnan, M., Sartory, G., van Beekum, A., Lohrmann, T., and Pietrowsky, R. (2012). Sleep-related cognitive function and the K-complex in schizophrenia. *Behav. Brain Res.* 234, 161–166. doi: 10.1016/j.bbr.2012.06.019

Rechtschaffen, A., and Kales, A. (1968). *A Manual of Standardized Terminology, Techniques and Scoring System for Sleep Stages of Human Subjects*. Washington DC: US Government Printing Office.

Rodenbeck, A., Binder, R., Geisler, P., Danker-Hopfe, H., Lund, R., Raschke, F., et al. (2006). A review of sleep EEG patterns. Part I: a compilation of amended rules for their visual recognition according to rechtschaffen and kales. *Somnologie* 10, 159–175. doi: 10.1111/j.1439-054x.2006.00101.x

Roth, M., Shaw, J., and Green, J. (1956). The form, voltage distribution and physiological significance of the K-complex. *Electroencephalogr Clin NeurophysioI* 8, 385–402. doi: 10.1016/0013-4694(56)90004-9

Ruan, J., Bludau, S., Palomero-Gallagher, N., Caspers, S., Mohlberg, H., Eickhoff, S. B., et al. (2018). Cytoarchitecture, probability maps, and functions of the human supplementary and pre-supplementary motor areas. *Brain Struct. Funct.* 223, 4169–4186. doi: 10.1007/s00429-018-1738-1736

Sallinen, M., Kaartinen, J., and Lyytinen, H. (1997). Precursors of the evoked K-complex in event-related brain potentials in stage 2 sleep. *Electroencephalogr Clin Neurophysi.* 102, 363–373. doi: 10.1016/s0013-4694(96)96614-6

Seneviratne, U., Cook, M., and D'Souza, W. (2016). Epileptiform K-Complexes and sleep spindles: an underreported phenomenon in genetic generalized epilepsy. *J Clin Neurophysiol.* 33, 156–161. doi: 10.1097/WNP.0000000000000239

Shackman, A. J., Salomons, T. V., Slagter, H. A., Fox, A. S., Winter, J. J., and Davidson, R. J. (2011). The integration of negative affect, pain and cognitive control in the cingulate cortex. *Nat. Rev. Neurosci.* 12, 154–167. doi: 10.1038/nrn2994

Siclari, F., and Tononi, G. (2017). Local aspects of sleep and wakefulness. *Curr. Opin. Neurobiol.* 44, 222–227. doi: 10.1016/j.conb.2017.05.008

Staresina, B. P., Ole Bergmann, T., Bonnefond, M., van der Meij, R., Jensen, O., Deuker, L., et al. (2015). Hierarchical nesting of slow oscillations, spindles and ripples in the human hippocampus during sleep. *Nat. Neurosci.* 18, 1679–1686. doi: 10.1038/nn.4119

Steele, J. D., and Lawrie, S. M. (2004). Segregation of cognitive and emotional function in the prefrontal cortex: a stereotactic meta-analysis. *Neuroimage* 21, 868–875. doi: 10.1016/j.neuroimage.2003.09.066

Steriade, M., and Amzica, F. (1998). Slow sleep oscillation, rhythmic K-complexes, and their paroxysmal developments. *J. Sleep Res.* 7 (Suppl 1), 30–35. doi: 10.1046/j.1365-2869.7.s1.4.x

Talairach, J., and Tournoux, P. (1988). *Co-planar Stereotaxic Atlas of the Human Brain: 3-Dimensional Proportional System - an Approach to Cerebral Imaging*. New York, NY: Thieme Medical Publishers.

Taylor, J. G., Ioannides, A. A., and Müller-Gärtner, H. W. (1999). Mathematical analysis of lead field expansions. *IEEE Trans. Med. Imaging* 18, 151–163. doi: 10.1109/42.759120

Taylor, S. F., Stern, E. R., and Gehring, W. J. (2007). Neural systems for error monitoring: Recent findings and theoretical perspectives. *Neuroscientist* 13, 160–172. doi: 10.1177/1073858406298184

Terzaghi, M., Sartori, I., Tassi, L., Rustioni, V., Proserpio, P., Lorusso, G., et al. (2012). Dissociated local arousal states underlying essential clinical features of non-rapid eye movement arousal parasomnia: an intracerebral stereo-electroencephalographic study. *J. Sleep Res.* 21, 502–506. doi: 10.1111/j.1365-2869.2012.01003.x

Tononi, G., and Cirelli, C. (2006). Sleep function and synaptic homeostasis. *Sleep Med. Rev.* 10, 49–62. doi: 10.1016/j.smrv.2005.05.002

Tzelepi, A., Ioannides, A. A., and Poghosyan, V. (2001). Early (N70m) neuromagnetic signal topography and striate and extrastriate generators following pattern onset quadrant stimulation. *Neuroimage* 13, 702-718. doi: 10.1006/nimg.2000.0735

Vogt, B. A., and Gabriel, M. (eds). (1993). *Neurobiology of Cingulate Cortex and Limbic Thalamus_ A Comprehensive Handbook*. Basel: Birkhäuser Boston.

Voysey, Z., Martín-López, D., Jiménez-Jiménez, D., Selway, R. P., Alarcón, G., and Valentín, A. (2015). Electrical stimulation of the anterior cingulate gyrus induces responses similar to K-complexes in awake humans. *Brain Stimul.* 8, 881-890. doi: 10.1016/j.brs.2015.05.006

Wauquier, A., Aloe, L., and Declerk, A. (1995). K-complexes: are they signs of arousal or sleep protective? *J. Sleep Res.* 4, 138–143. doi: 10.1111/j.1365-2869.1995.tb00162.x

Wennberg, R. (2010). Intracranial cortical localization of the human K-complex. *Clin. Neurophysiol.* 121, 1176–1186. doi: 10.1016/j.clinph.2009.12.039

Wennberg, R., and Cheyne, D. (2013). On noninvasive source imaging of the human K-complex. *Clin. Neurophysiol.* 124, 941–955. doi: 10.1016/j.clinph.2012.10.022

Wilson, M. T., Steyn-Ross, D. A., Sleigh, J. W., Steyn-Ross, M. L., Wilcocks, L. C., and Gillies, I. P. (2006). The K-complex and slow oscillation in terms of a mean-field cortical model. *J. Comput. Neurosci.* 21, 243–257. doi: 10.1007/s10827-006-7948-6

Wolfgang, K. (1999). EEG alpha and theta oscillations reflect cognitive and memory performance: a review and analysis. *Brain Res. Rev.* 29, 169–195. doi: 10.1016/S0165-0173(98)00056-53

Yoshida, H., Iramina, K., and Ueno, S. (1996). Source models of sleep spindles using MEG and EEG measurements. *Brain Topogr.* 8, 303–307. doi: 10.1007/bf01184789

Conflict of Interest Statement: AI and LL were employed by the company AAISCS.

The remaining author declares that the research was conducted in the absence of any commercial or financial relationships that could be construed as a potential conflict of interest.

Copyright © 2019 Ioannides, Liu and Kostopoulos. This is an open-access article distributed under the terms of the Creative Commons Attribution License (CC BY). The use, distribution or reproduction in other forums is permitted, provided the original author(s) and the copyright owner(s) are credited and that the original publication in this journal is cited, in accordance with accepted academic practice. No use, distribution or reproduction is permitted which does not comply with these terms.

frontiers in Neuroscience

OPINION
published: 20 August 2019
doi: 10.3389/fnins.2019.00813

Local Sleep Oscillations: Implications for Memory Consolidation

Maya Geva-Sagiv [1,2]* *and Yuval Nir* [2,3,4]*

[1] Department of Neurosurgery, University of California, Los Angeles, Los Angeles, CA, United States, [2] Sagol School of Neuroscience, Tel Aviv University, Tel Aviv, Israel, [3] Department of Physiology and Pharmacology, Sackler School of Medicine, Tel Aviv University, Tel Aviv, Israel, [4] Functional Neurophysiology and Sleep Research Lab, Tel-Aviv Sourasky Medical Center, Tel Aviv, Israel

Keywords: sleep, memory, spindles, ripples, coherence, regional

INTRODUCTION

Accumulating evidence suggests that sleep is important for plasticity and memory consolidation (Maquet, 2001; Walker and Stickgold, 2004; Datta and Maclean, 2007; Diekelmann and Born, 2010; Tononi and Cirelli, 2014; Dudai et al., 2015)—the transformation of new labile memories encoded in wakefulness into stable representations that integrate into long-term memory networks. A central model accounting for memory consolidation during sleep is that of coupling between hippocampal (HC) and neocortical networks (Buzsáki, 1996). According to this two-stage model of memory formation [also termed the hippocampal—neocortical dialogue model (Buzsáki, 1989)], the dominant direction of information flow across the brain differs between wake and sleep periods. During wakefulness, acquisition of sensory information mainly drives signal propagation from cortex to hippocampus (HC) (Buzsáki, 1998; Mormann et al., 2008). By contrast, during subsequent non-rapid eye movement (NREM) sleep, this model suggests a central role for information flow from HC to cortex especially around sharp-wave ripples (SWRs) events (Buzsáki, 1998). Accordingly, slow waves that originate in the neocortex repeatedly reactivate the newly encoded HC information when SWRs occur, driving subsequent activity in select cortical circuits (Siapas and Wilson, 1998). However, it is clear that information flow is not strictly unidirectional (Wagner et al., 2010) and may involve complex loops (Rothschild et al., 2017). HC reactivation tends to co-occur with sleep spindles that optimize plasticity (Seibt et al., 2017), resulting in long-term modification of synaptic efficacy. Thus, hippocampal–neocortical coupling requires interregional cross-frequency coordination between sleep oscillations, including slow waves and sleep spindles in thalamo-cortical circuits as well as HC ripples.

The underlying prevalent assumption is that sleep oscillations (slow waves in particular) are global events that co-occur nearly simultaneously across different brain regions. But in fact, they have been described as traveling waves propagating from anterior-to-posterior cortex (Massimini et al., 2004), and they typically occur out of phase across different cortical sites (Nir et al., 2011; Vyazovskiy et al., 2011; Malerba et al., 2019). How can we reconcile models requiring co-occurrence of sleep oscillations with accumulating evidence of non-uniform timing of oscillations across the brain? In this article, we first review the current data that sheds light on this question, and highlight recent studies that link *regional* coupling of sleep oscillations with consolidation of specific memories. Then, we highlight the gap between sleep and memory theory and experimental evidence. Based on studies that monitor and manipulate specific cortical circuits, we propose that coupling can occur between sleep oscillations in general, and between HC and cortex specifically, but that such coupling likely involves different brain regions at each point in time, contributing to memory consolidation in select circuits.

OPEN ACCESS

Edited by:
Giulio Bernardi,
IMT School for Advanced Studies Lucca, Italy

Reviewed by:
Roy Cox,
University of Bonn, Germany
Nicola Cellini,
University of Padova, Italy

***Correspondence:**
Maya Geva-Sagiv
mayagevasagiv@gmail.com
Yuval Nir
yuvalnir.tau@gmail.com

Specialty section:
This article was submitted to Sleep and Circadian Rhythms, a section of the journal Frontiers in Neuroscience

Received: *29 May 2019*
Accepted: *22 July 2019*
Published: *20 August 2019*

Citation:
Geva-Sagiv M and Nir Y (2019) Local Sleep Oscillations: Implications for Memory Consolidation. Front. Neurosci. 13:813. doi: 10.3389/fnins.2019.00813

SLOW WAVES, SPINDLES, AND THEIR REGIONAL MODULATION FOLLOWING LEARNING

Slow waves and sleep spindles constitute electroencephalographic (EEG) hallmarks of NREM sleep (Gibbs and Gibbs, 1950; Steriade, 2003). These robust oscillations are easily identified using non-invasive EEG and form the main criterion for sleep stage definition across mammalian species (Iber et al., 2007). Both oscillations are implicated in memory consolidation as we review below. While EEG represents summed activity across large cortical territories (Nunez, 1995), we will focus here on accumulating evidence that characterizes slow waves and spindles as local phenomena.

Neocortical slow waves reflect slow (1–4 Hz) alternations of cellular active (up-) and inactive (down-) states of neuronal activity (Steriade et al., 2001; Nir et al., 2011). Although not perfectly coherent, these oscillations represent the most synchronous event in the healthy brain, and traveling waves across large cortical territories may mediate diverse sleep functions including downregulation of synaptic strengths (Vyazovskiy et al., 2008; Norimoto et al., 2018), maintenance of cellular homeostasis (Tononi and Cirelli, 2014), and mediation of memory consolidation and synaptic plasticity (Diekelmann and Born, 2010).

Slow waves are thought to provide a temporal frame for a dialogue between the neocortex and subcortical structures, which is necessary for redistributing memories for long-term storage (Sirota et al., 2003; Sirota and Buzsáki, 2005; Marshall and Born, 2007): On a global scale, a strong increase in EEG coherence is observed during NREM sleep following learning in humans (Mölle et al., 2004, 2009). On a local scale, changes in sleep oscillations occur in specific cortical regions that were involved in encoding, both in rodents (Vyazovskiy et al., 2000; Hanlon et al., 2009) and in humans (Huber et al., 2004, 2006; Mölle et al., 2009). Although very commonly regarded as a global event occurring near-simultaneously across the cortex, cortical up-states are typically ignited locally in prefrontal cortex and spread to other cortical areas over tens to a few 100 ms (Massimini et al., 2004). Neural recordings in rodents were able to pinpoint the ignition source to layer 5 cells of cortex (Luczak et al., 2007; Chauvette et al., 2010; Beltramo et al., 2013). Intracranial recordings from epilepsy patients reveal that most slow waves, and the underlying active and inactive neuronal states, occur locally (Nir et al., 2011). This observation goes beyond potential confounds of epilepsy, since it is readily observed also in rodents and in cats (Chauvette et al., 2011; Vyazovskiy et al., 2011). Especially during late sleep, circumscribed slow waves are also detected via EEG recordings (Siclari et al., 2014; Bernardi et al., 2018).

Sleep spindles are classically defined as waxing-and-waning 10–16 Hz oscillations lasting 0.5–2 s (Gibbs and Gibbs, 1950). Sleep spindles are implicated in plasticity and trigger synaptic long-term potentiation via calcium transients that are believed to prime cortical networks for the long-term storage of memory representations (Timofeev et al., 2002; Rosanova and Ulrich, 2005; Ulrich, 2016; Niethard et al., 2018). On a global scale, increased spindle activity is observed during NREM sleep following learning of both declarative tasks and procedural motor skills (Gais et al., 2002; Eschenko et al., 2006; Fogel and Smith, 2006; Morin et al., 2008; Mölle et al., 2009). On a local scale, regional spindle activity correlates with offline improvement in consolidation of motor memories (Nishida and Walker, 2007). Importantly, despite the fact that spindles engage thalamo-cortical "loops," they are also mostly a local phenomenon occurring in select circuits at a time (Rasch and Born, 2013). Even when observed near-simultaneously across regions, their precise timings varies across cortical locations (Nir et al., 2011; Muller et al., 2016). Accordingly, learning different types of memories changes the properties of spindles in different topographically-restricted regions (Bergmann et al., 2012; Cox et al., 2014).

Not only are slow waves and sleep spindles each related to memory consolidation separately, recent evidence suggests that their precise interaction may play a role. For example, many sleep spindles tend to be "nested" in the "up" phase of the slow oscillation as revealed by phase-amplitude coupling (PAC) analysis (Diekelmann and Born, 2010; Staresina et al., 2015). However, slow wave and spindle oscillations behave as traveling waves at a whole-brain scale [for an extensive review see (Muller et al., 2018)], which translates to a delay of up to hundreds of milliseconds between oscillation peaks across different cortical areas. Thus, the temporal relationship between sleep oscillations across cortical regions varies substantially. Locally, within each brain region, the coupling of sleep spindles to slow wave up-states occurs in a topographically restricted fashion (Cox et al., 2014) and local slow waves coordinate spindle activity at virtually every cortical site (Cox et al., 2018). In contrast, coupling between distant brain regions does not necessarily occur regularly. For example, while parietal spindles are coupled to parietal slow waves, they are not necessarily coupled with frontal slow waves (**Figure 1**). Along this line, the strength of slow wave-spindle coupling differs between global and local slow waves, as well as between cortical locations (Malerba et al., 2019), highlighting the complexity of cross-frequency coupling between sleep oscillations across different brain regions.

INTERREGIONAL COUPLING BETWEEN HIPPOCAMPUS AND SPECIFIC CORTICAL REGIONS DURING SLEEP, AND ITS ROLE IN SUCCESSFUL MEMORY CONSOLIDATION

During NREM sleep, hippocampal (HC) activity is concentrated in sharp wave ripple (SWR) events, which correspond to a summed synchronous depolarization of a large fraction of the neurons in the CA1 sub region of the hippocampus (O'keefe and Nadel, 1978; Buzsáki et al., 1983; Buzsáki, 1986). Extensive animal research established a tight link between HC SWRs and memory consolidation in both wakefulness and sleep: SWRs accompany the sleep-associated re-activation of HC neuron ensembles that were active during the preceding awake learning experience (Nadasdy et al., 1999; Eschenko et al., 2008; Peyrache et al., 2009). SWRs occurrence increases in previously potentiated synaptic circuits (Behrens et al., 2005), and may

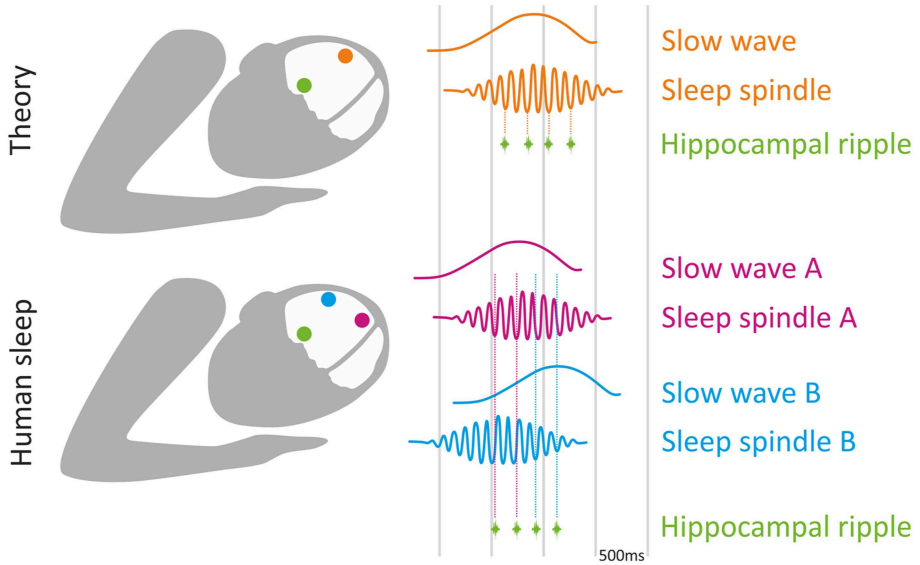

FIGURE 1 | Local sleep oscillations and memory consolidation: theory vs. experimental findings. **(Top)** Theory suggests that the nesting of hippocampal ripples (green) to sleep spindle troughs (orange), which in turn are nested in slow wave up-phase (orange), is critical for memory consolidation during sleep. **(Bottom)** Experimental data indicates that timing of both slow waves and spindles (as well as spindle nesting phase; Andrillon et al., 2011) varies across cortical regions (purple and blue), such that the nesting of each ripple (green) inevitably corresponds to different cortical locations (dashed vertical lines). Thus, each hippocampal ripple occurring at a specific time is associated with hippocampal-cortical coupling in different circuits, likely supporting memory consolidation related to that circuit.

further modulate synaptic strength (Buzsáki et al., 1987; King et al., 1999; Norimoto et al., 2018). Finally, selective manipulation of SWRs through electrical or optogenetic stimulation in HC modulates memory consolidation (Girardeau et al., 2009; Ego-Stengel and Wilson, 2010; Fernandez-Ruiz et al., 2019). Thus, SWRs represent important time epochs for offline HC activity, and their occurrence in NREM sleep carries a privileged role in plasticity and memory consolidation.

In deep layers of medial prefrontal cortex (mPFC), where most of the HC fibers make contacts, pyramidal cells respond phasically to SWRs (Siapas and Wilson, 1998; Mölle et al., 2006; Peyrache et al., 2011). Conversely, the occurrence of SWRs is modulated by neocortical inputs (Isomura et al., 2006), revealing bidirectional interactions between HC and cortex. Multiple studies revealed the fine temporal relationship between SWRs and neocortical sleep oscillations (Sirota et al., 2003; Sirota and Buzsáki, 2005; Staresina et al., 2015; Wang and Ikemoto, 2016), in which SWRs tend to be phase-locked to cortical spindle troughs, which in turn are phase-locked to slow wave up-states. Human studies are typically limited in SWR detection, as non-invasive EEG cannot reliably monitor local high-frequency activities in deep brain structures. Nevertheless, sleep studies in epilepsy patients implanted with intracranial electrodes support the notion that SWRs during sleep preferentially occur at specific times in relation to neocortical slow waves and spindles (Clemens et al., 2007, 2011; Nir et al., 2011; Staresina et al., 2015), extending the temporal tuning finding from rodents to human sleep. Given that spindles are mostly a local phenomenon, and their precise timing varies across cortical locations (Nir et al., 2011; Muller et al., 2016), temporal tuning between one cortical area and HC during a specific spindle does not necessarily imply temporal tuning between other cortical areas to HC at that time (**Figure 1**).

At present, a gap exists between theory on how hippocampal-cortical coupling supports memory consolidation (usually considering the entire cortex as a uniform entity) and the available experimental evidence highlighting that slow waves, spindles, and SWRs occur at different times in different regions.

COUPLING OF SLEEP OSCILLATIONS IN SELECT BRAIN REGIONS AND THE CONSOLIDATION OF SPECIFIC MEMORIES

A potential way to transcend this discrepancy is to consider that coupling between sleep oscillations may occur, but may involve select circuits at each given time—supporting memory consolidation in specific associated tasks. We illustrate this by considering two recent studies in rodents that causally link the coupling of sleep oscillations across specific regions to the consolidation of specific memories. A recent study (Maingret et al., 2016) established that co-occurrence of HC ripples and medial prefrontal cortex (mPFC) slow waves and spindles correlates with memory consolidation in a spatial learning task. Boosting this coupling by delivering SWR-triggered electrical stimulation to deep cortical layers causally improved memory performance on this hippocampus-dependent task (Maingret et al., 2016). Another study used a different closed-loop stimulation protocol to improve memory performance in a hippocampal dependent task: frontal slow waves triggered

optogenetic stimulation of the thalamic reticular nucleus during sleep, resulting in time-locked frontal sleep spindles, and HC SWRs (Latchoumane et al., 2017). Notably, these experiments, as well as studies selectively manipulating SWRs, report changes in coupling between SWRs in a specific hippocampal (HC) sub-field [mostly CA1 (Girardeau et al., 2009; Ego-Stengel and Wilson, 2010; Maingret et al., 2016)], and spindles in specific regions [either mPFC (Siapas and Wilson, 1998) or anterior cingulate cortex (Wang and Ikemoto, 2016)]. Thus, these findings demonstrate that although each SWR may be coupled with slow waves and spindle oscillations in different brain regions (**Figure 1**), HC-cortical coupling in select circuits may support memory consolidation in specific tasks.

Although the majority of sleep and memory experiments focus on temporal coupling between HC and cortex, several studies also demonstrate the importance of coherence between specific cortical regions. Miyamoto and colleagues demonstrated that coordinating slow wave activity between layer-5 primary somatosensory cortex and secondary motor cortex via synchronous optogenetic stimulation at 2 Hz enhances memory consolidation of a newly learned non-declarative skill. Asynchronous stimulation of these two regions (using opposite phases) reduced performance relative to the no-intervention controls (Miyamoto et al., 2016).

These experiments (Maingret et al., 2016; Miyamoto et al., 2016; Latchoumane et al., 2017) highlight the importance of both temporal and anatomical specificity of interventions designed to boost the coupling between sleep oscillations across two brain regions. Accordingly, a brief delay in stimulation timing was enough to abolish the memory enhancement that is observed when locking stimulation accurately to HC SWRs (Maingret et al., 2016).

HOW CAN WE IMPROVE CAUSAL INTERVENTIONS IN HUMANS LINKING SLEEP OSCILLATIONS TO LEARNING AND MEMORY?

Over the last decade, several studies have gone beyond demonstrating the existence of correlation between sleep oscillations (slow waves, spindles) and subsequent memory recall (e.g., Gais et al., 2002; Huber et al., 2004, 2006; Mölle et al., 2009; Fogel and Smith, 2011; Van Der Helm et al., 2011; Tamminen et al., 2013), to interventions that link an experimentally-induced increase in the amplitude of a sleep oscillation to human learning (Marshall et al., 2006; Ngo et al., 2013; Ladenbauer et al., 2017, but also see Bueno-Lopez et al., 2019). A recent study demonstrated that causal interventions affecting memory consolidation may also be applied locally. Unilateral olfactory stimulation induced "local targeted memory reactivation" and elicited both behavioral and EEG effects that were largely lateralized to one hemisphere (see preprint at - Bar et al., 2019). Such lateralization seems more difficult to demonstrate in the auditory modality (Simor et al., 2018), possibly because cortical auditory processing is less lateralized compared to vision and olfaction (Schnupp et al., 2011).

One line of causal interventions during sleep employs a temporally tuned approach, to perform "closed-loop" stimulation, phase-locked to endogenous sleep oscillations. For example, auditory stimulation in phase with slow wave up-states (as measured with scalp EEG) enhances slow wave activity and slow wave-spindle coupling, and improves the consolidation of declarative memory (Ngo et al., 2013; Lafon et al., 2017; Ketz et al., 2018; Goldi et al., 2019). Given that the timing of sleep oscillations differs across cortical regions, choosing a specific EEG channel to trigger stimulation, phase-locks the intervention to the timing of a specific cortical region. An elegant human study that took this into consideration shows degradation of learning efficiency following focal perturbation of slow wave activity over the motor cortex (Fattinger et al., 2017). Importantly, the perturbation was ineffective when targeting temporo-parietal cortex slow waves (Fattinger et al., 2017). Such an experimental approach draws our attention to the role of *local* sleep oscillations in specific cortical areas for consolidation of different types of memory tasks. The exact timing of intervention is critical for enhancing memory consolidation, and changing the stimulation phase may abolish memory effects completely (Ngo et al., 2013; Goldi et al., 2019).

Though impossible to directly compare, memory enhancement in humans appears to be modest and less pronounced compared to memory enhancement following interventions manipulating spindles and SWRs in rodents (Maingret et al., 2016; Latchoumane et al., 2017). We suggest that the precise timing of the intervention is critical for memory enhancement and may constitute an obstacle we need to overcome to obtain larger effects in human subjects. At present, human interventions typically rely on scalp EEG summating neuronal activity across wide regions, whereas animal studies track activity of specific neural populations in deep brain areas.

When studying coherence of EEG sleep oscillations between different cortical sites in humans, an important consideration is the tight and often underappreciated relation between (i) the amplitude of a sleep oscillation (e.g., slow wave or sleep spindle) as recorded with scalp EEG or intracranially, and (ii) its coherent occurrence across neuronal ensembles. Put simply, high-amplitude oscillations often reflect high synchronization between neuronal populations. Indeed we have shown, based on local iEEG recordings, that the amplitude of each slow wave recorded on the scalp is tightly correlated with the number of distant brain regions where this wave occurs near-simultaneously, such that high-amplitude slow waves are global (Nir et al., 2011). In the case of sleep spindles, high-amplitude events in scalp EEG likely reflect a precise coordination among neurons in cortex, thalamus, and reticular thalamic nucleus (Nunez, 1995). This means that many findings that link EEG slow wave or spindle amplitude/power in a given region to learning and memory may in fact imply stronger coherence within relevant neuronal circuits. Notwithstanding this, other factors also influence the amplitude of EEG sleep oscillations, as asynchronous local generators can also produce an unexpectedly large scalp signal (Von Ellenrieder et al., 2016). Further research is needed in order to separate the contribution of high

oscillatory power vs. high coherence between specific areas to memory consolidation.

FUTURE OUTLOOKS

Technological advances should allow accurate mapping of the roles of specific spatially-circumscribed cortical sleep events in the consolidation of long term memory in humans, and separate them from other functions carried out by events that travel and encompass the whole cortex. We expect that maturation of novel electrophysiology tools will improve both spatial and temporal resolutions of monitoring human brain activity in real-time (Khodagholy et al., 2017; Liu et al., 2018), thereby allowing accurate experimental interventions in humans and improving their electrophysiological and cognitive effects. For such advances to make an impact on basic scientific understanding and create genuine clinical utility, it is imperative that theory is fine-tuned according to the available data, and that we go beyond considering the sleeping brain as a uniform coherent entity.

AUTHOR CONTRIBUTIONS

All authors listed have made a substantial, direct and intellectual contribution to the work, and approved it for publication.

FUNDING

This study was supported by Sagol School of Neuroscience and The Naomi Foundation/GRTF Program at Tel Aviv University, The Rothschild Foundation (MG-S), Adelis Foundation, and the US-Israel Binational Science Foundation (BSF) grant # 2017628 (YN).

ACKNOWLEDGMENTS

We thank Anat Arzi and Aaron Krom for discussions and comments on the manuscript, and Sharon Tsach for graphics assistance.

REFERENCES

Andrillon, T., Nir, Y., Staba, R. J., Ferrarelli, F., Cirelli, C., Tononi, G., et al. (2011). Sleep spindles in humans: insights from intracranial EEG and unit recordings. *J. Neurosci.* 31, 17821–17834. doi: 10.1523/JNEUROSCI.2604-11.2011

Bar, E., Arzi, A., Perl, O., Livne, E., Sobel, N., Dudai, Y., et al. (2019). Local targeted memory reactivation in human sleep. *bioRxiv [Preprint]*. doi: 10.1101/539114

Behrens, C. J., Van Den Boom, L. P., De Hoz, L., Friedman, A., and Heinemann, U. (2005). Induction of sharp wave-ripple complexes *in vitro* and reorganization of hippocampal networks. *Nat. Neurosci.* 8, 1560–1567. doi: 10.1038/nn1571

Beltramo, R., D'urso, G., Dal Maschio, M., Farisello, P., Bovetti, S., Clovis, Y., et al. (2013). Layer-specific excitatory circuits differentially control recurrent network dynamics in the neocortex. *Nat. Neurosci.* 16, 227–234. doi: 10.1038/nn.3306

Bergmann, T. O., Mölle, M., Diedrichs, J., Born, J., and Siebner, H. R. (2012). Sleep spindle-related reactivation of category-specific cortical regions after learning face-scene associations. *Neuroimage* 59, 2733–2742. doi: 10.1016/j.neuroimage.2011.10.036

Bernardi, G., Siclari, F., Handjaras, G., Riedner, B. A., and Tononi, G. (2018). Local and widespread slow waves in stable NREM sleep: evidence for distinct regulation mechanisms. *Front. Hum. Neurosci.* 12:248. doi: 10.3389/fnhum.2018.00248

Bueno-Lopez, A., Eggert, T., Dorn, H., and Danker-Hopfe, H. (2019). Slow oscillatory transcranial direct current stimulation (so-tDCS) during slow wave sleep has no effects on declarative memory in healthy young subjects. *Brain Stimul.* 12, 948–958. doi: 10.1016/j.brs.2019.02.012

Buzsáki, G. (1986). Hippocampal sharp waves: their origin and significance. *Brain Res.* 398, 242–252. doi: 10.1016/0006-8993(86)91483-6

Buzsáki, G. (1989). Two-stage model of memory trace formation: a role for "noisy" brain states. *Neuroscience* 31, 551–570. doi: 10.1016/0306-4522(89)90423-5

Buzsáki, G. (1996). The hippocampo-neocortical dialogue. *Cereb. Cortex* 6, 81–92. doi: 10.1093/cercor/6.2.81

Buzsáki, G. (1998). Memory consolidation during sleep: a neurophysiological perspective. *J. Sleep Res.* 7(Suppl. 1), 17–23. doi: 10.1046/j.1365-2869.7.s1.3.x

Buzsáki, G., Haas, H. L., and Anderson, E. G. (1987). Long-term potentiation induced by physiologically relevant stimulus patterns. *Brain Res.* 435, 331–333. doi: 10.1016/0006-8993(87)91618-0

Buzsáki, G., Leung, L. W., and Vanderwolf, C. H. (1983). Cellular bases of hippocampal EEG in the behaving rat. *Brain Res.* 287, 139–171. doi: 10.1016/0165-0173(83)90037-1

Chauvette, S., Crochet, S., Volgushev, M., and Timofeev, I. (2011). Properties of slow oscillation during slow-wave sleep and anesthesia in cats. *J. Neurosci.* 31, 14998–15008. doi: 10.1523/JNEUROSCI.2339-11.2011

Chauvette, S., Volgushev, M., and Timofeev, I. (2010). Origin of active states in local neocortical networks during slow sleep oscillation. *Cereb. Cortex* 20, 2660–2674. doi: 10.1093/cercor/bhq009

Clemens, Z., Mölle, M., Eross, L., Barsi, P., Halasz, P., and Born, J. (2007). Temporal coupling of parahippocampal ripples, sleep spindles and slow oscillations in humans. *Brain* 130, 2868–2878. doi: 10.1093/brain/awm146

Clemens, Z., Mölle, M., Eross, L., Jakus, R., Rasonyi, G., Halasz, P., et al. (2011). Fine-tuned coupling between human parahippocampal ripples and sleep spindles. *Eur. J. Neurosci.* 33, 511–520. doi: 10.1111/j.1460-9568.2010.07505.x

Cox, R., Hofman, W. F., De Boer, M., and Talamini, L. M. (2014). Local sleep spindle modulations in relation to specific memory cues. *Neuroimage* 99, 103–110. doi: 10.1016/j.neuroimage.2014.05.028

Cox, R., Mylonas, D. S., Manoach, D. S., and Stickgold, R. (2018). Large-scale structure and individual fingerprints of locally coupled sleep oscillations. *Sleep* 41:zsy175. doi: 10.1093/sleep/zsy175

Datta, S., and Maclean, R. R. (2007). Neurobiological mechanisms for the regulation of mammalian sleep-wake behavior: reinterpretation of historical evidence and inclusion of contemporary cellular and molecular evidence. *Neurosci. Biobehav. Rev.* 31, 775–824. doi: 10.1016/j.neubiorev.2007.02.004

Diekelmann, S., and Born, J. (2010). The memory function of sleep. *Nat. Rev. Neurosci.* 11, 114–126. doi: 10.1038/nrn2762

Dudai, Y., Karni, A., and Born, J. (2015). The consolidation and transformation of memory. *Neuron* 88, 20–32. doi: 10.1016/j.neuron.2015.09.004

Ego-Stengel, V., and Wilson, M. A. (2010). Disruption of ripple-associated hippocampal activity during rest impairs spatial learning in the rat. *Hippocampus* 20, 1–10. doi: 10.1002/hipo.20707

Eschenko, O., Mölle, M., Born, J., and Sara, S. J. (2006). Elevated sleep spindle density after learning or after retrieval in rats. *J. Neurosci.* 26, 12914–12920. doi: 10.1523/JNEUROSCI.3175-06.2006

Eschenko, O., Ramadan, W., Mölle, M., Born, J., and Sara, S. J. (2008). Sustained increase in hippocampal sharp-wave ripple activity during slow-wave sleep after learning. *Learn. Mem.* 15, 222–228. doi: 10.1101/lm.726008

Fattinger, S., De Beukelaar, T. T., Ruddy, K. L., Volk, C., Heyse, N. C., Herbst, J. A., et al. (2017). Deep sleep maintains learning efficiency of the human brain. *Nat. Commun.* 8:15405. doi: 10.1038/ncomms15405

Fernandez-Ruiz, A., Oliva, A., Fermino De Oliveira, E., Rocha-Almeida, F., Tingley, D., and Buzsáki, G. (2019). Long-duration hippocampal sharp wave ripples improve memory. *Science* 364, 1082–1086. doi: 10.1126/science.aax0758

Fogel, S. M., and Smith, C. T. (2006). Learning-dependent changes in sleep spindles and Stage 2 sleep. *J. Sleep Res.* 15, 250–255. doi: 10.1111/j.1365-2869.2006.00522.x

Fogel, S. M., and Smith, C. T. (2011). The function of the sleep spindle: a physiological index of intelligence and a mechanism for sleep-dependent memory consolidation. *Neurosci. Biobehav. Rev.* 35, 1154–1165. doi: 10.1016/j.neubiorev.2010.12.003

Gais, S., Mölle, M., Helms, K., and Born, J. (2002). Learning-dependent increases in sleep spindle density. *J. Neurosci.* 22, 6830–6834. doi: 10.1523/JNEUROSCI.22-15-06830.2002

Gibbs, F. A., and Gibbs, E. L. (1950). *Atlas of Electroencephalography.* Cambridge, MA: Addison-Wesley Press.

Girardeau, G., Benchenane, K., Wiener, S. I., Buzsáki, G., and Zugaro, M. B. (2009). Selective suppression of hippocampal ripples impairs spatial memory. *Nat. Neurosci.* 12, 1222–1223. doi: 10.1038/nn.2384

Goldi, M., Van Poppel, E. A. M., Rasch, B., and Schreiner, T. (2019). Increased neuronal signatures of targeted memory reactivation during slow-wave up states. *Sci. Rep.* 9:2715. doi: 10.1038/s41598-019-39178-2

Hanlon, E. C., Faraguna, U., Vyazovskiy, V. V., Tononi, G., and Cirelli, C. (2009). Effects of skilled training on sleep slow wave activity and cortical gene expression in the rat. *Sleep* 32, 719–729. doi: 10.1093/sleep/32.6.719

Huber, R., Ghilardi, M. F., Massimini, M., Ferrarelli, F., Riedner, B. A., Peterson, M. J., et al. (2006). Arm immobilization causes cortical plastic changes and locally decreases sleep slow wave activity. *Nat. Neurosci.* 9, 1169–1176. doi: 10.1038/nn1758

Huber, R., Ghilardi, M. F., Massimini, M., and Tononi, G. (2004). Local sleep and learning. *Nature* 430, 78–81. doi: 10.1038/nature02663

Iber, C., Ancoli-Israel, S., Chesson, A. L., and Quan, S. F. (2007). *AASM Manual for the Scoring of Sleep and Associate Events. Rules, Terminology and Technical Specifications.* Westchester, IL: American Association of Sleep Medicine.

Isomura, Y., Sirota, A., Ozen, S., Montgomery, S., Mizuseki, K., Henze, D. A., et al. (2006). Integration and segregation of activity in entorhinal-hippocampal subregions by neocortical slow oscillations. *Neuron* 52, 871–882. doi: 10.1016/j.neuron.2006.10.023

Ketz, N., Jones, A. P., Bryant, N. B., Clark, V. P., and Pilly, P. K. (2018). Closed-loop slow-wave tacs improves sleep-dependent long-term memory generalization by modulating endogenous oscillations. *J. Neurosci.* 38, 7314–7326. doi: 10.1523/JNEUROSCI.0273-18.2018

Khodagholy, D., Gelinas, J. N., and Buzsáki, G. (2017). Learning-enhanced coupling between ripple oscillations in association cortices and hippocampus. *Science* 358, 369–372. doi: 10.1126/science.aan6203

King, C., Henze, D. A., Leinekugel, X., and Buzsáki, G. (1999). Hebbian modification of a hippocampal population pattern in the rat. *J. Physiol.* 521(Pt 1), 159–167. doi: 10.1111/j.1469-7793.1999.00159.x

Ladenbauer, J., Ladenbauer, J., Kulzow, N., De Boor, R., Avramova, E., Grittner, U., et al. (2017). Promoting sleep oscillations and their functional coupling by transcranial stimulation enhances memory consolidation in mild cognitive impairment. *J. Neurosci.* 37, 7111–7124. doi: 10.1523/JNEUROSCI.0260-17.2017

Lafon, B., Henin, S., Huang, Y., Friedman, D., Melloni, L., Thesen, T., et al. (2017). Low frequency transcranial electrical stimulation does not entrain sleep rhythms measured by human intracranial recordings. *Nat. Commun.* 8:1199. doi: 10.1038/s41467-017-01045-x

Latchoumane, C. V., Ngo, H. V., Born, J., and Shin, H. S. (2017). Thalamic spindles promote memory formation during sleep through triple phase-locking of cortical, thalamic, and hippocampal rhythms. *Neuron* 95, 424–35 e426. doi: 10.1016/j.neuron.2017.06.025

Liu, X., Lu, Y., and Kuzum, D. (2018). High-density porous graphene arrays enable detection and analysis of propagating cortical waves and spirals. *Sci. Rep.* 8:17089. doi: 10.1038/s41598-018-35613-y

Luczak, A., Bartho, P., Marguet, S. L., Buzsáki, G., and Harris, K. D. (2007). Sequential structure of neocortical spontaneous activity *in vivo*. *Proc. Natl. Acad. Sci. U.S.A.* 104, 347–352. doi: 10.1073/pnas.0605643104

Maingret, N., Girardeau, G., Todorova, R., Goutierre, M., and Zugaro, M. (2016). Hippocampo-cortical coupling mediates memory consolidation during sleep. *Nat. Neurosci.* 19, 959–964. doi: 10.1038/nn.4304

Malerba, P., Whitehurst, L. N., Simons, S. B., and Mednick, S. C. (2019). Spatio-temporal structure of sleep slow oscillations on the electrode manifold and its relation to spindles. *Sleep* 42:zsy197. doi: 10.1093/sleep/zsy197

Maquet, P. (2001). The role of sleep in learning and memory. *Science* 294, 1048–1052. doi: 10.1126/science.1062856

Marshall, L., and Born, J. (2007). The contribution of sleep to hippocampus-dependent memory consolidation. *Trends Cogn. Sci.* 11, 442–450. doi: 10.1016/j.tics.2007.09.001

Marshall, L., Helgadottir, H., Mölle, M., and Born, J. (2006). Boosting slow oscillations during sleep potentiates memory. *Nature* 444, 610–613. doi: 10.1038/nature05278

Massimini, M., Huber, R., Ferrarelli, F., Hill, S., and Tononi, G. (2004). The sleep slow oscillation as a traveling wave. *J. Neurosci.* 24, 6862–6870. doi: 10.1523/JNEUROSCI.1318-04.2004

Miyamoto, D., Hirai, D., Fung, C. C., Inutsuka, A., Odagawa, M., Suzuki, T., et al. (2016). Top-down cortical input during NREM sleep consolidates perceptual memory. *Science* 352, 1315–1318. doi: 10.1126/science.aaf0902

Mölle, M., Eschenko, O., Gais, S., Sara, S. J., and Born, J. (2009). The influence of learning on sleep slow oscillations and associated spindles and ripples in humans and rats. *Eur. J. Neurosci.* 29, 1071–1081. doi: 10.1111/j.1460-9568.2009.06654.x

Mölle, M., Marshall, L., Gais, S., and Born, J. (2004). Learning increases human electroencephalographic coherence during subsequent slow sleep oscillations. *Proc. Natl. Acad. Sci. U.S.A.* 101, 13963–13968. doi: 10.1073/pnas.0402820101

Mölle, M., Yeshenko, O., Marshall, L., Sara, S. J., and Born, J. (2006). Hippocampal sharp wave-ripples linked to slow oscillations in rat slow-wave sleep. *J. Neurophysiol.* 96, 62–70. doi: 10.1152/jn.00014.2006

Morin, A., Doyon, J., Dostie, V., Barakat, M., Hadj Tahar, A., Korman, M., et al. (2008). Motor sequence learning increases sleep spindles and fast frequencies in post-training sleep. *Sleep* 31, 1149–1156.

Mormann, F., Kornblith, S., Quiroga, R. Q., Kraskov, A., Cerf, M., Fried, I., et al. (2008). Latency and selectivity of single neurons indicate hierarchical processing in the human medial temporal lobe. *J. Neurosci.* 28, 8865–8872. doi: 10.1523/JNEUROSCI.1640-08.2008

Muller, L., Chavane, F., Reynolds, J., and Sejnowski, T. J. (2018). Cortical travelling waves: mechanisms and computational principles. *Nat. Rev. Neurosci.* 19, 255–268. doi: 10.1038/nrn.2018.20

Muller, L., Piantoni, G., Koller, D., Cash, S. S., Halgren, E., and Sejnowski, T. J. (2016). Rotating waves during human sleep spindles organize global patterns of activity that repeat precisely through the night. *Elife* 5:e17267. doi: 10.7554/eLife.17267

Nadasdy, Z., Hirase, H., Czurko, A., Csicsvari, J., and Buzsáki, G. (1999). Replay and time compression of recurring spike sequences in the hippocampus. *J. Neurosci.* 19, 9497–9507. doi: 10.1523/JNEUROSCI.19-21-09497.1999

Ngo, H. V., Martinetz, T., Born, J., and Mölle, M. (2013). Auditory closed-loop stimulation of the sleep slow oscillation enhances memory. *Neuron* 78, 545–553. doi: 10.1016/j.neuron.2013.03.006

Niethard, N., Ngo, H. V., Ehrlich, I., and Born, J. (2018). Cortical circuit activity underlying sleep slow oscillations and spindles. *Proc. Natl. Acad. Sci. U.S.A.* 115, E9220–E9229. doi: 10.1073/pnas.1805517115

Nir, Y., Staba, R. J., Andrillon, T., Vyazovskiy, V. V., Cirelli, C., Fried, I., et al. (2011). Regional slow waves and spindles in human sleep. *Neuron* 70, 153–169. doi: 10.1016/j.neuron.2011.02.043

Nishida, M., and Walker, M. P. (2007). Daytime naps, motor memory consolidation and regionally specific sleep spindles. *PLoS ONE* 2:e341. doi: 10.1371/journal.pone.0000341

Norimoto, H., Makino, K., Gao, M., Shikano, Y., Okamoto, K., Ishikawa, T., et al. (2018). Hippocampal ripples down-regulate synapses. *Science* 359, 1524–1527. doi: 10.1126/science.aao0702

Nunez, P. L. (1995). *Neocortical Dynamics and Human EEG Rhythms.* New York, NY: Oxford University Press.

O'keefe, J., and Nadel, L. (1978). *The Hippocampus as a Cognitive Map.* Oxford: Oxford University Press.

Peyrache, A., Battaglia, F. P., and Destexhe, A. (2011). Inhibition recruitment in prefrontal cortex during sleep spindles and gating of hippocampal inputs. *Proc. Natl. Acad. Sci. U.S.A.* 108, 17207–17212. doi: 10.1073/pnas.1103612108

Peyrache, A., Khamassi, M., Benchenane, K., Wiener, S. I., and Battaglia, F. P. (2009). Replay of rule-learning related neural patterns in the prefrontal cortex during sleep. *Nat. Neurosci.* 12, 919–926. doi: 10.1038/nn.2337

Rasch, B., and Born, J. (2013). About sleep's role in memory. *Physiol. Rev.* 93, 681–766. doi: 10.1152/physrev.00032.2012

Rosanova, M., and Ulrich, D. (2005). Pattern-specific associative long-term potentiation induced by a sleep spindle-related spike train. *J. Neurosci.* 25, 9398–9405. doi: 10.1523/JNEUROSCI.2149-05.2005

Rothschild, G., Eban, E., and Frank, L. M. (2017). A cortical-hippocampal-cortical loop of information processing during memory consolidation. *Nat. Neurosci.* 20, 251–259. doi: 10.1038/nn.4457

Schnupp, J., Nelken, I., and King, A. (2011). *Auditory Neuroscience : Making Sense of Sound.* Cambridge: MIT Press. doi: 10.7551/mitpress/7942.001.0001

Seibt, J., Richard, C. J., Sigl-Glockner, J., Takahashi, N., Kaplan, D. I., Doron, G., et al. (2017). Cortical dendritic activity correlates with spindle-rich oscillations during sleep in rodents. *Nat. Commun.* 8:684. doi: 10.1038/s41467-017-00735-w

Siapas, A. G., and Wilson, M. A. (1998). Coordinated interactions between hippocampal ripples and cortical spindles during slow-wave sleep. *Neuron* 21, 1123–1128. doi: 10.1016/S0896-6273(00)80629-7

Siclari, F., Bernardi, G., Riedner, B. A., Larocque, J. J., Benca, R. M., and Tononi, G. (2014). Two distinct synchronization processes in the transition to sleep: a high-density electroencephalographic study. *Sleep* 37, 1621–1637. doi: 10.5665/sleep.4070

Simor, P., Steinbach, E., Nagy, T., Gilson, M., Farthouat, J., Schmitz, R., et al. (2018). Lateralized rhythmic acoustic stimulation during daytime NREM sleep enhances slow waves. *Sleep* 41:zsy176. doi: 10.1093/sleep/zsy176

Sirota, A., and Buzsáki, G. (2005). Interaction between neocortical and hippocampal networks via slow oscillations. *Thalamus Relat. Syst.* 3, 245–259. doi: 10.1017/S1472928807000258

Sirota, A., Csicsvari, J., Buhl, D., and Buzsáki, G. (2003). Communication between neocortex and hippocampus during sleep in rodents. *Proc. Natl. Acad. Sci. U.S.A.* 100, 2065–2069. doi: 10.1073/pnas.0437938100

Staresina, B. P., Bergmann, T. O., Bonnefond, M., Van Der Meij, R., Jensen, O., Deuker, L., et al. (2015). Hierarchical nesting of slow oscillations, spindles and ripples in the human hippocampus during sleep. *Nat. Neurosci.* 18, 1679–1686. doi: 10.1038/nn.4119

Steriade, M. (2003). *Neuronal Substrates of Sleep and Epilepsy*. New York, NY: Cambridge University Press. doi: 10.1017/CBO9780511541711

Steriade, M., Timofeev, I., and Grenier, F. (2001). Natural waking and sleep states: a view from inside neocortical neurons. *J. Neurophysiol.* 85, 1969–1985. doi: 10.1152/jn.2001.85.5.1969

Tamminen, J., Lambon Ralph, M. A., and Lewis, P. A. (2013). The role of sleep spindles and slow-wave activity in integrating new information in semantic memory. *J. Neurosci.* 33, 15376–15381. doi: 10.1523/JNEUROSCI.5093-12.2013

Timofeev, I., Grenier, F., Bazhenov, M., Houweling, A. R., Sejnowski, T. J., et al. (2002). Short- and medium-term plasticity associated with augmenting responses in cortical slabs and spindles in intact cortex of cats *in vivo*. *J. Physiol.* 542, 583–598. doi: 10.1113/jphysiol.2001.013479

Tononi, G., and Cirelli, C. (2014). Sleep and the price of plasticity: from synaptic and cellular homeostasis to memory consolidation and integration. *Neuron* 81, 12–34. doi: 10.1016/j.neuron.2013.12.025

Ulrich, D. (2016). Sleep spindles as facilitators of memory formation and learning. *Neural Plast.* 2016:1796715. doi: 10.1155/2016/1796715

Van Der Helm, E., Gujar, N., Nishida, M., and Walker, M. P. (2011). Sleep-dependent facilitation of episodic memory details. *PLoS ONE* 6:e27421. doi: 10.1371/journal.pone.0027421

Von Ellenrieder, N., Dan, J., Frauscher, B., and Gotman, J. (2016). Sparse asynchronous cortical generators can produce measurable scalp EEG signals. *Neuroimage* 138, 123–133. doi: 10.1016/j.neuroimage.2016.05.067

Vyazovskiy, V., Borbely, A. A., and Tobler, I. (2000). Unilateral vibrissae stimulation during waking induces interhemispheric EEG asymmetry during subsequent sleep in the rat. *J. Sleep Res.* 9, 367–371. doi: 10.1046/j.1365-2869.2000.00230.x

Vyazovskiy, V. V., Cirelli, C., Pfister-Genskow, M., Faraguna, U., and Tononi, G. (2008). Molecular and electrophysiological evidence for net synaptic potentiation in wake and depression in sleep. *Nat. Neurosci.* 11, 200–208. doi: 10.1038/nn2035

Vyazovskiy, V. V., Olcese, U., Hanlon, E. C., Nir, Y., Cirelli, C., and Tononi, G. (2011). Local sleep in awake rats. *Nature* 472, 443–447. doi: 10.1038/nature10009

Wagner, T., Axmacher, N., Lehnertz, K., Elger, C. E., and Fell, J. (2010). Sleep-dependent directional coupling between human neocortex and hippocampus. *Cortex* 46, 256–263. doi: 10.1016/j.cortex.2009.05.012

Walker, M. P., and Stickgold, R. (2004). Sleep-dependent learning and memory consolidation. *Neuron* 44, 121–133. doi: 10.1016/j.neuron.2004.08.031

Wang, D. V., and Ikemoto, S. (2016). Coordinated interaction between hippocampal sharp-wave ripples and anterior cingulate unit activity. *J. Neurosci.* 36, 10663–10672. doi: 10.1523/JNEUROSCI.1042-16.2016

Conflict of Interest Statement: The authors declare that the research was conducted in the absence of any commercial or financial relationships that could be construed as a potential conflict of interest.

Copyright © 2019 Geva-Sagiv and Nir. This is an open-access article distributed under the terms of the Creative Commons Attribution License (CC BY). The use, distribution or reproduction in other forums is permitted, provided the original author(s) and the copyright owner(s) are credited and that the original publication in this journal is cited, in accordance with accepted academic practice. No use, distribution or reproduction is permitted which does not comply with these terms.

frontiers in Neuroscience

PERSPECTIVE
published: 13 September 2019
doi: 10.3389/fnins.2019.00949

Does the Mind Wander When the Brain Takes a Break? Local Sleep in Wakefulness, Attentional Lapses and Mind-Wandering

Thomas Andrillon[1], Jennifer Windt[2], Tim Silk[3,4,5], Sean P. A. Drummond[1], Mark A. Bellgrove[1] and Naotsugu Tsuchiya[1,6,7]*

[1] School of Psychological Sciences, Turner Institute for Brain and Mental Health, Monash University, Melbourne, VIC, Australia, [2] School of Philosophical, Historical and International Studies, Monash University, Melbourne, VIC, Australia, [3] School of Psychology, Deakin University, Melbourne, VIC, Australia, [4] Murdoch Children's Research Institute, Melbourne, VIC, Australia, [5] Department of Paediatrics, University of Melbourne, Melbourne, VIC, Australia, [6] Center for Information and Neural Networks (CiNet), National Institute of Information and Communications Technology (NICT), Osaka, Japan, [7] Advanced Telecommunications Research Computational Neuroscience Laboratories, Kyoto, Japan

Sleep has been classically described as an all-or-nothing global phenomenon. However, recent research strongly suggests that this view requires tempering. Invasive and non-invasive recordings in animals and humans show that neural activity typically associated with sleep can locally occur during wakefulness. Although local sleep is defined neuronally, it has been associated with impaired performance during cognitive tasks. Comparatively, the phenomenology of local sleep (i.e., what it feels like when your brain is partially asleep) has been less explored. Taking into account the literature on the neuronal and behavioral profile of local sleep intrusions in wakefulness, we propose that occurrences of local sleep could represent the neural mechanism underlying many attentional lapses. In particular, we argue that a unique physiological event such as local sleep could account for a diversity of behavioral outcomes from sluggish to impulsive responses. We further propose that local sleep intrusions could impact individuals' subjective experience. Specifically, we propose that the timing and anatomical sources of local sleep intrusions could be responsible for both the behavioral consequences and subjective content of attentional lapses and may underlie the difference between subjective experiences such as mind wandering and mind blanking. Our framework aims to build a parallel between spontaneous experiences in sleep and wakefulness by integrating evidence across neuronal, behavioral and experiential levels. We use the example of attention deficit hyperactivity disorder (ADHD) to illustrate how local sleep could explain complex cognitive profiles which include inattention, impulsivity, mind-wandering and mind-blanking.

Keywords: sleep, physiology, performance, wakefulness, phenomenology

OPEN ACCESS

Edited by:
Giulio Bernardi,
IMT School for Advanced Studies Lucca, Italy

Reviewed by:
Jean-Baptiste Eichenlaub, Université Savoie Mont Blanc, France
Angelica Quercia, D'Annunzio University of Chieti–Pescara, Italy

****Correspondence:***
Thomas Andrillon
thomas.andrillon@monash.edu

Specialty section:
This article was submitted to Sleep and Circadian Rhythms, a section of the journal Frontiers in Neuroscience

Received: *19 June 2019*
Accepted: *22 August 2019*
Published: *13 September 2019*

Citation:
Andrillon T, Windt J, Silk T, Drummond SPA, Bellgrove MA and Tsuchiya N (2019) Does the Mind Wander When the Brain Takes a Break? Local Sleep in Wakefulness, Attentional Lapses and Mind-Wandering. Front. Neurosci. 13:949. doi: 10.3389/fnins.2019.00949

INTRODUCTION

Sleep and wakefulness have been traditionally considered as mutually exclusive states. At the behavioral level, sleep is characterized by a transient loss of responsiveness to the environment (Carskadon and Dement, 2005; Cirelli and Tononi, 2008). This behavioral unresponsiveness was found to correspond, at the physiological level, to specific patterns of brain activity. Notably,

Non-Rapid Eye Movement (NREM) sleep, which amounts to 75–80% of the total time spent asleep in healthy adults (Ohayon et al., 2004; Carskadon and Dement, 2005), is characterized by the occurrence of high-amplitude slow oscillations. These so-called "slow waves" were initially described as alternations between moments of neuronal silencing and firing synchronized across the entire cortex (Steriade, 2003; Vyazovskiy and Harris, 2013).

Recent discoveries in animal and human sleep physiology have tempered the notion of slow waves as necessarily being a global physiological event (Nobili et al., 2012; Siclari and Tononi, 2017; Krueger et al., 2019). Within NREM sleep, some brain regions can show slow waves while others do not (Nir et al., 2011; Nobili et al., 2011). Such regional aspects of sleep activity had already been observed in certain animal species (e.g., dolphins who can enter unihemispheric sleep, sleeping in one brain hemisphere at a time) (Mascetti, 2016; Rattenborg et al., 2019) and in sleep pathologies (Terzaghi et al., 2009; Dodet et al., 2015; Castelnovo et al., 2016; Riedner et al., 2016). However, in the past few years, local sleep involving changes in sleep depth within NREM sleep has been robustly observed in individuals without sleep disorders (Huber et al., 2004; Nir et al., 2011). Even more striking is the observation of local sleep-like slow waves outside of NREM sleep, in wakefulness (Vyazovskiy et al., 2011; Hung et al., 2013; Bernardi et al., 2015; Quercia et al., 2018) or REM sleep (Funk et al., 2016; Bernardi et al., 2019). These slow waves are isolated (local in time) and spatially restricted (local in space) and consequently largely overlooked in standard classifications that focus on the global characteristics of sleep and wake states. The occurrence of local slow waves outside NREM sleep (i.e., in wakefulness or REM sleep) and the local modulation of the presence of slow waves within NREM sleep have been termed 'local sleep' (**Box 1**).

BOX 1 | Glossary: Some of the terms used in this Perspective are widely used but not systematically defined and the same terms may be used by behavioral, phenomenological and/or neurophysiological approaches to refer to slightly different target phenomena. Below we define each term to the extent that is acceptable across different disciplines in order to facilitate further interdisciplinary work, both theoretical and empirical.

Wakefulness: Wakefulness is a state in which individuals can rapidly and reliably react to environmental demands. At the physiological level, wakefulness is characterized by a pattern of brain activity dominated by fast, low-amplitude, desynchronized oscillations.

Sleep: Sleep is a state behaviorally defined by a transient loss of responsiveness. To induce responses, stimuli have to be more intense than during wakefulness. The recovery of responsiveness is usually associated with a reversal to neural patterns of wake activity. Neuronal activity during sleep is dominated by slow, high-amplitude, synchronized oscillations in Non-Rapid Eye Movement (NREM) sleep and by low-amplitude, theta (4–7 Hz) and mixed-frequency oscillations in Rapid Eye Movement (REM) sleep.

Local Sleep: A concept introduced by Huber et al. (2004) (in sleep) and Vyazovskiy et al. (2011) (in wakefulness). In its most general sense, local sleep refers to transient, regional neurophysiological states showing a mixture of features characteristic of (i) wakefulness and sleep, (ii) different sleep stages (NREM and REM sleep), or (iii) different sleep depths (light or deep sleep). Local sleep is local both in time and space. As a relatively new concept in the sleep literature, its precise definition is likely to evolve with time.

Microsleep: Microsleep is classically defined as a global shift in neuronal activity from wakefulness to light NREM sleep for a duration of 5 to 14 s. Above 14 s, the individual is considered asleep. Below 5 s, the individual is considered awake but could potentially show signs of local sleep (< 5 s).

Attentional lapse: Attentional lapses refer to the redirection of an individual's attention away from a specific task. These lapses are accompanied by a drop in objective performance as well as an increase in performance variability.

Mind-wandering: Mind-wandering is defined as spontaneous, dynamic and often associative thought. In the context of laboratory experiments, this is often operationalized as task- and/or stimulus independent thought. Mind-wandering can be considered as the phenomenological dimension of a large group of attentional lapses.

Mind-blanking: Mind-blanking refers to subjective reports of reduced awareness and a temporary absence of thought (empty mind) or lack of memory for immediately past thoughts. Mind-blanking can be considered as the phenomenological dimension of a distinct kind of attentional lapse compared to mind-wandering.

ADHD: Attention deficit hyperactivity disorder (ADHD) is a common neurodevelopmental disorder with a worldwide prevalence of approximately 5%. The diagnosis is based on age-inappropriate levels of inattention, hyperactivity and/or impulsivity.

Behavioral and Neuronal Effects of Local Sleep

Local sleep during wakefulness was originally defined based on the identification of a hallmark of NREM sleep within wakefulness: sleep slow waves (Vyazovskiy et al., 2011). These sleep slow waves can be observed in invasive intracranial recordings [local field potentials (LFP), electrocorticogram (ECoG)] or non-invasive scalp electroencephalography (EEG) in the form of high-amplitude, slow oscillations (< 4 Hz). At the level of individual neurons, these slow oscillations involve a brief episode of neuronal silencing (OFF period) followed by synchronous activation of neighboring neurons (Steriade, 2003; Vyazovskiy and Harris, 2013). OFF periods appear as the most unequivocal definition of local sleep intrusions during wakefulness as they directly show an increase in local synchrony and an interruption of neural activity similar to that which can be observed during sleep. However, these OFF periods cannot be recorded non-invasively.

Investigations in humans have therefore focused on the detection of local high-amplitude slow oscillations, which typically accompany OFF periods (Steriade, 2005). However, the exact frequency bands used to detect these waves differ from one study to another, with some studies focusing on the theta range (Hung et al., 2013; Bernardi et al., 2015), others on the delta range (Quercia et al., 2018), and yet others on a combination of the theta and delta range (Vyazovskiy et al., 2011; Nir et al., 2017). It is unclear if these so-called delta and theta waves refer to distinct events. Indeed, during normal sleep, slow waves have complex frequency profiles (e.g., a mixture of a delta component with faster oscillations) (Siclari et al., 2014; Halász, 2016). Further, there can be considerable variability when estimating the frequency of short-lived, isolated slow waves. Adding to the difficulty of comparing existing methods is the fact that the basic physiological properties of local sleep events in wakefulness are yet to be determined (topographical distribution, spatial extent, peak frequency, duration, etc). These parameters have been studied in sleep (Riedner et al., 2007; Siclari et al., 2014) but not in wakefulness. Existing studies suggest that local slow waves occur in both frontal and parietal regions (Vyazovskiy et al., 2011; Hung et al., 2013; Quercia et al., 2018),

with a larger number of waves in parietal regions (Vyazovskiy et al., 2011; Hung et al., 2013).

In summary, local sleep can be defined, at the level of neuronal networks, by the brief local appearance of events similar to sleep slow waves (delta and/or theta waves) which are in turn associated, at the level of single-neuron activity, with episodes of neuronal silencing (**Figure 1**). Local sleep is thus different from the concept of microsleep (**Box 1**) as it is defined by the local occurrence of a specific pattern of neural activity (slow wave) for, potentially, a much shorter period of time than microsleep. As is the case for microsleep, however, local sleep can be reliably induced by sleep deprivation. First, when examining scalp EEG, the power in the delta/theta band (corresponding to sleep slow waves) increases with time spent awake (Cajochen et al., 1995), a phenomenon thought to reflect the build-up of sleep pressure (Finelli et al., 2000) and potentially mediated by functional and structural changes in neuronal networks (Tononi and Cirelli, 2014). More recently, it has been shown that this increase in the power of slow oscillations is accompanied by the occurrence of isolated waves that bear a striking resemblance to sleep oscillations (Vyazovskiy et al., 2011; Hung et al., 2013; Bernardi et al., 2015; Quercia et al., 2018).

Interestingly, the occurrence of local sleep intrusions varies as a function of both the time spent awake and the degree to which a particular brain region has been activated by environmental demands (e.g., a specific task) (Hung et al., 2013; Bernardi et al., 2019). A recent study linked the occurrence of local slow waves during sleep with neuronal plasticity and learning (Quercia et al., 2018). Using a spatial memory task, Quercia et al. (2018) showed that local sleep occurrences in wakefulness are predictive of errors but can also be explained by learning-related processes. This is particularly interesting since similar use-dependent or learning-dependent regional modulations of slow waves have been observed during sleep (Huber et al., 2004; Bernardi et al., 2015). Altogether, these results support a link between local sleep and neuronal plasticity in both wakefulness and sleep. In a nutshell, the recruitment of a neuronal network by a given task would fatigue this network, particularly when the network is subject to plastic changes. This neuronal fatigue would translate in local sleep occurrences, which would negatively impact behavior in a region-specific, task-specific fashion.

At the same time, it is unlikely that extensive usage of local neural circuitry is the sole predictor of local sleep occurrences. Rather, it is more likely that local sleep is modulated by a combination of use-dependent and circadian factors. Sleep in general is known to be influenced by both time spent awake and circadian processes (Borbély, 1982). Consistent with this view, previous research has demonstrated the existence of local modulations of brain activity during the day, in response to both circadian rhythms and sleep pressure (Muto et al., 2016). However, this circadian viewpoint has not been taken into account by the majority of studies on local sleep and represents an important future research direction.

Although local sleep has been primarily defined at the physiological level, its occurrence during wake has been associated with impaired task performance: trials preceded by local slow waves typically show slower reaction times and increased error rates (Vyazovskiy et al., 2011; Hung et al., 2013; Bernardi et al., 2015; Nir et al., 2017; Quercia et al., 2018). These performance decrements were proposed to result from the transient period of neuronal silencing associated with local slow waves (Vyazovskiy et al., 2011). Indeed, during sleep, episodes of neuronal silencing accompanying slow waves have been associated with perturbations of sensory encoding and

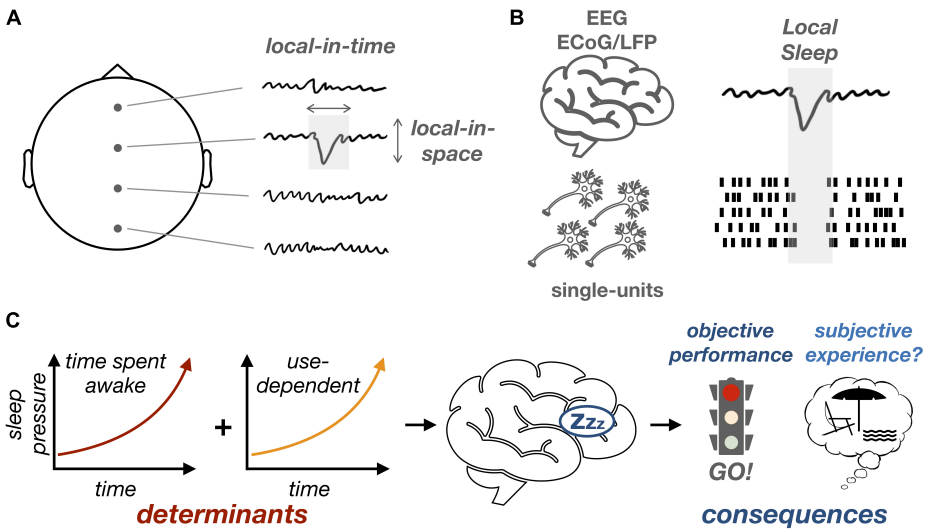

FIGURE 1 | Can local sleep in wakefulness affect behavior and subjective experience? **(A)** Isolated sleep-like slow waves (which are local in time and space) can be observed during wakefulness. **(B)** These slow waves can be observed in scalp EEG or intracranial recordings (ECoG/LFP, top) and are associated at the level of single-unit recordings (bottom) with episodes of neuronal silencing. **(C)** Local sleep increases with time spent awake, even more so in brain regions involved in a given recurrent task (use-dependent). The timing and location of local sleep occurrences could determine their impact on objective performance and, possibly, subjective experience.

information processing (McCormick and Bal, 1994) and it has been proposed that sleep slow waves could be the mechanism explaining sensory isolation (Schabus et al., 2012; Andrillon et al., 2016) and loss of consciousness (Tononi and Massimini, 2008) in NREM sleep. Importantly, the behavioral consequences of local sleep in rodents engaged in a specific task are region-specific: local sleep intrusions occurring in the neural networks involved in the task were more likely to lead to behavioral impairments (Vyazovskiy et al., 2011). Likewise, in humans, local sleep occurrences led to task-specific behavioral impairments (Hung et al., 2013; Bernardi et al., 2015).

Impact of Local Sleep on Phenomenology

Local modulations of sleep-like activity not only impact behavioral performance during wakefulness, but might also affect the contents or structure of subjective experience during sleep. Recent research, relying on subjective reports and serial-awakening paradigms (Siclari et al., 2013), has emphasized the diversity of sleep-related subjective experiences, ranging from immersive, narratively complex and often emotionally intense dreams to isolated thoughts and imagery, to a form of minimal subjective experience that lacks specific thought contents and imagery (Windt, 2015; Windt et al., 2016). We propose that local aspects of sleep could explain the emergence of different sleep-related experiences. For example, local modulations of slow-wave activity within NREM and REM sleep have been associated with the occurrence of dreams (Siclari et al., 2016). Specifically, a decrease in the number of slow waves (which can be interpreted as a regional reduction of sleep depth) in parietal regions is associated with subjective reports of dreaming upon awakening, although the causal nature of this relationship is debated (Boly et al., 2017; Wong et al., 2019). The spatio-temporal properties of the decrease in slow-wave activity are predictive not only of the occurrence of dreams but also of their content (Siclari et al., 2016) (e.g., a decrease in slow-wave activity in motor regions was associated with more reports of movements during dreams). These results suggest that local slow waves could act as a functional switch enabling or disabling specific cognitive processes during sleep, with direct consequences on oneiric contents (Siclari et al., 2016) but also the ability to process external stimuli (Andrillon et al., 2016, 2017; Tamaki et al., 2016; Blume et al., 2018).

Local sleep in wakefulness could be associated with similar changes in subjective experience. Indeed, spontaneous experiences in wakefulness and sleep share similar properties at the phenomenological level. Wakeful cognition is a highly dynamic process and fluctuations in spontaneous experience forming the so-called "stream of thought" (James, 1890) are at the core of mind-wandering research (Smallwood and Schooler, 2015) (**Box 1**). The sampling of conscious experiences during the day (Wamsley, 2013; Smallwood and Schooler, 2015), an approach similar to that used in dream research (Horikawa et al., 2013; Siclari et al., 2013), reveals that individuals spend on average 30–50% of their time thinking about something other than the task at hand (Killingsworth and Gilbert, 2010; Seli et al., 2013).

It has been suggested that dreaming and mind wandering could be placed on a continuum (Fox et al., 2013; Domhoff, 2018). First, dreaming and mind wandering seem supported by overlapping neural networks, including the Default Mode Network (DMN) (Fox et al., 2013). Second, from a phenomenological perspective, dreams are at core immersive, involving a simulated world centered on a simulated self (Windt, 2015; Windt et al., 2016). Similarly, daydreams tend to be focused on self-related concerns (D'Argembeau, 2018) and often contain vivid audio-visual imagery as well as emotions (Foulkes and Fleisher, 1975). Yet, daydreams lack the "here and now" quality of sleep dreams: in wakefulness, we don't lose touch with our actual environments or feel present in imagined ones as completely as we do in sleep-dreams. In this sense, dreams seem to be an intensified form of mind wandering.

Other sleep-experiences lack the immersive character of dreaming and hence have been termed dreamless sleep experiences. A subgroup of these is characterized by an absence of reportable content; these seem to involve simple or perhaps even minimal forms of subjective experience in which specific forms of thought contents or imagery are lacking (Windt, 2015; Windt et al., 2016). This subgroup of dreamless sleep experiences appears close to what has been termed mind-blanking in wakefulness, that is to say episodes in which individuals report a lack of conscious awareness (Ward and Wegner, 2013).

If sleep- and wake-related spontaneous experiences share similar properties at the phenomenological level, are they also related at the physiological level? More precisely, can local sleep explain the presence or absence (as well as content) of spontaneous experiences not just in sleep, but also in waking? This tantalizing question will need further investigation but initial results are promising. First of all, while the local decrease in slow-wave activity over parietal regions correlates with the occurrence of spontaneous experiences during sleep (dreams), a local increase during wakefulness over the same regions correlates with a reduction in spontaneous thoughts (Perogamvros et al., 2017). These results are in line with the involvement of the parietal cortex in multimodal integration (Alais et al., 2010) and consciousness (Koch et al., 2016; Boly et al., 2017). Other physiological indexes of vigilance have shown a link between fluctuations in attention or subjective experience and sleepiness. Attentional lapses in general have been associated with a diminution of noradrenergic activity using fMRI or pupillometry (Mittner et al., 2014, 2016), a proxy for noradrenergic activity (Varazzani et al., 2015; Joshi et al., 2016). This is particularly interesting as Noradrenaline (NA) is one of the key neuromodulators allowing sleep/wake transitions (Siegel, 2004) but also plays a central role in the modulation and orientation of attention (Sara, 2009; Sara and Bouret, 2012; Thiele and Bellgrove, 2018). At the phenomenological level, mind-blanking in particular has been associated with a reduction in pupil diameter and increase in subjective sleepiness (Unsworth and Robison, 2018). Here, we go one step further by hypothesizing that fluctuations in spontaneous experiences during wake not only correlate with states of low vigilance but

actually share common neuronal mechanisms with sleep-related spontaneous experiences.

Local Sleep as a Comprehensive Model of Attentional Lapses

We propose a multi-level model of attentional lapses from neurophysiology to behavior and phenomenology. In our framework, local sleep intrusions represent a unifying physiological mechanism that could not only predict the occurrence of attentional lapses but also describe these lapses in terms of their behavioral consequences and phenomenological properties. Other markers of low arousal have been proposed to predict attentional lapses. In particular, pupil size can predict the occurrence of attentional lapses and mind-wandering (Mittner et al., 2014; van den Brink et al., 2016). However, pupil size is a global, systemic index of arousal [although pupil diameter can be linked with specific components of behavior (van Kempen et al., 2019)] and our local sleep framework could help move beyond global indexes to offer a regional marker predictive of specific behavioral impairments (**Figure 2**). Interestingly, in this framework, a single physiological event can explain phenomena that have often been presented as opposed: impulsivity vs. sluggishness and mind-wandering vs. mind-blanking.

Previous studies investigating local sleep intrusions during wake focused mostly on task and region-specific effects, after forcing participants to continuously perform a single task [e.g., (Hung et al., 2013; Bernardi et al., 2015)]. The goal of such paradigms is to fatigue circumscribed neural networks engaged in the task, increasing the likelihood of local sleep intrusions which would then result in errors on that particular task. In this type of paradigm, local sleep occurring in a given set of brain regions is expected to have the same behavioral outcomes. However, most everyday tasks require complex behavior and engage different brain regions. Participants performing these tasks are prone to multiple types of action failures (Smith and Ratcliff, 2004), whose relationship with sleepiness are often unclear (Anderson and Horne, 2006; Anderson et al., 2010; Drummond et al., 2012). An alternative method is to observe the occurrence of local sleep, attentional lapses and sleep-like activity during wakefulness following sleep deprivation (Hung et al., 2013; Bernardi et al., 2015) or even under normal conditions (Quercia et al., 2018). Here, we propose that where and when local sleep occurs could predict not only the timing of errors but the type of error being made in a specific task.

In particular, local sleep occurrences could explain the occurrence of seemingly opposed behavioral failures such as omission errors (failure to produce a response) and commission errors (failure to control, select or suppress a response). The standard view is that commission errors are associated with executive control failure, whereas omission errors would rather mark the failure to maintain a more basic form of vigilance (Ballard, 2001; O'Connell et al., 2008; Van Schie et al., 2012). This view would predict that omission and commission errors occur in different contexts of vigilance. Research on the effects of sleep deprivation showed, however, that sleep loss could actually result in both impulsivity and sluggishness (Drummond et al., 2006; Anderson and Platten, 2011). According to our framework, the same neural mechanism (local sleep) occurring in different parts of the brain could explain both commission and omission errors associated with sleepiness. This is supported by previous research in humans showing that local sleep-like activity in perceptual areas leads to slower reaction times in a visual psychomotor vigilance task (Nir et al., 2017), whereas slow waves in motor areas lead to decreased motor performance and slow waves in frontal areas lead to inhibition errors (Bernardi et al., 2015).

Next, we hypothesize that local sleep can account not only for decreases in objective behavioral performance but also for changes in individuals' subjective experience. The impact of local sleep on subjective experience has been less frequently studied (Perogamvros et al., 2017) than its consequences on objective performance (Hung et al., 2013; Bernardi et al., 2015; Nir et al., 2017; Quercia et al., 2018). Previous work does acknowledge, however, that sleep restriction can lead to increased distractibility in various ways (e.g., increased sensitivity to environmental vs. endogenous distractors) (Anderson et al., 2010). A more systematic approach to record and analyze subjective experience is needed. Based on current findings, we suggest that it will be useful to distinguish: (i) lapses induced by environmental stimuli (or external distractions); (ii) spontaneous thoughts (mind-wandering); (iii) task-related interferences (e.g., performance monitoring), and (iv) mind-blanking. We stress here the importance of including the dimension of mind-blanking. By contrast, mind-wandering research usually assumes that the mind wanders somewhere

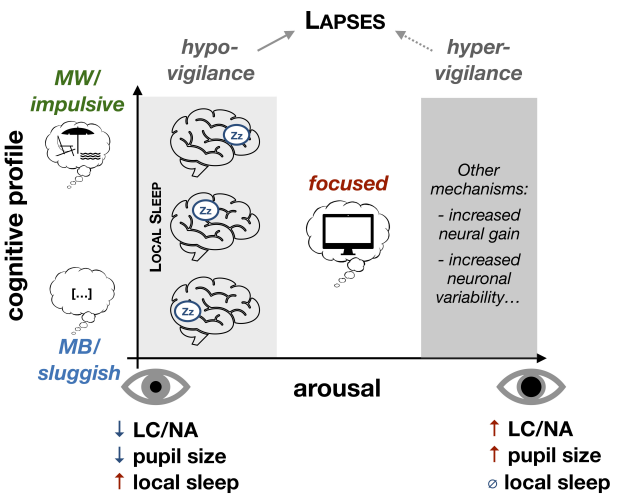

FIGURE 2 | Local sleep as a comprehensive model of attentional lapses under low levels of arousal. Under low levels of arousal (hypo-vigilance), the likelihood that local sleep intrusions occur increases. The spatial properties of these local sleep intrusions (which brain regions are affected) would determine the cognitive profile of attentional lapses (impact on objective performance and subjective experience). Global fluctuations of arousal could be determined by the level of activation of the Locus Coeruleus (LC) and the concentration in Noradrenaline (NA). Spatio-temporal properties of local sleep would further describe the cognitive profile of attentional lapses. Importantly, our model does not exclude the possibility that, under high levels of arousal (hyper-vigilance), objective performance and subjective performance can be affected by other neurophysiological mechanisms. MW, mind-wandering; MB, mind-blanking.

rather than nowhere (Ward and Wegner, 2013; Smallwood and Schooler, 2015), leading to a comparative neglect of mind blanking as compared to mind wandering.

Importantly, it has been previously suggested that these different types of subjective experiences correspond to different neural mechanisms and different levels of arousal. Mind-wandering has been proposed to be associated with a high level of arousal and fleeting or racing thoughts, whereas mind-blanking has been associated with decreased vigilance and low arousal (Mittner et al., 2016; Unsworth and Robison, 2018). However, this view is at odds with the fact that mind-wandering can occur in states or individuals with high sleep pressure (Braboszcz and Delorme, 2011; Carciofo et al., 2014; Poh et al., 2016) and typically increases when environmental demands decrease (e.g., easy or unmotivating tasks) (Antrobus et al., 1966). We offer here an alternative explanation to reconcile these views (**Figure 2**). We propose that the occurrence of mind-wandering is fully compatible with a low level of arousal and a state of subjective and objective fatigue and that local sleep intrusions could mechanistically account for both mind-wandering and mind-blanking. Similarly, as for behavioral outcomes, the subjective experience associated with a given local sleep occurrence would depend on the anatomical location of these local sleep intrusions, which is a well-defined, testable hypothesis.

ADHD: A Test Case for Our Novel Framework

Local sleep could also represent a powerful explanatory account of inter-individual differences in attentional lapses in conditions such as attention deficit hyperactivity disorder (ADHD). ADHD is a common neurodevelopmental disorder that affects 1–3% of adults and 3–7% of children (Loe and Feldman, 2007; Ebejer et al., 2012). It is characterized by age-inappropriate levels of inattention, hyperactivity and/or impulsivity, which result in substantial challenges in life (decreased socioeconomic status, increased lifetime comorbid psychiatric disorders and higher rates of premature death) (Dalsgaard et al., 2015). ADHD has a high genetic heritability (74%) (Faraone and Larsson, 2019) and is associated with changes in brain anatomy and neural communication (Faraone et al., 2000). However, the neural mechanisms underpinning the inattention and impulsivity which characterize the disorder remain unclear.

Key behavioral attributes of ADHD, established across numerous tasks, are the increase in omission errors, greater intra-individual variability in response timing, as well as more infrequent extremely slow responses (Bellgrove et al., 2005; Johnson et al., 2007a,b). At the phenomenological level, a recent study showed that both teenagers and adults diagnosed with ADHD also differ from non-ADHD individuals, showing increased levels of mind-blanking (Van den Driessche et al., 2017), at the expense of both attentive states and mind-wandering.

This behavioral and experiential fingerprint of ADHD involving sluggishness and mind-blanking portrays ADHD as hypo-vigilant. This could seem at odds with the popular association between ADHD and hyperactivity. However, the association between ADHD and hypo-vigilance fits well with the frequent observation of sleep disturbances in ADHD adults and children (Konofal et al., 2010; Hvolby, 2015; Virring et al., 2016; Gregory et al., 2017; Hiscock and Sciberras, 2019; Sciberras et al., 2019; Silk, 2019). In fact, as many as 73% of children with ADHD experience mild to severe sleep issues (Sung et al., 2008). Children diagnosed with ADHD who exhibit sleep problems also tend to have more severe ADHD symptoms as well as poorer daily functioning compared to ADHD children without sleep problems. In addition, treatments used in ADHD (e.g., methylphenidate) are also used to curb excessive daytime sleepiness in narcolepsy (Hvolby, 2015). Methylphenidate acts on the noradrenergic pathway, which controls attention and sleep/wake regulation (Siegel, 2004; Sara and Bouret, 2012), once again suggesting a mechanistic link between the regulation of attention and modulations of sleep/wake activity.

A key question in the ADHD literature is therefore whether these sleep problems are mere correlates of the attentional disorder or whether they could be at the root of the behavioral features of ADHD. In favor of the latter, it has been hypothesized that ADHD symptoms arise from a dysregulation of arousal (Geissler et al., 2014). Accordingly, ADHD patients may have elevated arousal levels at night, which could delay sleep onset and perturb sleep. As a consequence, these individuals would feel sleepy during the day, which could translate into an increase in local sleep intrusions and give rise to a pattern of sluggishness and impulsivity, mind-wandering and mind-blanking.

Thus, given that individuals with ADHD exhibit, when compared to healthy controls: (1) greater attentional lapses that affect task performance; (2) higher rates of mind-blanking; and (3) more sleep disturbances than healthy controls, local sleep could provide an interesting and largely overlooked neural mechanism for the behavioral phenotype in ADHD. This novel framework in ADHD research could also improve current therapeutic approaches, as current medications can improve daytime performance but can also perturb sleep (Hvolby, 2015). A more systematic investigation of the impact of ADHD treatments on nighttime sleep and daytime sleepiness could help reassess the costs and benefits of these treatments. Finally, current ADHD therapeutic approaches could be complemented with a focus on the improvement of both sleep quantity and quality.

DISCUSSION

We outline here testable hypotheses regarding the relationship between the occurrence of local sleep and the behavioral and phenomenological profiles of attentional lapses. We hypothesize that local sleep occurrences could not only predict attentional lapses but also the type of lapse depending on the anatomical location of local sleep intrusions. Our model could lead to a better understanding of phenomena such as mind wandering and mind blanking. Indeed, mind wandering has been associated with the recruitment of the DMN (Mason et al., 2007). Interestingly, it has been argued that similar patterns of brain activation can be accounted for by drowsiness in

resting-state functional Magnetic Resonance Imaging (fMRI) (Tagliazucchi and Laufs, 2014). In addition, it seems that DMN's activation is mirrored by a deactivation of attentional networks such as the dorsal attention network (Mittner et al., 2016). Local sleep occurrences within attentional networks could be the physiological trigger leading to the deactivation of attentional networks and the recruitment of the DMN, the combination of both resulting in an episode of mind wandering. Conversely, occurrences of local sleep within the DMN could prevent the emergence of spontaneous thoughts (mind wandering), leading to a state of mind blanking. Accordingly, previous findings (Perogamvros et al., 2017) show that an increase in slow-wave power in regions overlapping with the DMN can reduce endogenous thoughts in both wakefulness and sleep. Finally, as during sleep, the set of brain regions affected by an episode of local sleep could be predictive of the specific content of the associated thoughts. For example, local sleep occurrences in prefrontal cortices could be associated with a lack of awareness and agency such as in dreaming (Nir and Tononi, 2010; Voss et al., 2014). Local sleep occurrences in perceptual or associative areas, such as the "hot zone" identified by Siclari et al. (2016) (including sensory areas, precuneus, posterior cingulate), could lead to the occurrence of minimal subjective experience devoid of specific forms of imagery and thought contents (i.e., mind blanking) similar to white dreams during sleep (Windt et al., 2016; Fazekas et al., 2019).

We further propose that local sleep could account for inter-individual differences in the frequency and type of attentional lapses. In particular, focusing on individuals with ADHD, we hypothesize that the reported increase in mind-blanking, at the expense of both mind-wandering and a focused state (Van den Driessche et al., 2017), may be traced back to an increase in local sleep intrusions during the day. This larger propensity to enter mixed sleep/wake states could in turn be related to the sleep disturbances that often accompany the disorder. By showing that individuals with ADHD show more instances of local sleep, we could offer a more exhaustive account of their symptoms, which links daytime performance with disruptions of the restorative function of sleep.

Importantly, we do not argue here that all forms of attentional lapses can be explained by sleepiness and local sleep intrusions, nor that changes in subjective experience such as mind-wandering and mind-blanking are always associated with local sleep. It is of course possible that attentional lapses with similar behavioral consequences to those discussed here can occur in contexts of hyper-arousal rather than hypo-vigilance (**Figure 2**). Nonetheless, we propose that attentional lapses associated with hypo-vigilance might be more frequent.

Although promising, this framework needs to be further established. It has already been suggested that local sleep intrusions, depending on their location, can affect specific aspects of wake behavior (Vyazovskiy et al., 2011; Hung et al., 2013; Bernardi et al., 2015; Nir et al., 2017; Quercia et al., 2018). However, previous findings were obtained in different tasks or studies, or investigated the correlation between local sleep and performance across trials and individuals rather than on the single-trial level. Similarly, the link between local sleep and subjective experience is suggested by previous research but these studies focused mostly on subjective experiences occurring during sleep. Although there is a phenomenological similarity between mind-wandering, mind-blanking and sleep-related experiences and while it is suggestive that both mind-wandering and mind-blanking occur under conditions of low arousal (Braboszcz and Delorme, 2011; Poh et al., 2016; Unsworth and Robison, 2018), this needs to be established through simultaneous phenomenological and neural recordings. Furthermore, it is yet to be determined whether spatial properties of local sleep intrusions could predict changes in spontaneous experience in a region-specific fashion.

Finally, the conditions under which local sleep can be observed are yet unclear. Initial studies have shown local sleep intrusions following extensive sleep deprivation, with the first intrusions occurring only after a few hours of sleep restriction (Hung et al., 2013; Bernardi et al., 2015; Nir et al., 2017). A recent study, however, showed that local sleep can also occur during an experimental task after a normal night of sleep (Quercia et al., 2018). Is local sleep then an abnormal event, occurring when the brain is pushed to its limits or does it represent a normal component of the healthy brain's physiology? Does local sleep affect each of us or is it constrained to very specific contexts or sub-populations? To answer these questions, it is necessary to perform interdisciplinary studies, combining the methods and approaches of sleep, vigilance and attention research. For example, paradigms established in attention research (Robertson et al., 1997; O'Connell et al., 2009; Dockree et al., 2017) and seeking to explore the sub-processes of sensory processing and decision making can be modified to allow the probing of subjective experience with a comprehensive taxonomy of spontaneous cognition (Smallwood and Schooler, 2015). The parallel recording of brain activity and in particular of EEG and pupillometry could then allow to map changes at the behavioral and experiential levels to physiological markers of local sleep and arousal (Bernardi et al., 2015; van Kempen et al., 2019). Exploring local sleep with complementary brain imaging techniques such as Magnetoencephalography (MEG) or fMRI could help understand how local a given local sleep event is and how the occurrence of local sleep in one region can functionally affect connected regions. Our framework is designed to support a versatile methodology that could explore the impact of local sleep in various contexts (with or without sleep deprivation, with or without pharmacological treatments, in response to circadian manipulation, etc) and different populations (healthy individuals, ADHD, insomnia, etc).

AUTHOR CONTRIBUTIONS

All authors contributed to the review and discussion of the literature and to the proposition of future directions.

FUNDING

TA and NT are supported by Australian Research Council Discovery Projects (DP180104128 and DP180100396) and a Strategic Project Grant from Monash University. TA is supported by the Human Frontier Science Program (LT000362/2018-L). NT and JW are supported by Arts-Medicine Interdisciplinary Research Program from Monash University. NT, JW, and SD are supported by AFFINITY grant from Monash University. JW is supported by an Australian Research Council Discovery Early Career Researcher Award (DE170101254). MB is supported by a Senior Research Fellowship from the National Health and Medical Research Council of Australia (NHMRC) and his program of research is funded by the NHMRC, Australian Research Council (ARC), and the Office of Naval Research Global (ONR Global).

REFERENCES

Alais, D., Newell, F., and Mamassian, P. (2010). Multisensory processing in review: from physiology to behaviour. *Seeing Perceiving* 23, 3–38. doi: 10.1163/187847510X488603

Anderson, C., and Horne, J. A. (2006). Sleepiness enhances distraction during a monotonous task. *Sleep* 29, 573–576. doi: 10.1093/sleep/29.4.573

Anderson, C., and Platten, C. R. (2011). Sleep deprivation lowers inhibition and enhances impulsivity to negative stimuli. *Behav. Brain Res.* 217, 463–466. doi: 10.1016/j.bbr.2010.09.020

Anderson, C., Wales, A. W. J., and Home, J. A. (2010). PVT lapses differ according to eyes open, closed, or looking away. *Sleep* 33, 197–204. doi: 10.1093/sleep/33.2.197

Andrillon, T., Poulsen, A. T., Hansen, L. K., Leger, D., and Kouider, S. (2016). Neural markers of responsiveness to the environment in human sleep. *J. Neurosci.* 36, 6583–6596. doi: 10.1523/JNEUROSCI.0902-16.2016

Andrillon, T., Pressnitzer, D., Léger, D., and Kouider, S. (2017). Formation and suppression of acoustic memories during human sleep. *Nat. Commun.* 8:179. doi: 10.1038/s41467-017-00071-z

Antrobus, J. S., Singer, J. L., and Greenberg, S. (1966). Studies in the stream of consciousness: experimental enhancement and suppression of spontaneous cognitive processes. *Percept. Mot. Skills* 23, 399–417. doi: 10.2466/pms.1966.23.2.399

Ballard, J. C. (2001). Assessing attention: comparison of response-inhibition and traditional continuous performance tests. *J. Clin. Exp. Neuropsychol.* 23, 331–350. doi: 10.1076/jcen.23.3.331.1188

Bellgrove, M. A., Hawi, Z., Kirley, A., Gill, M., and Robertson, I. H. (2005). Dissecting the attention deficit hyperactivity disorder (ADHD) phenotype: sustained attention, response variability and spatial attentional asymmetries in relation to dopamine transporter (DAT1) genotype. *Neuropsychologia* 43, 1847–1857. doi: 10.1016/j.neuropsychologia.2005.03.011

Bernardi, G., Betta, M., Ricciardi, E., Pietrini, P., Tononi, G., and Siclari, F. (2019). Regional delta waves in human rapid eye movement sleep. *J. Neurosci.* 39, 2686–2697. doi: 10.1523/JNEUROSCI.2298-18.2019

Bernardi, G., Siclari, F., Yu, X., Zennig, C., Bellesi, M., Ricciardi, E., et al. (2015). Neural and behavioral correlates of extended training during sleep deprivation in humans: evidence for local, task-specific effects. *J. Neurosci.* 35, 4487–4500. doi: 10.1523/JNEUROSCI.4567-14.2015

Blume, C., Del Giudice, R., Wislowska, M., Heib, D. P. J., and Schabus, M. (2018). Standing sentinel during human sleep: continued evaluation of environmental stimuli in the absence of consciousness. *Neuroimage* 178, 638–648. doi: 10.1016/j.neuroimage.2018.05.056

Boly, M., Massimini, M., Tsuchiya, N., Postle, B. R., Koch, C., and Tononi, G. (2017). Are the neural correlates of consciousness in the front or in the back of the cerebral cortex? Clinical and neuroimaging evidence. *J. Neurosci.* 37, 9603–9613. doi: 10.1523/JNEUROSCI.3218-16.2017

Borbély, A. A. (1982). A two process model of sleep regulation. *Hum. Neurobiol.* 1, 195–204.

Braboszcz, C., and Delorme, A. (2011). Lost in thoughts: neural markers of low alertness during mind wandering. *NeuroImage* 54, 3040–3047. doi: 10.1016/j.neuroimage.2010.10.008

Cajochen, C., Brunner, D. P., Krauchi, K., Graw, P., and Wirz-Justice, A. (1995). Power density in theta/alpha frequencies of the waking EEG progressively increases during sustained wakefulness. *Sleep* 18, 890–894. doi: 10.1093/sleep/18.10.890

Carciofo, R., Du, F., Song, N., and Zhang, K. (2014). Mind wandering, sleep quality, affect and chronotype: an exploratory study. *PLoS One* 9:e91285. doi: 10.1371/journal.pone.0091285

Carskadon, M. A., and Dement, W. C. (2005). "Normal human sleep: an overview," in *Principles and Practice of Sleep Medicine*, eds M. H. Kryger, T. Roth, and W. C. Dement, (Philadelphia, PA: Elsevier Saunders), 13–23. doi: 10.1016/B0-72-160797-7/50009-4

Castelnovo, A., Riedner, B. A., Smith, R. F., Tononi, G., Boly, M., and Benca, R. M. (2016). Scalp and source power topography in sleepwalking and sleep terrors: a high-density EEG study. *Sleep* 39, 1815–1825. doi: 10.5665/sleep.6162

Cirelli, C., and Tononi, G. (2008). Is sleep essential? *PLoS Biol.* 6:e216. doi: 10.1371/journal.pbio.0060216

Dalsgaard, S., Østergaard, S. D., Leckman, J. F., Mortensen, P. B., and Pedersen, M. G. (2015). Mortality in children, adolescents, and adults with attention deficit hyperactivity disorder: a nationwide cohort study. *Lancet* 385, 2190–2196. doi: 10.1016/S0140-6736(14)61684-6

D'Argembeau, A. (2018). *Mind-Wandering and Self-Referential Thought*, eds K. Christoff, and K. C. R. Fox, (Oxford: Oxford University Press).

Dockree, P. M., Barnes, J. J., Matthews, N., Dean, A. J., Abe, R., Nandam, L. S., et al. (2017). The effects of methylphenidate on the neural signatures of sustained attention. *Biol. Psychiatry* 82, 687–694. doi: 10.1016/j.biopsych.2017.04.016

Dodet, P., Chavez, M., Leu-Semenescu, S., Golmard, J. L., and Arnulf, I. (2015). Lucid dreaming in narcolepsy. *Sleep* 38, 487–497. doi: 10.5665/sleep.4516

Domhoff, G. W. (2018). *Dreaming Is an Intensified Form of Mind-Wandering, Based in an Augmented Portion of the Default Network*, eds K. Christoff, and K. C. R. Fox, (Oxford: Oxford University Press).

Drummond, S. P. A., Anderson, D. E., Straus, L. D., Vogel, E. K., and Perez, V. B. (2012). The effects of two types of sleep deprivation on visual working memory capacity and filtering efficiency. *PLoS One* 7:e35653. doi: 10.1371/journal.pone.0035653

Drummond, S. P. A., Paulus, M. P., and Tapert, S. F. (2006). Effects of two nights sleep deprivation and two nights recovery sleep on response inhibition. *J. Sleep Res.* 15, 261–265. doi: 10.1111/j.1365-2869.2006.00535.x

Ebejer, J. L., Medland, S. E., van der Werf, J., Gondro, C., Henders, A. K., Lynskey, M., et al. (2012). Attention deficit hyperactivity disorder in australian adults: prevalence, persistence, conduct problems and disadvantage. *PLoS One* 7:e47404. doi: 10.1371/journal.pone.0047404

Faraone, S. V., Biederman, J., Spencer, T., Wilens, T., Seidman, L. J., Mick, E., et al. (2000). Attention-deficit/hyperactivity disorder in adults: an overview. *Biol. Psychiatry* 48, 9–20.

Faraone, S. V., and Larsson, H. (2019). Genetics of attention deficit hyperactivity disorder. *Mol. Psychiatry* 24, 562–575. doi: 10.1038/s41380-018-0070

Fazekas, P., Nemeth, G., and Overgaard, M. (2019). White dreams are made of colours: what studying contentless dreams can teach about the neural basis of dreaming and conscious experiences. *Sleep Med. Rev.* 43, 84–91. doi: 10.1016/j.smrv.2018.10.005

Finelli, L. A., Baumann, H., Borbély, A. A., and Achermann, P. (2000). Dual electroencephalogram markers of human sleep homeostasis: correlation between theta activity in waking and slow-wave activity in sleep. *Neuroscience* 101, 523–529. doi: 10.1016/s0306-4522(00)00409-7

Foulkes, D., and Fleisher, S. (1975). Mental activity in relaxed wakefulness. *J. Abnorm. Psychol.* 84, 66–75. doi: 10.1037/h0076164

Fox, K. C. R., Nijeboer, S., Solomonova, E., Domhoff, G. W., and Christoff, K. (2013). Dreaming as mind wandering: evidence from functional neuroimaging and first-person content reports. *Front. Hum. Neurosci.* 7:412. doi: 10.3389/fnhum.2013.00412

Funk, C. M., Honjoh, S., Rodriguez, A. V., Cirelli, C., and Tononi, G. (2016). Local slow waves in superficial layers of primary cortical areas during REM sleep. *Curr. Biol.* 26, 396–403. doi: 10.1016/j.cub.2015.11.062

Geissler, J., Romanos, M., Hegerl, U., and Hensch, T. (2014). Hyperactivity and sensation seeking as autoregulatory attempts to stabilize brain arousal in ADHD and mania? *Atten. Defic. Hyperact. Disord.* 6, 159–173. doi: 10.1007/s12402-014-0144-z

Gregory, A. M., Agnew-Blais, J. C., Matthews, T., Moffitt, T. E., and Arseneault, L. (2017). ADHD and sleep quality: longitudinal analyses from childhood to early adulthood in a twin cohort. *J. Clin. Child Adolesc. Psychol.* 46, 284–294. doi: 10.1080/15374416.2016.1183499

Halász, P. (2016). The K-complex as a special reactive sleep slow wave – a theoretical update. *Sleep Med. Rev.* 29, 34–40. doi: 10.1016/j.smrv.2015.09.004

Hiscock, H., and Sciberras, E. (2019). *Sleep and ADHD: an Evidence-Based Guide to Assessment and Treatment*. Available at: http://search.ebscohost.com/login.aspx?direct=true&scope=site&db=nlebk&db=nlabk&AN=1914230 (accessed April 15, 2019).

Horikawa, T., Tamaki, M., Miyawaki, Y., and Kamitani, Y. (2013). Neural decoding of visual imagery during sleep. *Science* 340, 639–642. doi: 10.1126/science.1234330

Huber, R., Ghilardi, M. F., Massimini, M., and Tononi, G. (2004). Local sleep and learning. *Nature* 430, 78–81. doi: 10.1038/nature02663

Hung, C.-S., Sarasso, S., Ferrarelli, F., Riedner, B., Ghilardi, M. F., Cirelli, C., et al. (2013). Local experience-dependent changes in the wake EEG after prolonged wakefulness. *Sleep* 36, 59–72. doi: 10.5665/sleep.2302

Hvolby, A. (2015). Associations of sleep disturbance with ADHD: implications for treatment. *Atten. Defic. Hyperact. Disord.* 7, 1–18. doi: 10.1007/s12402-014-0151-0

James, W. (1890). *The Principles of Psychology*. New York, NY: Henry Holt and Company.

Johnson, K. A., Kelly, S. P., Bellgrove, M. A., Barry, E., Cox, M., Gill, M., et al. (2007a). Response variability in attention deficit hyperactivity disorder: evidence for neuropsychological heterogeneity. *Neuropsychologia* 45, 630–638. doi: 10.1016/j.neuropsychologia.2006.03.034

Johnson, K. A., Robertson, I. H., Kelly, S. P., Silk, T. J., Barry, E., Dáibhis, A., et al. (2007b). Dissociation in performance of children with ADHD and high-functioning autism on a task of sustained attention. *Neuropsychologia* 45, 2234–2245. doi: 10.1016/j.neuropsychologia.2007.02.019

Joshi, S., Li, Y., Kalwani, R. M., and Gold, J. I. (2016). Relationships between pupil diameter and neuronal activity in the locus coeruleus, colliculi, and cingulate cortex. *Neuron* 89, 221–234. doi: 10.1016/j.neuron.2015.11.028

Killingsworth, M. A., and Gilbert, D. T. (2010). A wandering mind is an unhappy mind. *Science* 330, 932–932. doi: 10.1126/science.1192439

Koch, C., Massimini, M., Boly, M., and Tononi, G. (2016). Neural correlates of consciousness: progress and problems. *Nat. Rev. Neurosci.* 17, 307–321. doi: 10.1038/nrn.2016.22

Konofal, E., Lecendreux, M., and Cortese, S. (2010). Sleep and ADHD. *Sleep Med.* 11, 652–658. doi: 10.1016/j.sleep.2010.02.012

Krueger, J. M., Nguyen, J. T., Dykstra-Aiello, C. J., and Taishi, P. (2019). Local sleep. *Sleep Med. Rev.* 43, 14–21. doi: 10.1016/j.smrv.2018.10.001

Loe, I. M., and Feldman, H. M. (2007). Academic and educational outcomes of children with ADHD. *J. Pediatr. Psychol.* 32, 643–654. doi: 10.1093/jpepsy/jsl054

Mascetti, G. G. (2016). Unihemispheric sleep and asymmetrical sleep: behavioral, neurophysiological, and functional perspectives. *Nat. Sci. Sleep* 8, 221–238. doi: 10.2147/NSS.S71970

Mason, M. F., Norton, M. I., Van Horn, J. D., Wegner, D. M., Grafton, S. T., and Macrae, C. N. (2007). Wandering minds: the default network and stimulus-independent thought. *Science* 315, 393–395. doi: 10.1126/science.1131295

McCormick, D. A., and Bal, T. (1994). Sensory gating mechanisms of the thalamus. *Curr. Opin. Neurobiol.* 4, 550–556. doi: 10.1016/0959-4388(94)90056-6

Mittner, M., Boekel, W., Tucker, A. M., Turner, B. M., Heathcote, A., and Forstmann, B. U. (2014). When the brain takes a break: a model-based analysis of mind wandering. *J. Neurosci.* 34, 16286–16295. doi: 10.1523/JNEUROSCI.2062-14.2014

Mittner, M., Hawkins, G. E., Boekel, W., and Forstmann, B. U. (2016). A neural model of mind wandering. *Trends Cogn. Sci.* 20, 570–578. doi: 10.1016/j.tics.2016.06.004

Muto, V., Jaspar, M., Meyer, C., Kusse, C., Chellappa, S. L., Degueldre, C., et al. (2016). Local modulation of human brain responses by circadian rhythmicity and sleep debt. *Science* 353, 687–690. doi: 10.1126/science.aad2993

Nir, Y., Andrillon, T., Marmelshtein, A., Suthana, N., Cirelli, C., Tononi, G., et al. (2017). Selective neuronal lapses precede human cognitive lapses following sleep deprivation. *Nat. Med.* 23, 1474–1480. doi: 10.1038/nm.4433

Nir, Y., Staba, R., Andrillon, T., Vyazovskiy, V. V., Cirelli, C., Fried, I., et al. (2011). Regional slow waves and spindles in human sleep. *Neuron* 70, 153–169. doi: 10.1016/j.neuron.2011.02.043

Nir, Y., and Tononi, G. (2010). Dreaming and the brain: from phenomenology to neurophysiology. *Trends Cogn. Sci.* 14, 88–100. doi: 10.1016/j.tics.2009.12.001

Nobili, L., De Gennaro, L., Proserpio, P., Moroni, F., Sarasso, S., Pigorini, A., et al. (2012). Local aspects of sleep: observations from intracerebral recordings in humans. *Prog. Brain Res.* 199, 219–232. doi: 10.1016/B978-0-444-59427-3.00013-7

Nobili, L., Ferrara, M., Moroni, F., De Gennaro, L., Russo, G. L., Campus, C., et al. (2011). Dissociated wake-like and sleep-like electro-cortical activity during sleep. *NeuroImage* 58, 612–619. doi: 10.1016/j.neuroimage.2011.06.032

O'Connell, R. G., Bellgrove, M. A., Dockree, P. M., Lau, A., Fitzgerald, M., and Robertson, I. H. (2008). Self-alert training: volitional modulation of autonomic arousal improves sustained attention. *Neuropsychologia* 46, 1379–1390. doi: 10.1016/j.neuropsychologia.2007.12.018

O'Connell, R. G., Dockree, P. M., Robertson, I. H., Bellgrove, M. A., Foxe, J. J., and Kelly, S. P. (2009). Uncovering the neural signature of lapsing attention: electrophysiological signals predict errors up to 20 s before they occur. *J. Neurosci.* 29, 8604–8611. doi: 10.1523/JNEUROSCI.5967-08.2009

Ohayon, M. M., Carskadon, M. A., Guilleminault, C., and Vitiello, M. V. (2004). Meta-analysis of quantitative sleep parameters from childhood to old age in healthy individuals: developing normative sleep values across the human lifespan. *Sleep* 27, 1255–1273. doi: 10.1093/sleep/27.7.1255

Perogamvros, L., Baird, B., Seibold, M., Riedner, B., Boly, M., and Tononi, G. (2017). The phenomenal contents and neural correlates of spontaneous thoughts across wakefulness, NREM sleep, and REM sleep. *J. Cogn. Neurosci.* 29, 1766–1777. doi: 10.1162/jocn_a_01155

Poh, J.-H., Chong, P. L. H., and Chee, M. W. L. (2016). Sleepless night, restless mind: effects of sleep deprivation on mind wandering. *J. Exp. Psychol.* 145, 1312–1318. doi: 10.1037/xge0000207

Quercia, A., Zappasodi, F., Committeri, G., and Ferrara, M. (2018). Local use-dependent sleep in wakefulness links performance errors to learning. *Front. Hum. Neurosci.* 12:122. doi: 10.3389/fnhum.2018.00122

Rattenborg, N. C., van der Meij, J., Beckers, G. J. L., and Lesku, J. A. (2019). Local aspects of avian non-REM and REM sleep. *Front. Neurosci.* 13:567. doi: 10.3389/fnins.2019.00567

Riedner, B. A., Goldstein, M. R., Plante, D. T., Rumble, M. E., Ferrarelli, F., Tononi, G., et al. (2016). Regional patterns of elevated alpha and high-frequency electroencephalographic activity during nonrapid eye movement sleep in chronic insomnia: a pilot study. *Sleep* 39, 801–812. doi: 10.5665/sleep.5632

Riedner, B. A., Vyazovskiy, V. V., Huber, R., Massimini, M., Esser, S., Murphy, M., et al. (2007). Sleep homeostasis and cortical synchronization: III. A high-density EEG study of sleep slow waves in humans. *Sleep* 30, 1643–1657. doi: 10.1093/sleep/30.12.1643

Robertson, I. H., Manly, T., Andrade, J., Baddeley, B. T., and Yiend, J. (1997). "Oops!": performance correlates of everyday attentional failures in traumatic brain injured and normal subjects. *Neuropsychologia* 35, 747–758. doi: 10.1016/s0028-3932(97)00015-8

Sara, S. J. (2009). The locus coeruleus and noradrenergic modulation of cognition. *Nat. Rev. Neurosci.* 10, 211–223. doi: 10.1038/nrn2573

Sara, S. J., and Bouret, S. (2012). Orienting and reorienting: the locus coeruleus mediates cognition through arousal. *Neuron* 76, 130–141. doi: 10.1016/j.neuron.2012.09.011

Schabus, M., Dang-Vu, T. T., Heib, D. P. J., Boly, M., Desseilles, M., Vandewalle, G., et al. (2012). The fate of incoming stimuli during nrem sleep is determined by spindles and the phase of the slow oscillation. *Front. Neurol.* 3:40. doi: 10.3389/fneur.2012.00040

Sciberras, E., Heussler, H., Berthier, J., and Lecendreux, M. (2019). "Epidemiology and etiology of medical sleep problems in ADHD," in *Sleep and ADHD*, eds H. Hiscock, and E. Sciberras, (Amsterdam: Elsevier), 95–117. doi: 10.1016/B978-0-12-814180-9.00004-1

Seli, P., Carriere, J. S. A., Levene, M., and Smilek, D. (2013). How few and far between? Examining the effects of probe rate on self-reported mind wandering. *Front. Psychol.* 4:430. doi: 10.3389/fpsyg.2013.00430

Siclari, F., Baird, B., Perogamvros, L., Bernardi, G., LaRocque, J. J., Riedner, B., et al. (2016). The neural correlates of dreaming. *bioRxiv*

Siclari, F., Bernardi, G., Riedner, B. A., LaRocque, J. J., Benca, R. M., and Tononi, G. (2014). Two distinct synchronization processes in the transition to sleep: a high-density electroencephalographic study. *Sleep.* 37, 1621–1637. doi: 10.5665/sleep.4070

Siclari, F., Larocque, J. J., Postle, B. R., and Tononi, G. (2013). Assessing sleep consciousness within subjects using a serial awakening paradigm. *Front. Psychol.* 4:542. doi: 10.3389/fpsyg.2013.00542

Siclari, F., and Tononi, G. (2017). Local aspects of sleep and wakefulness. *Curr. Opin. Neurobiol.* 44, 222–227. doi: 10.1016/j.conb.2017.05.008

Siegel, J. M. (2004). The neurotransmitters of sleep. *J. Clin. Psychiatry* 65(Suppl. 16), 4–7.

Silk, T. J. (2019). "New frontiers: neurobiology of sleep in ADHD," in *Sleep and ADHD*, eds H. Hiscock and E. Sciberras (Amsterdam: Elsevier), 331–353. doi: 10.1016/B978-0-12-814180-9.00013-12

Smallwood, J., and Schooler, J. W. (2015). The science of mind wandering: empirically navigating the stream of consciousness. *Annu. Rev. Psychol.* 66, 487–518. doi: 10.1146/annurev-psych-010814-015331

Smith, P. L., and Ratcliff, R. (2004). Psychology and neurobiology of simple decisions. *Trends Neurosci.* 27, 161–168. doi: 10.1016/j.tins.2004.01.006

Steriade, M. (2003). *Neuronal Substrates of Sleep and Epilepsy*, 1st Edn. Cambridge: Cambridge University Press.

Steriade, M. (2005). Sleep, epilepsy and thalamic reticular inhibitory neurons. *Trends Neurosci.* 28, 317–324. doi: 10.1016/j.tins.2005.03.007

Sung, V., Hiscock, H., Sciberras, E., and Efron, D. (2008). Sleep problems in children with attention-deficit/hyperactivity disorder: prevalence and the effect on the child and family. *Arch. Pediatr. Adolesc. Med.* 162:336. doi: 10.1001/archpedi.162.4.336

Tagliazucchi, E., and Laufs, H. (2014). Decoding wakefulness levels from typical fMRI resting-state data reveals reliable drifts between wakefulness and sleep. *Neuron* 82, 695–708. doi: 10.1016/j.neuron.2014.03.020

Tamaki, M., Bang, J. W., Watanabe, T., and Sasaki, Y. (2016). Night watch in one brain hemisphere during sleep associated with the first-night effect in humans. *Curr. Biol.* 26, 1190–1194. doi: 10.1016/j.cub.2016.02.063

Terzaghi, M., Sartori, I., Tassi, L., Didato, G., Rustioni, V., LoRusso, G., et al. (2009). Evidence of dissociated arousal states during NREM parasomnia from an intracerebral neurophysiological study. *Sleep* 32, 409–412. doi: 10.1093/sleep/32.3.409

Thiele, A., and Bellgrove, M. A. (2018). Neuromodulation of attention. *Neuron* 97, 769–785. doi: 10.1016/j.neuron.2018.01.008

Tononi, G., and Cirelli, C. (2014). Sleep and the price of plasticity: from synaptic and cellular homeostasis to memory consolidation and integration. *Neuron* 81, 12–34. doi: 10.1016/j.neuron.2013.12.025

Tononi, G., and Massimini, M. (2008). Why does consciousness fade in early sleep? *Ann. N. Y. Acad. Sci.* 1129, 330–334. doi: 10.1196/annals.1417.024

Unsworth, N., and Robison, M. K. (2018). Tracking arousal state and mind wandering with pupillometry. *Cogn. Affect. Behav. Neurosci.* 18, 638–664. doi: 10.3758/s13415-018-0594

van den Brink, R. L., Murphy, P. R., and Nieuwenhuis, S. (2016). Pupil diameter tracks lapses of attention. *PLoS One* 11:e0165274. doi: 10.1371/journal.pone.0165274

Van den Driessche, C., Bastian, M., Peyre, H., Stordeur, C., Acquaviva, É, Bahadori, S., et al. (2017). Attentional lapses in attention-deficit/hyperactivity disorder: blank rather than wandering thoughts. *Psychol. Sci.* 28, 1375–1386. doi: 10.1177/0956797617708234

van Kempen, J., Loughnane, G. M., Newman, D. P., Kelly, S. P., Thiele, A., O'Connell, R. G., et al. (2019). Behavioural and neural signatures of perceptual decision-making are modulated by pupil-linked arousal. *eLife* 8:e42541. doi: 10.7554/eLife.42541

Van Schie, M. K. M., Thijs, R. D., Fronczek, R., Middelkoop, H. A. M., Lammers, G. J., and Van Dijk, J. G. (2012). Sustained attention to response task (SART) shows impaired vigilance in a spectrum of disorders of excessive daytime sleepiness: vigilance impairment in EDS. *J. Sleep Res.* 21, 390–395. doi: 10.1111/j.1365-2869.2011.00979.x

Varazzani, C., San-Galli, A., Gilardeau, S., and Bouret, S. (2015). Noradrenaline and dopamine neurons in the reward/effort trade-off: a direct electrophysiological comparison in behaving monkeys. *J. Neurosci.* 35, 7866–7877. doi: 10.1523/JNEUROSCI.0454-15.2015

Virring, A., Lambek, R., Thomsen, P. H., Møller, L. R., and Jennum, P. J. (2016). Disturbed sleep in attention-deficit hyperactivity disorder (ADHD) is not a question of psychiatric comorbidity or ADHD presentation. *J. Sleep Res.* 25, 333–340. doi: 10.1111/jsr.12377

Voss, U., Holzmann, R., Hobson, A., Paulus, W., Koppehele-Gossel, J., Klimke, A., et al. (2014). Induction of self awareness in dreams through frontal low current stimulation of gamma activity. *Nat. Neurosci.* 17, 810–812. doi: 10.1038/nn.3719

Vyazovskiy, V. V., and Harris, K. D. (2013). Sleep and the single neuron: the role of global slow oscillations in individual cell rest. *Nat. Rev. Neurosci.* 14, 443–451. doi: 10.1038/nrn3494

Vyazovskiy, V. V., Olcese, U., Hanlon, E. C., Nir, Y., Cirelli, C., and Tononi, G. (2011). Local sleep in awake rats. *Nature* 472, 443–447. doi: 10.1038/nature10009

Wamsley, E. J. (2013). Dreaming, waking conscious experience, and the resting brain: report of subjective experience as a tool in the cognitive neurosciences. *Front. Psychol.* 4:637. doi: 10.3389/fpsyg.2013.00637

Ward, A. F., and Wegner, D. M. (2013). Mind-blanking: when the mind goes away. *Front. Psychol.* 4:650. doi: 10.3389/fpsyg.2013.00650

Windt, J. M. (2015). *Dreaming: a Conceptual Framework for Philosophy of Mind and Empirical Research*. Cambridge, MA: MIT Press.

Windt, J. M., Nielsen, T., and Thompson, E. (2016). Does consciousness disappear in dreamless sleep? *Trends Cogn. Sci.* 20, 871–882. doi: 10.1016/j.tics.2016.09.006

Wong, W., Noreika, V., Móró, L., Revonsuo, A., Windt, J., Valli, K., et al. (2019). The dream catcher experiment: blinded analyses disconfirm markers of dreaming consciousness in EEG spectral power. *bioRxiv*.

Conflict of Interest Statement: The authors declare that the research was conducted in the absence of any commercial or financial relationships that could be construed as a potential conflict of interest.

Copyright © 2019 Andrillon, Windt, Silk, Drummond, Bellgrove and Tsuchiya. This is an open-access article distributed under the terms of the Creative Commons Attribution License (CC BY). The use, distribution or reproduction in other forums is permitted, provided the original author(s) and the copyright owner(s) are credited and that the original publication in this journal is cited, in accordance with accepted academic practice. No use, distribution or reproduction is permitted which does not comply with these terms.

frontiers in Neuroscience

ORIGINAL RESEARCH
published: 15 October 2019
doi: 10.3389/fnins.2019.01094

Local Gamma Activity During Non-REM Sleep in the Context of Sensory Evoked K-Complexes

Marco Laurino[1], *Andrea Piarulli*[2,3], *Danilo Menicucci*[2] *and Angelo Gemignani*[1,2*]

[1] Institute of Clinical Physiology, National Research Council, Pisa, Italy, [2] Department of Surgical, Medical, Molecular Pathology and Critical Care Medicine, University of Pisa, Pisa, Italy, [3] Coma Science Group, GIGA Consciousness, University of Liège, Liège, Belgium

K-complexes (KCs) and Sleep Slow Oscillations (SSOs) are the EEG expression of neuronal bistability during deeper stages Non-REM sleep. They are characterized by a deep negative deflection lasting about half-a-second, sustained, at the cortical level, by a widespread and synchronized neuronal hyperpolarization (i.e., electrical silence). The phase of hyperpolarization is followed by a period of intense and synchronized neuronal firing (i.e., depolarization phase) resulting at the EEG level, in a large positive deflection (lasting about 0.5 s) and a concurrent high frequency activity (i.e., spindles). Both KCs and SSOs rather than being "local" phenomena, propagate over large sections of the cortex. These features suggest that bistability is a large-scale network phenomenon, possibly driven by a propagating excitatory activity and involving wide populations of synchronized neurons. We have recently shown that KCs and SSOs include a positive bump preceding the negative peak and that for sensory-evoked KCs this bump coincides with the P200 wave. We demonstrated that the P200 has a sensory-modality specific localization, as it is firstly elicited in the primary sensory areas related to the stimulus, which in turn receive projections from the thalamic core. We observed that the P200 acts as a propagating excitatory activity and hypothesized that it could play a key role in inducing the opening of K+ channels, and hence the cortical hyperpolarization. Here we demonstrate that the P200 is sustained by a high-frequency excitation bringing further support to its role in triggering bistability. We show that the P200 has a higher power density in gamma band as compared to the P900 coherently for all sensory modalities, and we confirm that the latter wave is crowned by higher activity in sigma-beta bands. Finally, we characterize the P200 gamma activity at the cortical level in terms of spatial localization and temporal dynamics, demonstrating that it emerges in sensory stimulus-specific primary areas and travels over the cortical mantle spreading toward fronto-central associative areas and fading concurrently with the N550 onset.

Keywords: K-complex, slow oscillation, sensory processing, consciousness, source localization, gamma activity, sleep, down state

OPEN ACCESS

Edited by:
Michele Bellesi,
University of Bristol, United Kingdom

Reviewed by:
Brady A. Riedner,
University of Wisconsin-Madison, United States
Peter Halasz,
Hungarian Society for Sleep Medicine, Hungary

***Correspondence:**
Angelo Gemignani
angelo.gemignani@unipi.it

Specialty section:
This article was submitted to Sleep and Circadian Rhythms, a section of the journal Frontiers in Neuroscience

Received: *15 June 2019*
Accepted: *30 September 2019*
Published: *15 October 2019*

Citation:
Laurino M, Piarulli A, Menicucci D and Gemignani A (2019) Local Gamma Activity During Non-REM Sleep in the Context of Sensory Evoked K-Complexes. Front. Neurosci. 13:1094. doi: 10.3389/fnins.2019.01094

INTRODUCTION

Bistability is the activity modality proper of thalamic and cortical neurons during Non-REM (NREM) sleep (Vyazovskiy et al., 2007). This dynamic pattern consists of an alternation between states of neuronal hyperpolarization-electrical silence (down states) and states of depolarization characterized by intense neuronal firing and synaptic activity (up states)

(Steriade et al., 1993; Compte et al., 2003; Steriade and Timofeev, 2003). In humans, the down state lasts a few hundred milliseconds, and is followed by an up state of comparable duration. This bistable phenomenon is the neurobiological mechanism underlying both K-complexes (KCs) and Sleep Slow Oscillations (SSOs) (Amzica and Steriade, 1997a).

KCs and SSOs have been identified as synchronized-cortical-network phenomena (Amzica and Steriade, 1997b), involving large assemblies of neural circuits, so that their electrical patterns are easily detectable using surface EEG. Each KC/SSO is composed by a sharp negative wave (down state) followed by a large positive deflection crowned by high frequency activity (up state). While the former pattern is the EEG manifestation of a single event of bistable activity, the SSOs can either occur as single events or as trains of waves during periods of deepest NREM sleep (Crunelli and Hughes, 2010).

Several studies (e.g., Sejnowski and Destexhe, 2000; Steriade, 2004; Destexhe et al., 2007; Menicucci et al., 2013) have highlighted similarities between up states and wakefulness as they are both characterized by high-frequency activity with a similar spatio-temporal synchronization. In this framework, the up state high frequency activity has been hypothesized to play a fundamental role in memory consolidation (Mölle et al., 2011), with mentation as byproduct (Steriade, 2000).

The SSO/KC seem thus to subserve two different yet complimentary functions as it (1) maintains sleep and unconsciousness (down state), (2) plays a key role in the consolidation of recently acquired learning (up state).

While SSO/KC down and up states have been widely investigated unveiling the neuronal and network phenomena subtending their appearance and identifying their respective functions, the electrophysiological mechanisms responsible for the down state's ignition still remain to be fully elucidated.

In a previous study focused on temporally isolated SSOs events (Menicucci et al., 2013), we demonstrated that the down state is preceded by an early positive wave, that we named pre-down state. We showed that this early wave is characterized by the presence of a concurrent excitatory activation (beta to gamma) and hypothesized that this high-frequency excitatory activity could have a key role in triggering the opening of activity-dependent K+ channels, hence promoting the down state onset (Fröhlich et al., 2006; Sanchez-Vives et al., 2010).

During NREM sleep, simple sensory stimuli can evoke KCs, whose electrophysiological pattern consists of three distinctive waves: P200, N550, and P900 where the letter P (N) stands for positive (negative) deflection, and the number identifies the conventional latency of the wave peak in milliseconds (see Laurino et al., 2014).

The KC was first described by Loomis and colleagues (Loomis et al., 1935), and deeply investigated by Halász in recent years (Halász, 2005, 2016).

Amzica and Steriade (1997b), demonstrated that KCs and spontaneous SSOs originate from the same neurobiological mechanisms (hence the name evoked-SSOs for KCs), the KC counterparts of the down and up states corresponding, respectively to its N550 and P900 components (Laurino et al., 2014).

In Laurino et al. (2014), by using high-density EEG, we studied the quenching of sensory processing during NREM sleep in humans. We considered both stimulation events characterized by the evoked KC (eKC), elicitation (i.e., down and up state phases) and those where no response was evoked. We showed that, in both cases, the P200 is detectable and has the shortest latencies in stimulus-related primary sensory areas, acting as a wake-like activation traveling from primary sensory areas toward fronto-central regions. We observed that the elicitation of the biphasic component of the eKC (N550 and P900, respectively) depends on the P200 amplitude when it reaches areas with higher proneness to bistability (i.e., fronto-central areas), corresponding at the cortical level, to the insula and medial cingulate cortex Murphy et al., 2009. On this basis, we hypothesized that the triggering of the electrical silence (N550/down state) depends on the interaction between the level of excitatory activity sustaining the P200 (the higher the level, the higher the probability of triggering a down state) and the local proneness to bistability.

In this study, using the same eKC model of Laurino et al. (2014), we demonstrate that the P200 is a bottom-up excitatory cortical response to a sensory stimulation, while the P900 is associated to recursive cortico-thalamo-cortical activities. To this aim, we characterize and compare the P200 and P900 waves considering their spectral content at high frequencies (from sigma, to gamma bands) both in primary sensory areas and in fronto-central regions. We show that the P200 is characterized by higher gamma activity as compared to the P900, consistently across sensory modalities, and that this activity is already present in primary sensory areas and maintained throughout its cortical travel toward fronto-central regions. Conversely, we find that the P900 is characterized by higher sigma-beta activity as compared to the P200, consistently across sensory modalities and regions of interest. We finally characterize the P200 gamma activity at the cortical level in terms of temporo-spatial dynamics, demonstrating that it originates in stimulus-related primary sensory areas and travels over the cortex reaching fronto-central regions. These findings taken together suggest that the P200 is a purely cortical response composed by a slow positive deflection complemented by a concurrent excitatory activity in gamma band. We hypothesize that this excitatory activity acts as a trigger for the opening of K+ channels, thus favoring the local fall in down state and hence the quenching of sensory processing.

METHODS

Participants and Experimental Protocol

This work aims at shedding light on aspects of evoked K-Complexes not investigated in Laurino et al. (2014), where the focus was set on latencies/topologies of P200, N550, and P900. We first briefly recall methods and experimental protocols developed in our previous research that are used also in this study (for a detailed characterization of subjects and stimulation modalities, please refer to Laurino et al., 2014).

Fourteen healthy volunteers (right-handed males, age 20–26 years) without history of medical diseases, psychiatric or neurological disorders, audiological, and/or visual deficits were included in the study. Each subject slept for two consecutive

nights in the sleep laboratory (the first as an adaptation night). High-density sleep EEG recordings were collected in the second night (experimental session). The Local Ethical Committee approved the study, and the experimental procedures were in line with the tenets of the declaration of Helsinki.

During each experimental session, we performed a real-time EEG visual scoring continuously assessing the sleep stage (AASM criteria, Iber, 2007). Stimulation was carried out during N2 and N3 stages, but not during N1, awakenings or arousals, and consisted in sequences of auditory, tactile and visual stimuli delivered in a randomized order, with inter-stimulus intervals randomly sampled from a uniform distribution of allowed time intervals ranging from 15 to 20 s.

Acoustic stimuli were pure tones at 1,000 Hz with a 50 ms time-duration (rise and fall times 5 ms), delivered through in-ear headphones (XBA, Sony) and a sound pressure intensity of 60 dB. Tactile stimuli were achieved using mechanical vibrations (pallesthesia) at 300 Hz (50 ms of stimulation, rise and fall times 20 ms), delivered through an electrically driven vibrating device placed on the middle finger of the right hand. Visual stimuli consisted in light flashes (time-duration <1 ms) delivered with a photographic flash (32 Z-2, Metz), oriented toward the room ceiling.

EEG Recordings

High-density EEGs were recorded using a Net Amps 300 system (GES300, Electrical Geodesic Inc., Eugene, OR, USA) with a 128-electrode HydroCel Geodesic Sensor net.

EEG signals were acquired with a sampling rate of 500 Hz in the 0.01–500 Hz band, using Net Station software, Version 4.4.2 (Electrical Geodesic Inc., Eugene, OR, USA), taking the vertex as the online reference potential (Cz). Electrodes impedance were maintained below 50 KΩ throughout the recording, in line with Electrical Geodesics recommendations.

All offline analyses were conducted using tailored Matlab codes (MathWorks, Natick, MA, USA), and when dealing with cortical sources reconstruction, taking advantage of Brainstorm toolbox functions (Tadel et al., 2011) and of OpenMEEG software (Kybic et al., 2005; Gramfort et al., 2011).

Temporal Segmentation of eKCs

EEG sleep recordings were offline visually scored according to the AASM scoring criteria (Iber, 2007). After the removal of artifacted epochs, EEG signals were re-referenced to the mastoids' average, and trials consisting of full-fledged and temporally isolated eKCs (i.e., without any SSO event or delta wave occurring from 3 s before to 4 s after the eKC negative peak, see Laurino et al., 2014), were extracted.

For each retained event, three epochs of interest were selected (see **Figure 1**):

1) Baseline: 1 s window ending 100 ms before the stimulus;
2) P200: 300 ms window starting 50 ms after the stimulus (pre-down state);
3) P900: 1 s window starting 750 ms after the stimulus (up state);

Spectral Characterization of High Frequency Activity in Baseline, T200, and T900 Epochs

In line with the study hypotheses (the characterization of P200 and P900 waves considering their spectral content at high frequencies), three bands of interest were selected: sigma (9–18 Hz), beta (18–30 Hz), and gamma (30–45 Hz). Power spectra were estimated for each epoch of interest using the Fast Fourier Transform applied on a 300 ms Hamming-weighted sliding window. The length of the window was chosen as a trade-off between two opposite requirements: (i) provide an appropriate frequency resolution for a reliable power density estimation in the bands of interest, (ii) the window had to be wide enough to encompass the P200 wave and at the same time its time-limits had to be at a suitable distance both from the stimulus delivery and from the N550 peak.

For each subjects, electrode and epoch, band-limited power spectra were calculated as the sum of the power spectra over the frequency bins included in the band and then log-transformed.

For the P200, a single window was applied (the window length being equal to the epoch duration), while for the Baseline and the P900, power spectra were estimated using a 300 ms sliding window with a 33% overlap between contiguous ones. In this latter case (e.g., Baseline and P900), the mean power was obtained averaging among the windows pertaining to the epoch. The mean power densities in sigma, beta, and gamma bands were thus estimated for each subject, sensory-modality, electrode, and epoch (e.g., Baseline, P200, and P900), averaging over the related trials.

Two scalp regions of interest (ROI) were selected:

1) Primary Sensory Areas (PSA): electrodes over primary sensory areas with respect to each type of sensory stimulation: (i) electrodes related to acoustic stimuli were located over Brodmann areas (BAs) 41 and 42, (ii) electrodes related to tactile stimuli over BAs 3, 1, 2, and (iii) electrodes related to visual stimuli over BAs 17 and 18. Of note, these electrodes were those showing the shortest P200 latency in Laurino et al. (2014).
2) Frontal Central Areas (FCA): electrodes over fronto-central regions as these areas are characterized by a higher proneness to fall in down state (steeper Slope 1 in Laurino et al., 2014).

For each ROI, the mean power for each band of interest was estimated averaging among those of the electrodes included in the ROI.

NREM Sleep Band-Wise Comparisons

For each sensory modality, band-wise differences between the three epochs (baseline, P200, and P900) were evaluated for both FCA and PSA sites.

Pairwise comparisons between all couples of epochs were conducted for each band using two-sided Wilcoxon signed rank tests. *P*-values significance threshold was set at 0.05.

For each band and ROI three comparisons were thus performed:

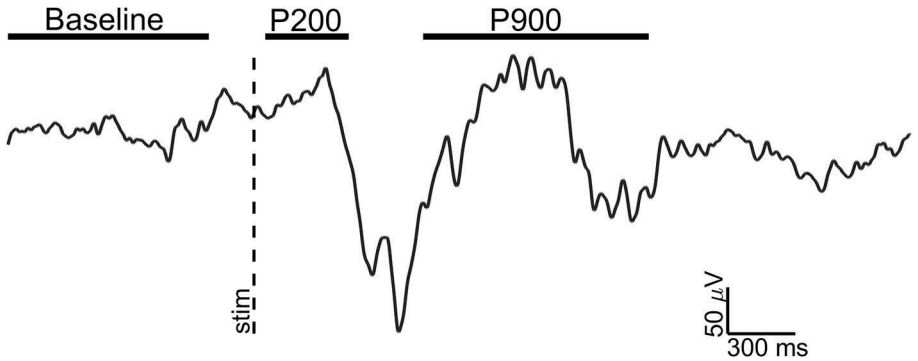

FIGURE 1 | Exemplary EEG trace (Fz electrode, signal filtered in 0.3–30 Hz band) of a visual evoked K-complex for showing the time windows of analysis. The stimulus onset (vertical dotted line) and time windows considered for Baseline (1 s), P200 (300 ms), and P900 (1 s) are shown.

i) P200 vs. Baseline.
ii) P900 vs. Baseline.
iii) P200 vs. P900.

Cortical Source Localization of Gamma Activity

Based on the hypothesis of the P200 being a purely cortical wake-like activity, we focused the P200 cortical source analyses on gamma band.

EEG signals were first band-pass filtered (Hamming filter with zero-phase lag) in gamma band (30–45 Hz). Note that the choice of the time-windows length for cortical level analyses is not constrained by any trade-off between frequency and temporal resolutions, allowing thus a more precise windowing. For cortical level characterization, the P200 epoch was defined as the time interval from 140 to 350 ms after the stimulus: the P200 was divided in three time-windows based on the P200 template, obtained averaging across stimulus modalities (see **Figures 3A**, **4A**, **5A**): (i) T140 (+140 to +210 ms); (ii) T210 (+210 to +280 ms); (iii) T280 (+280 to +350 ms).

Standardized cortical current densities of gamma signals were estimated applying the standardized low-resolution brain electromagnetic tomography (sLORETA, Pascual-Marqui, 2002) algorithm, using Brainstorm toolbox for Matlab (Tadel et al., 2011). A default anatomical MRI template "Colin27" (Holmes et al., 1998) was used to estimate a symmetrical boundary element head model with 15002 dipoles (modeled layers: cortical surface, inner skull, outer skull, and scalp) using OpenMEEG software (Kybic et al., 2005; Gramfort et al., 2011).

For each trial, the time-course of the cortical standardized current densities was estimated using sLORETA algorithm. For each subject and sensory modality, the mean time course of standardized current densities was estimated averaging across the related trials. Z-scores of averaged cortical sources time-course of P200 were estimated with respect to the corresponding Baseline. As a last step the mean z-scores of the three time-windows (T140, T210, and T280) enclosing the P200 were estimated for each sensory modality and subject, averaging among the time-samples pertaining to the window (see **Figures 3B**, **4B**, **5B**). Voxels with z-scores > 1.65 ($p < 0.05$, one-tailed) were considered significant. For each sensory modality and time-window, only cortical areas composed of at least 100 adjacent significant voxels were retained, avoiding thus spurious findings. From here on, we will refer to gamma z-scores at the cortical level as gamma activations.

RESULTS

We first verified whether the P200 and the P900 had different power at high frequencies with respect to the Baseline. For each band of interest (sigma, beta, and gamma), ROI (FCA and PSA) and sensory-modality (acoustic, tactile, visual), the power contents of the P200 and P900 were compared to that of the Baseline (**Figure 2**).

The P200 Shows a Massive Enhancement of Gamma Power

Comparisons between P200 and Baseline epochs yield three main findings:

1) no difference in sigma and beta power is found either for PSAs or FCAs coherently for all sensory modalities;
2) a significant increase of gamma power with respect to Baseline is observed consistently across all sensory modalities. This increase is already apparent in PSAs (the site of P200 emergence) and is maintained in FCAs (**Figure 2**, first column).

The P900 Is Accompanied by a Concurrent Increase of Power in Sigma-Beta Bands

Two main results emerge when considering P900-Baseline comparisons:

1) The P900 is characterized by a significant increase of power in sigma and beta bands. This increase holds for all sensory modalities both when considering PSAs and FCAs.
2) No significant difference between P900 and Baseline is apparent when considering gamma band (**Figure 2**, second column).

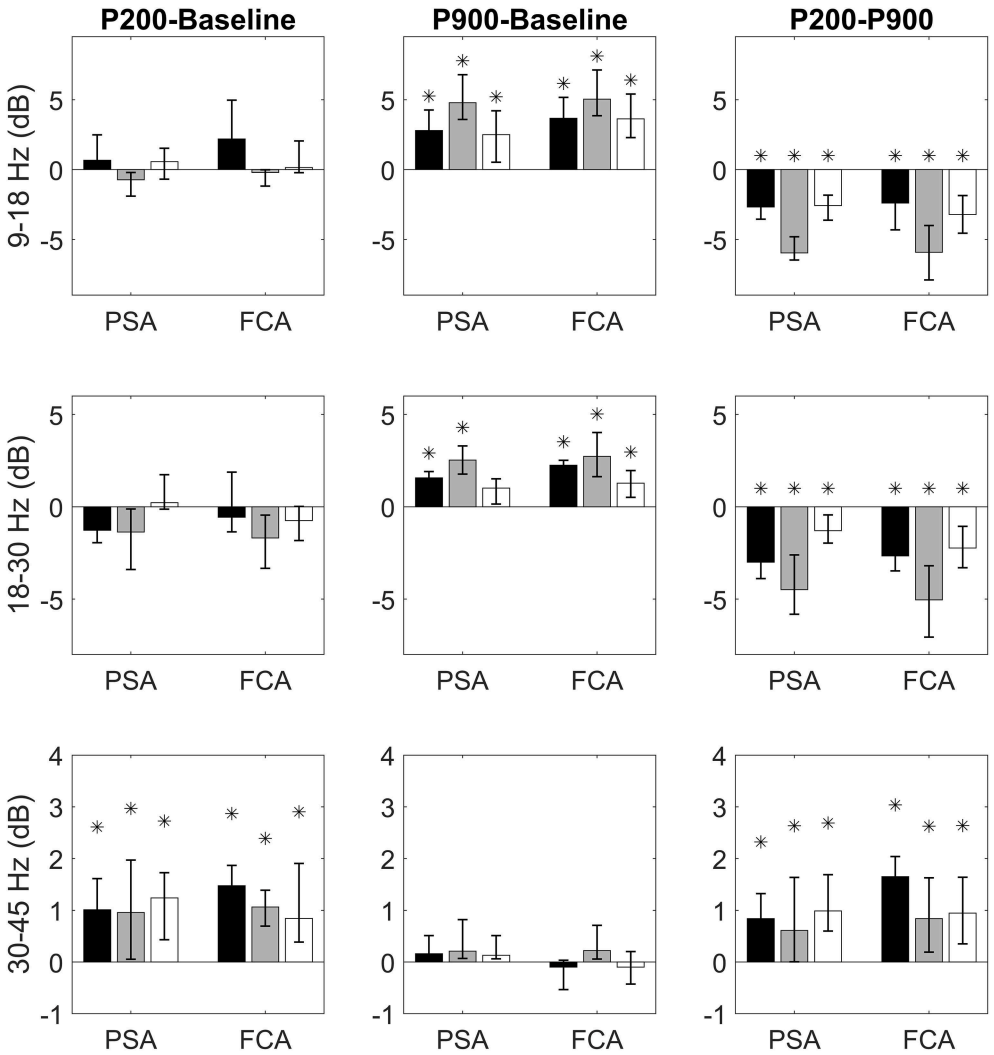

FIGURE 2 | Bandwise comparisons between couples of epochs are presented for PSAs and FCAs. Each bar represent the band-wise difference of spectral powers between P200 and Baseline (first column), P900 and Baseline (second column), and P200 and Baseline (third column). The bar color identifies the sensory modality: acoustic (black), tactile (gray), and visual (white). Comparisons in sigma (9–18 Hz), beta (15–30 Hz), and gamma (30–45 Hz) bands are presented, respectively in the first, second, and third row. Each comparison is performed for two regions of interest: Primary Sensory Area (PSA) and Fronto-Central Area (FCA). The PSA bars are related to only the electrodes of specific sensory modality (black PSA bars for acoustic PSA, gray PSA bars for tactile PSA, and white PSA bars for visual PSA). Data are expressed as median values and interquartile ranges. Significant (pairwise Wilcoxon signed rank test, $p < 0.05$) comparisons are highlighted by asterisks.

Band-Specific Differences Between P200 and P900

Finally, we focused on the identification of spectral differences between P200 and P900. The P200 shows higher power within gamma band while P900 is characterized by significantly higher power in sigma-beta bands. Both findings are consistent across sensory-modalities and ROIs (**Figure 2**, third column).

Source Localization of P200 Gamma Activity

We performed a cortical current source localization of gamma oscillations (30–45 Hz), for the three time-windows (T140, T210, T280) encompassing the P200 wave. Standardized current densities were transformed in z-scores (gamma activations) with respect to the Baseline epoch. In **Figures 3A**, **4A**, **5A** shows the grand-average templates of P200 for PSA (red) and FCA (in white) along with the analyzed time-window (T140 in **Figure 3**; T210 in **Figure 4**; T280 in **Figure 5**). Of note, the PSA's P200 peak precedes that of the FCA, indicating that PSA are always the first regions activated by thalamic excitatory sensory volleys. **Figures 3B**, **4B**, **5B** show for each sensory modality, cortical sources with significantly higher gamma activity as compared to Baseline. **Figures 3B**, **4B**, **5B** show the three consecutive phases of gamma cortical travel. In T140, significant gamma activations are predominantly localized over the stimulus-specific primary

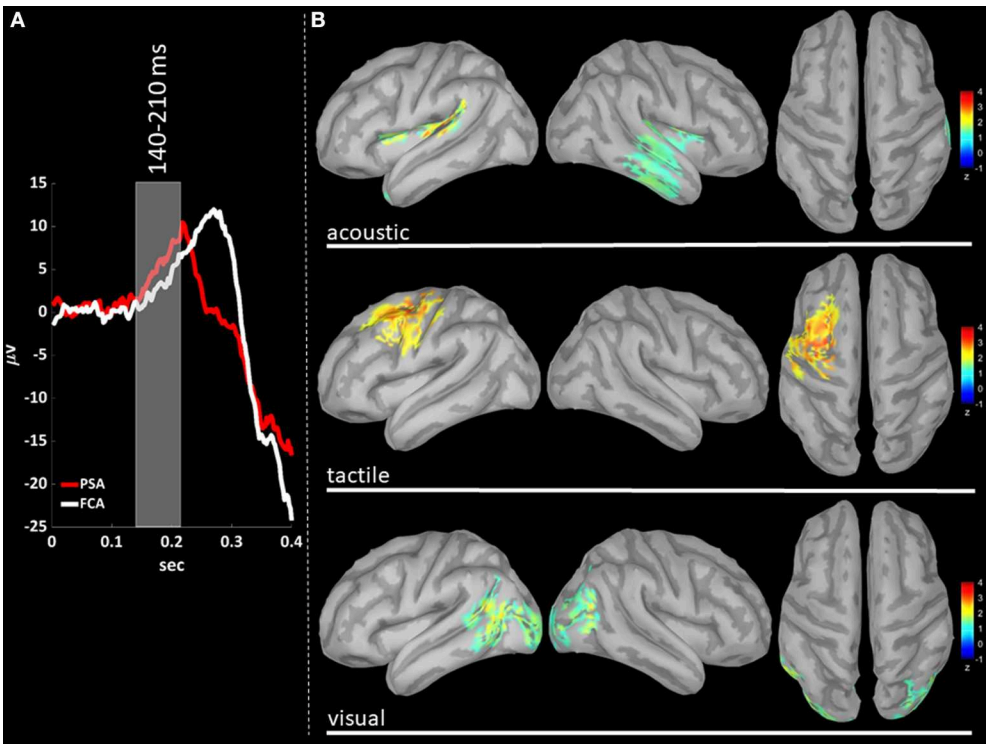

FIGURE 3 | (A) The time-courses of grand mean eKCs templates (averaged over sensory modalities) from the stimulus delivery to 0.4 s after the stimulus are presented for Primary Sensory Areas (PSAs, red line) and for Fronto-Central Areas (FCA, white line). The T140 time window (+140 to +210 ms) is identified by a gray panel. **(B)** Standardized cortical current densities of gamma (30–45 Hz) signals evaluated over the T140 time-window for acoustic (first row), tactile (second row), and visual (third row) sensory modalities. The standardized current densities are expressed as the mean z-scores averaged over the T140 with respect to the corresponding Baseline (see **Figure 1**). For each sensory modality, only cortical areas composed of at least 100 adjacent significant voxels were retained.

sensory areas (**Figure 3B**). When considering the interval spanning from 210 to 280 ms (T210, see **Figure 4B**), gamma activations spread from primary sensory areas toward central and anterior cortical regions coherently for all sensory modalities. Depending on the sensory modality, other cortical areas are involved:

- For the acoustic modality, further activations are observed in parieto-temporal areas including the secondary auditory cortex (superior edge of the lateral surface of the temporal lobe).
- In the tactile modality, the gamma activity spread involves also areas of the temporal gyri.
- In the case of visual modality, gamma activity spread includes large portions of the occipital lobe and of parieto-temporal regions.

In T280 time-window (**Figure 5B**), gamma activity is still detected mainly in fronto-central regions, even if an overall reduction of activations can be observed for all areas activated during the T210 time-window (this finding holds for all sensory modalities). Notably the T210, which includes the peaks of the P200 slow positive deflection, is the time-window where gamma activations spread over larger portions of the cortical mantle as compared to either T140 or T280.

DISCUSSION

Bistability is a paradigmatic dynamic of brain activity during NREM sleep, subtending both SSOs and KCs, which have been identified as highly synchronized-cortical-network phenomena involving large neuronal patches by Amzica and Steriade (1997b).

We have previously demonstrated that both SSOs (Menicucci et al., 2013), and KCs (Laurino et al., 2014) are triphasic waves, as the classical bistable pattern (down-state/N550, up-state/P900), is preceded by an early positive deflection (pre-down state/P200). It is fair to underline that the identification of the KC as a triphasic pattern (P200, N550, and P900) is not a novelty, as it was already observed by Loomis et al. (1935), and investigated by Roth et al. (1956). However, an exhaustive characterization of the P200 wave (and of its SSO counterpart, i.e., pre-down state) and the identification of its role, have been overlooked until recent years.

The role of P200, using the evoked K-complex model, was investigated by Riedner et al. (2011), and thoroughly characterized by our group (Laurino et al., 2014). We described temporal and morphological features of evoked KCs for three sensory modalities: acoustic, tactile and visual, demonstrating that the classical biphasic components of the KC (N550 and N900) are independent from the stimulus' sensory modality, showing a higher detection rate in fronto-central areas. On the

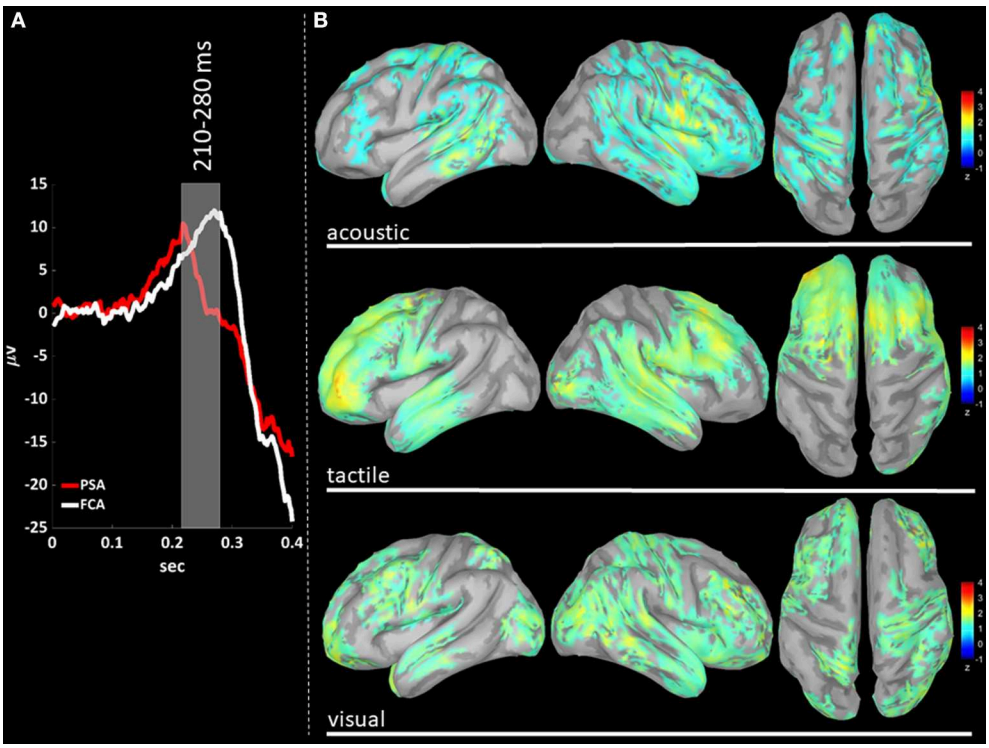

FIGURE 4 | (A) The time-courses of grand mean eKCs templates (averaged over sensory modalities) from the stimulus delivery to 0.4 s after the stimulus are presented for Primary Sensory Areas (PSAs, red line) and for Fronto-Central Areas (FCA, white line). The T210 time window (+210 to +280 ms) is identified by a gray panel. **(B)** Standardized cortical current densities of gamma (30–45 Hz) signals evaluated over the T210 time-window for acoustic (first row), tactile (second row), and visual (third row) sensory modalities. The standardized current densities are expressed as the mean z-scores averaged over the T210 with respect to the corresponding Baseline (see **Figure 1**). For each sensory modality, only cortical areas composed of at least 100 adjacent significant voxels were retained.

contrary, we observed that P200 topology is highly dependent on the stimulus sensory modality, with the earliest waves detected in the related primary sensory areas. We further demonstrated that the P200 is a wave rapidly traveling as a cortical excitatory activity over the whole cortex. We hypothesized that the P200 acts as a traveling cortical excitation whose function is the triggering of the bistable cortical response (N550-P900) which is in turn critical for quenching sensory processing (maintaining thus sleep and unconsciousness, N550/down-state), and favoring the consolidation of newly acquired abilities (spindle activity concurrent with the up-state).

As elegantly summarized by Halász (2016), "KCs have a Janus-faced nature: on the one hand they are evoked by an input-dependent traveling cortical excitation and on the other hand they represent an induced, cortical slow wave in the fronto-central region."

Several studies (e.g., Sejnowski and Destexhe, 2000; Destexhe et al., 2007) have characterized high-frequency activity crowning up states demonstrating its similarity to cortical activity during wakefulness. This high frequency activity (e.g., spindles), has been hypothesized to be deeply engaged in memory consolidation processes (Schabus et al., 2004; Steriade, 2006; Mölle et al., 2011; Lüthi, 2014).

On the contrary, the electrophysiological mechanisms responsible for the down state's ignition and the possible role of P200 (pre-down state in SSOs), remain to be fully elucidated. Based on our previous findings (Menicucci et al., 2013; Laurino et al., 2014), we herein provide further evidence that the P200 and specifically its high-frequency activity is a plausible candidate able to favor the down state ignition, and we demonstrate that the gamma band component of the P200 has striking analogies with that proper of wakefulness.

In this study, using the same eKC model of Laurino et al. (2014), we characterize the high-frequency spectral components of the two active states of eKCs, namely P200 and P900 waves (see **Figure 1**). We next identify the spatio-temporal dynamics of gamma activity cortical sources during the P200 wave.

Four main original results emerge from our study:

(i) The P200 is characterized by a significant increase of gamma activity in sensory-modality-primary sensory areas as well as in fronto-central regions, as compared to Baseline and P900 (**Figure 2**).

(ii) The P900 is characterized by a significant increase of sigma-beta activity in sensory-modality-primary sensory areas as well as in fronto-central regions, as compared to Baseline and P200 (**Figure 2**).

(iii) The distribution of gamma cortical activations is dependent on the sensory modality, with earliest activations detected in the stimulation-related primary sensory areas (**Figure 3**).

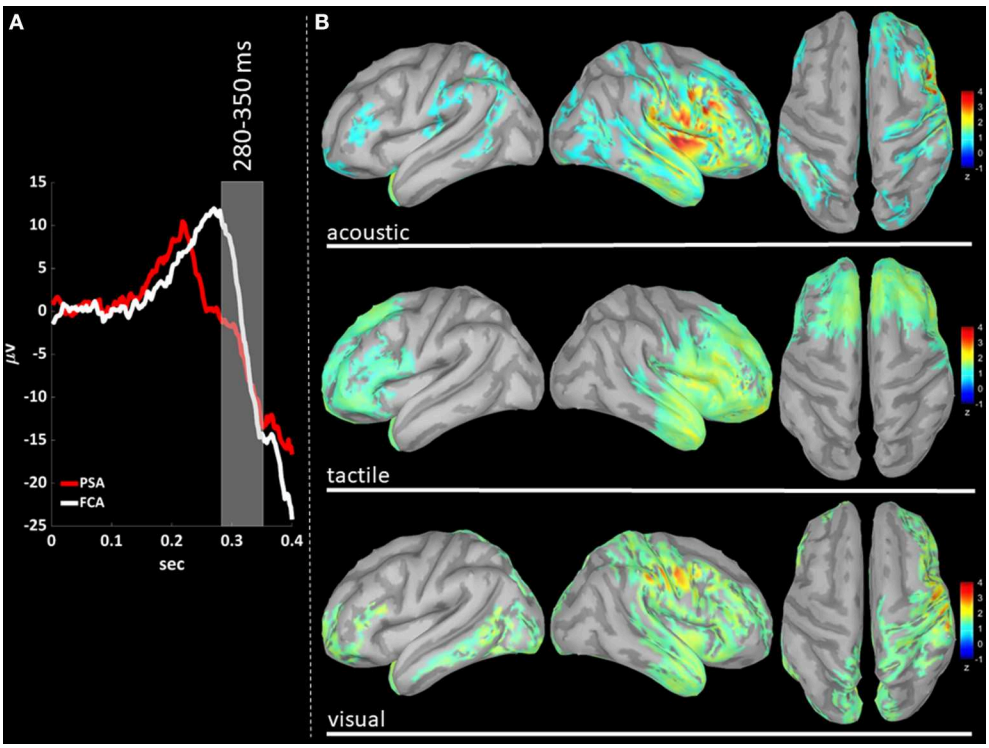

FIGURE 5 | (A) The time-courses of grand mean eKCs templates (averaged over sensory modalities) from the stimulus delivery to 0.4 s after the stimulus are presented for Primary Sensory Areas (PSAs, red line) and for Fronto-Central Areas (FCA, white line). The T280 time window (+280 to +350 ms) is identified by a gray panel. **(B)** Standardized cortical current densities of gamma (30–45 Hz) signals evaluated over the T280 time-window for acoustic (first row), tactile (second row), and visual (third row) sensory modalities. The standardized current densities are expressed as the mean z-scores averaged over the T280 with respect to the corresponding Baseline (see **Figure 1**). For each sensory modality, only cortical areas composed of at least 100 adjacent significant voxels were retained.

(iv) P200-related gamma activity travels on the cortical mantle as an excitatory activity (**Figures 4**, **5**), reaching its maximum cortical spreading in the time-window enclosing the P200 peak, and partially receding in the T280 windows (concurrently with the down state onset).

Based on these results, a global picture emerges: while on the one side P200 and P900 (pre-down state and up state in spontaneous SSOs, respectively) are both driven by the interplay between thalamus and cortex, each wave is subtended by different physiological mechanisms subserving different functional roles.

Let us now discuss the emerging picture in terms of an ideal bottom-up travel of a sensory input from periphery to cortical areas, for P200, and an ideal "top-down bottom-up cycle" between thalamus and cortex for P900. This allows us to pinpoint each finding in a unifying scenario and in an intuitive order.

P200 Gamma Activity as a Wake-Like Sensory Cortical Excitation

As described in our previous work (Laurino et al., 2014), the P200 is the first wave of the eKC, with shortest latencies detected in the primary sensory areas of stimulation. This result demonstrates that also during NREM sleep, sensory stimuli follow wake-like sensory pathways, ascending to primary sensory areas from core thalamic nuclei (Velluti, 1997): the specific wiring configuration of sensory inputs is arranged to minimize the processing time in term of perception during wakefulness (Kandel et al., 2000). The efficiency of this wiring configuration makes it the predominant sensory pathway also during NREM sleep (Laurino et al., 2014).

The hypothesized excitatory nature of the P200 gains further strength from the identification of a concurrent spectral component in gamma band: P200 gamma power is significantly higher both as compared to Baseline and to P900. This latter finding assumes a fundamental importance when considering that the high-frequency activities crowning the up states (P900) have been described as 'fragments of wakefulness' (Destexhe et al., 2007). This statement along with the fact that gamma rhythm is deeply involved in cortical processing during wakefulness (Bosman et al., 2014), strongly suggests that the gamma band rhythm proper of the P200 wave, is a real wake-like activity.

However, a limitation of our study should be noted: we did not stimulate systematically the subjects during wakefulness in order to show an analogous excitatory response with respect to NREM sleep. However, several studies have previously characterized the spectral activity of sensory processing in wakefulness. These studies have shown how specific gamma-band activity is typically evoked in human EEG as response to sensory stimulations.

During wakefulness, gamma oscillations are nearly ubiquitous, as they are involved in a wide range of low

(neural circuits) and high level (e.g., cognition, emotion, sensory processing) brain functions (see Bosman et al., 2014).

Gamma rhythms can be induced by sensory stimuli: sniffing-induced gamma rhythms were first described in the olfactory bulb and pyriform cortex of the hedgehog by Nobel laureate Adrian (1942), and induced gamma activity following sensory-specific stimulation has since been identified in human's visual (Adjamian et al., 2004; Hoogenboom et al., 2006), auditory (Pantev et al., 1991; Pantev, 1995), and somatosensory (Chen and Herrmann, 2001; Bauer et al., 2006) cortices. The increase in gamma activity has been demonstrated to be sensory modality-dependent: auditory stimuli induce larger activations in the temporal cortex, visual stimuli in primary visual cortex, and tactile stimuli in the somatosensory cortex (Jefferys et al., 1996; Whittington et al., 2011).

Our findings fit nicely with this scenario, as we find that gamma cortical current distribution is dependent on the sensory modality, with the earliest cortical activations detected in the related primary sensory area (T140, **Figure 3B**).

One of the most intriguing roles of gamma band is its capability to synchronize distributed neuronal patches thus promoting and regulating the flow of information between neuronal groups and contributing to brain computations. The flow of information is facilitated by gamma synchronization as it entrains the firing rate of the involved neurons at frequencies of 40–80 Hz, obtaining a precise spike synchronization among neighboring excitatory neurons. These sequences of synchronized spikes propagate to other neuronal groups, where the synchronization of the incoming spikes enhance the feedforward coincidence detection process, thereby favoring their efficacy in recruiting and entraining other neurons (Salinas and Sejnowski, 2001). Gamma synchronization has also a modulatory function as it affects the efficacy of the synaptic input to the group of synchronized neurons: when a group of neurons is synchronized in gamma band, its activity is strongly influenced by gamma-rhythmic inhibitory inputs (Hasenstaub et al., 2005). Excitatory inputs efficacy thus depends on their timing with respect to inhibitory activity (i.e., excitatory inputs are most effective when arriving out of phase with respect to the inhibitory barrier, Fries, 2009).

Again, an analogy with wakefulness can be drawn, as we find that gamma activity, after emerging in the stimulus-specific primary sensory areas, travels over the cortex mantle reaching fronto-central integrative regions. We can reasonably assume that the gamma activity cortical travel is sustained and driven by the same neurobiological mechanisms promoted by gamma synchronization during wakefulness.

P900 Sigma/Beta Activities Emerge From Cortico-thalamo-cortical Loops' Activity

The P900 is characterized by a significantly higher sigma and beta band power as compared to Baseline and P200. This finding is in line with an amount of studies both in animal models and humans (see Steriade, 2006), demonstrating that up states (P900 waves) are crowned by high frequency activity in sigma (spindle activity) and beta band.

From an electrophysiological point of view, the P900 slow positive deflection reflects the size of the underlying synchronized neuronal pool with membrane potentials shifting toward depolarization levels, a mechanism initiating in cortical neurons and reinforced cortico-thalamo-cortical loops (Timofeev and Chauvette, 2011). During the P900 (up state), both cortical mechanisms and volleys from subcortical structures (thalamus and hippocampus) facilitate the entry of Ca++ in dendrites of cortical neurons, thus favoring cellular and synaptic plasticity, which are the molecular mechanisms promoting the consolidation of newly acquired abilities (see Rasch and Born, 2013). Ca++ entry causes the depolarization of membrane potentials inducing a synchronized neural spiking, detectable by surface EEG as a high-frequency EEG activity crowning the up state mainly in sigma band (in the frequency range of thalamic spindle activity, see Lüthi, 2014), but extending also to beta (Mölle et al., 2002).

P200 Gamma Activity as a Trigger for Bistability

We have previously hypothesized that the fast traveling P200 wave acts as a trigger for the bistable complex (N550/N900 of eKCs). We showed that P200 along its travel has a waxing behavior, entraining progressively larger neuronal patches (by synchronizing their activity), and displaying larger amplitude in fronto-central areas, as their integrative nature promotes an electrical reverberation of recently generated up-scaled Hebbian circuits (Tononi and Cirelli, 2006).

We here demonstrate that the P200 wave is complemented by a significant gamma activity spreading over the cortical mantle as an excitatory activity (see **Figures 3–5**). This finding suggests a plausible mechanism able to induce the following hyperpolarization phase (N550), thus reinforcing the hypothesis on the P200 complex as a traveling trigger for bistability (Laurino et al., 2014).

In the last two decades, a growing number of studies has dealt with the identification of the electrophysiological mechanisms responsible for the onset of electrically silent states (down-state/N550) and ultimately for preserving unconsciousness. Sanchez-Vives et al. (2010), demonstrated that cortical down states are promoted by the synchronous opening of activity-dependent K+ channels, and that both the speed of transition to the silent state and its duration are modulated by the preceding electrical activity.

In a previous study, Vyazovskiy et al. (2009), were able to induce SSOs by delivering intracortical electrical pulses in sleeping rats. They concluded that volleys of electrical activity capable of excite and recruit sufficiently large neural populations, induce SSOs (and specifically down states) during natural sleep in rats.

Lemieux et al. (2015) identified, in cats under ketamine-xylazine anesthesia, three mechanisms that promote the down state onset: (1) a reduction of excitatory synaptic activity in large neuronal pools with a nearly simultaneous decrease of cortical neurons' firing, (2) an increase of inhibitory activity in subpopulations of neurons; (3) the delivery of an excitatory input effectively triggering the transition. In their study, Lamieux and colleagues, mimicked excitatory inputs by delivering pulse currents to neocortical sites during active states, and were able

to induce down states within tens of milliseconds from the stimulus onset.

Our hypothesis that P200 gamma activity spreading over the cortical mantle as a wake-like excitatory activity acts as a trigger for the onset of the down state is strongly supported by the above-mentioned findings. We conclude that also in humans' natural sleep, a sufficiently strong cortical excitatory electrical activity (able thus to excite and recruit large cortical neuronal populations) acts as a trigger for the down state ignition, hence preserving unconsciousness.

CONCLUDING REMARKS

Here, using the sensory-evoked K-complex model, we provide strong evidence that an excitatory cortical activity concurrent with the P200 wave is able to trigger the down state ignition during natural sleep in humans. We show that the P200 is complemented by a concurrent cortical activation in gamma band acting as a wake-like excitatory activity emerging from sensory stimulus-related primary sensory areas, rapidly spreading over the cortical mantle reaching fronto-central associative regions and fading concurrently with the down state onset. These findings demonstrate that pathways and neurobiological mechanisms sustaining the P200-related gamma activity are completely different from those subtending high-frequency activities crowning up-states (e.g., cortico-thalamo-cortical loops). We show that the P200 has a significantly higher gamma power as compared to P900, and conversely the latter is characterized by significantly higher power in sigma-beta bands.

Our hypothesis of the role of excitatory gamma activity as a trigger for down states gains further support from previous studies in the animal model showing that volleys of electrical activity able of exciting and thus recruiting sufficiently large neuronal pools, induce down states.

In our opinion, the findings and the hypothesis herein presented assume a special interest as, differently from the above-mentioned studies, they are drawn from an investigation on naturally sleeping humans, thus in a more ecological context.

At this point, we believe some considerations are due. The finding about a wake-like behavior of sensory-stimulus induced gamma activity, in terms of both cortical origins and mechanisms of cortical spreading, in no way implies a conscious information processing.

While a generalization of the results we obtained using the sensory-evoked KC model to all SSOs seems appropriate, as they are subtended by very same neurobiological mechanisms (Amzica and Steriade, 1997a,b), future studies focusing on down state ignition in spontaneous sleep slow oscillations are warranted. In this framework, a previous study from our group (Menicucci et al., 2013), suggests that the down state ignition in spontaneous SSO could be triggered by mechanisms similar (e.g., excitatory activity), to those herein presented.

Finally, we would like to point out that, while the excitatory activity mechanism is effective in initiating the down state, results from studies in the animal model (see Lemieux et al., 2015), show that other concurring or even alternative neurobiological mechanisms and/or conditions can favor the down state onset.

DATA AVAILABILITY STATEMENT

The datasets generated for this study are available on request to the corresponding author.

ETHICS STATEMENT

The studies involving human participants were reviewed and approved by Pisa local ethical committee. The patients/participants provided their written informed consent to participate in this study.

AUTHOR CONTRIBUTIONS

ML, AP, DM, and AG contributed to the design, implementation of the study, analysis of the results, and writing of the manuscript.

FUNDING

This present work is co-funded by "LAID-Smart Bed Project: an integrated platform for evaluating sleep quality in the general population" (Tuscany Region POR CREO FESR 2014–2020 call 1).

REFERENCES

Adjamian, P., Holliday, I. E., Barnes, G. R., Hillebrand, A., Hadjipapas, A., and Singh, K. D. (2004). Induced visual illusions and gamma oscillations in human primary visual cortex. *Eur. J. Neurosci.* 20, 587–592. doi: 10.1111/j.1460-9568.2004.03495.x

Adrian, E. D. (1942). Olfactory reactions in the brain of the hedgehog. *J. Physiol.* 100, 459–473. doi: 10.1113/jphysiol.1942.sp003955

Amzica, F., and Steriade, M. (1997a). The K-complex: its slow (<1-Hz) rhythmicity and relation to delta waves. *Neurology* 49, 952–959. doi: 10.1212/WNL.49.4.952

Amzica, F., and Steriade, M. (1997b). Cellular substrates and laminar profile of sleep K-complex. *Neuroscience* 82, 671–686. doi: 10.1016/S0306-4522(97)00319-9

Bauer, M., Oostenveld, R., Peeters, M., and Fries, P. (2006). Tactile spatial attention enhances gamma-band activity in somatosensory cortex and reduces low-frequency activity in parieto-occipital areas. *J. Neurosci.* 26, 490–501. doi: 10.1523/JNEUROSCI.5228-04.2006

Bosman, C. A., Lansink, C. S., and Pennartz, C. M. (2014). Functions of gamma-band synchronization in cognition: from single circuits to functional diversity across cortical and subcortical systems. *Eur. J. Neurosci.* 39, 1982–1999. doi: 10.1111/ejn.12606

Chen, A. C., and Herrmann, C. S. (2001). Perception of pain coincides with the spatial expansion of electroencephalographic dynamics in human subjects. *Neurosci. Lett.* 297, 183–186. doi: 10.1016/S0304-3940(00)01696-7

Compte, A., Sanchez-Vives, M. V., McCormick, D. A., and Wang, X. J. (2003). Cellular and network mechanisms of slow oscillatory activity (<1 Hz) and wave propagations in a cortical network model. *J. Neurophysiol.* 89, 2707–2725. doi: 10.1152/jn.00845.2002

Crunelli, V., and Hughes, S. W. (2010). The slow (<1 Hz) rhythm of non-REM sleep: a dialogue between three cardinal oscillators. *Nat. Neurosci.* 13:9. doi: 10.1038/nn.2445

Destexhe, A., Hughes, S. W., Rudolph, M., and Crunelli, V. (2007). Are corticothalamic 'up'states fragments of wakefulness?. *Trends Neurosci.* 30, 334–342. doi: 10.1016/j.tins.2007.04.006

Fries, P. (2009). Neuronal gamma-band synchronization as a fundamental process in cortical computation. *Annu. Rev. Neurosci.* 32, 209–224. doi: 10.1146/annurev.neuro.051508.135603

Fröhlich, F., Bazhenov, M., Timofeev, I., Steriade, M., and Sejnowski, T. J. (2006). Slow state transitions of sustained neural oscillations by activity-dependent modulation of intrinsic excitability. *J. Neurosci.* 26, 6153–6162. doi: 10.1523/JNEUROSCI.5509-05.2006

Gramfort, A., Papadopoulo, T., Olivi, E., and Clerc, M. (2011). Forward field computation with OpenMEEG. *Comput. Intell. Neurosci.* 2011:923703. doi: 10.1155/2011/923703

Halász, P. (2005). K-complex, a reactive EEG graphoelement of NREM sleep: an old chap in a new garment. *Sleep Med. Rev.* 9, 391–412. doi: 10.1016/j.smrv.2005.04.003

Halász, P. (2016). The K-complex as a special reactive sleep slow wave–a theoretical update. *Sleep Med. Rev.* 29, 34–40. doi: 10.1016/j.smrv.2015.09.004

Hasenstaub, A., Shu, Y., Haider, B., Kraushaar, U., Duque, A., and McCormick, D. A. (2005). Inhibitory postsynaptic potentials carry synchronized frequency information in active cortical networks. *Neuron* 47, 423–435. doi: 10.1016/j.neuron.2005.06.016

Holmes, C. J., Hoge, R., Collins, L., Woods, R., Toga, A. W., and Evans, A. C. (1998). Enhancement of MR images using registration for signal averaging. *J. Comput. Assist. Tomogr.* 22, 324–333. doi: 10.1097/00004728-199803000-00032

Hoogenboom, N., Schoffelen, J. M., Oostenveld, R., Parkes, L. M., and Fries, P. (2006). Localizing human visual gamma-band activity in frequency, time and space. *Neuroimage* 29, 764–773. doi: 10.1016/j.neuroimage.2005.08.043

Iber, C. (2007). The AASM manual for the scoring of sleep and associated events: rules, terminology and technical specifications. *Am. Acad. Sleep Med.* 1, 23–31.

Jefferys, J. G., Traub, R. D., and Whittington, M. A. (1996). Neuronal networks for induced '40 Hz'rhythms. *Trends Neurosci.* 19, 202–208. doi: 10.1016/S0166-2236(96)10023-0

Kandel, E. R., Schwartz, J. H., and Jessell, T. M. (2000). *Principles of Neural Science,Vol. 4*. New York, NY: McGraw-Hill.

Kybic, J., Clerc, M., Abboud, T., Faugeras, O., Keriven, R., and Papadopoulo, T. (2005). A common formalism for the integral formulations of the forward EEG problem. *IEEE Trans. Med. Imaging* 24, 12–28. doi: 10.1109/TMI.2004.837363

Laurino, M., Menicucci, D., Piarulli, A., Mastorci, F., Bedini, R., Allegrini, P., et al. (2014). Disentangling different functional roles of evoked K-complex components: mapping the sleeping brain while quenching sensory processing. *Neuroimage* 86, 433–445. doi: 10.1016/j.neuroimage.2013.10.030

Lemieux, M., Chauvette, S., and Timofeev, I. (2015). Neocortical inhibitory activities and long-range afferents contribute to the synchronous onset of silent states of the neocortical slow oscillation. *J. Neurophysiol.* 113, 768–779. doi: 10.1152/jn.00858.2013

Loomis, A. L., Harvey, E. N., and Hobart, G. (1935). Potential rhythms of the cerebral cortex during sleep. *Science* 81, 597–598. doi: 10.1126/science.81.2111.597

Lüthi, A. (2014). Sleep spindles: where they come from, what they do. *Neuroscientist* 20, 243–256. doi: 10.1177/1073858413500854

Menicucci, D., Piarulli, A., Allegrini, P., Laurino, M., Mastorci, F., Sebastiani, L., et al. (2013). Fragments of wake-like activity frame down-states of sleep slow oscillations in humans: new vistas for studying homeostatic processes during sleep. *Int. J. Psychophysiol.* 89, 151–157. doi: 10.1016/j.ijpsycho.2013.01.014

Mölle, M., Bergmann, T. O., Marshall, L., and Born, J. (2011). Fast and slow spindles during the sleep slow oscillation: disparate coalescence and engagement in memory processing. *Sleep* 34, 1411–1421. doi: 10.5665/SLEEP.1290

Mölle, M., Marshall, L., Gais, S., and Born, J. (2002). Grouping of spindle activity during slow oscillations in human non-rapid eye movement sleep. *J. Neurosci.* 22, 10941–10947. doi: 10.1523/JNEUROSCI.22-24-10941.2002

Murphy, M., Riedner, B. A., Huber, R., Massimini, M., Ferrarelli, F., and Tononi, G. (2009). Source modeling sleep slow waves. *Proc. Natl. Acad. Sci. U.S.A.* 106, 1608–1613. doi: 10.1073/pnas.0807933106

Pantev, C. (1995). Evoked and induced gamma-band activity of the human cortex. *Brain Topogr.* 7, 321–330. doi: 10.1007/BF01195258

Pantev, C., Makeig, S., Hoke, M., Galambos, R., Hampson, S., and Gallen, C. (1991). Human auditory evoked gamma-band magnetic fields. *Proc. Natl. Acad. Sci. U.S.A.* 88, 8996–9000. doi: 10.1073/pnas.88.20.8996

Pascual-Marqui, R. D. (2002). Standardized low-resolution brain electromagnetic tomography (sLORETA): technical details. *Methods Find. Exp. Clin. Pharmacol.* 24(Suppl. D), 5–12.

Rasch, B., and Born, J. (2013). About sleep's role in memory. *Physiol. Rev.* 93, 681–766. doi: 10.1152/physrev.00032.2012

Riedner, B. A., Hulse, B. K., Murphy, M. J., Ferrarelli, F., and Tononi, G. (2011). "Temporal dynamics of cortical sources underlying spontaneous and peripherally evoked slow waves," in *Progress in Brain Research, Vol. 193*, eds E. J. W. Van Someren, Y. D. Van Der Werf, P. R. Roelfsema, H. D. Mansvelder, and F. H. Lopes Da Silva (Elsevier), 201–218. doi: 10.1016/B978-0-444-53839-0.00013-2

Roth, M., Shaw, J., and Green, J. (1956). The form, voltage distribution and physiological significance of the K-complex. *Electroencephalogr. Clin. Neurophysiol.* 8, 385–402. doi: 10.1016/0013-4694(56)90004-9

Salinas, E., and Sejnowski, T. J. (2001). Correlated neuronal activity and the flow of neural information. *Nat. Rev. Neurosci.* 2, 539–550 doi: 10.1038/35086012

Sanchez-Vives, M. V., Mattia, M., Compte, A., Perez-Zabalza, M., Winograd, M., Descalzo, V. F., et al. (2010). Inhibitory modulation of cortical up states. *J. Neurophysiol.* 104, 1314–1324. doi: 10.1152/jn.00178.2010

Schabus, M., Gruber, G., Parapatics, S., Sauter, C., Klosch, G., Anderer, P., et al. (2004). Sleep spindles and their significance for declarative memory consolidation. *Sleep* 27, 1479–1485. doi: 10.1093/sleep/27.7.1479

Sejnowski, T. J., and Destexhe, A. (2000). Why do we sleep? *Brain Res.* 886, 208–223. doi: 10.1016/S0006-8993(00)03007-9

Steriade, M. (2000). Neuronal basis of dreaming and mentation during slow-wave (non-REM) sleep. *Behav. Brain Sci.* 23, 1009–1011. doi: 10.1017/S0140525X00894029

Steriade, M. (2004). Acetylcholine systems and rhythmic activities during the waking-sleep cycle. *Prog. Brain Res.* 145, 179–196. doi: 10.1016/S0079-6123(03)45013-9

Steriade, M. (2006). Grouping of brain rhythms in corticothalamic systems. *Neuroscience* 137, 1087–1106. doi: 10.1016/j.neuroscience.2005.10.029

Steriade, M., Nunez, A., and Amzica, F. (1993). A novel slow (<1 Hz) oscillation of neocortical neurons *in vivo*: depolarizing and hyperpolarizing components. *J. Neurosci.* 13, 3252–3265. doi: 10.1523/JNEUROSCI.13-08-03252.1993

Steriade, M., and Timofeev, I. (2003). Neuronal plasticity in thalamocortical networks during sleep and waking oscillations. *Neuron* 37, 563–576. doi: 10.1016/S0896-6273(03)00065-5

Tadel, F., Baillet, S., Mosher, J. C., Pantazis, D., and Leahy, R. M. (2011). Brainstorm: a user-friendly application for MEG/EEG analysis. *Comput. Intell. Neurosci.* 2011:879716. doi: 10.1155/2011/879716

Timofeev, I., and Chauvette, S. (2011). Thalamocortical oscillations: local control of EEG slow waves. *Curr. Top. Med. Chem.* 11, 2457–2471. doi: 10.2174/156802611797470376

Tononi, G., and Cirelli, C. (2006). Sleep function and synaptic homeostasis. *Sleep Med. Rev.* 10, 49–62. doi: 10.1016/j.smrv.2005.05.002

Velluti, R. (1997). Interactions between sleep and sensory physiology. *J. Sleep Res.* 6, 61–77. doi: 10.1046/j.1365-2869.1997.00031.x

Vyazovskiy, V. V., Faraguna, U., Cirelli, C., and Tononi, G. (2009). Triggering slow waves during NREM sleep in the rat by intracortical electrical stimulation: effects of sleep/wake history and background activity. *J. Neurophysiol.* 101, 1921–1931. doi: 10.1152/jn.91157.2008

Vyazovskiy, V. V., Riedner, B. A., Cirelli, C., and Tononi, G. (2007). Sleep homeostasis and cortical synchronization: II. A local field potential study of sleep slow waves in the rat. *Sleep* 30, 1631–1642. doi: 10.1093/sleep/30.12.1631

Whittington, M. A., Cunningham, M. O., LeBeau, F. E., Racca, C., and Traub, R. D. (2011). Multiple origins of the cortical gamma rhythm. *Dev. Neurobiol.* 71, 92–106. doi: 10.1002/dneu.20814

Conflict of Interest: The authors declare that the research was conducted in the absence of any commercial or financial relationships that could be construed as a potential conflict of interest.

Copyright © 2019 Laurino, Piarulli, Menicucci and Gemignani. This is an open-access article distributed under the terms of the Creative Commons Attribution License (CC BY). The use, distribution or reproduction in other forums is permitted, provided the original author(s) and the copyright owner(s) are credited and that the original publication in this journal is cited, in accordance with accepted academic practice. No use, distribution or reproduction is permitted which does not comply with these terms.

frontiers in Neuroscience

MINI REVIEW
published: 18 October 2019
doi: 10.3389/fnins.2019.01086

Sleepiness as a Local Phenomenon

Sasha D'Ambrosio[1†], Anna Castelnovo[2*†], Ottavia Guglielmi[3], Lino Nobili[4,5], Simone Sarasso[1*] and Sergio Garbarino[3]*

[1] Dipartimento di Scienze Biomediche e Cliniche "L. Sacco", Università Degli Studi di Milano, Milan, Italy, [2] Sleep and Epilepsy Center, Neurocenter of Southern Switzerland, Civic Hospital (EOC) of Lugano, Lugano, Switzerland, [3] Department of Neuroscience, Rehabilitation, Ophthalmology, Genetics and Maternal/Child Sciences, University of Genoa, Genoa, Italy, [4] Department of Neuroscience (DINOGMI), University of Genoa, Genoa, Italy, [5] IRCCS, Child Neuropsychiatry Unit, Giannina Gaslini Institute, Genoa, Italy

Sleep occupies a third of our life and is a primary need for all animal species studied so far. Nonetheless, chronic sleep restriction is a growing source of morbidity and mortality in both developed and developing countries. Sleep loss is associated with the subjective feeling of sleepiness and with decreased performance, as well as with detrimental effects on general health, cognition, and emotions. The ideas that small brain areas can be asleep while the rest of the brain is awake and that local sleep may account for at least some of the cognitive and behavioral manifestations of sleepiness are making their way into the scientific community. We herein clarify the different ways sleep can intrude into wakefulness, summarize recent scientific advances in the field, and offer some hypotheses that help framing sleepiness as a local phenomenon.

Keywords: local sleep, sleepiness, microsleep, EEG slowing, sleep loss, prolonged wakefulness, OFF-periods, performance

OPEN ACCESS

Edited by:
Michele Bellesi, University of Bristol, United Kingdom

Reviewed by:
Vincenzo Muto, University of Liège, Belgium
Valentina Alfonsi, Sapienza University of Rome, Italy

***Correspondence:**
Sasha D'Ambrosio
sasha.dambrosio@unimi.it
Anna Castelnovo
anna.castelnovo@eoc.ch
Simone Sarasso
simone.sarasso@unimi.it

† These authors have contributed equally to this work

Specialty section:
This article was submitted to Sleep and Circadian Rhythms, a section of the journal Frontiers in Neuroscience

Received: *20 March 2019*
Accepted: *26 September 2019*
Published: *18 October 2019*

Citation:
D'Ambrosio S, Castelnovo A, Guglielmi O, Nobili L, Sarasso S and Garbarino S (2019) Sleepiness as a Local Phenomenon. Front. Neurosci. 13:1086. doi: 10.3389/fnins.2019.01086

INTRODUCTION

Epidemiological data have shown that, over the last decades, we are seeing a concerning decrease in both the duration and the quality of sleep in developed and developing countries (Dinges, 1995; Broman et al., 1996; Dinges et al., 1997; Liu and Zhou, 2002; Krueger and Friedman, 2009; Maric et al., 2017). The progressive shift toward "24-h societies" has been accompanied by an increase in "sleepiness" and its associated detrimental effects on the individual's performance, cognition, emotions, and general health (Dinges et al., 1997; Van Dongen et al., 2003a; Chee and Choo, 2004; Banks and Dinges, 2007; Bernert and Joiner, 2007; Knutson et al., 2007; Goel et al., 2009, 2014; Couyoumdjian et al., 2010; Grandner et al., 2010; Krause et al., 2017). Thus, understanding the regulatory mechanisms of sleepiness and their implications for human health is urgent and of utmost importance (Garbarino et al., 2016).

Although the concept of sleepiness might sound intuitive, at a closer look its definition is far from trivial, and neither is the answer to fundamental issues like what sleepiness is from a neurobiological standpoint. Attempts to operationalize the subjective feeling of sleepiness for clinical and research purposes have led to the development of a number of tools, some based on subjective ratings (e.g., the Epworth Sleepiness Scale), others on objective measures like cognitive performance (e.g., reaction time test, driving-simulators) and electroencephalography [e.g., multiple sleep latency test (MSLT) or polysomnography (PSG)]. Despite the reliability of these validated measures, their agreement remains poor as they capture different aspects of sleepiness,

differentially influenced by endogenous, exogenous, and situational factors. For tackling and overcoming the complex phenomenon of sleepiness, previous studies have employed and suggested a twofold approach of identifying "sleepy" patients based on combined subjective and objective sleepiness and/or physiological and biochemical biomarkers (Olson et al., 1998; Kritikou et al., 2014); this approach may be more valuable than any single measure of sleepiness (Fleming et al., 2016) but is not yet exhaustive.

In the last few years, science has produced compelling evidence supporting the idea that both sleep and wakefulness are under local regulation (Siclari and Tononi, 2017; Krueger et al., 2019). These ideas were influenced by studies performed during the transition between wake and sleep, where it was found that some brain areas may fall asleep, or awaken, before others (Pigarev et al., 1997; Magnin et al., 2010; Marzano et al., 2013; Sarasso et al., 2014a,b; Siclari et al., 2014). In further support of this view, sleep homeostasis can be modulated on a local level by active or passive tasks or via local synaptic potentiation (Kattler et al., 1994; Miyamoto et al., 2003; Huber et al., 2004, 2006, 2007; De Gennaro et al., 2008; Vyazovskiy and Tobler, 2008; Hanlon et al., 2009; Lesku et al., 2011).

The presence of local sleep was also demonstrated through the observation that slow waves and spindles, the two major spontaneous electroencephalographic oscillations of sleep that arise from complex re-entrant circuits in the thalamocortical system, often occur out-of-phase in different brain regions (Andrillon et al., 2011; Nir et al., 2011).

This case is particularly compelling as both sleep spindles and slow waves are dependent on the hyperpolarization of thalamic relay and cortical neurons, respectively. This occurs during NREM sleep due to the progressive decrease of noradrenergic, serotonergic, and cholinergic neuromodulation from brainstem activating systems. As such, being under the influence of diffuse neuromodulatory systems, their occurrence, particularly for slow waves, has been long assumed to be an ubiquitous feature of virtually every neural cell of the sleeping brain (Steriade et al., 1993) occurring in a remarkably synchronous way (Volgushev et al., 2006).

Even more dramatically, during non-rapid eye movement (NREM) sleep, slow waves may coexist with transient local wake-like activity (Rector et al., 2005, 2009; Nobili et al., 2011; Peter-Derex et al., 2015). Similarly, local isles of sleep may intrude upon wakefulness (Rector et al., 2005, 2009; Vyazovskiy et al., 2011a; Hung et al., 2013; Quercia et al., 2018).

We herein clarify the different ways sleep can physiologically intrude into wakefulness, summarize the main findings on this topic, and offer a global framework to interpret sleepiness as a local phenomenon.

THE INTRUSION OF SLEEP INTO WAKEFULNESS

From a neuro-physiological standpoint, sleep may intrude upon wakefulness in the form of local sleep, electroencephalogram (EEG) slowing, and microsleep.

Local Sleep During Wakefulness

Local sleep is a complex physiological phenomenon occurring within anatomically discrete brain locations (Krueger et al., 2019). Experiments in isolated cortical slabs (Kristiansen and Courtois, 1949), as well as in slice preparations (Steriade et al., 1993) and cell cultures (Corner et al., 2008; Hinard et al., 2012), confirmed that slow waves—a key electrophysiological graphoelement characterizing the sleep state—is essentially an intrinsic property of cortical cells ensembles. Rector et al. (2005) provided the first indirect evidence of local sleep in living intact animals using surface evoked potentials (SEP) in rats. They showed that, while on average, wakefulness is characterized by low SEP amplitude and NREM sleep by high SEP amplitude (Hall and Borbely, 1970), SEP amplitude fluctuates over time during both states and is frequently different between hemispheres and nearby cortical columns. Moreover, the longer a cortical column produces low-amplitude wake-like SEP the more it will begin to produce large-amplitude sleep-like SEP (Rector et al., 2005).

Further indirect evidence in favor of local sleep emerged from cortical multiunit recordings in rats during sleep deprivation (SD): firing rates increased continuously for the first 3 h of SD and showed no further significant change in the last hour. This "ceiling-effect" was interpreted as the consequence of the increase in the number of local neuronal silent periods (or OFF-periods) (Vyazovskiy et al., 2009).

Local sleep had been observed more directly in rats in 2011 (Vyazovskiy et al., 2011a,b). After a period of prolonged wakefulness, cortical neurons tended to fall silent for brief periods, as they do during NREM sleep. These OFF-periods were associated with slow oscillations in the slow/theta range in local field potential (LFP) recordings, as also confirmed by a study applying micro-stimulation during prolonged wakefulness (Vyazovskiy et al., 2013). Local OFF-periods occurred asynchronously across brain regions and increased with time spent awake. Most strikingly, they occurred in behaviorally awake animals, and their presence over motor areas negatively affected motor performance during a sugar pellet reaching task.

More recently, use-dependent, local sleep-like EEG theta events have been found to occur during prolonged wakefulness in humans (Hung et al., 2013). As in the former studies on rodents, also in humans the occurrence of these events over frontal or posterior scalp regions was selectively associated with negative behavioral outcomes on executive functions or visuomotor control tasks, respectively (Bernardi et al., 2015; Quercia et al., 2018).

These findings lead to the intriguing hypothesis that deficits in sensory, psychomotor, and cognitive aspects of behavior after SD may arise as a result of altered neuronal responsiveness to incoming stimuli due to these OFF-periods.

Global and Local EEG Slowing

Under SD conditions, which are similar to what occurs during NREM sleep, the firing rates of neurons in ON-periods, as well as the number and duration of OFF-periods, the number of neurons participating synchronously in OFF-periods and the low-frequency content (particularly in the theta range) of the

EEG increase (Vyazovskiy et al., 2011b). At odds with NREM sleep, though, is the fact that during SD these events typically involve an isolated portion of the cortex possibly reflecting the occurrence of more or less widespread local cortical isles of sleep during prolonged wakefulness. In further support of this hypothesis, an fMRI connectivity analysis indicated that prolonged wakefulness is associated with a decrease in measures representing the mean strength of coupling among brain areas, resembling the breakdown in connectivity typical of slow waves sleep (Bernardi et al., 2015; Kaufmann et al., 2016).

In humans (Cajochen et al., 1995; Aeschbach et al., 1997; Finelli et al., 2000; Strijkstra et al., 2003; Fattinger et al., 2017), as in rats (Franken et al., 1991; Vyazovskiy and Tobler, 2005), EEG power in the lower frequency bands (especially theta) progressively increase with the time spent in quiet waking. This slowing can be captured by surface EEG and is paralleled by subjective sleepiness—at least in humans (Aeschbach et al., 1996; Bernardi et al., 2015)—and by a decrease in behavioral performance (Gorgoni et al., 2014; Fattinger et al., 2017). Transcranial magnetic stimulation (TMS) measures converge with EEG measures in indicating that SD has severe effects on cortical activity. SD is associated with an increased TMS resting motor threshold and cortical facilitation, at least in females, and these changes clearly predict changes in EEG theta activity (De Gennaro et al., 2007).

The increase in low frequencies in the EEG is associated with the subsequent homeostatic increase of sleep slow-wave activity (SWA) during NREM sleep in both humans (Finelli et al., 2000) and rats (Borbély et al., 1984; Tobler and Borbely, 1986), as well as with the increase of theta and delta power during REM sleep (Tinguely et al., 2006). Notably, superimposed to the homeostatic process, several studies reported a strong circadian modulation of the waking EEG (Aeschbach et al., 1996; Dumont et al., 1999; Cajochen et al., 2002) so that the intrusion of low frequencies is restrained when sustained wakefulness coincides with the biological day, while it is completely free to manifest itself during the biological night (Cajochen et al., 2002). Similarly, cortical excitability assessed using TMS coupled with scalp EEG is robustly correlated with circadian dynamics and with endocrine markers of circadian amplitude (Ly et al., 2016).

Interestingly, these regulatory mechanisms may act locally. The aforementioned increase in low frequencies has a fronto-central predominance, mainly in the theta range during wakefulness (Finelli et al., 2000; Strijkstra et al., 2003) and in the SWA range during subsequent recovery sleep (Cajochen et al., 1999; Finelli et al., 2000; Leemburg et al., 2010), and it can be observed also after repeated partial sleep restriction (Plante et al., 2016).

More recently, studies performed in humans showed that the increase in waking theta EEG activity during SD displayed regional, use-dependent changes (Hung et al., 2013; Gorgoni et al., 2014; Bernardi et al., 2015; Nir et al., 2017). A first study took advantage of high-density EEG technology to show an increase in theta power over left frontal brain regions after a language-based task and over posterior parietal regions after a visuomotor task. The same regions displayed local increases in SWA power during subsequent recovery sleep (Hung et al., 2013). A subsequent study demonstrated that the occurrence of theta waves in task-related regions coincided with specific performance errors in humans (Bernardi et al., 2015). Another study used intra-cranial electrodes in human neurosurgical patients performing a psychomotor vigilance task (PVT) at baseline and during SD. Cognitive lapses involved local state-dependent changes in neuronal activity in the medial temporal lobe (MTL). Specifically, immediately before cognitive lapses the spiking responses of individual neurons were attenuated, delayed, and lengthened while, during cognitive lapses, LFPs showed a relative local increase in slow activity (Nir et al., 2017).

In line with these findings, a study using a driving simulator to evaluate the effect of sleepiness at the wheel, found that a local increase in theta EEG activity over the motor regions (as localized by EEG source modeling techniques) was associated with an increased risk of line departures (Ahlstrom et al., 2017).

Microsleep

In this review, microsleeps are defined as short episodes of sleep-like activity that satisfy criteria for stage 1 sleep (theta replacing alpha rhythm) except for their short duration of up to 15 s (Priest et al., 2001; Blaivas et al., 2007; Hertig-Godeschalk et al., 2019). Usually, blinking artifacts characteristic of full wakefulness disappear, often accompanied by the appearance of slow eye movements. However, behavioral changes, such as eye-closure and nodding-off, are not defining features of microsleeps, as they may or may not be present during microsleep episodes (Torsvall and Akerstedt, 1988; Boyle et al., 2008). Regardless, microsleeps may be associated with significant cognitive impairment—e.g., poorer performance during a continuous task under driving-simulator conditions (Boyle et al., 2008)—and are strictly associated with subjective sleepiness. Indeed, some evidence suggests that microsleeps analysis in MSLT might be a more sensitive and specific test for excessive daytime sleepiness (EDS) as compared to MSLT alone (Tirunahari et al., 2003).

Microsleep episodes are more frequent after a sleep-restricted night compared to a normally rested night (Friedman et al., 1978; Horne and Pettitt, 1985; Poudel et al., 2018) and can be followed by a brief recovery in performance (Poudel et al., 2018).

Traditionally, microsleeps have been hypothesized to be global brain phenomena that reflect the transient shutdown of activating systems, with the parallel activation of sleep promoting centers (Sechenova, 2011; Silkis, 2013). However, recent evidence describes microsleep in terms of intermediate states between sleep and wakefulness (Hertig-Godeschalk et al., 2019), possibly reflecting their local nature. Supporting this notion, a recent fMRI study during one night of SD described local decreased activation over frontal, parietal, and occipital associative cortices as well as increased activation in the default mode network (DMN) associated with slow reaction times responses at the PVT (typically reflecting the occurrence of microsleeps), showing how these different patterns of activation and deactivation could depend on circadian phases as well as homeostatic sleep pressure and the interactions between the two (Zhu et al., 2018).

NEUROBIOLOGY AND NEUROPHYSIOLOGY OF SLEEPINESS

In simple terms, just as hunger is the physiological need for food, sleepiness can be described as the physiological need for sleep. Very few theoretical constructs about sleepiness are available in the literature (Cluydts et al., 2002; De Valck and Cluydts, 2003). Conceptually, sleepiness is the consequence of an imbalance between the sleep drive (level of activation of sleep circuits) and the wake drive (level of activation of arousal systems) (Cluydts et al., 2002). When wake still prevails but sleep pressure is high we experience sleepiness.

The concept of sleepiness, therefore, closely relates to the concept of "sleep debt." While Horne originally proposed that sleep debt was uniquely the consequence of the loss of "core" or "obligatory sleep" (referred as the first 4–5 h of sleep) but not of "optional" or "facultative" sleep, which "fills the tedious hours of darkness until sunrise" (Horne, 1985), empirical research indicated that sleep debt accumulates linearly. Although clearly influenced and modulated by circadian factors (Shekleton et al., 2013), according to this line of research, sleep debt may be defined as the cumulative hours of sleep loss with respect to a subject-specific daily need for sleep (Van Dongen et al., 2003b).

Another closely related concept of sleepiness is "sleep inertia," a physiological condition of subjective drowsiness, decreased alertness, and impaired cognitive and sensory-motor performance that arises during the transition between sleep to wakefulness. It has been shown that the subjective feeling of sleep inertia lasts on average 15–30 min, although objective measure of alertness and performance do not return to waking baseline until 2–4 h after waketime (Jewett et al., 1999). Electroencephalographic, evoked potential, and neuroimaging studies suggested that sleep inertia involves the intrusion of sleep patterns during wakefulness (Trotti, 2017), bringing the concepts of sleepiness and sleep inertia even closer and further corroborating the notion that vigilance states are not necessarily discrete.

But how does this translate from a neurophysiological standpoint? According to the data presented in the previous section, sleepiness may be associated with the occurrence of local sleep during wakefulness in the presence of a positive sleep debt. We will now focus on possible regulatory mechanisms of local sleep and their interaction with global processes.

Local Regulation of Sleep

Great progress has been made in characterizing the brain centers responsible for the orchestration of sleep and wakefulness as global behavioral states (Jones, 2005; Saper et al., 2005; Szymusiak and McGinty, 2008; Siegel, 2009; Brown et al., 2012). Although anatomically widespread, these centers act in a coordinated fashion in modulating whole-brain activity, thus allowing for a clear behavioral distinction between wake and sleep states (for a review see Saper et al., 2001; Scammell et al., 2017; Eban-Rothschild et al., 2018). According to Saper's flip-flop switch model, sleep regulation depends on a mutually inhibitory interaction between sleep centers and the components of the arousal systems (Saper et al., 2001), located both in cortical and subcortical structures.

Although the described mechanisms may orchestrate sleep globally, sleep is fundamentally an intrinsic property of the cerebral neurons and can be regulated locally at the level of cortical areas as small as cortical columns (Krueger et al., 2008). This columnar state segregation is favored by the fact that the functional intracolumnar connections are denser than intercolumnar connections allowing greater activity and state synchrony between cells pertaining to the same column (Panzeri et al., 2003).

The very first model-based postulation of local sleep was published in 1993 and 1995 by Krueger and Obal (1993) and Krueger et al. (2008), who postulated that sleep begins as a local neuronal group event involving oscillations of inhibition and excitation and is thus "quantal" in nature. From this perspective, these authors considered sleepiness as a statistical phenomenon, the perception of which arises when a sufficient number of neuronal groups become "bistable."

Coordination of neuronal group sleep results from both neuronal and humoral systems. As proposed by the Synaptic Homeostasis Hypothesis (SHY; Tononi and Cirelli, 2003, 2006), when neuronal plasticity during wakefulness is increased or decreased in specific brain areas, sleep intensity, as reflected by the amount of SWA, selectively increases or decreases in those areas (Kattler et al., 1994; Huber et al., 2004; Vyazovskiy and Tobler, 2008; Hanlon et al., 2009; Lesku et al., 2011). Indeed, increased synaptic connectivity means more synchronous oscillations and increased slow wave activity. Alternatively (or additionally), local slow wave generation could be due to a change in the excitability or amount of adaptation of individual neurons. Along these lines, a build-up in the need for cellular maintenance could cause individual neurons to show lower excitability and stronger adaptation (Vyazovskiy et al., 2013). OFF-periods would therefore occur locally were most needed, thus providing a potential explanation for local sleep patterns. Similarly, as soon as individual neurons fall below a certain cellular stress threshold, their excitability is restored, leading to a more wake-like pattern of activity.

Considerable evidence also suggests a role for local paracrine signaling pathways in the regulation of both global and local sleep. In this vein, it is known that sleep pressure correlates with the concentration of—among others—nitric oxide (NO) (Gautier-Sauvigné et al., 2005; Kalinchuk et al., 2011), adenosine, and various cytokines (Imeri and Opp, 2009) such as interleukin-1 (IL-1) and tumor necrosis factor (TNF). These substances are synthesized by metabolically or synaptically active cells and are released in a local fashion (Latini and Pedata, 2001; Porkka-Heiskanen and Kalinchuk, 2011). Again, Krueger et al. (1995b) played a pivotal role in delineating this humoral component (Krueger, 2008). They hypothesized that sleep at the neuronal group level is regulated by paracrine substances whose production and catabolism rates are synaptic use-dependent (Krueger et al., 1995a).

According to their model, Adenosine 5′-γ-ThiotriPhosphate (ATP) released during neurotransmission and acting on purine P2 receptors induces the release of IL1 and TNF. These cytokines

in turn act on neurons to change their intrinsic properties (Krueger, 2008), directly or indirectly, altering the production of neuroendocrine substances and neurotransmitters, for example the growth hormone releasing hormone and NO, which are known to be involved in sleep-wake regulation (Krueger et al., 1995b). More recent evidences in support of this model have been shown by Nguyen et al. (2019).

Finally, there is another mechanism able to explain regional sleep differences, especially the aforementioned frontal predominance of the low frequency effect. Different regions might be more susceptible to sleep due to intrinsic differences in some of their activating inputs. In other words, even widespread projections from centers regulating sleep globally may present with topographical differences that may affect sleep-wake regulation at the level of cortical macro-areas. For example, recent evidence suggested a region-specific dissociation between cortical noradrenaline levels during the sleep/wake cycle (Bellesi et al., 2016). Compared to the motor cortex, in the medial Prefrontal Cortex (mPFC) noradrenaline levels are higher and changes in its concentration during sleep and wake are slower. Furthermore, SD leads to a decrease in noradrenaline only at the level of mPFC, suggesting that noradrenergic neurons targeting the prefrontal cortex may undergo fatigue earlier or more markedly than other projecting cells from locus coeruleus. An increased susceptibility of noradrenergic projections to the frontal cortex might explain frontal cognitive executive function impairments associated with sleepiness (Jones and Harrison, 2001) and why the frontal lobes display more evident electrophysiological signs of deep sleep after prolonged wakefulness (Plante et al., 2016). These mechanisms may, alone or in combination, explain the occurrence of local sleep during wakefulness, leading to the subjective feeling of sleepiness.

As a last note, it is worth mentioning here that, despite the fact that we mainly focused on the cortex when we tried to explain the origins of local sleep, NREM sleep patterns *in vivo* emerge from the interplay between the cortex and the thalamus, more specifically the thalamic reticular nucleus (TRN). It has been reviewed recently how cellular and functional TRN heterogeneity may account for some features of local NREM sleep (Vantomme et al., 2019). By experimentally modulating the activation and firing of the TRN neurons, it was indeed possible to rapidly induce slow wave activity (Lewis et al., 2015) as well as sleep spindles (Fernandez et al., 2018) in spatially restricted regions of the cortex. However, at the current state of the art, it remains unclear how the TRN contributes in terms of physiological conditions and what the signals that activate TRN neurons locally are. Further research will need to clarify these aspects and disentangle the causative role—if there is one —of TRN and the cortex in this loop-network.

Interplay Between Local and Global Regulation

Having highlighted local sleep regulatory mechanisms, it remains to be discussed how they interact with the different processes orchestrating sleep in a global fashion.

According to Saper's model (Saper et al., 2005), sleep regulation relies on three main streams: the "homeostatic" (Porkka-Heiskanen et al., 1997, 2000; Huang et al., 2007, 2011, 2014), the "circadian" (Chou et al., 2003; Fuller et al., 2006), and the "cognitive/emotional" (Chou et al., 2002; Sakurai et al., 2005; Yoshida et al., 2006). Each drive can potentially act globally as well as locally. Aside from the well-known homeostatic local sleep modulation discussed above, there is evidence of regional modulation of brain circadian rhythmicity. This has been demonstrated by a recent fMRI study quantifying changes in brain responses to a sustained-attention task across the circadian cycle, during baseline wakefulness, SD, and after recovery sleep (Muto et al., 2016). Subcortical areas exhibited a dominant circadian modulation that closely followed the melatonin profile but had no significant influence on sleep debt. Cortical responses also showed significant circadian rhythmicity, the phase of which varied across brain regions, as well as a widespread negative influence exerted by sleep pressure. The mechanisms of this local modulation are unknown, although the authors suggested the potential role of clock gene expression. Intriguingly, an EEG study showed that circadian rhythms modulate the incidence amplitude, frequency, and slope of slow waves (the latter being the most accurate marker of synaptic strength), with a dominant effect on central and occipital areas (Lazar et al., 2015).

Moreover, global regulatory mechanisms, particularly regarding the homeostatic and the circadian components, may influence local sleep regulation. In this respect, the extent of brain areas displaying sleep features (and thus the associated behavioral impairments and subjective feeling of sleepiness) may rest on the level of synchronization between global regulatory mechanisms. As such, asynchrony and shift of phase between the homeostatic and the circadian drive may result in local sleep without a global state transition (see **Figure 1**, conceived for schematizing these concepts without fitting any biological data for the sleep drives or for the number of neurons in OFF-periods). Likewise, the cognitive/emotional system may modulate the interaction between the homeostatic and the circadian drives and keep the subject awake despite strong circadian and homeostatic sleep-promoting inputs, accentuating their desynchronization (Horne, 1985).

In summary, local sleep may arise as an intrinsic property of each regulatory drive of the slow-wave cycle or by the desynchronization between these drives acting globally.

In turn, local sleep may affect brain centers responsible for sleep and wake as global behavioral states. As such, the occurrence of isolated local OFF-periods during wakefulness could subsequently lead to global sleep through the involvement of neuro-modulatory systems responsible for the generation of NREM sleep (Saper et al., 2010; Brown et al., 2012). Similar to focal onset seizures with impaired awareness, local changes in cortical activity may lead to profound global alteration of the vigilance state associated with loss of consciousness through the progressive involvement of other brain regions such as midline subcortical structures including the thalamus, the hypothalamus, and the brainstem (Englot and Blumenfeld, 2009). Recordings in the ventrolateral preoptic nucleus (VLPO) neurons showed that their firing rates increase during sleep, almost doubling during

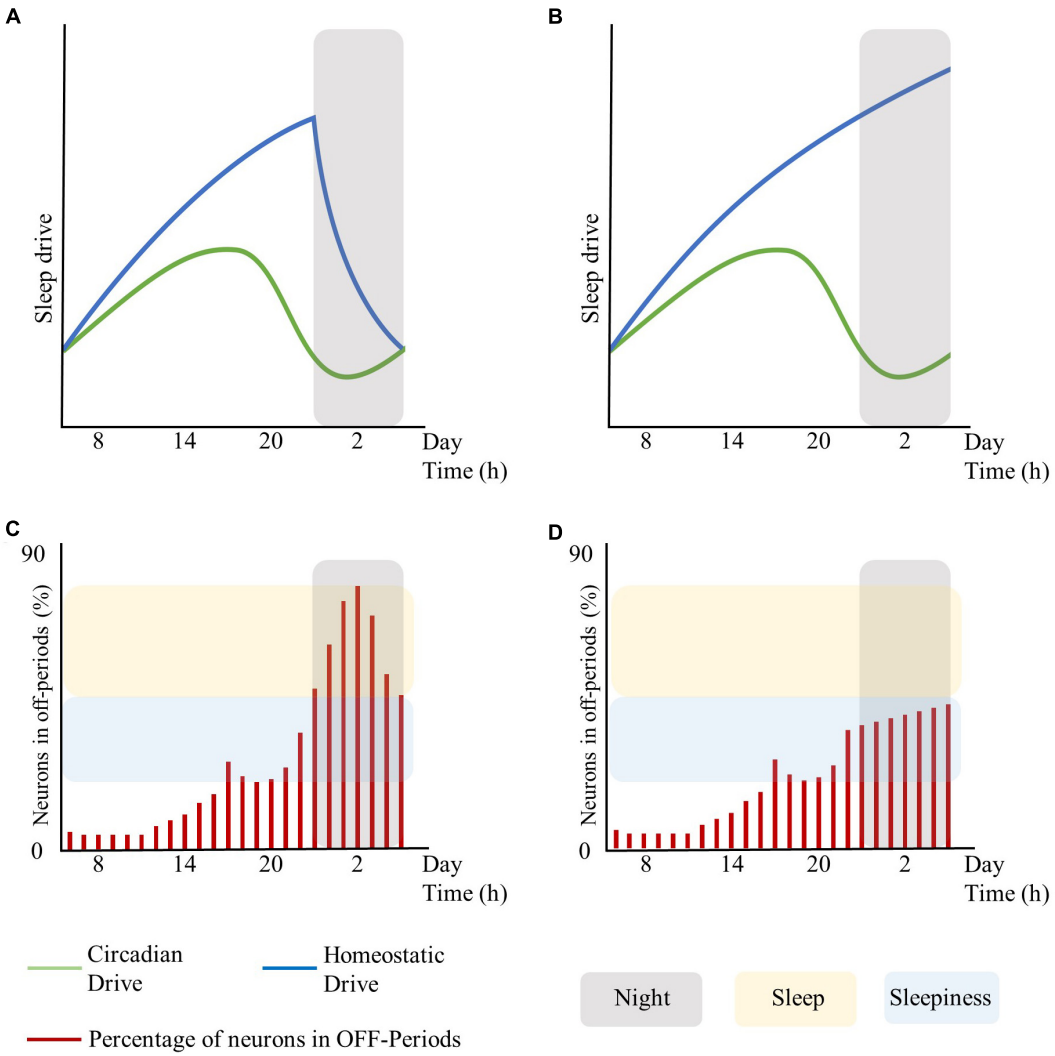

FIGURE 1 | Interplay between global sleep drivers and cortical neuronal firing. The figure is intended to schematize the concepts described in this work without fitting any biological data for sleep drives or the number of neurons in OFF-periods. Top panels represent the time-course of the circadian and homeostatic drive over 24 h. Bottom panels represent the percentage of neurons in OFF-periods across 24 h. **(A)** circadian and homeostatic drives under physiological conditions. **(B)** circadian and homeostatic drives out of phase due to sustained wakefulness. **(C)** percentage of cortical neurons in OFF-periods under physiological conditions. **(D)** percentage of cortical neurons in OFF-periods during sustained wakefulness. Red bars: percentage of cortical neurons in OFF-periods. Blue lines: homeostatic drive. Green lines: circadian drive. Gray areas: night period. Yellow areas: sleep. Light-blue areas: sleepiness. The figure has been realized by fitting the mathematical function published in Daan et al. (1984).

recovery sleep after SD, but did not increase during prolonged wakefulness. Thus, as homeostatic sleep drive accumulates, it may influence other neurons in the brain, such as the median preoptic neurons, which provide input to the VLPO (Saper et al., 2010). Alternatively, there could be a threshold in the number of areas showing sleep signs during wakefulness, which may imply behavioral impairments and sleepiness at first, and only when passing the threshold of the transition to global sleep. Specifically, it is hypothesized that whole organism sleep is an emergent property of the collective neuronal assemblies (Rector et al., 2009), as when networks of neuronal assemblies are coupled they will tend to synchronize (Roy et al., 2008). As such, when the number of neuronal groups entering the sleep state exceeds a significant threshold, other groups will follow (Rector et al., 2009) thus enabling the full-fledged transition from wakefulness to sleep (see **Figure 1**, conceived for schematizing these concepts without fitting any biological data for the sleep drives or number of neurons in OFF-periods).

Sleepiness typically arises in conditions of SD and/or prolonged wakefulness. The prevalence of the so called "insufficient sleep syndrome" is estimated to be between 1 and 4% of the population (Ohayon, 2008) and two to four times higher in individuals sleeping less than 6 h per night compared to individuals sleeping between 7 and 8 h per night (Ohayon, 2012).

The great majority of sleep disorders determine sleepiness through the curtailment of total sleep time and/or sleep

fragmentation without primarily affecting the function of sleep-promoting centers. Examples are sleep breathing disorders like obstructive sleep apnoea, circadian rhythm sleep-wake disorders like shift-work disorder, sleep related movement disorders like restless leg syndrome, and objective insomnia. Central disorders of hypersomnolence like narcolepsy type 1 and 2 or idiopathic hypersomnia involve instead a pathologic imbalance between sleep promoting and wake promoting pathways in favor of the former, determining an increased sleep need and/or the abrupt intrusion of sleep into wakefulness due to an instability of the switching mechanisms between sleep and wakefulness. Also, parasomnias like sleepwalking and sleep terrors have been associated with subjective daytime sleepiness, via as of yet unknown mechanisms (Carrillo-Solano et al., 2016).

Sleepiness is also related to mental and organic diseases that may directly or indirectly affect sleep (Ohayon, 2012). These disorders may cause a disruption of the sleep-wake schedule due to changes in behavior, dysregulate sleep centers orchestrating sleep due to neurological lesions or more subtle abnormalities, or nociceptive, immunomodulatory, or other modulatory inputs.

CONCLUSION AND FUTURE DIRECTIONS

While familiar to all on a subjective level, sleepiness is a complex matter that science is just beginning to understand. We have herein summarized how, during prolonged wakefulness, the occurrence of local neuronal OFF-periods may relate to the well-known negative consequences on performance observed in this state. As suggested by the reviewed literature, this phenomenon of local sleep during wake may account for at least some of the cognitive and behavioral manifestations of sleepiness. Under this perspective, sleepiness may reflect the transition between different vigilance states, being an epiphenomenon of these "fluid boundaries" (Sarasso et al., 2014a).

This interpretation is probably the key that will help develop new measures to quantify sleepiness in the near future. From a clinical perspective, high-density EEG, which allows an optimal spatial and temporal resolution to capture local isles of EEG slowing, may represent a valuable technological support. Moreover, a better characterization of the role of the circadian rhythm and of its interaction with other drives that modulate the sleep-wake cycle is warranted. Finally, a promising future line of research will be on the linking of the neurophysiological concepts of local sleep and sleepiness to interindividual variability in susceptibility to sleepiness (Van Dongen et al., 2004; Kuna et al., 2012; Rupp et al., 2012; Goel et al., 2013; Spaeth et al., 2015). This will open the way to a more personalized sleep medicine that will have a considerable impact on human health and promote occupational well-being, benefiting the society as a whole.

AUTHOR CONTRIBUTIONS

AC and SD'A wrote the first draft of the manuscript. OG, SG, LN, and SS wrote sections of the manuscript. All authors contributed to the manuscript revision, read, and approved the submitted version of the manuscript.

FUNDING

This work was supported by "Sinergia" CRSII3_160803/1 of the Swiss National Science Foundation to SD'A.

REFERENCES

Aeschbach, D., Cajochen, C., Landolt, H., and Borbely, A. A. (1996). Homeostatic sleep regulation in habitual short sleepers and long sleepers. *Am. J. Physiol.* 270, R41–R53.

Aeschbach, D., Matthews, J. R., Postolache, T. T., Jackson, M. A., Giesen, H. A., and Wehr, T. A. (1997). Dynamics of the human EEG during prolonged wakefulness: evidence for frequency-specific circadian and homeostatic influences. *Neurosci. Lett.* 239, 121–124. doi: 10.1016/s0304-3940(97)00904-x

Ahlstrom, C., Jansson, S., and Anund, A. (2017). Local changes in the wake electroencephalogram precedes lane departures. *J. Sleep Res.* 26, 816–819. doi: 10.1111/jsr.12527

Andrillon, T., Nir, Y., Staba, R. J., Ferrarelli, F., Cirelli, C., Tononi, G., et al. (2011). Sleep spindles in humans: insights from intracranial EEG and unit recordings. *J. Neurosci.* 31, 17821–17834. doi: 10.1523/JNEUROSCI.2604-11.2011

Banks, S., and Dinges, D. F. (2007). Behavioral and physiological consequences of sleep restriction. *J. Clin. Sleep Med.* 3, 519–528.

Bellesi, M., Tononi, G., Cirelli, C., and Serra, P. A. (2016). Region-specific dissociation between cortical noradrenaline levels and the sleep/wake cycle. *Sleep* 39, 143–154. doi: 10.5665/sleep.5336

Bernardi, G., Siclari, F., Yu, X., Zennig, C., Bellesi, M., Ricciardi, E., et al. (2015). Neural and behavioral correlates of extended training during sleep deprivation in humans: evidence for local, task-specific effects. *J. Neurosci.* 35, 4487–4500. doi: 10.1523/JNEUROSCI.4567-14.2015

Bernert, R. A., and Joiner, T. E. (2007). Sleep disturbances and suicide risk: a review of the literature. *Neuropsychiatr. Dis. Treat.* 3, 735–743. doi: 10.2147/ndt.s1248

Blaivas, A. J., Patel, R., Hom, D., Antigua, K., and Ashtyani, H. (2007). Quantifying microsleep to help assess subjective sleepiness. *Sleep Med.* 8, 156–159. doi: 10.1016/j.sleep.2006.06.011

Borbély, A. A., Tobler, I., and Hanagasioglu, M. (1984). Effect of sleep deprivation on sleep and EEG power spectra in the rat. *Behav. Brain Res.* 14, 171–182. doi: 10.1016/0166-4328(84)90186-4

Boyle, L. N., Tippin, J., Paul, A., and Rizzo, M. (2008). Driver Performance in the Moments Surrounding a Microsleep. *Transp. Res. Part F Traffic Psychol. Behav.* 11, 126–136. doi: 10.1016/j.trf.2007.08.001

Broman, J. E., Lundh, L. G., and Hetta, J. (1996). Insufficient sleep in the general population. *Neurophysiol. Clin.* 26, 30–39. doi: 10.1016/0987-7053(96)81532-2

Brown, R. E., Basheer, R., Mckenna, J. T., Strecker, R. E., and Mccarley, R. W. (2012). Control of sleep and wakefulness. *Physiol. Rev.* 92, 1087–1187. doi: 10.1152/physrev.00032.2011

Cajochen, C., Brunner, D. P., Krauchi, K., Graw, P., and Wirz-Justice, A. (1995). Power density in theta/alpha frequencies of the waking EEG progressively increases during sustained wakefulness. *Sleep* 18, 890–894. doi: 10.1093/sleep/18.10.890

Cajochen, C., Khalsa, S. B., Wyatt, J. K., Czeisler, C. A., and Dijk, D. J. (1999). EEG and ocular correlates of circadian melatonin phase and human performance decrements during sleep loss. *Am. J. Physiol.* 277, R640–R649.

Cajochen, C., Wyatt, J. K., Czeisler, C. A., and Dijk, D. J. (2002). Separation of circadian and wake duration-dependent modulation of EEG activation during wakefulness. *Neuroscience* 114, 1047–1060. doi: 10.1016/s0306-4522(02)00209-9

Carrillo-Solano, M., Leu-Semenescu, S., Golmard, J.-L., Groos, E., and Arnulf, I. (2016). Sleepiness in sleepwalking and sleep terrors: a higher sleep pressure? *Sleep Med.* 26, 54–59. doi: 10.1016/j.sleep.2015.11.020

Chee, M. W., and Choo, W. C. (2004). Functional imaging of working memory after 24 hr of total sleep deprivation. *J. Neurosci.* 24, 4560–4567. doi: 10.1523/jneurosci.0007-04.2004

Chou, T. C., Bjorkum, A. A., Gaus, S. E., Lu, J., Scammell, T. E., and Saper, C. B. (2002). Afferents to the ventrolateral preoptic nucleus. *J. Neurosci.* 22, 977–990. doi: 10.1523/jneurosci.22-03-00977.2002

Chou, T. C., Scammell, T. E., Gooley, J. J., Gaus, S. E., Saper, C. B., and Lu, J. (2003). Critical role of dorsomedial hypothalamic nucleus in a wide range of behavioral circadian rhythms. *J. Neurosci.* 23, 10691–10702. doi: 10.1523/jneurosci.23-33-10691.2003

Cluydts, R., De Valck, E., Verstraeten, E., and Theys, P. (2002). Daytime sleepiness and its evaluation. *Sleep Med. Rev.* 6, 83–96. doi: 10.1053/smrv.2002.0191

Corner, M. A., Baker, R. E., and Van Pelt, J. (2008). Physiological consequences of selective suppression of synaptic transmission in developing cerebral cortical networks in vitro: differential effects on intrinsically generated bioelectric discharges in a living 'model' system for slow-wave sleep activity. *Neurosci. Biobehav. Rev.* 32, 1569–1600. doi: 10.1016/j.neubiorev.2008.06.008

Couyoumdjian, A., Sdoia, S., Tempesta, D., Curcio, G., Rastellini, E., De Gennaro, L., et al. (2010). The effects of sleep and sleep deprivation on task-switching performance. *J. Sleep Res.* 19, 64–70. doi: 10.1111/j.1365-2869.2009.00774.x

Daan, S., Beersma, D. G., and Borbely, A. A. (1984). Timing of human sleep: recovery process gated by a circadian pacemaker. *Am. J. Physiol.* 246, R161–R183.

De Gennaro, L., Fratello, F., Marzano, C., Moroni, F., Curcio, G., Tempesta, D., et al. (2008). Cortical plasticity induced by transcranial magnetic stimulation during wakefulness affects electroencephalogram activity during sleep. *PLoS One* 3:e2483. doi: 10.1371/journal.pone.0002483

De Gennaro, L., Marzano, C., Veniero, D., Moroni, F., Fratello, F., Curcio, G., et al. (2007). Neurophysiological correlates of sleepiness: a combined TMS and EEG study. *Neuroimage* 36, 1277–1287. doi: 10.1016/j.neuroimage.2007.04.013

De Valck, E., and Cluydts, R. (2003). Sleepiness as a state-trait phenomenon, comprising both a sleep drive and a wake drive. *Med. Hypotheses* 60, 509–512. doi: 10.1016/s0306-9877(02)00444-9

Dinges, D. F. (1995). An overview of sleepiness and accidents. *J. Sleep Res.* 4, 4–14. doi: 10.1111/j.1365-2869.1995.tb00220.x

Dinges, D. F., Pack, F., Williams, K., Gillen, K. A., Powell, J. W., Ott, G. E., et al. (1997). Cumulative sleepiness, mood disturbance, and psychomotor vigilance performance decrements during a week of sleep restricted to 4-5 hours per night. *Sleep* 20, 267–277.

Dumont, M., Macchi, M. M., Carrier, J., Lafrance, C., and Hebert, M. (1999). Time course of narrow frequency bands in the waking EEG during sleep deprivation. *Neuroreport* 10, 403–407. doi: 10.1097/00001756-199902050-00035

Eban-Rothschild, A., Appelbaum, L., and De Lecea, L. (2018). Neuronal Mechanisms for Sleep/Wake Regulation and Modulatory Drive. *Neuropsychopharmacology* 43, 937–952. doi: 10.1038/npp.2017.294

Englot, D. J., and Blumenfeld, H. (2009). Consciousness and epilepsy: why are complex-partial seizures complex? *Prog. Brain Res.* 177, 147–170. doi: 10.1016/S0079-6123(09)17711-7

Fattinger, S., Kurth, S., Ringli, M., Jenni, O. G., and Huber, R. (2017). Theta waves in children's waking electroencephalogram resemble local aspects of sleep during wakefulness. *Sci. Rep.* 7:11187. doi: 10.1038/s41598-017-11577-3

Fernandez, L. M., Vantomme, G., Osorio-Forero, A., Cardis, R., Béard, E., and Lüthi, A. (2018). Thalamic reticular control of local sleep in mouse sensory cortex. *eLife* 7:e39111. doi: 10.7554/eLife.39111

Finelli, L. A., Baumann, H., Borbely, A. A., and Achermann, P. (2000). Dual electroencephalogram markers of human sleep homeostasis: correlation between theta activity in waking and slow-wave activity in sleep. *Neuroscience* 101, 523–529. doi: 10.1016/s0306-4522(00)00409-7

Fleming, W. E., Ferouz-Colborn, A., Samoszuk, M. K., Azad, A., Lu, J., Riley, J. S., et al. (2016). Blood biomarkers of endocrine, immune, inflammatory, and metabolic systems in obstructive sleep apnea. *Clin. Biochem.* 49, 854–861. doi: 10.1016/j.clinbiochem.2016.05.005

Franken, P., Dijk, D. J., Tobler, I., and Borbely, A. A. (1991). Sleep deprivation in rats: effects on EEG power spectra, vigilance states, and cortical temperature. *Am. J. Physiol.* 261, R198–R208.

Friedman, L., Bergmann, B. M., and Rechtschaffen, A. (1978). Effects of sleep deprivation on sleepiness, sleep intensity, and subsequent sleep in the rat. *Sleep* 1, 369–391. doi: 10.1093/sleep/1.4.369

Fuller, P. M., Gooley, J. J., and Saper, C. B. (2006). Neurobiology of the sleep-wake cycle: sleep architecture, circadian regulation, and regulatory feedback. *J. Biol. Rhythms* 21, 482–493. doi: 10.1177/0748730406294627

Garbarino, S., Lanteri, P., Durando, P., Magnavita, N., and Sannita, W. G. (2016). Co-Morbidity, mortality, quality of life and the healthcare/welfare/social costs of disordered sleep: a rapid review. *Int. J. Environ. Res. Public Health* 13:E831. doi: 10.3390/ijerph13080831

Gautier-Sauvigné, S., Colas, D., Parmantier, P., Clement, P., Gharib, A., Sarda, N., et al. (2005). Nitric oxide and sleep. *Sleep Med. Rev.* 9, 101–113.

Goel, N., Abe, T., Braun, M. E., and Dinges, D. F. (2014). Cognitive workload and sleep restriction interact to influence sleep homeostatic responses. *Sleep* 37, 1745–1756. doi: 10.5665/sleep.4164

Goel, N., Basner, M., Rao, H., and Dinges, D. F. (2013). Circadian rhythms, sleep deprivation, and human performance. *Prog. Mol. Biol. Transl. Sci.* 119, 155–190. doi: 10.1016/b978-0-12-396971-2.00007-5

Goel, N., Rao, H., Durmer, J. S., and Dinges, D. F. (2009). Neurocognitive consequences of sleep deprivation. *Semin. Neurol.* 29, 320–339. doi: 10.1055/s-0029-1237117

Gorgoni, M., Ferlazzo, F., Ferrara, M., Moroni, F., D'Atri, A., Fanelli, S., et al. (2014). Topographic electroencephalogram changes associated with psychomotor vigilance task performance after sleep deprivation. *Sleep Med.* 15, 1132–1139. doi: 10.1016/j.sleep.2014.04.022

Grandner, M. A., Hale, L., Moore, M., and Patel, N. P. (2010). Mortality associated with short sleep duration: the evidence, the possible mechanisms, and the future. *J. Sleep Med. Rev.* 14, 191–203. doi: 10.1016/j.smrv.2009.07.006

Hall, R. D., and Borbely, A. A. (1970). Acoustically evoked potentials in the rat during sleep and waking. *Exp. Brain Res.* 11, 93–110.

Hanlon, E. C., Faraguna, U., Vyazovskiy, V. V., Tononi, G., and Cirelli, C. (2009). Effects of skilled training on sleep slow wave activity and cortical gene expression in the rat. *Sleep* 32, 719–729. doi: 10.1093/sleep/32.6.719

Hertig-Godeschalk, A., Skorucak, J., Malafeev, A., Achermann, P., Mathis, J., and Schreier, D. R. (2019). Microsleep episodes in the borderland between wakefulness and sleep. *Sleep* doi: 10.1093/sleep/zsz163 [Epub ahead of print].

Hinard, V., Mikhail, C., Pradervand, S., Curie, T., Houtkooper, R. H., Auwerx, J., et al. (2012). Key electrophysiological, molecular, and metabolic signatures of sleep and wakefulness revealed in primary cortical cultures. *J. Neurosci.* 32, 12506–12517. doi: 10.1523/JNEUROSCI.2306-12.2012

Horne, J., and Pettitt, A. N. (1985). High incentive effects on vigilance performance during 72 hours of total sleep deprivation. *Acta Psychol.* 58, 123–139. doi: 10.1016/0001-6918(85)90003-4

Horne, J. A. (1985). Sleep function, with particular reference to sleep deprivation. *Ann. Clin. Res.* 17, 199–208.

Huang, Z. L., Urade, Y., and Hayaishi, O. (2007). Prostaglandins and adenosine in the regulation of sleep and wakefulness. *Curr. Opin. Pharmacol.* 7, 33–38. doi: 10.1016/j.coph.2006.09.004

Huang, Z. L., Urade, Y., and Hayaishi, O. (2011). The role of adenosine in the regulation of sleep. *Curr. Top. Med. Chem.* 11, 1047–1057.

Huang, Z. L., Zhang, Z., and Qu, W. M. (2014). Roles of adenosine and its receptors in sleep-wake regulation. *Int. Rev. Neurobiol.* 119, 349–371. doi: 10.1016/B978-0-12-801022-8.00014-3

Huber, R., Esser, S. K., Ferrarelli, F., Massimini, M., Peterson, M. J., and Tononi, G. (2007). TMS-induced cortical potentiation during wakefulness locally increases slow wave activity during sleep. *PLoS One* 2:e276. doi: 10.1371/journal.pone.0000276

Huber, R., Ghilardi, M. F., Massimini, M., Ferrarelli, F., Riedner, B. A., Peterson, M. J., et al. (2006). Arm immobilization causes cortical plastic changes and locally decreases sleep slow wave activity. *Nat. Neurosci.* 9, 1169–1176. doi: 10.1038/nn1758

Huber, R., Ghilardi, M. F., Massimini, M., and Tononi, G. (2004). Local sleep and learning. *Nature* 430, 78–81. doi: 10.1038/nature02663

Hung, C. S., Sarasso, S., Ferrarelli, F., Riedner, B., Ghilardi, M. F., Cirelli, C., et al. (2013). Local experience-dependent changes in the wake EEG after prolonged wakefulness. *Sleep* 36, 59–72. doi: 10.5665/sleep.2302

Imeri, L., and Opp, M. R. (2009). How (and why) the immune system makes us sleep. *Nat. Rev. Neurosci.* 10, 199–210. doi: 10.1038/nrn2576

Jewett, M. E., Wyatt, J. K., Ritz-De Cecco, A., Khalsa, S. B., Dijk, D. J., and Czeisler, C. A. (1999). Time course of sleep inertia dissipation in human performance and alertness. *J. Sleep Res.* 8, 1–8. doi: 10.1111/j.1365-2869.1999.00128.x

Jones, K., and Harrison, Y. (2001). Frontal lobe function, sleep loss and fragmented sleep. *Sleep Med. Rev.* 5, 463–475. doi: 10.1053/smrv.2001.02

Jones, B. E. (2005). From waking to sleeping: neuronal and chemical substrates. *Trends Pharmacol. Sci.* 26, 578–586. doi: 10.1016/j.tips.2005.09.009

Kalinchuk, A. V., Mccarley, R. W., Porkka-Heiskanen, T., and Basheer, R. (2011). The time course of adenosine, nitric oxide (NO) and inducible NO synthase changes in the brain with sleep loss and their role in the non-rapid eye movement sleep homeostatic cascade. *J. Neurochem.* 116, 260–272. doi: 10.1111/j.1471-4159.2010.07100.x

Kattler, H., Dijk, D. J., and Borbely, A. A. (1994). Effect of unilateral somatosensory stimulation prior to sleep on the sleep EEG in humans. *J. Sleep Res.* 3, 159–164. doi: 10.1111/j.1365-2869.1994.tb00123.x

Kaufmann, T., Elvsåshagen, T., Alnæs, D., Zak, N., Pedersen, P. Ø, Norbom, L. B., et al. (2016). The brain functional connectome is robustly altered by lack of sleep. *Neuroimage* 127, 324–332. doi: 10.1016/j.neuroimage.2015.12.028

Knutson, K. L., Spiegel, K., Penev, P., and Van Cauter, E. (2007). The metabolic consequences of sleep deprivation. *Sleep Med. Rev.* 11, 163–178. doi: 10.1016/j.smrv.2007.01.002

Krause, A. J., Simon, E. B., Mander, B. A., Greer, S. M., Saletin, J. M., Goldstein-Piekarski, A. N., et al. (2017). The sleep-deprived human brain. *Nat. Rev. Neurosci.* 18, 404–418. doi: 10.1038/nrn.2017.55

Kristiansen, K., and Courtois, G. (1949). Rhythmic electrical activity from isolated cerebral cortex. *Electroencephalogr. Clin. Neurophysiol.* 1, 265–272. doi: 10.1016/0013-4694(49)90038-3

Kritikou, I., Basta, M., Vgontzas, A. N., Pejovic, S., Liao, D., Tsaoussoglou, M., et al. (2014). Sleep apnoea, sleepiness, inflammation and insulin resistance in middle-aged males and females. *ERJ* 43, 145–155. doi: 10.1183/09031936.00126712

Krueger, J. M. (2008). The role of cytokines in sleep regulation. *Curr. Pharm. Des.* 14, 3408–3416. doi: 10.2174/138161208786549281

Krueger, J. M., Nguyen, J. T., Dykstra-Aiello, C. J., and Taishi, P. (2019). Local sleep. *Sleep Med. Rev.* 43, 14–21. doi: 10.1016/j.smrv.2018.10.001

Krueger, J. M., Obál, F. Jr., Kapás, L., and Fang, J. (1995a). Brain organization and sleep function. *Behav. Brain Res.* 69, 177–185. doi: 10.1016/0166-4328(95)00015-1

Krueger, J. M., Takahashi, S., Kapás, L., Bredow, S., Roky, R., Fang, J., et al. (1995b). Cytokines in sleep regulation. *Adv. Immunol.* 5, 171–188.

Krueger, J. M., and Obal, F. (1993). A neuronal group theory of sleep function. *J. Sleep Res.* 2, 63–69. doi: 10.1111/j.1365-2869.1993.tb00064.x

Krueger, J. M., Rector, D. M., Roy, S., Van Dongen, H. P., Belenky, G., and Panksepp, J. (2008). Sleep as a fundamental property of neuronal assemblies. *Nat. Rev. Neurosci.* 9, 910–919. doi: 10.1038/nrn2521

Krueger, P. M., and Friedman, E. M. (2009). Sleep duration in the United States: a cross-sectional population-based study. *Am. J. Epidemiol.* 169, 1052–1063. doi: 10.1093/aje/kwp023

Kuna, S. T., Maislin, G., Pack, F. M., Staley, B., Hachadoorian, R., Coccaro, E. F., et al. (2012). Heritability of performance deficit accumulation during acute sleep deprivation in twins. *Sleep* 35, 1223–1233. doi: 10.5665/sleep.2074

Latini, S., and Pedata, F. (2001). Adenosine in the central nervous system: release mechanisms and extracellular concentrations. *J. Neurochem.* 79, 463–484. doi: 10.1046/j.1471-4159.2001.00607.x

Lazar, A. S., Lazar, Z. I., and Dijk, D.-J. (2015). Circadian regulation of slow waves in human sleep: topographical aspects. *Neuroimage* 116, 123–134. doi: 10.1016/j.neuroimage.2015.05.012

Leemburg, S., Vyazovskiy, V. V., Olcese, U., Bassetti, C. L., Tononi, G., and Cirelli, C. (2010). Sleep homeostasis in the rat is preserved during chronic sleep restriction. *Proc. Natl. Acad. Sci. U.S.A.* 107, 15939–15944. doi: 10.1073/pnas.1002570107

Lesku, J. A., Vyssotski, A. L., Martinez-Gonzalez, D., Wilzeck, C., and Rattenborg, N. C. (2011). Local sleep homeostasis in the avian brain: convergence of sleep function in mammals and birds? *Proc. Biol. Sci.* 278, 2419–2428. doi: 10.1098/rspb.2010.2316

Lewis, L. D., Voigts, J., Flores, F. J., Schmitt, L. I., Wilson, M. A., Halassa, M. M., et al. (2015). Thalamic reticular nucleus induces fast and local modulation of arousal state. *eLife* 4:e08760. doi: 10.7554/eLife.08760

Liu, X., and Zhou, H. (2002). Sleep duration, insomnia and behavioral problems among Chinese adolescents. *Psychiatry Res.* 111, 75–85. doi: 10.1016/s0165-1781(02)00131-2

Ly, J. Q., Gaggioni, G., Chellappa, S. L., Papachilleos, S., Brzozowski, A., Borsu, C., et al. (2016). Circadian regulation of human cortical excitability. *Nat. Commun.* 7:11828. doi: 10.1038/ncomms11828

Magnin, M., Rey, M., Bastuji, H., Guillemant, P., Mauguiere, F., and Garcia-Larrea, L. (2010). Thalamic deactivation at sleep onset precedes that of the cerebral cortex in humans. *Proc. Natl. Acad. Sci. U.S.A.* 107, 3829–3833. doi: 10.1073/pnas.0909710107

Maric, A., Montvai, E., Werth, E., Storz, M., Leemann, J., Weissengruber, S., et al. (2017). Insufficient sleep: enhanced risk-seeking relates to low local sleep intensity. *Ann. Neurol.* 82, 409–418. doi: 10.1002/ana.25023

Marzano, C., Moroni, F., Gorgoni, M., Nobili, L., Ferrara, M., and De Gennaro, L. (2013). How we fall asleep: regional and temporal differences in electroencephalographic synchronization at sleep onset. *Sleep Med.* 14, 1112–1122. doi: 10.1016/j.sleep.2013.05.021

Miyamoto, H., Katagiri, H., and Hensch, T. (2003). Experience-dependent slow-wave sleep development. *Nat. Neurosci.* 6, 553–554. doi: 10.1038/nn1064

Muto, V., Jaspar, M., Meyer, C., Kussé, C., Chellappa, S. L., Degueldre, C., et al. (2016). Local modulation of human brain responses by circadian rhythmicity and sleep debt. *Science* 353, 687–690. doi: 10.1126/science.aad2993

Nguyen, J., Gibbons, C. M., Dykstra-Aiello, C., Ellingsen, R., Koh, K. M. S., Taishi, P., et al. (2019). Interleukin-1 receptor accessory proteins are required for normal homeostatic responses to sleep deprivation. *J. Appl. Physiol.* 127, 770–780. doi: 10.1152/japplphysiol.00366.2019

Nir, Y., Andrillon, T., Marmelshtein, A., Suthana, N., Cirelli, C., Tononi, G., et al. (2017). Selective neuronal lapses precede human cognitive lapses following sleep deprivation. *Nat. Med.* 23, 1474–1480. doi: 10.1038/nm.4433

Nir, Y., Staba, R. J., Andrillon, T., Vyazovskiy, V. V., Cirelli, C., Fried, I., et al. (2011). Regional slow waves and spindles in human sleep. *Neuron* 70, 153–169. doi: 10.1016/j.neuron.2011.02.043

Nobili, L., Ferrara, M., Moroni, F., De Gennaro, L., Russo, G. L., Campus, C., et al. (2011). Dissociated wake-like and sleep-like electro-cortical activity during sleep. *Neuroimage* 58, 612–619. doi: 10.1016/j.neuroimage.2011.06.032

Ohayon, M. M. (2008). From wakefulness to excessive sleepiness: what we know and still need to know. *Sleep Med. Rev.* 12, 129–141. doi: 10.1016/j.smrv.2008.01.001

Ohayon, M. M. (2012). Determining the level of sleepiness in the American population and its correlates. *J. Psychiatr. Res.* 46, 422–427. doi: 10.1016/j.jpsychires.2011.06.008

Olson, L., Cole, M., and Ambrogetti, A. (1998). Correlations among Epworth sleepiness scale scores, multiple sleep latency tests and psychological symptoms. *J. Sleep Res.* 7, 248–253. doi: 10.1046/j.1365-2869.1998.00123.x

Panzeri, S., Petroni, F., Petersen, R. S., and Diamond, M. E. (2003). Decoding neuronal population activity in rat somatosensory cortex: role of columnar organization. *Cereb. Cortex* 13, 45–52. doi: 10.1093/cercor/13.1.45

Peter-Derex, L., Magnin, M., and Bastuji, H. (2015). Heterogeneity of arousals in human sleep: a stereo-electroencephalographic study. *Neuroimage* 123, 229–244. doi: 10.1016/j.neuroimage.2015.07.057

Pigarev, I. N., Nothdurft, H. C., and Kastner, S. (1997). Evidence for asynchronous development of sleep in cortical areas. *Neuroreport* 8, 2557–2560. doi: 10.1097/00001756-199707280-00027

Plante, D. T., Goldstein, M. R., Cook, J. D., Smith, R., Riedner, B. A., Rumble, M. E., et al. (2016). Effects of partial sleep deprivation on slow waves during non-rapid eye movement sleep: a high density EEG investigation. *Clin. Neurophysiol.* 127, 1436–1444. doi: 10.1016/j.clinph.2015.10.040

Porkka-Heiskanen, T., and Kalinchuk, A. V. (2011). Adenosine, energy metabolism and sleep homeostasis. *Sleep Med. Rev.* 15, 123–135. doi: 10.1016/j.smrv.2010.06.005

Porkka-Heiskanen, T., Strecker, R. E., and Mccarley, R. W. (2000). Brain site-specificity of extracellular adenosine concentration changes during sleep deprivation and spontaneous sleep: an in vivo microdialysis study. *Neuroscience* 99, 507–517. doi: 10.1016/s0306-4522(00)00220-7

Porkka-Heiskanen, T., Strecker, R. E., Thakkar, M., Bjorkum, A. A., Greene, R. W., and Mccarley, R. W. (1997). Adenosine: a mediator of the sleep-inducing effects of prolonged wakefulness. *Science* 276, 1265–1268. doi: 10.1126/science.276.5316.1265

Poudel, G. R., Innes, C. R. H., and Jones, R. D. (2018). Temporal evolution of neural activity and connectivity during microsleeps when rested and following sleep restriction. *Neuroimage* 174, 263–273. doi: 10.1016/j.neuroimage.2018.03.031

Priest, B., Brichard, C., Aubert, G., Liistro, G., and Rodenstein, D. O. (2001). Microsleep during a simplified maintenance of wakefulness test. A validation study of the OSLER test. *Am. J. Respir. Crit. Care Med.* 163, 1619–1625. doi: 10.1164/ajrccm.163.7.2007028

Quercia, A., Zappasodi, F., Committeri, G., and Ferrara, M. (2018). Local use-dependent sleep in wakefulness links performance errors to learning. *Front. Hum. Neurosci.* 12:122. doi: 10.3389/fnhum.2018.00122

Rector, D. M., Schei, J. L., Van Dongen, H. P., Belenky, G., and Krueger, J. M. (2009). Physiological markers of local sleep. *Eur. J. Neurosci.* 29, 1771–1778. doi: 10.1111/j.1460-9568.2009.06717.x

Rector, D. M., Topchiy, I. A., Carter, K. M., and Rojas, M. J. (2005). Local functional state differences between rat cortical columns. *Brain Res.* 1047, 45–55. doi: 10.1016/j.brainres.2005.04.002

Roy, S., Krueger, J. M., Rector, D. M., and Wan, Y. (2008). A network model for activity-dependent sleep regulation. *J. Theor. Biol.* 253, 462–468. doi: 10.1016/j.jtbi.2008.03.033

Rupp, T. L., Wesensten, N. J., and Balkin, T. J. (2012). Trait-like vulnerability to total and partial sleep loss. *Sleep* 35, 1163–1172. doi: 10.5665/sleep.2010

Sakurai, T., Nagata, R., Yamanaka, A., Kawamura, H., Tsujino, N., Muraki, Y., et al. (2005). Input of orexin/hypocretin neurons revealed by a genetically encoded tracer in mice. *Neuron* 46, 297–308. doi: 10.1016/j.neuron.2005.03.010

Saper, C. B., Cano, G., and Scammell, T. E. (2005). Homeostatic, circadian, and emotional regulation of sleep. *J. Comp. Neurol.* 493, 92–98. doi: 10.1002/cne.20770

Saper, C. B., Chou, T. C., and Scammell, T. E. (2001). The sleep switch: hypothalamic control of sleep and wakefulness. *Trends Neurosci.* 24, 726–731. doi: 10.1016/s0166-2236(00)02002-6

Saper, C. B., Fuller, P. M., Pedersen, N. P., Lu, J., and Scammell, T. E. (2010). Sleep state switching. *Neuron* 68, 1023–1042. doi: 10.1016/j.neuron.2010.11.032

Sarasso, S., Pigorini, A., Proserpio, P., Gibbs, S. A., Massimini, M., and Nobili, L. (2014a). Fluid boundaries between wake and sleep: experimental evidence from Stereo-EEG recordings. *Arch. Ital. Biol.* 152, 169–177. doi: 10.12871/0002982920142311

Sarasso, S., Proserpio, P., Pigorini, A., Moroni, F., Ferrara, M., De Gennaro, L., et al. (2014b). Hippocampal sleep spindles preceding neocortical sleep onset in humans. *Neuroimage* 86, 425–432. doi: 10.1016/j.neuroimage.2013.10.031

Scammell, T. E., Arrigoni, E., and Lipton, J. O. (2017). Neural Circuitry of Wakefulness and Sleep. *Neuron* 93, 747–765. doi: 10.1016/j.neuron.2017.01.014

Sechenova, I. M. (2011). Rossiiskii Fiziologicheskii Zhurnal. *Transl. Silkis* 97, 472–482.

Shekleton, J. A., Rajaratnam, S. M. W., Gooley, J. J., Van Reen, E., Czeisler, C. A., and Lockley, S. W. (2013). Improved neurobehavioral performance during the wake maintenance zone. *J. Clin. Sleep Med.* 9, 353–362. doi: 10.5664/jcsm.2588

Siclari, F., Bernardi, G., Riedner, B. A., Larocque, J. J., Benca, R. M., and Tononi, G. (2014). Two distinct synchronization processes in the transition to sleep: a high-density electroencephalographic study. *Sleep* 37, 1621–1637. doi: 10.5665/sleep.4070

Siclari, F., and Tononi, G. (2017). Local aspects of sleep and wakefulness. *Curr. Opin. Neurobiol.* 44, 222–227. doi: 10.1016/j.conb.2017.05.008

Siegel, J. M. (2009). The neurobiology of sleep. *Semin. Neurol.* 29, 277–296.

Silkis, I. G. (2013). Generation of ponto-geniculo-occipital (pgo) waves as a possible cause of impairments to visual perception during microsleep. *Neurosci. Behav. Physiol.* 43, 122–128. doi: 10.1007/s11055-012-9701-0

Spaeth, A. M., Dinges, D. F., and Goel, N. (2015). Phenotypic vulnerability of energy balance responses to sleep loss in healthy adults. *Sci. Rep.* 5:14920. doi: 10.1038/srep14920

Steriade, M., Nunez, A., and Amzica, F. (1993). A novel slow (< 1 Hz) oscillation of neocortical neurons in vivo: depolarizing and hyperpolarizing components. *J. Neurosci.* 13, 3252–3265. doi: 10.1523/jneurosci.13-08-03252.1993

Strijkstra, A. M., Beersma, D. G., Drayer, B., Halbesma, N., and Daan, S. (2003). Subjective sleepiness correlates negatively with global alpha (8-12 Hz) and positively with central frontal theta (4-8 Hz) frequencies in the human resting awake electroencephalogram. *Neurosci. Lett.* 340, 17–20. doi: 10.1016/s0304-3940(03)00033-8

Szymusiak, R., and McGinty, D. (2008). Hypothalamic regulation of sleep and arousal. *Ann. N. Y. Acad. Sci.* 1129, 275–286. doi: 10.1196/annals.1417.027

Tinguely, G., Finelli, L. A., Landolt, H. P., Borbely, A. A., and Achermann, P. (2006). Functional EEG topography in sleep and waking: state-dependent and state-independent features. *Neuroimage* 32, 283–292. doi: 10.1016/j.neuroimage.2006.03.017

Tirunahari, V. L., Zaidi, S. A., Sharma, R., Skurnick, J., and Ashtyani, H. (2003). Microsleep and sleepiness: a comparison of multiple sleep latency test and scoring of microsleep as a diagnostic test for excessive daytime sleepiness. *Sleep Med.* 4, 63–67. doi: 10.1016/s1389-9457(02)00250-2

Tobler, I., and Borbely, A. A. (1986). Sleep EEG in the rat as a function of prior waking. *Electroencephalogr. Clin. Neurophysiol.* 64, 74–76. doi: 10.1016/0013-4694(86)90044-1

Tononi, G., and Cirelli, C. (2003). Sleep and synaptic homeostasis: a hypothesis. *Brain Res. Bull.* 62, 143–150. doi: 10.1016/j.brainresbull.2003.09.004

Tononi, G., and Cirelli, C. (2006). Sleep function and synaptic homeostasis. *Sleep Med. Rev.* 10, 49–62. doi: 10.1016/j.smrv.2005.05.002

Torsvall, L., and Akerstedt, T. (1988). Extreme sleepiness: quantification of EOG and spectral EEG parameters. *Int. J. Neurosci.* 38, 435–441. doi: 10.3109/00207458808990704

Trotti, L. M. (2017). Waking up is the hardest thing I do all day: sleep inertia and sleep drunkeness. *Sleep Med. Rev.* 35, 76–84. doi: 10.1016/j.smrv.2016.08.005

Van Dongen, H. P., Baynard, M. D., Maislin, G., and Dinges, D. F. (2004). Systematic interindividual differences in neurobehavioral impairment from sleep loss: evidence of trait-like differential vulnerability. *Sleep* 27, 423–433.

Van Dongen, H. P., Maislin, G., Mullington, J. M., and Dinges, D. F. (2003a). The cumulative cost of additional wakefulness: dose-response effects on neurobehavioral functions and sleep physiology from chronic sleep restriction and total sleep deprivation. *Sleep* 26, 117–126. doi: 10.1093/sleep/26.2.117

Van Dongen, H. P., Rogers, N. L., Dinges, D. F. J. S., and Rhythms, B. (2003b). Sleep debt: theoretical and empirical issues. *Sleep Biol. Rhythm* 1, 5–13. doi: 10.1046/j.1446-9235.2003.00006.x

Vantomme, G., Osorio-Forero, A., Lüthi, A., and Fernandez, L. M. J. (2019). Regulation of Local Sleep by the Thalamic Reticular Nucleus. *Front. Neurosci.* 13:576. doi: 10.3389/fnins.2019.00576

Volgushev, M., Chauvette, S., Mukovski, M., and Timofeev, I. (2006). Precise long-range synchronization of activity and silence in neocortical neurons during slow-wave sleep. *J. Neurosci.* 26, 5665–5672. doi: 10.1523/jneurosci.0279-06.2006

Vyazovskiy, V. V., Cirelli, C., and Tononi, G. (2011a). Electrophysiological correlates of sleep homeostasis in freely behaving rats. *Prog. Brain Res.* 193, 17–38. doi: 10.1016/B978-0-444-53839-0.00002-8

Vyazovskiy, V. V., Olcese, U., Hanlon, E. C., Nir, Y., Cirelli, C., and Tononi, G. (2011b). Local sleep in awake rats. *Nature* 472, 443–447. doi: 10.1038/nature10009

Vyazovskiy, V. V., Olcese, U., Cirelli, C., and Tononi, G. (2013). Prolonged wakefulness alters neuronal responsiveness to local electrical stimulation of the neocortex in awake rats. *J. Sleep Res.* 22, 239–250. doi: 10.1111/jsr.12009

Vyazovskiy, V. V., Olcese, U., Lazimy, Y. M., Faraguna, U., Esser, S. K., Williams, J. C., et al. (2009). Cortical firing and sleep homeostasis. *Neuron* 63, 865–878. doi: 10.1016/j.neuron.2009.08.024

Vyazovskiy, V. V., and Tobler, I. (2005). Theta activity in the waking EEG is a marker of sleep propensity in the rat. *Brain Res.* 1050, 64–71. doi: 10.1016/j.brainres.2005.05.022

Vyazovskiy, V. V., and Tobler, I. (2008). Handedness leads to interhemispheric EEG asymmetry during sleep in the rat. *J. Neurophysiol.* 99, 969–975. doi: 10.1152/jn.01154.2007

Yoshida, K., Mccormack, S., Espana, R. A., Crocker, A., and Scammell, T. E. (2006). Afferents to the orexin neurons of the rat brain. *J. Comp. Neurol.* 494, 845–861. doi: 10.1002/cne.20859

Zhu, Y., Xi, Y., Fei, N., Liu, Y., Zhang, X., Liu, L., et al. (2018). Dynamics of cerebral responses to sustained attention performance during one night of sleep deprivation. *J. Sleep Res.* 27, 184–196. doi: 10.1111/jsr.12582

Conflict of Interest: The authors declare that the research was conducted in the absence of any commercial or financial relationships that could be construed as a potential conflict of interest.

Copyright © 2019 D'Ambrosio, Castelnovo, Guglielmi, Nobili, Sarasso and Garbarino. This is an open-access article distributed under the terms of the Creative Commons Attribution License (CC BY). The use, distribution or reproduction in other forums is permitted, provided the original author(s) and the copyright owner(s) are credited and that the original publication in this journal is cited, in accordance with accepted academic practice. No use, distribution or reproduction is permitted which does not comply with these terms.

frontiers in Neuroscience

ORIGINAL RESEARCH
published: 29 October 2019
doi: 10.3389/fnins.2019.01161

Surveillance During REM Sleep for the First-Night Effect

*Masako Tamaki and Yuka Sasaki**

Department of Cognitive, Linguistic, and Psychological Sciences, Brown University, Providence, RI, United States

We experience disturbed sleep in a new place, and this effect is known as the first-night effect (FNE) in sleep research. We previously demonstrated that the FNE is associated with a surveillance system in one brain hemisphere during NREM sleep, which manifests as interhemispheric asymmetry in sleep depth in the default-mode network (DMN) and increased vigilance toward monitoring external stimuli. This surveillance system may be useful for protecting vulnerable sleepers from abnormal events in unfamiliar environments. The present study investigated whether a similar surveillance system is exhibited during rapid eye movement (REM) sleep. The impacts of the FNE could be different between the phasic period, in which eyes move rapidly, and the tonic period, in which eye movement ceases, of REM sleep; without the FNE, vigilance to external stimuli is generally reduced during the phasic period but not the tonic period. Thus, REM sleep was split into phasic and tonic periods. First, we replicated previous findings showing interhemispheric asymmetry in delta activity in the DMN associated with the FNE during NREM sleep. However, during REM sleep, interhemispheric asymmetry in delta activity or theta activities, two oscillatory activities during REM sleep, was not found during the phasic or tonic periods. Next, we tested whether vigilance, as measured by evoked brain responses (P2) to deviant tones, associated with the FNE was increased in one hemisphere during REM sleep. The P2 amplitudes during the phasic period were augmented by the FNE on day 1 and were significantly larger than those on day 2 when the FNE was not present. In contrast, the P2 amplitudes during the tonic period were not different across days. The P2 amplitudes showed no interhemispheric asymmetry during the phasic or tonic periods. These results suggest that while the surveillance system exhibits interhemispheric asymmetry in sleep depth and vigilance during NREM sleep, this system shows no interhemispheric asymmetry in oscillatory activities and exhibits increased vigilance in both hemispheres only during the phasic period of REM sleep. Therefore, the surveillance system associated with the FNE may involve different mechanisms during NREM and REM sleep.

Keywords: first-night effect, REM sleep, evoked brain response, theta activity, delta activity, default-mode network

OPEN ACCESS

Edited by:
Francesca Siclari,
Lausanne University Hospital (CHUV), Switzerland

Reviewed by:
Luigi De Gennaro,
Sapienza University of Rome, Italy
Thomas Andrillon,
Monash University, Australia
Brady A. Riedner,
University of Wisconsin–Madison, United States

***Correspondence:**
Yuka Sasaki
yuka_sasaki@brown.edu

Specialty section:
This article was submitted to Sleep and Circadian Rhythms, a section of the journal Frontiers in Neuroscience

Received: *12 June 2019*
Accepted: *14 October 2019*
Published: *29 October 2019*

Citation:
Tamaki M and Sasaki Y (2019) Surveillance During REM Sleep for the First-Night Effect. Front. Neurosci. 13:1161. doi: 10.3389/fnins.2019.01161

INTRODUCTION

Sleep is crucial for the maintenance of daily life (Stickgold, 2005; Imeri and Opp, 2009). The psychological and behavioral consequences of a decline in sleep quality may be severe (Carskadon and Dement, 1981; Drummond et al., 2000; Buysse et al., 2011; Okawa, 2011; Czeisler, 2013). However, sleep quality may be decreased as a protective mechanism under specific circumstances,

for example, sleeping deeply in only one brain hemisphere when an environment is not safe for the animal to sleep deeply in both hemispheres (Rattenborg et al., 1999; Peever and Fuller, 2017). One form of this mechanism is the first-night effect (FNE), which is widely known in human sleep research (Agnew et al., 1966; Carskadon and Dement, 1979; Tamaki et al., 2005a,b, 2014, 2016). The FNE is a temporary sleep disturbance that occurs specifically in the first session of sleep experiments in young healthy adults, and it manifests in prolonged sleep-onset latency, frequent arousal, and decreased deep non-rapid eye movement (NREM) sleep (Roth et al., 2005). Our previous study demonstrated that the FNE was not merely a sleep disturbance but a manifestation of a surveillance system in one hemisphere that remains less asleep and more vigilant than the other hemisphere (Tamaki et al., 2016). This surveillance system in one vigilant brain hemisphere may be useful for monitoring unfamiliar surroundings to protect sleepers in their most vulnerable state and to detect deviant events (Tamaki et al., 2016). We found that slow-wave activity or delta activity, which is an index of sleep depth, decreases in the left hemisphere compared to the right hemisphere regionally in the default-mode network (DMN) during NREM stage 3 sleep (stage N3 or slow-wave sleep) as part of the FNE on day 1, and this decrease causes interhemispheric asymmetry in slow-wave activity. The amplitude of an evoked brain response during stage N3 correlates with vigilance, and the amplitude was increased in one hemisphere on day 1, which caused interhemispheric asymmetry in vigilance. These interhemispheric asymmetries in local sleep depth and vigilance in monitoring the external world function as a surveillance system to counteract vulnerability during deep NREM sleep (Tamaki et al., 2016).

In contrast to NREM sleep, whether the FNE influences brain activities during rapid eye movement (REM) sleep and its possible mechanisms are less well-understood. Approximately 30 studies investigated the FNE during REM sleep in healthy young adults. The characteristics of the FNE during REM sleep include decreased time spent in REM sleep (Rechtschaffen and Verdone, 1964; Kales et al., 1967b; Sforza et al., 2008), delayed onset of REM sleep (Agnew et al., 1966; Kales et al., 1967b), and increased microarousals during REM sleep (Sforza et al., 2008). To the best of our knowledge, only two papers (Toussaint et al., 1997; Curcio et al., 2004) have investigated brain activities quantitatively during REM sleep. However, the results from these studies are contradictory. One study showed that the FNE decreased electroencephalography (EEG) power in a wide range of frequency bands, including delta (0.5–3.5 Hz), theta (4–7.5 Hz), and beta (13–21.5 Hz) bands (Toussaint et al., 1997). The other study reported that the FNE increased theta power (5 Hz) (Curcio et al., 2004). No study has investigated brain activities separately for each hemisphere or whether the FNE altered vigilance during REM sleep. Therefore, whether the FNE alters sleep depth and vigilance levels during REM sleep, acting as a surveillance system in an analogous manner to asymmetries in NREM sleep, is not known.

Notably, it is suggested that the ability to process external stimuli differs depending on whether REMs appear (phasic period) or not (tonic period) during REM sleep (Price and Kremen, 1980; Sallinen et al., 1996; Takahara et al., 2002, 2006b; Wehrle et al., 2007). First, the amplitudes of evoked brain responses differ significantly between the phasic and tonic periods; that is, much smaller brain responses are observed during the phasic period than during the tonic period (Sallinen et al., 1996; Takahara et al., 2002, 2006b). The amplitudes of evoked potentials correlate with the degree of vigilance (Nielsen-Bohlman et al., 1991; Michida et al., 2005). Thus, finding smaller potentials during the phasic period suggests that the degree of vigilance to external stimuli is significantly lower when the eyes are moving rapidly during the phasic period compared to tonic periods during REM sleep without the FNE (Michida et al., 2005). Second, one study investigated blood-oxygen-level dependency (BOLD) responses to acoustic stimulations (Wehrle et al., 2007) and reported that acoustic stimulations during the tonic period induced BOLD activations in the auditory cortex to some degree. In contrast, BOLD activations in the auditory cortex during the phasic period were only minimal. Thus, the ability to process external stimuli may be reduced significantly during the phasic period but sustained to some extent during the tonic period. These reports suggest that it is important to split REM sleep into phasic and tonic periods for the examination of evoked brain responses.

The present study investigated whether the FNE affected oscillatory activity and vigilance during REM sleep and whether decreased oscillatory activity or enhanced vigilance, if any, shows interhemispheric asymmetry in an analogous manner to that seen during NREM sleep. Theta activity was investigated because it is one of the major spontaneous brain oscillations during REM sleep (Takahara et al., 2006a). We also investigated delta activity during REM sleep because previous studies have shown that delta activity also occurs during REM sleep (Simor et al., 2016; Bernardi et al., 2019). We targeted the DMN for the analysis of theta and delta activities during REM sleep because a previous study (Tamaki et al., 2016) suggested that the DMN may be involved in the surveillance system. The study suggested that brain activities may need to be source-localized using individual anatomical brain information for the detection of asymmetry in delta activity. Moreover, interhemispheric asymmetry in delta activity is difficult to identify on the sensor space, at least in the case of NREM sleep (Tamaki et al., 2016). Therefore, we tested whether the FNE involved interhemispheric asymmetry in oscillatory activity in the DMN during REM sleep using a source-localization technique that combines EEG, structural MRI, and polysomnography (PSG) in the sleeping brain. To test whether the FNE altered vigilance, we measured evoked brain responses to external stimuli using an oddball paradigm during tonic and phasic periods. An evoked brain potential during REM sleep, the latency of which is approximately 200 ms (hereafter, P2), is elicited to deviant tones during REM sleep (Bastuji et al., 1995; Sallinen et al., 1996; Takahara et al., 2002, 2006b). Previous studies have found that the amplitude of P2 reflects the degree of vigilance during REM sleep (Takahara et al., 2006b). Thus, we used the P2 amplitude to test whether vigilance was enhanced in one hemisphere in the FNE during REM sleep analogous to that seen during NREM sleep. We also tested whether the

impact of the FNE on brain responses differed between the phasic and tonic periods because the FNE may differentially influence these periods.

MATERIALS AND METHODS

Participants

Twenty-four subjects participated in the present study. Twelve subjects participated in Experiment 1 (nine females; 23.3 ± 0.99 years old, mean ± SEM), and the other 12 subjects participated in Experiment 2 (six females; 24.8 ± 0.67 years old, mean ± SEM). An experimenter thoroughly described the purpose and procedures of the experiment to the candidate subjects, and they were asked to complete questionnaires about their sleep-wake habits for screening, including usual sleep and wake times, regularity of their sleep-wake habits and lifestyle, nap-taking habits, and information on their physical and psychiatric health, including sleep complaints. The exclusion criteria included having physical or psychiatric disease, currently receiving medical treatment, having a suspected sleep disorder, and having a habit of consuming alcoholic beverages before sleep or smoking. Eligible people had regular sleep-wake cycles, i.e., the difference between average bedtimes and sleep durations on weekdays and weekends was less than 2 h, and the average sleep duration regularly ranged from 6 to 9 h. All subjects gave written informed consent for their participation in the experiments. Data collection was performed at Brown University. The institutional review board approved the research protocol.

Four subjects' data from day 1 and another 2 subjects' data from day 2 were excluded from Experiment 2, resulting in complete data sets from 8 participants on day 1 and 10 participants on day 2. The data omitted from day 1 and day 2 were from different subjects. Therefore, there were 6 subjects whose data were available for both day 1 and day 2 in Experiment 2. Data were omitted because of a lack of REM sleep ($n = 5$) or because the measured brain responses were too noisy ($n = 1$).

Experimental Design

Subjects in Experiments 1 and 2 were instructed to maintain their regular sleep-wake schedule, i.e., their daily wake/sleep time and sleep duration, until the study was over. The sleep-wake schedule of the subjects were monitored using a sleep log for 3 days prior to the experiment. Subjects were instructed to refrain from alcohol consumption, unusual excessive physical exercise, and naps on the day before the sleep session. Caffeine consumption was not allowed on the day of the experiments.

Both Experiments 1 and 2 were conducted with a nap design in accordance with a previous study (Tamaki et al., 2016), which found interhemispheric asymmetry in delta activity during NREM sleep with increased vigilance in one hemisphere in association with the FNE during the first nap session. To fairly compare NREM sleep and REM sleep, we used a daytime nap design in the current study. The impact of the FNE does not seem to be significantly different between daytime nap and night sleep (Tamaki et al., 2016).

Experiment 1

We tested whether there was hemispheric asymmetry in delta or theta activity in the DMN during REM sleep with the FNE. In addition, we tested whether interhemispheric asymmetry in delta activity in the DMN could be replicated during NREM sleep. All the subjects took a nap for the first time in the sleep laboratory. Subjects came to the experimental room at approximately 1 pm for PSG preparations. Room lights were turned off at approximately 2 pm, and the 90-min sleep session began. The time for the sleep session was chosen due to the known "mid-afternoon dip," which would facilitate the onset of sleep, even in subjects who do not customarily nap (Horikawa et al., 2013). Structural MRI was measured on another day after the sleep session (see section "Anatomical MRI Acquisition and Region of Interest"). Approximately 1 week later, the same subjects came to the experiment room again and participated in a learning experiment. After the learning experiment, at approximately 1 pm, PSG was prepared, and the subjects were asked to go to sleep at approximately 2 pm for 90 min. These sleep sessions were performed approximately 1 week apart so that any effects of napping during the first sleep session would not carry over into the second sleep session. We only used the sleep-onset latency from the PSG data from the second sleep session to confirm the FNE on day 1. Other data, including oscillatory activities and the sleep structure during the second sleep session, were not analyzed for the current study, as the learning experiment prior to the sleep session was likely to modulate the results.

Experiment 2

We measured the evoked brain responses in each hemisphere during REM sleep using an oddball paradigm. We tested whether the evoked brain responses to deviant tones were larger on day 1 than on day 2. Subjects participated in two experimental sleep sessions (day 1 and day 2). These sessions were performed approximately 1 week apart so that any effects of napping during the first sleep session would not carry over into the second sleep session.

Subjects came to the experimental room at approximately 1 pm on both days, and electrodes were attached for PSG measurements (see section "PSG Measurement"). Subjects were taken to a sleep chamber after the electrodes were attached. Subjects were informed that faint beeping sounds may be presented through earphones while they slept, but they were instructed to ignore these sounds. Room lights were turned off at approximately 2 pm, and the 90-min sleep session began, as in Experiment 1. PSG was monitored, and experienced experimenters scored sleep stages in real time during the sleep session. Sound presentations (see "Auditory Stimuli") began after at least 5 min of uninterrupted NREM stage 2 sleep. Sounds were presented during NREM and REM sleep, but sound presentations were stopped every time a lighter stage of sleep (stage W or NREM stage 1 sleep) or a period of arousal were observed. This procedure was repeated throughout the sleep session. See **Supplementary Figure 1** for the total number of sound presentations for the tonic and phasic periods for all the subjects on days 1 and 2 (see section "Classification of Phasic and Tonic Periods").

PSG Measurement

Polysomnography was recorded in a soundproof and shielded room. PSG consisted of EEG, electrooculogram (EOG), electromyogram (EMG), and electrocardiogram (ECG) measurements. EEG was recorded at 64 scalp sites, according to the 10% electrode position (Sharbrough et al., 1991), using active electrodes (actiCap, Brain Products, LLC) with a standard amplifier (BrainAmp Standard, Brain Products, LLC). The online reference was Fz, which was re-referenced to the average of the left and right mastoids offline after recording. The sampling frequency was 500 Hz. The impedance was kept below 20 kΩ because the active electrodes included a new type of integrated impedance converter that allowed the EEG signal to be transmitted with significantly lower levels of noise than traditional passive electrode systems. The data quality obtained using the active electrodes was as good as the 5 kΩ quality obtained using passive electrodes, which were used for EOG and EMG recordings (BrainAmp ExG, Brain Products, LLC). The horizontal EOG was recorded from two electrodes placed at the outer canthi of each eye. The vertical EOG was measured from two electrodes 3 cm above and below each eye. EMG was recorded from the mentum (chin). ECG was recorded from two electrodes placed at the right clavicle and the left rib bone. The impedance was kept below 10 kΩ for the passive electrodes. Brain Vision Recorder software (Brain Products, LLC) was used for recording. The data were filtered between 0.1 and 40 Hz.

Sleep-Stage Scoring and Sleep Parameters

Sleep stages were scored for every 30-s epoch, following standard criteria (Rechtschaffen and Kales, 1968; Iber et al., 2007), into the stages of wakefulness (stage W), NREM stage 1 sleep (stage N1), NREM stage 2 sleep (stage N2), NREM stage 3 sleep (stage N3), and REM sleep. The following variables were calculated for each subject to assess basic sleep structure (**Table 1**): the duration (min) and percentage (%) of time in each sleep stage, latency to REM sleep (min), sleep onset latency (SOL, min), wake time after sleep onset (WASO, min), sleep efficiency (SE,%), and time in bed (TIB, min).

TABLE 1 | Sleep parameters.

	Experiment 1	Experiment 2	
	Day 1 (Mean ± SEM)	Day 1 (Mean ± SEM)	Day 2 (Mean ± SEM)
Stage W (min)	10.6 ± 1.91	10.8 ± 1.83	5.0 ± 0.85
Stage N1 (min)	5.8 ± 1.78	8.9 ± 2.02	4.9 ± 1.07
Stage N2 (min)	36.6 ± 3.98	34.5 ± 2.42	30.3 ± 3.15
Stage N3 (min)	12.7 ± 3.57	12.6 ± 2.12	19.5 ± 2.88
REM sleep (min)	14.8 ± 2.20	9.3 ± 1.83	15.4 ± 2.87
Stage W (%)	12.5 ± 2.19	12.9 ± 1.96	7.0 ± 1.37
Stage N1 (%)	11.6 ± 1.81	15.2 ± 2.32	8.7 ± 1.47
Stage N2 (%)	43.0 ± 4.20	42.5 ± 3.11	39.6 ± 2.96
Stage N3 (%)	15.4 ± 4.43	17.2 ± 3.10	25.4 ± 3.23
REM sleep (%)	17.4 ± 2.43	11.8 ± 2.25	19.5 ± 3.50
REM latency (min)	59.3 ± 7.94	63.4 ± 3.17	62.1 ± 3.82
SOL (min)	11.6 ± 1.53	8.9 ± 1.20	5.2 ± 1.02
WASO (min)	3.8 ± 1.13	5.4 ± 1.49	2.4 ± 0.68
SE (%)	87.5 ± 2.19	87.1 ± 1.96	93.0 ± 1.37
TIB (min)	84.8 ± 2.55	79.6 ± 2.69	80.1 ± 3.59

Sleep parameters were obtained from the first sleep cycle because not all subjects had a second sleep cycle. REM latency, latency to REM sleep onset; SOL, sleep-onset latency; WASO, wake time after sleep onset; SE, sleep efficiency. TIB, time in bed, which indicates the duration of each sleep session (the time interval between lights-off and lights-on).

Anatomical MRI Acquisition and Region of Interest

Anatomical MRI data in Experiment 1 were acquired and used to determine the conductor geometry for the boundary element model (BEM) of the head (Hamalainen and Sarvas, 1989) and to register the EEG sensor locations with the individual subject's anatomy (Dale et al., 1999; Fischl et al., 1999). Subjects were scanned in a 3T MR scanner (Trio, Siemens) using a 32-ch head coil. T1-weighted MR images (MPRAGE; TR = 2.531 s, TE = 3.28 ms, flip angle = 7°, TI = 1100 ms, 256 slices, voxel size = 1.3 mm × 1.3 mm × 1.0 mm) were acquired. The cortical surface was inflated for each subject for brain parcelation to localize individual gyri and sulci (Fischl et al., 2004).

Regions within the DMN were individually anatomically determined *a priori* based on previously published papers using an automated parcelation method (Fischl et al., 2004; Destrieux et al., 2010; Tamaki et al., 2016). We defined the DMN as a circuit that included the medial prefrontal, inferior parietal, and posterior parietal cortices, according to previous research (Mason et al., 2007; Raichle and Snyder, 2007; Tamaki et al., 2016). The medial prefrontal cortex consists of the anterior part of the superior frontal gyrus and the anterior cingulate gyrus and sulcus. The inferior parietal cortex consists of the inferior parietal gyrus and angular gyrus. The posterior parietal cortex consists of the precuneus gyrus, posterior-dorsal cingulate gyrus, and sup-parietal sulcus.

Source Localization of EEG

To compute the strength of brain activities during sleep in the DMN, EEG data were subjected to the Morlet wavelet analysis in Experiment 1 and source localization using the minimum-norm estimate (MNE) of individual MRI information (see section "Anatomical MRI Acquisition and Region of Interest"). The Morlet wavelet analysis was applied to raw EEG data (Lin et al., 2004; Ahveninen et al., 2007; Tamaki et al., 2013) every 3 s to obtain the MNE strength at the peak frequency of 6 Hz (theta activity) and 1–4 Hz (1 Hz bin, delta activity) during REM sleep and every 30 s to obtain the MNE strength at 1–4 Hz (delta activity) during NREM sleep. The window width in the Morlet wavelet analysis was specified as 10 such that the MNE strength at 6 Hz would cover activities from 5 to 7 Hz, which corresponds to the theta band, and the strength at 1–4 Hz should cover activities from 1 to 4 Hz in the delta band. EEG during REM sleep was measured at a better temporal resolution (3 s) than that during NREM sleep because we classified REM sleep into tonic and phasic periods (see section "Classification of Phasic and Tonic

Periods" below). To localize the current sources underlying the EEG signals, the cortically constrained MNE was used on EEGs using individual anatomical MRIs and constrained the current locations to the cortical mantle (Lin et al., 2004; Ahveninen et al., 2007). Information from the EEG sensor locations and structural MRI segmentation were used to compute the forward solutions for all source locations using a three-layer model of the boundary element method (BEM) (Hamalainen and Sarvas, 1989). The individual forward solutions constituted the rows of the gain (lead-field) matrix. The noise covariance matrix was computed from raw EEG data for 30 s during wakefulness. These two matrices were used to calculate the inverse operator to yield the estimated source activity during sleep, as a function of time, on a cortical surface (Lin et al., 2004; Ahveninen et al., 2007). The theta and delta-band activities were then averaged for tonic and phasic periods during REM sleep (see section "Classification of Phasic and Tonic Periods" below).

Classification of Phasic and Tonic Periods

To classify EEG recordings during REM sleep into the phasic and tonic periods, we first detected eye movements during REM sleep automatically. First, a bandpass filter (0.5–8 Hz) was applied to the vertical and horizontal EOG electrodes during REM sleep. We then measured the amplitudes of eye movements. If the amplitude was 20 μV or higher, then it was counted as 1 movement. Eye movements that occurred within a brief time window (within 100 ms) were counted as only 1 movement. Based on the eye movements, the recordings during REM sleep were classified into a phasic or tonic period every 3 s according to previous studies (Takahara et al., 2002, 2006b). If at least one eye movement was detected within a 3-s epoch, the period was classified as a phasic period, and if no eye movements were detected within a 3-s epoch, the period was classified as a tonic period. We measured the percentage of phasic periods in REM sleep (**Supplementary Table 1**). We also measured the REM density by measuring the number of REMs divided by (1) the total duration of REM sleep (min) and (2) the duration of the phasic periods (min) that occurred during REM sleep. We compared these two types of REM density measures on day 1 in Experiments 1 vs. 2.

Auditory Stimuli

Auditory stimuli were controlled using MATLAB (The MathWorks, Inc.) software and were presented through earphones (HAFR6A, JVC Americas, Corp.). The stimuli consisted of 2000-Hz deviant (presented at 10% probability) and 1000-Hz standard (presented at 90% probability) pure tones, all of which were 50 ms in duration (10 ms rise/fall). These sounds were presented monaurally every 1 s (1 trial = 1000 ms, fixed ISI = 950 ms). The probabilities of the sound type (deviant or standard) and the presented ear (left or right) were pseudorandomized every 30 s, which corresponded to the sleep-stage scoring epoch (see section "Sleep-Stage Scoring and Sleep Parameters"). More concretely, 30 sounds were presented in total, 15 per ear, in a given 30-s epoch. The probability of a deviant sound occurring was 10%, and at least one deviant sound was presented to each ear.

The sound intensity was approximately 35 dB (Extech 407740, Digital Sound Level Meter, Extech Instruments, Corp.), which was lower than that presented in previous studies that also used an oddball paradigm during REM sleep (50–100 dB) (Sallinen et al., 1996; Cote and Campbell, 1999a; Cote et al., 1999, 2001; Takahara et al., 2002, 2006b) to prevent subjects from waking. It was confirmed that 35 dB was sufficiently quiet to maintain sleep in each subject before the sleep session began.

Analysis of Brain Responses to Auditory Stimuli

We examined the evoked brain potential known as P2 (Takahara et al., 2002, 2006b) from EEG data recorded during REM sleep using the oddball paradigm in Experiment 2. P2 is a positive brain potential that appears during REM sleep, and its amplitude increases to rare and salient stimuli (Takahara et al., 2002, 2006b). Therefore, P2 responses are used as an index of vigilance during REM sleep in humans (Takahara et al., 2006b).

To obtain the P2 amplitudes, first, six channels (three channels per hemisphere) from the central site (left: C1, C3, and C5; right: C2, C4, and C6) were analyzed. This site was chosen because it had the largest amplitudes in the previous study (Takahara et al., 2006b). Second, we also measured the P2 amplitudes from fronto-central electrodes (left: FC1, FC3, and FC5; right: FC2, FC4, and FC6) because this site also showed higher amplitudes in the topographic maps (see **Figure 3**). All data were examined visually for each trial, and any trials that included arousal (Bonnet et al., 1992; Iber et al., 2007) or motion artifacts were excluded from further analyses.

Analyses of brain responses followed a previous study (Tamaki et al., 2016). The EEG amplitudes during the 200-ms prestimulus period (−200 to 0 ms) were averaged. The mean EEG amplitude from the prestimulus period was subtracted from the EEG amplitudes from the 0- to 1000-ms post-stimulus period to apply baseline correction to the signal amplitude for each of the 1-s trials (0 to 1000-ms post-stimulus). These values were averaged for each sound type (deviant and standard), hemisphere (left and right), day (day 1 and day 2), and period (tonic and phasic) during REM sleep to compute averaged brain responses. The maximum value (peak) of the 150–250 ms post-stimulus time window from the brain responses was used as the P2 amplitude. We chose this time window because it roughly corresponded to the P2 window defined in previous studies (Bastuji et al., 1995; Perrin et al., 1999; Crowley and Colrain, 2004; Takahara et al., 2006b). Averaged values were obtained for each of the phasic and tonic periods (see section "Classification of Phasic and Tonic Periods"). For visualization purposes (**Figure 2** and **Supplementary Figure 2**), a moving average with a 50-ms window (2 ms step size) was applied to amplitude values to smooth the waveforms. The area under the curve (**Figure 5** and **Supplementary Figure 7**) was measured by summing all the positive values in a 150–250 ms window for the deviant trials for each hemisphere, period, and day.

Topographic maps (**Figure 3** and **Supplementary Figures 3, 4**) were made for the P2 amplitudes across electrode locations.

For each electrode, the peak in the 150–250 ms post-stimulus time window was averaged across subjects. To control for interindividual differences in amplitudes across electrode locations, the values were z-transformed for each subject across all the electrode locations. Z-transformation was applied only for the data used to make the topographic maps.

Statistical Analyses

An α level (type-I error rate) of 0.05 was set for all statistical analyses. In Experiment 1, a two-tailed paired *t*-test was performed for analyses of delta activity during stage N3 sleep in the left vs. right hemispheres. Three-way repeated measures ANOVA on the measured delta and theta strengths during REM sleep (factors: frequency, period, hemisphere) was performed. In Experiment 2, a paired *t*-test was performed on sleep parameters. Three-way repeated measures ANOVA was used on each of the P2 amplitudes and the area under the curve. For *post hoc* analysis, two-tailed *t*-tests were used with Bonferroni correction as a multiple comparisons test. When the Bonferroni correction was used, the p values shown were adjusted values multiplied by the number of comparisons. When a *t*-test indicated a statistically significant difference, the effect size was calculated using Cohen's *d* (Cohen, 1988), which indicates the magnitude of the difference between the two groups. This result is interpreted as having a large effect size when Cohen's $d \geq 0.8$ and as having a medium effect size when $d \geq 0.5$.

RESULTS

Confirmation of the FNE

In Experiment 1, we compared the sleep-onset latency between day 1 and day 2. We found that the sleep-onset latency, which is a critical measure of the FNE (Schmidt and Kaelbling, 1971; Webb and Campbell, 1979; Tamaki et al., 2005a), was significantly longer on day 1 (11.6 ± 1.53 min) than on day 2 (7.3 ± 1.56 min) [paired *t*-test, $t(11) = 2.42$, $p = 0.034$, Cohen's $d = 0.70$], confirming the FNE in Experiment 1. In addition, we found an interhemispheric asymmetry in delta activity during NREM sleep, a signature of the FNE, in Experiment 1 (see below, **Figure 1A**).

To confirm that the FNE occurred in Experiment 2, we compared sleep-onset latency between day 1 and day 2. We found that the sleep-onset latency was significantly longer on day 1 than day 2 [paired *t*-test, $t(11) = 5.01$, $p < 0.001$, Cohen's $d = 1.47$]. Thus, we confirmed that the FNE had occurred in Experiment 2 (**Table 1**).

Additionally, in Experiment 2, the WASO was significantly larger [paired *t*-test, $t(11) = 2.74$, $p = 0.019$, Cohen's $d = 0.79$, uncorrected for multiple comparisons], and the percentage of time spent in stage N3 sleep was significantly lower [paired *t*-test, $t(11) = 2.20$, $p = 0.049$, Cohen's $d = 0.64$, uncorrected for multiple comparisons] on day 1 than day 2. These results indicate that it took longer to fall asleep on day 1 than on day 2, sleep was more fragmented, and deep sleep was reduced, in accordance with previous studies (Kales et al., 1967a; Scharf et al., 1975; Webb and Campbell, 1979; Tamaki et al., 2016). However, there was no significant difference in the duration of [paired *t*-test, $t(11) = 1.15$, $p = 0.151$] or latency to [paired *t*-test, $t(17) = 0.27$, $p = 0.794$] REM sleep. Although we did not compare between days in Experiment 1 statistically, the sleep parameters on day 1 in Experiment 1 were similar to those on day 1 in Experiment 2 (e.g., sleep-onset latency, stage N3%). See **Table 1** for the results of all the sleep parameters for Experiments 1 and 2.

Experiment 1

Source-Localized Delta and Theta Activity

Experiment 1 examined whether there was interhemispheric asymmetry in delta or theta activity in the DMN during REM sleep in association with the FNE. This experiment also examined whether interhemispheric asymmetry in delta activity was present during stage N3 of NREM sleep, as in the previous study (Tamaki et al., 2016). We measured delta (1–4 Hz) and theta activity (∼5–7 Hz) originating in the DMN in each hemisphere during REM sleep and measured delta activity (1–4 Hz) during stage N3 sleep (see section "Source Localization of EEG").

First, we performed a two-tailed paired *t*-test on the measured delta strength during stage N3 between the left and right hemispheres. Because one subject did not show stage N3 sleep, the analysis of delta strength included data from only 11 subjects. We confirmed that interhemispheric asymmetry was present in delta activity in the DMN during stage N3 of NREM sleep [$t(10) = 2.34$, $p = 0.042$, Cohen's $d = 0.70$]. Delta activity was significantly lower in the left than the right hemisphere (**Figure 1A**). This result replicates previous findings (Tamaki et al., 2016).

Second, we performed three-way repeated measures ANOVA on the delta and theta strengths during REM sleep (factors: Frequency, Period, Hemisphere, see **Figures 1B,C**). The ANOVA results indicated that the main effects of Period [$F(1,11) = 20.22$, $p = 0.001$] and Frequency [$F(1,11) = 63.14$, $p < 0.001$] were significant. Other factors or interactions between factors were not significant [a main effect of Hemisphere: $F(1,11) = 2.61$, $p = 0.134$; Frequency × Period: $F(1,11) = 0.78$, $p = 0.396$; Frequency × Hemisphere: $F(1,11) = 1.07$, $p = 0.324$; Period × Hemisphere: $F(1,11) = 1.44$, $p = 0.256$; Frequency × Period × Hemisphere: $F(1,11) = 0.142$, $p = 0.713$; **Figures 1B,C**]. These results demonstrate that delta and theta activity during REM sleep did not show interhemispheric asymmetry, while delta activity during stage N3 NREM sleep replicated previous findings showing interhemispheric asymmetry.

Experiment 2

Evoked Brain Responses

We measured the P2 amplitude, which is one of the primary evoked components seen during REM sleep (Takahara et al., 2002, 2006b). The amplitude of P2 may differ based on the eye movement state. Thus, we analyzed brain responses during the tonic (no REMs) and phasic (1 or more REMs) periods of REM sleep (see section "Classification of Phasic and Tonic Periods" and **Supplementary Table 1** for the percentage of time spent in the phasic period). To test whether the brain was more vigilant in

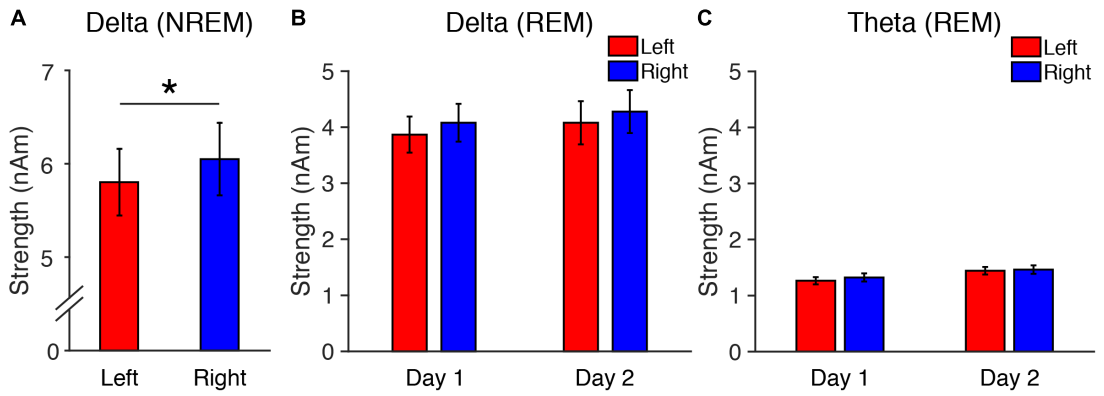

FIGURE 1 | Source-localized oscillatory activity in the DMN in Experiment 1. **(A)** Delta strength during NREM sleep on Day 1, and delta **(B)** and theta **(C)** strength during REM sleep. $N = 12$. $^*p < 0.05$.

one hemisphere during REM sleep with the FNE and whether the level of vigilance differed based on the eye movement state, we measured the mean amplitudes of P2 for each hemisphere (left vs. right), period (phasic vs. tonic), and sound type (deviant vs. standard) (see section "Analysis of Brain Responses to Auditory Stimuli" for measurement of amplitude). Statistical tests were performed using six subjects whose data were available for both day 1 and day 2 for within-subjects comparisons. However, the figures are shown in the following two ways: (1) data using the six subjects and (2) using all the available data treated independently in **Supplementary Figures** ($n = 8$ for day 1, and $n = 10$ for day 2).

The sleep session on day 2 was treated as a normal sleep without the FNE. On day 2, a clear P2 was elicited to deviant tones during the tonic period (**Figure 2C** and **Supplementary Figure 2C**), and no visible P2 was elicited during the phasic period (**Figure 2D** and **Supplementary Figure 2D**) in the ground-averaged brain responses and topographic maps (**Figures 3C,D** and **Supplementary Figures 3C,D**). However, on day 1, with the FNE, a large P2 was elicited to deviant tones during both tonic and phasic periods [**Figures 2A,B** and **Supplementary Figures 2A,B** in the ground-averaged brain responses, and **Figures 3A,B** and **Supplementary Figures 3A,B** for the topographic maps, **Supplementary Figure 4** for the topographic maps that indicate day difference (day 1 minus day 2)].

We next tested whether the FNE impacts P2 amplitudes. For the statistical tests below, we used six subjects' data, as their data were available for both days 1 and 2. We first examined the P2 amplitudes measured from the central electrodes. Three-way repeated measures ANOVA was conducted with the within-subjects factors of Period (tonic, phasic), Hemisphere (left, right), and Day (day 1 vs. day 2). If there was interhemispheric asymmetry in the P2 amplitudes associated with the FNE, then a significant Day × Hemisphere interaction should be present. If the amplitudes in a period were different between days, then a significant Day × Period interaction should be present. The statistical results showed that the Day × Hemisphere interaction was not significant [**Figure 4A**, $F(1,5) < 0.01$, $p = 0.99$]. However, there was a significant Period × Day interaction [**Figure 4B**, $F(1,5) = 7.43$, $p = 0.042$]. None of the main factors or other interactions [Hemisphere: $F(1,5) = 0.62$, $p = 0.466$; Period: $F(1,5) = 1.06$, $p = 0.350$; Day: $F(1,5) = 3.70$, $p = 0.112$; Hemisphere × Period: $F(1,5) = 0.64$, $p = 0.462$; Day × Hemisphere × Period: $F(1,5) = 0.88$, $p = 0.390$] were significant.

Because the Period × Day interaction was significant, we performed *post hoc* analyses to investigate the source of this interaction. Because no significant effect of Hemisphere was found in the above ANOVA, data from the left and the right hemispheres were pooled for subsequent analyses. *Post hoc* *t*-tests indicated a significant difference in the P2 amplitude between day 1 and day 2 in the phasic period [orange bars in **Figure 4B**; paired *t*-test, $t(11) = 4.05$, $p = 0.008$, Cohen's $d = 1.17$; Bonferroni correction for four comparisons] and between the phasic and tonic periods on day 2 [**Figure 4B**; paired *t*-test, $t(11) = 3.12$, $p = 0.039$, Cohen's $d = 0.90$, Bonferroni correction for four comparisons]. There was no significant difference between days in the tonic period [blue bars, **Figure 4B**; paired *t*-test, $t(11) = 0.27$, $p = 1.00$, Bonferroni correction for the four comparisons] or between the tonic and phasic periods on day 1 [**Figure 4B**; paired *t*-test, $t(11) = 0.27$, $p = 1.00$; Bonferroni correction for four comparisons]. We performed one-sample *t*-tests on the P2 amplitudes for each of the periods and days to investigate whether P2 was elicited, i.e., whether P2 amplitude was significantly different from zero (**Figure 4B**). The P2 amplitude was significantly different from 0 during the tonic period on day 1 [$t(11) = 7.70$, $p < 0.001$, Cohen's $d = 2.22$, Bonferroni correction for the following four comparisons] and day 2 [$t(11) = 3.25$, $p = 0.031$, Cohen's $d = 0.94$, Bonferroni correction for four comparisons] and was significantly different from zero during the phasic period on day 1 [$t(11) = 6.43$, $p < 0.001$, Cohen's $d = 1.86$, Bonferroni correction for four comparisons] but not on day 2 [$t(11) = 0.71$, $p = 1.00$, Bonferroni correction for four comparisons]. Thus, the P2 amplitude was larger on day 1 than day 2 during the phasic period. See **Supplementary Figures 5A,B** for the results using all the available data ($n = 8$ on day 1, $n = 10$ on day 2).

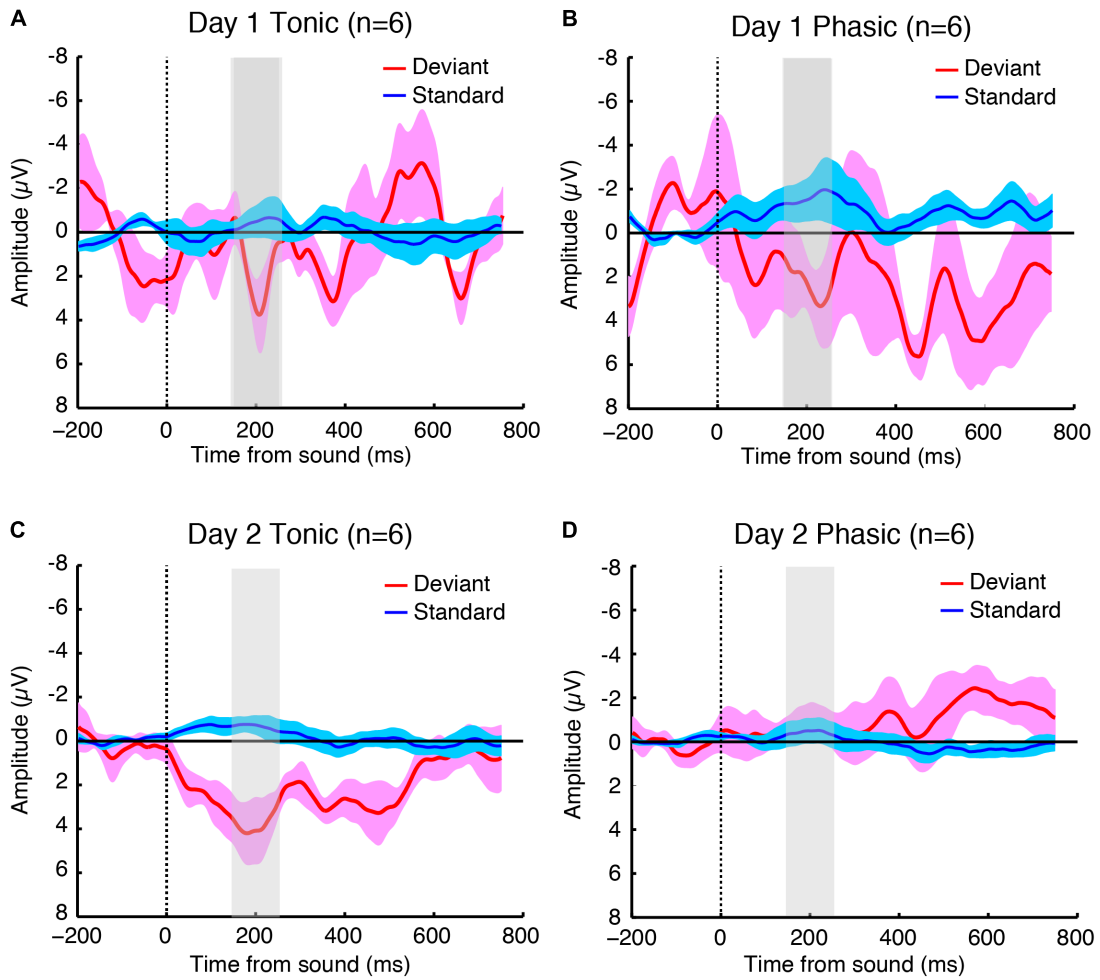

FIGURE 2 | Grand-averaged brain responses of six subjects (averaged across both hemispheres because the statistical tests indicated no significant difference between hemispheres) to deviant (red) and standard (blue) tones time-locked to sound onset during the **(A)** tonic and **(B)** phasic periods on day 1, and the **(C)** tonic and **(D)** phasic periods on day 2 during REM sleep. The shaded part indicates 150–250 ms window where the P2 amplitudes were measured. $N = 6$.

In addition, we next examined the P2 amplitudes measured from the fronto-central electrodes, as the topographic maps suggest that this site shows higher amplitudes of P2. Three-way repeated measures ANOVA was performed on the P2 amplitudes from the fronto-central electrodes with the within-subjects factors of Period (tonic, phasic), Hemisphere (left, right), and Day (day 1 vs. day 2). If the amplitudes in a period were different between days, then a significant Day × Period interaction should be present. There was indeed a significant Period × Day interaction [$F(1,5) = 9.08$, $p = 0.030$]. The Day × Hemisphere interaction was not significant [**Figure 4C**; $F(1,5) = 0.01$, $p = 0.938$]. None of the main factors or other interactions [Hemisphere: $F(1,5) = 0.04$, $p = 0.848$; Period: $F(1,5) = 0.96$, $p = 0.372$; Day: $F(1,5) = 2.22$, $p = 0.848$; Hemisphere × Period: $F(1,5) = 0.35$, $p = 0.580$; Day × Hemisphere × Period: $F(1,5) = 0.42$, $p = 0.548$] were significant.

Because the Period × Day interaction was significant, we performed *post hoc* analyses to investigate the source of this interaction. Because no significant effect of Hemisphere was found in the above ANOVA, data from the left and the right hemispheres were pooled for subsequent analyses. *Post hoc* t-tests indicated a significant difference in the amplitude between day 1 vs. day 2 in the phasic period [**Figure 4D**; paired t-test, $t(11) = 4.60$, $p = 0.003$, Cohen's $d = 1.46$; Bonferroni correction for the following four comparisons] and between the phasic and tonic periods on day 2 [**Figure 4D**; paired t-test, $t(11) = 2.98$, $p = 0.0496$, Cohen's $d = 0.83$, Bonferroni correction for four comparisons]. There was no significant difference between days in the tonic period [**Figure 4D**; paired t-test, $t(11) = 0.64$, $p = 1.00$, Bonferroni correction for the four comparisons] or between the tonic and phasic periods on day 1 [**Figure 4D**; paired t-test, $t(11) = 2.76$, $p = 0.072$; Bonferroni correction for four comparisons]. We performed one-sample t-tests on the amplitudes for each of the periods and days to investigate whether P2 was elicited, i.e., whether P2 amplitude was significantly different from zero (**Figure 4D**). The amplitude was significantly different from 0 during the tonic period on day 1 [$t(11) = 9.11$, $p < 0.001$, Cohen's $d = 2.63$, Bonferroni correction for four

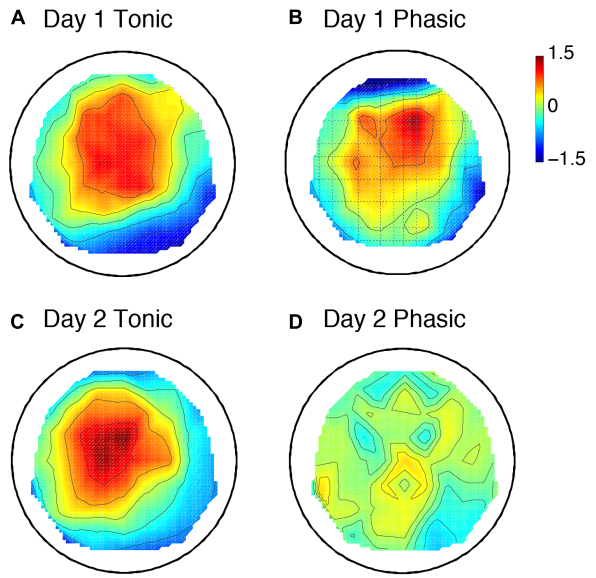

FIGURE 3 | Topographic maps including 6 subjects' data for the P2 amplitude. Day 1 tonic **(A)** and phasic **(B)**, and day 2 tonic **(C)** and phasic **(D)**. $N = 6$. The values are z-transformed (see section "Materials and Methods").

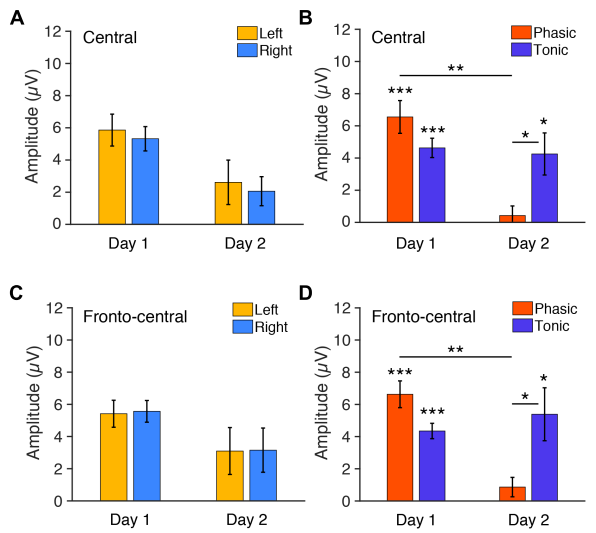

FIGURE 4 | Mean P2 amplitudes to deviant tones during REM sleep measured from **(A,B)** central and **(C,D)** fronto-central electrodes. **(A)** The amplitudes for each hemisphere on days 1 and 2 (phasic and tonic periods averaged). $N = 6$. **(B)** The amplitudes for each phasic and tonic period on days 1 and 2 (hemispheres averaged). $N = 6$. *Post hoc* paired *t*-test, $^{***}p < 0.001$, $^{**}p < 0.01$, $^{*}p < 0.05$ (Bonferroni correction). **(C)** The amplitudes for each hemisphere on days 1 and 2 (phasic and tonic periods averaged). $N = 6$. **(D)** The amplitudes for each phasic and tonic period on days 1 and 2 (hemispheres averaged). $N = 6$. *Post hoc* paired *t*-test, $^{***}p < 0.001$, $^{**}p < 0.01$, $^{*}p < 0.05$ (Bonferroni correction).

comparisons] and day 2 [$t(11) = 3.27$, $p = 0.030$, Cohen's $d = 0.94$, Bonferroni correction for four comparisons], and was significantly different from zero during the phasic period on day 1 [$t(11) = 7.97$, $p < 0.001$, Cohen's $d = 2.30$, Bonferroni correction for four comparisons], but not on day 2 [$t(11) = 1.43$, $p = 0.722$, Bonferroni correction for four comparisons]. Thus, the P2 amplitude was larger on day 1 than day 2 during the phasic period also in the fronto-central electrodes. See **Supplementary Figures 5C,D** for the results of the fronto-central P2 using all the available data ($n = 8$ on day 1, $n = 10$ on day 2). Together, these results demonstrate that vigilance during REM sleep, especially during the phasic period, was enhanced on day 1 with the FNE, but there was no interhemispheric asymmetry.

We conducted additional analyses to confirm that these P2 results were due to the FNE, but not due to noises. First, we tested whether the increased P2 amplitudes to deviant tones during the phasic period on day 1 were due to noises caused by smaller number of trials for deviant tones compared to those for the standard tones. We used the same number of trials (randomly selected) for the standard tones as for the deviant tones and measured the amplitude of P2 to the standard tones. We did not find any evidence that indicates that the P2 amplitude is elicited by smaller number of trials for standard tones (see **Supplementary Figure 6**). We conducted three-way ANOVA (factors: day, period, hemisphere) on the P2 amplitudes elicited to the standard tones with the smaller number of trials. Neither a significant main effect nor an interaction was found [Period: $F(1,5) = 0.14$, $p = 0.727$; Day: $F(1,5) < 0.01$, $p = 0.986$; Hemisphere: $F(1,5) = 0.21$, $p = 0.668$; Period × Day: $F(1,5) = 0.30$, $p = 0.610$; Period × Hemisphere: $F(1,5) = 1.09$, $p = 0.344$; Day × Hemisphere: $F(1,5) = 4.34$, $p = 0.092$; Period × Hemisphere × Day: $F(1,5) = 0.94$, $p = 0.378$]. Thus, we believe that P2 elicited to deviant tones during sleep is not due to noise induced by using a smaller number of trials. This result is consistent with previous studies showing that ERPs elicited by standard tones in the oddball paradigm are very small during sleep (Takahara et al., 2002; Tamaki et al., 2016) and during wakefulness (Tamaki et al., 2016). It has been shown that ERP amplitude is larger to infrequent events and very small to frequent events (Squires et al., 1975). Second, we investigated whether the significant amplitude increase to deviant tones on day 1 during the phasic period was due to fluctuations in brain responses during the prestimulus period. We measured the averaged amplitude during the prestimulus baseline period for each condition (phasic and tonic periods on day 1 and day2) measured from central electrodes. Then we tested whether the averaged amplitude was significantly different from zero using a one sample *t*-test. The results showed that the prestimulus baseline amplitudes were not significantly different from zero 0 in any of the conditions [one-sample *t*-test, hemisphere averaged, Tonic day 1, $t(5) = 0.15$, $p = 0.890$; Tonic day 2, $t(5) = 0.64$, $p = 0.549$; Phasic day 1, $t(5) = 0.08$, $p = 0.936$; Phasic day 2, $t(5) = 0.41$, $p = 0.700$]. These results indicate that the significant increase of P2 amplitudes on day 1 during the phasic period was not due to smaller number of trials used or the fluctuations in brain response during prestimulus baseline period.

We further measured the area under the curve of ERPs by summing all the positive values within a 150–250 ms window for each hemisphere, period, and day. Three-way repeated measures ANOVA with the within-subjects factors of Period (tonic, phasic),

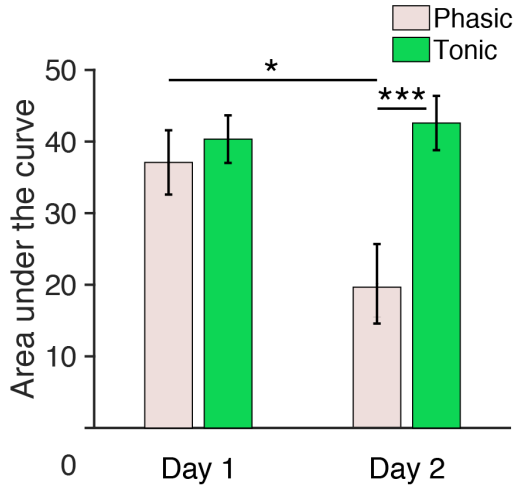

FIGURE 5 | Area under the curve (150–250 ms) during REM sleep measured from central electrodes. The area under the curve for $n = 6$. *Post hoc* paired *t*-test, $^{***}p < 0.001$, $^{*}p < 0.05$ (Bonferroni correction).

Hemisphere (left, right) and Day (day 1, day 2) was performed on the areas under the curve elicited by deviant tones (**Figure 5**). The statistical results were similar to the results for P2 amplitudes described above. There was a significant Period × Day interaction [$F(1,5) = 8.80$, $p = 0.031$]. The main effect of Period was also significant [$F(1,5) = 7.48$, $p = 0.041$]. None of the other main factors or interactions [Hemisphere: $F(1,5) = 0.07$, $p = 0.801$; Day: $F(1,5) = 2.33$, $p = 0.188$; Day × Hemisphere; $F(1,5) = 0.03$, $p = 0.872$; Hemisphere × Period: $F(1,5) = 3.06$, $p = 0.141$; Day × Hemisphere × Period: $F(1,5) = 0.59$, $p = 0.478$] were significant.

Because the Period × Day interaction was significant, we performed *post hoc* analyses to investigate the source of this interaction. Because no significant effect of Hemisphere was found in the above ANOVA, data from the left and the right hemispheres were pooled for subsequent analyses. *Post hoc t*-tests indicated a significant difference in the area under the curve between day 1 and day 2 during the phasic period [pale pink bars, **Figure 5**; paired *t*-test, $t(11) = 3.01$, $p = 0.047$, Cohen's $d = 0.87$; Bonferroni correction for the following four comparisons] and between the phasic and tonic periods on day 2 [paired *t*-test, $t(11) = 4.17$, $p < 0.001$, Cohen's $d = 1.20$; Bonferroni correction for four comparisons]. There was no significant difference in the area under the curve between days in the tonic period [green bars, **Figure 5**, paired *t*-test, $t(11) = 0.90$, $p = 1.00$, Bonferroni correction for four comparisons] or between the tonic and phasic periods on day 1 [paired *t*-test, $t(11) = 1.05$; Bonferroni correction for four comparisons]. See **Supplementary Figure 7** for the area under the curve measured from all the subjects available. Together, these results demonstrate that the area under the curve for P2 during the phasic period was enhanced on day 1 with the FNE without interhemispheric asymmetry.

We next examined whether the FNE alters the latency to the P2 peak (**Table 2**). The latency to the P2 peak was measured for each hemisphere (left vs. right), period (phasic vs. tonic), and day (day 1 vs. day 2). Statistical tests were conducted using six subjects' data (whose data are available for both days 1 and 2) as follows. Three-way repeated measures ANOVA was performed on the P2 latencies, with the within-subjects factors of Period (tonic, phasic), Hemisphere (left, right), and Day (day 1, day 2). None of the main effects or interactions were significant [Hemisphere: $F(1,5) = 0.69$, $p = 0.446$; Period: $F(1,5) = 0.95$, $p = 0.375$; Day: $F(1,5) = 1.15$, $p = 0.333$; Period × Day: $F(1,5) = 0.48$, $p = 0.520$; Day × Hemisphere: $F(1,5) = 0.06$, $p = 0.816$; Hemisphere × Period: $F(1,5) = 2.36$, $p = 0.185$; Day × Hemisphere × Period: $F(1,5) = 0.36$, $p = 0.574$]. See **Supplementary Table 2** for the P2 latency measured from all the available subjects.

REM Density

One may wonder whether sound presentations increased REM density (**Table 3**). We measured REM density in the following two ways: (1) the number of REMs divided by the total REM sleep duration (min) and (2) the number of REMs divided by the total duration of the combined phasic periods during REM sleep (min). Then, we compared REM densities on day 1 in Experiment 1 to those on day 1 in Experiment 2. We conducted an unpaired *t*-test on the REM densities. We did not find a significant difference between experiments [see **Table 3**; all REM sleep, $t(18) = 0.16$, $p = 0.877$; only the phasic period, $t(18) = 1.94$, $p = 0.069$].

DISCUSSION

The present study found that the level of vigilance during REM sleep was higher on day 1 than day 2, specifically during the phasic period. However, interhemispheric asymmetry in evoked

TABLE 2 | P2 latency (Mean ± SEM, ms).

	Tonic				Phasic			
	Day 1		Day 2		Day 1		Day 2	
	Left	Right	Left	Right	Left	Right	Left	Right
Mean	209.8	201.5	210.2	191.8	204.3	227.8	170.2	201.6
SE	10.14	11.79	12.63	11.43	16.74	13.23	7.11	12.00

N = 6. See the main text for statistical results.

TABLE 3 | REM density on Day 1 (Mean ± SE, number per min).

	Experiment 1 (*N* = 12)	Experiment 2 (*N* = 8)
REM density (all REM sleep)	12.1 (2.36)	12.1 (3.32)
REM density (only phasic period)	24.0 (2.07)	31.0 (3.52)

REM density for all REM sleep was measured by the number of rapid eye movements divided by the total REM sleep duration in minutes (the first row). The REM density was only measured during phasic REM sleep and was determined by the number of rapid eye movements divided by the duration of phasic REM sleep in minutes.

brain responses was not found during REM sleep. Neither delta nor theta activity during REM sleep showed interhemispheric asymmetry, but we replicated previous findings showing interhemispheric differences in delta activity during NREM sleep.

Notably, although brain responses to auditory stimuli did not show interhemispheric asymmetry associated with the FNE during REM sleep, a larger response to rare stimuli was found, specifically during the phasic period. Because the amplitude of an evoked brain response to deviant stimuli during sleep correlates with the degree of vigilance (Nielsen-Bohlman et al., 1991; Michida et al., 2005), the present results suggest that the FNE augments vigilance during REM sleep, especially when REMs are observed. These results demonstrate that a surveillance system using both hemispheres exists during the phasic period of REM sleep.

We found that the amplitudes of brain responses were larger on day 1 than on day 2, specifically during the phasic period. Why did the phasic period, but not the tonic period, show augmented evoked brain responses in association with the FNE? The brain is more sensitive in the monitoring of external stimuli during the tonic period than in the phasic period during normal sleep without the FNE (Takahara et al., 2002). This suggests that there may be no additional capacity available for information processing or attention to external stimuli during the tonic period, as the attention capacity is likely to be limited (Kahneman, 1973; Marois and Ivanoff, 2005). If attentional resources are not available for external monitoring during the tonic period, when there is a need to increase vigilance even further, such as when sleeping in an unfamiliar environment, this increase would have to occur outside the tonic period, i.e., during the phasic period. This compensatory action might explain why vigilance was enhanced during the phasic period during REM sleep in association with the FNE.

There are several differences between the current ERP findings and those in previous studies. First, previous studies (Cote and Campbell, 1999a; Cote et al., 2001) indicated that P300 was elicited during REM sleep in an oddball paradigm. However, we do not think that the P300 component was elicited in the present study. The P300 component is known to be distributed over the posterior site, and its latency could be as early as 250 ms (Polich, 2007). However, the topographic maps did not indicate that the peak of the component in the present study was around the posterior site during the tonic or phasic periods. Second, previous studies (Sallinen et al., 1996; Takahara et al., 2006b) showed that a small P2 was elicited during both the tonic and phasic periods during REM sleep. However, P2 was not significantly elicited during the phasic period on day 2 in the present study. These inconsistencies could be due to the difference in the intensity of the sounds used across studies. It has been shown that the intensity of sounds affects ERP amplitudes during REM sleep (Cote and Campbell, 1999b). Indeed, previous studies have used much louder sounds (50–100 dB) (Sallinen et al., 1996; Cote and Campbell, 1999a; Cote et al., 1999, 2001; Takahara et al., 2002, 2006b) than those used in the present study (∼35 dB). In particular, these previous studies that showed P300 during REM sleep used very loud sounds (95∼100 dB). We speculate that loud sounds could increase vigilance during REM sleep and might even wake up subjects. This possible increase in vigilance might result in P300 during the phasic periods in the previous studies.

The phasic period of normal REM sleep without the FNE is linked to subjective mental activities (Berger and Oswald, 1962; Weinstein et al., 1988). Notably, a previous study suggested that sensitivity to external stimuli was lower during sleep-onset dreaming (Michida et al., 2005). Thus, the reason for a very small brain responses during the phasic period of normal REM sleep without the FNE may be due to ongoing mental activities, including dreaming, which may interfere with the monitoring of the external environments (Sallinen et al., 1996; Michida et al., 2005). However, a large brain response was elicited during the phasic period during REM sleep in association with the FNE. This result suggests that resources for internal mental activities are deployed for external monitoring when sleeping in an unfamiliar environment leading to the FNE.

We did not find clear interhemispheric asymmetry in delta or theta activity or in the amplitudes of the evoked potentials between hemispheres during REM sleep in association with the FNE. These results contrast our previous study (Tamaki et al., 2016), in which we found interhemispheric asymmetry in regional slow-wave activity and vigilance during deep NREM sleep. This difference suggests that different mechanisms are involved in surveillance during REM sleep and deep NREM sleep. It may be the case that since the arousal threshold may be too high and costly during deep NREM sleep to increase vigilance in both hemispheres, only one hemisphere is used for surveillance. However, resources for dreaming and mental activity are already available during REM sleep. These resources may be easily deployed for surveillance without much sacrifice in sleep. Thus, the surveillance is present in both hemispheres during REM sleep.

Some may wonder whether the circadian timing may affect the surveillance system associated with the FNE during REM sleep. A previous study (Tamaki et al., 2016) indicated that the FNE occurs regardless of whether a sleep period occurred during daytime nap or at night. Another previous study (Toussaint et al., 1997) did not show a significant effect of sleep cycle on the FNE during REM sleep (see Figure 1 in Toussaint et al., 1997). These studies suggest that the effect of the circadian rhythm on the FNE during REM sleep may not be large enough to alter the findings of the present study. However, how circadian phases influence the surveillance system with the FNE during REM sleep needs to be systematically clarified in future research.

The present study targeted the DMN for the analysis of brain activities during REM sleep, because a previous study (Tamaki et al., 2016) suggested that the DMN may be involved in the surveillance system in association with the FNE. However, whether the responsive brain network related to the FNE during REM sleep resides specifically in the DMN is still speculative. Other brain networks need to be investigated in future research.

CONCLUSION

The protective surveillance system activated during REM sleep may involve a different mechanism than that activated during deep NREM sleep. A surveillance system was shown to increase vigilance in both hemispheres throughout REM sleep, specifically during the phasic period. This REM-specific surveillance system may be based on resources available for internal mental activity.

DATA AVAILABILITY STATEMENT

The datasets generated for this study are available on request to the corresponding author.

ETHICS STATEMENT

The studies involving human participants were reviewed and approved by Institutional review board, Brown University. The patients/participants provided their written informed consent to participate in this study.

AUTHOR CONTRIBUTIONS

MT and YS designed the research and wrote the manuscript. MT performed the experiments and analyzed the data.

FUNDING

This work was supported by NIH (R21EY028329).

SUPPLEMENTARY MATERIAL

The Supplementary Material for this article can be found online at: https://www.frontiersin.org/articles/10.3389/fnins.2019.01161/full#supplementary-material

REFERENCES

Agnew, H. W. Jr., Webb, W. B., and Williams, R. L. (1966). The first night effect: an EEG study of sleep. *Psychophysiology* 2, 263–266.

Ahveninen, J., Lin, F. H., Kivisaari, R., Autti, T., Hamalainen, M., Stufflebeam, S., et al. (2007). MRI-constrained spectral imaging of benzodiazepine modulation of spontaneous neuromagnetic activity in human cortex. *Neuroimage* 35, 577–582.

Bastuji, H., Garcia-Larrea, L., Franc, C., and Mauguiere, F. (1995). Brain processing of stimulus deviance during slow-wave and paradoxical sleep: a study of human auditory evoked responses using the oddball paradigm. *J. Clin. Neurophysiol.* 12, 155–167.

Berger, R. J., and Oswald, I. (1962). Eye movements during active and passive dreams. *Science* 137:601.

Bernardi, G., Betta, M., Ricciardi, E., Pietrini, P., Tononi, G., and Siclari, F. (2019). Regional delta waves in human rapid eye movement sleep. *J. Neurosci.* 39, 2686–2697. doi: 10.1523/JNEUROSCI.2298-18.2019

Bonnet, M., Carley, D., Carskadon, M., Easton, P., Guilleminault, C., Harper, R., et al. (1992). EEG arousals: scoring rules and examples: a preliminary report from the sleep disorders atlas task force of the American Sleep Disorders Association. *Sleep* 15, 173–184.

Buysse, D. J., Germain, A., Hall, M., Monk, T. H., and Nofzinger, E. A. (2011). A neurobiological model of insomnia. *Drug Discov. Today Dis. Models.* 8, 129–137. doi: 10.1016/j.ddmod.2011.07.002

Carskadon, M. A., and Dement, W. C. (1979). Effects of total sleep loss on sleep tendency. *Percept. Mot. Skills* 48, 495–506. doi: 10.2466/pms.1979.48.2.495

Carskadon, M. A., and Dement, W. C. (1981). Cumulative effects of sleep restriction on daytime sleepiness. *Psychophysiology* 18, 107–113.

Cohen, J. (1988). *Statistical Power Analysis for the Behavioral Sciences*. Hillsdale: Lawrence Erlbaum and Associates.

Cote, K. A., and Campbell, K. B. (1999a). P300 to high intensity stimuli during REM sleep. *Clin. Neurophysiol.* 110, 1345–1350.

Cote, K. A., and Campbell, K. B. (1999b). The effects of varying stimulus intensity on P300 during REM sleep. *Neuroreport* 10, 2313–2318.

Cote, K. A., de Lugt, D. R., Langley, S. D., and Campbell, K. B. (1999). Scalp topography of the auditory evoked K-complex in stage 2 and slow wave sleep. *J. Sleep Res.* 8, 263–272.

Cote, K. A., Etienne, L., and Campbell, K. B. (2001). Neurophysiological evidence for the detection of external stimuli during sleep. *Sleep* 24, 791–803.

Crowley, K. E., and Colrain, I. M. (2004). A review of the evidence for P2 being an independent component process: age, sleep and modality. *Clin. Neurophysiol.* 115, 732–744. doi: 10.1016/j.clinph.2003.11.021

Curcio, G., Ferrara, M., Piergianni, A., Fratello, F., and De Gennaro, L. (2004). Paradoxes of the first-night effect: a quantitative analysis of antero-posterior EEG topography. *Clin. Neurophysiol.* 115, 1178–1188. doi: 10.1016/j.clinph.2003.12.018

Czeisler, C. A. (2013). Perspective: casting light on sleep deficiency. *Nature* 497, S13. doi: 10.1038/497S13a

Dale, A. M., Fischl, B., and Sereno, M. I. (1999). Cortical surface-based analysis. *Neuroimage* 9, 179–194. doi: 10.1006/nimg.1998.0395

Destrieux, C., Fischl, B., Dale, A., and Halgren, E. (2010). Automatic parcellation of human cortical gyri and sulci using standard anatomical nomenclature. *Neuroimage* 53, 1–15. doi: 10.1016/j.neuroimage.2010.06.010

Drummond, S. P., Brown, G. G., Gillin, J. C., Stricker, J. L., Wong, E. C., and Buxton, R. B. (2000). Altered brain response to verbal learning following sleep deprivation. *Nature* 403, 655–657. doi: 10.1038/35001068

Fischl, B., Sereno, M. I., and Dale, A. M. (1999). Cortical surface-based analysis. *Neuroimage* 9, 195–207. doi: 10.1006/nimg.1998.0396

Fischl, B., van der Kouwe, A., Destrieux, C., Halgren, E., Segonne, F., Salat, D. H., et al. (2004). Automatically parcellating the human cerebral cortex. *Cereb. Cortex* 14, 11–22. doi: 10.1093/cercor/bhg087

Hamalainen, M. S., and Sarvas, J. (1989). Realistic conductivity geometry model of the human head for interpretation of neuromagnetic data. *IEEE Trans. Biomed. Eng.* 36, 165–171. doi: 10.1109/10.16463

Horikawa, T., Tamaki, M., Miyawaki, Y., and Kamitani, Y. (2013). Neural decoding of visual imagery during sleep. *Science* 340, 639–642. doi: 10.1126/science.1234330

Iber, C., Ancoli-Israel, S. S., Chesson, A., and Quan, S. F. (2007). *The AASM Manual for the Scoring of Sleep and Associated Events: Rules, Terminology, and Technical Specifications*. Westchester: American Academy of Sleep Medicine.

Imeri, L., and Opp, M. R. (2009). How (and why) the immune system makes us sleep. *Nat. Rev. Neurosci.* 10, 199–210. doi: 10.1038/nrn2576

Kahneman, D. (1973). *Attention and Effort*. Upper Saddle River, NJ.: Prentice-Hall.

Kales, A., Heuser, G., Jacobson, A., Kales, J. D., Hanley, J., Zweizig, J. R., et al. (1967a). All night sleep studies in hypothyroid patients, before and after treatment. *J. Clin. Endocrinol. Metab.* 27, 1593–1599. doi: 10.1210/jcem-27-11-1593

Kales, A., Jacobson, A., Kales, J. D., Kun, T., and Weissbuch, R. (1967b). All-night EEG sleep measurements in young adults. *Psychon. Sci.* 7, 67–68.

Lin, F. H., Witzel, T., Hamalainen, M. S., Dale, A. M., Belliveau, J. W., and Stufflebeam, S. M. (2004). Spectral spatiotemporal imaging of cortical oscillations and interactions in the human brain. *Neuroimage* 23, 582–595. doi: 10.1016/j.neuroimage.2004.04.027

Marois, R., and Ivanoff, J. (2005). Capacity limits of information processing in the brain. *Trends Cogn. Sci.* 9, 296–305. doi: 10.1016/j.tics.2005.04.010

Mason, M. F., Norton, M. I., Van Horn, J. D., Wegner, D. M., Grafton, S. T., and Macrae, C. N. (2007). Wandering minds: the default network and stimulus-independent thought. *Science* 315, 393–395. doi: 10.1126/science.1131295

Michida, N., Hayashi, M., and Hori, T. (2005). Effects of hypnagogic imagery on the event-related potential to external tone stimuli. *Sleep* 28, 813–818.

Nielsen-Bohlman, L., Knight, R. T., Woods, D. L., and Woodward, K. (1991). Differential auditory processing continues during sleep. *Electroencephalogr. Clin. Neurophysiol.* 79, 281–290. doi: 10.1016/0013-4694(91)90124-M

Okawa, M. (2011). Delayed sleep phase syndrome and depression. *Sleep Med.* 12, 621–622. doi: 10.1016/j.sleep.2011.03.014

Peever, J., and Fuller, P. M. (2017). The biology of REM Sleep. *Curr. Biol.* 27, R1237–R1248. doi: 10.1016/j.cub.2017.10.026

Perrin, F., Garcia-Larrea, L., Mauguiere, F., and Bastuji, H. (1999). A differential brain response to the subject's own name persists during sleep. *Clin. Neurophysiol.* 110, 2153–2164.

Polich, J. (2007). Updating P300: an integrative theory of P3a and P3b. *Clin. Neurophysiol.* 118, 2128–2148. doi: 10.1016/j.clinph.2007.04.019

Price, L. J., and Kremen, I. (1980). Variations in behavioral response threshold within the REM period of human sleep. *Psychophysiology* 17, 133–140.

Raichle, M. E., and Snyder, A. Z. (2007). A default mode of brain function: a brief history of an evolving idea. *Neuroimage* 37, 1083–1090. doi: 10.1016/j.neuroimage.2007.02.041

Rattenborg, N. C., Lima, S. L., and Amlaner, C. J. (1999). Half-awake to the risk of predation. *Nature* 397, 397–398. doi: 10.1038/17037

Rechtschaffen, A., and Kales, A. (1968). *A Manual of Standardized Terminology, Techniques, and Scoring System for Sleep Stages of Human Subjects*. Washington, DC: US Government Printing Office.

Rechtschaffen, A., and Verdone, P. (1964). Amount of dreaming: effect of incentive, adaptation to laboratory, and individual differences. *Percept. Mot. skills* 19, 947–958.

Roth, T., Stubbs, C., and Walsh, J. K. (2005). Ramelteon (TAK-375), a selective MT1/MT2-receptor agonist, reduces latency to persistent sleep in a model of transient insomnia related to a novel sleep environment. *Sleep* 28, 303–307.

Sallinen, M., Kaartinen, J., and Lyytinen, H. (1996). Processing of auditory stimuli during tonic and phasic periods of REM sleep as revealed by event-related brain potentials. *J. Sleep Res.* 5, 220–228.

Scharf, M. B., Kales, A., and Bixler, E. O. (1975). Readaptation to the sleep laboratory in insomniac subjects. *Psychophysiology* 12, 412–415.

Schmidt, H. S., and Kaelbling, R. (1971). The differential laboratory adaptation of sleep parameters. *Biol. Psychiatry* 3, 33–45.

Sforza, E., Chapotot, F., Pigeau, R., and Buguet, A. (2008). Time of night and first night effects on arousal response in healthy adults. *Clin. Neurophysiol.* 119, 1590–1599. doi: 10.1016/j.clinph.2008.03.010

Sharbrough, F. C. G. E., Lesser, R. P., Lüders, H., Nuwer, M., and Picton, T. W. (1991). American electroencephalographic society guidelines for standard electrode position nomenclature. *J. Clin. Neurophysiol.* 8, 200–202.

Simor, P., Gombos, F., Szakadat, S., Sandor, P., and Bodizs, R. (2016). EEG spectral power in phasic and tonic REM sleep: different patterns in young adults and children. *J. Sleep Res.* 25, 269–277. doi: 10.1111/jsr.12376

Squires, N. K., Squires, K. C., and Hillyard, S. A. (1975). Two varieties of long-latency positive waves evoked by unpredictable auditory stimuli in man. *Electroencephalogr. Clin. Neurophysiol.* 38, 387–401. doi: 10.1016/0013-4694(75)90263-1

Stickgold, R. (2005). Sleep-dependent memory consolidation. *Nature* 437, 1272–1278. doi: 10.1038/nature04286

Takahara, M., Kanayama, S., Nittono, H., and Hori, T. (2006a). REM sleep EEG pattern: examination by a new EEG scoring system for REM sleep period. *Sleep Biol. Rhythms* 4, 105–110.

Takahara, M., Nittono, H., and Hori, T. (2006b). Effect of voluntary attention on auditory processing during REM sleep. *Sleep* 29, 975–982.

Takahara, M., Nittono, H., and Hori, T. (2002). Comparison of the event-related potentials between tonic and phasic periods of rapid eye movement sleep. *Psychiatry Clin. Neurosci.* 56, 257–258.

Tamaki, M., Bang, J. W., Watanabe, T., and Sasaki, Y. (2014). The first-night effect suppresses the strength of slow-wave activity originating in the visual areas during sleep. *Vis. Res.* 99, 154–161. doi: 10.1016/j.visres.2013.10.023

Tamaki, M., Bang, J. W., Watanabe, T., and Sasaki, Y. (2016). Night watch in one brain hemisphere during sleep associated with the first-night effect in humans. *Curr. Biol.* 26, 1190–1194. doi: 10.1016/j.cub.2016.02.063

Tamaki, M., Huang, T. R., Yotsumoto, Y., Hamalainen, M., Lin, F. H., Nanez, J. E., et al. (2013). Enhanced spontaneous oscillations in the supplementary motor area are associated with sleep-dependent offline learning of finger-tapping motor-sequence task. *J. Neurosci.* 33, 13894–13902. doi: 10.1523/JNEUROSCI.1198-13.2013

Tamaki, M., Nittono, H., Hayashi, M., and Hori, T. (2005a). Examination of the first-night effect during the sleep-onset period. *Sleep* 28, 195–202.

Tamaki, M., Nittono, H., and Hori, T. (2005b). The first-night effect occurs at the sleep-onset period regardless of the temporal anxiety level in healthy students. *Sleep Biol. Rhythms* 3, 92–94.

Toussaint, M., Luthringer, R., Schaltenbrand, N., Nicolas, A., Jacqmin, A., Carelli, G., et al. (1997). Changes in EEG power density during sleep laboratory adaptation. *Sleep* 20, 1201–1207.

Webb, W. B., and Campbell, S. S. (1979). The first night effect revisited with age as a variable. *Waking Sleeping* 3, 319–324.

Wehrle, R., Kaufmann, C., Wetter, T. C., Holsboer, F., Auer, D. P., Pollmacher, T., et al. (2007). Functional microstates within human REM sleep: first evidence from fMRI of a thalamocortical network specific for phasic REM periods. *Eur. J. Neurosci.* 25, 863–871. doi: 10.1111/j.1460-9568.2007.05314.x

Weinstein, L., Schwartz, D., and Ellman, S. J. (1988). The development of scales to measure the experience of self-participation in sleep. *Sleep* 11, 437–447.

Conflict of Interest: The authors declare that the research was conducted in the absence of any commercial or financial relationships that could be construed as a potential conflict of interest.

Copyright © 2019 Tamaki and Sasaki. This is an open-access article distributed under the terms of the Creative Commons Attribution License (CC BY). The use, distribution or reproduction in other forums is permitted, provided the original author(s) and the copyright owner(s) are credited and that the original publication in this journal is cited, in accordance with accepted academic practice. No use, distribution or reproduction is permitted which does not comply with these terms.

frontiers in Neuroscience

ORIGINAL RESEARCH
published: 20 December 2019
doi: 10.3389/fnins.2019.01380

Pathway-Dependent Regulation of Sleep Dynamics in a Network Model of the Sleep–Wake Cycle

*Charlotte Héricé and Shuzo Sakata**

Strathclyde Institute of Pharmacy and Biomedical Sciences, University of Strathclyde, Glasgow, United Kingdom

Sleep is a fundamental homeostatic process within the animal kingdom. Although various brain areas and cell types are involved in the regulation of the sleep–wake cycle, it is still unclear how different pathways between neural populations contribute to its regulation. Here we address this issue by investigating the behavior of a simplified network model upon synaptic weight manipulations. Our model consists of three neural populations connected by excitatory and inhibitory synapses. Activity in each population is described by a firing-rate model, which determines the state of the network. Namely wakefulness, rapid eye movement (REM) sleep or non-REM (NREM) sleep. By systematically manipulating the synaptic weight of every pathway, we show that even this simplified model exhibits non-trivial behaviors: for example, the wake-promoting population contributes not just to the induction and maintenance of wakefulness, but also to sleep induction. Although a recurrent excitatory connection of the REM-promoting population is essential for REM sleep genesis, this recurrent connection does not necessarily contribute to the maintenance of REM sleep. The duration of NREM sleep can be shortened or extended by changes in the synaptic strength of the pathways from the NREM-promoting population. In some cases, there is an optimal range of synaptic strengths that affect a particular state, implying that the amount of manipulations, not just direction (i.e., activation or inactivation), needs to be taken into account. These results demonstrate pathway-dependent regulation of sleep dynamics and highlight the importance of systems-level quantitative approaches for sleep–wake regulatory circuits.

Keywords: sleep regulatory circuits, computational model, brain state, sleep/wake cycle, Python programing language

OPEN ACCESS

Edited by:
Michele Bellesi,
University of Bristol, United Kingdom

Reviewed by:
Umberto Olcese,
University of Amsterdam, Netherlands
Aleksander Domanski,
University of Bristol, United Kingdom

***Correspondence:**
Shuzo Sakata
shuzo.sakata@strath.ac.uk

Specialty section:
This article was submitted to Sleep and Circadian Rhythms, a section of the journal Frontiers in Neuroscience

Received: *10 September 2019*
Accepted: *05 December 2019*
Published: *20 December 2019*

Citation:
Héricé C and Sakata S (2019) Pathway-Dependent Regulation of Sleep Dynamics in a Network Model of the Sleep–Wake Cycle. Front. Neurosci. 13:1380. doi: 10.3389/fnins.2019.01380

INTRODUCTION

Global brain states vary dynamically on multiple timescales. Humans typically exhibit a daily cycle between three major behavioral states: wakefulness, REM sleep and NREM sleep. This daily cycle is regulated by a circadian rhythm and a homeostatic sleep pressure (Borbély, 1982; Achermann and Borbely, 1990). These states alternate on a timescale of several hours called an ultradian rhythm (Borbély, 1982; Archermann and Borbely, 2017; Carskadon, 2017). Thus, complex interactions between homeostatic, circadian, and ultradian processes are involved in the sleep-wake cycle generation. However, it remains elusive how these states are regulated in the brain.

Over the past several decades, various cell types, neurotransmitters and neuropeptides have been identified as part of the sleep–wake regulating circuits within the brain (Saper et al., 2001; Brown et al., 2012; Luppi et al., 2013; Weber and Dan, 2016; Scammell et al., 2017; Herice et al., 2019). Sleep- or wake-promoting neurons show state-dependent firing and contribute to the induction and/or maintenance of a particular state (Jouvet, 1962; McCarley and Hobson, 1971; Hobson et al., 1975; Saper et al., 2001; Brown et al., 2012; Weber and Dan, 2016; Herice et al., 2019). To gain a better understanding of sleep–wake regulation, it is fundamental not just to identify and characterize each component of sleep–wake regulating circuits, but to also investigate how each pathway between neural populations contributes to state regulation.

Although controlling neural activity has provided mechanistic insights into sleep–wake regulation, their results are sometimes contradictory: for example, the role of pontine cholinergic neurons in REM sleep has been debated (Grace et al., 2014; Grace, 2015; Grace and Horner, 2015; Van Dort et al., 2015). Even recent studies with opto- and chemogenetic approaches do not resolve this long-standing issue (Van Dort et al., 2015; Kroeger et al., 2017). Even though this discrepancy may be simply due to differences in animal models and experimental techniques, it is technically challenging to manipulate neurons or specific pathways precisely across different laboratories.

A computational approach may be a viable alternative for gaining insights into the mechanism of sleep–wake regulation. Since pioneering work in the 1970s and 1980s (McCarley and Hobson, 1975; Borbély, 1982; Archermann and Borbely, 2017), various computational models have been developed (Tamakawa et al., 2006; Diniz Behn et al., 2007; Diniz-Behn and Booth, 2010; Robinson et al., 2011; Booth and Diniz Behn, 2014; Archermann and Borbely, 2017; Booth et al., 2017; Herice et al., 2019): conceptually, a homeostatic sleep-dependent process and a circadian process play a key role in sleep regulation (Borbély, 1982; Archermann and Borbely, 2017). Reciprocal excitatory-inhibitory connections (McCarley and Hobson, 1975; Diniz Behn et al., 2007; Diniz-Behn and Booth, 2010; Diniz Behn and Booth, 2012; Booth et al., 2017) and mutual inhibitory interactions (Saper et al., 2001) can be recognized as key network motifs within sleep–wake regulating circuits. Although their dynamics have been explored (Diniz Behn and Booth, 2012; Diniz Behn et al., 2013; Weber, 2017), and those models can replicate sleep architecture of humans and animals (Diniz-Behn and Booth, 2010) as well as state-dependent neural firing (Tamakawa et al., 2006), few studies have investigated how the strength of synaptic connections between wake- and sleep-promoting populations contribute to sleep dynamics. As controlling neural activity at high spatiotemporal resolution *in vivo* becomes feasible experimentally, computational approaches can be considered as complementary approaches for investigating the role of specific neural pathways in sleep–wake regulation.

To this end, we utilize a simplified network model (Diniz Behn and Booth, 2012; Costa et al., 2016) (**Figure 1**) and systematically manipulate the strength of every pathway. Because neurons within the sleep–wake regulating circuits typically project to a wide range of neural populations (Schwarz and Luo, 2015; Scammell et al., 2017; Herice et al., 2019), their contributions to the sleep–wake cycle may also vary depending on the pathway. Therefore, we set out to test the hypothesis that the sleep–wake cycle is regulated in a pathway-dependent manner.

Although the present model is highly abstract, it captures the following key features of sleep–wake regulating circuits: while the interaction between neuronal populations in the brainstem and the hypothalamus governs the sleep–wake regulation, some of the populations can be recognized as wake- or sleep-promoting (Brown et al., 2012; Luppi et al., 2013, 2017; Scammell et al., 2017; Herice et al., 2019). To reflect the populations' state-dependent

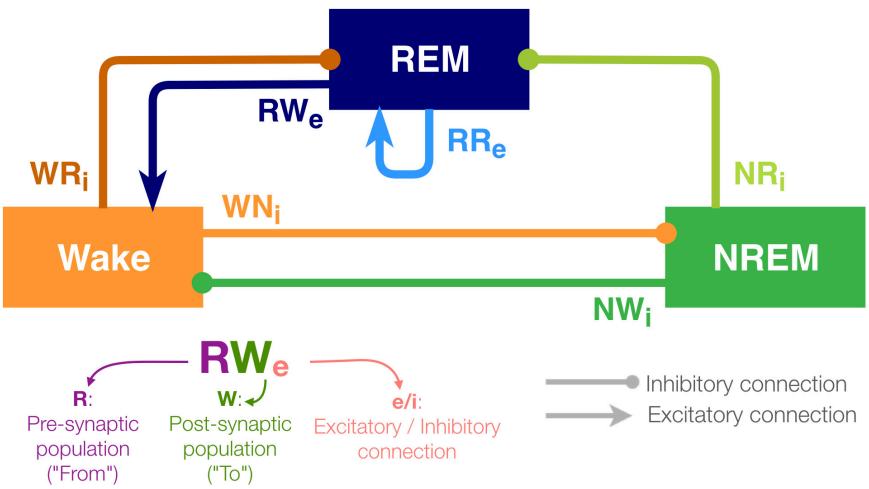

FIGURE 1 | Architecture of the sleep regulatory network. Three neural populations are connected with excitatory and inhibitory synapses. Each neural population is named as the state they promote. The arrows and circles represent excitatory and inhibitory connections, respectively. The synapses are named with two uppercase and one lowercase letters: first letter of the pre-synaptic population (where the synapse is from), first letter of the post-synaptic population (where the synapse is going to) and "e" if it is excitatory or sign "i" if inhibitory.

firing, the model contains three neuronal populations (REM, NREM and Wake). The activity in these populations defines the state of the network (see section Materials and Methods).

With respect to connectivity between these populations, Saper et al. (2001) proposed that the mutual inhibition between wake-promoting and sleep-promoting populations acts as a flip-flop switch for the regulation of transitioning between wakefulness and NREM sleep. Hence, in this model, the outputs from the Wake-promoting and NREM-promoting populations are considered as inhibitory. Because pontine REM-active cholinergic neurons provide excitatory connections to the sublaterodorsal nucleus (SLD), a key component of REM sleep-regulating circuits (Boissard et al., 2002), the REM-promoting population has a recurrent excitatory connection. Glutamatergic neurons project rostrally to several wake-promoting nuclei, such as the intralaminar nuclei of the thalamus and basal forebrain, and the REM population also provides excitatory outputs onto the Wake population (Boissard et al., 2002; Lu et al., 2006). In addition, because recent studies have shown that GABAergic inputs play a role in REM sleep induction (Weber et al., 2015), the REM-promoting population also receives inhibitory inputs from both the wake-promoting and NREM-promoting populations in this model. Based on this simplified model, we report that the effects of synaptic weight alterations on sleep architecture are highly pathway-dependent. We also discuss implications for future biological experiments.

MATERIALS AND METHODS

We implemented a computational model of the sleep/wake cycle containing three neuronal populations whose activity by several differential equations. Numerical simulations were computed with the Runge–Kutta integration method (4th order), with a time step of 1 ms and a simulation duration of 24 h. For these simulations and a part of the data processing, we used the Python programing language (version 3.6.8). In order to run multiple simulations for all the conditions, we implemented a script Bash (version 3.2.57). The majority of the data processing, the plots were performed with R (version 3.5.1) and MATLAB (R2018b, Mathworks). All details about the tools and libraries used for this work are summarized in **Supplementary Table S1**. Codes are available at https://github.com/Sakata-Lab/sleep-model.

Firing Rate Formalism

All three populations are promoting the sleep–wake cycle corresponding to their name and are associated with a specific neurotransmitter. The REM-promoting population releases the excitatory neurotransmitters RX_e whereas the NREM- and Wake-promoting populations release the inhibitory ones NX_i and WX_i, respectively.

Firing rate F_X of population X is described as follows:

$$\frac{dF_X}{dt} = \frac{F_{X\infty}(I_X) - F_X}{\tau_X},$$

where $F_{X\infty}$ is a steady state firing rate function for each population (see below). τ_X is the membrane time constant of the population X. The synaptic input I_X is a weighted sum of neurotransmitter concentrations released by the pre-synaptic populations Y and is described as follows:

$$I_W = g_{NW_i} \cdot C_{NX_i} + g_{RW_e} \cdot C_{RX_e} + \xi(t)$$

$$I_N = g_{WN_i} \cdot C_{WX_i} + \xi(t)$$

$$I_R = g_{WR_i} \cdot C_{WX_i} + g_{NR_i} \cdot C_{NX_i} + g_{RR_e} \cdot C_{RX_e} + \xi(t),$$

where $C_{YXe/i}$ represents the neurotransmitter concentration involved in the pathway from population Y to X with synaptic weight $g_{YXe/i}$. The parameter $\xi(t)$ provides a weak Gaussian noise (mean of 0.01 Hz and standard deviation of 0.005 Hz) to mimics the variability of the biological networks.

For each population, the steady state firing rate function $F_{X\infty}$ is modeled with the following equations:

$$F_{W\infty} = W_{\max} \cdot \left(0.5 \cdot (1 + \tanh\left[(I_W - \beta_W)/\alpha_W\right])\right)$$

$$F_{R\infty} = R_{\max} \cdot \left(0.5 \cdot (1 + \tanh\left[(I_R - \beta_R)/\alpha_R\right])\right)$$

$$F_{N\infty} = N_{\max} \cdot \left(0.5 \cdot (1 + \tanh\left[(I_N - k_N \cdot H(t))/\alpha_N\right])\right),$$

where W_{max}, N_{max} and R_{max} are constant values to set the maximum firing rates of the populations. α and β are slope and threshold parameters of the hyperbolic tangent function for the population X, respectively. Because the NREM population is linked to the homeostatic sleep drive, the steady state firing function also depends on the homeostatic sleep drive variable $H(t)$ (see below).

All parameter values are provided in **Supplementary Table S2**.

Homeostatic Sleep Drive

In the model, the sleep–wake transition is driven by the homeostatic sleep drive $H(t)$. This process can be described by the following equation:

$$\frac{dH}{dt} = \frac{H_{\max} - H}{\tau_{hw}} \cdot \mathcal{H}(F_W - \theta_W) - \frac{H}{\tau_{hs}} \cdot \mathcal{H}(\theta_W - F_W),$$

where $\mathcal{H}(z)$ stands for the Heaviside function, which returns 0 if $z < 0$ and 1 if $z \geq 0$. θ_W is a constant to set the sleep drive threshold. $H_{\max}$ is a constant value to set the maximum value for the homeostatic force. T_{hw} and T_{hs} are time constants of sleep drive built up during wakefulness and declined during sleep, respectively. Hence, the homeostatic force value increases during wakefulness due to a high activity of the wake-promoting population, and decreases during sleep when this activity is lower.

Action of Neurotransmitters

The neurotransmitter concentration $C_{YX}(t)$ from the populations Y to X is described as following:

$$\frac{dC_{YX}}{dt} = \frac{C_{YX_\infty}(F_Y) - C_{YX}}{\tau_{YX}},$$

where C_{YX8} is a saturating function to provide the steady state of the neurotransmitter release from the population Y to the population X as a function of F_Y. This function is described as:

$$C_{YX_\infty} = \tanh(F_Y/\tau_{YX}),$$

TABLE 1 | Synaptic weights for the different alterations.

Conditions	Eighth	Quarter	Half	Double	Quadruple	Octuple
Symbols	**g/8**	**g/4**	**g/2**	**g*2**	**g*4**	**g*8**
RR_e	0.2	0.4	0.8	3.2	6.4	12.8
RW_e	0.125	0.25	0.5	2.0	4.0	8.0
WN_i	−0.25	−0.5	−1.0	−4.0	−8.0	−16.0
WR_i	−0.5	−1.0	−2.0	−8.0	−16.0	−32.0
NR_i	−0.1625	−0.325	−0.65	−2.6	−5.2	−10.4
NW_i	−0.21	−0.42	−0.84	−3.36	−6.72	−13.44

*Initials values can be found in the **Supplementary Table S2** with the model parameters.*

where T_{YX} is a time constant. The concentration of each neurotransmitter was normalized between 0 and 1 and is expressed in arbitrary unit (a.u.) (Diniz-Behn and Booth, 2010).

Alterations of Synaptic Weights in the Network

To investigate pathway-dependent regulation of sleep architecture in the network model, we systematically altered the synaptic weight g in the network as shown in **Table 1**.

We also simulated a lesion of each pathway by setting g to 0. For each condition, we run 8 simulations.

Determination of Sleep–Wake States

The state of the network was determined according to Diniz-Behn and Booth (2010): If firing rate of the Wake-promoting population is above 2 Hz, the state of the network is Wake. If not, the state is either NREM or REM sleep: if firing rate of the REM-promoting population is above 2 Hz, the state is REM sleep. If not, the state is NREM sleep.

Statistical Analyses

All statistical analyses were performed using R scripts (version 3.5.1). Data are presented as the means (plain curves) ± s.e.m. (shaded curves). One-way analysis of variance (ANOVA) were used to analyze the synaptic weights alterations depending on the sleep state or transition. Following the ANOVA, Tukey *post hoc* tests were performed for pairwise comparisons to the control conditions (no synaptic weights manipulations). *P*-values less than 0.05 were considered significant. If it is not the case, the sign "NS" was added on the graphs, otherwise there was a significant difference compared to the control condition.

RESULTS

We utilized the network architecture as reported in previous studies (Diniz Behn and Booth, 2012; Costa et al., 2016). As shown in **Figure 1**, this model contained three neuronal populations (labeled REM, NREM and Wake). The activity of these populations was characterized by differential equations describing the population firing rates which defined the state of the network (see Materials and Methods). These equations have been proved to be components of suitable sleep/wake regulatory computational models in previous studies (Diniz Behn et al., 2007, 2013; Diniz-Behn and Booth, 2010; Diniz Behn and Booth, 2012; Costa et al., 2016). The pathways from one population to the other were either excitatory or inhibitory. The concentrations of excitatory and inhibitory neurotransmitters were directly related to the population firing rates of the neural populations and a homeostatic sleep drive. Each population also received random Gaussian noise (**Supplementary Figure S1**).

Sleep Dynamics Under Initial Conditions

Before manipulating synaptic weights across pathways, we confirmed the sleep–wake cycle in our model (**Figure 2**). The initial parameter setting in our model was the same as that in previous reports (Diniz Behn and Booth, 2012; Costa et al., 2016) (**Supplementary Table S2**). As shown in **Figure 2**, this network always started with wakefulness where activity in the Wake-promoting population was high. As the homeostatic force gradually built up, the Wake-promoting population dropped its activity and the network entered NREM sleep. During sleep, the homeostatic force gradually decreased while alternations between NREM sleep and REM sleep appeared before the network exhibited wakefulness again. As expected, the concentration of neurotransmitters was well correlated with the firing rate of neural populations.

In the following sections, to assess the effect of synaptic weight alterations on sleep architecture, we measured the following quantities, all of which are measurable experimentally:

- the total duration of each state (**Figure 3** and **Supplementary Figure S2**),
- the percentage of the time spent in these states (**Figures 4A**, **5A**, **6A**),
- the number of episodes (**Figures 4B**, **5B**, **6B**),
- the number of transitions between states (**Figures 4C**, **5C**, **6C**), and
- the NREM and REM sleep latencies (**Figure 7**).

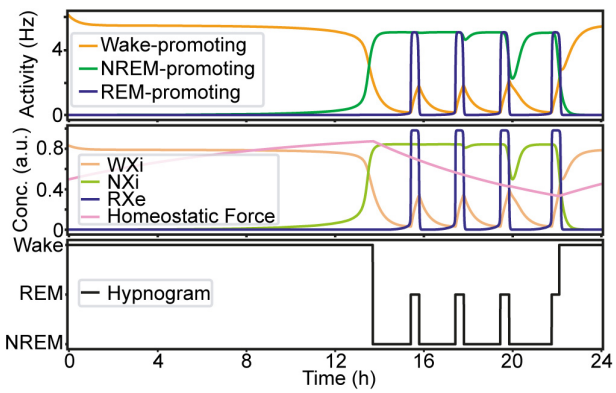

FIGURE 2 | An example of the sleep–wake cycle generated by the network with the initial parameters. Top, the firing rate of each population as a function of time. Middle, the concentration of the neurotransmitters and the homeostatic force. Bottom, a hypnogram which was determined based on firing rates of the three neural populations.

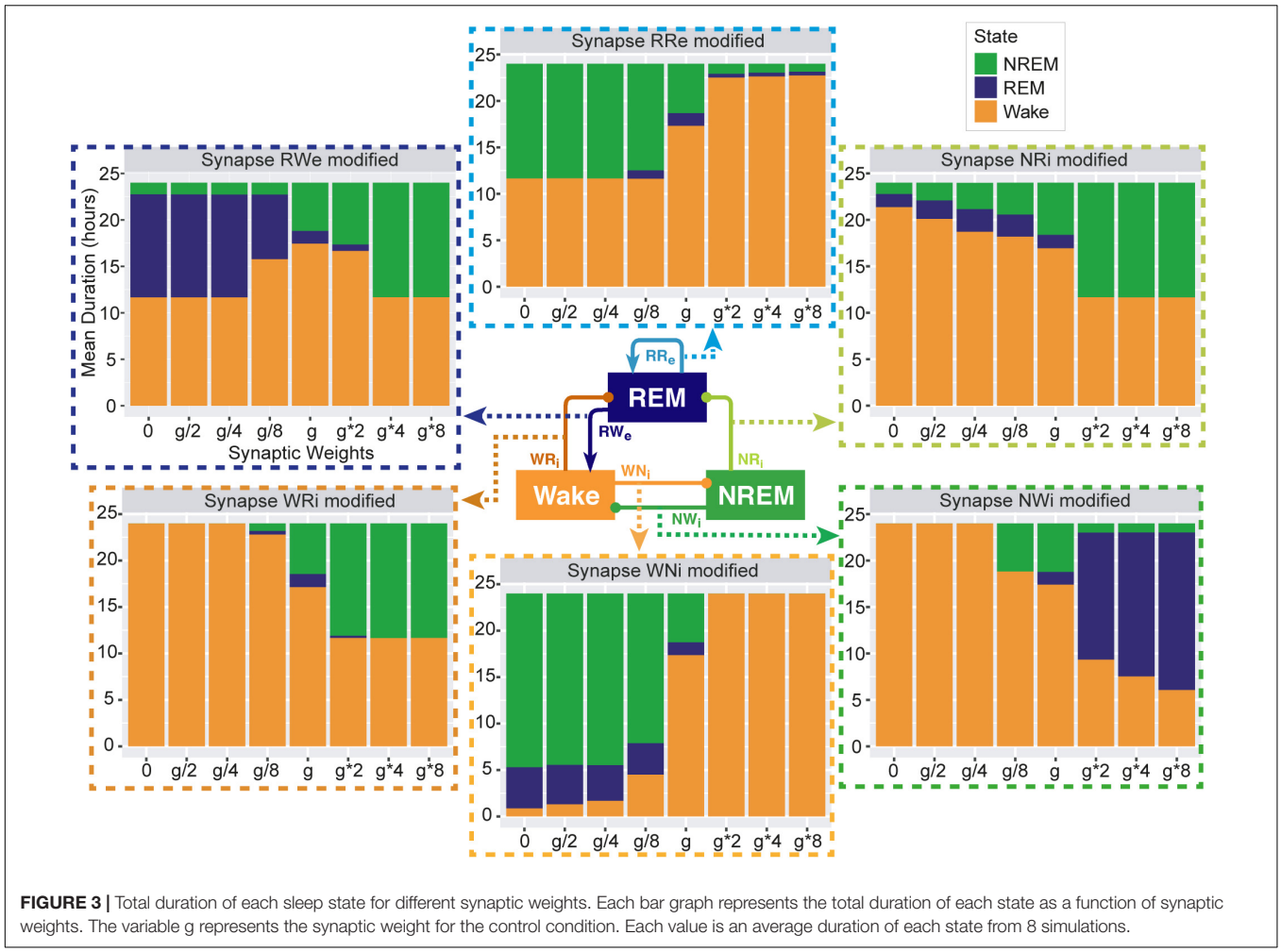

FIGURE 3 | Total duration of each sleep state for different synaptic weights. Each bar graph represents the total duration of each state as a function of synaptic weights. The variable g represents the synaptic weight for the control condition. Each value is an average duration of each state from 8 simulations.

In the following sections, we describe how synaptic weight alterations affect sleep architecture in this network with respect to these measurements.

Effects of Synaptic Weight Alteration on Total Sleep–Wake Duration

To investigate pathway-dependent regulation of sleep, we systematically modified the synaptic weight across pathways: the modified weight span from 0 to 8 times while g was the initial condition. We performed 24-h simulations (n = 8) in each condition.

To assess the overall sleep architecture, we measured the total duration of each state (**Figure 3**). While each neural population had two output pathways (**Figure 1**), the effect of weight alterations on sleep architecture was highly pathway-dependent: in the case of the outputs from the Wake population, although stronger weights in the Wake → NREM (WNi) pathway led to longer wakefulness ($F_{1,7}$ = 911.4, p < 0.0001, one-way ANOVA), the Wake → REM (WRi) pathway showed an opposite trend ($F_{1,7}$ = 88.7, p < 0.0001, one-way ANOVA). The WNi pathway was necessary to induce Wake whereas the WRi pathway was necessary to induce sleep states.

In the outputs from the NREM populations, stronger weights in the NREM → REM (NRi) connection led to longer NREM ($F_{1,7}$ = 14985.8, p < 0.0001, one-way ANOVA) whereas stronger weights in the NREM → Wake (NWi) connection were associated with longer REM ($F_{1,7}$ = 2290812, p < 0.0001, one-way ANOVA).

In the outputs from the REM population, to our surprise, strong recurrent excitatory (RRe) connection shortened the duration of REM sleep ($F_{1,7}$ = 189.2, p < 0.0001, one-way ANOVA). Rather, weaker weighting in the REM → Wake (RWe) connection promoted longer REM sleep ($F_{1,7}$ = 94156.8, p < 0.0001, one-way ANOVA). Thus, the effects of synaptic weight alterations on overall sleep architecture were highly pathway-dependent. We also assessed how simultaneous alterations of two output pathways from each neural population affect sleep dynamics (**Supplementary Figure S3**) (see below Section "Joint Alterations of Two Output Pathways From Each Population and Sleep Architecture" for comprehensive simultaneous alterations). The outcomes deviated from those of individual pathway manipulations, suggesting pathway-dependent regulation in the sleep dynamics. In the next sections, we explore detailed sleep architecture of this model with varied synaptic weights.

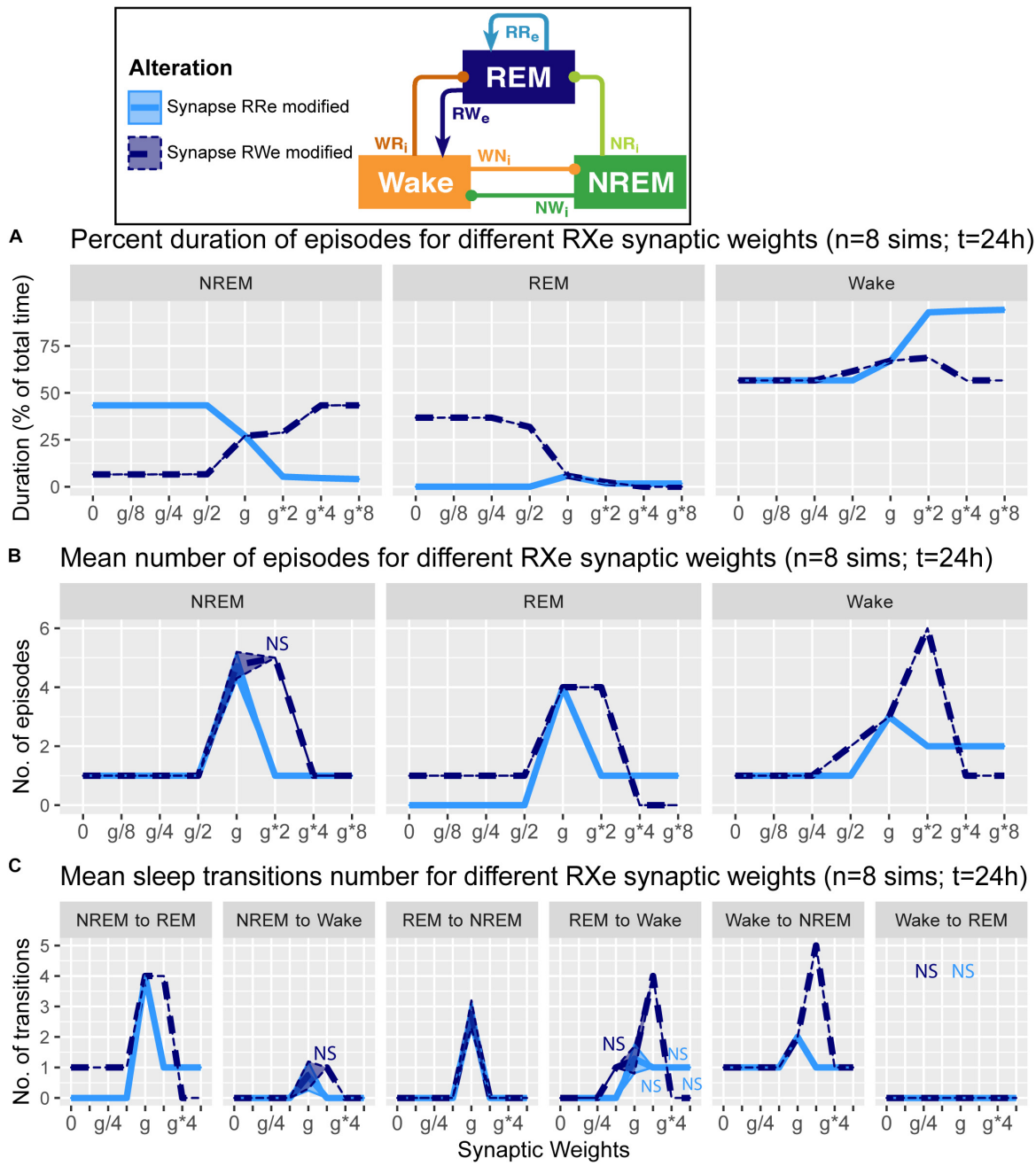

FIGURE 4 | Effects of synaptic weight alterations of the REM population on sleep architecture. The percentage of time spent in each state **(A)**, the number of episodes **(B)**, and the number of state transitions **(C)** as a function of synaptic weights. Each profile was based on eight 24 h simulations. Data presents mean ± s.e.m. Light blue, RRe pathway; dark blue, RWe pathway. NS, non-significant (one-way ANOVA).

Alterations of REM Population Output Pathways and Overall Sleep Architecture

How does the output from the REM population contribute in the sleep architecture? To address this, we quantified the effect of synaptic weight alterations in the REM population outputs on the sleep architecture, with respect to the percentage of time spent in each state (**Figure 4A**), the number of episodes (**Figure 4B**), and the number of state transitions (**Figure 4C**).

When we manipulated the synaptic weight in the RRe pathway (light blue in **Figure 4**), the percentage of NREM sleep decreased as a function of the synaptic weight ($F_{1,7}$ = 1.93e5, $p < 0.0001$, one-way ANOVA) whereas the percentage of Wake increased ($F_{1,7}$ = 8.63e5, $p < 0.0001$, one-way ANOVA) (**Figure 4A**). We observed only small changes in the percentage of REM sleep. The number of all episodes were generally reduced (**Figure 4B**): it was similar for NREM sleep no

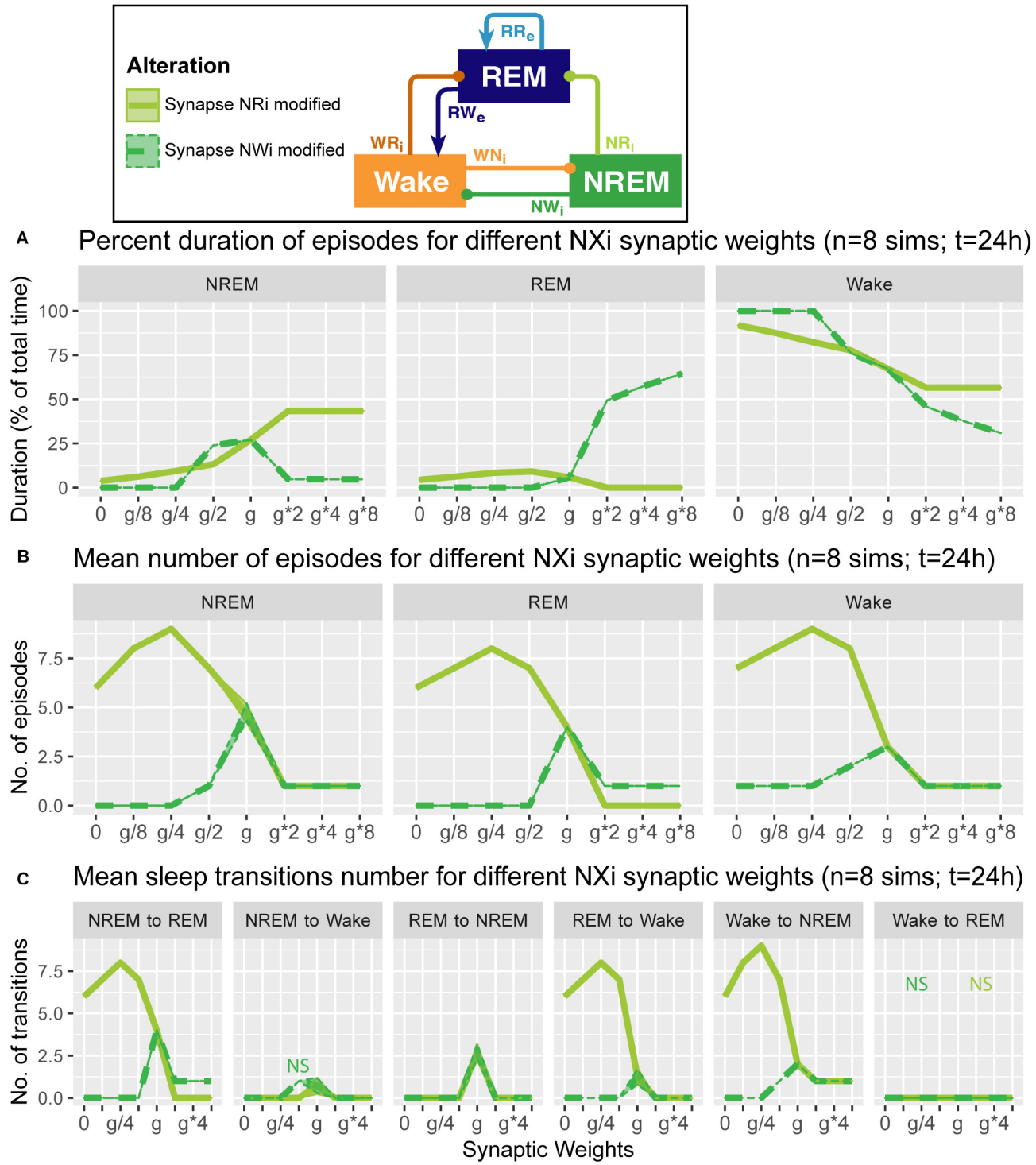

FIGURE 5 | Effects of synaptic weight alterations of the NREM population on sleep architecture. The percentage of time spent in each state **(A)**, the number of episodes **(B)**, and the number of state transitions **(C)** as a function of synaptic weights. Each profile was based on eight 24 h simulations. Data presents mean ± s.e.m. Light green, NRi pathway; green, NWi pathway. NS, non-significant (one-way ANOVA).

matter the synaptic weights ($F_{1,7}$ = 4.78e2, $p < 0.0001$, one-way ANOVA), but we observed a smaller reduction in REM sleep and Wake episodes for stronger weights ($F_{1,7}$ = 5.6 and $F_{1,7}$ = 5.4 respectively, $p < 0.0001$ for both, one-way ANOVA). These results correlated with a similar reduction in the number of transitions between the states

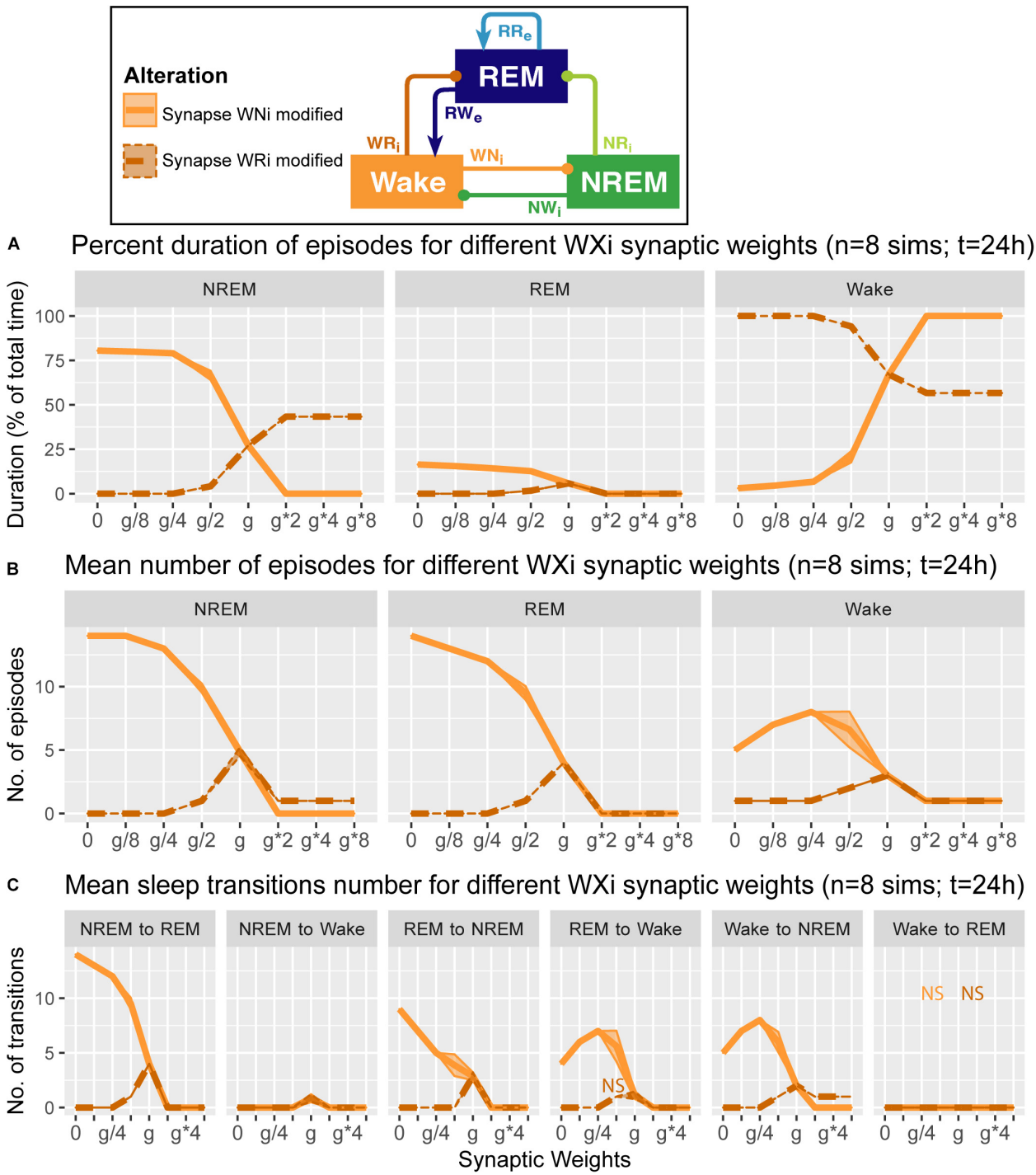

FIGURE 6 | Effects of synaptic weight alterations of the Wake population on sleep architecture. The percentage of time spent in each state **(A)**, the number of episodes **(B)**, and the number of state transitions **(C)** as a function of synaptic weights. Each profile was based on eight 24 h simulations. Data presents mean ± s.e.m. Orange, WNi pathway; brown, WRi pathway. NS, non-significant (one-way ANOVA).

(**Figure 4C**). Thus, the manipulation of the RRe pathway stabilized the network state.

When we manipulated the synaptic weight in the RWe pathway (dark blue in **Figure 4**), the percentage of REM sleep decreased as a function of the synaptic weight ($F_{1,7}$ = 9.31e5, p < 0.0001, one-way ANOVA) whereas the percentage of NREM sleep increased ($F_{1,7}$ = 1.26e5, p < 0.0001, one-way ANOVA) (**Figure 4A**). The weaker weight in the RWe

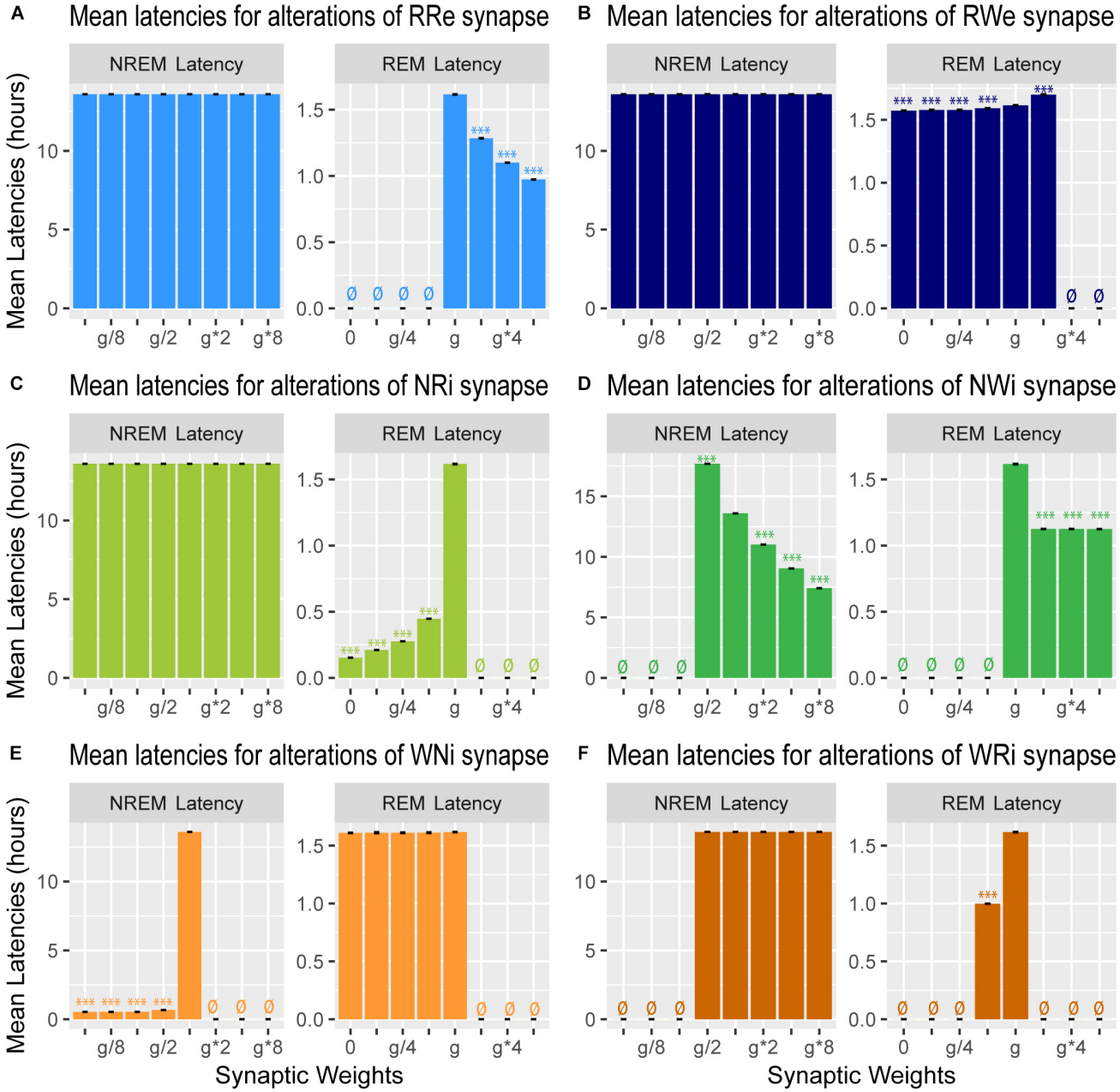

FIGURE 7 | Effects of synaptic weight alterations on sleep latency. Bar graphs represent mean latency for NREM (left) and REM (right) as a function of synaptic weights in modifications of RRe **(A)**, RWe **(B)**, NRi **(C)**, NWi **(D)**, WNi **(E)**, and WRi pathways **(F)**. Error bars, s.e.m.; ø, no occurrence of the state.

pathway extended the duration of REM sleep ($F_{1,7}$ = 9.31e5, $p < 0.0001$, one-way ANOVA). Although the time spent in REM sleep decreased with g^*2 ($F_{1,7}$ = 9.31e5, $p < 0.0001$, one-way ANOVA with *post hoc* Tukey HSD test), the number of REM episodes ($F_{1,7}$ = 6.9, $p < 0.0001$, one-way ANOVA) (**Figure 4B**) and transitions (**Figure 4C**) increased. Hence stronger RWe pathway caused a fragmented sleep–wake cycle although g^*4 and g^*8 provided a different picture, suggesting an optimal range of synaptic strengths to induce the fragmentation of the sleep–wake cycle. Therefore, effects of alterations of REM population output pathways on sleep architecture were highly pathway-dependent.

Alterations of NREM Population Output Pathways and Sleep Architecture

What are the effects of variation in the outputs from the NREM population in the sleep architecture and genesis? Here, we also examined how alterations of the output strengths from the

NREM population contributed to sleep/wake transition, with respect to the percentage of time spent in each state (**Figure 5A**), the number of episodes (**Figure 5B**), and the number of state transitions (**Figure 5C**).

Strengthening the NRi pathway (light green in **Figure 5**) increased the percentage of time spent in NREM ($F_{1,7}$ = 6.93e5, $p < 0.0001$, one-way ANOVA) and decreased that in REM ($F_{1,7}$ = 4.62e5, $p < 0.0001$, one-way ANOVA) and Wake ($F_{1,7}$ = 7.67e5, $p < 0.0001$, one-way ANOVA) (**Figure 5A**). This was associated with the reduction in state transitions (**Figures 5B,C**), meaning state stabilization. On the other hand, weakening the pathway increased the number of sleep episodes ($F_{1,7}$ = 9.20e2, $p < 0.0001$, one-way ANOVA) and transitions (**Figures 5B,C**), meaning fragmentation.

Strengthening the NWi pathway (green in **Figure 5**) increased the percentage of time spent in REM sleep ($F_{1,7}$ = 7.13e5, $p < 0.0001$, one-way ANOVA) and decreased that in NREM ($F_{1,7}$ = 4.88e5, $p < 0.0001$, one-way ANOVA) and Wake ($F_{1,7}$ = 7.37e5, $p < 0.0001$, one-way ANOVA) (**Figure 5A**). Weakening this pathway eliminated sleep episodes completely, meaning that this pathway is essential for sleep genesis.

Alterations of Wake Population Output Pathways and Sleep Architecture

We also examined how alterations of the output strengths from the Wake population contributed to sleep architecture, with respect to the percentage of time spent in each state (**Figure 6A**), the number of episodes (**Figure 6B**), and the number of state transitions (**Figure 6C**).

When we manipulated the synaptic weights in the WNi pathway (orange in **Figure 6**), the percentage of Wake increased as the synaptic weight increased ($F_{1,7}$ = 1.34e4, $p < 0.0001$, one-way ANOVA) (**Figure 6A**). On the other hand, as the synaptic weight decreased, the more the number of episodes increased across three states ($F_{1,7}$ = 9750.7 for REM, $F_{1,7}$ = 8.12e3 for NREM, $F_{1,7}$ = 3.14e2 for Wake, $p < 0.0001$ for all, one-way ANOVA) (**Figure 6B**), with longer sleep states ($F_{1,7}$ = 1.41e4, $p < 0.0001$, one-way ANOVA) (**Figure 6A**).

Contrary to these, when we increased the synaptic weight in the WRi pathway (brown in **Figure 6**), the percentage of Wake decreased ($F_{1,7}$ = 5.72e5, $p < 0.0001$, one-way ANOVA) (**Figure 6A**). There was an optimal range to increase the numbers of sleep episodes ($F_{1,7}$ = 1.27e3, $p < 0.0001$, one-way ANOVA) (**Figure 6B**). Again, the effects of alterations of Wake population output pathways on sleep architecture were pathway-dependent.

Effects of Synaptic Modifications on the Sleep Latency

We also measured the latency of NREM and REM (**Figure 7**): the former is the latency of the first NREM episode since the beginning of the simulation whereas the latter is the latency of the first REM episode since the onset of the first NREM episode.

Strengthening the RRe pathway decreased the REM latency ($F_{7,56}$ = 7.22e5, $p < 0.0001$, one-way ANOVA) (**Figure 7A**) whereas strengthening the RWe pathway increased the REM latency at g*2 ($F_{7,56}$ = 1.11e5, $p < 0.0001$, one-way ANOVA with *post hoc* Tukey HSD test) (**Figure 7B**). As expected, we did not observe any effect on the NREM latency by the manipulation of either pathway (**Figures 7A,B**). Thus, the output pathways from the REM population contributed only to the REM latency.

Weakening the NRi pathway decreased the REM latency ($F_{7,56}$ = 4.43e5, $p < 0.0001$, one-way ANOVA) whereas the NREM latency was not changed (**Figure 7C**). Strengthening the NWi pathway decreased the NREM latency ($F_{7,56}$ = 9,63e7, $p < 0.0001$, one-way ANOVA) whereas the REM latency was also reduced and remained consistent across different weights ($F_{7,56}$ = 5.33e5, $p < 0.0001$, one-way ANOVA) (**Figure 7D**). Thus, the output pathways from the NREM population exhibited complex contributions to the NREM and REM latencies depending on output pathways.

Finally, weakening the WNi pathway decreased the NREM latency ($F_{7,56}$ = 1.53e8, $p < 0.0001$, one-way ANOVA) whereas the REM latency was not affected as long as sleep was induced (**Figure 7E**). While strengthening the WRi pathway did not affect the NREM latency, the REM latency increased at *g*2* ($F_{7,56}$ = 8.29e5, $p < 0.0001$, one-way ANOVA with *post hoc* Tukey HSD test). Thus, the output pathways from the Wake population contributed to the latency of sleep state which was directly influenced.

Effects of Synaptic Modifications on the Dynamics of Population Activity

Investigating the effect of synaptic modifications on the sleep architecture (**Figures 4–6**) and sleep latency (**Figure 7**), we noticed at least two non-trivial responses of the system. First, the strength of the RRe pathway did not correlate with the duration of REM sleep (**Figure 4**). Second, the stronger NWi pathway led to longer REM sleep, rather than longer NREM sleep (**Figure 5**).

To gain insight into the underlying mechanism, we analyzed the firing rate dynamics of three populations (**Figure 8**). With respect to the manipulation of the RRe pathway (**Figure 8A**), in the default condition, the firing rate of the REM-promoting population quickly decreased. This was due to the inhibitory effect from the WRi pathway as the firing rate of the Wake-promoting population increased. However, when the strength of the RRe pathway increased, the firing rate of the REM-promoting population kept high along with increasing the firing rate of the Wake-promoting population. Therefore, by definition, the system entered and kept Wake. Thus, increasing the strength of the RRe pathway led to a pathological state where both the REM-promoting and Wake-promoting populations stay active.

With respect to the manipulation of the NWi pathway (**Figure 8B**), when the strength of the NWi pathway increased, the firing rate of the Wake-promoting population remained low and decreased due to the inhibitory effect of the NWi pathway. This resulted in the saturated firing rate of the REM-promoting population and therefore longer REM sleep. From these two analyses, an optimal range of activation in the Wake-promoting population plays a key role in the regulation of REM sleep.

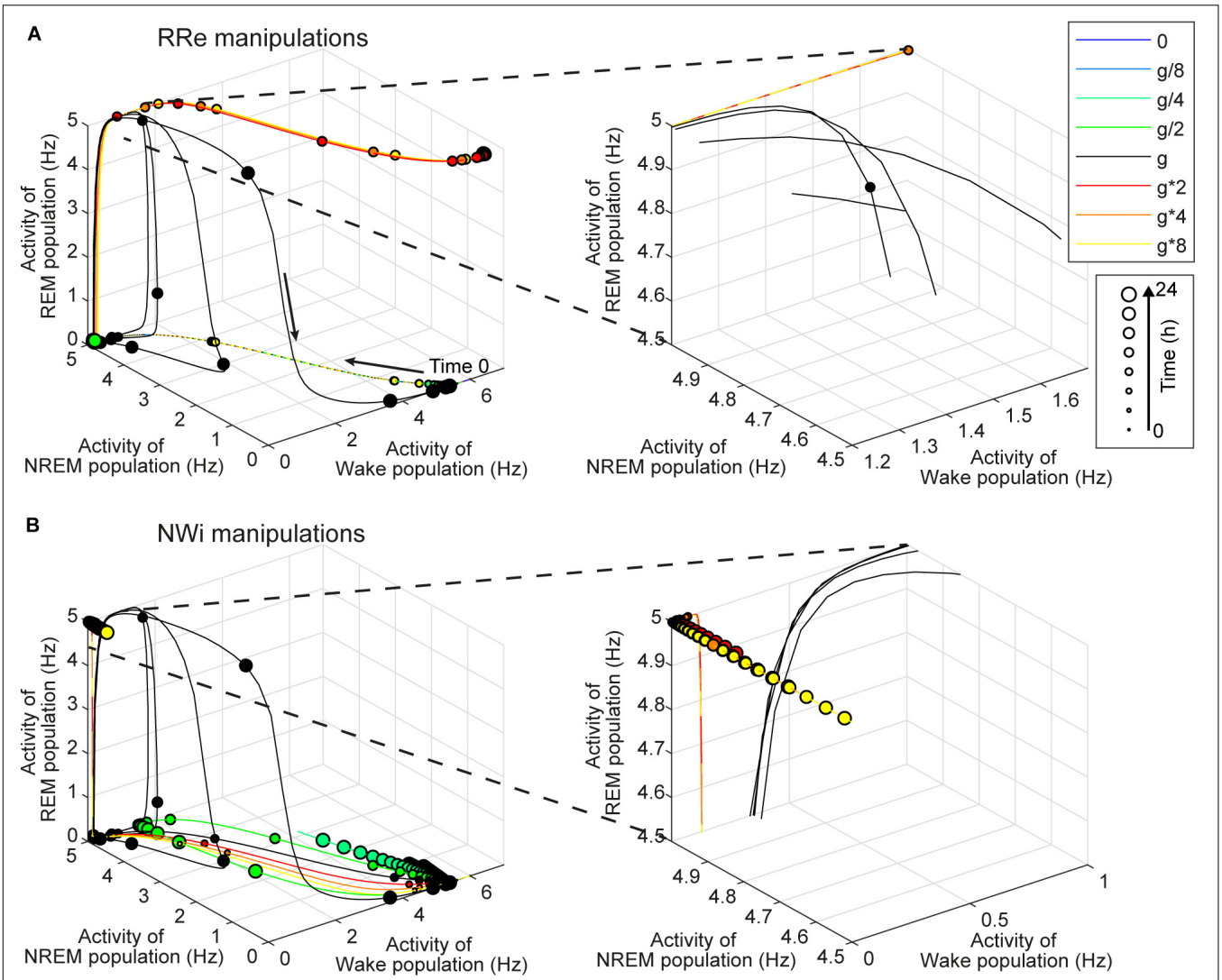

FIGURE 8 | Effects of synaptic modifications on the dynamics of population activity. **(A)** Modifications of RRe pathway. **(B)** Modifications of NWi pathway. In each plot, the firing rate dynamics of three populations are shown in three-dimensional space. Line colors indicate types of synaptic modifications. Every 30-min time point is marked and their sizes represent time points of the simulation. Right panels show the magnified traces.

Joint Alterations of Two Output Pathways From Each Population and Sleep Architecture

Finally, to gain further insight into the role of each pathway in the behavior of this model, we manipulated the strength of the two output pathways from each population (**Figure 9**). Two types of joint manipulations could increase the total duration of REM sleep: first, the stronger RRe pathway with the weaker RWe pathway increased the duration of REM sleep (**Figure 9A**). This was consistent with the intuition obtained above (**Figure 8A**). Second, the weaker NRi pathway with the stronger NWi pathway also increased the duration of REM sleep (**Figure 9B**). To increase the total duration of NREM sleep, in addition to the weaker RRe pathway or stronger inhibitory synapses from the NREM-promoting population, the stronger WRi pathway with the weaker WNi pathway also lead to longer NREM sleep (**Figure 9C**). These results indicate that the balance between two outputs is crucial to determine the sleep architecture.

DISCUSSION

In this study, we have introduced a modeling framework to investigate the dynamics of the sleep–wake cycle and the effects of internal network manipulations (i.e., synaptic weight variations) on its regulation. We have implemented a simple computational model with three interconnected neural populations (**Figure 1**), each one promoting a different state of the sleep–wake cycle (wakefulness, REM and NREM sleep). We have comprehensively assessed how the manipulation of synaptic weight affects the dynamics of the sleep–wake cycle in our model. We found

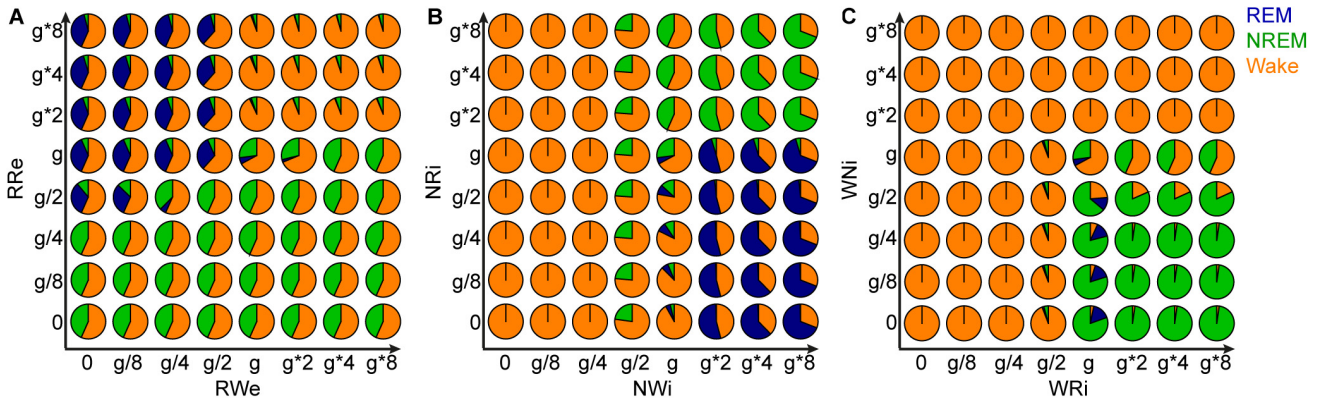

FIGURE 9 | Effects of joint manipulation of two output pathways on the percentage of vigilance states. **(A)** The manipulation of output pathways from REM-promoting population. Each pie chart shows the percentage of three vigilance states at a certain joint manipulation. **(B)** The manipulation of output pathways from NREM-promoting population. **(C)** The manipulation of output pathways from Wake-promoting population.

that effects of synaptic weight alterations on the sleep dynamics depend on the pathway where the synapse belongs (**Figures 2–9**). For example, the manipulation of the two outputs from the Wake-promoting population showed opposite outcomes: one was lengthening the wakefulness state whereas the other was shortening it. Thus, the sleep–wake dynamics is regulated in a pathway-dependent manner.

Implications of the Current Study

In previous studies, the performances of network models have been explored (Diniz Behn and Booth, 2012; Diniz Behn et al., 2013; Weber, 2017) and these models can replicate sleep dynamics (Diniz-Behn and Booth, 2010) as well as state-dependent neural firing (Tamakawa et al., 2006). However, few studies have reported how the strength of synaptic connections between wake- and sleep-promoting populations contribute to the sleep architectures. The present or similar studies may lead to at least two directions: first, this type of simulations may provide insight into the underlying mechanisms of inter-species differences in sleep dynamics as well as pathological sleep conditions in humans. Second, given the advent of recent technological advance, such as optogenetics and chemogenetics, addressing this issue *in silico* may provide insight into the design of new experiments.

For example, the REM-promoting population in the current model presumably represents pontine cholinergic populations. Experimentally, the involvement of pontine cholinergic populations in the initiation and maintenance of REM sleep has been actively debated (Grace and Horner, 2015): lesion and pharmacological studies have provided inconsistent and contradictory results (Amatruda et al., 1975; Webster and Jones, 1988; Boissard et al., 2002; Grace et al., 2014). Even recent chemogenetic and optogenetic experiments also provided conflicting observations (Van Dort et al., 2015; Kroeger et al., 2017): chemogenetic activation has no effect on REM sleep whereas optogenetic activation can trigger REM sleep. Our observations (**Figures 4**, **8**, **9**) demonstrated that the activation of both pathways had little effect on REM sleep whereas a more specific manipulation can increase the duration of REM sleep (**Figure 9**). These results suggest that the complex balance of the synaptic strength between the RRe and RWe pathways may determine the duration of REM sleep. Therefore, it would be interesting to adopt pathway-specific manipulations of cholinergic activity to reconcile this issue in future.

Another intriguing observation is that measuring the latency of sleep states provided relatively intuitive outcomes. For example, strengthening the RRe pathway could reduce the REM latency without increasing the duration of REM sleep (**Figure 7A**), consistent with recent experimental observations (Carrera-Cañas et al., 2019). Strengthening the NWi pathways also reduced the NREM latency (**Figure 7D**). Thus, measuring the latency to change states may provide insights into the role of the manipulated pathway in sleep regulation.

Another general implication can be derived from the results that the pathways which are not directly connected to the REM population can contribute to the duration of REM sleep. It is possible that any manipulations can make distal impacts, resulting in unexpected state alternations. This effect is called "Diaschisis" or "shocked throughout," describing the sudden loss of function in another portion of the brain through being linked with a distal, (directly) affected brain region (Carrera and Tononi, 2014; Otchy et al., 2015). This implies that experimental observations may need to be interpret with care. Our simulations directly demonstrated such indirect effects even in our simple model.

Limitations and Possible Improvements

One of the major limitations in the present study is that the network model did not fully capture biological sleep-wake regulation. For example, the duration of REM sleep episodes typically increases during the sleep period. Our model did not implement such a homeostatic regulation of REM sleep. Therefore, some of our observations do not necessarily predict the behavior of biological circuits. To address these issues, it would be important to extend the network size to reflect more biological observations (Tamakawa et al., 2006).

For example, the reciprocal interaction present in our model between Wake and REM promoting populations has been hypothesized to be a part of the REM sleep regulation, which can be under the control of a circadian modulation (Lu et al., 2006; Sapin et al., 2009; Costa et al., 2016). The model presented here does include an homeostatic sleep drive through the NREM-promoting population, but does not have any circadian modulation, which is known to be another important sleep drive (Fuller et al., 2006; Scammell et al., 2017; Weber et al., 2018; Herice et al., 2019). These effects could be implemented into the model by adding some corresponding populations such as the suprachiasmatic nucleus (SCN), which heavily influences the sleep/wake transitions (Fleshner et al., 2011; Booth and Diniz Behn, 2014).

In addition to the extension of the network, it would be interesting to refine the formalism of the model. Indeed, in this study we focused on the activity of the neural populations and network dynamics rather than on the activity of single neurons. Such a model with a more detailed formalism (with spiking neurons for example) would be attractive but its implementation would require more parameters derived from experimental work. More quantitative experimental data are certainly required to create even more realistic networks (Herice et al., 2019).

Another limitation to the present work is that we manipulated the synaptic strength during the entire simulation period. In biological experiments, however, manipulations can be transient, such as in optogenetic experiments (Adamantidis et al., 2007; Van Dort et al., 2015; Weber et al., 2015). It would be interesting to manipulate synaptic weights transiently in the network model.

Relating to this point, it may be also interesting to reconsider the definition of the state in the model. In particular, if the activity of each neural population is manipulated, the current definition (see section Materials and Methods) cannot be adopted because the activity of each population itself defines the state. To address this issue, it would be interesting to connect the modeled sleep–wake regulating circuit to cortical circuits and muscle units, through which the state of the system can be defined based on the activity of the cortical circuits or muscle units as in biological experiments. This direction will become an important topic to better understand how subcortical sleep-regulating circuits and cortical circuits interact with each other across the sleep–wake cycle and how recent closed-loop stimulation approaches affect neural circuit dynamics as well as connectivity (Marshall et al., 2006; Ngo et al., 2019).

CONCLUSION

In conclusion, utilizing a simple network model of the sleep–wake cycle, we found pathway-dependent effects of synaptic weight manipulations on sleep architecture. Given the fact that even the simple network model can provide complex behaviors, designing *in vivo* experiments and interpreting the outcomes require careful considerations about the complexity of sleep–wake regulating circuits. A similar computational approach could complement to make specific predictions for *in vivo* experiments.

DATA AVAILABILITY STATEMENT

The datasets generated and analyzed for this study can be found on GitHub (https://github.com/Sakata-Lab/sleep-model) and at https://doi.org/10.15129/f3fe4727-a05e-469e-b762-6b2c8a9b5b5f.

AUTHOR CONTRIBUTIONS

SS and CH designed the project, performed the simulations, analyzed the data, and wrote the manuscript. CH developed the code.

FUNDING

This work was supported by BBSRC (BB/M00905X/1), Leverhulme Trust (RPG-2015-377), and Alzheimer's Research UK (ARUK-PPG2017B-005) to SS.

ACKNOWLEDGMENTS

We thank Arno Onken, William Berg, Aimee Bias, and Emma Mitchell for critical reading of the manuscript. This manuscript has been released as a Pre-Print at BioRxiv (Héricé and Sakata, 2019).

SUPPLEMENTARY MATERIAL

The Supplementary Material for this article can be found online at: https://www.frontiersin.org/articles/10.3389/fnins.2019.01380/full#supplementary-material

REFERENCES

Achermann, P., and Borbely, A. A. (1990). Simulation of human sleep: ultradian dynamics of electroencephalographic slow-wave activity. *J. Biol. Rhythms* 5, 141–157. doi: 10.1177/074873049000500206

Adamantidis, A. R., Zhang, F., Aravanis, A. M., Deisseroth, K., and de Lecea, L. (2007). Neural substrates of awakening probed with optogenetic control of hypocretin neurons. *Nature* 450, 420–424. doi: 10.1038/nature06310

Amatruda, T. T. III, Black, D. A., McKenna, T. M., McCarley, R. W., and Hobson, J. A. (1975). Sleep cycle control and cholinergic mechanisms: differential effects of carbachol injections at pontine brain stem sites. *Brain Res.* 98, 501–515. doi: 10.1016/0006-8993(75)90369-8

Archermann, P., and Borbely, A. A. (2017). "Sleep homeostasis and models of sleep regulation," in *Principles and Practice of Sleep Medicine*, eds M. Kryger, T. Roth, and W. C. Dement (Philadelphia, PA: Elsevier), 377–387.

Boissard, R., Gervasoni, D., Schmidt, M. H., Barbagli, B., Fort, P., and Luppi, P. H. (2002). The rat ponto-medullary network responsible for paradoxical sleep onset and maintenance: a combined microinjection and functional neuroanatomical study. *Eur. J. Neurosci.* 16, 1959–1973. doi: 10.1046/j.1460-9568.2002.02257.x

Booth, V., and Diniz Behn, C. G. (2014). Physiologically-based modeling of sleep-wake regulatory networks. *Math. Biosci.* 250, 54–68. doi: 10.1016/j.mbs.2014.01.012

Booth, V., Xique, I., and Diniz Behn, C. G. (2017). One-dimensional map for the circadian modulation of sleep in a sleep-wake regulatory network model for human sleep. *Siam J. Appl. Dyn. Syst.* 16, 1089–1112. doi: 10.1137/16m1071328

Borbély, A. A. (1982). A two process model of sleep regulation. *Hum neurobiol* 1, 195–204.

Brown, R. E., Basheer, R., McKenna, J. T., Strecker, R. E., and McCarley, R. W. (2012). Control of sleep and wakefulness. *Physiol. Rev.* 92, 1087–1187. doi: 10.1152/physrev.00032.2011

Carrera, E., and Tononi, G. (2014). Diaschisis: past, present, future. *Brain* 137(Pt 9), 2408–2422. doi: 10.1093/brain/awu101

Carrera-Cañas, C., Garzón, M., and de Andrés, I. (2019). The transition between slow-wave sleep and REM sleep constitutes an independent sleep stage organized by cholinergic mechanisms in the rostrodorsal pontine tegmentum. *Front. Neurosci.* 13:748. doi: 10.3389/fnins.2019.00748

Carskadon, M. A. (2017). "Normal human sleep: an overview," in *Principles and Practice of Sleep Medicine*, eds M. Kryger, T. Roth, and W. C. Dement (Philadelphia, PA: Elsevier), 15–24.

Costa, M. S., Born, J., Claussen, J. C., and Martinetz, T. (2016). Modeling the effect of sleep regulation on a neural mass model. *J. Comput. Neurosci.* 41, 15–28. doi: 10.1007/s10827-016-0602-z

Diniz Behn, C. G., Ananthasubramaniam, A., and Booth, V. (2013). Contrasting existence and robustness of rem/non-rem cycling in physiologically based models of rem sleep regulatory networks. *SIAM J. Appl. Dyn. Syst.* 12, 279–314. doi: 10.1137/120876939

Diniz Behn, C. G., and Booth, V. (2012). A fast-slow analysis of the dynamics of REM sleep. *Siam J. Appl. Dyn. Syst.* 11, 212–242. doi: 10.1016/j.mbs.2014.01.012

Diniz Behn, C. G., Brown, E. N., Scammell, T. E., and Kopell, N. J. (2007). Mathematical model of network dynamics governing mouse sleep-wake behavior. *J. Neurophysiol.* 97, 3828–3840. doi: 10.1152/jn.01184.2006

Diniz-Behn, C. G., and Booth, V. (2010). Simulating microinjection experiments in a novel model of the rat sleep-wake regulatory network. *J. Neurophysiol.* 203, 1937–1953. doi: 10.1152/jn.00795.2009

Fleshner, M., Booth, V., Forger, D. B., and Diniz-Behn, C. G. (2011). Circadian regulation of sleep-wake behaviour in nocturnal rats requires multiple signals from suprachiasmatic nucleus. *Philos. Trans. R. Soc. A* 369, 3855–3883. doi: 10.1098/rsta.2011.0085

Fuller, P. M., Gooley, J. J., and Saper, C. B. (2006). Neurobiology of the sleep-wake cycle: sleep architecture, circadian regulation, and regulatory feedback. *J. Biol. Rhythms* 21, 482–493. doi: 10.1177/0748730406294627

Grace, K. P. (2015). How useful is optogenetic activation in determining neuronal function within dynamic circuits? *Proc. Natl. Acad. Sci. U.S.A.* 112, E3755.

Grace, K. P., and Horner, R. L. (2015). Evaluating the evidence surrounding pontine cholinergic involvement in REM sleep generation. *Front. Neurol.* 6:190. doi: 10.3389/fneur.2015.00190

Grace, K. P., Vanstone, L. E., and Horner, R. L. (2014). Endogenous cholinergic input to the pontine REM sleep generator is not required for REM sleep to occur. *J. Neurosci.* 34, 14198–14209. doi: 10.1523/JNEUROSCI.0274-14.2014

Herice, C., Patel, A. A., and Sakata, S. (2019). Circuit mechanisms and computational models of REM sleep. *Neurosci. Res.* 140, 77–92. doi: 10.1016/j.neures.2018.08.003

Héricé, C., and Sakata, S. (2019). Pathway-dependent regulation of sleep dynamics in a network model of the sleep-wake cycle. *bioRxiv[Preprints]*. doi: 10.1101/705822

Hobson, J. A., McCarley, R. W., and Wyzinski, P. W. (1975). Sleep cycle oscillation: reciprocal discharge by two brainstem neuronal groups. *Science* 189, 55–58. doi: 10.1126/science.1094539

Jouvet, M. (1962). [Research on the neural structures and responsible mechanisms in different phases of physiological sleep]. *Arch. Ital. Biol.* 100, 125–206.

Kroeger, D., Ferrari, L. L., Petit, G., Mahoney, C. E., Fuller, P. M., Arrigoni, E., et al. (2017). Cholinergic, glutamatergic, and GABAergic neurons of the pedunculopontine tegmental nucleus have distinct effects on sleep/wake behavior in mice. *J. Neurosci.* 37, 1352–1366. doi: 10.1523/JNEUROSCI.1405-16.2016

Lu, J., Sherman, D., Devor, M., and Saper, C. B. (2006). A putative flip–flop switch for control of REM sleep. *Nature* 441:589. doi: 10.1038/nature04767

Luppi, P. H., Clement, O., and Fort, P. (2013). Paradoxical (REM) sleep genesis by the brainstem is under hypothalamic control. *Curr. Opin. Neurobiol.* 23, 786–792. doi: 10.1016/j.conb.2013.02.006

Luppi, P. H., Peyron, C., and Fort, P. (2017). Not a single but multiple populations of GABAergic neurons control sleep. *Sleep Med. Rev.* 32, 85–94. doi: 10.1016/j.smrv.2016.03.002

Marshall, L., Helgadottir, H., Molle, M., and Born, J. (2006). Boosting slow oscillations during sleep potentiates memory. *Nature* 444, 610–613. doi: 10.1038/nature05278

McCarley, R. W., and Hobson, J. A. (1971). Single neuron activity in cat gigantocellular tegmental field: selectivity of discharge in desynchronized sleep. *Science* 174, 1250–1252. doi: 10.1126/science.174.4015.1250

McCarley, R. W., and Hobson, J. A. (1975). Neuronal excitability modulation over the sleep cycle: a structural and mathematical model. *Science* 189, 58–60. doi: 10.1126/science.1135627

Ngo, H. V., Seibold, M., Boche, D. C., Molle, M., and Born, J. (2019). Insights on auditory closed-loop stimulation targeting sleep spindles in slow oscillation up-states. *J. Neurosci. Methods* 316, 117–124. doi: 10.1016/j.jneumeth.2018.09.006

Otchy, T. M., Wolff, S. B., Rhee, J. Y., Pehlevan, C., Kawai, R., Kempf, A., et al. (2015). Acute off-target effects of neural circuit manipulations. *Nature* 528, 358–363. doi: 10.1038/nature16442

Robinson, P. A., Phillips, A. J., Fulcher, B. D., Puckeridge, M., and Roberts, J. A. (2011). Quantitative modelling of sleep dynamics. *Philos. Trans. A Math. Phys. Eng. Sci.* 369, 3840–3854. doi: 10.1098/rsta.2011.0120

Saper, C. B., Chou, T. C., and Scammell, T. E. (2001). The sleep switch: hypothalamic control of sleep and wakefulness. *Trends Neurosci.* 24, 726–731. doi: 10.1016/s0166-2236(00)02002-6

Sapin, E., Lapray, D., Bérod, A., Goutagny, R., Léger, L., Ravassard, P., et al. (2009). Localization of the brainstem GABAergic neurons controlling paradoxical (REM) sleep. *PLoS One* 4:e4272. doi: 10.1371/journal.pone.0004272

Scammell, T. E., Arrigoni, E., and Lipton, J. O. (2017). Neural circuitry of wakefulness and sleep. *Neuron* 93, 747–765. doi: 10.1016/j.neuron.2017.01.014

Schwarz, L. A., and Luo, L. (2015). Organization of the locus coeruleus-norepinephrine system. *Curr. Biol.* 25, R1051–R1056. doi: 10.1016/j.cub.2015.09.039

Tamakawa, Y., Karashima, A., Koyama, Y., Katayama, N., and Nakao, M. (2006). A quartet neural system model orchestrating sleep and wakefulness mechanisms. *J. Neurophysiol.* 95, 2055–2069. doi: 10.1152/jn.00575.2005

Van Dort, C. J., Zachs, D. P., Kenny, J. D., Zheng, S., Goldblum, R. R., Gelwan, N. A., et al. (2015). Optogenetic activation of cholinergic neurons in the PPT or LDT induces REM sleep. *Proc. Natl. Acad. Sci. U.S.A.* 112, 584–589. doi: 10.1073/pnas.1423136112

Weber, F. (2017). Modeling the mammalian sleep cycle. *Curr. Opin. Neurobiol.* 46, 68–75. doi: 10.1016/j.conb.2017.07.009

Weber, F., Chung, S., Beier, K. T., Xu, M., Luo, L., and Dan, Y. (2015). Control of REM sleep by ventral medulla GABAergic neurons. *Nature* 526, 435–438. doi: 10.1038/nature14979

Weber, F., and Dan, Y. (2016). Circuit-based interrogation of sleep control. *Nature* 538, 51–59. doi: 10.1038/nature19773

Weber, F., Do, J. P. H., Chung, S., Beier, K. T., Bikov, M., Doost, M. S., et al. (2018). Regulation of REM and Non-REM sleep by periaqueductal GABAergic neurons. *Nat. Commun.* 9:354. doi: 10.1038/s41467-017-02765-w

Webster, H. H., and Jones, B. E. (1988). Neurotoxic lesions of the dorsolateral pontomesencephalic tegmentum-cholinergic cell area in the cat. II. Effects upon sleep-waking states. *Brain Res.* 458, 285–302. doi: 10.1016/0006-8993(88)90471-4

Conflict of Interest: The authors declare that the research was conducted in the absence of any commercial or financial relationships that could be construed as a potential conflict of interest.

Copyright © 2019 Héricé and Sakata. This is an open-access article distributed under the terms of the Creative Commons Attribution License (CC BY). The use, distribution or reproduction in other forums is permitted, provided the original author(s) and the copyright owner(s) are credited and that the original publication in this journal is cited, in accordance with accepted academic practice. No use, distribution or reproduction is permitted which does not comply with these terms.

Advantages of publishing in Frontiers

OPEN ACCESS
Articles are free to read for greatest visibility and readership

FAST PUBLICATION
Around 90 days from submission to decision

HIGH QUALITY PEER-REVIEW
Rigorous, collaborative, and constructive peer-review

TRANSPARENT PEER-REVIEW
Editors and reviewers acknowledged by name on published articles

Frontiers
Avenue du Tribunal-Fédéral 34
1005 Lausanne | Switzerland

Visit us: www.frontiersin.org
Contact us: info@frontiersin.org | +41 21 510 17 00

REPRODUCIBILITY OF RESEARCH
Support open data and methods to enhance research reproducibility

DIGITAL PUBLISHING
Articles designed for optimal readership across devices

FOLLOW US
@frontiersin

IMPACT METRICS
Advanced article metrics track visibility across digital media

EXTENSIVE PROMOTION
Marketing and promotion of impactful research

LOOP RESEARCH NETWORK
Our network increases your article's readership